ON THE MECHANISMS OF MINOR MORAINE FORMATION IN HIGH-MOUNTAIN ENVIRONMENTS OF THE EUROPEAN ALPS

Cianna E. Wyshnytzky

Submitted in partial fulfilment of the
requirements of the Degree of
Doctor of Philosophy
in Geography

Queen Mary University of London
2017

I, Cianna E. Wyshnytzky, confirm that the research included within this thesis is my own work or that where it has been carried out in collaboration with, or supported by others, that this is duly acknowledged below and my contribution indicated. Previously published material is also acknowledged below.

I attest that I have exercised reasonable care to ensure that the work is original, and does not to the best of my knowledge break any UK law, infringe any third party's copyright or other Intellectual Property Right, or contain any confidential material.

I accept that the College has the right to use plagiarism detection software to check the electronic version of the thesis.

I confirm that this thesis has not been previously submitted for the award of a degree by this or any other university.

Signature: Cianna E. Wyshnytzky
Date: 30 December 2016

Details of collaboration and publications:
Dr. Kathryn Adamson at Manchester Metropolitan University processed ground-penetrating radar data. All subsequent figures and interpretations presented in the text are my own.

ABSTRACT

Groups of closely spaced minor moraines allow for observations of moraine formation and ice-marginal fluctuations on short timescales, helping to better understand glacier retreat and predict its geomorphological effects. Some minor moraines can be classified as annual moraines given sufficient chronological control, which implies a seasonal climatic driver of ice-marginal fluctuations. This leads to moraines being utilised as very specific, short-term records of glacier fluctuations and climate change. This research is common in lowland, maritime settings, but remains sparse in high-mountain settings.

This study presents the detailed geomorphological and sedimentological results of minor moraines at two high-mountain settings in the European Alps. Geomorphological investigations included mapping and measurements through field observations and remotely-sensed imagery. Detailed sedimentological investigations followed excavation of moraines and include multiple scales of observation and measurements to support interpretations of sediment transport and deposition. Additionally, ground-penetrating radar data were collected in one foreland.

Minor moraines at Schwarzensteinkees, Austria, formed as push or combined push and freeze-on moraines in two groups between approximately 1850 and 1930. The existence of a former proglacial lake appears to have exerted a strong control on moraine formation. Modern minor moraines at Silvrettagletscher, Switzerland, exist primarily on reverse bedrock slopes and have formed since approximately 1850 through push, freeze-on, and controlled moraine mechanisms. The presence of these bedrock slopes, and in some areas englacial debris septa, appear to exert the primary controls on moraine formation. The foreland of Gornergletscher, Switzerland, has been revisited using aerial imagery to assess if moraines are still forming annually, and this has been confirmed.

These findings show a range of mechanisms responsible for moraine formation, which are then compared to previously published research on minor moraines to elucidate any common drivers of minor and annual moraine formation globally. This includes a global database of forelands where minor moraines have been studied, created as part of this research and presented as a table and Google Earth file, both easily accessible and freely available online, for use by other researchers when exploring similar topics.

ACKNOWLEDGEMENTS

A list of thanks would be inadequate without starting with my supervisor, Sven Lukas. It was his continued interest in the topic, after one brief visit to Gornergletscher, which sparked the idea for this project and the drive to find a graduate student to continue work on “annual” moraines in the Alps. Other specific thanks include proofreading my German writing, handling hydrofluoric acid in the lab so that I didn’t have to, and meetings over coffee. Mostly, thank you for helping me grow as a researcher, writer, and educator.

This research would not have been possible without funding from various organizations, which are wholly thanked for their contributions. Fieldwork in Austria was possible through the QMUL Postgraduate Research Fund and Expeditions Fund, the BSG Postgraduate Research Grant, and the Gilchrist Educational Trust Grants For Expeditions. Fieldwork in Switzerland was possible through the RGS Dudley Stamp Award, the QRA New Research Worker’s Award, and the IAS Postgraduate Grant Scheme. Funding to attend the EGU Annual Meeting was partially provided by the EGU Early Career Scientist’s Travel Award and the IAS Travel Grant. All of these organizations made up for the shortcomings of governmental powers that be in the United Kingdom, who would prefer not to support foreign students contributing to scientific research at their institutions.

The Berliner Hütte, Austria, and Silvrettahütte, Switzerland, provided wonderful fieldwork accommodations, food, and logistical support. Many individuals helped during or preparing for fieldwork as part of TEAM ALPS 2014, 2015, and 2016 (Harry McMahon, John Groves, Josh Leigh, Marie Busfield, Michelle Day, Niall Lehane, Sven Lukas, Tom Howlin), and a special thanks to Lindsey Harrington for accompanying me for a day and night in Switzerland. Other members of the physical geography contingent of QMUL are thanked for discussion, ideas, trouble-shooting, and breaks from office work. Kathryn Adamson (Manchester Metropolitan University) is thoroughly thanked for processing GPR data. The summer weather systems of the Alps are thanked for giving at least a few relatively decent days to conduct fieldwork free from blinding fog, torrential downpour, and blizzard conditions. My lack of formal glacial coursework is not thanked, although self-taught disciplines hold merit in their own. To my bags of sand trapped in the dark: It’s not my fault you have been abandoned. I will resurrect you eventually.

A special thanks to my family and other half for enduring three years of my general absence from the United States. Although modern technology easily facilitates communication and visits across an ocean, the separation by a large body of water cannot truly be reconciled. No list of acknowledgements for the years behind this thesis would be possible without the greatest thanks to a specific canine, but that deserves a page in itself…

DEDICATION

To the one that kept me sane, because we were not meant for this place.

Let's move back to some mountains.

You deserve this as much as I do, dog.

Congratulations, Dr. Geomorphologist Labradorite Wyshnytzky (MSc, PhD)!

TABLE OF CONTENTS

LIST OF FIGURES

Page

LIST OF TABLES

Page

CHAPTER 1. Introduction

"And the mountains said I will find you here. They whispered the snow and leaves in my ear.
I traced my fingers along your trails, and your body was the map. I was lost in it.
Floating over your rocky spine. The glaciers made you and now you're mine."
Your Rocky Spine by Great Lake Swimmers

Understanding the evolution of a glacial landscape is critical in accurately reconstructing modern- and palaeoenvironmental records and glacier dynamics (Owen et al., 2009). Glaciers are sensitive to climate change, as changes in mass balance and ice front position are primarily driven by changes in temperature and precipitation. However, where direct ice measurements do not exist, an accurate chronological framework for geomorphological evolution of a glacier foreland is imperative to trace landscape evolution and ties to climate records. Fortunately, landforms can sometimes be used in one specific field area or across a region as geochronological markers and markers of former ice extent.

Moraines are accumulations of sediment once carried subglacially, englacially, or supraglacially prior to deposition by a glacier, or they can comprise proglacial sediment deformed by the glacier. Moraines can therefore demarcate former and present ice-margin positions in frontal or lateral positions, or additionally as a combined latero-frontal moraine (Evans and Benn, 2004; Bennett and Glasser, 2009; Benn and Evans, 2010). Research on moraines informs our understanding of ice-marginal dynamics and moraine formation, and also inherently includes investigation of the interaction between proglacial ice-marginal and glaciofluvial environments through deformation and evolution of the glacier foreland, deformation of proglacial sediments, and the role of proglacial fluvial systems in enhancing or limiting preservation potential of landforms (Owen et al., 2009). Understanding these factors may also help in assessing the role of subglacial, supraglacial, and englacial sediments in landscape evolution.

The term "minor moraines" in this thesis refers to groups of end moraines < 4 m high, differentiated from the broader category of "moraines" by their occurrence in clusters and small sizes. This definition refers to modern observation, and acknowledges that moraines may degrade or completely erode through time, as discussed throughout this thesis. Minor moraines may help further the understanding of climate influences on glacier dynamics, particularly when they are shown to be annually formed. Such annual moraines, as the name implies, record ice-marginal and climate fluctuations from year to year, and thus represent the most dynamic end-member response of glaciers to the effects of precipitation and temperature (Krüger, 1995; Bradwell, 2004; Beedle et al., 2009; Lukas, 2012; Bradwell et al., 2013; Reinardy et al., 2013; Chandler et al., 2016a). Modern annual

moraines therefore present a suitable landform to connect to climate forcing on a yearly timescale and through the several years that their groups span, as many exist during the period of modern climate recordings. An understanding of annual moraine formation in regards to the physical processes of ice motion and glaciotectonic deformation of foreland sediments compared to climate data helps ascertain if and how climatic drivers influence the position of the ice front and thus moraine formation and which climate signals annual moraines record. Research on modern annual moraines may also help inform studies of similar features in a Pleistocene context by refining glacier reconstructions and the interpretations of similar and larger Pleistocene landforms (Ham and Attig, 2001; Evans et al., 2014) and palaeoclimatology (Bennett, 2001).

Understanding glacial systems is increasingly important in a modern context, as most glaciers across the world are retreating (Zemp et al. 2008). Detailed investigations of modern minor moraines are especially important during this period of global glacier retreat, as they allow a down-scaled glimpse into moraine formation and ice-marginal fluctuations on short timescales and the duration of individual events (Reinardy et al., 2013; Chandler et al., 2016a). Suites of minor moraines allow a way to assess the role of ice-marginal fluctuations during periods of overall retreat, therefore providing means to predict how retreating ice may influence the future landscape and how glaciers may respond to a warming climate. This research can also inform on the implications of glacier change for communities that depend on meltwater for personal and agricultural uses (e.g. Huss et al., 2010; Aizen, 2011) and the snow sports and tourism industries that rely on glaciers and snowfields (e.g. Steiger and Mayer, 2008; Fox, 2013; Stewart et al., 2016).

1.1 Literature review and global minor moraines database

As introduced above, minor moraines are small-scale ice-marginal landforms formed during periods of overall glacier retreat punctuated by small-scale and short-lived readvances. These landforms have been studied since 1967 in modern environments (Hewitt, 1967) and 1942 in Pleistocene settings (Gwynne, 1942). The term “annual moraines” has been used to describe groups of minor moraines in which one moraine forms every year (Andersen and Sollid, 1971; Worsley, 1974; Birnie, 1977; Sharp, 1984; Ono, 1985; Boulton, 1986; Gordon and Timmis, 1992; Krüger, 1995; Evans et al., 1999a; Evans et al., 1999b; Bradwell, 2004; Evans and Hiemstra, 2005; Beedle et al., 2009; Lukas, 2012; Schomacker et al., 2012; Bradwell et al., 2013; Reinardy et al., 2013; Chandler et al., 2016a).

To date, no systematic research has been done on minor moraines on a scale that exceeds the local, despite their aforementioned significance. Therefore, one of the primary objectives of this thesis is to assess minor moraine formation globally. The literature review

and global minor moraines database (GLOMMAD16) presented in this thesis are designed to compile studies that present information about annual moraines, minor moraines, or allusions to either and work together as an overview in tabular format and more detail regarding author methods and interpretations in written format. This surveyed publications in the English language, as these publications are available to the largest audience. This compilation will then inform a review and synthesis of global minor moraine research in Section 1.1.4 and be referred to in Chapter 7 when incorporating the study areas presented in this thesis.

This literature review and GLOMMAD16 are organised by country, in alphabetical order, with minor moraines reported in modern settings presented first and those in Pleistocene ice sheet settings second. Subgroupings organise specific research by mountain range or ice cap, in alphabetical order. This division aids in geographical comparisons amongst study areas (Section 1.1.3) and most clearly showcases the relative number of studies in each broader setting.

The literature review and database do not include previous work that discusses minor moraines in several specific settings. Minor moraines formed by surging glaciers (e.g. Jónsson et al., 2014; Flink et al., 2015) are not discussed because the dynamics of surging systems vary considerably from non-surging glacial systems and are not clearly understood (Sevestre and Benn, 2015). The global minor moraines database also omits previous work from glaciers that terminate in large bodies of water (e.g. Boulton, 1986; Flink et al., 2015), as they include different dynamics at the ice front than terrestrially-terminating glaciers due to the influences of calving, grounding lines, and circulation patterns of the aqueous environment on ice front dynamics (Benn et al., 2007). This compilation additionally omits research that discusses the creation of minor moraines during overall periods of ice advances punctuated by periods of short-lived retreat, leaving no landform record due to obliterative overlap, and therefore only observable through detailed remote sensing or field observations at the time of advance (e.g. Winkler and Nesje, 1999). Lastly, this database does not include groups of closely spaced recessional moraines formed during former periods of glaciation for which seasonal ice margin oscillations have not been suggested or inferred by the authors, such as Younger Dryas moraines in Scotland (e.g. Lukas, 2005; Benn and Lukas, 2006; Lukas and Benn, 2006; Finlayson et al., 2011; Boston et al., 2015). Although, it should be noted that Lukas (2005) recognizes the exciting possibility that some of these moraines may reflect annual fluctuations of the ice margin, but that this cannot be resolved.

1.1.1 Modern settings

Canada: Canadian Rockies

Minor moraines at Athabasca Glacier are recorded by several researchers (Welch, 1967; Kucera, 1972, 1981; Luckman, 1988; Luckman, 2017) but described in more detail by the Luckman (1988, 2017). The moraines formed during the periods 1924-1930/31 (Luckman, 1988), 1962-1981, and 1999-2007 and are composed of till and unconsolidated foreland sediment (Luckman, 2017). Luckman (1988, 2017) ascribes a pushing mechanisms of moraine formation, although the sedimentological architecture of the moraines is not further described. An example photograph shows the well-defined ridges of the 1962-1981 period. Luckman (1988, 2017) states that documentary evidence, aerial photographs, and annual or biannual surveys of the ice front from 1945 to 1980 conducted by the Water survey of Canada reveal annual moraine formation, and therefore assigns these landforms the term "annual moraines," but this evidence is not presented beyond the statement.

Canada: Columbia Mountains

The information presented about the minor moraines at Castle Creek Glacier is sparse. The moraines formed from 1959 to 2007 on top of till sheets, but the sedimentological composition of the moraines themselves is not presented (Beedle et al., 2009). The authors mention that the moraine dimensions are similar to push moraines formed in Iceland and attribute the formation of the Castle Creek moraines to pushing, without presenting any concrete evidence. The authors present an example photograph that shows annual formation of the moraines, and thereby discuss the landforms as "annual moraines." An assessment of climate factors shows that ablation season temperature controls changes in glacier length on an annual scale and that accumulation-season precipitation may control recession with a decadal response time.

Iceland: Myrdalsjökull Ice Cap

Previous work describes minor moraines in four forelands of the Myrdalsjökull Ice Cap. One study notes the presence of minor moraines at Slettjökull on the northeastern side of the Myrdalsjökull Ice Cap (Krüger, 1995), and two others note the presence of other minor moraines in three forelands of outlet glaciers: Öldufellsjökull (Evans et al., 1999a), Sandfellsjökull (Evans et al., 1999a), and Sólheimajökull (Schomacker et al., 2012).

The minor moraines at Slettjökull formed from 1928 to 1984 and are composed of till, glaciolacustrine sediment from a proglacial pond, and mass movement deposits, which were observed through excavating sections (Krüger, 1994; Krüger, 1995). Although section logs and photographs are presented (Krüger, 1994) and sedimentological relationships are described, comprehensive information regarding the geometries of the minor moraines is not presented (Krüger, 1995). The author describes four mechanisms of minor moraine formation, which may work independently or in combination: (1) pushing, (2) squeezing, (3) basal freezing (Figure 1.1), and (4) debris band melt out. Krüger (1995) does, however, mention that a squeezing mechanism is speculative, as no observations at the time supported this method of formation. Krüger (1995) shows that summer temperature controls ice-marginal retreat rates and advances creating minor moraines, and these advances may also be influenced by cold winters. Additional controls on minor moraine formation include ice front thickness and the ice surface slope (Krüger, 1995). Although the moraines were not observed forming due to the timing of field seasons, geomorphological mapping using aerial photographs and field observations shows that 1-4 moraines formed every year, leading Krüger (1995) to eventually call these "annual moraines," although evidence shows that they may in fact be sub-annual, and no example aerial photographs of moraines formed annually or sub-annually are presented.

The information presented about the minor moraines at Öldufellsjökull and Sandfellsjökull is sparse, as they were not the primary focus of research in the forelands (Evans et al., 1999a). Lichenometric dating was used to establish ages of the moraines, which shows that those at Öldufellsjökull formed between 1923 and 1949, whereas the moraines at Sandfellsjökull formed earlier, from 1896 to 1916 or 1925. No information is provided about the sedimentological composition or geometries of the moraines, however they are mentioned to have formed from pushing, and are therefore referred to as "push moraines." No further information is provided regarding specific formation mechanisms or specific controls on moraine formation. The minor moraines at Sólheimajökull formed in 1850 and later and between 1995 and 2012 and are composed of diamicton and till on top of a glaciofluvial outwash plain (Schomacker et al., 2012). Sedimentological logs and explanations detail the internal structures of excavated moraines, however the geometries of some of the moraines are only discussed as having a sawtooth shape. The authors ascribe minor moraine formation to a combination of thrusting and dumping. Schomacker et al. (2012) present some images that show the location of the ice margin through time and describe how the combined analysis of DEM data, aerial photographs, glacier length change measurements, and field observations confirm annual formation of moraines during winter advances; however, controls on moraine formation are not discussed.

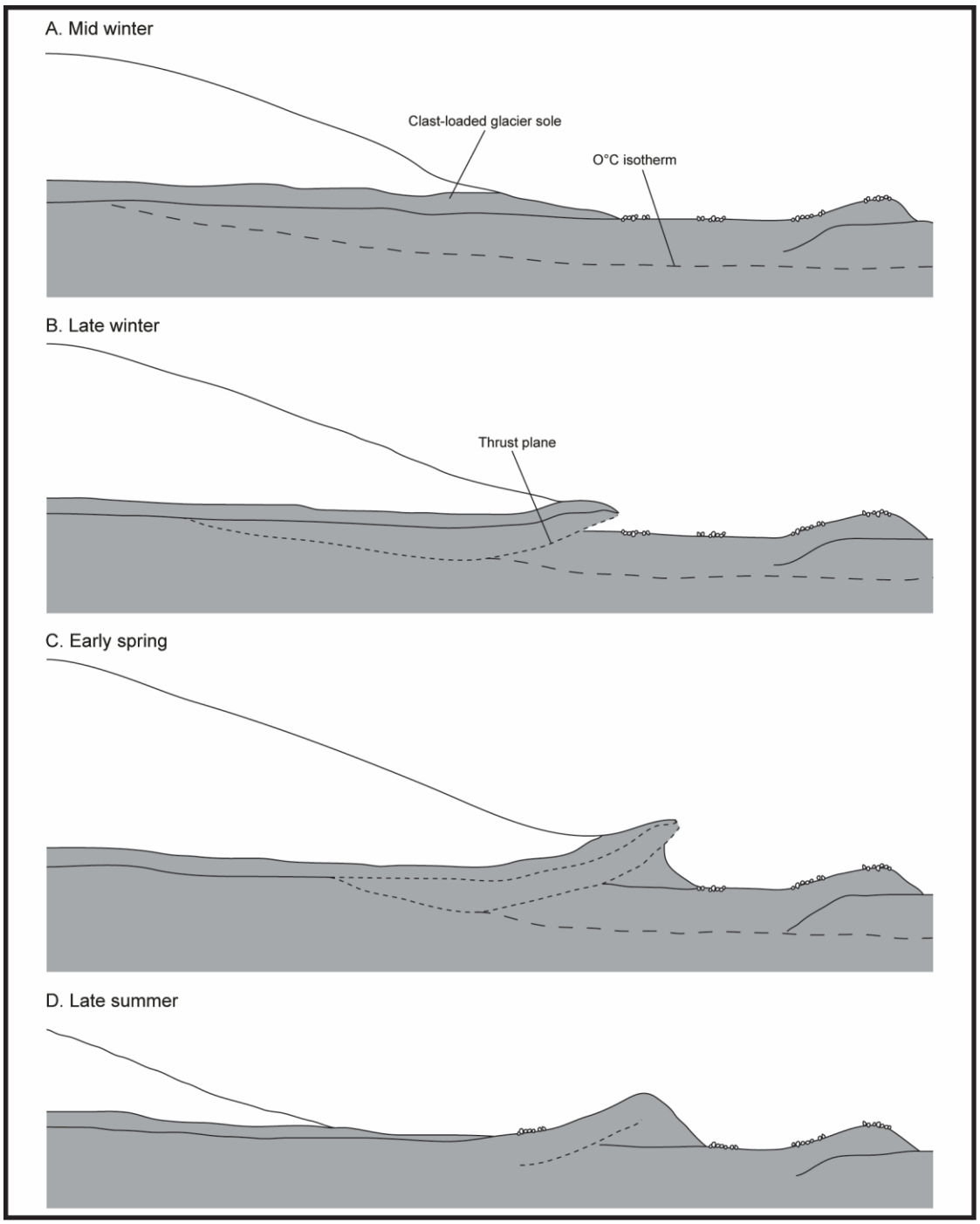

Figure 1.1. Conceptual diagram of minor moraine formation in the Slettjökull foreland, Iceland, showing a combined freeze-on and push mechanism of formation. Modified from Krüger (1995).

Iceland: Vatnajökull Ice Cap

Previous work describes minor moraines in five forelands of Vatnajökull Ice Cap outlet glaciers and three outlet glacier forelands of the joint Vatnajökull and Öraefajökull Ice Caps. The minor moraines in the Breiðamerkurjökull foreland have been described with varying degrees of detail in three different studies. The minor moraines described by Boulton

(1986) formed from 1965 to 1983 and are composed of till and outwash sediment, although detailed information about sedimentological composition and geometries of moraines are not presented. The moraines formed as either individual landforms or as composite ridges, both attributed to pushing, although no data to support this formation mechanism are presented. Boulton (1986) calls these landforms "annual moraines" but does not provide any evidence to support this designation. Evans et al. (1999b) also mention the minor moraines in the Breiðamerkurjökull foreland as "annual moraines" formed through pushing, but only by citing the research presented by Boulton (1986). Evans and Twigg (2002) slightly update the original work and present three different periods of minor moraine formation as 1890-1934, 1930-1960, and 1965 and later, with chronological constraint derived from geomorphological mapping and lichenometric methods. The moraines contain outwash and diamictic sediment; however, no detailed information is presented. The authors do, however, describe the geometries of the moraines as crenulated, lobate, or saw-toothed, which they attribute to the presence of longitudinal crevasses at the ice front and potential push or squeeze mechanisms of moraine formation, without elaborating on evidence to support these interpretations. Evans and Twigg (2002) call these landforms both "low amplitude marginal moraines" and "push moraines," and cite Boulton (1986) when mentioning that the moraines may be annual in some areas, without presenting any new information to confirm or deny this designation.

Evans et al. (1999a) mention minor moraines in the Heinabergsjökull foreland. They describe these moraines as having formed sometime before the late 1930s to sometime before the early 1970s through pushing mechanisms. They also state that relatively warm summers may control front variations responsible for minor moraine formation, and refer to the moraines as "push moraines," which may have been deposited sub-annually in places. The authors do not, however, provide any information to substantiate their interpretations of formation mechanisms.

Minor moraines at Lambatungnajökull formed from 1932 to 1950 and are composed of clay-rich diamicton (Bradwell, 2004). Bradwell (2004) describes the sedimentological composition, including clast measurement data, of some moraines and mentions the sawtooth shape of the moraines, however does not provide this information visually, as photographs or sedimentological logs. Despite this lack of detail, squeezing is described as the mechanism of moraine formation. Bradwell (2004) uses moraine spacing as a proxy for recession rates and then describes that summer air temperature controls glacier ablation rates, which may influence moraine formation, and that a debris-free glacier surface may also exert a control on moraine deposition. These landforms are referred to as "annual moraines" after presenting this information and discussing a suite of aerial

photographs that confirms annual formation, although no example aerial photographs are presented (Bradwell, 2004).

Sharp (1984) and Chandler et al. (2016a) both describe minor moraines in the Skálafellsjökull foreland. Sharp (1984) defines the period of moraine formation as 1913-1984, whereas Chandler et al. (2016a) break this down into more specific periods of before 1945, 1945-1964, and 1969-1974, with newer moraine formation during 2006-2012. Although both present sedimentological and geomorphological data, those presented by Chandler et al. (2016a) are considerably more detailed and should serve as a framework for future minor moraine studies. The moraines described by Sharp (1984) contain till and debris flow deposits and are interpreted to have formed through squeeze, snow-bank push, push, and subglacial shearing mechanisms (Figure 1.2). The sedimentological composition seems to have been assessed only through examining the particle size in cores collected from several moraines, and no sedimentological logs or photographs are presented as examples. Chandler et al. (2016a) document moraines composed of till and glaciofluvial sediment and diamicton and glaciofluvial sediment and attribute formation to push, combined push and squeeze, and freeze-on mechanisms (Figure 1.3). The composition of these moraines is documented through the use of detailed sedimentological logs. Sharp (1984) and Chandler et al. (2016a) agree that changes in the ice-front are most sensitive to summer air temperatures, and Chandler et al. (2016a) expand this to also discuss the influences of sea surface temperatures and North Atlantic Oscillation, as well as below-average winter-spring temperatures for moraines formed after 2012. Chandler et al. (2016a) further note that a reverse bedrock slope and thin ice front in some areas may also exert a control on minor moraine formation. Sharp (1984) describes that these landforms seem to have a formed annually, whereas the detailed work by Chandler et al. (2016a) allows for more refined designations, as they describe the landforms as small-scale recessional moraines, and describe how some are conclusively annual moraines or even sub-annual moraines, supported by a collection of aerial photographs used as examples.

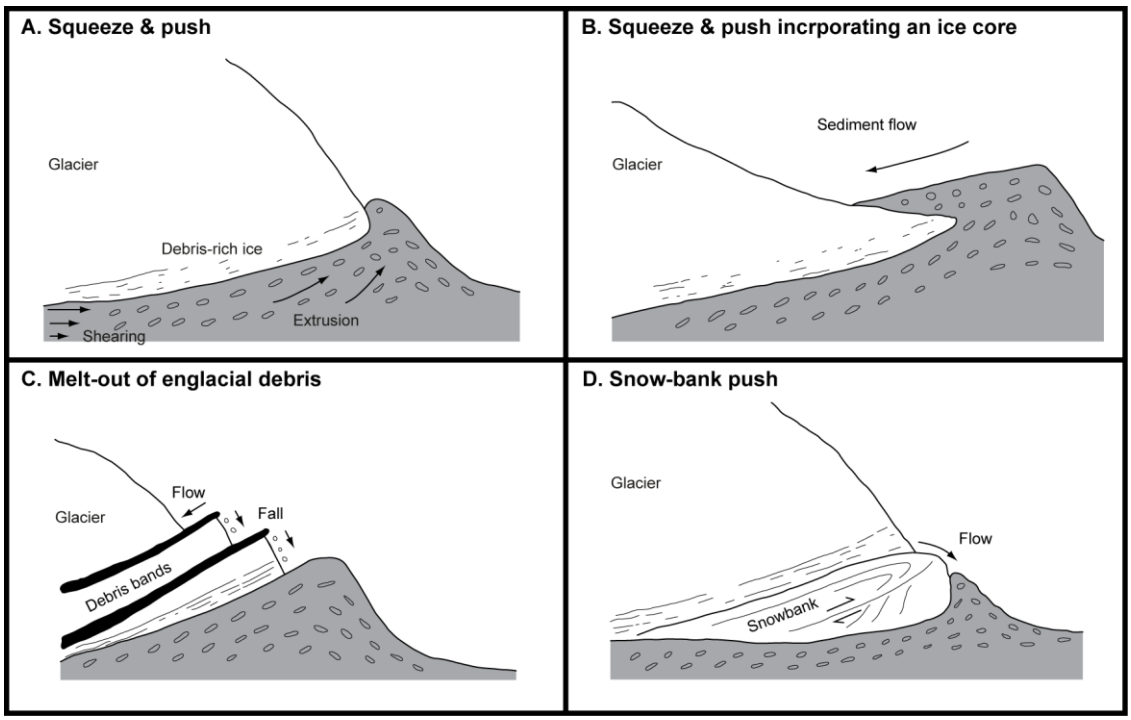

Figure 1.2. Conceptual diagrams of minor moraine formation in the Skálafellsjökull foreland, Iceland, showing A.) a combined squeeze and push mechanism of formation; B.) a combined squeeze and push mechanism of formation incorporating an ice core; C.) melt-out of englacial debris forming a ridge; and D.) a snow-bank push mechanism of formation. Modified from Sharp (1984).

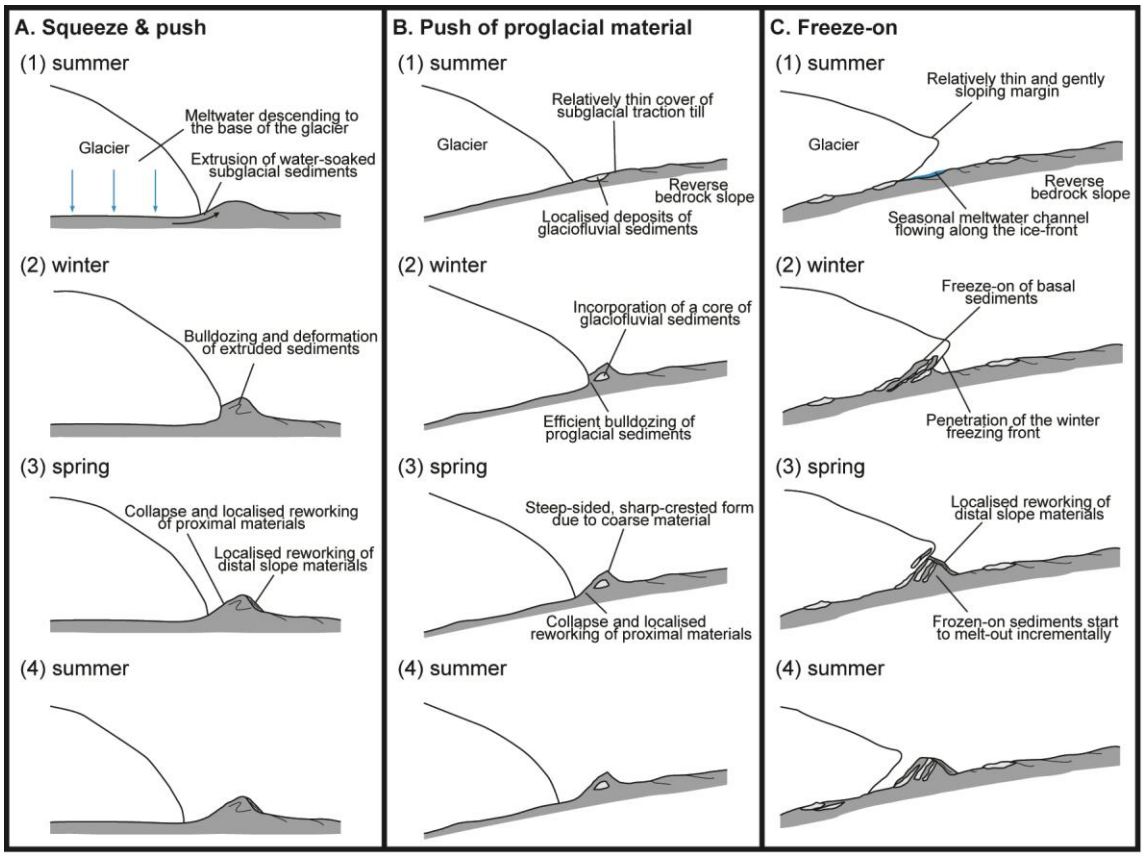

Figure 1.3. Conceptual diagrams of minor moraine formation in the Skálafellsjökull foreland, Iceland, showing A.) A combined squeeze and push mechanism of formation; B.) Push moraine formation on a reverse bedrock slope; and C.) A freeze-on mechanism of formation on a reverse bedrock slope. Modified from Chandler et al. (2016a).

Iceland: Vatnajökull-Öraefajökull Ice Cap

Price (1970) and Evans and Twigg (2002) both describe minor moraines in the Fjallsjökull foreland. Price (1970) defines the period of moraine formation as 1900-1970, although it is unclear how this was determined, whereas Evans and Twigg (2002) present a shifted and shorter period of 1890-1934, determined through lichenometric dating. The moraines observed by Price (1970) contain glaciofluvial material and till and are interpreted to have formed through squeezing, however no sedimentological logs or photographs are presented and the composition is only discussed through clast orientations and relative sediment size. Further confusion arises as the author does not provide evidence of till, despite referring to clast measurements from till units, and instead describes ridges comprising gravel in a sandy matrix. The author supports the interpretation of a squeezing mechanism through the washboard-style shape of the moraines, the orientation of clasts in the moraines, and observations of moraine formation during several fieldwork seasons (Figure 1.4). Throughout this work, Price (1970) refers to the landforms simply as "moraines," although discusses the temptation to describe them as "annual moraines." The author recognises that it is not possible to conclusively support annual formation solely through the agreement of number of moraines and years elapsed. Evans and Twigg (2002) claim that moraines are often, although not always, produced annually, which is presumably concluded from assessments of maps and aerial photographs.

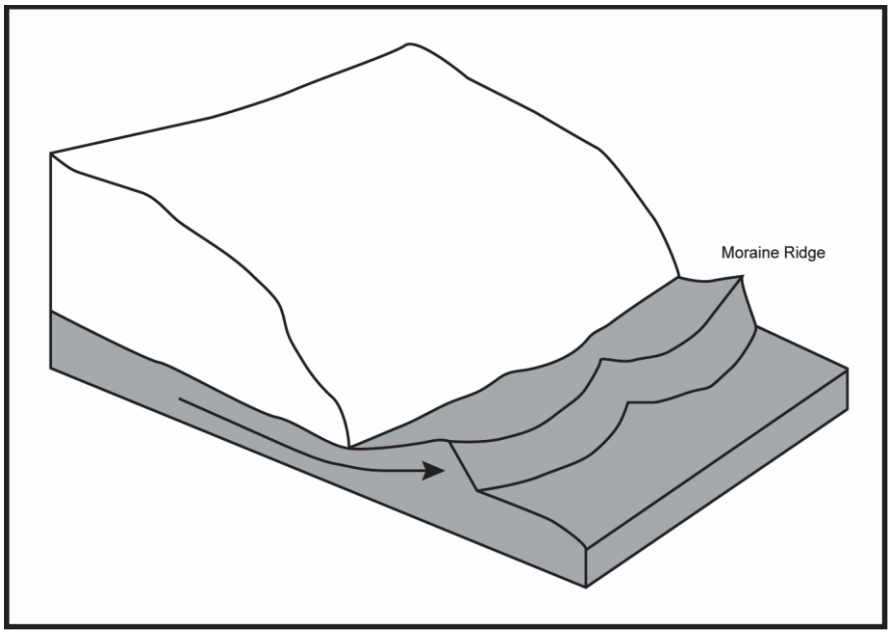

Figure 1.4. Conceptual diagram of minor moraine formation in the Fjallsjökull foreland, Iceland, showing a till squeezing mechanism of moraine formation. Modified from Price (1970).

Minor moraines in the Kvíárjökull foreland formed from 1870 to 1977, based on lichenometric measurements (Evans et al., 1999a). No information regarding the sedimentological composition or geomorphological form of the moraines is presented, yet the authors interpret these landforms as push moraines and refer to them as "recessional push moraines" that may be influenced by the effect of cold winters on ice-marginal fluctuations.

Minor moraines in the Virkisjökull–Falljökull foreland formed from 1935 to 1945 and 1991 to 2004 and are composed of subglacial, supraglacial, and glaciofluvial sediment (Bradwell et al., 2013). Bradwell et al. (2013) discuss some detailed sedimentological analyses of the minor moraines, including clast shape of gravels, but do not present any sedimentological logs or example photographs and do not specify if their observations are from exposed sections. The geomorphological observations are more robustly drawn from aerial photographs and field observations and surveys. The authors interpret these moraines to have formed through a pushing mechanism, through similarities with previous work, but do not present specific examples from the present study. Bradwell et al. (2013) discuss how these moraines likely formed on an annual basis, supported through their assessment of ice-front measurements, the geomorphological record and aerial photographs, field photographs, lichenometric measurements, and similarity to other annual moraines in Iceland, for various time periods. They additionally present some evidence of moraine formation through example aerial photographs, but voice their reservations in conclusively supporting annual formation, as they recognise that some ridges were occupied by the ice front more than once and some may have been modified by ice front dynamics on numerous occasions. Assuming annual formation, Bradwell et al. (2013) use the moraines as a proxy for retreat rates to compare their formation to climate records, and show that summer temperatures, with less than a half-year response time, influence ice-front position. The authors also mention the presence of a reverse bedrock slope that may additionally influence the ice front.

Nepal: Himalaya

Two studies record the presence of minor moraines in three glacier forelands of the Himalaya, Nepal. Fushimi (1977) mentions clusters of small moraine ridges at Dzonglha Glacier and Gyajo Glacier but does not present the periods of moraine formation. The author briefly mentions the sedimentological composition of the moraines and the geometry of the Gyajo moraines, however this research lacks detail overall. Both sets of moraines contain outwash sediments, and the Gyajo moraines additionally contain some lacustrine sediment. Despite the sparse data, Fushimi (1977) speculates that these groups of minor moraines

likely reflect short term climate changes. Slightly more data exist about the minor moraines in the Yala (Dakpatsen) Glacier foreland (Ono, 1985). These moraines formed between 1850 and 1985 and contain till and englacial gravel. Ono (1985) attributes moraine formation to pushing, through field observations and till fabric analysis, however the author only vaguely describes field observations and does not present sedimentological logs or photographs. Furthermore, the author assumes that the height of an individual moraine reflects the distance of ice advance, but does not quantify moraine dimensions. Ono (1985) first refers to these landforms as minor moraines, before mentioning their similarity to annual moraines in the Himalaya, particularly at Gyajo Glacier (Fushimi, 1977). The author then compares the minor moraines at Yala Glacier to the 1976 advance at Gyajo Glacier and the surrounding minor moraines and recognises that this chronological comparison rests on assumption of synchronicity, but follows on to designate these landforms as "annual moraines" regardless.

Norway: Hardangerjøkulen Ice Cap

Two studies describe minor moraines in the Midtdalsbreen foreland. Andersen and Sollid (1971) describe minor moraines formed from 1955 to 1968 composed of till and glaciofluvial sediment through some assessment of the composition and form of the moraines. The authors determine that the minor moraines formed annually through analysis of aerial photography, although only provide one example photograph, and therefore refer to these landforms as "annual moraines." Andersen and Sollid (1971) do, however, approach this term with caution, as they discuss that some moraines may be formed through multiple years, multiple moraines may be formed in a single year, and some may be eroded due to low preservation potential. Reinardy et al. (2013) revisit this study area to assess how the foreland has evolved since previous work. The authors describe subglacial diamicton, i.e. not conclusively till, and glaciofluvial sediment and also include moraine formation during 2010/2011. Reinardy et al. (2013) provide considerably more detailed information about the sedimentological composition and geomorphological form of minor moraines in the foreland than Andersen and Sollid (1971). Both groups interpret a freeze-on mechanism of moraine formation (Figure 1.5), providing multiple veins of evidence to support this interpretation, and describe the role of reverse slopes and ice cores in moraine formation and evolution, and Reinardy et al. (2013) additionally mention the effects of a thin glacier front and aspect across the ice front. Throughout their work, Reinardy et al. (2013) call these landforms "annual moraines." The authors do not, however, provide evidence for annual formation, and presumably used this terminology based on the original work by Andersen and Sollid (1971) and assessment of air photos from 1988 onwards.

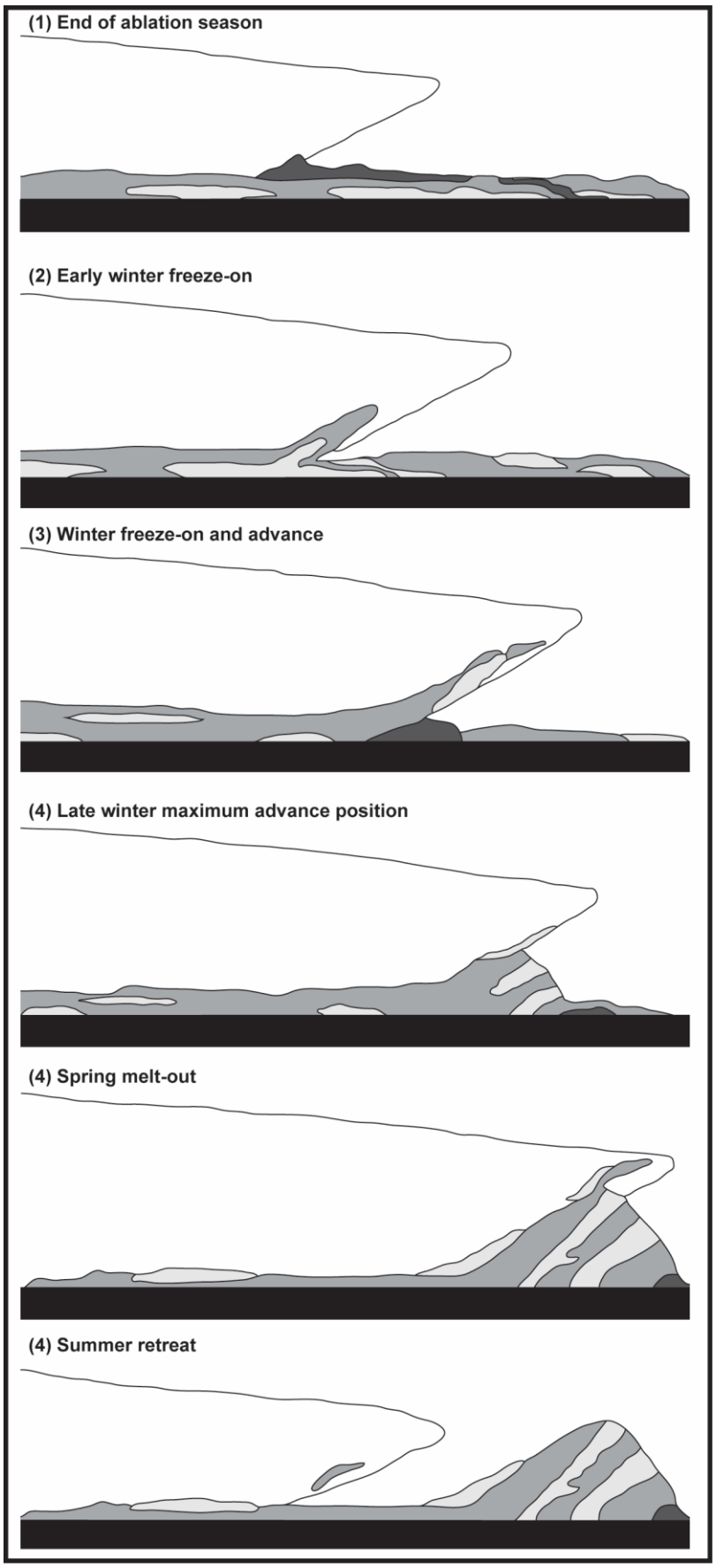

Figure 1.5. Conceptual diagram of minor moraine formation in the Midtdalsbreen foreland, Norway, showing a freeze-on mechanism of moraine formation. Modified from Reinardy et al. (2013).

Norway: Jostedalsbreen Ice Cap

Three forelands of outlet glaciers from the Jostedalsbreen Ice Cap contain fewer than five minor moraines, however the moraines are discussed here due to their small statures, designation as "minor moraines" by the authors, and similarity with minor moraines in other studies, particularly in Norway. The minor moraines in the Bergsetbreen and Kjenndalsbreen forelands formed from 1997 to 2000, and the period of moraine formation in the Tuftebreen foreland is not presented (Winkler and Matthews, 2010). No detailed sedimentological or geomorphological data about the minor moraines are presented. The moraines are all interpreted to have formed through pushing, and are composed of foreland sediment at Bergsetbreen, supraglacial material at Kjenndalsbreen, and proglacial material overlying bare bedrock at Tuftebreen. The moraines at Bergstebreen were monitored annually from 1991/92 onwards by one of the authors, and are described as one larger composite moraine composed of smaller ridges formed during seasonal advances. The authors therefore call these landforms "terminal moraines" (Winkler and Matthews, 2010). The Kjenndalsbreen foreland was similarly monitored and is also described as having a larger, multi-ridge moraine, with additional chronological constraint on individual ridges through ice front variation measurements and aerial photographs. The authors consequently call these landforms "terminal moraines," and suggest that they are likely annually deposited (Winkler and Matthews, 2010). In contrast, data about the moraines in the Tuftebreen foreland is derived from sparse observation by one of the authors, which is why chronological constraint was not possible. The authors mention that obtaining some chronological constraint was attempted using lichenometric measurements, but discuss the uncertainty in these ages due to samples that could have been derived from previous sediment and incorporated into moraines during pushing (Winkler and Matthews, 2010). The interpretation of push moraine formation in this foreland is derived from assessing the composition of the moraines, which the authors suggest is consistent with bulldozing, however they do not provide sufficient information about the composition. Regardless, the authors call these landforms small seasonal moraines and suggest that they are likely annually deposited (Winkler and Matthews, 2010). The authors show some example photographs of moraines forming at the ice front, and the interpretation of annual formation would be further strengthened with photographs of formation during consecutive years.

Norway: Jotunheimen

Two of the glacier forelands in Jotunheimen contain fewer than eight minor moraines, but are discussed here due to their small sizes and similarity with other minor moraines, particularly in Norway. The minor moraines in the Bøverbreen and Storjuvbreen forelands formed after 2001 and from 1994 to 2000, respectively (Winkler and Matthews, 2010). Both forelands were monitored annually since 1994 by one of the authors; however, no detailed sedimentological or geomorphological data about these landforms are presented. The moraines at Bøverbreen are composed of till and have been interpreted to have formed through basal freeze-on and push mechanisms. The authors refer to these landforms as "terminal moraines" that formed during seasonal advances, as observed during fieldwork, and the freezing mechanism of moraine formation is supported by fieldwork observations. The moraines at Storjuvbreen comprise supraglacial debris, englacial debris, and till, and have been interpreted to have formed through dumping of supraglacial debris, melting-out of englacial debris, and pushing (Winkler and Matthews, 2010). The authors refer to these landforms as "terminal moraines" and also note an ice core present in one moraine.

The minor moraines in the Storbreen foreland formed in the 1980s and 1990s and are composed of till (Hiemstra et al., 2015). The described sedimentological work was detailed, as this research was focused on sediment fingerprinting and those data are presented clearly, however sedimentological logs or example photographs of clearly visible till slabs are not presented. Similarly, detailed geomorphological observations are not presented, but an example photograph depicts the form of the moraine ridges well (Hiemstra et al., 2015). The authors interpret the ridges to have formed as individual landforms as part of a larger composite moraine, through a freeze-on mechanism (Figure 1.6), supported by sediment fingerprinting analyses and the observation of till slabs. Any potential climatic or other influences on moraine formation are not discussed. The authors call these landforms "annual moraines," because the number of ridges and years available for formation mostly correspond with one ridge forming each year (Hiemstra et al., 2015).

The minor moraines in the Styggedalsbreen foreland formed from 10.3 ka to 9.0 ka, 1250 to 1850, and 1931 to 1972 (Matthews et al., 1995), and from 1997 to 2007 (Hiemstra et al., 2015). Matthews et al. (1995) describe the older minor moraines as composed of glaciofluvial sediments and diamicton/till and mention ice cores, and Hiemstra et al. (2015) observe till making up the younger minor moraines. Both groups support a freeze-on mechanism of formation (Figures 1.6-1.7). Matthews et al. (1995) describe that only shallow excavations through moraines were possible due to ice cores and present some clast measurement data comparing the moraine sediments to control environments, however no sedimentological logs or example photographs showcase the composition of moraines.

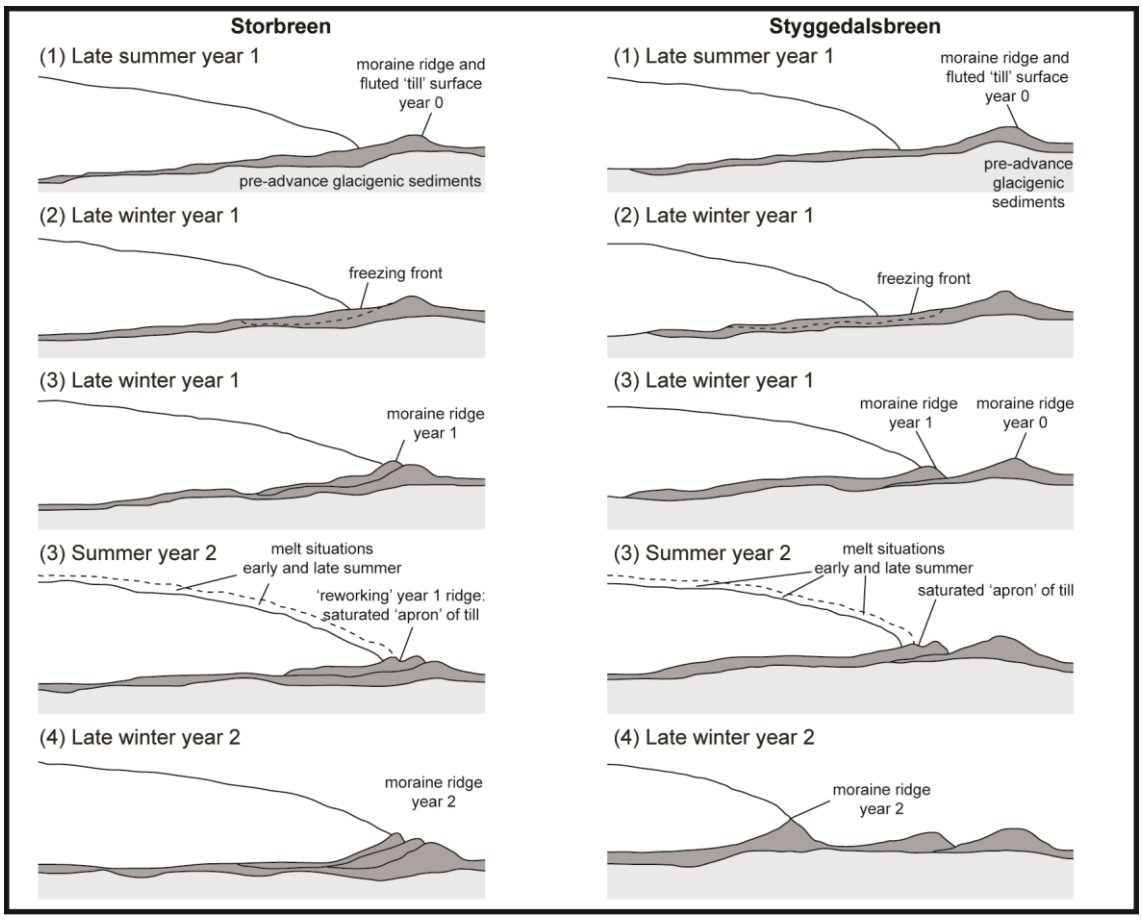

Figure 1.6. Conceptual diagrams of minor moraine formation in the Storbreen and Styggedalsbreen forelands, Norway, showing a freeze-on mechanisms of moraine formation. Individual moraine ridges at Strobreen form a larger composition moraine landforms, whereas those at Styggedalsreen form as discrete individual moraines Modified from Hiemstra et al. (2015).

The geometries of the moraines are briefly described, and the authors include some example photographs that show the geomorphology of these landforms well. The interpretation of a freezing mechanism responsible for moraine formation is drawn from evidence for prolific seasonal ground freezing in the foreland, the morphology of the ice front, and thick, frozen sediment layers in the moraines and foreland (Matthews et al., 1995). Matthews et al. (1995) describe that strong summer ablation and insufficiently cold winters may provide favourable conditions for minor moraine formation, and cite field observations and previous studies to support seasonal oscillations of the ice margin. The authors call the older landforms "terminal moraines," presumably due to the lack of accurate chronological constraint, but refer to the 1934-1972 moraines as "annual moraines." They draw this conclusion from the size of the moraines and speed of retreat, but do not present evidence that conclusively shows annual formation. Similar to their work at Storbreen, Hiemstra et al. (2015) present detailed data regarding sediment fingerprinting, but unfortunately do not show examples of clearly visible till slabs, whether as example photographs or sedimentological logs. They do, however, provide an example

photograph of the form of these moraines, but do not discuss the geometries in detail. No speculation regarding potential climate or other influences on moraine formation is presented (Hiemstra et al., 2015). The authors call these landforms “annual moraines”, but this is derived from counting back from the known 2007 moraine (Hiemstra et al., 2015). This approach should be cautioned, as more than one moraine may form in a year, some years may not have a moraine formed, and some moraines may have been eroded.

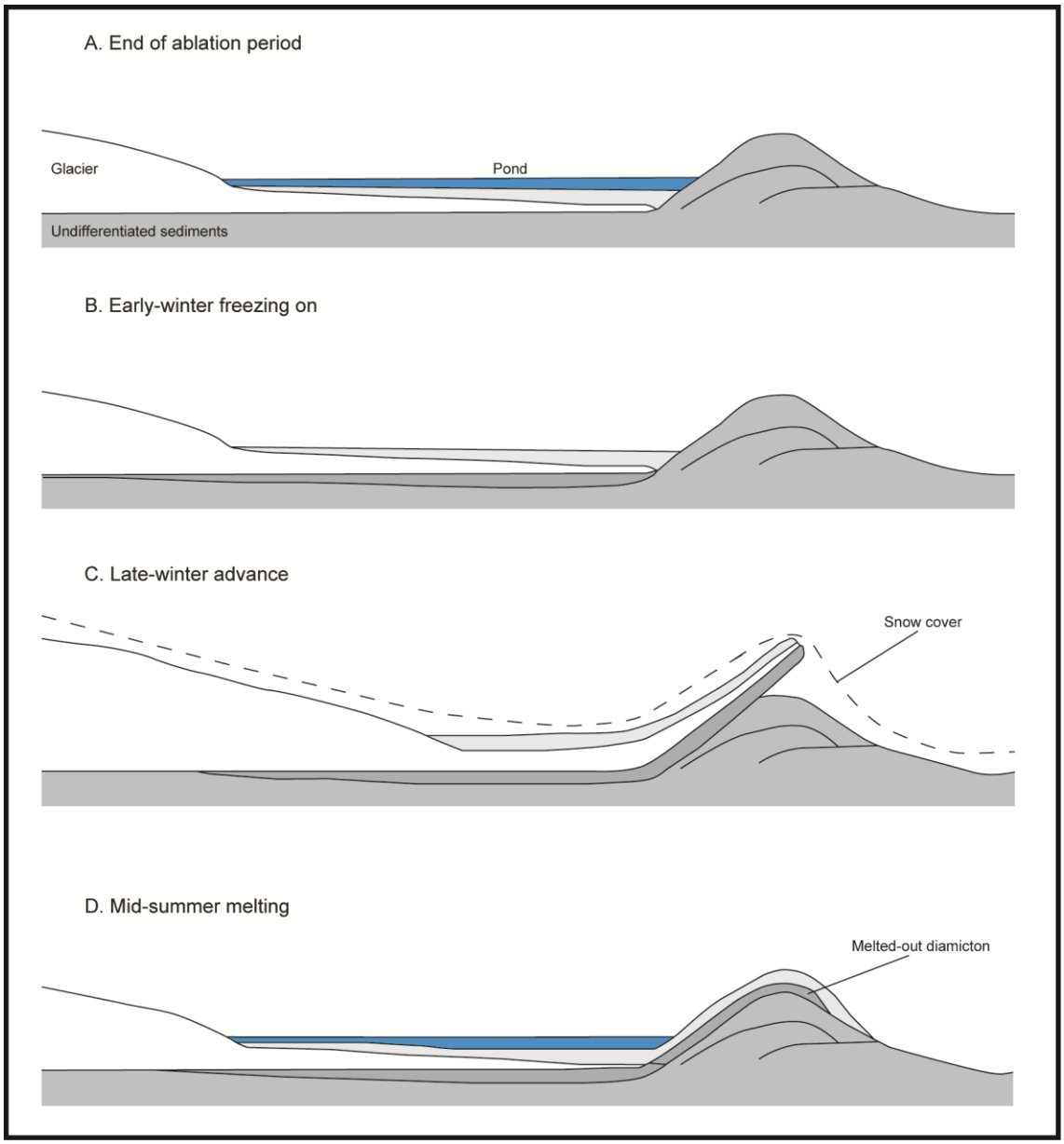

Figure 1.7. Conceptual diagram of minor moraine formation in the Styggedalsbreen forelamd, Norway, showing a freeze-on mechanism of moraine formation. Modified from Matthews et al. (1995).

Norway: Okstindbreen Ice Cap

Minor moraines have been described in one foreland of an Okstindbreen Ice Cap outlet

glacier. Minor moraines in the Austre Okstindbreen foreland formed from 1957 to 1970 and are composed of till derived from the underlying till sheet, although no more detail is provided (Worsley, 1974). Worsley (1974) does not describe the dimensions of ridges, but does mention that they are easier to recognise in aerial photographs than on the ground, and that the modern geometries of these minor moraines are likely not representative of original deposition due to erosion. The author speculates that the moraines were formed primarily through pushing, but does not reject a squeezing mechanism. He also admits that these hypotheses are drawn from previously described mechanisms of minor moraine formation as the data did not allow for conclusions about these mechanisms in the present study area. Chronological control on moraine formation is derived from aerial photographs, and these photographs and field observations show that moraines did not form during the summer. Worsley (1974) eventually calls these landforms "annual moraines" but with reservations that highlight the uncertainties of chronological controls in the foreland.

Pakistan: Karakoram Mountains

One study describes minor moraines in the Karakoram Mountains, Pakistan. Minor moraines in the Biafo Glacier foreland formed around 1961 and are composed of proglacial outwash, ice-contact lake sediments, other ice-contact deposits, and talus. However, the relationships between these sediments are only described as a thin veneer covering cohesive material or minor ridges of large blocks (Hewitt, 1967). The geometry of the moraines is not discussed, but an example photograph shows the form of the moraines well. Hewitt (1967) describes the incorporation of new and overridden material at the ice front in a manner that sounds like pushing, but without using the common words "push" or "bulldoze." Hewitt (1967) speculates that these moraines are related to seasonal climate variations and also mentions some control on moraine formation from proglacial relief, sediment availability, volume and structure of ice and rates of ice movement, and patterns and rates of ice melt.

South Georgia: Allaroyce and Salvesen Ranges

Two studies describe minor moraines on South Georgia, with two forelands in the Allaroyce Range (Glacier Col and Lucas Glacier), three in the Salvesen Range (Graae Glacier, Nachtigal Glacier, and Ross Glacier), and one on the border of the two (Cook Glacier). Birnie (1977) began research on minor moraines on South Georgia at Lucas Glacier, however does not provide details on the period of moraine formation. These moraines are composed of what Birnie (1977) calls till, although evidence supporting this designation is not presented and

this could therefore be a bracketing term for "glacial sediment". Two photographs show examples of excavated sections through moraines. Unfortunately, no more information about the sedimentological compositions or geometries of the moraines is provided. Birnie (1977) describes a mechanism of "snow bank push" in which a snow bank acts as an obstacle that impedes the glacier pushing sediment at the ice-front, supported by snow-cored ridges, observations of snow-bank deformation, observations of the evolution of a snow-bank at another glacier through a stationary camera, and painted clasts used to trace the evolution of a snow-bank moraine ridge. The timing of fieldwork observations and the presence of partially decomposed seal pups in an excavated section suggests that these moraines are formed in winter, although specific climate controls on moraine formation are not explored. The author does, however, mention that other controls on moraine formation may include snow depth and the influence of the topographic setting on ice front thickness. Birnie (1977) calls these landforms "annual moraines" without presenting evidence for annual formation, but additionally voices reservations in this designation, as the chronological constraint on these moraines is limited.

Gordon and Timmis (1992) present information about minor moraines in other forelands of South Georgia, but the data presented are sparse. The minor moraines at Cook Glacier (1975-1881), Glacier Col (1980-1982), Graae Glacier (1953) and Nachtigal Glacier (1977-1982) formed around the same time, and the timing of minor moraine formation at Ross Glacier is just described as likely reflecting the Little Ice Age (approximately 1850). The authors do not describe the sedimentological composition or geomorphological form of minor moraines, and only briefly speculate on mechanisms of minor moraine formation when stating that the moraines at Graae Glacier may have formed through a snow-bank pushing mechanism similar to that described by Birnie (1977). Gordon and Timmis (1992) do, however, describe that seasonal temperature variations control the mass balance of glaciers on South Georgia, and also mention the form of the ice front, debris cover, and effects of shading as influencing moraine formation in the Nachitgal Glacier foreland. The authors refer to the minor moraines as "annual moraines," except for those in the Ross Glacier foreland, where they merely mention a group of more subdued ridges, but this designation is not supported by evidence.

Switzerland: European Alps

Minor moraines in the European Alps have been observed in two forelands. Findelengletscher and Gornergletscher are both located in the Pennine Alps in Switzerland, on the border with Italy. Although the minor moraines in the Findelengletscher foreland have not been studied, their presence was noted by previous researchers (Schlüchter, 1983;

Lukas et al., 2012; personal communication, 2014), but only two of the larger moraines are still visible on Google Earth imagery. This imagery also reveals a newer set of minor moraines close to the modern ice margin.

Lukas (2012) conducted pioneering research while pairing detailed geomorphological and sedimentological assessment of minor moraines to understand processes of formation at Gornergletscher, creating the foundation for the most robust subsequent research on similar landforms (Reinardy et al., 2013; Chandler et al., 2016a). The moraines have been forming since 1980 or earlier at the subsidiary northern ice front and contain proglacial outwash and debris flow material. The sedimentological architectures of these moraines are well documented through the use of detailed logs. Lukas (2012) describes three mechanisms of minor moraine formation: (1) push moraine formation with dead-ice incorporation, (2) push moraine formation without dead-ice incorporation, and (3) terrestrial ice-contact fan formation (Figure 1.8). An assessment of climate factors that may influence ice-marginal retreat rates shows that winter temperatures control retreat and therefore exert a control on moraine formation, however ice surface slope and a reverse bedrock slope also influence mechanisms of formation. Lukas (2012) mentions that aerial photographs reveal annual deposition of minor moraines, and therefore assigns these landforms the term “annual moraines”, but these images are not presented.

1.1.2 Pleistocene ice sheet settings

Four studies in three settings specifically mention the presence of minor moraines along the Laurentide Ice Sheet (LIS) margin. It is important to note that accurate and precise chronological controls on these moraines do not exist, and therefore none of the studies incorporate discussion on specific climate controls potentially driving ice-marginal fluctuations of the larger Laurentide Ice Sheet, smaller lobes, or individual glaciers.

Evans et al. (1999b) describe minor moraines near Frank Lake, Alberta, Canada, on the southwestern edge of the LIS, but provide no information about the geomorphological form or sedimentological composition of the moraines. They liken the moraines to modern annual moraines in two Icelandic forelands (Breidamerkurjökull and Sandfellsjökull) and, from these modern analogues, interpret that the moraines most likely formed through a pushing mechanism. The authors speculate that the moraines formed during most winters or every winter, similar to the Icelandic examples, although do not support this claim with chronological information and do not ever commit to the terminology of “annual moraines,” opting instead for “minor moraines” and “recessional moraines.”

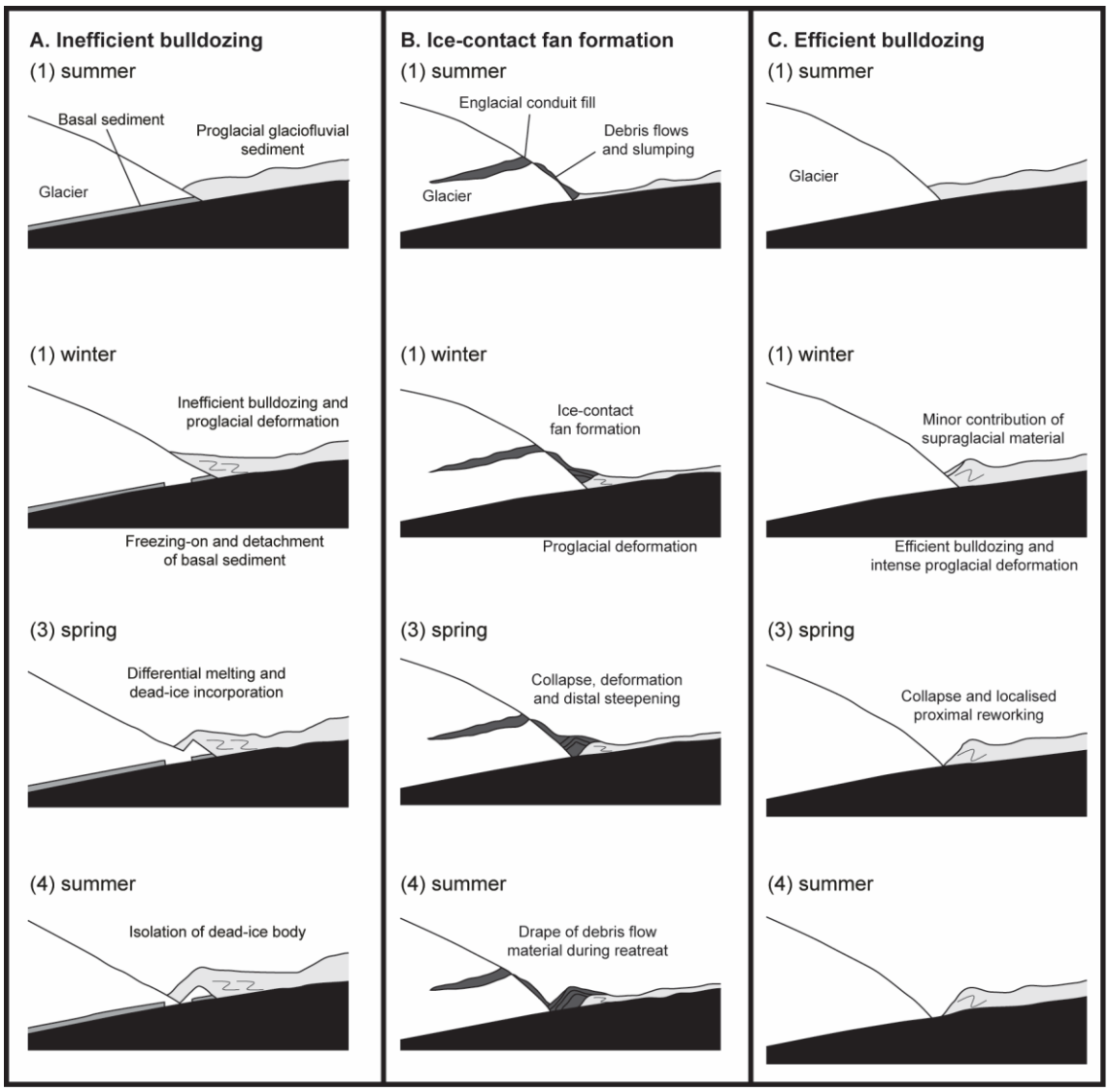

Figure 1.8. Conceptual diagrams of minor moraine formation in the Gornergletscher foreland, Switzerland, showing A.) Push moraine formation through inefficient bulldozing, incorporating an ice core; B.) Melt-out of englacial material and ice-contact fan formation; and C.) Push moraine formation through efficient bulldozing. Modified from Lukas (2012).

Christiansen (1956) describes minor moraines near Moose Mountain, Saskatchewan, Canada, in an area that was part of the Weyburn Lobe of the LIS. The author describes the moraines as composed of till, but it is unclear what observations led to this claim or if this term is used more as a bracketing term for "glacial sediment". The author additionally provides some information about the geometries of the moraines, but no specific examples of the sedimentological composition or geomorphological form of the moraines are presented. Christiansen (1956) interprets that these moraines formed through a pushing mechanism, which seems primarily derived through citing previous work that discusses push moraines formed during overall retreat. The author therefore calls these landforms "minor recessional ridges" and states that they are likely annual.

Minor moraines in Iowa, United States, are described in an area that was part of what is referred to the Mankato Lobe of the LIS by Gwynne (1942) or the Des Moines Lobe by Stewart et al. (1988). The interpretation of the formation of these landforms is inconsistent between the two studies. Both authors describe the landforms as composed of till, and the detailed sedimentological work by Stewart et al. (1988) additionally reveals glaciofluvial material. Stewart et al. (1988) provide detailed sedimentological information about the moraines through till fabric analysis and stratigraphic columns, whereas Gwynne (1942) only briefly mentions till with little supporting information. Gwynne (1942) interprets parallel moraines and the inferred ice margin, as well as their closely spaced nature, to represent seasonal push of pre-existing till and consequently calls these landforms "seasonal minor recessional moraines". Stewart et al. (1988) dismiss these previous interpretations and instead interpret a mechanism of formation through which till and glaciofluvial sediment are deposited into cracks and crevasses at the base of the ice, which are then deposited during retreat and/or stagnation, which may not represent the location of the ice front. The authors therefore refer to these landforms as "corrugation ridges", which describes their planform geometries and appear to have formed through the mechanisms later described in detail by Rea and Evans (2011). The data presented by Stewart et al. (1988) are considerably more detailed and the mechanisms of formation better supported than those presented by Gwynne (1942). Neither author mentions potential climate controls on moraine formation, but Stewart et al. (1988) speculate that a deformable bed, a thin and flat ice front, and rapid advance creating basal cracks are critical for moraine formation in this setting.

Ham and Attig (2001) describe minor moraines near Irma Hill, Wisconsin, United States, in an area that was part of the Wisconsin Lobe of the Laurentide Ice Sheet. The authors describe the moraines as composed of till, proglacial sediments, and debris flow deposits. Although they present detailed descriptions of the sedimentological composition of moraines, sedimentological logs are absent. Ham and Attig (2001) also describe the geometries of the moraines, with the benefit of a clear example aerial photograph. The moraines are interpreted to have formed through push and freeze-on mechanisms (Figure 1.9) similar to the minor moraines formed at Myrdalsjökull (Krüger, 1995), and the authors additionally note that topography likely exerted a control on ridge orientation in the study area (Ham and Attig, 2001). Although specific climate influences are not discussed, Ham and Attig (2001) speculate that cyclic processes, likely relating to temperature (according to modern minor moraine studies), must control ice-marginal fluctuations, due to the close and repetitive spacing of moraines in this setting. The authors speculate that these moraines formed annually, but this interpretation is derived from comparison to modern

environments, and the chronological constraint on moraines in this study is insufficient to support this claim.

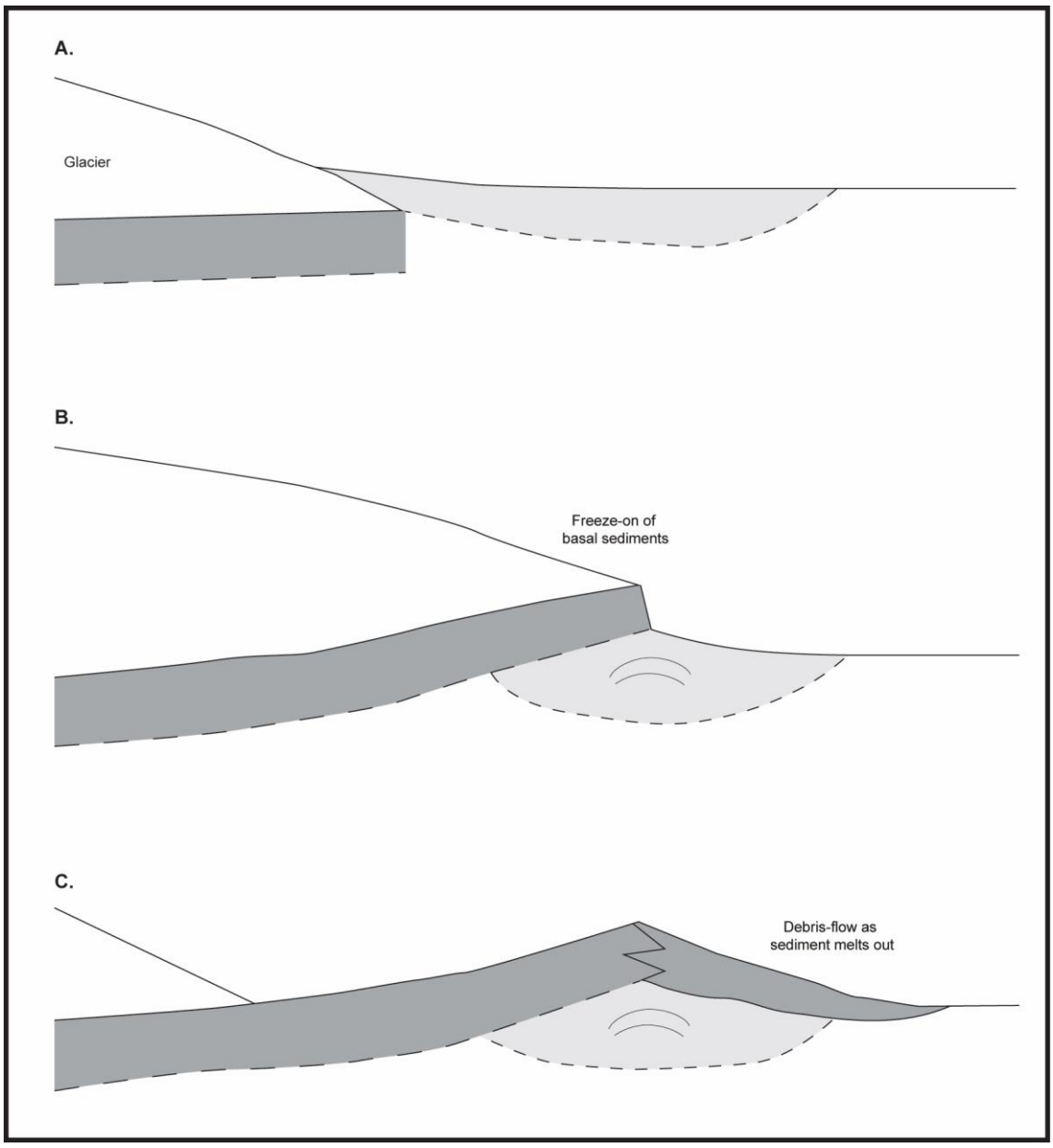

Figure 1.9. Conceptual diagram of minor moraine formation at the edge of the Wisconsin Lobe of the Laurentide Ice Sheet showing a freeze-on mechanism of formation. Modified from Ham and Attig (2001).

1.1.3 GLOMMAD16

The literature review and GLOMMAD16 are designed to complement each other, and the study areas are organised in the same way between the two (Tables 1.1-1.2). Where the literature review provides more detailed information about authors' observations and interpretations, the database provides more information about glacier and moraine measurements. This database firstly includes location of the modern ice front (modern

coordinate location at the ice front and climate regime) and glacier metrics (length and area). The database then includes information about the minor moraines in the glacier forelands. Depending on the data in the original literature, this includes the period of moraine formation, detailed sedimentological and geomorphological observations and analyses, the length, width, height, and relative proximal and distal slope steepness of moraines, the spacing between ridges, and the sedimentological composition. Finally, the database presents the authors' interpretations regarding mechanisms of formation, if climate controls on moraine formation were noted or assessed, and other controls on moraine formation, and what term(s) the authors use to refer to these landforms.

1.1.4 Synthesis of minor moraine formation mechanisms

Previous research has documented minor moraines in 41 different study areas, in 35 different studies. Pushing or bulldozing is the most frequently described mechanism of minor moraine formation (Christiansen, 1956; Hewitt, 1967; Worsley, 1974; Sharp, 1984; Ono, 1985; Evans et al., 1999a; Evans et al., 1999b; Ham and Attig, 2001; Evans and Twigg, 2002; Beedle et al., 2009; Winkler and Matthews, 2010; Lukas, 2012; Bradwell et al., 2013; Chandler et al., 2016a). Pushing up a reverse bedrock slope (Lukas, 2012; Bradwell et al., 2013) and incorporating snow banks (Birnie, 1977; Gordon and Timmis, 1992) specifically have also been described. Freezing of subglacial sediment has also been described as a mechanism of minor moraine formation (Andersen and Sollid, 1971; Matthews et al., 1995; Ham and Attig, 2001; Winkler and Matthews, 2010; Reinardy et al., 2013; Hiemstra et al., 2015; Chandler et al., 2016a), and Lukas (2012) mentions freezing of proglacial sediment to the ice front. Additional mechanisms of minor moraine formation include shearing and/or thrusting of sediment planes from subglacial to proglacial positions (Sharp, 1984; Schomacker et al., 2012), squeezing of till at the ice front (Worsley, 1974; Sharp, 1984; Bradwell, 2004; Chandler et al., 2016a), and dumping of supraglacial debris (Winkler and Matthews, 2010).

It is important to reiterate that not all studies of minor moraines present detailed sedimentological evidence to support interpretations of formation mechanisms. Credit is due to several authors who recognized the importance of this vein of research and utilized similar techniques in their work on minor moraines (Krüger, 1995; Ham and Attig, 2001; Lukas, 2012; Schomacker et al., 2012; Reinardy et al., 2013; Chandler et al., 2016a). This previous work formed the framework for the research in this thesis. Several other authors also assessed the sedimentological composition of minor moraines, albeit in less detail (Price, 1970; Andersen and Sollid, 1971; Sharp, 1984; Ono, 1985; Matthews et al., 1995; Schlüchter et al., 1999; Evans and Twigg, 2002; Bradwell, 2004; Bradwell et al., 2013;

Hiemstra et al., 2015). The absence of detailed sedimentological investigation of minor moraines in some studies may lessen the veracity of interpretations of formation mechanisms, but this can only be checked by revisiting these study sites and expanding the previously conducted research.

1.1.4.1 Spatial distribution of minor moraine study areas

As the literature review shows, the majority of minor moraine research has been conducted in Iceland and Norway. Previous research on minor moraines is notably absent from several areas: much of the polar latitudes, mid-latitudes, and mountain ranges along the Pacific Ocean or strongly influenced by Pacific Ocean climate controls. It is important to note, however, that the lack of evidence of minor moraines does not mean that these features do not exist in these regions, either in isolated valleys or more prolifically. This may reflect areas that have not been visited for geomorphological and/or glaciological research or study in areas in which minor moraines have not been recognized or further explored. For example, Nussbaumer et al. (2016) mentioned the presence of annual moraines in one study area in Chile, during an oral presentation at a conference, and recall similar moraines in areas further north, in the tropical Andes (Nussbaumer, personal communication). This example shows that perhaps researchers have noted minor/annual moraines in their study areas, but have either not realized their significance or have not decided to investigate these comparatively subtle landforms to develop larger understandings of landscape evolution and glacial history in their study areas. Furthermore, additional potential study sites have been revealed in the Alps (see Chapter 2) and South Georgia when scanning Google Earth imagery, and Beedle et al. (2009) mention that similar scanning of aerial photographs shows that minor moraine sequences are common in western Canada. Alternatively, the dearth of minor moraine studies as opposed to those on larger moraines and other glacier landforms (e.g. drumlins) may simply reflect that these minor moraines are not as widespread as other landforms.

Table 1.1. Published work on minor moraines in modern settings, part of GLOMMAD16.

Name	Coordinates	Area (km^2)	Length (km)	Period of moraine formation	Moraine length (m)	Moraine width (m)	Moraine height (m)	Steeper slope	Spacing (m)	Sediment	Methods	Formation	Climate control	Other control	Designation	Study
CANADIAN ROCKIES, Canada																
Athabasca Glacier	52°12'37.91"N	14.9	9.3	1924-1930/31	> 100 m		< 1		10-30	till		push			annual moraines	Luckman (1988; 2017)
	117°14'2.2""W	1956	1956	1962-1981					< few	unconsolidated foreland						Welch (1967)
				1999-2007												Kucera (1972, 1981)
COLUMBIA MOUNTAINS, Canada																
Castle Creek Glacier	53°1'40.98"N	9.4	5.8	1959-2007		0.61-4.39	0.07-1.10			deposited on till sheets		push	ablation season temperature controlling annual length change		annual moraines	Beedle et al. (2009)
	120°26'22.96"W	(2009)	(2009)										March precipitation			
													accumulation season preciptation with decadal delay			
													(all modulated by bed slope)			
MYRDALSJÖKULL ICE CAP, Iceland																
Öldufellsjökull	63°43'41.57"N			1923-1949								push			push moraines	Evans et al. (1999a)
	18°51'22.04"W															
Sandfellsjökull	63°39'59.94"N			1896-1916/1925								push			push moraines	Evans et al. (1999a)
	18°56'12.60"W															
Slettjökull	63°46'21.01"N	600		1928-1984	100-200	1.6-18.65	0.3-0.7	distal	< 10 - 50	till	✓ DS	basal freeze-on	summer temperature controls retreat rate	ice front thickness	annual moraines	Krüger (1995)
	18°55'34.19"W	(1995)								glaciolacustrine (pond)		push & basal freeze-on	cold winters			
										mass movement		melt-out of englacial debris				
Sólheimajökull	63°32'13.17"N		11	1850 and later	≤ 400	5-10	1-2			diamicton	✓ DS	till thrusting & dumping			annual moraines	Schomacker et al. (2012)
	19°21'43.98"W		(2012)	1995-2012	≤ 200	0.5-1	≤ 0.4			till						
VATNAJÖKULL ICE CAP, Iceland																
Breiðamerkurjökull	64°5'9.66"N	160 ^		1965-1983			1-2	distal	10	till		push	winter temperature; series of cold winters		annual moraines	Boulton (1986)
	16°19'10.73"W	(1995)								outwash						
												push			annual moraines (based on Boulton 1986)	Evans et al. (1999b)
		160 ^		since 1965	> 3		< 5			outwash	● SS	push & squeezing			low amplitude marginal moraines; push moraines	Evans and Twigg (2002)
		(1996)		1890-1934						pre-existing diamictons		push				
				1930-1960												
Fjallsjökull*	64°2'4.42"N	48		1900-1970		4-8	1-10	distal		glaciofluvial	● SG ● SS	till squeezing		pre-existing topography	moraines	Price (1970)
	16°24'22.31"W	(1995)								till ??				shape of ice front		
										outwash						
				1890-1934	> 3		< 5			pre-existing diamictons	● SS	push & squeezing			low amplitude marginal moraines; push moraines	Evans and Twigg (2002)
												push				
Fláajökull	64°19'27.40"N	213.3	29									push			annual moraines	Ewertowski et al. (2016)
	15°34'47.63"W	(2013)	(2013)													
Heinabergsjökull	64°17'26.13"N			< early 1970s								push	relatively warmer summers		push moraines	Evans et al. (1999a)
	15°40'16.03"W															
Kviárjökull*	63°56'47.18"N	22	13	1870-1977								push	colder winters		recessional push moraines	Evans et al. (1999a)
	16°27'55.03"W	(2012)	(2012)													
Lambatungnajökull	64°29'40.90"N	100 (W)		1932-1950			< 3	distal	6-60	clay-rich diamicton	● SS	squeezing	summer air temperature controls ablation	debris cover on ice	annual moraines	Bradwell (2004)
	15°17'54.19"W	(1995)														
													spacing from summer retreat			
Skálafellsjökull	64°16'25.45"N	100		1913-1984		1.6-18.65	0.4-5.25	distal		till	● SG ● SS	push & squeezing	summer temperature controls ridge spacing	can incorporate ice core	annual moraines	Sharp (1984)
	15°40'12.63"W	(1995)								debris-flow deposits		melt-out of englacial debris				
												snow-bank push				
		100.6	24.4	pre-1945	≤ 530	2-18	0.2-1.5	symm.	3-35	till and glaciofluvial	✓ DG ✓ DS	push	summer air temperature (most sensitive)	ice surface slope	smalls-scale recessional moraines / minor moraines	Chandler et al. (2016)
		(2010)	(2010)	1945-1964	(3-20 fragments)			distal		diamicton and glaciofluvial		push & squeezing	sea surface temperature	reverse bedrock slope	SOME conclusively annual moraines	
				1969-1974						till and glaciofluvial		basal freeze-on	North Atlantic Oscillation	ice front thickness	some sub-annual moraines	
				2006-2012									below average winter/spring temperatures (2012/13)	reverse bedrock slope		

Name	Coordinates	Area (km^2)	Length (km)	Period of moraine formation	Moraine length (m)	Moraine width (m)	Moraine height (m)	Steeper slope	Spacing (m)	Sediment	Methods	Formation	Climate control	Other control	Designation	Study
Skeiðarárjökull	63°59'56.93"N	850 (E)														Thorarinsson (1967)
		(1995)														
	17°13'18.92"W	44 (W)														
		(1995)														
		530 (M)														
		(2010)														
Virkisjökull–Falljökull*	63°58'4.98"N	5		1991-2004	100-400	2.0-8.0	0.5-2.0	distal	1-33	subglacial	• SG • SS	push	summer temperatures with <0.5 yr response time for ice front position	reverse bedrock slope	annual moraines	Bradwell et al. (2013)
	16°48'46.47"W	(shared accumulation area of the two before a split at a bedrock ridge and then recombine)								supraglacial			periods of elevated summer temperatures			
		(2013)		1935-1945	60-250	4-8	0.4-2.1	distal	17-50	glaciofluvial			periods of elevated summer temperatures			
HIMALAYA, Nepal																
Dzonglha Glacier	27°55'57.08"N									terrace-like sediments						Fushimi (1977)
	86°46'39.08"E									general outwash?						
Gyajo Glacier	27°54'51.45"N					2-3	1-2			lacustrine						Fushimi (1977)
	86°40'9.02"E															
Yala (Dakpatsen) Glacier	28°14'7.70"N	1.9		1850-1985	>250				1.3-9.1	till	• SS	push	summer temperature (influence on if precipitation falls as snow	distance of ice advance	annual moraines	Ono (1985)
	85°36'15.43"E	(1996)								englacial gravel			or rain during monsoon season)			
HARDANGERJØKULEN ICE CAP, Norway																
Midtdalsbreen	60°34'22.72"N	7.1		1955-1968	vary greatly		≤ 1	distal		till	• SG • SS	basal freeze-on		reverse bedrock slope	annual moraines, with reservations	Andersen and Sollid (1971)
	7°28'7.83"E	(2000)		(and before or after)			vary greatly			glaciofluvial						
		6.7		probably 1960s	10s		0.35-1.25	distal	1.3-26	subglacial diamicton	✓DG ✓DS	basal freeze-on	modulated by shading, aspect, debris cover on ice	ice front thickness	annual moraines	Reinardy et al. (2013)
		(2011)		(pre-1985)						glaciofluvial				sediment availability		
				2010/2011										debris cover on ice		
JOSTEDALSBREEN ICE CAP, Norway																
Bergsetbreen	61°38'35.01"N 7°	10.5	4.8	1997-2000			1-3			general foreland		push	seasonal advances		terminal moraines; multi-ridge composite moraine	Winkler and Matthews (2010)
	7'59.56"E	(1988)	(1988)													
Kjenndalsbreen	61°43'58.48"N	19.06	6.9	1997-2000			3			supraglacial		push			terminal moraines; multi-ridge composite moraine	Winkler and Matthews (2010)
	7°1'41.31"E	(1988)	(1988)												essentially annual moraines	
Tuftebreen	61°39'26.99"N	6.59	6.5							proglacial on bare bedrock		push			small seasonal moraines	Winkler and Matthews (2010)
	7°9'20.07"E	(1988)	(1988)												"essentially annual moraines"	
JOTUNHEIMEN, Norway																
Bøverbreen	61°33'23.17"N 8°	4.87	7	after 2001			1-3			till		basal freeze-on	seasonal advances		terminal moraines	Winkler and Matthews (2010)
	2'55.23"E	(1988)	(1988)									some push				
Storbreen	61°34'55.71"N 8°	5		1980s			<0.5			till		basal freeze-on			annual moraines in composite moraine	Hiemstra et al. (2015)
	9'51.98"E	(2015)		1990s			≤ 2									
Storjuvbreen	61°39'56.27"N	4.48	4.3	1994-2000			1-3			supraglacial		supraglacial dumping		ice core	terminal moraines	Winkler and Matthews (2010)
	8°17'55.55"E	(1988)	(1988)							englacial		englacial melt-out				
										till		push				
Styggedalsbreen	61°29'24.06"N	1.8		LIA			≤ 8	distal		ice core	• SG • SS	basal freeze-on	strong summer ablation, insufficiently cold winters	thin glacier snout	terminal moraines	Matthews et al. (1995)
	7°52'38.05"E	(1995)		10.3-9 ka			<0.5			glaciofluvial			seasonal oscillation of the ice margin	topography at ice front	annual moraine ridges (1934-1972)	
				1834-1972						diamicton (till)						
		<2		1997-2007						till	• SS	basal freeze-on			annual moraines	Hiemstra et al. (2015)
		(2015)														
OKSTINDBREEN ICE CAP, Norway																
Austre Okstindbreen	66°2'46.89"N			1957-1970		0.6-1.0	0.1-1.0			till		push primarily			annual moraines	Worsley (1974)
	14°19'30.01"E											till squeezing not rejected				
KARAKORAM MOUNTAINS, Pakistan																
Biafo Glacier	35°43'22.16"N		58	1961	<100		<4	symm.		proglacial outwash		push	seasonal variations	pre-existing topography	minor moraines	Hewitt (1967)
	75°53'29.78"E		(1967)							ice-contact deposit				sediment availability		
										ice-contact lacustrine				shape of the ice front		

Name	Coordinates	Area (km^2)	Length (km)	Period of moraine formation	Moraine length (m)	Moraine width (m)	Moraine height (m)	Steeper slope	Spacing (m)	Sediment	Methods	Formation	Climate control	Other control	Designation	Study
ALLAROYCE RANGE, South Georgia																
Cook Glacier**	54°26'53.00"S		1	1975-1981?		0.75-2	0.25-0.5						seasonal temperature variations controlling mass balances		annual moraines	Gordon and Timmis (1992)
	36°11'35.75"W		(1992)													
Glacier Col	54°20'41.02"S		1.25	1980-1982									seasonal temperature variations controlling mass balances		annual moraines	Gordon and Timmis (1992)
	36°32'2.05"W		(1992)													
Lucas Glacier	54° 4'7.40"S						0.2-2.5	distal		till		snow-bank push		snow depth	annual moraines (with reservations)	Birnie (1977)
	37°18'6.59"W													pre-existing topography		
														ice front thickness		
SALVESEN RANGE, South Georgia																
Graae Glacier	54°49'4.89"S		6	1953-1981								snow-bank push possible	seasonal temperature variations controlling mass balance		annual moraines	Gordon and Timmis (1992)
	36°12'7.41"W		(1992)													
Nachtigal Glacier	54°28'47.54"S		4	1977-1982									seasonal temperature variations controlling mass balance		annual moraines	Gordon and Timmis (1992)
	36°9'57.75"W		(1992)										(modulated by shading, form of ice front, debris cover on ice)			
Ross Glacier	54°33'36.62"S		12	around 1850			1-2						seasonal temperature variations controlling mass balance		series of more subdued ridges	Gordon and Timmis (1992)
	36°7'4.61"W		(1992)													
EUROPEAN ALPS, Switzerland																
Findelengletscher	46° 0'37.45"N	13	8	around 1978								push			annual moraines	Schlüchter (1983)
(Switzerland)	7°49'24.58"E	(2012)	(2010)												annual moraines	Lukas (pers. comm.)
Gornergletscher	45°58'40.37"N	38.25	14.1	1980-present	up to several ^	≤ 6	0.5-1.5	symm.	4.5-15	proglacial outwash	✓ DG ✓ DS	push	winter temperature (modulated by reverse bedrock slope and	ice front thickness	annual moraines	Lukas (2012)
(Switzerland)	7°48'15.06"E	(2012)	(2012)					distal		debris flow material			and possible shading and hypsometry)	ice surface slope		
														reverse bedrock slope		
												freeze-on		ice front thickness		
												ice-contact fan deposition		sediment availability		

* Óraefajökull/Vatnajökull Ice Cap (joint)
** Allaroyce-Salvesen Range (joint)
^ Western lobe

E = East
W = West
M = Middle

✓ DG = detailed geomorphology
● SG = somewhat detailed geomorphology
✓ DS = detailed sedimentology
● SS = somewhat detailed sedimentology

Table 1.2. Published work on minor moraines in Pleistocene settings, part of GLOMMAD16.

Name	Coordinates	Area (km^2)	Length (km)	Period of moraine formation	Moraine length (m)	Moraine width (m)	Moraine height (m)	Steeper slope	Spacing (m)	Sediment	Methods	Formation	Climate control	Other control	Designation	Study
LAURENTIDE ICE SHEET																
Frank Lake (Alberta)	50°33'35.32"N											push	stable system responding to predominant climate conditions		minor moraines; recessional moraines	Evans et al. (1999b)
(Canada)	113°42'38.45"W															
Moose Mountain (Saskatchewan)	50°56'17.66"N				sometimes	30	1.5-6		~90-100	till		push			minor recessional ridges (likely annual)	Christiansen (1956)
(Weyburn Lobe)	114°50'5.71"W				fragmented											
Des Moines Lobe (Iowa)	42° 3'29.47"N			LGM		20-90	1-<6		30-180	till	● SG ✓ DS	basal cracks & crevasses		deformable bed	corrugation ridges	Stewart et al. (1988)
(Mankato in Gwynne, 1942; USA)	93°35'11.67"W									glaciofluvial				thin and flat ice front		
														rapid advance creating basal cracks		
Irma Hill (Wisconsin)	45°21'4.62"N			late Pleistocene	≤ 1km		1-4	proximal	30-80	till	✓ DS	push & freeze-on	winter temperature	pre-existing topography	annual moraines	Ham and Attig (2001)
(Wisconsin Valley Lobe; USA)	89°39'15.02"W				(one ridge up to 10 km long)					sorted proglacial			summer tempearture controls spacing	ice front thickness		
Mankato Lobe (Iowa)	42° 3'31.47"N			LGM			<3-5			till		push			seasonal minor recessional moraines	Gywnne (1942)
(Des Moines in Stewart et al. 1988; USA	93°36'0.01"W															

✓ DG = detailed geomorphology

● SG = somewhat detailed geomorphology

✓ DS = detailed sedimentology

● SS = somewhat detailed sedimentology

1.1.4.2 Controls on minor moraine formation

Most groups of minor moraines reflect successive positions of the ice front during a longer period of recession, punctuated by small readvances or still stands. Ice front fluctuations are inherently related to glacial dynamics dominantly driven by climate, although other factors may control the style of moraine formation or modulate climate signals of ice front variation. Both the potential climatic controls and other controls on minor moraine formation are therefore assessed below. Groups of closely spaced minor moraines may also reflect subglacial sedimentation (Stewart et al., 1988). These moraines are not discussed in a climatological context, as they do not strictly reflect ice front positions.

Before assessing controls on minor moraine formation, i.e. specifically why and how these moraines form, it is important to understand the distribution of minor moraine formation mechanisms. Some previous research has not reported mechanisms of formation, so those are omitted from the following totals. The investigation of the spatial distribution of minor moraine study areas can be deepened by assessing which specific countries or mountain ranges contain specific mechanisms of formation and how potential controls on minor moraine formation may be reflected in the global distribution of minor moraines (Table 1.3). Moraines formed through pushing dominate reported mechanisms of minor moraine formation (26) followed by freeze-on (9). All other mechanisms of formation have been reported three or fewer times (Table 1.3). Minor push moraines are found in all previously studied settings, whereas other mechanisms of formation are more localised.

Table 1.3. Mechanisms of minor moraine formation organised by country or mountain range. Areas with no reported instances of a specific formation mechanism are shaded grey.

Formation Mechanism	IS	NO	SG	CA	E.A.	NP	PK	LIS	Total
Push	7	6	2	1	1	1	1	3	**22**
Freeze-on	2	4			1				**7**
Squeezing	1	1							**2**
Combined push-squeeze	2								**2**
Combined push-freeze on	1							1	**2**
Thrusting/shearing	1								**1**
Englacial melt out	1	1			1				**3**
Dumping		1							**1**
Basal cracks and crevasses								1	**1**
Total	**15**	**13**	**2**	**1**	**3**	**1**	**1**	**5**	**41**

IS = Iceland
NO = Norway
SG = South Georgia
CA = Canada
E.A. = European Alps
NP = Nepal
PK = Pakistan
LIS = Laurentide Ice Sheet

The distribution of freeze-on moraines is notable, as these occur primarily in Norway, in four forelands (Andersen and Sollid, 1971; Matthews et al., 1995; Winkler and Matthews, 2010; Reinardy et al., 2013; Hiemstra et al., 2015), and also two forelands in Iceland (Krüger, 1995; Chandler et al., 2016a) and one in the Alps (Lukas, 2012). Previous work recognizes that freeze-on processes are responsible for moraine formation when freezing is able to penetrate sediment underlying the ice front (Krüger, 1995; Ham and Attig, 2001; Lukas, 2012; Reinardy et al., 2013; Chandler et al., 2016a), which implies the necessity of seasonally cold temperatures that allow freezing during the cold season but do not sustain permafrost.

The distribution of a squeezing mechanism of moraine formation is also outstanding. These moraines occur in three forelands in Iceland (Price, 1970; Sharp, 1984; Evans and Twigg, 2002; Bradwell, 2004; Chandler et al., 2016a), and are only otherwise reported potentially, i.e. without definitive evidence or confidence from the author, from one foreland in Norway (Worsley, 1974). Chandler et al. (2016a) discuss the importance of meltwater saturating till at the ice front, which then allows this semi-plastic till to be squeezed out at the ice margin.

Climatic controls on minor moraine formation

Previous work has speculated or recognized how climate factors may influence ice margin fluctuations that form suites of minor moraines. Most studies that have assessed climatic controls on minor moraine formation discuss **ablation season temperature** as the dominant control, and most of the glaciers are in Iceland: Slettjökull by Krüger (1995), Lambatungnajökull by Bradwell (2004), Skálafellsjökull by Sharp (1984) and Chandler et al. (2016a), and Virkisjökull-Falljökull by Bradwell et al. (2013), with the addition of Castle Creek Glacier in Canada by Beedle et al. (2009). More specifically, particularly high ablation season temperatures influencing moraine formation are discussed by several researchers in Iceland (Heinabergsjökull by Evans et al. (1999a) and Lambatungnajökull by Bradwell (2004)) and one setting in Norway (Styggedalsbreen by Matthews et al. (1995)). The detailed work by Bradwell et al. (2013) was able to show that the Virkisjökull- Falljökull system responds to changes in ablation season temperatures with a response time of less than half a year.

The influence of **accumulation season temperature** on minor moraine formation is also mentioned in several studies. Lukas (2012) shows that the dominant control on ice-marginal fluctuations creating moraines in the Gornergletscher foreland is accumulation season temperature, and that **average annual temperature** may also influence moraine formation. Evans et al. (1999b) specifically target particularly cold winters as a dominant

control on moraine formation in the Kvíárjökull foreland, and this climate influence is echoed as a subsidiary influence on minor moraine formation at Slettjökull (Krüger, 1995) and Skálafellsjökull (Chandler et al., 2016a) (both after ablation season temperature). In contrast, Matthews et al. (1995) highlight particularly warm winters as a subsidiary control (after ablation season temperature) on moraine formation in the Styggedalsbreen foreland.

Few studies have assessed the influence of precipitation on ice-marginal fluctuations responsible for forming minor moraines (Beedle et al., 2009; Chandler et al., 2016a). Beedle et al. (2009) show that **March precipitation** is the secondary driver of ice front change at Castle Creek Glacier, after ablation season temperatures, and that **accumulation season precipitation** is also an influence, with an approximate decadal delay of ice front reaction. Chandler et al. (2016a) show that precipitation does not play a significant role on ice front variations responsible for moraine formation in the Skálafellsjökull foreland. Although not explicitly studied, the importance of precipitation on ice-marginal fluctuations is mentioned by Krüger (1995), and Lukas (2012) speculates that differences between temperature drivers of ice front variation between Gornergletscher (ablation temperature) and lowland, maritime sites (accumulation temperature) could be due to lower precipitation and potential lower mass turnover in the high mountain setting, which may mute accumulation season front variations by superimposing longer-term climate signals on the overall ice-front variation record.

Several studies more generally mention that advances producing minor moraines are likely seasonal, but without linking this to climate data: Winkler and Matthews (2010) at Bergsetbreen and Gordon and Timmis (1992) on South Georgia and Evans et al. (1999b), Gwynne (1942), and Ham and Attig (2001) for lobes of the LIS. Ham and Attig (2001) additionally state that cyclic temperature changes may have controlled moraine formation by the LIS Wisconsin Lobe, which is supported solely through comparison to modern environments in Iceland, primarily following research at Myrdralsjökull by Krüger (1995).

The most robust studies with regard to assessing climate signals on minor moraine formation are those by Beedle et al. (2009) at Castle Creek Glacier and Chandler et al. (2016a) at Skálafellsjökull, which both assess multiple climate factors on ice front variations through systematic statistical analyses using moraine spacing as a proxy for retreat rates. By comparing both lagged and un-lagged climate factors, Beedle et al. (2009) were able to show that the ice front responds immediately to ablation season temperatures and changes in ablation season mass balance, which is superimposed on an approximate decadal delay of ice margin response to accumulation season precipitation. This research also compared mass balance and glacier length change from other regional glaciers to assess if the results at Castle Creek Glacier are regionally representative, which has shown that ablation season temperature dominantly controls glacier recession. The authors do not, however, discuss

more localized factors that may affect moraine spacing or speculate as to why annual moraines are not found in these other forelands. Chandler et al. (2016a) extend assessment of climate influences on ice margin location to those beyond local temperature and precipitation by assessing annual, ablation season, and accumulation season temperatures and precipitation along with sea surface temperature (SST) and the North Atlantic Oscillation (NAO). This research shows that Skálafellsjökull dominantly responds to inter-annual variations in ablation season temperature, which corresponds to similar results at other Icelandic glaciers. Through the extension of their climate analyses, Chandler et al. (2016a) show that SST and NAO also influence Skálafellsjökull ice front variations, however the links between these climate factors need to be further tested to assess potential interrelationships of climate variables that collectively influence ice front fluctuations.

Reinardy et al. (2013) show another effect of climate influencing minor moraine formation at Midtdalsbreen, after the primary influence of climate on mass balance and ice margin fluctuations. The influence on climate here is particularly important in altering the ice front geometry by creating a thinner and more gently sloping margin, allowing freeze-on to occur and minor moraines to be created.

These detailed studies comparing climate and glacier response have yielded important results to better understand the controls on minor moraine formation in the study areas, as well as furthering our understanding of how glacial systems may respond on a larger scale to climate influences. Where possible, similar methods can be used in the future to help further build our understanding of minor moraine formation globally, which would then allow for a more thorough assessment of connections among study areas. This vein of research is only possible, however, where detailed and long time-series of temperature and precipitation data exist, the annual nature of moraine formation can be proven, and for some more specific analyses, the mass balance and front variation of the glacier through time has been recorded.

Non-climatic controls on minor moraine formation

Although climate signals control glacier fluctuations overall, other factors have been shown to influence where, when, why, and how individual minor moraines and groups of minor moraines form, regardless of region or climate realm. Non-climatic controls on minor moraine formation sometimes influence multiple mechanisms of formation, but they may exclusively influence one. Non-climatic controls on minor moraine formation, as presented in previous work and noted in this thesis, are therefore discussed here with regards to specific formation mechanisms.

Push / bulldozing

Glacier morphology, topography, and sediment may affect push moraine formation or the specific style of push moraine formation. Hewitt (1967) generally mentions that drastic changes to ice front shape during summer influence sediment delivery rates and the style of pushing. Ice front thickness may also influence the style of push moraine formation, where a thicker ice front may cause more folding in the sediment or snow pile than a thin ice front (Birnie, 1977), or a thin ice front may be buried by slumped proglacial sediment during pushing, resulting in an ice-cored moraine (Lukas, 2012; Chapter 5). A gently-sloping ice front facilitates this slumping and inefficient bulldozing in some locations at Gornergletscher (Lukas, 2012), whereas the relatively steeper ice margin at Skálafellsjökull ensures no burial of the ice front (Chandler et al., 2016a).

Pre-existing topography may also influence minor push moraine formation either by generally affecting "resultant forms" (Birnie, 1977) or ice front sedimentation (Hewitt, 1967) or in more specific ways. Topography may influence the orientations and distribution of minor push moraine ridges (Ham and Attig, 2001). Additionally, surface irregularity, either as topographic or sedimentary obstacles, (Schlüchter et al., 1999) may be necessary to generate push moraines. Some work specifically discusses reverse bedrock slopes, which may cause proximal moraine slopes to be longer than distal slopes and influence the slumping of proglacial sediment onto the ice front, potentially creating ice-cored moraines (Lukas, 2012).

Sediment availability also inherently influences push moraine formation, as no moraines would form if sediment was not present, and larger moraines hold larger volumes of sediment than smaller moraines. Hewitt (1967) also discusses the importance of sediment availability in minor push moraine formation when mentioning an abundance of sediment released at the ice front in the summer, which facilitates subsequent moraine formation and can depend on the amount and composition of proglacial sediment. The composition of sediment would also affect permeability, which Schlüchter et al. (1999) list as an "important prerequisite" for push moraine formation.

Basal freeze-on

Glacier morphology, topography, and sediment may all also affect moraines formed through basal freeze-on, although in considerably different ways than push moraine formation. Ice front thickness is commonly mentioned as critical for basal freeze-on to occur, as the ice front needs to be thin enough (<15 m) to allow for the freezing front to penetrate to

underlying sediment (Krüger, 1995; Ham and Attig, 2001; Lukas, 2012; Reinardy et al., 2013; Chandler et al., 2016a; Chapter 5).

Similar to minor moraine formation through pushing, topography may influence the orientations and distribution of minor moraines formed through basal freeze-on or combined freezing and pushing mechanisms (Ham and Attig, 2001). Reverse bedrock slopes also influence minor moraines formed through freeze-on, as the reverse slope may contribute to the necessary thin ice front (Chandler et al., 2016a). Andersen and Sollid (1971) note that the largest moraines in their study area are on reverse bedrock slopes, although this is not elaborated on.

The role of sediment on minor moraines formed through basal freeze-on mechanisms is only discussed in one study. Firstly, the presence of supraglacial debris may inhibit minor ice margin fluctuations that produce minor moraines, and in the Midtdalsbreen study area, moraines formed exclusively through basal freeze-on mechanisms, by creating complex down-wasting patterns at the ice front (Reinardy et al., 2013). Sediment availability may also be important in varying sedimentological composition of minor freeze-on moraines in individual forelands, where supraglacial sediment that slumped off of the ice front and englacial and subglacial sediment that melted out at the ice front may later be incorporated into freeze-on moraines (Reinardy et al., 2013).

Till squeezing

Price (1970) very briefly mentions that slope angles and aspect may influence the distribution of moraines. Reverse bedrock slopes may also play an important role in minor moraine formation through till squeezing. Chandler et al. (2016a) explain how meltwater cannot penetrate bedrock and consequently flows and accumulates towards the ice front, creating highly saturated submarginal and subglacial sediments. This viscous till with high pore-water pressure then lends itself to squeezing at the ice margin, which may then be pushed into a more distinct moraine by the ice front. This does, however, also occur in areas without a reverse bedrock slope.

Potential sedimentological influences on minor moraines formed through till squeezing are not prolifically discussed. Bradwell (2004), however, mentions that a low amount of supraglacial debris both influenced moraine formation and aided in moraine preservation. Although Bradwell (2004) does not discuss this in more detail, this may imply that differential ablation associated with supraglacial material did not create stagnant ice bodies or hummocky moraine through differential ablation (e.g. Benn, 1992; Bennett, 2001;

Evans and Twigg, 2002; Evans, 2005; Winkler and Matthews, 2010), instead allowing for the formation of sharper moraines through till squeezing.

Melt-out of englacial debris

The melt-out of englacial debris forming minor moraines is reliant on sediment availability. Although not explicitly stated by authors, moraines formed through englacial sediment melting out at an ice front, then being pushed into a ridge or incorporated into a ridge through other means, require the presence of an englacial conduit (Krüger, 1995; Winkler and Matthews, 2010; Lukas, 2012).

Non-climatic controls modulating climatic controls

These previous examples show that non-climatic factors may influence mechanisms of minor moraine formation and thereby modulate the geomorphological record. It is also important to consider that some of these non-climate factors can modulate or obscure otherwise more dominant climate signals on ice margin fluctuations, and that topography is frequently discussed as modulating climate signals on glacial dynamics that may produce minor moraines. Despite the lack of caution from some authors, the potential of these non-climatic controls on ice margin flucuations, across multiple study areas, emphasizes the need to intergrate, or at least recognize the presence of, localised glaciology, topography, and sediment dyanmics when connecting minor moraine or annual moraine formation to potential climatic controls on glacier dynamics and landscape evolution.

Different directions and degrees of bed slope are mentioned in several studies. Beedle et al. (2009) more generally discusses how bed slope can affect ice flow velocities and therefore ice margin fluctuations. However, the authors found no relation between bed slope and glacier length change in their study area. Additionally, Lukas (2012) first discussed how reverse bedrock slopes may modulate the rate of ice-marginal fluctuations and therefore superimpose a topographic signal on any potential climate signal, as supported through glaciological research (Huss, 2005). This idea is then subsequently mentioned by Bradwell et al. (2013) and Chandler et al. (2016a).

Other topography is also mentioned as potentially modulating climate signals in ways that have not been discussed in specific mechanisms of minor moraine formation. Gordon and Timmis (1992) were the first researchers on minor moraines to mention that shading may influence ice front fluctuations by creating differential ablation across the glacier. This is subsequently mentioned by Reinardy et al. (2013), along with aspect, another non-climatic influence on the geomorphological record. Additionally, Lukas, (2012)

speculates that the role of shading, and perhaps hypsometry, at Gornergletscher may influence some of the differences in how this glacier, and potentially others in high-mountain settings, react to climate signals in comparison to lowland, maritime glaciers that also form annual/minor moraines. Supraglacial sediment cover is also mentioned as a non-climate control that can affect ablation rates across a glacier, and therefore perhaps obscure climate signals of ice front variations (Gordon and Timmis, 1992; Reinardy et al., 2013).

1.2 Research gaps

GLOMMAD16 and the accompanying literature review are a compilation of previously conducted research on minor moraines and provide a quick view of gaps in minor moraine research. This database is considered again in Chapter 7 when comparing the findings of this thesis to minor moraine formation globally.

GLOMMAD16 highlights differences in study methods. Only recent studies have combined detailed sedimentological and geomorphological observations (Lukas, 2012; Reinardy et al., 2013; Chandler et al., 2016a), and some older studies have used less detail while still combining sedimentological and geomorphological assessments (Price, 1970; Andersen and Sollid, 1971; Sharp, 1984; Evans and Twigg, 2002; Bradwell et al., 2013). Several studies have incorporated detailed sedimentological observations (Krüger, 1995; Ham and Attig, 2001; Schomacker et al., 2012), and others incorporated less detailed sedimentological assessment (Ono, 1985; Bradwell, 2004; Hiemstra et al., 2015). Many studies, however, do not describe the sedimentological composition or form of minor moraines and instead only mention or describe their presence (Hewitt, 1967; Worsley, 1974; Birnie, 1977; Boulton, 1986; Beedle et al., 2009), although some of these did not have a primary research focus on investigating annual or minor moraines or seasonal fluctuations of the ice front (Christiansen, 1956; Fushimi, 1977; Gordon and Timmis, 1992; Evans et al., 1999a; Evans et al., 1999b; Winkler and Matthews, 2010).

The role of climate controls and other controls on moraine formation and specific mechanisms of formation are also mentioned by most authors, as summarised by GLOMMAD16. Several authors discuss both climate controls and other controls on moraine formation (Hewitt, 1967; Gordon and Timmis, 1992; Krüger, 1995; Matthews et al., 1995; Ham and Attig, 2001; Bradwell, 2004; Lukas, 2012; Bradwell et al., 2013; Chandler et al., 2016a). Some studies only find or discuss climate controls on moraine formation (Sharp, 1984; Ono, 1985; Boulton, 1986; Evans et al., 1999a; Evans et al., 1999b; Beedle et al., 2009; Winkler and Matthews, 2010), and other studies do the same with other controls on moraine formation (Price, 1970; Andersen and Sollid, 1971; Birnie, 1977; Schlüchter et al., 1999; Reinardy et al., 2013).

Study methodologies, specific mechanisms of formation, and controls on minor moraine formation are explored further in Chapter 7 when comparing minor moraines in a global context and synthesising GLOMMAD16 and the new research presented in this thesis.

1.3 Research objectives and goals

As the review of previous research on minor moraines demonstrates, the processes that form minor moraines remain incompletely understood, presumably mainly due to the dearth of studies on the subject when compared to other glacial landforms. Most studies have been conducted in Iceland and Norway, so in addition to establishing controls on minor moraine formation, the leading question is where and why minor moraines exist in high-mountain settings and what information minor moraines in this setting may provide about Quaternary glacial dynamics. The potential of minor moraines as terrestrial archives of glacier fluctuations and ice-margin dynamics showcases the need to examine the characteristics of minor moraines in a diversity of settings and the potential to extract valuable insight into recent ice-marginal retreat.

This calls for investigation in other areas to test existing interpretations of minor moraine formation against observations in the nearly un-investigated high-mountain setting. This thesis therefore contributes to the following research questions, objectives, and goals:

(1) Do minor moraines exist in other high-mountain settings of the European Alps?

Section 1.1.1 shows that most research concerning minor moraines records these landforms in Iceland and Norway. High-mountain, more inland examples of minor moraines are comparatively sparse. Lukas (2012) presents detailed research regarding minor moraines in one foreland in Switzerland. This study suggests that minor moraines may be found in other Alpine forelands, despite some researchers suggesting that minor moraines should not be found in high-mountain settings due to climate controls on low mass balance gradients and diminished ice flow velocities, which should not allow for significant short-term (e.g. seasonal or annual) advance and retreat cycles (Boulton, 1986; Bennett, 2001). This research therefore seeks to establish where minor moraines exist in other forelands of in the European Alps.

(2) What can the geomorphological presence and sedimentological composition of minor moraines in glacier forelands in the European Alps reveal about glacier dynamics?

Previous research has studied minor moraines using geomorphological, sedimentological, and climatological methods, but the combination of these complementary methods is limited to only three studies (Lukas, 2012; Reinardy et al., 2013; Chandler et al., 2016a). The importance of the links between the composition of landforms and their surficial characteristics is imperative in accurately interpreting processes of formation. Several studies note the presence of minor moraines and assess these features primarily or solely through their geomorphological characteristics. This research therefore uses the framework of detailed geomorphological and sedimentological methods in these three previous studies to explore mechanisms of minor moraine formation in the European Alps. If these mechanisms differ from those previously published, conceptual models will be created to describe the genetic processes of formation.

(3) How do the mechanisms of minor moraine formation in study areas in the European Alps relate to the mechanisms of minor moraine formation in previously published work? Are there similarities linking minor moraine formation globally in terms of where, when, why, and how minor moraines form?

Comparing moraine formation in multiple areas is critical in assessing whether common mechanisms of moraine formation create minor moraines or if more localised factors, e.g. local climate or geomorphology, control their formation. This includes comparisons of glacier locations and size, specific mechanisms of moraine formation, and potential climate and other controls on minor moraine formation. Additionally, in what context and with what supporting evidence can minor moraines conclusively be given the term "annual moraines?" This includes assessing the use of the term "annual moraines" in previously published research, as well as considering if the minor moraines of the two newly studied glacier forelands in this thesis have been formed or are forming annually. This also includes consideration of the implications that the term "annual moraines" holds in understanding glacial dynamics, whether appropriately or inappropriately used. As the literature review has shown, this thesis considers both annual moraines and groups of closely spaced minor moraines, referring to them as minor moraines until sufficient evidence is presented to show that the moraines formed annually.

In assessing these questions and meeting these research objectives and goals, this thesis will contribute to a better understanding of glacier behaviour in a changing climate by

contributing to the broader disciplines of glacial sedimentology and geomorphology, physical geography and earth surface sciences, and climate studies.

1.4 Thesis structure

This thesis is divided into eight chapters. This chapter has introduced the key conceptual frameworks and current knowledge gaps driving the research objectives and goals. Chapter 2 describes the methods used in selecting study sites, mapping the geomorphology of study sites, analysing the sedimentological composition of minor moraines, and comparing the geomorphological record to climate data. Chapter 3 describes the three study sites of this research.

The results of this research are divided into three chapters. Chapter 4 assesses the geomorphological evolution of the Schwarzensteinkees foreland, Austria, and presents evidence and interpretations of minor moraine formation in the foreland. Chapter 5 presents evidence and interpretations of minor moraine formation in the foreland of Silvrettagletscher, Switzerland. Chapter 6 assesses the continued evolution of the foreland of Gornergletscher, Switzerland, since fieldwork was last conducted in 2007 by Lukas (2012).

Chapter 7 synthesises the results of Chapters 4-6 and places these findings in the wider context by comparing mechanisms of minor moraine formation globally to assess how our understanding of minor moraines contributes to the knowledge of glacier dynamics in various settings. The research throughout this thesis is summarised in Chapter 8, which also includes avenues for future research in both current and new field areas.

CHAPTER 2. Methods

"Standing on the edge of a million landscapes, emptying,
and the water from the glacier fills my shoes."
Lonely At The Top by Conor Oberst

Recent studies of minor moraines have used a well-developed, comprehensive combination of geomorphological mapping and sedimentological logging to detail minor moraine characteristics and interpret mechanisms of minor moraine formation (Lukas, 2012; Reinardy et al., 2013; Chandler et al., 2016a). This study follows a similar design for the most robust, accurate understanding of minor moraine formation. This is first accomplished by mapping and measuring the geomorphological characteristics of the moraines in the field and with remotely-sensed data. This is then followed by excavating sections through moraines for sedimentological assessment. Finally, the geomorphological record is compared to climate data to assess the roles of temperature and precipitation on moraine formation, where possible.

2.1 Study area selection

The review of previously-published studies on minor moraines (Chapter 1) reveals a relative scarcity of work in high-mountain when compared to more lowland environments. The research presented in Chapter 1 suggests that either minor moraines in high-mountain continental settings are more prolific than published research suggests, or that minor moraines in high-mountain, continental settings are not widespread. Of the studies in high-mountain settings, Lukas (2012) presents the most detailed information about minor moraine formation, for the moraines in the foreland of Gornergletscher, Switzerland. The present research therefore uses the Gornergletscher study as a framework to assess if more forelands containing minor moraines exist in the European Alps, and if so, whether these forelands provide prolific research opportunities.

Study sites were selected following a systematic search for minor moraines in all glacierised valleys of the European Alps. Google Earth was used as a platform of freely-available, easily-accessible, and easily-utilised aerial imagery to efficiently visually assess the entirety of the mountain range. This research includes only visual assessment of imagery in Google Earth. It is therefore recognised that this imagery may be too low resolution to resolve minor moraines in some areas and that minor moraines may exist in formerly glaciated valleys.

The results of this scanning are presented as a Google Earth database (Appendix A). Figure 2.1 shows the extent of surveying, whereas Figure 2.2 shows areas without minor moraines and Figure 2.3 shows areas that may contain or conclusively contain minor moraines, or where low resolution imagery, snow cover, clouds, or shadows do not allow for a good visual assessment through available years. Each glacierised valley was assessed individually, but the database may indicate larger areas (i.e. multiple valleys) classified as not having minor moraines, instead of representing this with an individual point for each valley. Some valleys are labelled as potentially having minor moraines, but a more definitive designation cannot be obtained due to the resolution of the imagery.

The assessment of glacierised valleys of the European Alps reveals that only four valleys conclusively contain at least ten minor moraines: Schwarzensteinkees in Austria, an unnamed glacier in Italy, and Findelengletscher, Gornergletscher, and Silvrettagletscher in Switzerland (Figure 2.3).

This project focuses primarily on the Schwarzensteinkees foreland, Austria, and the Silvrettagletscher foreland, Switzerland, for several reasons. Most importantly, these two valleys contain many (greater than 50) definitive minor moraines clearly visible when compiling the database (Figures 2.4-2.5). Additionally, both forelands are easily accessible, are included in the World Glacier Monitoring Service (WGMS) database, and have been the focus of some previous work about the glacier and/or geomorphological history. This research additionally includes the Gornergletscher foreland, Switzerland, to update the findings of Lukas (2012) by addressing questions associated with preservation potential, minor moraine alteration, and continued minor moraine genesis.

2.2 Geomorphological mapping

Geomorphological mapping assists in measuring the dimensions and orientations of and between landforms and in recording any outstanding features of landforms (Hubbard and Glasser, 2005). The most robust geomorphological mapping incorporates multiple methods of landform observation, measurement, and analysis. Previous studies have shown the benefits of pairing remote sensing and field mapping for vigorous geomorphological assessment of minor moraines. However, this level of detail is sparse in such settings (Lukas, 2012; Bradwell et al., 2013; Reinardy et al., 2013; Chandler et al., 2015; Chandler et al., 2016a).

Geomorphological mapping in the Schwarzensteinkees foreland has benefited from combining field observations with 1 m resolution digital elevation model (DEM) data provided by the government of Tirol, Austria, historical imagery, and historical maps.

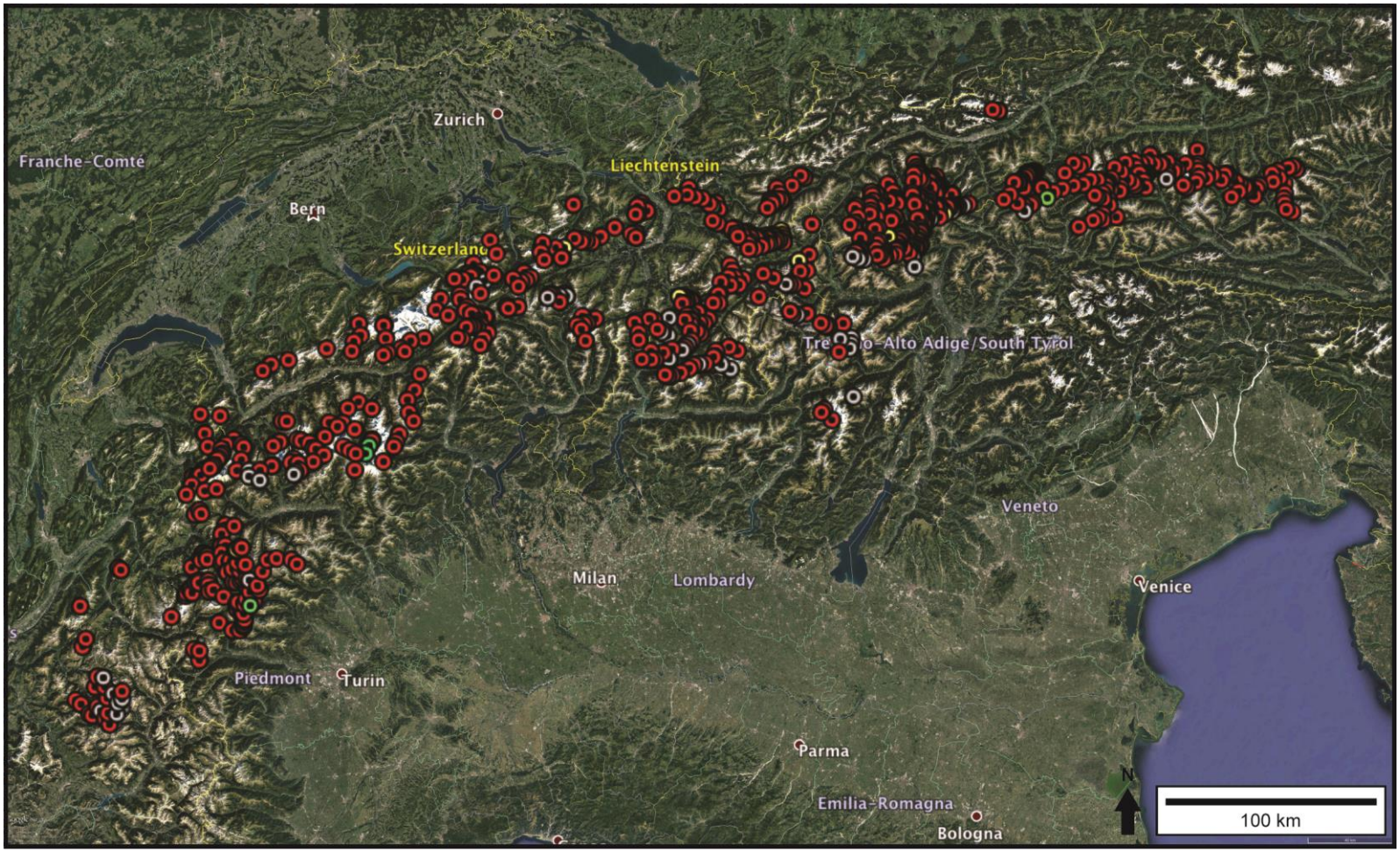

Figure 2.1. Map of scanning for minor moraines in the European Alps. Grey points indicate where a good visual assessment was not possible. Red points indicate individual valleys or a group of valleys with no minor moraines. Yellow points indicate valleys that potentially have minor moraines. Green points indicate valleys that conclusively contain 10 or more minor moraines. This dataset is available to explore in Google Earth (Appendix A). Dataset created in Google Earth, with current extent using Landsat imagery (SIO et al., 2015).

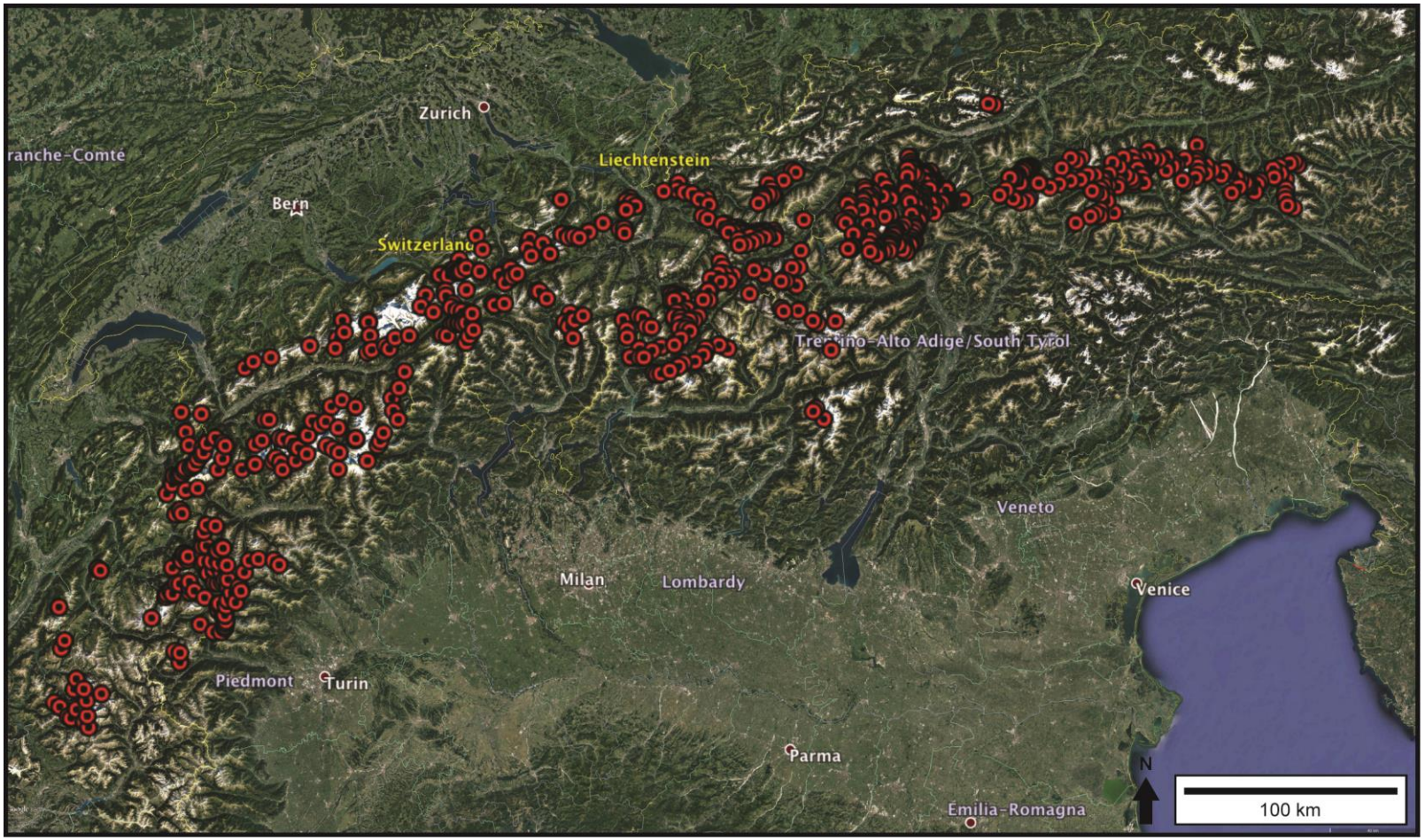

Figure 2.2. The European Alps, showing only individual valleys or a group of valleys with no minor moraines (red points). This dataset is available to explore in Google Earth (Appendix A). Dataset created in Google Earth, with current extent using Landsat imagery (SIO et al., 2015).

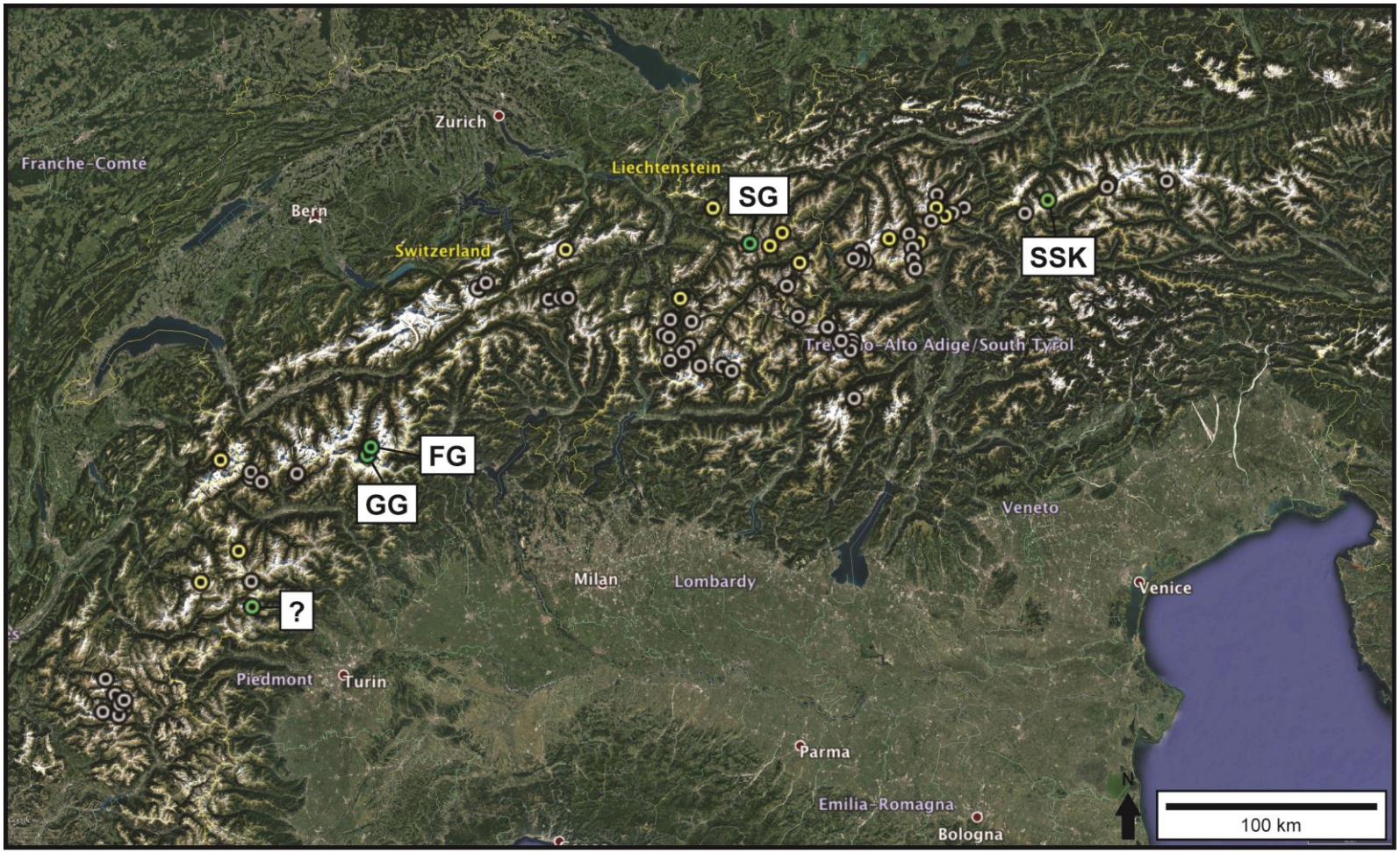

Figure 2.3. The European Alps, showing valleys that potentially have minor moraines (yellow points) and valleys that conclusively contain 10 or more minor moraines (green points). Grey points indicate where a good visual assessment was not possible. Labels refer to valleys that contain minor moraines: "?" unnamed, Italy; "GG" Gornergletscher, "FG" Findelengletscher, "SG" Silvrettagletscher, Switzerland; "SSK" Schwarzensteinkees, Austria. This dataset is available to explore in Google Earth (Appendix A). Dataset created in Google Earth, with current extent using Landsat imagery (SIO et al., 2015).

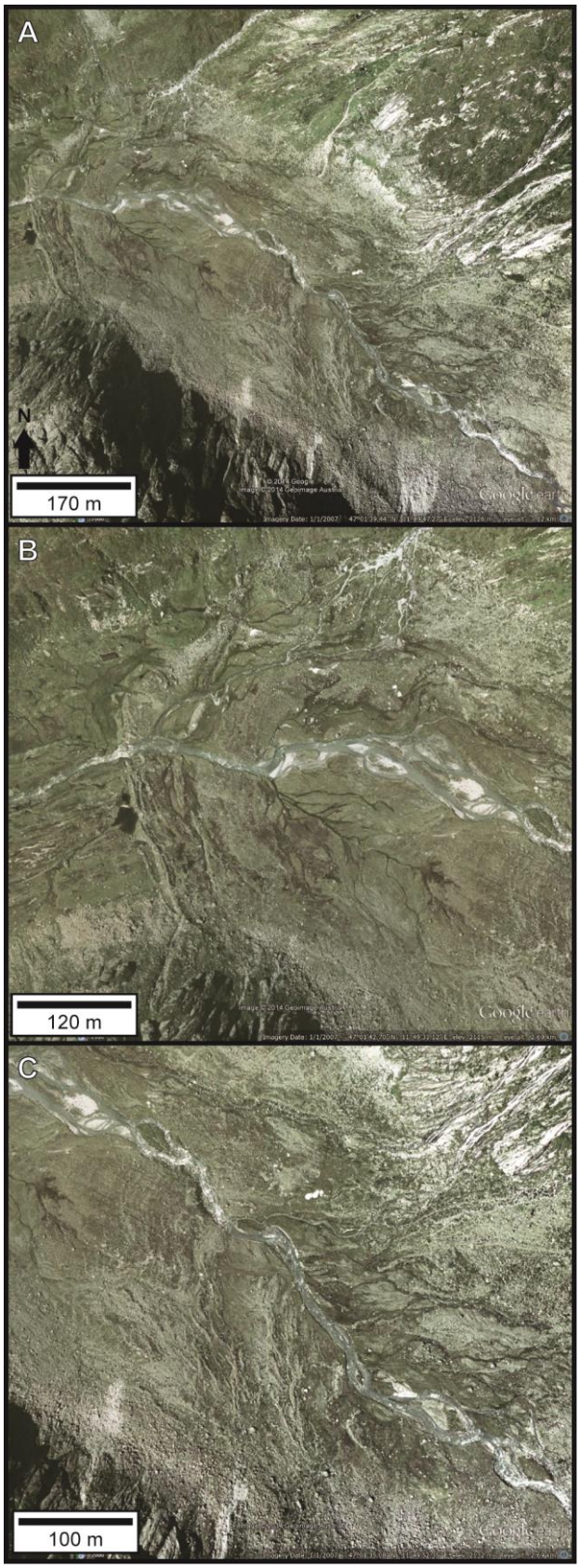

Figure 2.4. The Schwarzensteinkees foreland, Austria, and minor moraines as seen in Google Earth. A) The foreland downvalley of the portion dominated by bedrock, showing two groups of minor moraines. The glacier is located in the bedrock extent (southeast), approximately 860 m upvalley; B) The downvalley group of minor moraines; C) The upvalley group of minor moraines. Imagery from 2007 (Geoimage Austria and Google Earth, 2014).

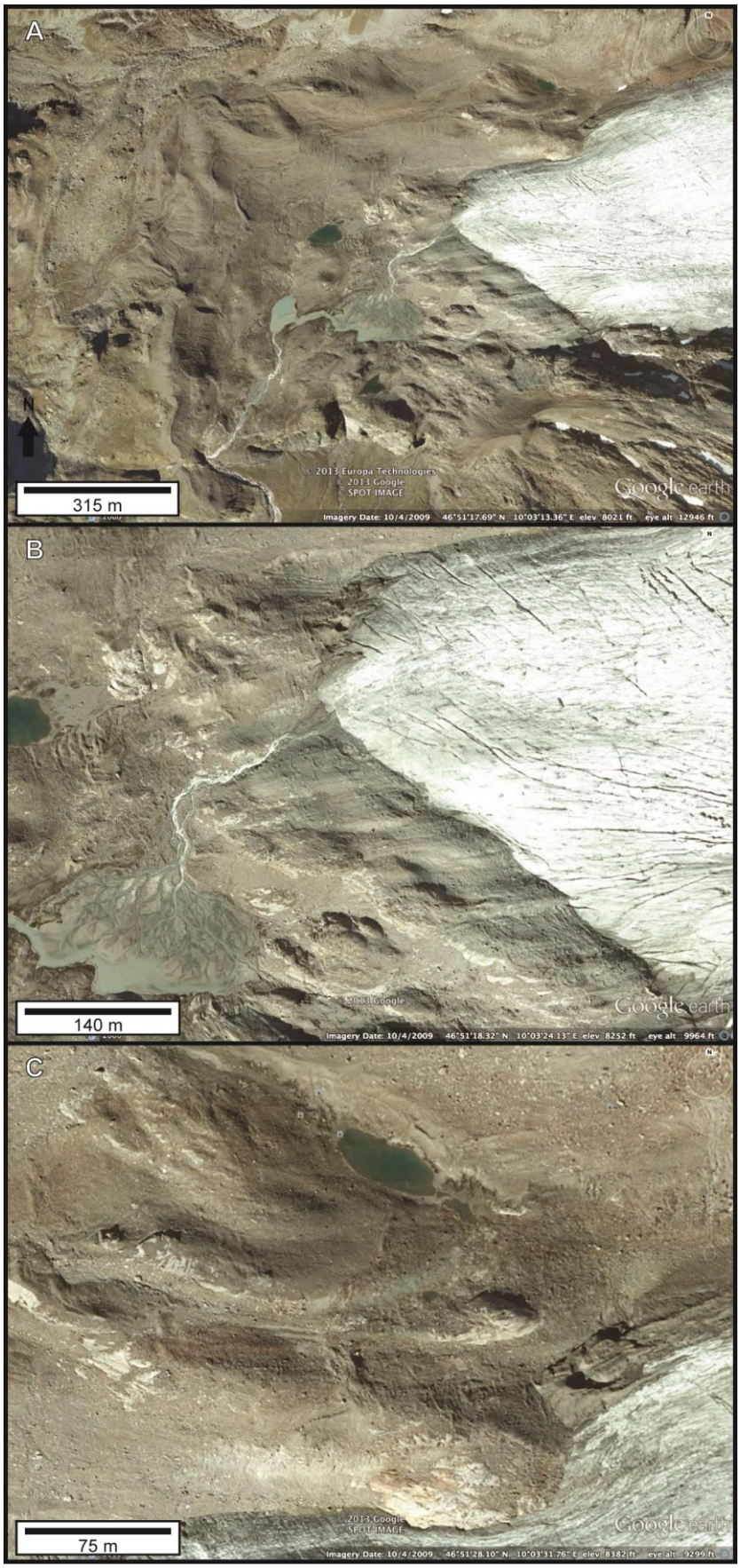

Figure 2.5. The Silvrettagletscher foreland, Switzerland, and minor moraines as seen in Google Earth. A) Silvrettagletscher and foreland; B) Modern minor moraines at the southern (lower) ice front; C) Modern minor moraines at the northern (upper) ice front. Imagery from 2009 (Europa Technologies et al., 2013).

Geomorphological mapping in the Silvrettagletscher foreland has combined field observations with remotely-sensed data provided by the Glaciology section of ETH Zürich. No historical data are available. The new geomorphological map of the Gornergletscher foreland uses newly available remotely-sensed data provided by the Glaciology section of ETH Zürich since the published map by Lukas (2012), which was originally created by combining field observations in 2007 and remotely-sensed data up to 2007.

2.2.1 Field mapping

Field maps were drawn on top of Google Earth imagery, which provided the highest resolution base layer available at the time of fieldwork. This mapping focused on minor moraines, but also included fluvial channels and terraces, exposed bedrock, flutings, prominent boulders, foreland sediment cover, medial and controlled moraines, and the position of the ice front. A handheld GPS (Garmin eTrex 10) was used to record moraine locations where the moraines were recognizable in the field but not on imagery, although the +/- 3 m accuracy may not be of sufficient resolution for these small landforms.

Detailed geomorphological measurements were taken in the field for moraines that were excavated for sedimentological analysis. Individual moraines were measured using a tape measure on the length of the entire moraine and width in representative locations (defined by visual assessment), as well as measurements of exposures through moraines. A clinometer (Silva Expedition 15TDCL) with an assumed accuracy of +/- 5° was used to measure slope angles at representative locations (defined by visual assessment) and on slopes delineating exposures, a technique commonly used to measure moraine slopes (Hubbard and Glasser, 2005). The low accuracy may not be of high enough resolution to discuss relative slope angles. A compass (Silva Expedition 15TDCL) was used to measure the orientation of minor moraines as a whole or in segments if orientation markedly changed.

Field mapping in the Schwarzensteinkees foreland occurred during July 2014, 2015, and 2016. The foreland was entirely snow-free during these periods. Field mapping in the Silvrettagletscher foreland occurred during June and September 2015. Much of the foreland was covered in snow in June. Therefore, only large ridges and the approximate ice front could be mapped. The foreland was snow-free by September allowing for detailed field mapping to take place, with the exception of several days of snowfall.

2.2.2 Remotely-sensed data

Remotely-sensed data commonly used in geomorphological mapping include aerial photographs, satellite imagery, and DEMs. These types of data can be used individually or together to enhance digital mapping. When using such data, it is important to consider the scale of mapping and which types of data are most useful for the intended map. For example, satellite imagery is typically more useful in mapping larger-scale features in large field areas, whereas aerial imagery may be more useful in distinguishing smaller-scale landforms (Hubbard and Glasser, 2005).

Aerial imagery of the Schwarzensteinkees foreland from 2007 was extracted from Google Earth (Google Earth and Geoimage Austria, 2007), as this imagery was clearer than that available from 2000, 2012, and 2015. Google Earth shows an imagery date of 1 January 2007, which is deemed inaccurate due to the foreland and surrounding slopes being dominantly snow-free, which would be highly unusual for this area known for winter ski touring. However, these moraines are historical and the position of the ice front is not being assessed, so the timestamp of the imagery is not critical. A 1 m DEM from 2007 is also available (Amt der Tiroler Landesregierung, 2007). A combination of the aerial imagery and DEM were used as modern data to map geomorphological features.

Aerial imagery of the Silvrettagletscher foreland is available from the Glaciology section of ETH Zürich for snow-free periods for 2003 at an unknown resolution, 2010 at an unknown resolution, and 2012 and 2013 at 25 cm resolution. Google Earth imagery was also used (Geoimage Austria and Google Earth, 2000; Google Earth, 2009), however the years stated on this imagery could not be verified against the known ages of the aforementioned imagery and were therefore deemed unreliable. Google has not yet responded to a request for review of these timestamps. These images were therefore used without firm chronological implications, and were instead compared to images of known age to place in relative chronological order.

Aerial imagery of the Gornergletscher foreland is available from the Glaciology section of ETH Zürich for snow-free periods for 2012, 2013, and 2014 at 25 cm resolution, which is the same source used by Lukas (2012).

2.2.3 Historical documents

Historical documents, which include pictorial records and written work, can assist in reconstructing glacier extent (Hubbard and Glasser, 2005). Using historical documents in assessing geomorphological evolution inherently involves exerting caution, as any depictions may include objectivity of the artist or author. The reliability of these sources is discussed when they are used in analyses in this thesis.

Geomorphological mapping in the Schwarzensteinkees foreland benefits from a wealth of historical imagery, including topographic maps, photographs, sketches, and paintings available from the early 19th century forward. Historic topographic maps extending back to 1807/08 (Timár et al., 2006) show approximate ice front locations and landforms in the foreland. Some maps of high enough resolution provide important information about the evolution of the Schwarzensteinkees foreland, and are presented in Chapter 4 in more detail. Additionally, several paintings, photographs, and sketches depict the glacier and its foreland and provide some clues to the evolution of the valley, as presented in Chapter 4.

2.3 Sedimentological composition of minor moraines

Sedimentological fieldwork includes field-scale observations and measurements to interpret sediment transportational and depositional processes. Sedimentological investigation followed similar techniques to previous studies on minor moraines that have provided substantial detail about the internal composition and architecture of these landforms (Krüger, 1995; Lukas, 2012; Schomacker et al., 2012; Reinardy et al., 2013; Chandler et al., 2016a). This approach follows from research in other glacial environments that has highlighted that the most accurate interpretations of sediment transport and deposition arise from the multiple scales of observation across an individual landform and collective landsystems (e.g. Lawson, 1979; Benn, 1992; Benn and Ballantyne, 1993; Benn and Ballantyne, 1994; Menzies, 2002; Spedding and Evans, 2002; Evans and Benn, 2004; Lukas, 2005; Lukas, 2007; Owen et al., 2009; Shulmeister et al., 2009; Lukas, 2012; Reinardy et al., 2013; Chandler et al., 2016a).

Five exposures through minor moraines in the Schwarzensteinkees foreland were obtained by manually excavating sections perpendicular to the ridge crests, where possible, to maintain consistency with inferred ice flow direction. The minor moraines described were chosen for thorough analysis because the sediment of each was partially exposed prior to further excavation. All but one of the exposures were cut perpendicular to the trend of the moraine ridge crest, due to faces already partially excavated by the channel. Seven exposures through moraines in the Silvrettagletscher foreland were manually excavated perpendicular to the ridge crests. The minor moraines described were chosen for thorough analysis following preliminary assessment of test pits. The Gornergletscher foreland was not visited during the course of this research, and therefore no new sedimentological data following the research conducted by Lukas (2012) are presented.

Sedimentological observations and measurements record sedimentary and deformation structures and sedimentary bed and facies architecture (e.g. deposit type,

thickness, geometry, contacts, and deformation structures). Sediments were analysed using a lithofacies approach and recorded using lithofacies codes for clear representation and to aid interpretations of depositional processes and landform formation (Evans and Benn, 2004) (Figure 2.6). Individual facies were grouped into facies associations, where applicable, to help interpret transport and deposition processes.

These sedimentological observations and measurements were recorded on exposure logs. Sections were logged on grid-paper with the assistance of fixed tape measures along the height and length of the exposures. Individual sections were then digitally overlain on photographs of the respective exposures to maintain the most accurate digital representation when producing the final two-dimensional exposure logs.

2.3.1 Clast morphology

Detailed analysis of clasts contained within landforms can elucidate information about provenance, flow regimes of glacial and fluvial systems, and mechanisms of erosion, transport, and deposition (Lukas et al., 2013). This approach necessitates the collection of control samples collected from locations where the processes of erosion, transport, and deposition can be unequivocally constrained (Lukas et al., 2013).

Fifty clasts were randomly selected at each sample location. Clast size was restricted to a-axes of 2.5-25 cm long (Lukas et al., 2013), as clast size may influence shape (Benn and Ballantyne, 1994; Benn, 2004). Lithology may exert controls on clast shape (Benn and Ballantyne, 1994; Benn, 2004; Lukas et al., 2013). Therefore, only granite clasts were measured in the Schwarzensteinkees foreland, and only meta-granite clasts were measured in the Silvrettagletscher foreland. These represent the dominant rock types found in the respective field areas. Measurements of clast morphology include relative roundness (well rounded, rounded, sub-rounded, sub-angular, angular, and very angular) (Benn and Ballantyne, 1994) and form (length of a-, b-, and c-axes). Roundness was determined visually, and the axis lengths were measured using a ruler.

Control samples were also collected from the dominant lithologies mentioned above. Control samples in the Schwarzensteinkees foreland include samples from two modern channel locations and two talus slope deposits originating from bedrock in the Schwarzensteinkees valley and two supraglacial and two subglacial samples from neighbouring Hornkees, as Schwarzensteinkees was inaccessible and the same lithology is present in both catchments (Chapter 4). Two alluvial fans in the Schwarzensteinkees foreland were also sampled to assess if there were similarities between these clasts and those in the moraines, and are included as “control samples,” as these may be potential clast sources for moraines lower in the foreland.

Facies Code	Description
Diamictons	*Very poorly sorted mixture of wide grain-size range*
Dmm	Matrix-supported, massive
Dcl	Matrix-supported, laminated
Dcm	Clast-supported, massive
Boulders	*Particles >256 mm (b-axis)*
Bms	Matrix-supported, massive
Bcm	Clast-supported, massive
Gravels	*Particles of 8-256 mm*
Gms	Matrix-supported, massive
Gm	Clast-supported, massive
Gh	Horizontally bedded
Gp	Planar cross-bedded
Gfu	Upward-fining (normal grading)
Gcu	Upward-coarsening (reverse grading)
Go	Openwork gravels
Granules	*Particles of 2-8 mm*
GRm	Massive
Gh	Horizontally bedded
GRo	Openwork structure
Sands	*Particles of 0.063-2 mm*
Sh	Very fine to very coarse and horizontally/planar bedded or low angle cross-lamination
Sl	Horizontal and draped lamination
Sm	Massive
Sd	Deformed bedding
Sc	Steeply dipping planar cross-bedding
Silts & Clays	*Particles of <0.063 mm*
Fm	Massive
Fl	Fine laminations
Fd	Deformed

Symbology	Description		
	Boulder	**Sm**	Facies code
	Weathered bedrock	A	Photo
	Diamicton	C1	Clast measurements
	Sand		Fault
	Gravel		Bedding or laminations

Figure 2.6. Facies codes and symbols used in this research. Facies codes used in text and on exposure logs adapted from Evans and Benn (2004). Symbols are used on exposure logs. Colours consistent between exposure logs and conceptual diagrams of moraine formation.

Control samples in the Silvrettagletscher foreland include two modern channel samples, three subglacial samples, and two supraglacial samples. Two sample locations each from medial moraine and englacial debris septa debris cone locations were also

measured and are included as "control samples," as these are potential clast sources for moraines in this study area (Chapter 5). Englacial and subglacial fluvial clasts could not be safely sampled.

Clasts measurements are displayed on ternary diagrams with end member shapes of blocky (a ≈ b ≈ c), platy (a ≈ b > c), and elongated (a > b ≈ c) clasts (Benn and Ballantyne, 1994; Benn, 2004; Lukas et al., 2013). The diagrams follow the basic principles of Sneed and Folk (1958) through a version by Lukas et al. (2013) modified from Graham and Midgley (2000). The C_{40} index, included on these diagrams, records clasts with c:a axis ratios ≤0.4 to assist in distinguishing between actively- and passively-transported glacial sediment (Ballantyne, 1982; Evans and Benn, 2004). Clast roundness is also useful to distinguish between sediment transport regimes (Evans and Benn, 2004). For these purposes, histograms depicting clast roundness were created. Additionally, the RA index (percentage of angular and very angular clasts) (Benn and Ballantyne, 1994; Lukas et al., 2013) and the RWR index (percentage of rounded and well-rounded clasts) (Benn, 2004; Lukas et al., 2013) were calculated and are displayed on covariance plots with the C_{40} index. Both RA and RWR indices are presented, as Lukas et al. (2013) show that the RA index is most useful in discriminating between subglacially- and supraglacially-transported clasts, whereas the RWR index is best for discriminating between subglacially- and fluvially-transported clasts, depending on the amount of fluvial reworking.

2.3.2 Ground-penetrating radar

Ground-penetrating radar (GPR) can be used as a non-invasive way to assess subsurface stratigraphic architecture and can therefore help reconstruct depositional environments in a variety of settings (Neal, 2004). GPR uses electromagnetic energy to probe the shallow subsurface and record electrical discontinuities by generating and transmitting an electromagnetic pulse through the ground, from a transmitter antenna, and then recording the reflection from layer boundaries and other inhomogeneities as a two-way travel time, with a receiver antenna (Neal, 2004; Annan, 2009). Water and clay content primarily control dielectric permittivity of sedimentary layers and as such also the reflectivity measured with GPR, allowing for detection of various grain size and texture differences of layers. The use of GPR to investigate glacial sediments in high-mountain settings in the Alps is sparse. This method therefore builds on the techniques for investigating moraine composition with GPR developed by Lukas and Sass (2011), which investigated lateral moraines at Gornergletscher.

GPR was used in the Schwarzensteinkees foreland to assess the subsurface stratigraphy along one transect through a flat area (Chapter 4) to elucidate processes and hypotheses of how this unusual area formed. Logistical complications of transporting field

equipment and consideration for landscape aesthetics in a moderately-trafficked hiking and mountaineering setting did not allow coring or large-scale excavation. Therefore, GPR was chosen as a non-invasive method of assessing the sediment underlying this surface. The transect was chosen to capture the maximum longitudinal extent of this flat area.

The Sensors & Software pulseEKKO PRO system was used for the measurements. Three different transmission frequencies were used: 50 MhZ, 100 MhZ, and 200 MhZ. Data were collected using the common offset method as a copolarised, perpendicular broadside survey (Neal, 2004), in which the transmitter and receiver are moved the same distance between collection points. For the 50 MhZ frequency, the transmitter and receiver were separated by 2 m, and a 12.5 cm step size between data collection points was used. For the 100 MhZ frequency, the transmitter and receiver were separated by 1 m, and a 25 cm step size between data collection points was used. For the 200 MhZ frequency, the transmitter and receiver were separated by 50 cm, and a 50 cm step size between data collection points was used. A handheld GPS (Garmin eTrex 10) was used to record elevation measurements along the transect.

A conversion must be applied to convert two-way travel time, measured from the method above, to depth. The common midpoint (CMP) technique, in which the transmitter and receiver are moved apart in fixed horizontal increments from a common midpoint, was used to measure the propagation velocity of radar waves (Annan and Davis, 1976; Neal, 2004), which could then be used for conversion of two-way travel time to depth specifically pertaining to the sediment investigated. This was performed for each frequency with a start spacing of 50 cm and a step spacing of 25 cm. The wide-angle reflection and refraction (WARR) technique was also used, in which one antenna is fixed and the other is moved away (Annan and Davis, 1976; Davis and Annan, 1989). This was performed for each frequency with a start spacing of 25 cm and a step spacing of 25 cm.

GPR data were processed by Kathryn Adamson at Manchester Metropolitan University to produce two-dimensional radar reflection profiles. WARR measurements provided more reliable data for time-to-depth conversions and were used for hyperbola velocity calibration functions, which resulted in velocity measurements of 0.059 m/ns for 50 MhZ frequency measurements, 0.057 m/ns for 100 MhZ frequency measurements, and 0.058 m/ns for 200 MhZ frequency measurements. All data were dewowed to remove low frequency signals that obscured main signals in the data (Annan, 2009; Sandmeier, 2010). Topographic correction was applied for prominent boundary locations along the transect. These elevation measurements may not be accurate however, given low vertical accuracy of the GPS unit (+/- 3 m). The final images presented were created with spreading and exponential compensation correction (SEC2), as this yielded clearer results than when automatic gain correction (ACG) was applied (Cassidy, 2009). Background subtraction

(filter width = 741 m) was applied to 200 MhZ data. The three radar reflection profiles (50, 100, and 200 MhZ) are shown, followed by a combined interpretation.

2.4 Moraine spacing, front variation, and climatological measurement comparisons

The geomorphological record of minor moraines in the Schwarzensteinkees and Silvrettagletscher forelands is compared to front variation measurements collected by the WGMS (Zemp et al., 2012; Zemp et al., 2013). Front variation measurement data were overlain on the geomorphological map of minor moraines using chronological constraint as starting points. In the Schwarzensteinkees foreland, chronological constraint on latero-frontal moraines from previous work (see Chapter 4) and interpreted connections between moraine ridge fragments were used to pin front variation measurement transects at 1913 and 1926.

In the Silvrettaglescher foreland, the 1959 and 1981 ice positions marked along an education path, the Gletscherlehrpfad (Silvrettahütte, 2016), were extrapolated to transects of moraines, and ice front variation transects were pinned at these locations. A second transect for 1986-1992 was placed over a nearby transect of moraines for comparison. Two younger (1993-2009) transects were overlain on the geomorphological map using the first moraine in front of the 2009 ice front, as see in aerial imagery, as a pinning point, under the assumption that this moraine formed in 2009. The transect locations were chosen due to the prolific number of moraines present when compared to other locations in the foreland and their positions in front of areas of clean ice, to lessen the effects of sediment cover at the ice front. This was only possible with extant aerial imagery for the younger transect, and may not stand true for the older transect. In both locations of the younger transects, additional transects were created again using the first moraine in front of the 2009 ice position as a starting point, then counting back under the assumption of annual formation, with each moraine representing one year.

The geomorphological record of minor moraines in the Silvrettagletscher foreland, front variation and mass balance measurements of Silvrettagletscher, and climate data are compared to assess any potential influences of temperature and precipitation on moraine formation, following the approaches outlined by Lukas (2012) and Chandler et al. (2016a) that suggest the spacing of moraines may be used as a proxy for ice margin retreat rates. This analysis was not possible for the Schwarzensteinkees study area, because no local monitoring stations record both temperature and precipitation during the applicable time period. Comparisons to climate data include average annual temperature, ablation season temperature, accumulation season temperature, average annual precipitation, ablation season precipitation, and accumulation season precipitation. Ablation season is defined as

May-September, whereas accumulation season is defined as October-April. Correlation was assessed both visually (as graphs) and statistically (through the calculation of R^2 and p-values). Climate data were obtained from the Weissfluhjoch monitoring station (46°50'/9°48', 2,691 m) (MeteoSwiss, 2015b), the nearest station to Silvrettagletscher that records both monthly temperature and precipitation and is similar in elevation (20 km away, 2,691 m elevation), and the Davos monitoring station (46°49'/9°51', 1,594 m; 18 km away) (MeteoSwiss, 2015a), for comparison to previous work (Huss and Bauder, 2009). In addition to a comparison of moraine spacing, annual average, ablation-season average, and accumulation-season average temperature and precipitation were compared to front variation measurements available from 1960 to 2010 (Zemp et al., 2012; Zemp et al., 2013) and mass balance measurements available from 1918 (Huss et al., 2015) or 1960 to 2010 (Zemp et al., 2012; Zemp et al., 2013).

CHAPTER 3. Study areas

"Women could read about glaciers in the Alps, but they were not fit for glaciological research, field science, or even alpine tourism."
(Carey et al., 2016)

The European Alps represent one of the world's most well-known mountain ranges. They span approximately 800 km from east to west and approximately 200 km from north to south, passing through eight European countries in an arc shape (Figure 3.1). This mountain range is the result of Late Cretaceous and Tertiary collision between the Adriatic Plate (part of the African Plate) and European Plate, which created the complex structural and lithological patterns of continental and oceanic crust seen today. Resulting peaks commonly reach over 4,000 m (with Mont Blanc as the highest, 4,810 m), and the western Alps generally contain the highest peaks (Pfiffner, 2014).

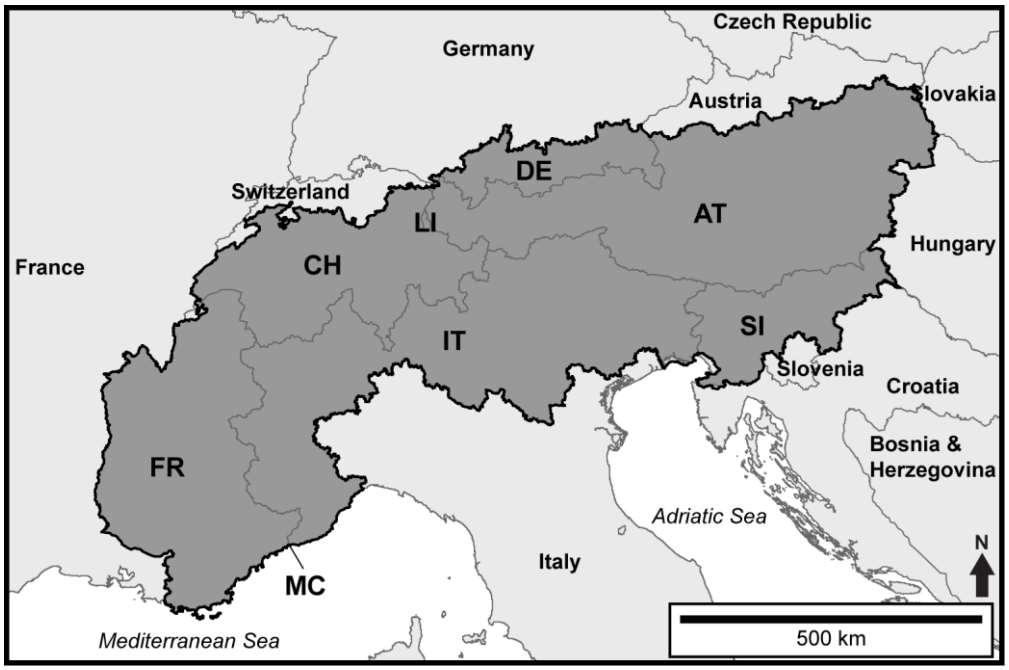

Figure 3.1. Overview map of the European Alps. Darker grey area shows extent of the European Alps. Country borders in light grey. Lighter grey area distinguishes countries from seas (white). Countries labelled outside of the Alps with full names and inside the Alps with country codes. Countries shapefile from Esri and DeLorme Publishing Company Inc. (n.d.). Alps shapefile from European Soil Data Centre (ESDAC, 2005).

The Quaternary history of the Alps was dominated by repeated glaciations that created the spectacular glacial legacy characteristically associated with this mountain range. Glaciers covered approximately 126,000 km^2 of the Alps during the last glacial maximum (Late Würmian, 30-18 ka), a period marked by temperatures approximately 15°C lower than present day and 70-80% less precipitation throughout the region (Haeberli and

Penz, 1985; Ivy-Ochs et al., 2008; Ivy-Ochs et al., 2009). This was followed by rapid glacial retreat until a readvance at 17 ka with moraine stabilisation by 15.4 ka (Gschnitz stadial) and two readvances (Clavadel/Senders and Daun stadials, >14.6 ka) until the Younger Dryas readvance (Egesen stadial, 12.9-11.7 ka) (Ivy-Ochs et al., 2008; Ivy-Ochs et al., 2009; Schindelwig et al., 2012; Heiri et al., 2014; Moran et al., 2016).

The Holocene record shows a prominent glacier advance at 10.8 ka (Kromer/Kartell stadial) (Ivy-Ochs et al., 2008), and that glaciers were smaller than modern for most of 10.5-3.3 ka, with minor advances occurring locally and more prolifically with smaller glaciers 9.6-9.3 ka, 8.85 ka and 8.40 ka, 6.3-5.0 ka, and 3.8-3.4 ka (Hormes et al., 2001; Joerin et al., 2006; Kerschner and Ivy-Ochs, 2008; Nicolussi and Schlüchter, 2012). Several other advances (3.0-2.3 ka, 500-600 AD, 800-900 AD, 1100-1200 AD) occurred before the prominent Little Ice Age (LIA) advances in the 14th, 17th, and 19th centuries in Switzerland and mid-15th and 17th centuries in Austria (Ivy-Ochs et al., 2009). The LIA in the Alps, with an end around 1850, was followed by an overall period of retreat punctuated by prominent advances in the 1890s, 1920s, and 1970s-80s, which all remained upvalley of LIA extents (Zemp et al., 2006).

Precipitation in the Alps varies regionally and distinguishes the northern and southern Alps from other zones. Westerlies from the North Atlantic Ocean deliver precipitation to the northern and western Alps, whereas lee-side cyclogenesis in the Gulf of Genoa controls precipitation delivery to the southern and eastern Alps (Ivy-Ochs et al., 2008). Due to orographic effects on precipitation, the inner Alps are drier than the northern and southern Alps, which experience similar annual precipitation (Fliri, 1974; Frei and Schär, 1998).

Based on a thorough review of potential study areas presented in Chapter 2, the following three study areas have been selected. These study sites also show a transect from east to west. Glacier length ranges from 2.5-14.1 km, area ranges from 2.7-38.2 km^2, annual average temperature at the nearest monitored weather station ranges from -1.6-7.7°C, and average annual precipitation ranges from 635-1,380 mm. These differences allow for assessing variations in minor moraine formation across the Alps.

3.1 Schwarzensteinkees, Austria

Schwarzensteinkees is one of three glaciers in the upper Zemmgrund (valley) in the central Zillertal Alps region of Austria (Figure 3.2A). Schwarzensteinkees (47°00'36.65"N, 11°51'1.87"E) is 2.5 km long (1999) with an area of 4.5 km^2 (1999) (WGMS, 2015) and has an approximately northwestern aspect. The highest peak of the watershed is Schwarzenstein (3,370 m), which straddles the border between Austria and Italy.

Schwarzensteinkees is located in an area underlain by metagranodiorite-metatonalite bedrock (Geologische Bundesanstalt, 2005), and the foreland subsurface additionally comprises metagranite, granitic gneiss, and migmatitic gneiss (Moser and Pavlik, 2005). The Zemmbach (river) flows northwest out of the valley, and then continues to flow northeast before joining the Ziller (river).

The 1971-2000 average annual temperature in Mayrhofen, the closest monitored weather station to Schwarzensteinkees (14 km, 643 m elevation), was 7.7°C (ZAMG, n.d.), with July as the warmest month and January the coldest overall. The 1971-2001 average annual precipitation in Mayrhofen was 1,043.7 mm (ZAMG, n.d.), with July as the wettest month and January the driest. These climate patterns are supported by additional weather stations near Schwarzensteinkees recording temperature and precipitation data since 1958, showing June-August as the wettest and warmest period and December-February as the driest and coldest period (Auer et al., 2007).

Previous work in the upper Zemmgrund has focused on establishing ice positions through time and dating glacial geomorphological features, primarily in the Hornkees and Waxeggkees forelands (Wintges, 1985; Pindur and Heuberger, 2008; Mahaney et al., 2011), with the first description of glacial landforms of these three forelands in 1929 (Kinzl, 1929). Pindur and Heuberger (2010) provide the most comprehensive compilation of glacially related data published about the upper Zemmgrund field area and create a glacial history for the three main upper Zemmgrund glaciers.

The Schwarzensteinkees foreland contains various glacial landforms, including larger moraines that pre- and post-date the LIA (Pindur and Heuberger, 2008; Mahaney et al., 2011), prominent lateral moraines, flutings, a potential drumlin, and two groups of closely spaced minor moraines (Figure 2.4). These moraines were first mentioned by Pindur and Heuberger (2008) as “winter moraines” or “retreat moraines” that were deposited after 1850, around 1890, and around 1920; the authors do not, however, explore this terminology further. These small, closely spaced moraines form the basis of this research. The observations and data from these previous studies are assessed and incorporated into this study in Chapter 4.

Despite previous work establishing chronological constraint of the glacial history of this valley, albeit modest, nothing has been reported about landform structure and composition. Chapter 4 explores the glacial history and evolution of the valley since approximately 1800 while focusing primarily on the presence of these two groups of closely spaced minor moraines and the mechanisms of minor moraine formation in the foreland.

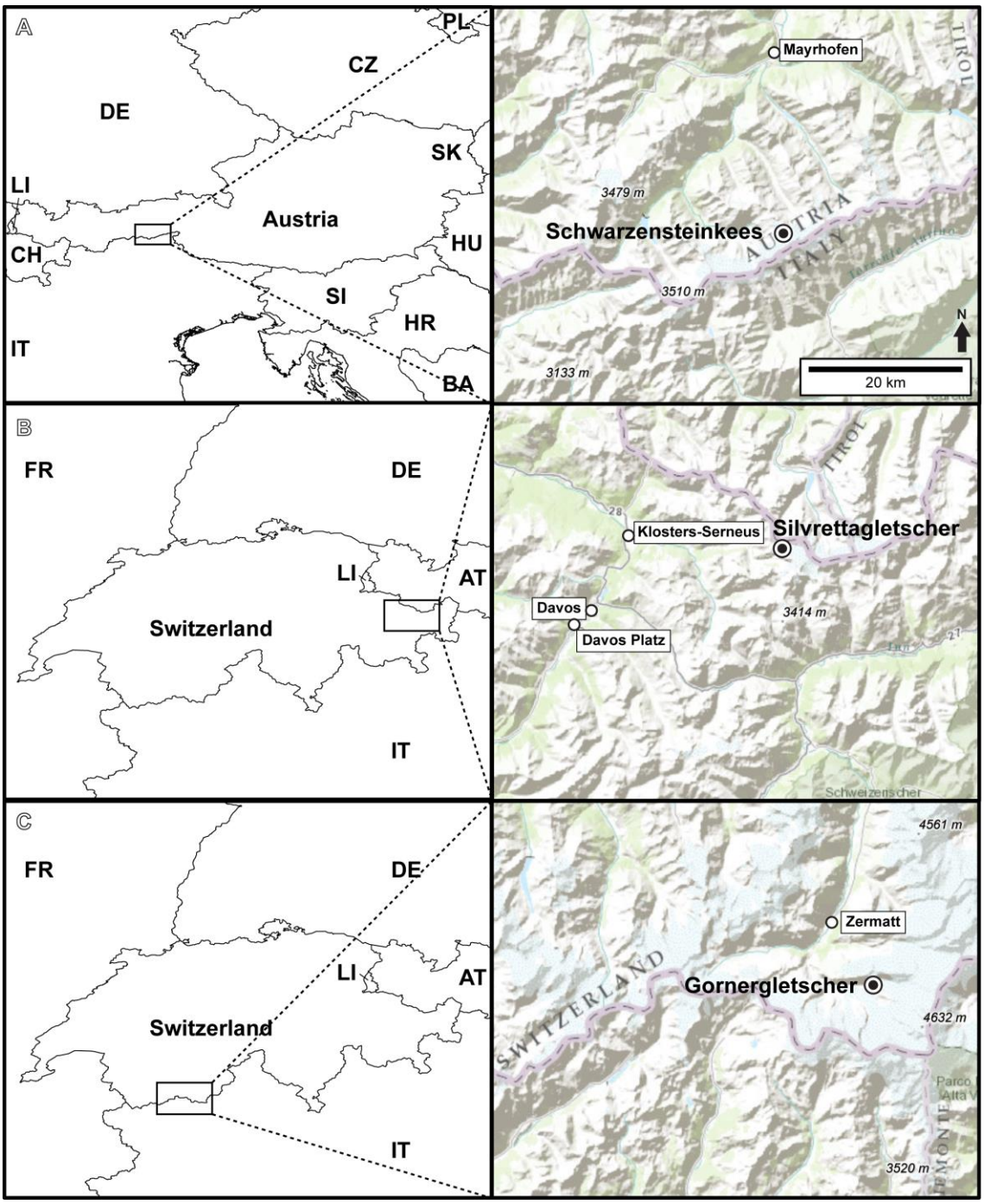

Figure 3.2. Locations of the three study areas, showing location in country on the left and more specific location on the right. A) Schwarzensteinkees, Austria, near the border between Austria and Italy; B) Silvrettagletscher, Switzerland, near the border between Switzerland and Austria; C) Gornergletscher, Switzerland, near the border between Switzerland and Italy. Nearest towns and cities labelled. Countries shapefile (left) for all from Esri and DeLorme Publishing Company Inc. (n.d.). Topographic base map (right) for all from Esri et al. (2015).

Table 3.1. Measurements for studied glaciers. Length and area from WGMS (2015) and elevation range from Google Earth (Digital Globe, 2016).

Glacier	Aspect	Length (km)	Area (km^2)	Elevation range (m)
Schwarzensteinkees	NW	2.5 (1999)	4.5 (1999)	2,530-3,100 (2015)
Silvrettagletscher	W	3.5 (1975)	2.7 (2013)	2,530-3,080 (2015)
Gornergletscher	NW	14.1 (2012)	38.2 (2013)	2,345-4,340 (2013)

3.2 Silvrettagletscher, Switzerland

Silvrettagletscher is one of three glaciers in the upper Verstanclabach valley in the Silvretta Alps region of Switzerland (Central Eastern Alps) (Figure 3.2B). Silvrettagletscher (46°51'20.78"N, 10°3'53.12"E) is 3.5 km long (1975) with an area of 2.7 km^2 (2013) (WGMS, 2015) and has an approximately western aspect. The highest peak of the watershed is Silvrettahorn (3,244 m). Silvrettagletscher and its foreland sediments currently overlie Paleozoic metagranodiorite, metagabbro, metabasalt, meta-ultrabasite, and some gneiss and mica schist (Swisstopo, 2005). Glacial meltwater and runoff feed the Verstanclabach (river), which flows west until joining with the Vereinbach (river) to create the Landquart (river) near the town of Klosters-Serneus.

Weissfluhjoch (2,691 m) hosts the closest monitored weather station to Silvrettagletscher (20 km) that records both temperature and precipitation at a similar elevation (2,691 m) to Silvrettagletscher. The average annual temperature for 2000-2014 was -1.6°C, with August as the warmest month and February as the coldest, generally (MeteoSwiss, 2015b). The average annual precipitation was 1,380.4 mm, with August as the wettest month and March and December the driest, generally (MeteoSwiss, 2015b).

A mass-balance monitoring program has been providing publically available data from Silvrettagletscher since 1959 as part of the Swiss Glacier Monitoring Network, the World Glacier Monitoring Service, and the Laboratory of Hydraulics, Hydrology, and Glaciology of ETH Zurich. Previous research regarding Silvrettagletscher has included developing mass-balance models (Huss and Bauder, 2009; Huss, 2013) and connecting mass-balance changes to climate (Farinotti et al., 2009; Huss et al., 2010).

Despite extensive research in this valley regarding mass balance changes of Silvrettagletscher, all published data remains glaciological, i.e. pertaining to the ice itself. No studies have examined glacial landforms in the foreland. The Silvrettagletscher foreland contains various glacial landforms, including prominent and more subdued moraines and

flutings, as well as bedrock striae. Several clusters of numerous, closely spaced minor moraines in the foreland form the focus of this research (Figure 2.5). Chapter 5 explores the mechanisms of minor moraine formation in the foreland of Silvrettalgetscher, Switzerland, through geomorphological and sedimentological analyses.

3.3 Gornergletscher, Switzerland

Gornergletscher (45°58'1.28"N, 7°47'49.43"E) is the second largest glacial system in the European Alps and is 14.1 km long (2012) with an area of 38.2 km^2 (2013) (WGMS, 2015), with an approximately northwestern aspect. The highest peak of the watershed is Dufourspitze (4,634 m). Gornergletscher is the largest glacier that feeds the Gornera (river) in the Pennine Alps region of Switzerland (Western Alps) (Figure 3.2C). Gornergletscher and its foreland sediments currently overlie Palaeozoic metaperidotite, metagabbro, gneiss and mica schist, and meta-granite and Permian chalk (Bearth, 1953; Ebert, 2001; Swisstopo, 2005).

Zermatt (1,608 m) has the closest monitored weather station to Gornergletscher (5 km) that records both temperature and precipitation. The average annual temperature for 1983-2015 was 4.4°C, with July as the warmest month and January as the coldest, generally (MeteoSwiss, 2015c). The average annual precipitation was 631.5 mm, with May as the wettest month and February and March the driest, generally (MeteoSwiss, 2015c).

The front variation of Gornergletscher has been measured since 1883 and the thickness change has been derived since 1931 as part of the Swiss Glacier Monitoring Network and the Laboratory of Hydraulics, Hydrology, and Glaciology of ETH Zurich. Previous research regarding Gornergletscher has included developing remote-sensing monitoring of glacier mass balance (Huss et al., 2013), the drainage of an ice-marginal lake (e.g. Bauder et al., 2007; Riesen et al., 2010; Sugiyama et al., 2008, 2007), and considerable research on glaciology and subglacial hydrology (e.g. Eisen et al., 2009; Walter et al., 2010, 2008). Previous geomorphological and sedimentological work at Gornergletscher has also assessed the formation of lateral moraines (Lukas and Sass, 2011) and annual moraines (Lukas, 2012).

The northernmost subsidiary snout of Gornergletscher had been forming moraines annually from 1977-2007 (Lukas, 2012). Chapter 6 builds on and updates the research presented by Lukas (2012) about annual moraines in the Gornergletscher foreland by assessing moraine formation and degradation in the foreland since 2007.

CHAPTER 4. Mechanisms of minor moraine formation in the Schwarzensteinkees foreland, Austria

4.1. Geomorphological features of the Schwarzensteinkees foreland and changes through time

The most prominent features of the Schwarzensteinkees foreland are two groups of minor moraines. The foreland contains nearly 190 moraine ridge fragments, not including the eight fragments distinguished as marking the Little Ice Age position (Figure 4.1). The length of these ridge fragments ranges from 9 m to 108 m, with an average of 29 m. The width ranges from 1 m to 14 m, with an average of 6.1 m. Distal moraine slopes are typically steeper than proximal slopes. The moraine hosting Exposure B (described below) has a bifurcating crestline.

The foreland is divided into seven zones, listed here from downvalley to upvalley: Minor Moraines 1 (MM1), Irregular Zone 1 (IZ1), Flat Zone 1 (FZ1), Long Sloping Zone (LSZ), Irregular Zone 2 (IZ2), Minor Moraines 2 (MM2), Flat Zone 2 (FZ2). It is important to recognize that the minor moraines may have been deposited as fragments. The evolution of these zones is assessed throughout time using historical topographic maps, photographs, and illustrations and modern observations during fieldwork and mapping.

4.1.1 1783-1820: Little Ice Age fluctuations

The maps from 1807/08 and 1817 show one or two ridges at the end of the Schwarzensteinkees valley (Figure 4.2). Pindur and Heuberger (2008) assign these moraines the vague ages of "2nd half of the 18th Century," based on extrapolating several sources of historical evidence and their own lichenometry measurements. No historical documents (maps, descriptions, illustrations etc.) of the upper Zemmgrund exist prior to 1783, providing the only lower age limit on the advances that deposited these moraines. Additionally, a report states primary source observations that Schwarzensteinkees grew significantly during five years, presumably immediately prior to 1820 (i.e. 1815-1820), and secondary source observations, by a hunter who frequented the area, state that the glacier advanced continuously, approximately 125 m total, for 30 years, presumably immediately prior to 1819 (i.e. 1789-1819) (Klettner, 1820 in Slupetzky and Slupetzky, 1995). These observations suggest that the glacier was advancing since at least 1790.

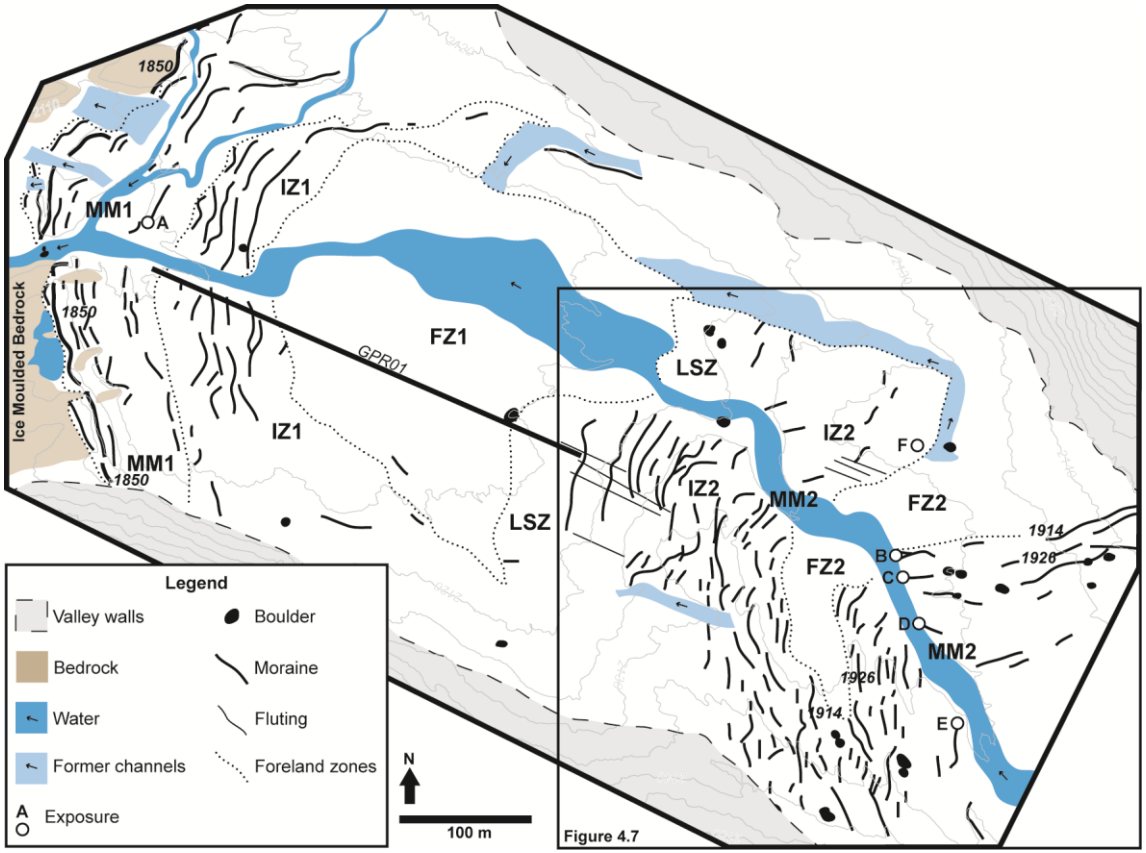

Figure 4.1. Geomorphological map of the Schwarzensteinkees foreland. This map focuses on the presence of different zones in the foreland and the location of minor moraines: "MM1" first group of minor moraines, "IZ1" first Irregular Zone, "FZ1" first Flat Zone, "LSZ" Long Sloping Zone, "IZ2" second Irregular Zone, "MM2" second group of minor moraines, "FZ2" Flat Zone 2. Dashed lines show approximate valley walls. Dotted lines delineate different zones discussed in the text and labeled on the map. The thicker moraine line shows the Little Ice Age (1850) ridge. Thinner lines indicate minor moraines. Moraines are labelled with approximate ages, as discussed in the text. Thick straight line indicates location of a GPR transect (GPR01).

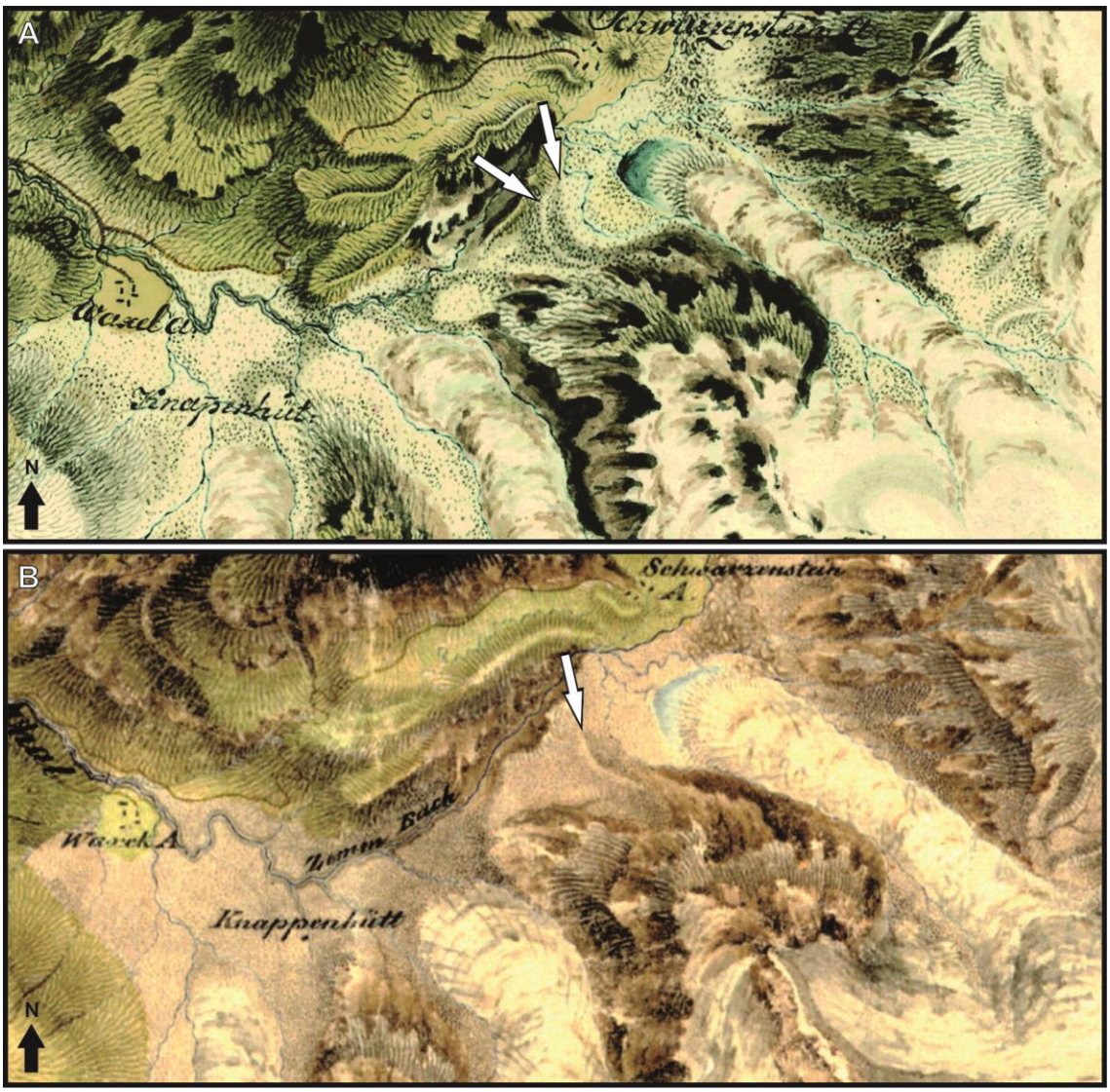

Figure 4.2. Historic topographic maps of the upper Zemmgrund, 1807/08 and 1817. A) Map from 1807/08 that shows two moraines at the end of the Schwarzensteinkees valley, as indicated by arrows, and a proglacial lake (Timár et al., 2006); B) Map from 1817 that shows one moraine at the bottom of the Schwarzensteinkees valley, as indicated by an arrow. The proglacial lake is smaller than in 1807/08, and the ice appears to extend farther downvalley (Martensteig, 1817).

These lowermost moraines illustrated on the historic maps, mapped by Pindur and Heuberger (2008), and mapped in this study (Figure 4.1) therefore were likely deposited prior to 1790 and with time to account for the glacier retreating upvalley and then advancing for at least 30 years until observation in 1819. Soil weathering profile analysis and lichenometry by Mahaney et al. (2011) support the vague age assignments of these moraines to the 18th Century. The 1807/08 and 1817 maps additionally both show an immediately proglacial lake in the Schwarzensteinkees foreland (Figure 4.2), however the exact location of the lake and the ice front is not discernible, as the maps do not have contour lines or other features that would allow unequivocal topographic links.

4.1.2 1820-1850: The final Little Ice Age advance

In addition to the continued advance of Schwarzensteinkees described by the hunter (see above), a journal entry and paintings provide clues to the extent of Schwarzensteinkees during the final Little Ice Age (LIA) advance. An unpublished journal entry found by Pindur and Heuberger (2008) describes that the Hornkees and Waxeggkees glaciers were joined in their forelands in 1840 (Kreidl, 1941), which suggests that the Schwarzensteinkees limit was quite far down valley as well. Two watercolour paintings from 1841 show the Schwarzensteinkees ice front (Figure 4.3) (Ender, 1841a; Ender, 1841b in Pindur and Heuberger, 2008). One of these paintings depicts what may be a small proglacial lake (Figure 4.3A), perhaps remnant from the more extensive lake in 1817 (Figure 4.2), whereas the second depicts the proglacial fluvial system and a potential moraine at the ice front (Figure 4.3B). These paintings show the ice front near what is mapped as the 1850 moraine (Figure 4.1), but do not contain any more specific clues to position, and also show the primary proglacial channel established in the same location as the modern channel.

Two geomorphological studies place an approximate 1850 age on the largest moraine in the valley, providing the most specific geochronological reference for the lower foreland as the terminal LIA advance (Pindur and Heuberger, 2008; Mahaney et al., 2011). Pindur and Heuberger (2008) describe this dominant moraine in the downvalley-most reach of the Schwarzensteinkees foreland and assign a "middle of the 19th century" age to this landform based on lichenometry, as they were unable to excavate the moraine for more detailed observation. Mahaney et al. (2011) also assign an 1850 age for this same moraine, based on weathering rind measurements and lichenometry. This moraine is therefore labelled in this study as the 1850 moraine (Figure 4.1).

4.1.3 1850-1940: Glacier retreat and minor moraines

A group of minor moraines exists immediately upvalley of the 1850 moraine (MM1). There are at least 11 of these small landforms on valley left, and at least six on valley right (Figure 4.1). Pindur and Heuberger (2008) briefly mention these landforms as "winter" or "retreat" moraine fragments that were deposited after 1850, but before 1890. These moraines, and some further upvalley, are the focus of this chapter.

The first map following the 1850 advance was drawn in 1872 and shows the ice front at 2,105 m elevation and the faint presence of what likely corresponds to the 1850 moraine at the bottom of the valley (Figure 4.4A). This elevation is deemed unreliable, however, as modern elevation measurements show the 1850 moraine near 2,115 m and no

elevation upvalley of this moraine less than 2,115 m. Regardless, the map does show ice retreat from the 1850 position.

Photographs from 1874-1883 (Figure 4.5A) and 1880-1889 (Figure 4.5B) do not resolve minor moraines but do show the ice front in FZ1 and/or LSZ. Both photographs confirm the presence of some of FZ1 (for the portion visible) and show a proglacial fluvial system smaller than the modern one. The photograph from 1874-1883 shows a moraine at the right edge of FZ1, approximately parallel to the valley axis (Figure 4.5A), which is noted on the geomorphological map (Figure 4.1) and on subsequent photographs.

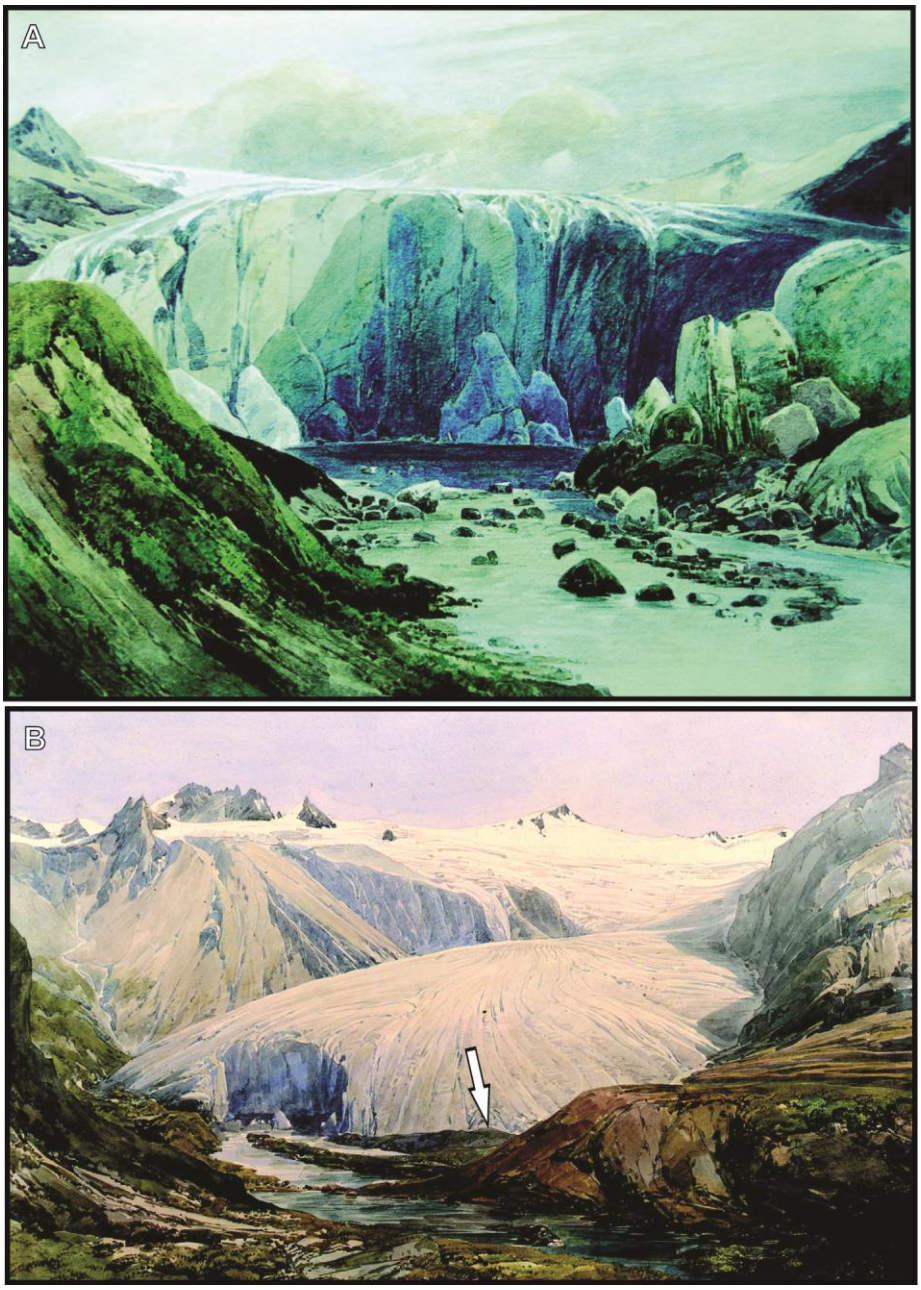

Figure 4.3. Watercolour paintings of the Schwarzensteinkees ice front, 1841. A) The ice front appears to extend to just upvalley of the ice moulded bedrock area (Figure 4.1) (Ender, 1841a). B) A view from slightly further away reveals a potential moraine, as marked by an arrow (Ender, 1841b).

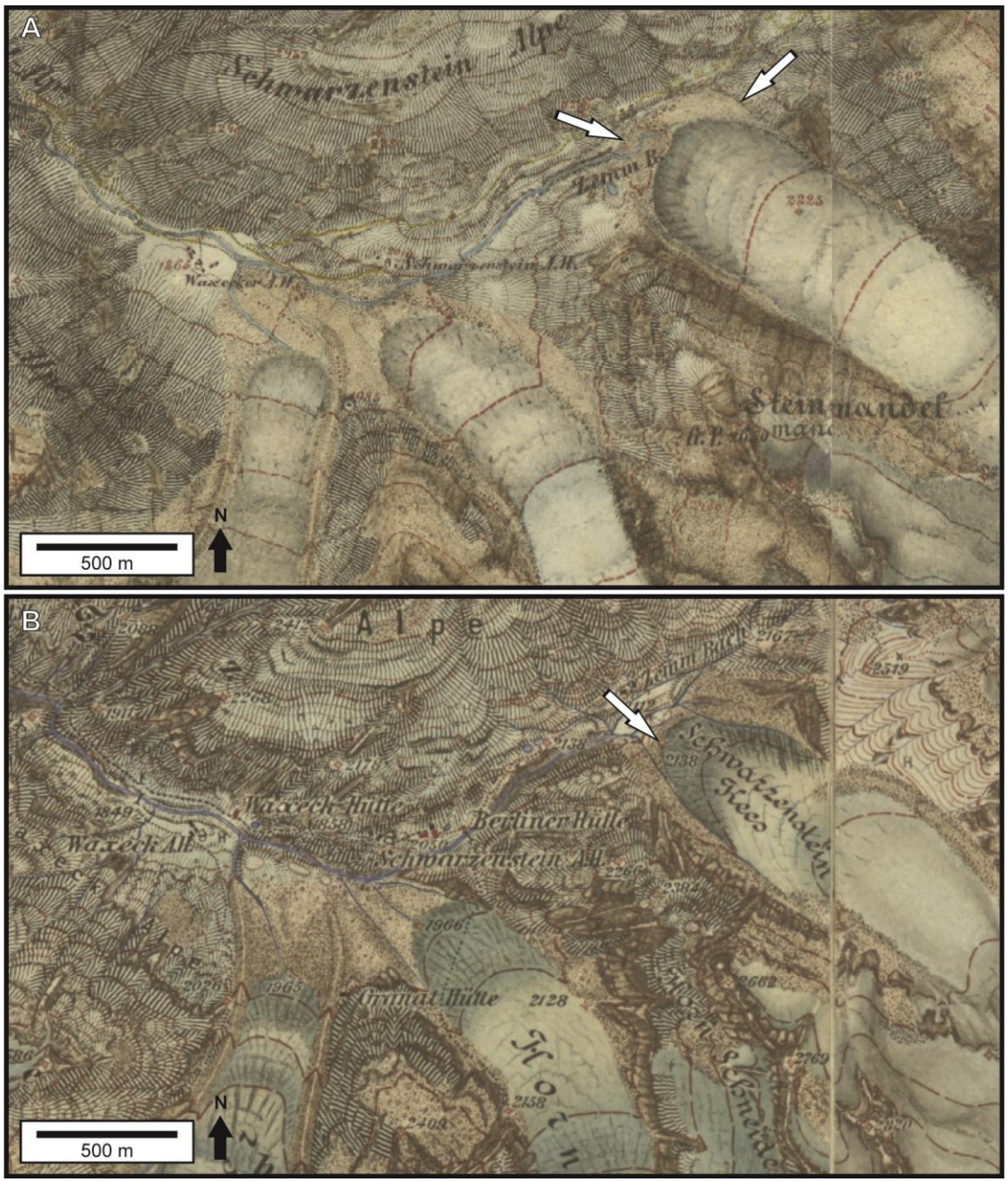

Figure 4.4. Historic topographic maps of the upper Zemmgrund, 1872 and 1888. A) Map from 1872 that shows the ice front at 2,150 m and the faint presence of what likely corresponds to the 1850 moraine at the end of the Schwarzensteinkees valley, indicated with arrows (Fromm and Wuczinicz, 1872; Wanick and Wuczinicz, 1872; Wuczinicz, 1872a; Wuczinicz, 1872b); B) Map from 1888 that shows the Schwarzensteinkees ice front at 2,138 m, at a marker indicated with the arrow.

The photograph from 1880-1889 additionally shows that the main channel had already cut through the 1850 moraine in the same location as the modern channel (Figure 4.5B).

The map drawn in 1888 shows the ice front at 2,138 m elevation (Figure 4.4B), which places it nearer to MM2 than MM1 (Figure 4.1) when compared to modern elevation measurements. This elevation is questionable, however, as the extent of the mapped glacier does not correspond to the location of MM2 viewed today.

Figure 4.5. Photographs of Schwarzensteinkees and its foreland, 1874-1883 and 1880-1889. A) Photograph from 1874-1883 that shows FZ1 and a latero-frontal, as indicated with an arrow (Johannes, 1874-1883); B) Photograph from 1880-1889 that notably shows FZ1 and that the channel cut through the 1850 moraine sometime before this photograph was taken. Dashed lines indicate lower extent of the FZ1 and the 1850 moraine. Arrow indicates direction of channel flow ("Blick auf den Schwarzenstein und den Schwarzensteinkees", 1880-1889).

Both this map and the map from 1872 (Figure 4.4A) are therefore not considered wholly accurate representations of ice terminus and elevation, which could be due to a combination

of resolution, map scale, and map style. Regardless, a comparison of the 1872 and 1888 maps shows relative retreat during this period (Figure 4.4).

Front variation measurements from 1882 onwards show Schwarzensteinkees retreating overall during this minor moraine period (1850-1930) (Figure 4.6; Table 4.1). These data support the assessment of historical maps and images, which depict retreat from the 1850 position.

A second group of minor moraines (MM2) exists further up the valley, nearly 500 m upvalley of MM1. There are at least 25 of these minor moraines on valley left and at least 10 on valley right. The moraines on valley left are split by a flat area (FZ2), whereas those on valley right begin just upvalley of the flat zone (Figure 4.1).

Pindur and Heuberger (2008) map these landforms on aerial imagery as "winter/retreat" moraine fragments related to two periods, around 1890 and around 1920. The authors base these chronologic assignments on lichenometry measurements of two larger latero-frontal moraines that they mapped and labelled as the 1914 and 1926 ice advances (Pindur and Heuberger, 2008). A more detailed comparison of the Schwarzensteinkees front variation measurements and geomorphological map of the foreland shows general correlation between the datasets (Figure 4.7). Interpreted moraine chains that appear to match front variation measurement positions (23) outnumber those that do not (14), although measurements for 23 years are not reported. This analysis suggests that Exposure B was formed in 1913 and 1914, Exposure C in 1921, Exposure D in 1930, and Exposure E in 1937.

The first maps from this period were drawn in 1894 and 1905 and show that a small lake may have existed in the lowest reaches of the valley (Figure 4.8). This potential lake is also depicted in several other maps until 1937, discussed separately and chronologically. However, any potential lake is not present on a more detailed map from 1932. The scale and resolution of these maps make it difficult to distinguish if this is, in fact, a lake, or if the maps instead depict two channels separated by land. The maps from 1913 and 1914 also show this potential lake at the ice front (Figure 4.9), and the map from 1913 (Figure 4.9A) additionally depicts the ice front at 2,138 m elevation, showing the same marking point as the map from 1888 (Figure 4.4B). This contradicts the front variation data, which show over 130 m retreat from 1888 to 1913 (Figure 4.6, Table 4.1) and therefore shows that either or both maps are not accurate. The map from 1925 depicts the same 2,138 m ice front (Figure 4.10A), despite front variation data from 1913 to 1925 recording over 50 m of retreat. The maps from 1914 (Figure 4.9B) and 1925/26 (Figure 4.10B) similarly show an unchanged ice front. Analysing the maps in relation to landscape evolution and the extent of Schwarzensteinkees may therefore not always be fruitful when the relationship between the ice front, the glacier foreland, and the lake (or lack thereof) is difficult to assess due to

map style, scale, and resolution. The veracity of historical mapping in this area is particularly important to question if the location of the ice front does not change through time, despite front variation measurements showing changes during the periods in question.

A photograph of Schwarzensteinkees and its foreland in 1925 shows the ice front somewhere above the LSZ, which corresponds to an elevation of at least 2,130 m (Figure 4.11). Comparing the position of the ice front in this photograph to that mapped in 1925 (Figure 4.10) further suggests that the maps do not accurately depict the position of the ice front, and instead use the furthest downvalley extent from previous maps. This photograph does not show a proglacial lake, and instead clearly shows the 1850 and earlier moraine, IZ1, FZ1, and LSZ (Figure 4.11).

The WGMS data on front variation of Schwarzensteinkees from 1890 to 1930 show retreat for most years (Zemp et al., 2012; Zemp et al., 2013). However, 1915 and 1920 both show a slight positive (0.3 m) front variation. Small measurements such as these may, however, be problematic when considering accuracy during these older years without high-resolution GPS devices and no indication of where ice front measurements were specifically taken each year. The data from 17 years are missing (Figure 4.6, Table 4.1).

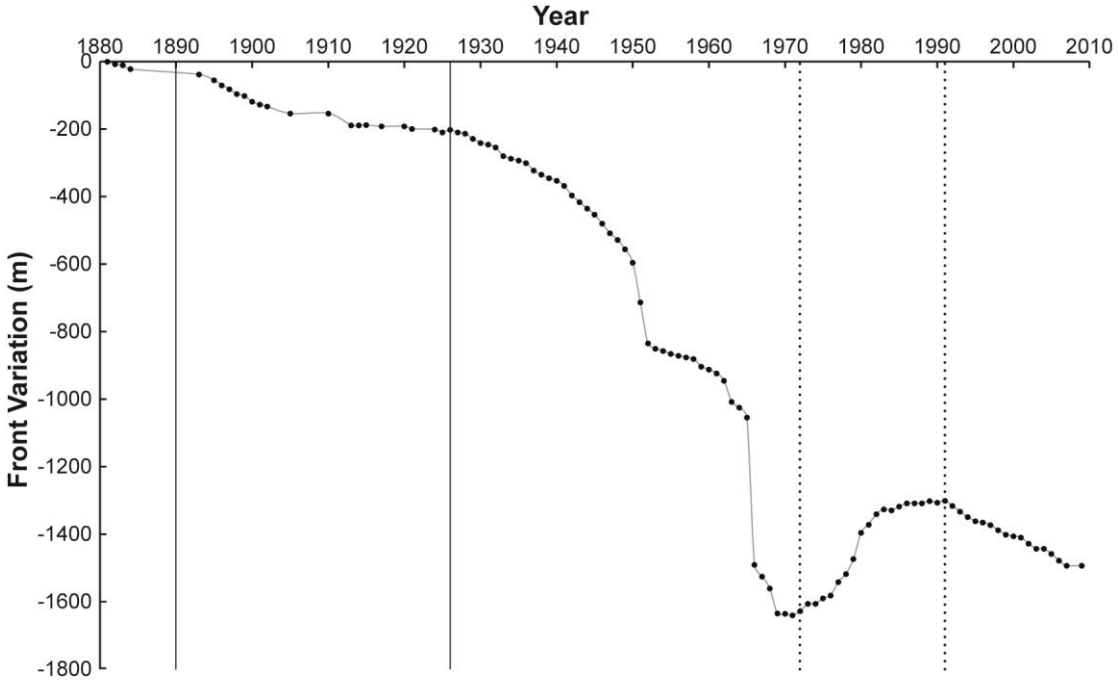

Figure 4.6. Front variation of Schwarzensteinkees, 1882-2009. Solid lines separate periods described in the text: pre-1890 glacier retreat and minor moraines, 1890-1926 glacier retreat and minor moraines, and 1926-present dominant glacier retreat. Dotted border shows dominantly positive front variation from 1972 to 1991. Data from the WGMS (Zemp et al., 2012; Zemp et al., 2013).

Table 4.1. Front variation of Schwarzensteinkees, 1882-2009. Solid lines separate periods described in text: pre-1890 glacier retreat and minor moraines, 1890-1926 glacier retreat and minor moraines, and 1926-present dominant glacier retreat. Dotted border shows dominantly positive front variation from 1972 to 1991. The WGMS data span 1882 to 2009, with some years omitted and others without data or with no net change (Zemp et al., 2012; Zemp et al., 2013). The WGMS does not clarify what these spaces represent.

Year	Front Variation (m)	Year	Front Variation (m)	Year	Front Variation (m)
1882	-8	1939	-9.7	1974	
1883	-2.2	1940	-7.4	1975	17
1884	-12	1941	-16	1976	8
1893	-15.7	1942	-28.4	1977	40
1895	-17.1	1943	-19.2	1978	24
1896	-15	1944	-19.2	1979	44
1897	-11.4	1945	-18	1980	78
1898	-14.3	1946	-26.9	1981	24
1899	-6.1	1947	-28	1982	31
1900	-17.1	1948	-20	1983	14.5
1901	-8	1949	-28	1984	-3
1902	-5.9	1950	-39	1985	11.5
1905	-20.7	1951	-118	1986	9
1910		1952	-121	1987	0
1913	-34.9	1953	-16.2	1988	0
1914		1954	-6.5	1989	7
1915	0.3	1955	-9.2	1990	-5
1917	-3.7	1956	-5.2	1991	5.5
1920	0.3	1957	-4.7	1992	-15
1921	-7.5	1958	-4.8	1993	-17
1924	-1.7	1959	-22.7	1994	-16
1925	-8.4	1960	-8.8	1995	-12
1926	7.5	1961	-11	1996	-4
1927	-8.3	1962	-22.3	1997	-8
1928	-3	1963	-62	1998	-15
1929	-15.4	1964	-17	1999	-13
1930	-12.6	1965	-30	2000	-5
1931	-4.8	1966	-436	2001	-4
1932	-8.8	1967	-35	2002	-18
1933	-25.2	1968	-35	2003	-15
1934	-7.5	1969	-74	2004	
1935	-6.1	1970	-1	2005	-15
1936	-7.1	1971	-5	2006	-20
1937	-21.9	1972	13	2007	-15
1938	-12.8	1973	21	2009	

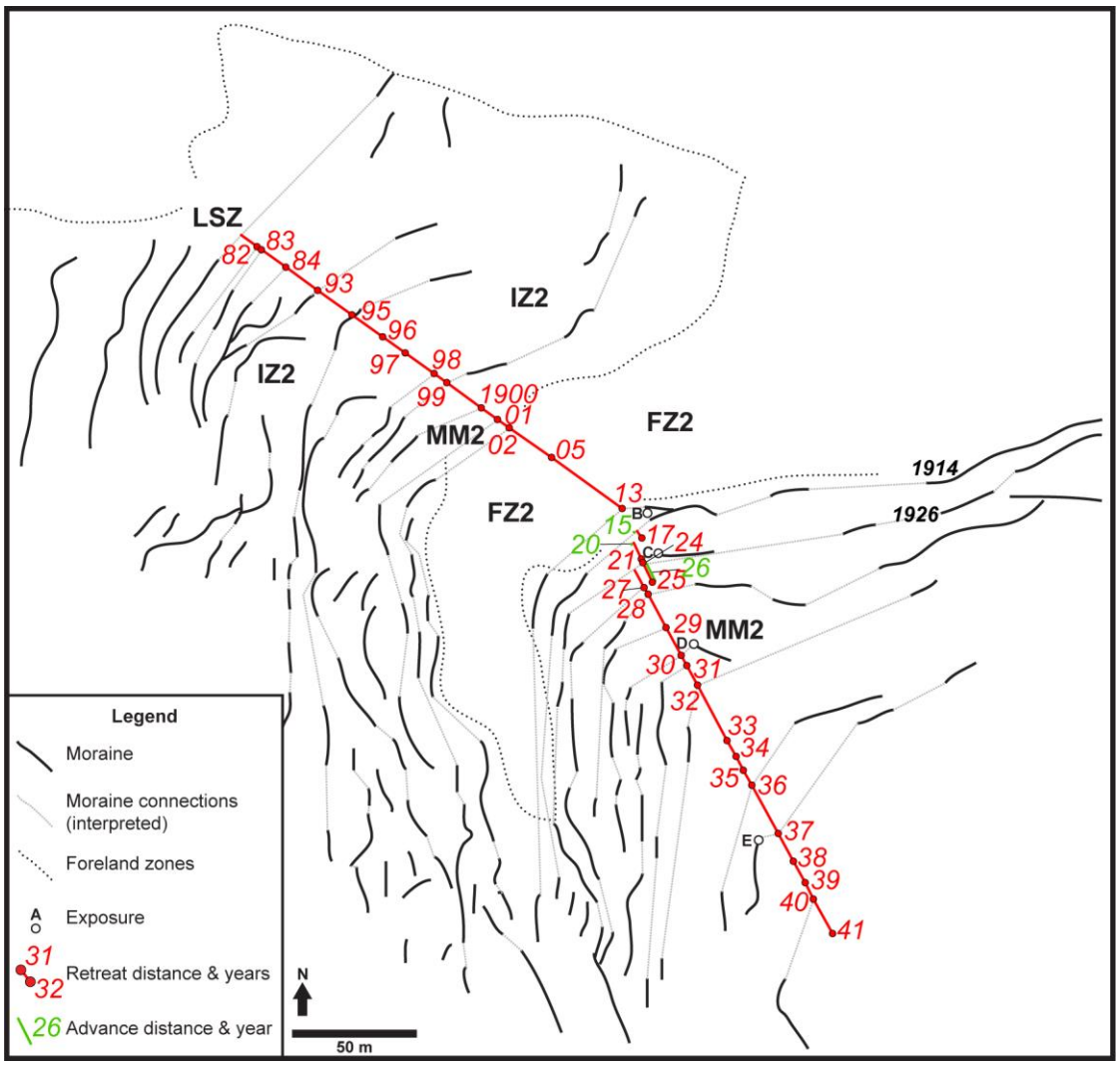

Figure 4.7. Front variation of Schwarzensteinkees overlain on geomorphological map. Red points represent retreat measurements. Green points represent advance measurements. See Figure 4.1 for larger geomorphological map. Front variation data from the WGMS (Zemp et al., 2012; Zemp et al., 2013).

Table 4.2. Comparison of front variation of Schwarzensteinkees and mapped moraines derived from Figure 4.7 map. Front variation data from the WGMS (Zemp et al., 2012; Zemp et al., 2013).

Year	Match	No Match	No Data	Year	Match	No Match	No Data
1882	x			1912			x
1883	x			1913	x		
1884	x			1914	x		
1885			x	1915		x	
1886			x	1916			x
1887			x	1917		x	
1888			x	1918			x
1889			x	1919			x
1890			x	1920		x	
1891			x	1921	x		
1892			x	1922			x
1893	x			1923			x
1894			x	1924	x		
1895	x			1925		x	
1896		x		1926		x	
1897		x		1927	x		
1898	x			1928	x		
1899	x			1929	x		
1900	x			1930	x		
1901	x			1931	x		
1902	x			1932	x		
1903			x	1933		x	
1904			x	1934		x	
1905		x		1935		x	
1906			x	1936	x		
1907			x	1937	x		
1908			x	1938		x	
1909			x	1939		x	
1910			x	1940	x		
1911			x	1941		x	

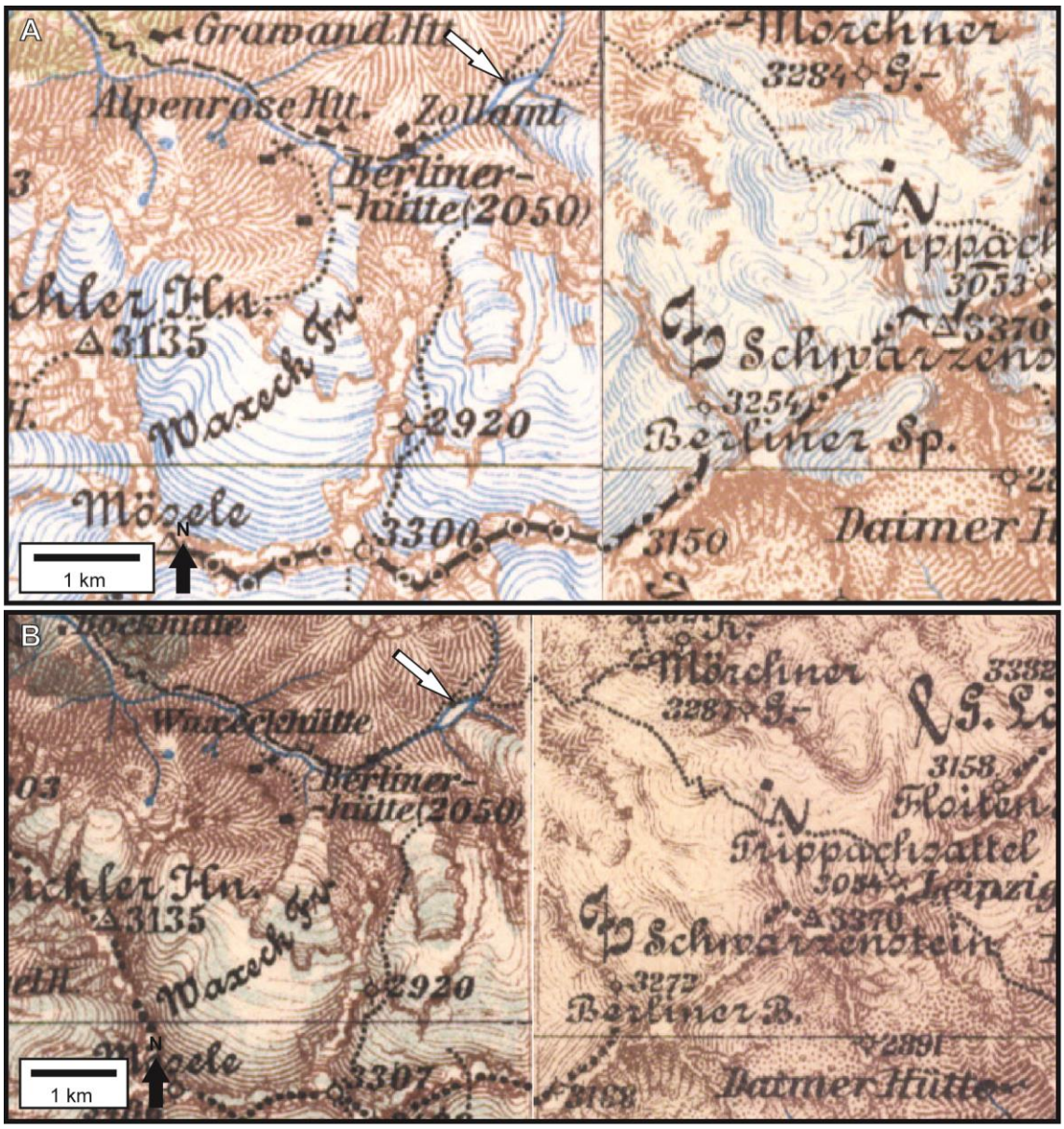

Figure 4.8. Historic topographic maps of the upper Zemmgrund, 1894 and 1905. A) Map from 1894 that potentially shows a small proglacial lake at the Schwarzensteinkees ice front, indicated with an arrow ("Generalkarte von Mitteleuropa," 1894); B) Map from 1905 that potentially shows a small proglacial lake at the Schwarzensteinkees ice front, indicated with an arrow (Mühlberger, 1905).

Figure 4.9. Historic topographic maps of the upper Zemmgrund, 1913 and 1914. A) Map from 1913 that potentially shows a small proglacial lake at the Schwarzensteinkees ice front, indicated with an arrow, and shows the ice front at 2,138 m, at a marker indicated with an arrow (Heinrich, 1913); B) Map from 1914 that potentially shows a small proglacial lake at the Schwarzensteinkees ice front, indicated with an arrow (Triltsch, 1914).

Figure 4.10. Historic topographic maps of the upper Zemmgrund, 1925 and 1925/26 A) Map from 1925 that potentially shows a small proglacial lake at the Schwarzensteinkees ice front, indicated with an arrow, and shows the ice front at 2,138 m, at a marker indicated with an arrow ("Bruneck (5248)," 1925; "Hippach und Wildgerlos-Spitze (5148)," 1925; "Matrei (5147)," 1925; "Sterzing und Franzensfeste (5247)," 1925); B) Map from 1925/26 that potentially shows a small proglacial lake at the Schwarzensteinkees ice front, indicated with an arrow ("Generalkarte von Mitteleuropa," 1925).

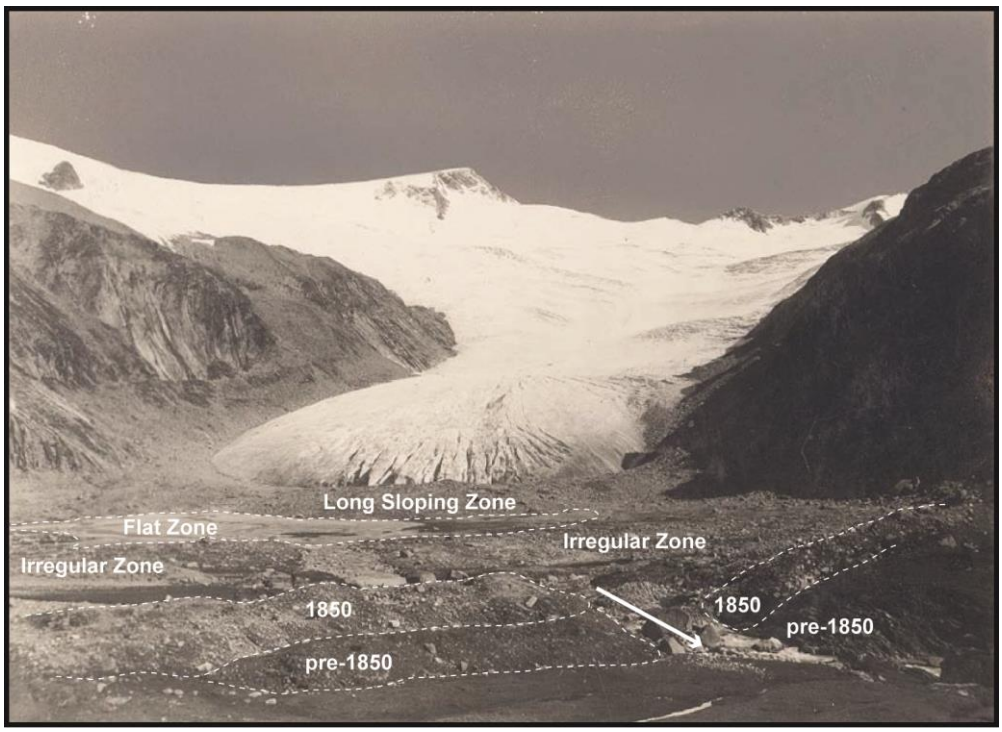

Figure 4.11. Photograph of Schwarzensteinkees and its foreland, 1925. The ice front is somewhere above the LSZ, and FZ1, IZ1, and 1850 moraine are clearly noticeable. Dashed lines indicate extents of FZ1, IZ1, 1850 moraine, and a pre-1850 moraine. Arrow indicates direction of channel flow (Lichtenecker, 1925).

4.1.4 1940 to present: Dominant glacier retreat

The first map following deposition of MM2 supports the deposition of these minor moraines by 1932 and is the only historical map to resolve these landforms (Figure 4.12). This map shows the ice front at 2,140 m elevation, above the elevation of MM2. The map also clearly shows the presence of two distinct sets of minor moraines (MM1 and MM2) separated by a flat zone (FZ1), and an elevation measurement marking the highest minor moraine in the valley at 2,139 m. Figure 4.7 suggests that the furthest up-valley minor moraine was deposited in 1940. It cannot be discounted that moraines formed after this time and have since been eroded, but any evidence is lacking.

Maps from 1935 and 1937 (Figure 4.13) show the potential lake and ice extent as mapped in other, older maps, whereas the 1932 map only depicts channels in the foreland (Figure 4.12). The 1935 and 1937 maps, however, more closely fit the two distinct artistic styles of older, lower-resolution maps, and the 1932 map is more detailed and similar to subsequent maps. This suggests that the 1935 and 1937 maps may not be accurate and instead transferred landforms and ice position from older maps without renewed mapping. A photograph from 1936 supports the ice position as mapped in 1932, near the upper limit of MM2 (Figure 4.14). This is also the first photograph to show multiple MM2 moraines in the foreland, with the lighting most emphasizing ridges trending in the approximate

direction of the valley axis, which may include the moraine hosting Exposure D (Figure 4.1). This photograph also clearly shows both Flat Zones.

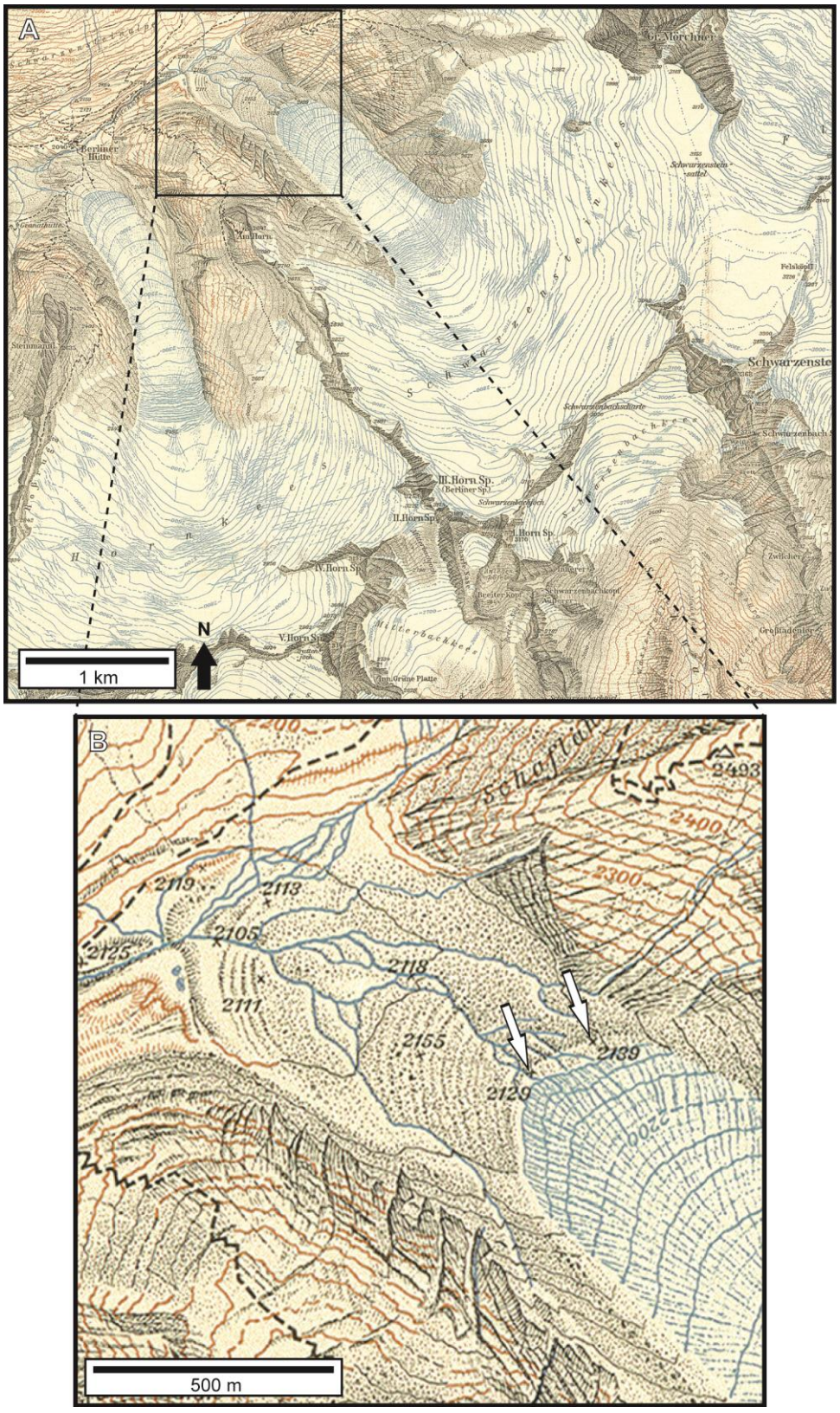

Figure 4.12. Historic topographic map of the upper Zemmgrund, 1932. The lower map provides a closer view of the Schwarzensteinkees foreland, which reveals the two groups of minor moraines, separated by a flat area and a larger moraine (1850) at the end of the valley. An elevation point marks the elevation of the highest minor moraine at 2,139 m, as indicated by arrows ("Karte der Zillertaler-Alpen Mittleres Blatt," 1932).

Figure 4.13. Historic topographic maps of the upper Zemmgrund, 1935 and 1937. A) Map from 1935 that potentially shows a small proglacial lake at the Schwarzensteinkees ice front, indicated with an arrow, and shows the ice front at 2,138 m, at a marker indicated with an arrow ("Matrei, Tirol," 1935); B) Map from 1937 that potentially shows a small proglacial lake at the Schwarzensteinkees ice front, indicated with an arrow ("Generalkarte von Mitteleuropa 1937," 1937).

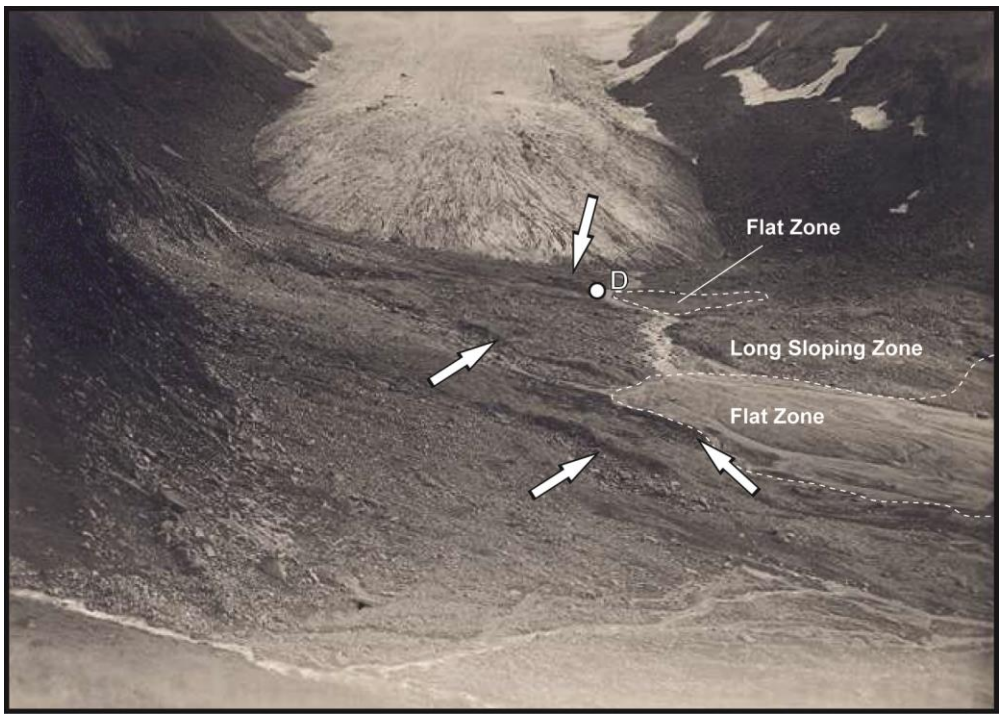

Figure 4.14. Photograph of Schwarzensteinkees and its foreland, 1936. The ice front is somewhere near the upper limit of the second group of minor moraines. Dashed lines indicate extents of the two Flat Zones. Arrows indicate moraines, and the location of Exposure D is noted (Figure 4.1) (Sander, 1936).

A measured sketch derived from ice front variation measurements depicts the changing position and shape of the ice front from 1935 to 1939 (Figure 4.15). Some overlap of the ice front between 1937 and 1938 may suggest that these subtle variations are not uncommon at the Schwarzensteinkees margin, which illustrates the importance of considering obliterative overlap erasing some moraines from the geomorphological record. This sketch emphasizes that ice front measurements may depend on the specific point of measurement, creating another potential source of error when considering ice front position and geomorphological evolution of the valley. This sketch portrays measurements across the ice front, but shows that an individual point measurement representing a single year may vary considerably, as the different retreat rates of the portal and rest of the ice front from 1936 to 1937 show (Figure 4.15).

Several photographs from 1942 and 1946 show the ice front above MM2 and a lack of moraine deposition around this time, corresponding to the highest mapped minor moraines (Figure 4.1). A photograph of Schwarzensteinkees and its foreland in 1942 is the first photograph that clearly depicts the second set of minor moraines, as well as the two Flat Zones, IZ2, and LSZ (Figure 4.16). It is unclear whether any moraines lie immediately in front of the glacier. The furthest upvalley moraine on this photograph may correspond to that mapped at 2,139 m in 1932 (Figure 4.12), based on its continuity and stark presence on valley right, although this cannot be definitively proven.

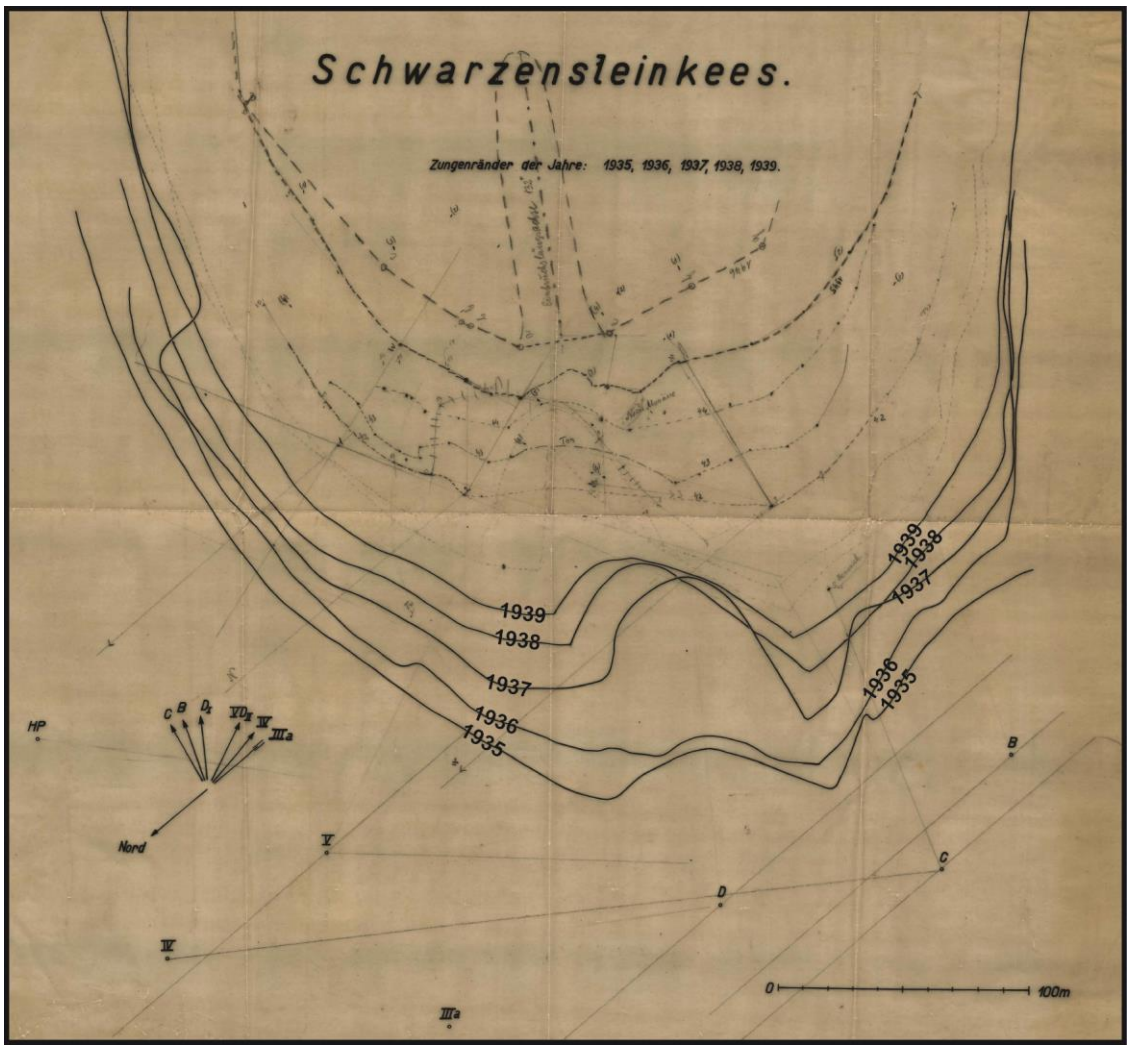

Figure 4.15. Sketch of the Schwarzensteinkees ice front positions relative to each other from 1935 to 1939. Figure modified from Felkel and Rotter (1946e).

Two photographs from 1946 show a closer view of the ice front than the photograph from 1942 (Figure 4.17). These photographs depict the ice collapsing near the centre of the ice front and a lack of moraines in this part of the foreland, which suggests a cessation of moraine formation prior to 1946. However, the photograph from 1942 shows that the glacier portal had likely already collapsed and widened, which questions the chronological designation of these photographs (Figure 4.16).

Additional photographs from 1946 show the lower area of the foreland and clearly depict FZ1, IZ1, and MM1 enclosed by the 1850 moraine at the bottom of the valley (Figure 4.18). Ridges in IZ1, particularly on valley right, are quite clear when compared to today.

Two photographs from 1951 (Figure 4.19) show the ice front considerably retreated from the 1946 position, corresponding to retreat of 370 m overall according to ice front variation measurements (Figure 4.6, Table 4.1). These photographs both also depict FZ2, and one photograph shows several moraines bordering this area (Figure 4.19B). A photograph from 1953 further emphasizes the retreating glacier, as the second group of

minor moraines is not shown (Figure 4.20). The map from 1964 (Figure 4.21) is nearest in age to this photograph and emphasizes a considerably retreated ice front (at 2,160 m) when compared to the next oldest map in 1937, although as previously described, the veracity of the extent of Schwarzensteinkees as depicted on the 1937 map is questionable (Figure 4.13B). The front variation data also show considerable retreat (around 700 m) from 1937 to 1964 (Figure 4.6; Table 4.1).

Not long after the map from 1964 was drawn, a photograph from 1969 shows that the ice had reached its bedrock extent by this time (Figure 4.22). The age of this photograph and the extent of the glacier shown in the photograph from 1953 (Figure 4.20) shows that the glacier retreated into the bedrock reach during this period, during which the glacier retreated more than 780 m, which includes nearly 436 m of retreat from 1965 to 1966, derived from ice front variation measurements (Figure 4.6; Table 4.1).

Today, the modern channel and bedrock dominate the Schwarzensteinkees foreland upvalley of the second group of minor moraines. Alluvial fans and talus cones constitute most of the surface valley fill and are the only landform assemblages of the upper valley recorded during fieldwork. Although the various zones of the foreland are well defined, the landforms appear more muted than in previous photographs, particularly when attempting to trace ridges in the Irregular Zones (Figure 4.23-4.23).

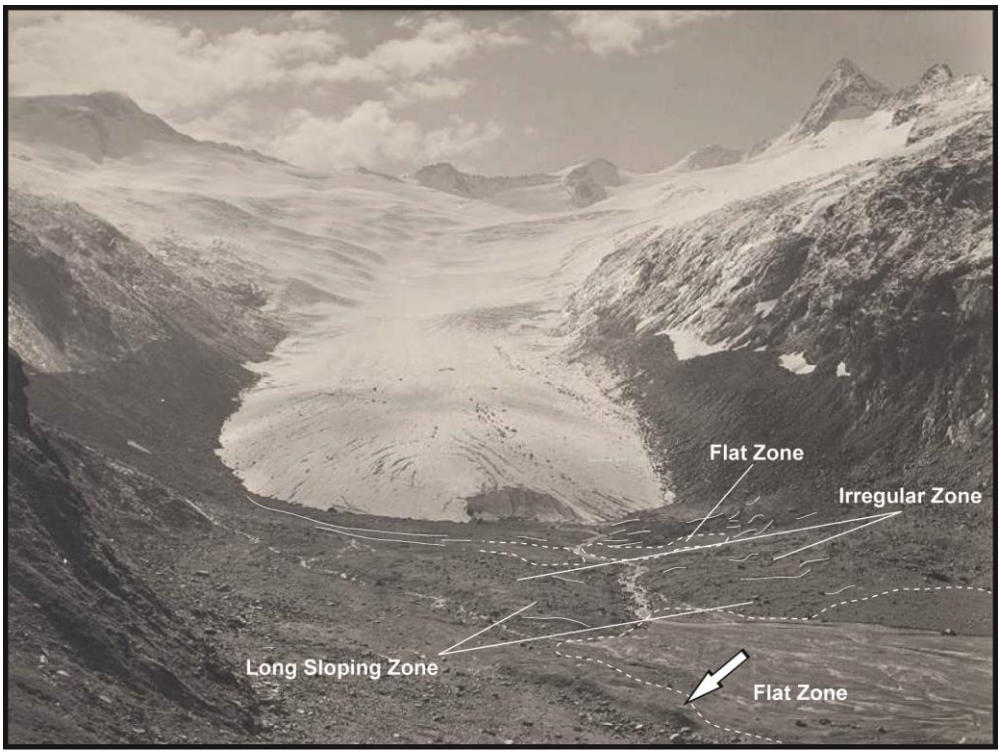

Figure 4.16. Photograph of Schwarzensteinkees and its foreland, 1942. The ice front is somewhere near the upper limit of the second group of minor moraines. Dashed lines indicate extents of the two Flat Zones. The arrow indicates a prominent moraine at the edge of FZ1 (Figure 4.1). Thin lines show numerous moraine ridges in MM2 (Schatz, 1942).

Figure 4.17. Photographs of the Schwarzensteinkees ice front, 1946. A) A portion of the ice front collapsing (Felkel and Rotter, 1946a); B) Closer view of the collapsed ice front (Felkel and Rotter, 1946b). The lack of moraines in front of the ice in both views suggests an end of minor moraine formation prior to 1946. Arrows indicate direction of channel flow.

Today, the glacier sits in the bedrock reach of the valley (Figure 4.24) with a lowest elevation of approximately 2,360 m. The WGMS data on front variation of Schwarzensteinkees from 1926 to 2009 show retreat for most years. The glacier did dominantly advance from 1972 to 1989, however (Figure 4.6; Table 4.1). Positive front variations suggest that Schwarzensteinkees had been advancing for nearly three decades,

but the advance appears to have left no geomorphological signature, likely due to the glacier's position in the bedrock reaches of the valley.

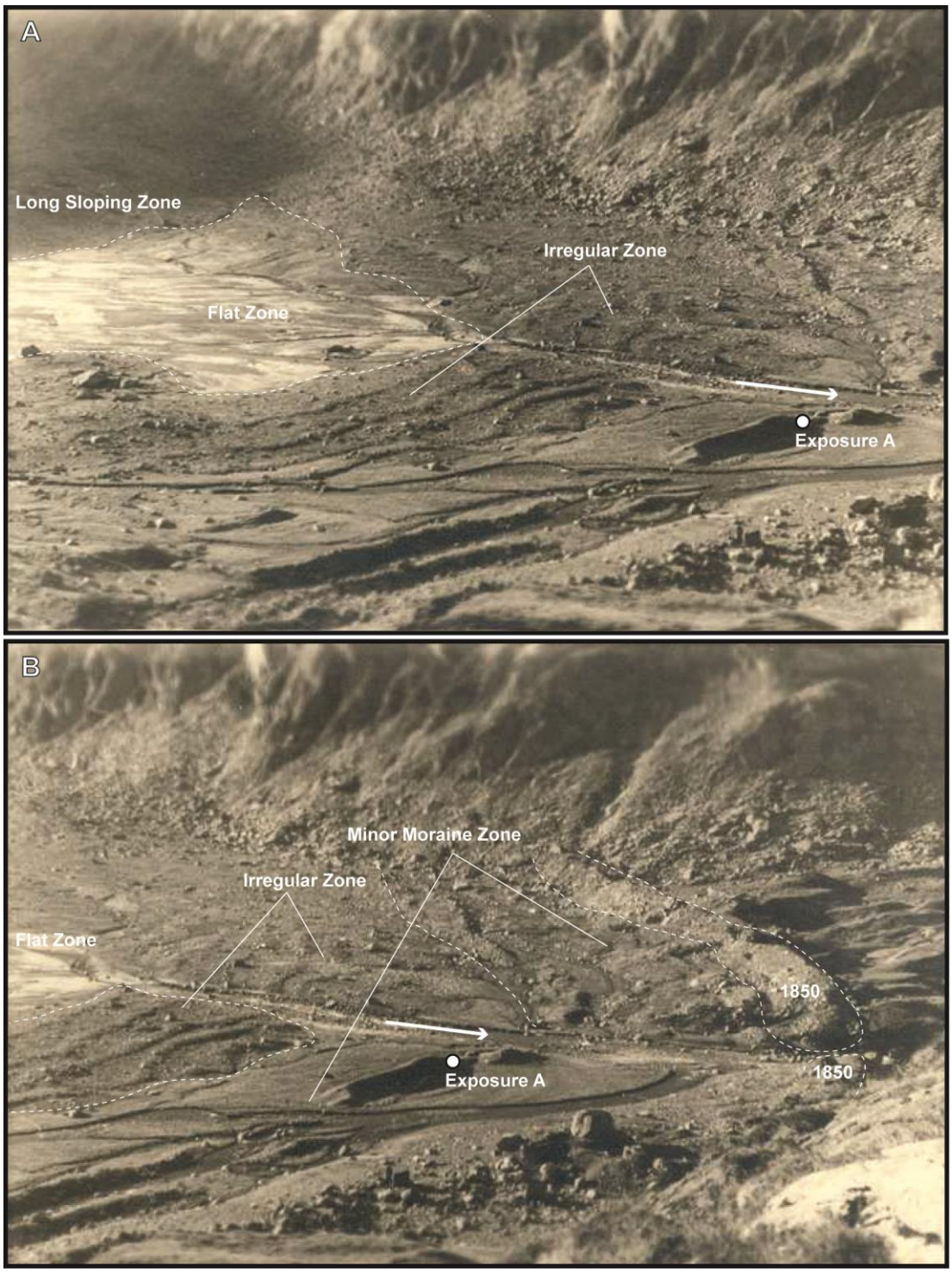

Figure 4.18. Photographs of the Schwarzensteinkees foreland, 1946. A) View of the foreland from the bottom end of the LSZ to near the moraine hosting Exposure A (Felkel and Rotter, 1946c); B) View of the foreland from the bottom of FZ1 to near the 1850 moraine (Felkel and Rotter, 1946d). Dashed lines indicate extent of various zones or the 1850 moraine (B). The location of Exposure A (Figure 4.1) is indicated and labelled. Arrows indicate direction of flow of the main channel.

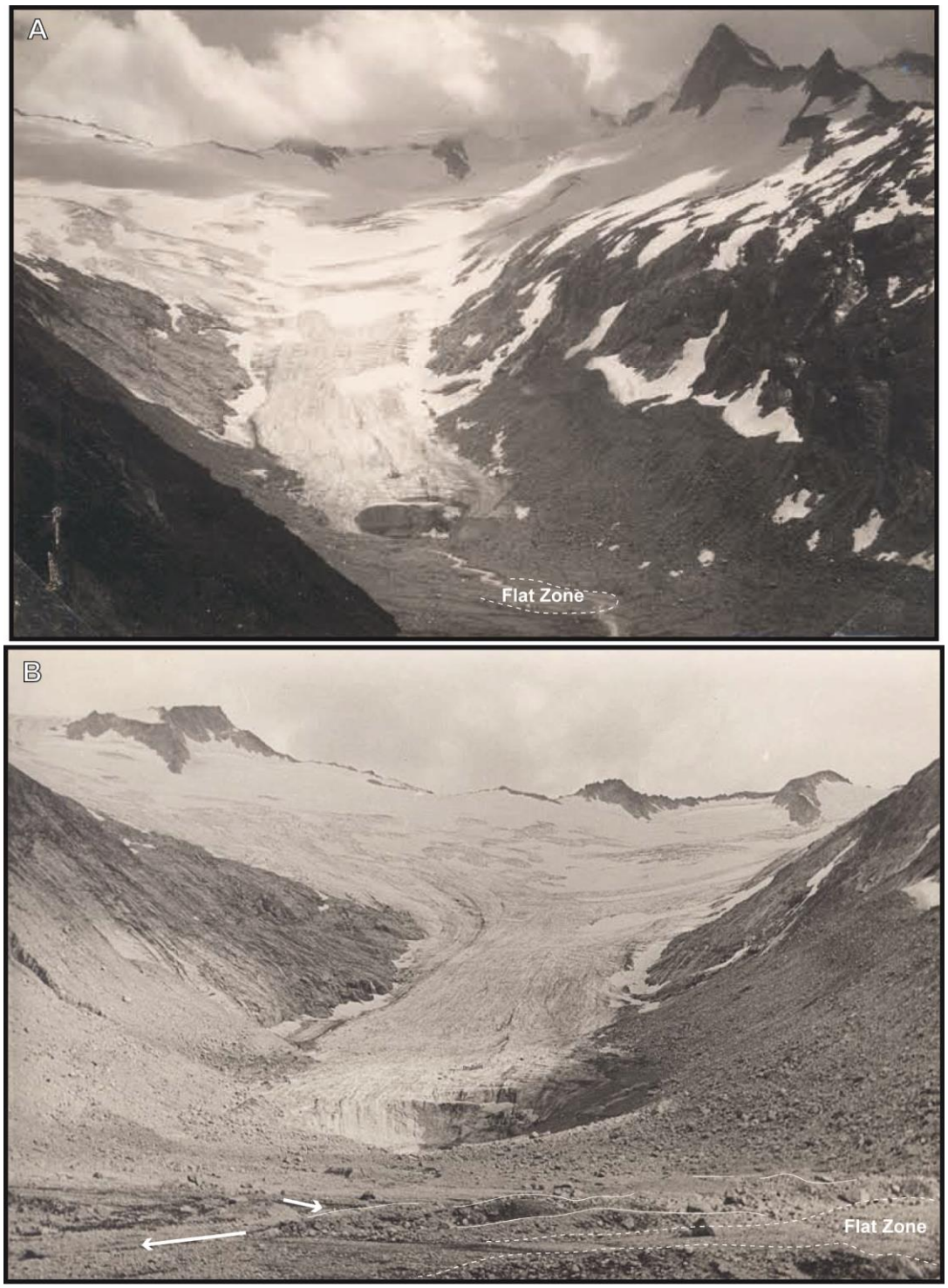

Figure 4.19. Photographs of Schwarzensteinkees and its foreland, 1951. A) Distant view looking down and into the valley, showing FZ2 (Karl, 1951); B) View of the glacier and foreland from near the downvalley extent of MM2 showing FZ2 (dashed lines) and minor moraine ridges (thin lines). Arrows indicate flow direction of meandering channel (Kinzl, 1951).

Figure 4.20. Photographs of Schwarzensteinkees and its foreland, 1953. This view captures the glacier considerably upvalley of the second group of minor moraines, which are out of the frame (Drong, 1953).

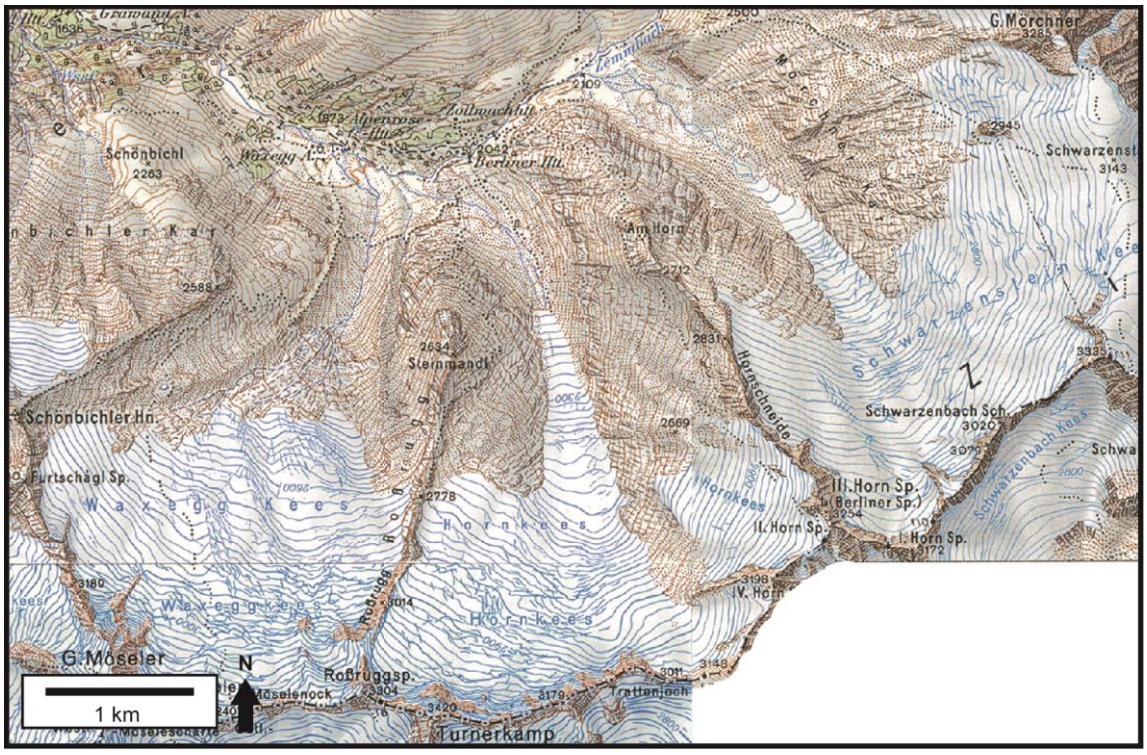

Figure 4.21. Historic topographic map of the upper Zemmgrund, 1964. This map shows the glacier significantly retreated from the position on the next oldest map in 1937, with the Schwarzensteinkees ice front indicated by an arrow (Figure 4.13B). Modified from "Österreichische Karte" (1964).

Figure 4.22. Photograph of Schwarzensteinkees and its foreland, 1969, showing that the ice had reached its bedrock extent (dashed line) by this time (Lässer, 1969).

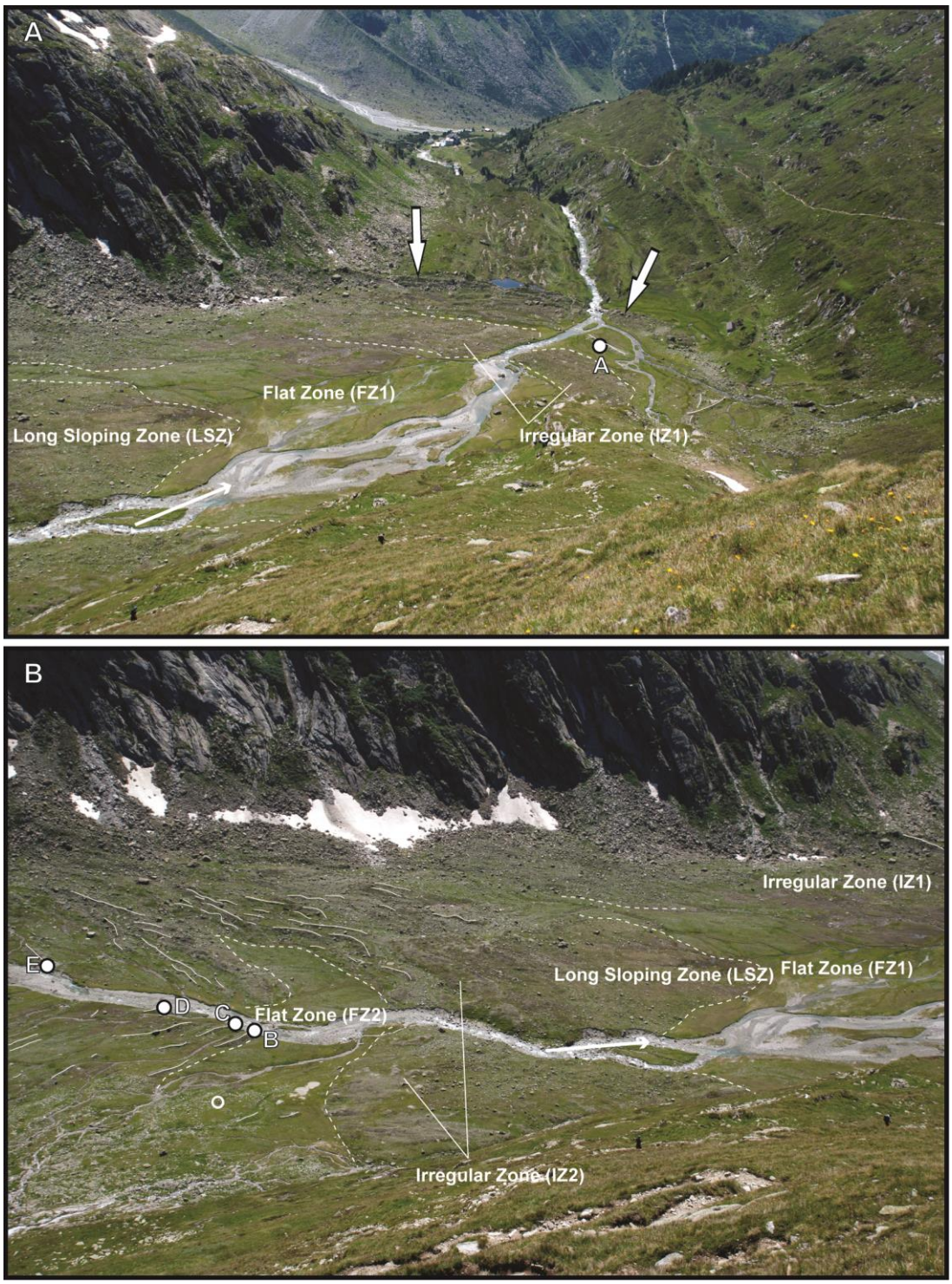

Figure 4.23. Photographs of the Schwarzensteinkees foreland, 2014. A) Photograph showing the lowermost extent of the valley, including the 1850 moraine, as indicated by arrows, IZ1, FZ1, and LSZ. Exposure A indicated. Arrow indicates flow direction of modern channel; B) Photograph showing the second group of minor moraines, including the locations of Exposures B-E, IZ1, FZ1, LSZ, IZ2, and FZ2. Horse for scale indicated by white-outlined circle. Arrow indicates flow direction of modern channel. Photographs taken in July 2014 from the northeastern valley wall.

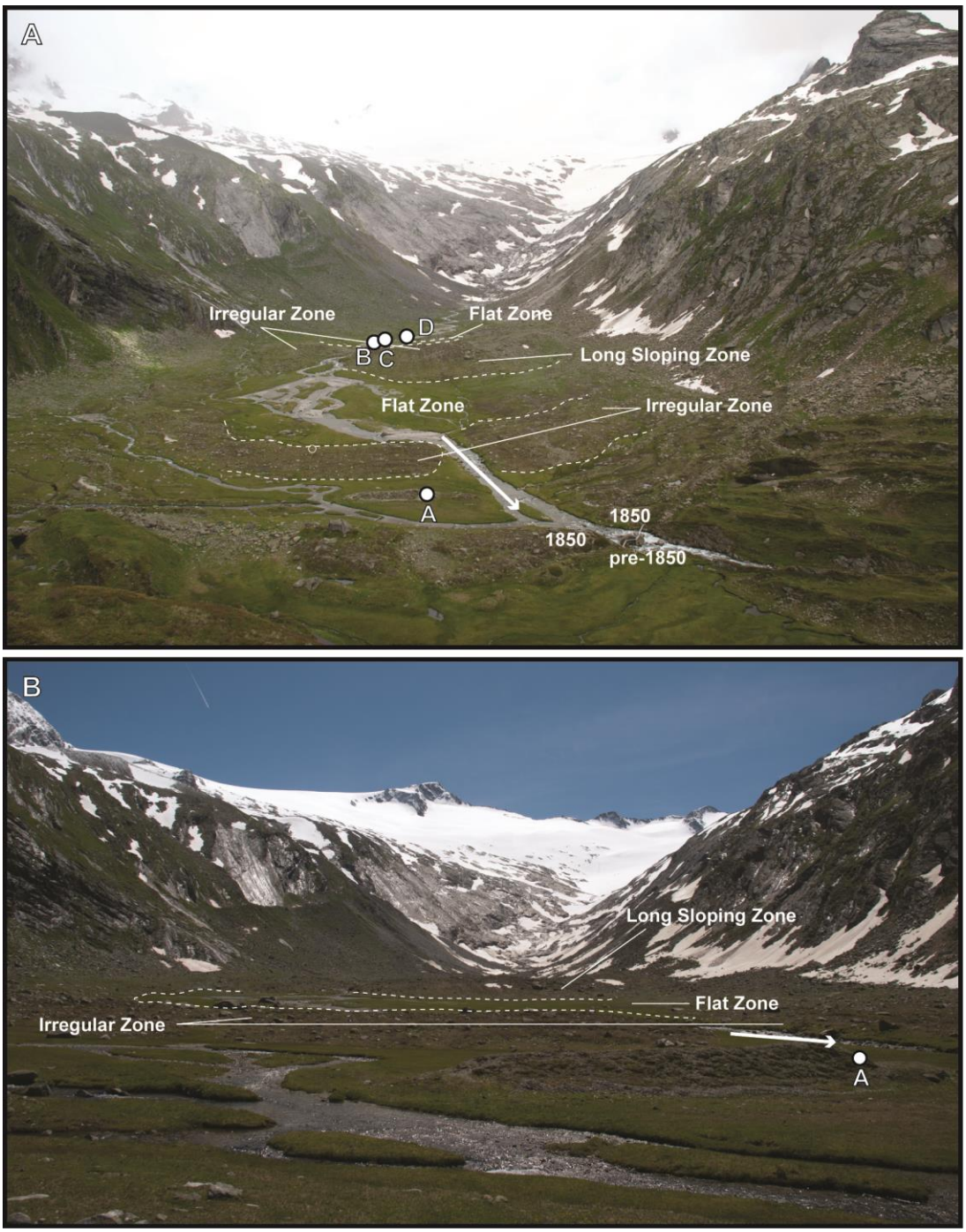

Figure 4.24. Photographs of Schwarzensteinkees and its foreland, 2014. A) Photograph highlighting multiple zones of the foreland (dashed lines) and showing the location of Exposures A-D. Horse for scale indicated by small circle, and arrow shows direction of main channel flow; B) Photograph from ground level showing the morphologies of the Irregular Zone, Flat Zone, and Long Sloping Zone (dashed lines) and the location of Exposure A. Arrow shows flow direction of main channel. Photographs taken in July 2014.

4.2 Ground-penetrating radar transect through the lower Flat Zone (FZ1)

Results from ground-penetrating radar measurements are presented for one transect through part of IZ1, FZ1, and part of LSZ (GPR01, Figure 4.1) as radar reflection profiles (Figure 4.25). Radar reflection profiles reveal a prominent reflector approximately 1.8-2.8 m deep generally constrained within the FZ1 boundaries as measured while collecting GPR data (81.5-313.0 m on 50 MhZ radargram, 72.5-318.5 m on 100 MhZ radargram, and 60.0-300.0 m on 200 MhZ radargram). This reflector marks a very prominent boundary to the underlying elements of the subsurface. Everything below this reflector is considered radar facies (RF) 1, whereas anything above is labelled as RF 2. Two other RF are noted as homogeneous sediment in IZ1 (RF3) and LSZ (RF4). The combined interpretation of radar reflection profiles are presented in Section 4.5.1.

4.3. Sedimentological composition of the Schwarzensteinkees minor moraines

The composition and architecture of moraines in the Schwarzensteinkees foreland is described for each excavated moraine. Interpretations of notable features in the exposures are presented in Section 4.4. These interpretations are then compiled and extrapolated on in discussion of specific mechanisms of minor moraine formation in Section 4.5.2.1. All clast measurement data can be found in Appendix B.

4.3.1. Exposure A

This moraine consists of three discontinuous ridge fragments on valley right and two or three ridge fragments on valley left, separated by the modern channel (Figure 4.1). The ridge fragment hosting this exposure is 41 m long with an average width of 11 m, and the straight ridge trends 200°. Overall, the proximal slope is slightly shallower (25°) than the distal slope (27°), although +/- 5° clinometer accuracy must be considered (Chapter 2). There is a notable accumulation of clasts on the valley floor along the distal slope of the landform. This exposure consists of 14 different FA and contains mostly gravel, with some sand beds and a distinct diamicton FA (Figure 4.26).

FAs 1-9 comprise the lower section of the exposure. FA 1 and FA 2 are located in the lowest ice-distal portion of the exposure. FA 1 is a horizontal bed of massive, matrix-supported boulders (Bmm), with poorly-sorted medium to coarse sand as the matrix. The longest exposed axes of the boulders range from 18 cm to 29 cm. FA 2 is a horizontal bed of massive, well-sorted fine to medium sand (Sm). FAs 3-6 and FA 8 are located in the lowest ice-proximal portion of the exposure. FA 3 is a diamicton that contains matrix-supported,

poorly-sorted pebbles and cobbles (maximum a-axis length 9.8 cm), with a laminated, moderately-sorted silty to fine sandy matrix (Dml). Weak laminations are present throughout FA 3. FA 4 consists of moderately-sorted coarse sand to granules and medium to coarse sand that is thinly horizontally bedded in places (GRh, Sh, Sm).

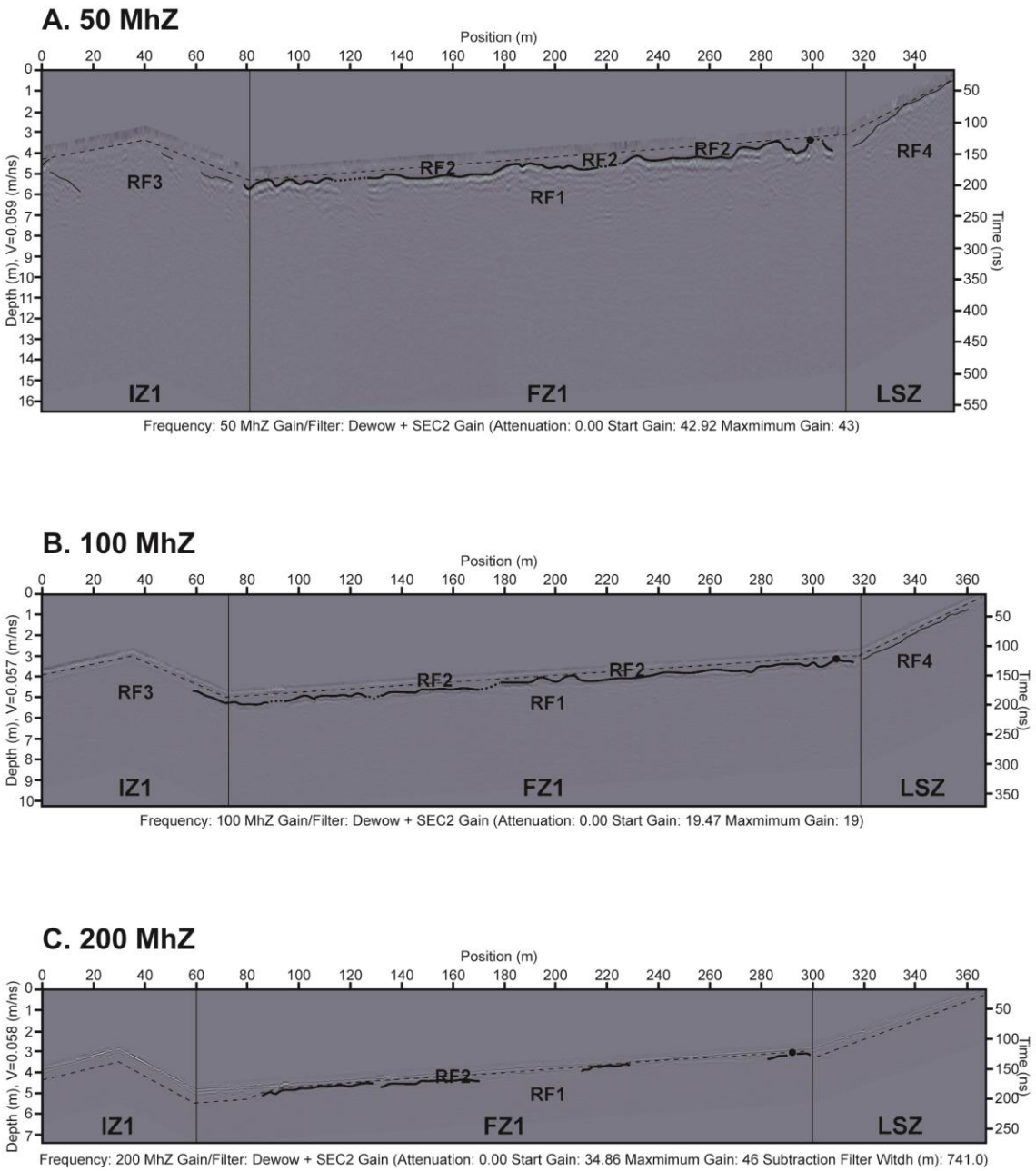

Figure 4.25. Ground-penetrating radar reflection profiles along the transect GPR01. A) 50 MhZ radargram. B) 100 MhZ radargram. C) 200 MhZ radargram. Upper thin, dashed line shows boundary between air and ground wave and underlying material. Boundaries of zones on the geomorphological map (Figure 4.1) labelled and demarcated with vertical lines. Black circle indicates prominent surface boulder, as noted during data collection. Thick line shows prominent reflector, and dashed thick line shows inferred connection between visible prominent reflectors. Thin lines show other reflectors. Prominent radar facies labelled.

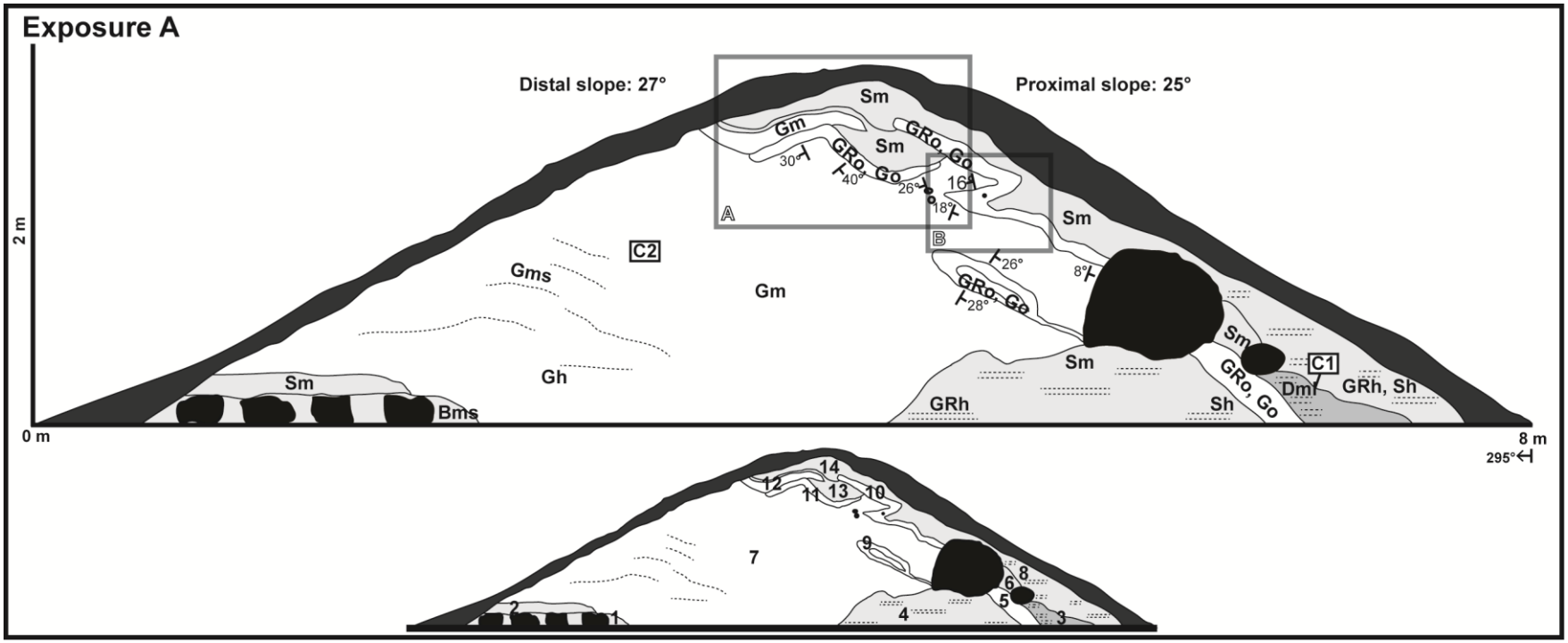

Figure 4.26. Exposure A representative log. FAs are labelled with facies codes (top) and FA numbers (bottom) and are described in the text in stratigraphic order from bottom to top. FA colours correspond to dominant grain-size class. Chapter 2 shows facies codes and symbols key (Figure 2.6). Labelled boxes indicate approximate clast measurement locations. Labelled photograph locations refer to the photographs in Figure 4.27.

The wedge of FA 5 is recognizable beginning under a boulder and separating FA 3 and FA 4, extending from a boulder at the base of the exposure in an orientation similar to the proximal slope of the landform. This FA contains openwork, moderately-sorted granules and pebbles (GRo, Go). FA 6 consists of massive, well-sorted medium sand (Sm). FA 7 dominates the exposure, particularly the ice-distal side. This FA contains matrix-supported, poorly-sorted pebbles and cobbles (Gms), with well-sorted coarse sand as the matrix, and clast-supported, poorly-sorted pebbles and cobbles (Gm). The FA contains some vague horizontal and slightly dipping beds in places (Gh), however bedding was immeasurable due to the highly friable nature of the sediment. FA 8 is present on the most proximal side of the exposure, however its upper contact with FA 14 is unclear. This FA contains moderately-sorted coarse sand to granule and medium to coarse sand zones, and thin horizontal bedding in places (GRh, Sh, Sm). FA 9 exists in FA 7, and contains massive, openwork, poorly-sorted granules and small pebbles (GRo, Go). This FA is folded into itself, creating an enclosed loop, with a limb that extends to a boulder.

FAs 10-14 comprise the ridge crest zone of the exposure, and FA 10, FA 11, and FA 13 are notably folded beds (Figure 4.27). FA 10 is found in the upper ice-proximal side of the exposure and contains massive, openwork, poorly-sorted granules to small pebbles (GRo, Go) with some coarse sand. This FA is folded, with three distinct limbs (Figure 4.27B). The outer limbs mimic the proximal slope of the moraine. FA 11 forms the upper centre part of the exposure and consists of massive, openwork, poorly-sorted granules to cobbles (GRo, Go). This FA is folded, and the fold limbs dip at 30°, 40°, and 26° (Figure 4.27A). FA 12 is found in the upper ice-distal part of the exposure and contains massive, clast-supported, poorly-sorted pebbles to cobbles (Gm) with some sand. This FA appears folded from an originally horizontal bed, although the fold limbs are diffuse and were not measured (Figure 4.27A). FA 13 is found in the upper centre part of the exposure and contains massive, well-sorted medium sand (Sm). FA 14 comprises the uppermost part of the exposure and extends to a boulder. The contact or transition between FA 14 and FA 8 is unclear. FA 14 consists of massive, moderately-sorted fine to medium sand (Sm).

Figure 4.27. Photographs from Exposure A. Photographs correspond to locations on Figure 4.26. Dashed lines show contact between FAs. A) Folding in the ridge crest. Trowel for scale, 23.0 cm long; B) Folding along the proximal slope. Pencil for scale, 14.7 cm long.

4.3.2. Exposure B

The landform hosting Exposure B comprises one ridge towards the right (eastern) side of the valley, which splits into two ridges closer to the modern channel (Figure 4.1). This landform cannot be traced to any ridges on the other side of the channel. The individual

ridge fragment is 22 m long with a width of 8 m and has a generally straight crestline that trends 280°. The upvalley ridge fragment is 4 m long and 7 m wide, and the generally straight crestline has a 250° trend. The downvalley ridge fragment is 8 m long and 11 m wide, and the generally straight crestline trends 285°. Considering the landform as a whole, proximal slopes are steeper (28°), on average, than distal slopes (25°), although +/- 5° clinometer accuracy must be considered (Chapter 2). The individual ridge fragment has a notable collection of clasts along its distal slope, whereas clasts accumulate along proximal slopes once the ridge splits into two segments. The exposure was partially created by fluvial erosion by the modern channel and includes both ridge fragments. Exposure B as a whole consists of 28 FAs and contains mostly gravel, with some sand. These FAs are labelled for each of the two exposed landforms, from bottom to top (Figure 4.28). FA 11 in the ice-distal exposure and FA 4 in the ice-proximal exposure are the same, connecting the two landforms.

The ice-distal exposure contains 17 FAs (Figure 4.28). FAs 1-4 are differentiated by dominant clast size and grain size of matrix material. FA 1 is the most ice-distal FA and extends from the unexposed base. This FA contains massive, matrix-supported, moderately-sorted pebbles (Gms), with moderately-sorted coarse sand to granules as the matrix. FA 2 is found in the ice-distal part of the exposure and also extends from the soil to below the exposure. This FA consists of massive, clast-supported, poorly-sorted pebbles with some cobbles and coarse sand (Gm). FA 3 is found in the lower ice-distal portion of the exposure and consists of massive, matrix-supported, poorly-sorted pebbles and few cobbles (Gms), with fine to medium sand as the matrix. FA 4 extends from the soil to below the exposure and contains massive, matrix-supported, poorly-sorted pebbles and few cobbles (Gms), with medium to coarse sand as the matrix. FA 5 and FA 6, by contrast, are openwork gravels. FA 5 contains massive, moderately-sorted pebble to cobble clasts (Go) and is a distinct lens that extends at an angle downwards from a boulder. FA 6 extends from the soil zone to below the exposure and contains massive, poorly-sorted granule to pebble clasts, with some cobbles (GRo, Go).

FAs 7-9 comprise the ice-proximal side of the downvalley moraine, and FA 11 underlies the junction between the downvalley and upvalley ridges. These FAs are differentiated by dominant clast size and matrix material. FA 7 is found in the lowermost part of the exposure and contains massive, clast-supported, moderately-sorted cobbles (Gm) with fine to medium sand. FA 8 is bound by boulders and FA 9 at its upper ice-distal extent and extends below the exposure. The contact between FA 8 and FA 11, at the upper ice-proximal extent of FA 8 is sharp at its upper end, but is diffuse lower in the exposure. FA 8 consists of massive, matrix-supported, moderately-sorted cobbles (Gms), with medium to coarse sand as the matrix, whereas the matrix of FA 9 is distinctly medium to coarse sand (Gms). FA 9 is a vague zone surrounding a prominent boulder. FA 10 is a distinct lens of

massive, moderately-sorted, fine to medium sand (Sm) under a boulder. FA 11 underlies the confluence of the two moraine ridges and constitutes a portion of both exposures. This FA contains massive, clast-supported, moderately-sorted cobbles (Gm) (maximum a-axis length 16.0 cm) with medium to coarse sand.

FAs 12-17 (with the exception of isolated FA 10, described above) generally constitute the core of the downvalley moraine and are differentiated by dominant clast size and matrix material. FA 12 dominates the upper centre of the exposure and consists of massive, matrix-supported, moderately-sorted cobbles, with medium to coarse sand as the matrix, fining upwards to massive, matrix-supported, moderately-sorted cobbles, with medium sand as the matrix (Gms, Gfu). FA 13 separates FA 12 and FA 14 and is a pocket of clast-supported, moderately-sorted cobbles (Gm) with some medium sand. FA 14 extends from the soil zone to FA 13 and contains massive, matrix-supported, moderately-sorted cobbles (Gms), with well-sorted medium sand as the matrix. FA 15 is a pocket of massive, clast-supported, poorly-sorted pebbles to cobbles (Gm) with some coarse sand that begins in the soil zone. FA 16 is a horizontal lens of massive, clast-supported, moderately-sorted cobbles (Gm) with coarse sand that underlies most of FA 17 and separates FA 12 and FA 17. FA 17 underlies the ridge crest and the upper proximal slope of the downvalley moraine. FA 17 contains massive, matrix-supported, moderately-sorted cobbles (Gms), with poorly-sorted, medium to coarse sand as the matrix.

The ice-proximal exposure contains 12 FAs (Figure 4.28). FA 1 comprises a majority of the lower ice-proximal part of this exposure and contains massive, matrix-supported, poorly-sorted pebbles to boulders (Gms, Bms), with poorly-sorted medium to coarse sand as the matrix. FA 2 and FA 3 are distinct layers of massive, moderately-sorted fine to medium sand (Sm) in FA 1. FA 2 is oriented similar to the proximal slope of the landform, whereas FA 3 is horizontal.

FA 4 of the ice-proximal exposure is also FA 11 of the ice-distal exposure (see description for FA 11 above). FAs 5-7 are distinct sand FAs in FA 4 and are all massive, moderately-sorted fine to medium sand (Sm). FA 5 is oriented similar to the ice-proximal slope of the landform, whereas FA 6 is an approximately horizontal wedge and FA 7 is a distinct horizontal lens. FA 8 extends from the soil zone at its ice-distal extent to a boulder at its ice-proximal extent. This FA contains massive, clast-supported, poorly-sorted pebbles to cobbles (Gm) with coarse sand and granules. FA 9 overlies FA 8 with an undulating basal contact and extends beyond two prominent boulders (Figure 4.29). This FA contains massive, well-sorted fine to medium sand (Sm) with lenses of coarse sand (Sh).

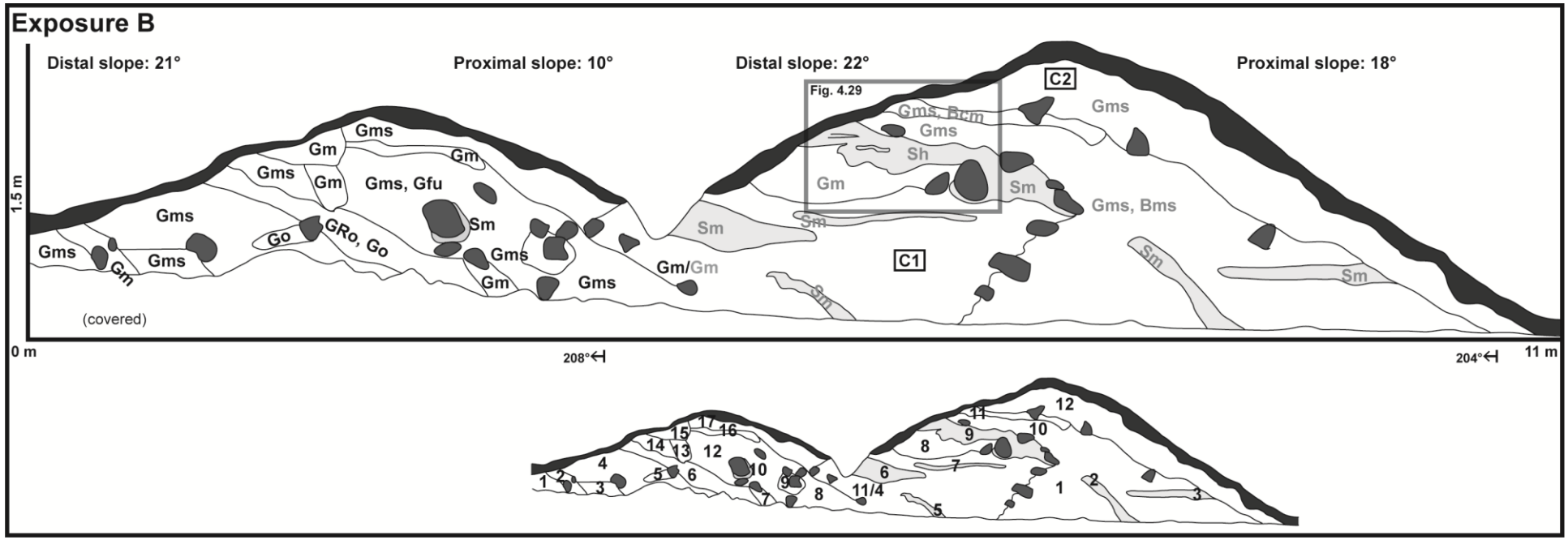

Figure 4.28. Exposure B representative log. FAs are labelled with facies codes (top) and FA numbers (bottom) and are described in the text in stratigraphic order from bottom to top. Black codes label facies in the ice-distal exposure and grey codes label facies in the ice-proximal exposure. FA colours correspond to dominant grain-size class. Chapter 2 shows a facies codes and symbols key (Figure 2.6). Labelled boxes indicate approximate clast measurement locations. Labelled photograph location refers to the photograph in Figure 4.29.

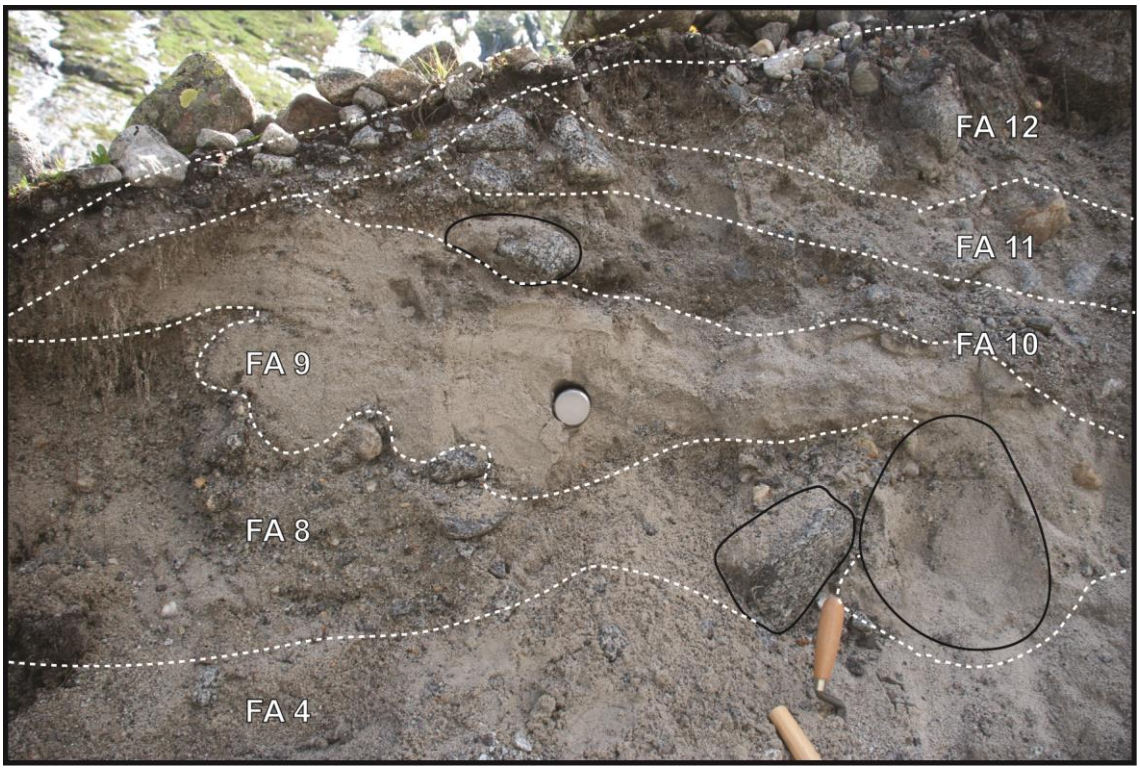

Figure 4.29. Photograph from Exposure B. This photograph corresponds to the indicated location on Figure 4.28. The photograph highlights the deformed contact between FA 8 and FA 9 of the ice-proximal landform. Dashed lines show contacts between FAs. Solid lines demarcated boulders. Trowel (23 cm long) and OSL tube (5 cm diameter) for scale.

FAs 10-12 (and perhaps FA 1) generally underlie the ridge crest and constitute the core of the landform. The boundary between FA 10 and FA 1 is unclear and diffusive. FA 10 contains massive, matrix-supported, moderately-sorted pebbles with some cobbles (Gms), with coarse sand to granules as the matrix. FA 11 is an approximately horizontal layer overlying FA 10 and contains massive, clast-supported, poorly-sorted cobbles to boulders (Gms, Bcm). FA 12 directly underlies the ridge crest and follows the proximal slope of the landform to the base of the exposure. This FA contains massive, clast-supported, poorly-sorted pebbles to cobbles (Gms) (maximum a-axis length 19.0 cm) with coarse sand to granules.

The ice-distal landform of Exposure B shows FA 16 and FA 17 capping the exposure and following the shape of the ridge crest and proximal slope. The ice-proximal landform shows FA 12 following the shape of the ridge crest and the proximal slope. Additionally, the ice-distal landform of Exposure B shows FA 2, FA 6, and FA 7 in the same orientation as the proximal slope, although this is less conclusive for FA 7 due to the small amount exposed, and the presence of the boulder at the top of the FA may have affected the orientation of the FA. The ice-proximal exposure of this landform shows that two distinct sand FAs, FA 2 and FA 5, follow the orientation of the proximal slope.

4.3.3. Exposure C

This moraine consists of one ridge on valley right that cannot be connected with confidence to any ridges on the other side of the modern channel (Figure 4.1). The ridge fragment hosting this exposure is 24 m long with an average width of 6 m, and the generally straight crestline has an average trend of 280°. The proximal and distal slopes are equal in length (3 m), however the proximal slope angle is steeper (30°), on average, than the distal slope (26°), although +/- 5° clinometer accuracy must be considered (Chapter 2). There is a notable accumulation of clasts on the valley floor along both the proximal and the distal slopes of the landform. Most of the exposure was created by erosion from the modern channel. Exposure C consists of 15 FAs and contains mostly gravel, with some sand (Figure 4.30).

FAs 1-4 are differentiated by dominant clast size, and the contacts between these FAs, where apparent, are dipping approximately following the morphology of the proximal slope. FA 1 is the lowest ice-distal FA and extends from the upper landform surface to below the exposure. This FA contains massive, clast-supported, poorly-sorted pebbles and cobbles (Gm) with coarse sand. FA 2 overlies FA 1 and extends from the soil to below the exposure. This FA consists of massive, clast-supported boulders (Bcm) with coarse sand. FA 3 overlies FA 2 and extends from the soil to below the exposure. This FA contains clast-supported, poorly-sorted pebbles to cobbles (Gm, Gh), with coarse sand. Vague horizontal beds are noticeable towards the bottom contact with FA 2. FA 4 overlies FA 3 and extends from the soil to below the exposure. This FA contains clast-supported boulders (Bh) with coarse sand, and some horizontal beds are noticeable. The basal contact with FA 3 is vague. The longest exposed axis of the largest boulder in this FA is 28 cm.

In contrast to the previous four FAs, FA 5 consists of massive, matrix-supported, poorly-sorted pebbles to cobbles (Gms) with poorly-sorted coarse sand to granules as the matrix. FA 5 overlies FA 4 and extends from the soil zone to below the exposure, and also shares contacts with FA 6 and FA 7 at its lower ice-proximal end.

FA 6 contains massive, openwork, poorly-sorted pebbles and few cobbles (Go) and describes a vague channel structure at the bottom of the exposure. FA 7 overlies FA 6 and is easily distinguishable as the dominant sand layer in the exposure and consists of poorly-sorted, fine to medium sand with few pebbles and poorly-sorted coarse sand to granule lenses (Sh). The most ice-distal zone contains planar-dipping beds and also describes a vague channel form. The contact between FA 7 and FA 8 is not apparent; however, FA 8 differs from FA 7 in that it contains no bedding or distinguishable lenses and instead contains massive, poorly-sorted fine to medium sand with few cobbles (Sm).

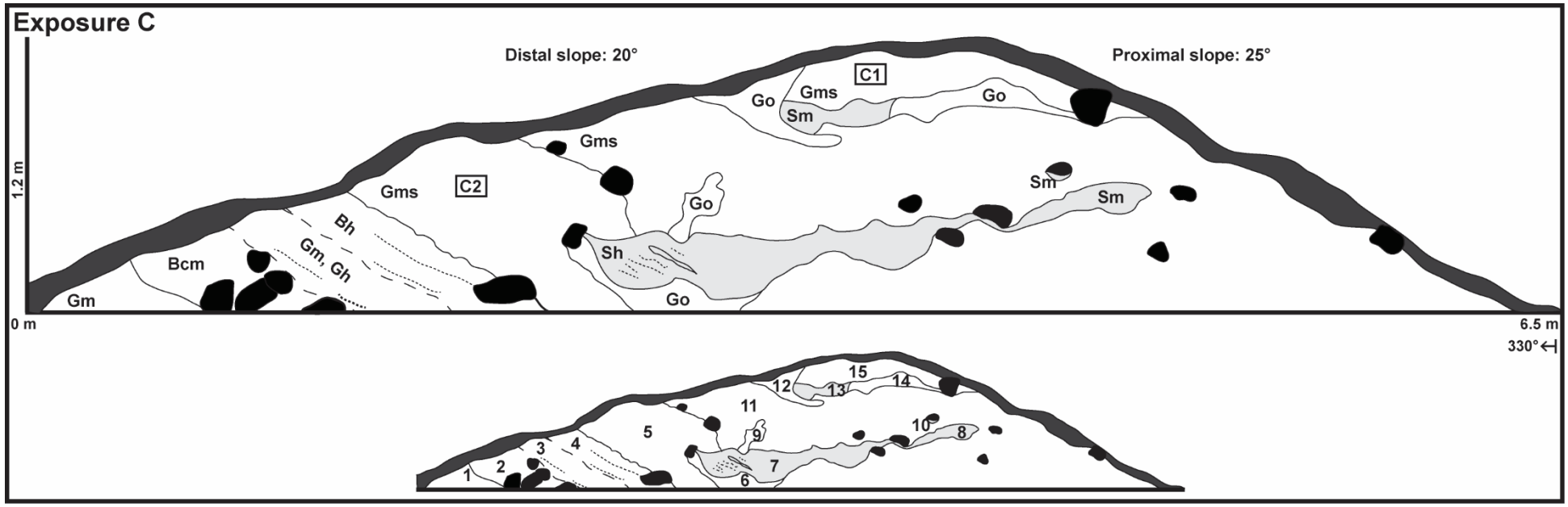

Figure 4.30. Exposure C representative log. FAs are labelled with facies codes (top) and FA numbers (bottom) and are described in the text in stratigraphic order from bottom to top. FA colours correspond to dominant grain-size class. Chapter 2 shows a facies codes and symbols key (Figure 2.6). Labelled boxes indicate approximate clast measurement locations.

FA 9 is a small pocket of massive, openwork, moderately-sorted pebbles and cobbles (Go) that is largely contained by FA 11 but also shares a basal contact with FA 7. FA 10 is a small pocket of massive, poorly-sorted medium to coarse sand (Sm) with few pebbles under a boulder in the ice-proximal side of the exposure.

FA 11 dominates the exposure and contains FAs 7-10. FA 11 contains massive, matrix-supported, moderately-sorted pebbles to cobbles (Gms), with moderately-sorted medium to coarse sand as the matrix. FAs 12-14 comprise the ridge-crest zone of the exposure. FA 12 extends from the soil zone to below FA 13 and is a pocket of massive, openwork, moderately-sorted pebbles with some cobbles (Go). FA 13 extends from FA 12 on its ice-distal side to FA 14 on its ice-proximal side. This FA consists of massive, poorly-sorted coarse sand with some medium sand and cobbles (Sm). FA 14 extends from FA 13 in the centre of the exposure to a prominent boulder and contains massive, openwork, moderately-sorted pebbles and few cobbles with minimal granules (Go). FA 15 immediately underlies the ridge crest and contains massive, matrix-supported, poorly-sorted pebbles and some cobbles (Gms), with poorly-sorted coarse sand to granules as the matrix.

4.3.4. Exposure D

This moraine consists of one ridge that may be connected with a ridge on the other side of the modern channel (Figure 4.1). The landform hosting Exposure D is 19 m long with a trend of 305°. The exposure, however, is not perpendicular to the ridge crest and is instead an oblique cut through the landform due to the location of the main channel, which partially excavated this face. Therefore, the width of the full ridge could not be measured. The distal slope, however, was 3 m long in a representative location. The average proximal slope of the landform was 28°, and the average distal slope was 20°, although +/- 5° clinometer accuracy must be considered (Chapter 2). Exposure D contains six gravel FAs differentiated by clast size and matrix material (Figure 4.31) and two prominent boulders (Figures 4.31).

FA 1 is a small zone at the base of the exposure that contains massive, matrix-supported, moderately-sorted pebbles (Gms), with well-sorted medium sand as the matrix. FA 2 is a pocket between the two boulders that contains massive, matrix-supported, moderately-sorted pebbles and few cobbles (Gms), with poorly-sorted medium to coarse sand with some granules as the matrix. FA 3 overlies two boulders. This FA contains massive, matrix-supported, moderately-sorted pebbles (Gms), with poorly-sorted medium to coarse sand and some fine sand as the matrix. FA 4 extends from a boulder to the ice proximal end of the exposure and below the base of the exposure.

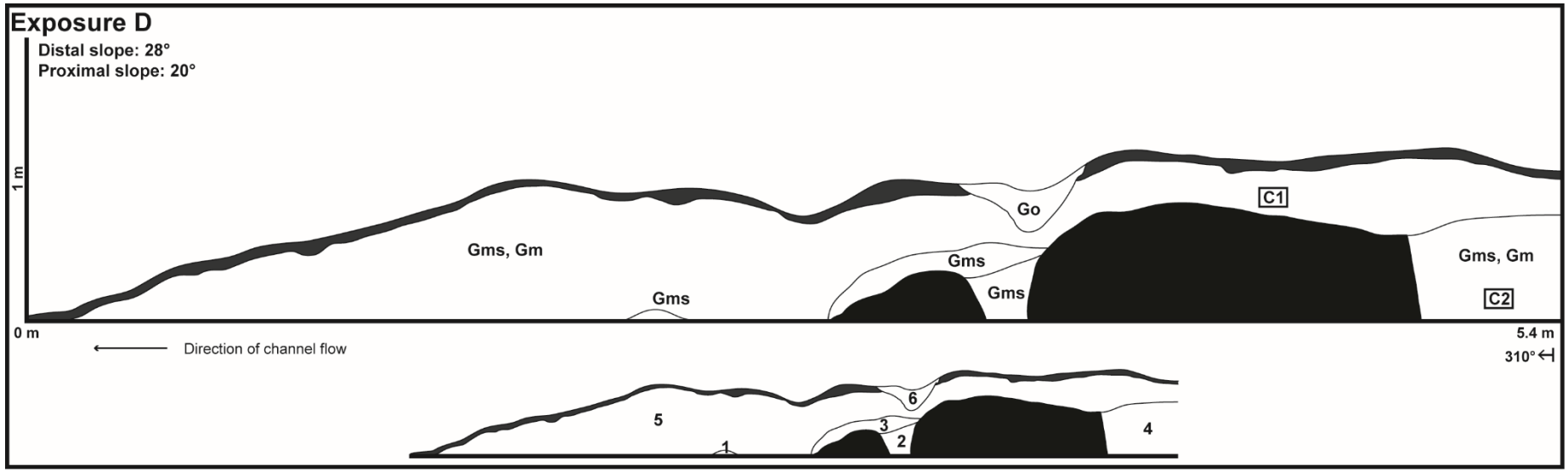

Figure 4.31. Exposure D representative log. FAs are labelled with facies codes (top) and FA numbers (bottom) and are described in the text in stratigraphic order from bottom to top. FA colours correspond to dominant grain-size class. Chapter 2 shows a facies codes and symbols key (Figure 2.6). Labelled boxes indicate approximate clast measurement locations.

This FA contains dominantly massive, matrix-supported, poorly-sorted pebbles to cobbles with some granules (Gms), with moderately-sorted medium to coarse sand as the matrix, and some massive, clast-supported, poorly-sorted pebbles to cobbles with medium to coarse sand and some granules (Gm). FA 5 dominates the exposure and consists of dominantly massive, clast-supported, poorly-sorted pebbles to cobbles with medium to coarse sand and some granules (Gm) and some massive, matrix-supported, poorly-sorted pebbles to cobbles with some granules (Gms), with poorly-sorted medium to coarse sand as the matrix. FA 6 is a wedge of massive, openwork, moderately-sorted cobbles with few pebbles (Go) that interrupts the otherwise continuous soil zone of the exposure.

Figure 4.32. Photograph from Exposure D. This photograph shows the two prominent boulders in the exposure and surrounding sediment (Figure 4.31). Trenching tool for scale (39.5 cm long).

4.3.5. Exposure E

This moraine consists of one ridge on valley-left that cannot be connected with confidence to any ridges on the other side of the modern channel (Figure 4.1). The moraine hosting Exposure E is 25 m long with an average width of 9.5 m, and the generally straight crestline trends 30°. The proximal slope is 22° and the distal slope is 18° as measured at the exposure, although +/- 5° clinometer accuracy must be considered (Chapter 2). Clast accumulation was noticeable on the valley floor along both proximal and distal flanks, but was greater on the distal flank. The orientation of this landform in relation to the face that had already been exposed by fluvial erosion did not allow for a full cross-section profile to be excavated, and the most ice-proximal portion of the landform therefore remains covered.

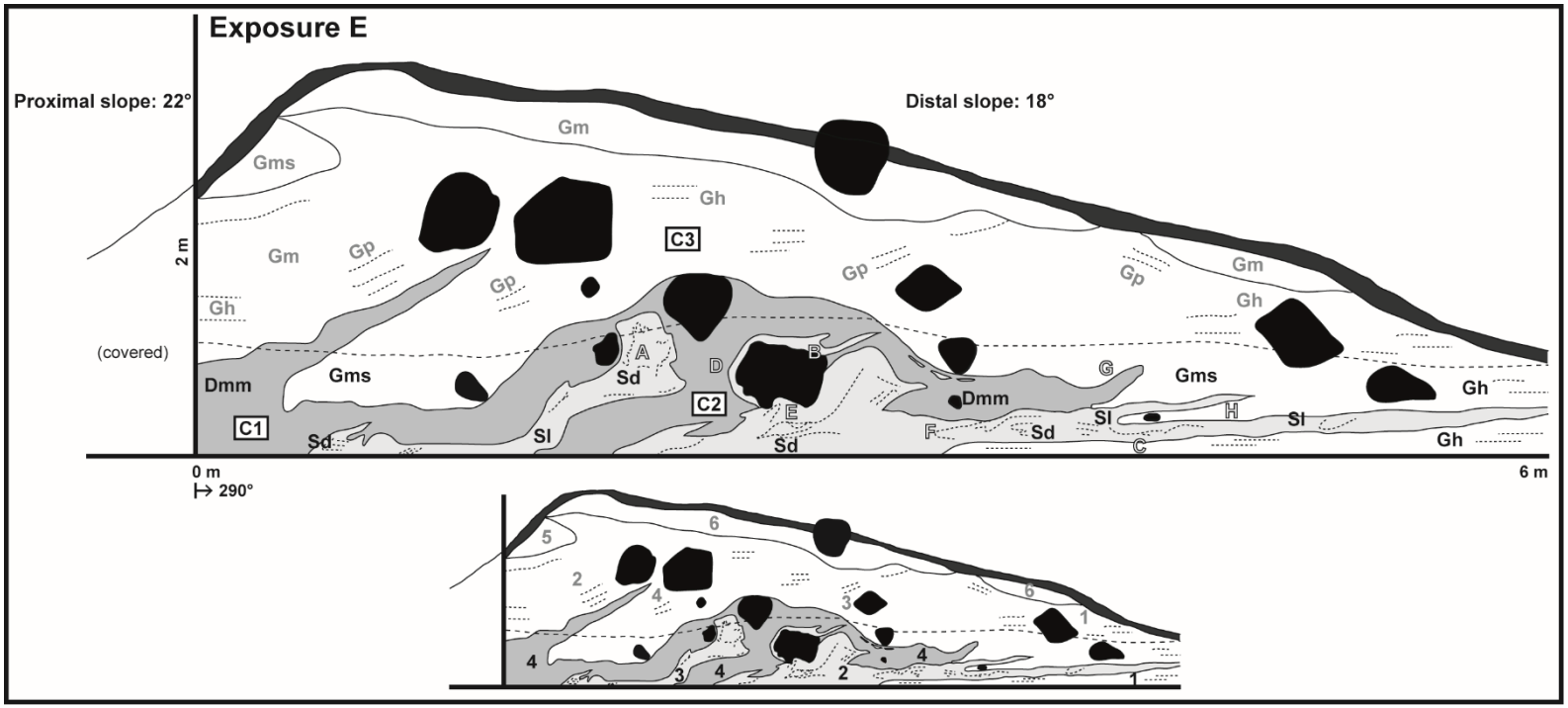

Figure 4.33. Exposure E representative log. FAs are labelled with facies codes (top) and FA numbers (bottom) and are described in the text in stratigraphic order from bottom to top. Black codes indicate the underlying sediment, grey codes indicate the moraine FAs. FA colours correspond to dominant grain-size class. Chapter 2 shows a facies codes and symbols key (Figure 2.6). Labelled boxes indicate approximate clast measurement locations. Photograph locations refer to photographs in Figure 4.34.

Exposure E consists of 10 FAs total and contains gravel, sand, and diamicton. FAs are labelled in two distinct groups, from bottom to top: FAs 1-4 of the underlying sediment and FAs 1-6 of the moraine sediment (Figure 4.33).

The sediment underlying the landform contains four different FAs. FA 1 is the lowermost ice-distal FA, is massive in places and horizontally-bedded in others, and contains clast-supported, poorly-sorted granules to pebbles with some cobbles and coarse sand (Gm, Gh) (Figure 4.34A). FA 2 overlies FA 1 towards the ice-distal part of the exposure and extends below the exposure elsewhere. This FA contains well-sorted fine to medium sand with horizontal (Sl) and deformed planar laminations (Sd) (Figure 4.34A-F). FA 3 contains the same sediment as FA 2, and also extends below the exposure towards the ice-proximal extent. FA 2 and FA 3 may be the same sand package, but the relationship is not seen due to the depth of exposure (Figure 4.34G).

FA 4 forms the base of the ice-proximal extent of the exposure and extends towards the ice-distal extent of the exposure while interfingering with FA 2 and FA 3. This massive diamicton FA contains zones of matrix-supported, poorly-sorted cobbles (Dmm). The matrix varies from silt to fine sand. This FA is consolidated and fissile, and is therefore considered till (Figure 4.34G-H).

The exposure contains six FAs of the moraine landform that overlie the aforementioned underlying four FAs. Sharp contacts between FAs differentiate FA 8 and FA 9 from the others, whereas the other FAs are distinguishable based only on dominant composition, due to the very friable nature of the sediments. Therefore, this may be considered one larger gravel deposit. The descriptions below are provided to emphasize sediment characteristics varying throughout the exposure.

FA 1 is the lowest FA and exists in the ice-distal part of the exposure. This FA consists of matrix-supported, moderately-sorted pebbles to cobbles with vague horizontal bedding near the base of two boulders (Gh) and vague, dipping planar beds towards the upper extent of the landform (Gp). The matrix is composed of poorly-sorted medium to coarse sand. This FA extends below the landform and interfingers with FA 2 and FA 4 of the underlying sediment. FA 2 is the lowest FA of the ice-proximal part of the landform. This FA contains clast-supported, poorly-sorted pebbles to cobbles with coarse sand to granules. FA 2 shows some planar dipping beds (Gp) and some horizontal beds (Gh) but is otherwise massive. FA 3 is a zone near the centre of the exposure and contains matrix-supported, moderately-sorted pebbles to cobbles with some dipping beds (Gp), with poorly-sorted medium to coarse sand as the matrix. FA 4 contains matrix-supported, moderately-sorted pebbles to cobbles with some clast-supported zones (Gh, Gp). The matrix, where present, varies between well-sorted coarse sand and moderately-sorted medium to coarse sand. This FA

contains some horizontal bedding towards the top of the exposure and planar bedding under a boulder.

Figure 4.34. Photographs from Exposure E. Photographs correspond to the indicated locations on Figure 4.33. These photographs highlight deformation structures in sand FAs and the contacts between various FAs of the underlying sediment. Thicker dashed lines show contacts between FAs, thinner lines show laminations. Pencil (14.7 cm long), trowel (23 cm long), and lens cap (4.2 cm diameter) for scale.

This FA extends below the landform, sharing a contact with underlying FA 4. FA 5 is a wedge of massive, matrix-supported, moderately-sorted pebbles (Gms), with a silt matrix, towards the upper ice-proximal side of the exposure. FA 6 underlies the ridge crest and most of the upper surface of the landform. FA 6 contains massive, clast-supported, moderately-sorted pebbles to cobbles with coarse sand (Gm) and has an orientation that follows the ridge crest but thins to the distal end of the exposure.

FA 6 of the landform caps the other FAs and follows the shape of the ridge and the distal slope. Additionally, some beds in gravel FAs 2-4 of the moraine landform trend vaguely in the same orientation as the proximal slope. By contrast, some vague horizontal bedding of gravel in FAs 1-4 of the moraine landform is maintained. These FAs are individually differentiated from surrounding FAs by the dominant facies present, with diffusive and unclear boundaries between.

4.3.6 Clast characteristics of control and moraine samples

All clast measurement data can be found in Appendix B. Clasts were measured from six different control environments (Figure 4.35). Alluvial fans may provide sediment to the valley bottom that may be incorporated into minor moraines, and are therefore included as control clasts (Chapter 2). Clasts from bedrock-derived talus are dominantly sub-angular, with some angular and sub-rounded and few very angular clasts. The RA values are 30% and 28%, and the C_{40} values are 28% and 34%. All RWR values are 0% (Figure 4.36). Clasts in the modern channel are dominantly sub-angular, with significant sub-rounded clasts and some angular clasts. The RA values are 6% and 28%, and the C_{40} values are both 14%. All RWR values are 0% (Figure 4.36). Clasts in the alluvial fans are dominantly sub-angular, with some sub-rounded and angular clasts. The RA values are 26% and 16%, and the C_{40} values are both 18% and 20%. All RWR values are 0% (Figure 4.36).

Subglacial clasts are dominantly sub-angular, with frequent sub-rounded clasts, few angular clasts, and negligible rounded clasts. The RA values range from 0% to 30%, and the C_{40} values range from 4% to 26% (Figure 4.37). Supraglacial clasts are dominantly angular, with some very angular clasts, few sub-angular clasts, and negligible sub-rounded clasts. The RA values range from 74% to 100%, and the C_{40} values range from 70% to 80%. All RWR values are 0% (Figure 4.37).

Clasts were measured in 11 locations in the five exposed moraines. Clasts in the FA 3 diamicton of Exposure A range from angular to sub-rounded, but are dominantly sub-angular, and have an RA index of 20% and a C_{40} index of 36% (Figure 4.38). Clasts in the FA 7 gravel were measured in the massive zone of this FA and range from angular to sub-

rounded, but are dominantly sub-angular, with an RA index of 6% and a C40 index of 2% (Figure 4.38)

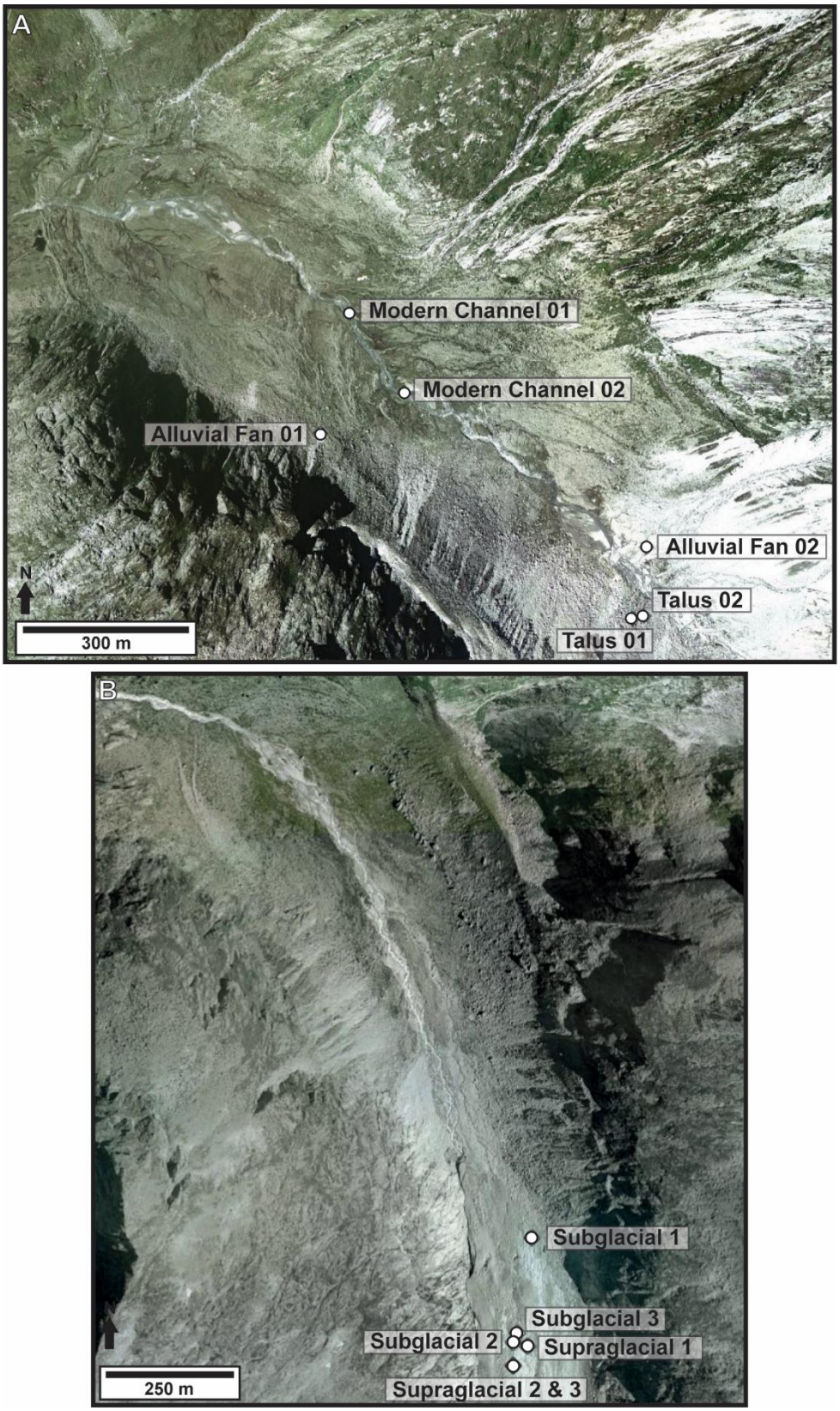

Figure 4.35. Locations of all clast measurement control samples from the Schwarzensteinkees and Hornkees forelands. A.) Environments sampled in the Schwarzensteinkees foreland include: modern channel, alluvial fan, and talus. B.) Subglacial and supraglacial clasts were measured in the Hornkees valley, as they were not accessible in the Schwarzensteinkees valley. Fifty clasts were measured at each location. Imagery obtained from Google Earth (Geoimage Austria and Google Earth, 2014).

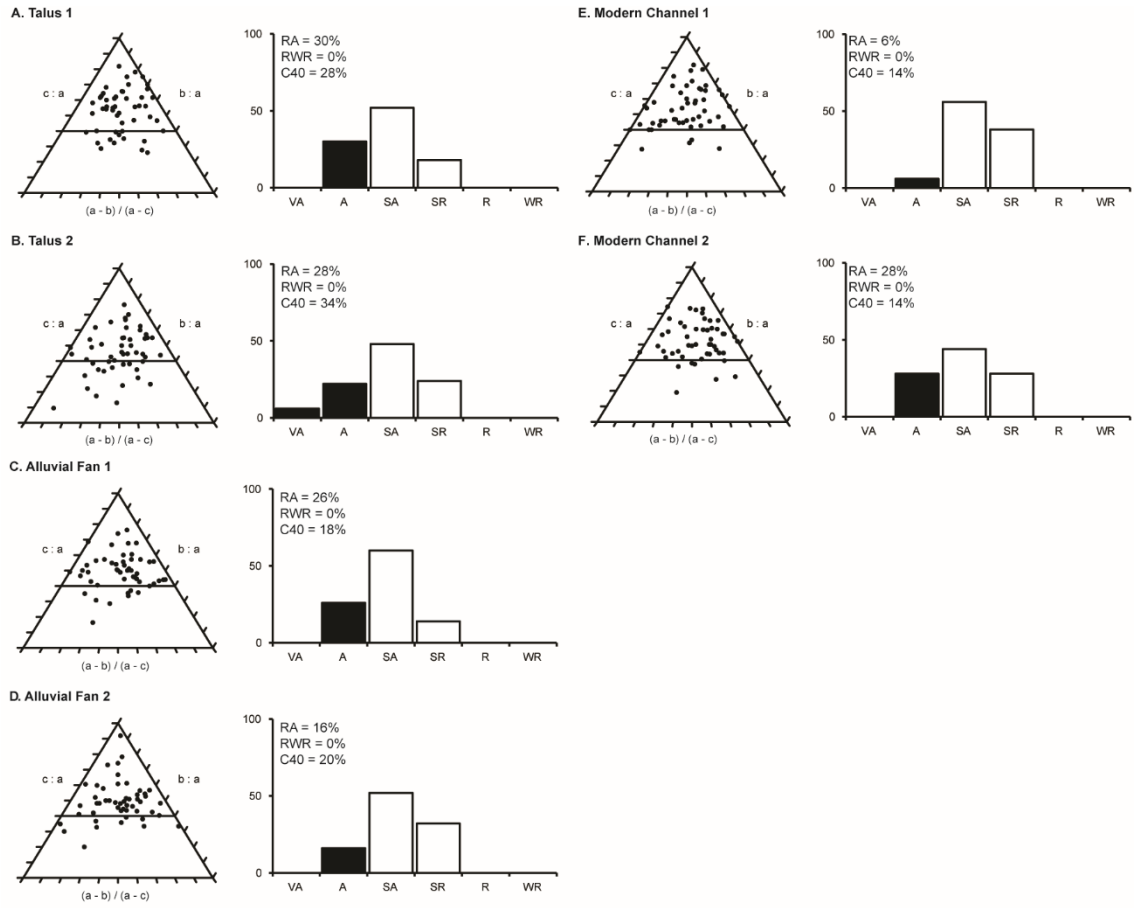

Figure 4.36. Clast measurement data for non-glacial control samples in the Schwarzensteinkees foreland. Sample locations are indicated on Figure 4.35A.

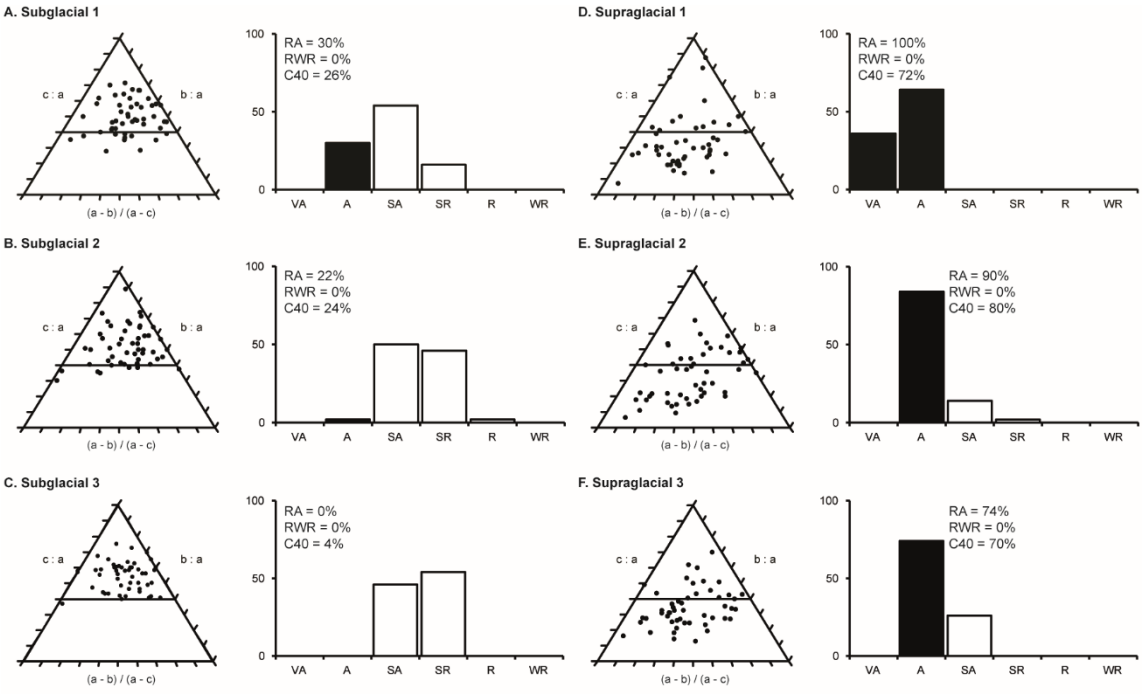

Figure 4.37. Clast measurement data for glacial control samples in the Hornkees foreland. Sample locations are indicated on Figure 4.35B.

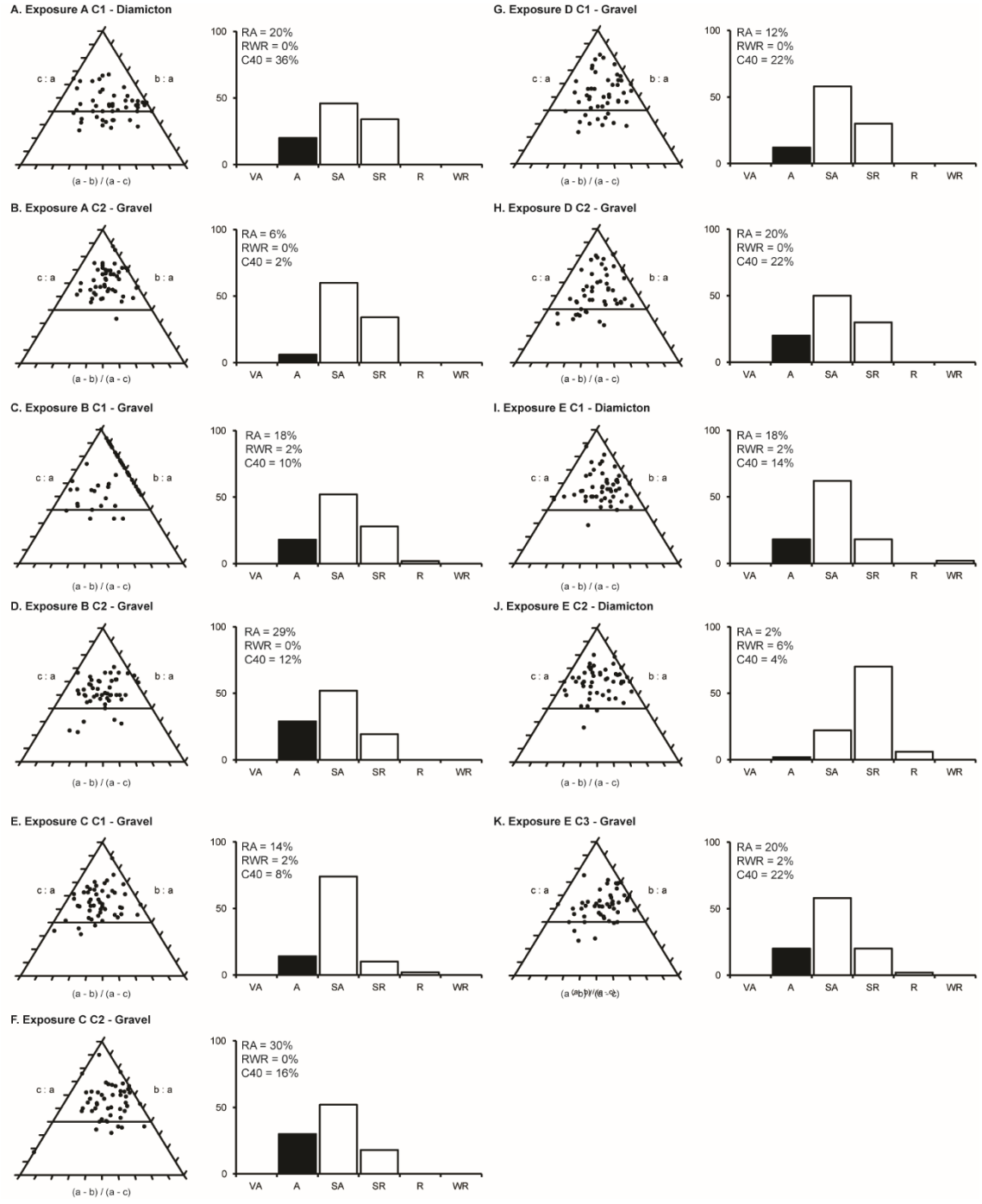

Figure 4.38 Clast measurement data for all exposures through moraines in the Schwarzensteinkees foreland. Sample locations are indicated on corresponding exposure logs.

Clasts from Exposures B, C, and D were sampled from gravel FAs. Clasts in FA 11 of Exposure B range from angular to rounded, but are dominantly sub-angular (Figure 4.38) and have an RA index of 18%, an RWR index of 2%, and a C_{40} index of 10%, and clasts in FA 12 range from angular to sub-rounded, but are dominantly sub-angular and have an RA index of 29% and a C_{40} index of 12% (Figure 4.38). Clasts in FA 5 of Exposure C range from angular to rounded, but are dominantly sub-angular and have an RA index of 14%, an RWR

index of 2%, and a C_{40} index of 8% (Figure 4.38), and clasts in FA 15 range from angular to sub-rounded but are dominantly sub-angular with an RA index of 30% and a C_{40} index of 16% (Figure 4.38). Clasts from FA 4 of Exposure D range from angular to sub-rounded, but are dominantly sub-angular and have an RA index of 20% and a C_{40} index of 22% (Figure 4.38). Clasts from FA 5 range from angular to sub-rounded, but are dominantly sub-angular and have an RA index of 12% and a C_{40} index of 22% (Figure 4.38).

Clasts from Exposure E were measured from a diamicton FA and a gravel FA. Two locations of FA 4 of the underlying sediment were sampled. In the first location, clasts range from angular to well-rounded, but are dominantly sub-angular with an RA index of 18%, an RWR index of 2%, and a C_{40} index of 14% (Figure 4.38). In the second location, clasts range from angular to rounded, but are dominantly sub-rounded with an RA index of 2%, an RWR index of 6%, and a C_{40} index of 4% (Figure 4.38). Clasts were also sampled from gravel FA 4 of the moraine sediment, and range from angular to rounded, but are dominantly sub-angular with an RA index of 20%, an RWR index of 2%, and a C_{40} index of 22% (Figure 4.38).

4.3.7 Exposure F

The downvalley margin of FZ 2 on valley right was trampled by horses, creating a sand pit with a sharp wall on its downvalley side (Figure 4.1). Part of this wall was excavated and revealed six distinct FAs, dominantly composed of sand (Figure 4.39).

FA 1 comprises the lower section and majority of the exposure. FA 1 contains dominantly poorly-sorted fine to coarse sand, but also lenses, pockets, and strands of openwork granules (GRo) and massive granules (GRm). The sand is laminated in places and massive (Sm) in others, and the laminations are deformed by folding throughout the exposure (Sd) (Figure 4.40A-D). FA 2 is a lens of massive, poorly-sorted granules (GRm) and pebbles (Gm) that arches up towards the top of the exposure towards the right (Figure 4.40E). FA 3 is a lens of laminated, well-sorted silt (Fl) and fine sand (Sd) with deformed laminations that follows the same shape as underlying FA 2 (Figure 4.40E). FA 4 is a lens of moderately-sorted, massive medium to coarse sand (Sm) towards the left of the exposure (Figure 4.40E), with planar bedding towards the right of the FA (Sp). This FA also contains a pod of openwork granules (GRo). FA 5 spans much of the upper exposure and comprises laminated, moderately-sorted silt (Fl) and fine to medium sand (Sl). The laminations are deformed through folding towards the left of the exposure (Sd/l, Fd/l) with a lens of massive sand (Sm). The laminations are approximately horizontal throughout the rest of the exposure (Sl, Fl). FA 6 overlies FA 5 on the right side of the exposure and comprises laminated, well-sorted silt and fine to medium sand, although dominantly sand in planar cross-beds (Sc) (Figure 4.39F).

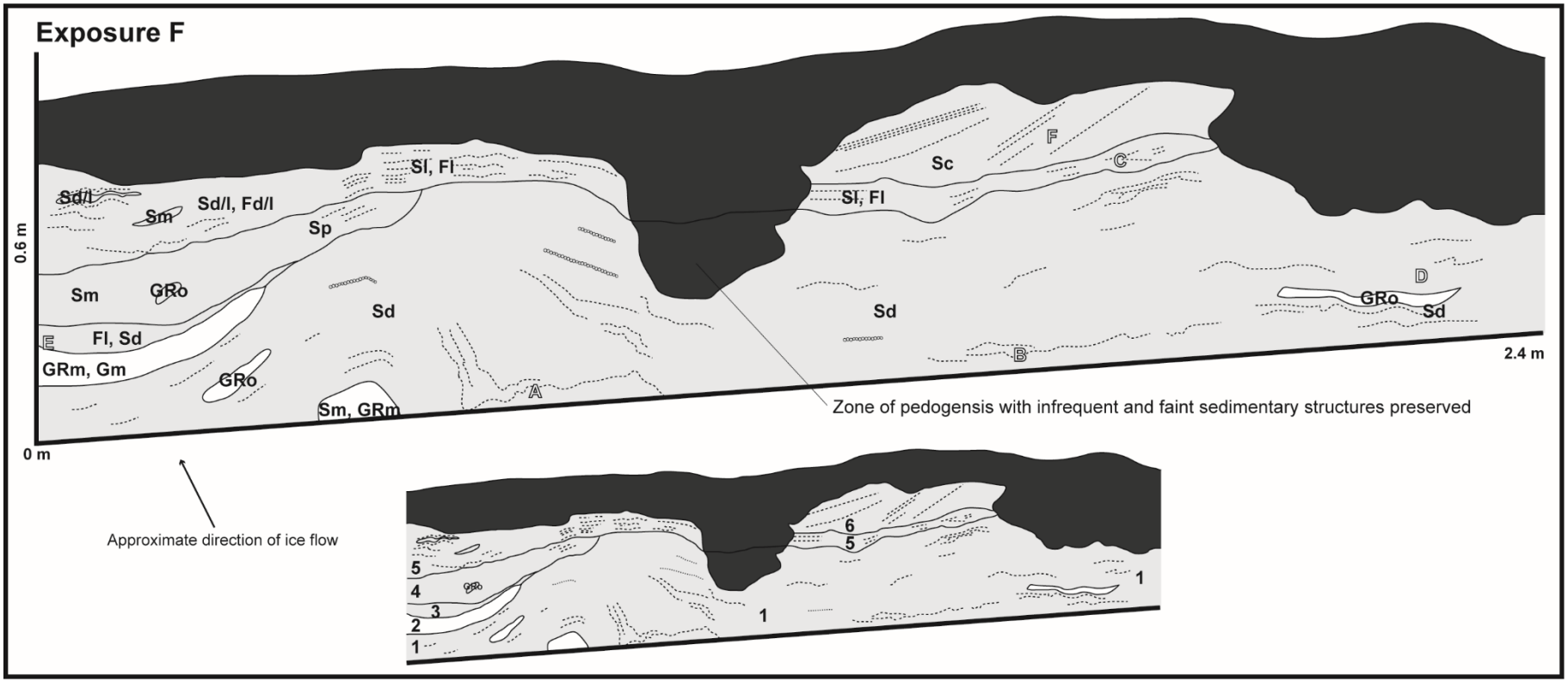

Figure 4.39. Exposure F representative log. FAs are labelled with facies codes (top) and FA numbers (bottom) and are described in the text in stratigraphic order from bottom to top. FA colours correspond to dominant grain-size class. Chapter 2 shows a facies codes and symbols key (Figure 2.6). Photograph locations refer to photographs in Figure 4.40.

Figure 4.40. Photographs from Exposure F. Photographs correspond to the locations indicated on Figure 4.39. A-D only show FA 1. Thicker dashed lines show contacts between FAs, thinner lines show laminations. Pencil for scale (14.7 cm long).

4.4 Synthesis

Mechanisms of minor moraine formation are the primary focus of this research in the Schwarzensteinkees foreland. The following sections first present conceptual models of minor moraine formation, by integrating interpretations of the sedimentological composition of individual moraines with general models of formation. The mechanisms of formation then lead to consideration of the greater geomorphological evolution of the foreland and how this influenced moraine formation and the extant landform configuration.

4.4.1 Mechanisms of minor moraine formation in the Schwarzensteinkees foreland

All exposures contain recurring FAs, dominated by gravel units, with some sand units, characterised with varying degrees of bedding, sorting, and deformation structures and varying clast and grain sizes. These FAs are interpreted as outwash, due to differences in clast and grain sizes representing deposition through varying flow velocities influencing stream competence or carrying capacities (Knighton, 1998; Benn and Evans, 2010) and in different depositional settings within a proglacial fluvial system (Church and Gilbert, 1975; Rust, 1975; Brodzikowski and van Loon, 1991; Knighton, 1998; Maizels, 2002; Benn and Evans, 2010).

Clast measurements support interpretation of a proglacial outwash origin of these sediments, as the roundness and form of gravel in the exposures most closely compares to the modern channel control samples (Figures 4.35-4.37). The gravels in the exposures and fluvial control samples are dominantly blocky and sub-angular, with significant sub-rounded clasts (Figure 4.38). Clasts from diamicton FAs are also dominantly blocky and contain significant sub-angular and sub-rounded clasts (Figure 4.38). These characteristics of both gravel and diamicton clasts from the exposures agree with those of the fluvial control samples (Figure 4.36) and are also similar to those from the subglacial control samples (Figure 4.37). Other non-glacial control samples are also dominantly blocky, however with more variation and more platy and elongated clasts (Figure 4.36). Supraglacial clasts are the most distinct of any sample, with a high concentration of platy clasts compared to any other sample, as reflected in the highest C_{40} values of any clasts measured (Figure 4.37).

The C_{40} versus RA covariance diagram further illustrates the similarities between exposure, modern channel, and subglacial clasts (Figure 4.41). The exposure clasts are clustered near the modern channel clasts, with some relationship to alluvial fan and subglacial clasts as the C_{40} value increases. The majority of exposure samples appear distinctly unrelated to the supraglacial and talus control samples. The C_{40} versus RWR covariance diagram is less effective at illustrating relationships between the samples, as few rounded and well-rounded clasts were present. This diagram does, however, further emphasize the distinct dissimilarity of supraglacial clasts to others measured (Figure 4.41).

The comparison of clast shape and roundness between exposure clasts and control clasts shows that exposure clasts are most similar to clasts from the modern, proximal, proglacial channel and subglacial samples collected beneath Hornkees. This relationship is consistent with push moraines formed from pre-existing proximal proglacial outwash sediment, in which sediment is transported from beneath the glacier to the foreland through the glaciofluvial system and then pushed into a moraine by advancing ice. This could

indicate that the clasts are therefore experiencing two environments that produce similar shapes and roundness, which signatures overprint those from other points of origin (e.g. supraglacial) or that considerable fluvial reworking that would have formed more rounded and well-rounded clasts played a limited role in this environment due to ice-proximal outwash deposition. Similarity between fluvial and subglacial samples of a catchment in a high-mountain setting has been previously described for high-mountain areas (Lukas et al., 2013), and also specifically for Findelengletscher in the Swiss Alps, which is echoed by the present study in the Schwarzensteinkees foreland.

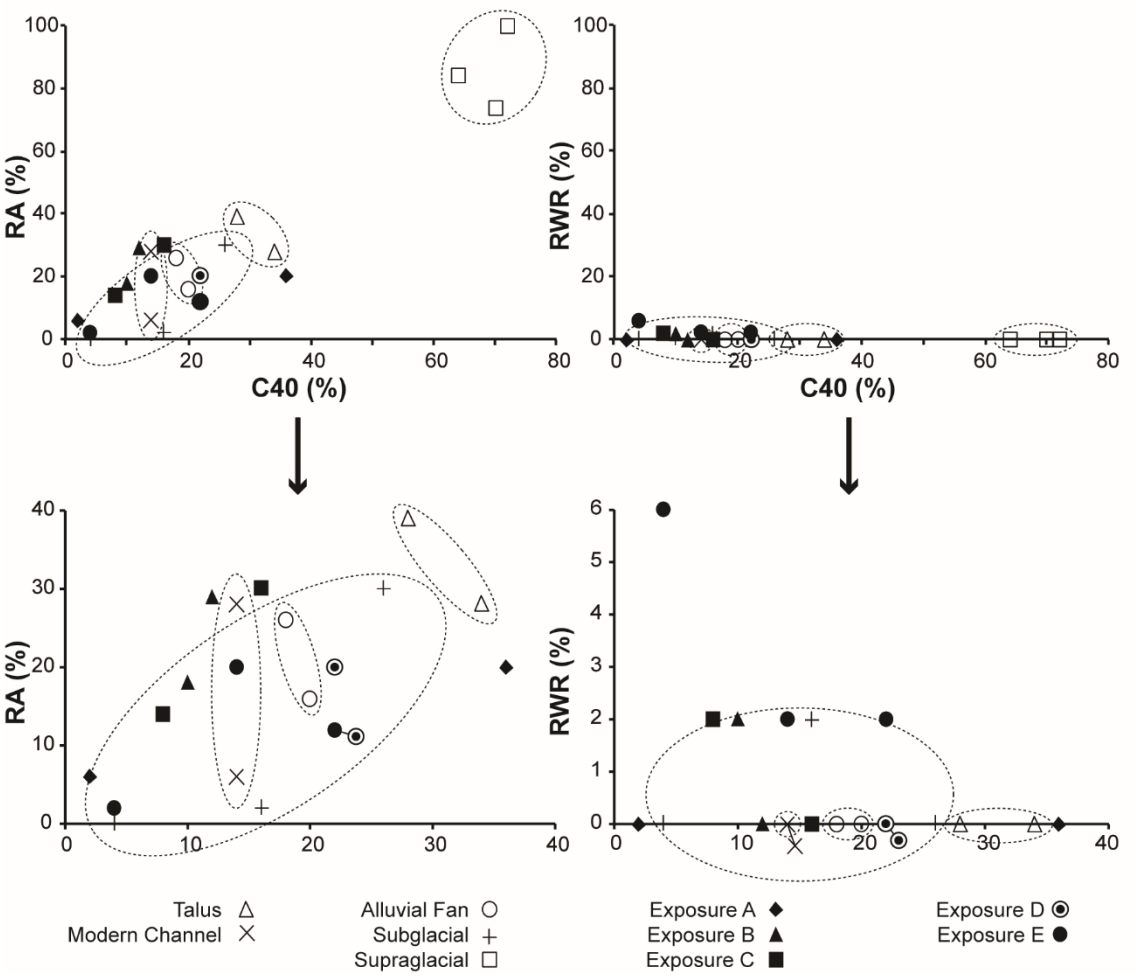

Figure 4.41. RA versus C_{40} and RWR versus C_{40} covariance plots for all clast measurements. Each data set has a unique symbol; control samples have no fill, whereas exposure samples are filled. Dashed lines group control samples as envelopes. Refer to ternary diagrams and histograms for clasts samples from control environments (Figures 4.35-4.36) and exposures (Figure 4.38) for more specific information.

The geomorphological expression of moraines in the Schwarzensteinkees foreland cannot alone be used to interpret mechanisms of moraine formation. When considering minor moraines formed solely through pushing, several authors describe dominantly

steeper distal slopes (Boulton, 1986; Lukas, 2012; Bradwell et al., 2013) or symmetrical slopes (Hewitt, 1967; Lukas, 2012; Chandler et al., 2016a). However, moraine slopes are not always diagnostic of formation mechanisms, and steeper distal slopes have also been noted for minor moraines formed through freeze-on (Andersen and Sollid, 1971; Krüger, 1995; Matthews et al., 1995) and squeezing mechanisms (Price, 1970; Sharp, 1984; Bradwell, 2004; Chandler et al., 2016a). It is also important to note that post-depositional modification through erosion (see Chapter 8) may have altered original morphologies of these moraines, whereas stabilization, in the Schwarzensteinkees foreland notably through soil development and plant colonization, may have helped preserve original moraine morphologies.

The crestline bifurcation of the Exposure B moraine supports interpretations of a dynamic and oscillating ice margin, which has already been noted by the presence of the groups of closely spaced minor moraines in this foreland. This crestline bifurcation may therefore support push moraine formation, albeit in one isolated incident in the foreland, as crestline bifurcations represent differential retreat or advance along the ice front (Bennett and Boulton, 1993; Lukas, 2007; Boston, 2012). When part of the ice front advances beyond the rest, while pushing sediment, and encounters an extant moraine, the newly forming moraine can be "welded" onto the older moraine, creating two distinct ridges that appear joined where the ice front was stable (Benn and Lukas, 2006; Boston, 2012).

The sedimentological analysis of moraine exposures provides more specific evidence and support for mechanisms of moraine formation. Sedimentological evidence reinforces and refines interpretations of some pushing of proglacial outwash sediment and also show evidence for how till is incorporated into one of the exposures. Although not all of the moraines in the Schwarzensteinkees foreland could be exposed for sedimentological analyses, the five minor moraines exposed for further analysis form a representative sample of the moraines in the foreland, supported by observations of their sedimentology in test excavations and the geomorphology of all moraines in the valley. Both the downvalley set and upvalley set of minor moraines are represented, with Exposure A as part of the downvalley group of moraines and Exposures B-E in the upvalley group. Four of the five exposures have similar sedimentological compositions and are dominantly composed of gravel from the outwash plain, with some sandy and few diamictic FAs.

Sedimentological descriptions and the discussion of deformation and lack thereof in the Schwarzensteinkees minor moraines allows for interpretation of two general mechanisms of moraine formation: push and a combined push and freeze-on mechanism. The following steps and conceptual models describe these mechanisms of formation in the Schwarzensteinkees foreland.

4.4.1.1 Push of outwash sediment

Sedimentological analysis of four out of the five moraines investigated shows a pure pushing mechanism of formation, Exposures A-D reveal similar deformation structures that support push moraine formation, as well as sediment that appears undisturbed from its original depositional architecture, which may also help support pushing.

Deformation structures

Deformation structures support push moraine formation of the Schwarzensteinkees minor moraines. Push moraine formation inherently involves the glacier pushing material from upvalley, which should be reflected in the orientation of deformation structures within the moraines. Several similarities in the sedimentary architectures of the minor moraines suggest similar mechanisms of formation.

Most exposures have FAs or bedding within FAs that follow the shape of the ridge crest or mimic the orientation of the proximal slope. In Exposure A, the dominant trend of folded FA 9, the two primary limbs of folded FA 10, and the middle portion of folded FA 11 follow the shape of the proximal slope (Figure 4.26). In Exposure B, FA 2 and FA 5 of the upvalley landform are both small lenses that parallel the proximal slope orientation (Figure 4.28). Exposure E shows the ice proximal portion of FA 2 and FA 3, both of the sediment underlying the landform, mimicking the shape of the proximal slope. In the landform sediment, some bedding of FAs 2-4 also approximately parallels the proximal slope orientation (Figure 4.33). Bedding and fold limbs that mimic proximal slope orientation may represent destabilization of the moraine slope and reworking of the uppermost sediments following ice retreat (Bennett, 2001; Lukas, 2005; Benn and Evans, 2010; Lukas, 2012; Reinardy et al., 2013; Chandler et al., 2016a), yet still maintaining the contacts between beds of an outwash plain due to compositional differences (Church and Gilbert, 1975; Rust, 1975; Brodzikowski and van Loon, 1991; Knighton, 1998; Maizels, 2002; Benn and Evans, 2010).

Similarly, two exposures contain FAs that directly underlie and also follow the orientations of proximal or distal slopes and the ridge crest. This is particularly evident in the orientation of FA 14 of Exposure A, underlying and following the proximal slope orientation (Figure 4.26). This is also observed in FA 12 of the upvalley landform and FA 17 of the downvalley landform in Exposure B (Figure 4.28), which underlie the soil mantles of the proximal slopes and maintain the same orientation of the proximal slopes. This may represent post-depositional cascading of sediment down the slope of the landform following ice retreat and destabilization of the sediment pile (Bennett, 2001; Lukas, 2005;

Benn and Evans, 2010; Lukas, 2012; Reinardy et al., 2013; Chandler et al., 2016a). Exposure C shows FAs 13-15 capping the exposure and generally following the shape of the ridge crest (Figure 4.30). FAs that mimic the shape of the ridge crest and/or comprise the ridge crest or mimic proximal slope shapes, either in distinct sedimentary beds or limbs of individual folds, may have also developed orientations at right angles to ice flow as inferred from valley orientation and geomorphological relationships between the moraines and modern channel. The relationship between the ridge crests (geomorphology) and beds that mimic their shape (sedimentology) therefore shows a direction of principle compressional stress responsible for push moraine formation (e.g. Schlüchter et al., 1999; Lukas, 2012). In Exposure E, FA 6 of the moraine landform underlies the ridge crest and distal slope, and maintains the same orientation as the distal slope (Figure 4.33). This could support redistribution of that sediment down the distal slope during pushing and associated with more passive gravitation processes (Benn, 1992; Bennett, 2001; Lukas, 2005; Lukas, 2007; Benn and Evans, 2010; Lukas, 2012; Reinardy et al., 2013; Chandler et al., 2016a), but maintaining original depositional contacts on the outwash plain due to sedimentological differences that distinguish the FAs (Church and Gilbert, 1975; Rust, 1975; Brodzikowski and van Loon, 1991; Knighton, 1998; Maizels, 2002; Benn and Evans, 2010).

Additional examples of deformation occur in individual landforms, and dominantly in the upper and central zones of exposures. The presence of most folded layers in Exposure A in the upper half of the landform, with the exception of FA 9 (Figure 4.26, Figure 4.27), could represent the presence of distinct sedimentary FAs or beds or the friable nature of FA 7 not preserving deformation structures. Contacts between FAs that are quite undulating when compared to more generally straight contacts are not compatible with an original depositional architecture of an outwash plain (Brodzikowski and van Loon, 1991; Maizels, 2002) and may instead have several explanations. The geometry of the contact between the distinctly sandy FA 8 and gravel FA 9 in the ice-proximal section of Exposure B (Figure 4.30) suggests ductile density-driven soft-sediment deformation or dewatering structures, which would have occurred during loading of saturated sediment (Lowe, 1975; Johnson and Menzies, 2002). Another explanation is that deformation during push moraine formation influenced this contact more than others in the exposure due to the distinct differences in rheology between the two FAs. FAs spanning the centre of Exposure C may show slight deformation of the core of this landform (Figure 4.30). FAs 6-8 appear to have been deposited as channel forms on the outwash plain (Brodzikowski and van Loon, 1991; Maizels, 2002), and then slightly deformed during the bulldozing stage of push moraine formation (Figure 4.30). The orientation of FA 9 may simply represent a pocket of openwork gravel in a larger gravel FA of the outwash plain from this section of the channel, but this FA shows no tangible evidence of subsequent deformation (Figure 4.30). Lukas (2012) also

records increased deformation in the centre and increasing near the crestline of minor push moraines composed of bulldozed outwash sediment. The similarities between these two study areas, in which push moraines are composed of proglacial outwash sediment, suggests that this type of deformation may be common in high-mountain settings.

Lack of deformation structures

The lack of deformation structures, whether absence of faulting or FAs and bedding that maintain approximate original horizontality from deposition in the outwash plain (Church and Gilbert, 1975; Rust, 1975; Brodzikowski and van Loon, 1991; Maizels, 2002), may provide important information about the mechanisms of moraine formation, in addition to deformation structures.

Regarding Exposure D, the oblique cut of this exposure through the ridge and the gravel facies do not show deformation structures, revealing no specific support for push moraine formation (Figure 4.31) (Lukas, 2012; Chandler et al., 2016a). The massive structure may itself represent deformation from an original depositional architecture, which was not observed due to the friable nature of the FAs, or originally massive deposition in the outwash plain (Church and Gilbert, 1975; Rust, 1975; Brodzikowski and van Loon, 1991; Maizels, 2002; Benn and Evans, 2010).

Some exposures have FAs or bedding within FAs that maintain their original horizontal depositional orientations as part of the outwash plain (Church and Gilbert, 1975; Rust, 1975; Brodzikowski and van Loon, 1991; Maizels, 2002). Three FAs in Exposure A maintain horizontal bedding of an outwash plain (Church and Gilbert, 1975; Rust, 1975; Brodzikowski and van Loon, 1991; Maizels, 2002): FA 1-4 and FA 8 are all in the lower half of Exposure A (Figure 4.26), which suggests that these remained undisturbed as the higher FAs were pushed by the advancing glacier. Horizontal FAs in the lower half of Exposure B suggest that pushing during moraine formation did not deform these sediments relative to the upper sediments of the main body of the moraine (Figure 4.29). FA 11 in the upper half of ice-proximal Exposure B is generally horizontal, which could relate the sedimentology of FA 11 being less affected by force from bulldozing ice than the surrounding FAs, as it notably contains both gravel (Gms) and boulder (Bcm) FAs, whereas the others are gravel FAs with few boulders. Similarly, lack of deformation in massive FAs may suggest that their sedimentology simply does not preserve deformation structures (Lukas, 2012; Chandler et al., 2016a) or that they were originally deposited in the outwash plain as massive (Church and Gilbert, 1975; Rust, 1975; Brodzikowski and van Loon, 1991; Maizels, 2002; Benn and Evans, 2010). As already mentioned, Exposure E shows the rarely observable contact between underlying sediment (five FAs) and the sediments that comprise the moraine

landform (nine FAs) (Figure 4.33). The most distal part of this underlying sediment shows undeformed, horizontal contacts between sand and gravel outwash beds and similarly intact horizontal laminations and bedding of the FAs, thus maintaining the depositional architecture of the former outwash plain orientation and channel depositional regimes (Church and Gilbert, 1975; Rust, 1975; Brodzikowski and van Loon, 1991; Knighton, 1998; Maizels, 2002; Benn and Evans, 2010).

The persistence of horizontal bedding from original deposition in the proglacial fluvial system through push moraine formation implies lack of significant stresses in these sedimentary packages or increased cohesiveness of specific FAs. The horizontal FAs are dominantly found in the lower parts of the moraines. Sediments in Exposure A and Exposure E additionally maintain horizontal geometries at the most distal extent of the exposures. Stress and resistance both increase with depth, suggesting here that the resisting forces may have been greater than those imparted by the glacier and overlying sediments, resulting in perceived higher stability. Additionally or alternatively, the sedimentology of each facies may also determine whether horizontality was maintained during and after push moraine formation, where more cohesive and/or more compacted gravel layers resisted deformation more than surrounding sediments.

Exposure C appears to show preservation of the fluvial system by recording channel forms (Brodzikowski and van Loon, 1991; Maizels, 2002). Potential slight deformation in the core of this landform (FAs 6-8) was described above, however the general channel shape is maintained (Figure 4.30). The uppermost FAs (FAs 12-14) may also be related to the larger channel form as distinct sedimentological zones. The most ice-distal FAs in Exposure C all follow the same orientation, which also approximates the ice-distal shapes of FA 6 and FA 7 of the aforementioned channel form. This suggests that FAs 1-4 may represent part of a larger channel form that has been pushed and slightly altered into the moraine landform, but all the while maintaining the overall channel form. Alternatively, the distinct FAs 1-4 and their contacts may represent another mechanism of moraine formation unrelated to pushing, followed by a pushing component, explored as an alternate explanation in Section 4.5.1.2.

Only the sediment underlying the moraine at Exposure E shows faulting, whereas none of the other described exposures in the Schwarzensteinkees foreland contain noticeable faults. Reinardy et al. (2013) also note a lack of faulting in moraines composed of outwash in Norway, which they use to support the interpretation that these moraines were *not* formed through bulldozing. Lukas (2012), however, notes various types and locations of faulting in the moraine exposures in the Gornergletscher foreland, which are composed of similar sediments to the moraines of this study, and are also interpreted to have formed as minor push moraines. The sediments in the Gornergletscher moraines, however, are

finer-grained and more cohesive that those in the Schwarzensteinkees moraines, so the lack of deformation here may be due to different rheology. The lack of faulting in the moraines of the Schwarzensteinkees foreland may therefore be due to the unconsolidated nature of the dominantly gravel landforms, which may be too friable to preserve fault structures (Lukas, 2012; Chandler et al., 2016a). Horizons of finer sediment, which could be used as tracers critical in detecting deformation structures, are absent in the Schwarzensteinkees exposures.

Several studies also specifically note the presence of boulders on top of moraines, interpreted to have formed as a result of gravitational dumping at the ice front during push moraine formation (Hewitt, 1967; Sharp, 1984; Lukas, 2012; Bradwell et al., 2013; Reinardy et al., 2013), and boulders may be the dominant or sole constituents of some ridges, what remains of some ridges, or deposited between distinct ridges in areas where there was no other material to bulldoze or where meltwater channels evacuated smaller material (Sharp, 1984). Boulders were found on ridge crests, along the bases of moraine slopes, and as the dominant constituents of some ridges in the Schwarzensteinkees foreland. Two boulders dominate Exposure D (Figure 4.31). These boulders could have been deposited during moraine formation, indicating a powerful ice-front capable of moving such large sediment. The boulders are sub-angular, suggesting that they were not dumped at the ice front from a supraglacial position (e.g. Winkler and Matthews, 2010) but perhaps instead melted out at the ice front before being incorporated into a moraine (e.g. Sharp, 1984). This interpretation is further supported by the general absence of boulder chains in the foreland (e.g. Sharp, 1984; Lukas, 2012) and instead more isolated boulders spread among the moraines.

Conceptual model of minor push moraine formation

The following conceptual model of push moraine formation in the Schwarzensteinkees foreland draws from the aforementioned sedimentological analyses of Exposures A-E (Figure 4.42). Exposures C and E are also revisited as having formed through separate, but related, mechanisms of minor moraine formation in Sections 4.5.1.2 and 4.5.1.3.

(1) The proglacial fluvial system deposits sediments onto the outwash plain in horizontal beds or channel forms (Brodzikowski and van Loon, 1991; Maizels, 2002; Benn and Evans, 2010).
(2) The glacier advances, bulldozing sediments as it progresses downvalley.
(3) Continued ice advance responsible for differential stress within individual moraines creates deformation and folded beds indicative of compressional stress in some

places, while maintaining horizontal bedding or showing no deformation in others (Bennett, 2001; Lukas, 2012).

(4) The glacier retreats, finally depositing sediment as push moraines. The proximal slope is exposed as the ice retreats, destabilizing surface sediments and causing them to cascade down the slope. Sediments may also be redistributed down the distal slope through more passive gravitational processes.

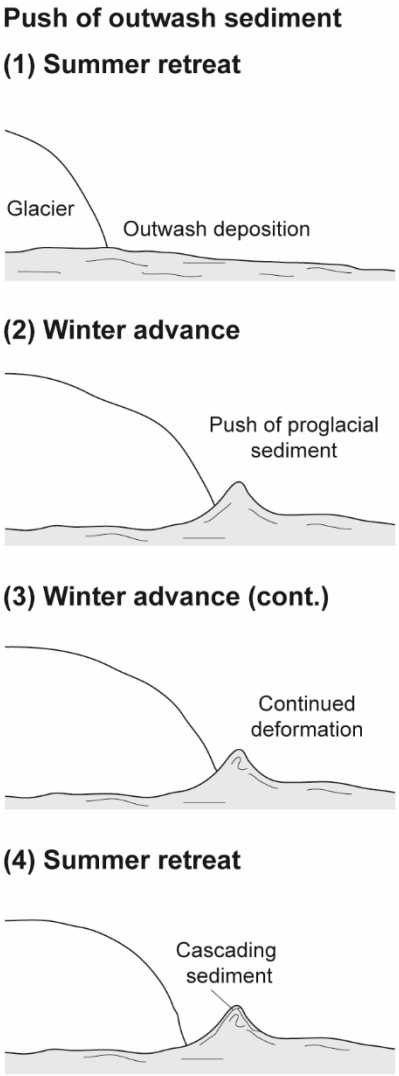

Figure 4.42. Conceptual diagram of minor push moraine formation in the Schwarzensteinkees foreland incorporating exclusively outwash sediment.

The minor push moraines in the Schwarzensteinkees foreland are generally consistent with other previously described mechanisms of minor push moraine formation (Worsley, 1974; Birnie, 1977; Sharp, 1984; Ono, 1985; Boulton, 1986; Lukas, 2012; Bradwell et al., 2013; Chandler et al., 2016a). Glaciofluvial outwash sediments have seldom been recorded in minor moraines, especially in those formed as push moraines in lowland settings (Bradwell, 2004; Reinardy et al., 2013; Chandler et al., 2016a). Lukas (2012),

however, records glaciofluvial outwash sediments in the high-mountain moraines at Gornergletscher in the Swiss Alps. The present study, therefore, highlights a primary similarity with groups of minor moraines in high-mountain environments of the Alps, as the minor moraines at both Schwarzensteinkees and Gornergletscher are composed dominantly of deformed, pre-existing proglacial outwash sediments. This suggests that the sedimentological composition of valley fill may influence the style of push moraine formation, and the loose, unconsolidated nature of outwash deposits may increase both the efficiency of the pushing ice front and the likelihood of sediment re-distribution down the proximal slope following ice retreat.

4.4.1.2 Stacking and push of outwash sediment

The following conceptual model of stacking and pushing creating a minor moraine in the Schwarzensteinkees foreland is derived from analysis of sediments in Exposure C (Figure 4.30) as a possible explanation for how this moraine was formed. As previously introduced, this moraine could have also formed solely through pushing (Section 4.4.1.1).

Deformation structures

If a channel structure does not explain the orientation of these FAs, the orientation of each FA away from a presumed approximate original horizontality could be explained by stacked sediment packages. The tilt of each of the FAs consistent with the direction of ice movement (Figure 4.30) would represent deformation and transport away from the original location and orientation to deposition as inclined slabs (Hiemstra et al., 2015), which is elaborated on below.

The possible deformation of a channel form in the centre of this exposure, FAs 6-8 (Section 4.5.1.1; Figure 4.30) may represent some deformation during pushing, which would have followed emplacement of the more distal stacked sediment packages.

Lack of deformation structures

The four most ice-distal FAs in Exposure C (FAs 1-4) all maintain sharp contacts and similar orientations as distinct sediment slabs. Bedding, where present, in these FAs follows the same orientations as the FAs. This preservation of original depositional features, here as bedding and sharp contacts, is more likely in a freeze-on scenario than through other mechanisms of moraine formation (i.e. pushing or squeezing), as stresses from advancing

ice would not be transmitted into the sediment package(s) if frozen to the base of ice (Matthews et al., 1995; Hiemstra et al., 2015).

Conceptual model of minor moraine formation through stacking and push of outwash sediment

The following conceptual model of moraine formation through stacking and push of outwash sediment (Figure 4.443) in the Schwarzensteinkees foreland draws from the aforementioned sedimentological analysis of Exposure C (Figure 4.30). This provides an alternative explanation for the formation of this moraine to that discussed in Section 4.5.1.1 above.

(1) The proglacial fluvial system deposits sediments onto the outwash plain in horizontal beds or channel forms (Brodzikowski and van Loon, 1991; Maizels, 2002; Benn and Evans, 2010).
(2) The glacier advances, bulldozing sediments as it progresses downvalley and forming a small push moraine/mound (Matthews et al., 1995).
(3) Winter freezing may penetrate the ice front and freeze overridden proglacial sediment to the base of the ice, which is then carried forward during ice advance (Krüger, 1995; Matthews et al., 1995; Lukas, 2012; Reinardy et al., 2013; Chandler et al., 2016a). The ice and frozen-on sediment slab may become slightly elevated or up-arched when encountering small push moraine feature (Matthews et al., 1995).
(4) The glacier retreats, and the once frozen-on till melts off as an individual FA on top of the originally pushed sediment mound, representing one phase of the moraine building event.
(5) Retreat continues, and new sediment may be deposited between the moraine and ice front as proglacial outwash.
(6-9) This sequence may repeat itself as the ice front remains thin enough, temperatures remain cold enough, and oscillations of the ice front remain small enough, resulting in the deposition of "stacked" packages of sediment that mimic the shape of the up-arched ice front. Exposure C shows that this may have occurred at least three times
(10) When the conditions above change, and likely related to changes in temperature and/or ice front thickness, the ice front may revert back to pushing proglacial outwash sediment when it advances.
(11) Continued ice advance and pushing may build this sediment pile and potentially deform any horizontal bedding or contacts or channel form structures.

(12) The glacier retreats, finally depositing pushed sediment on top of the previously stacked sediment sequence.

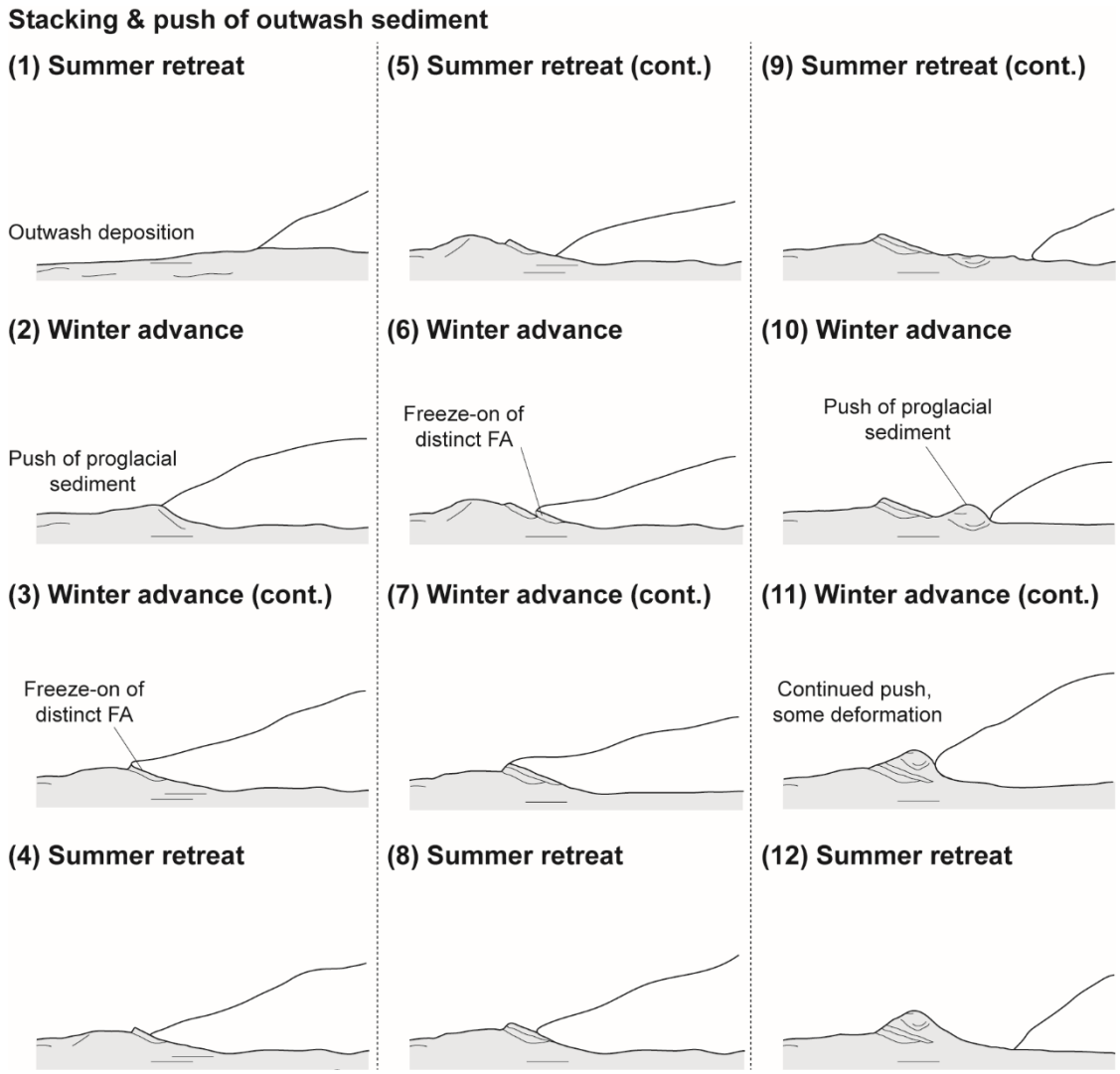

Figure 4.43. Conceptual diagram of minor moraine formation in the Schwarzensteinkees foreland through a combined stacking and pushing mechanism.

Multiple moraine building events present in this one composite moraine could have occurred during small oscillations within one year, continuous years, or with a longer gap. Figure 4.27 suggests that this moraine formed in 1921 or 1924, which are separated by only 1.7 m of measured ice retreat and no data presented for the intermediate years (Table 4.1). The close proximity of the ice front positions in these two years and the number of potential moraine building events, if considering the stacked FAs and group of pushed FAs with the conceptual model presented above, supports a composite moraine built during these four years' ice front oscillations. As such, FA 1 and FA 2 may represent a small pushed mound and subsequent sediments lab emplacement, respectively, in one year (1921), followed by sediment slabs stacked once each in the following two years (FA 3 in 1922 and FA 4in 1923),

and the remaining sediment pushed on topped of the stack sequence the following year (1924) to end the composition moraine building period.

Matthews et al. (1995) describe a similar sequence of multiple years the ice front advancing to the approximate same position as the previous year contributing to moraine growth through pushing of proglacial and/or subglacial sediment stacking of frozen-on sediment packages. A combined proglacial sediment push and freeze-on mechanisms, whether till or proglacial sediment is being frozen, has been previously described as a mechanism of moraine formation in other previous work as well (Andersen and Sollid, 1971; Krüger, 1995; Winkler and Matthews, 2010; Reinardy et al., 2013; Hiemstra et al., 2015; Chandler et al., 2016a), and is described in slightly different scenario pertaining to Exposure E, in Section 4.5.1.3 below.

4.4.1.3 Push of outwash sediment and freeze-on of till

The Exposure E moraine contains similar sediments to the other four moraines, as previously mentioned, but additionally reveals till, which was not found in any other exposure (Figure 4.33). This sedimentological disparity, where outwash dominates the foreland in comparison to till, may represent localised till deposition in the foreland and/or sampling strategy. Only five moraines were fully exposed, test excavations did not extend to the full depth of moraines, and each exposure only shows a two-dimensional slice of the landforms. Therefore, the absence of till in the other exposures does not necessarily exclude its existence in other sections of the moraines. This unit is interpreted as a till due to its high compaction, fissility, and macroscopically massive structure (Evans et al., 2006).

Exposure E reveals deformation structures and lack of deformation structures similar to those described above for a purely pushing mechanism of minor moraine formation. The assessment of the till unit(s) in this exposure suggests a combined push and freeze-on mechanism of moraine formation. Exposure E contains additional support for moraines composed of bulldozed proglacial outwash sediment. The exposure through this moraine continued into the sediment underlying the landform, creating a unique opportunity to view the sedimentology of the landform, the sedimentology of the underlying sediment, and the relationships between the two (Figure 4.33). Such an exposure has not been described in other minor moraine or push moraine studies.

Deformation structures

FA 2 and FA 4 of the moraine landform both follow the shape of the proximal slope, which could represent destabilisation of the proximal slope and redistribution of the sediment

down this slope (Bennett, 2001; Lukas, 2005; Benn and Evans, 2010; Lukas, 2012; Reinardy et al., 2013; Chandler et al., 2016a), which may be present here as two separated events.

The sediment underlying the moraine is deformed in the proximal and central extents of the exposure (Figure 4.33). The contacts between FAs are sharp, although irregular, showing considerable deformation. Parts of FA 2 dips following the orientation of the proximal slope and bedding in gravel FAs of the overlying sediment. Laminations in the two sand FAs (FA 2 and FA 3) are also extensively deformed. Deformation includes noticeable z-, m- and s-folds, other less-clear folding, and low-angle thrust faults, all indicative of compressional stress. Other laminations remain horizontal or follow the overall shape of contacts with overlying and underlying FAs (Figure 4.33). The massive nature of FA 4 does not show internal deformation, however a zone of boudinaged sand is present towards the centre of the exposure (Figure 4.33), a deformation structure indicative of longitudinal extension or shearing that can occur during glaciotectonism (van der Wateren, 2002; Glasser and Hambrey, 2005; van der Wateren, 2005; Lukas et al., 2012), which may here relate to cannibilazation by the overlying, deforming till (FA4) (Evans et al., 2006).

Lack of deformation structures

Some sediment underlying this moraine preserved the proglacial outwash plain as distinct beds of sand and gravel (Figure 4.33). Gravel FA 1 and sand FA 2 maintain dominantly horizontal bedding and orientations at the most distal end of the exposure. What is seen here is similar to what was observed in the field as part of the modern proglacial channel network on channel bars, within the channel, and along channel banks and what is common in proglacial outwash systems (Church and Gilbert, 1975; Rust, 1975; Brodzikowski and van Loon, 1991; Knighton, 1998; Maizels, 2002; Benn and Evans, 2010). This suggests little to minimal deformation of the distal section of the exposure, further supported by the most distal portion of gravel FA 1 in the moraine also maintaining horizontal bedding, preserved from original deposition as part of the outwash plain (Church and Gilbert, 1975; Rust, 1975; Brodzikowski and van Loon, 1991; Maizels, 2002).

Portions of FA 1-4 of the moraine sediment also maintain horizontal bedding. Horizontal bedding and clast size differences, typical of an outwash plain (Church and Gilbert, 1975; Rust, 1975; Brodzikowski and van Loon, 1991; Knighton, 1998; Maizels, 2002; Benn and Evans, 2010), suggest that the sedimentology of each layer determined whether horizontality was maintained during and after push moraine formation (e.g. Lukas 2012), where more cohesive and/or more compacted gravel layers resisted deformation more than surrounding sediments.

The shape and orientation of a till unit in Exposure E maintains original depositional architecture as a frozen-on slab that takes the shape of the up-arched ice front (Matthews et al., 1995; Reinardy et al., 2013), a process described in more detail in below. This sharp form suggests no subsequent deformation following deposition and therefore the final stages of moraine formation. The presence of till here, its distinct upglacier dip in two places, and its sharp boundaries in comparison to surrounding sediments (Figure 4.33) suggests that it was frozen on to the ice front as distinct slabs and subsequently emplaced during retreat (Krüger, 1995; Matthews et al., 1995; Lukas, 2012; Reinardy et al., 2013; Chandler et al., 2016a).

Conceptual model of combined push and freeze-on minor moraine formation

The following conceptual model of combined push and freeze-on minor moraine formation in the Schwarzensteinkees foreland draws from the aforementioned sedimentological analysis of Exposure E (Figure 4.44).

(1) The proglacial fluvial system deposits sediments onto the outwash plain in horizontal beds or channel forms (Brodzikowski and van Loon, 1991; Maizels, 2002; Benn and Evans, 2010).
(2) Winter freezing may penetrate the ice front and freeze till to the base of the ice, which is then carried forward during ice advance (Krüger, 1995; Lukas, 2012; Reinardy et al., 2013; Chandler et al., 2016a). The ice and till may become slightly elevated when encountering and pushing outwash sediment.
(3) The glacier continues to advance, which forms the outwash into a more distinct ridge and may deform any original depositional architecture present on the outwash plain.
(4) The glacier retreats, depositing the pushed sediment as a moraine, and the once frozen-on till melts off as a separate unit on the ice-proximal side of the sediment pile. The proximal slope is exposed as the ice retreats, destabilizing surface sediments and causing them to cascade down the slope and till unit.
(5) Continued retreat upvalley allows more outwash to be deposited between the ice and newly formed moraine.
(6) The process repeats itself as the glacier advances to the same location as the previously deposited moraine. The extant moraine causes pronounced up-arching of the ice front (Matthews et al., 1995; Reinardy et al., 2013), and the frozen-on till inherently follows this shape.

(7) The glacier continues to advance, which deforms the previous moraine and builds this sediment and the newer outwash into a larger moraine.

(8) The glacier retreats, and the second till slab melts out on the ice-proximal side of the now composite moraine. Following ice retreat, the proximal side of the moraine may destabilize, causing some sediment from the ridge crest to cascade down the slope.

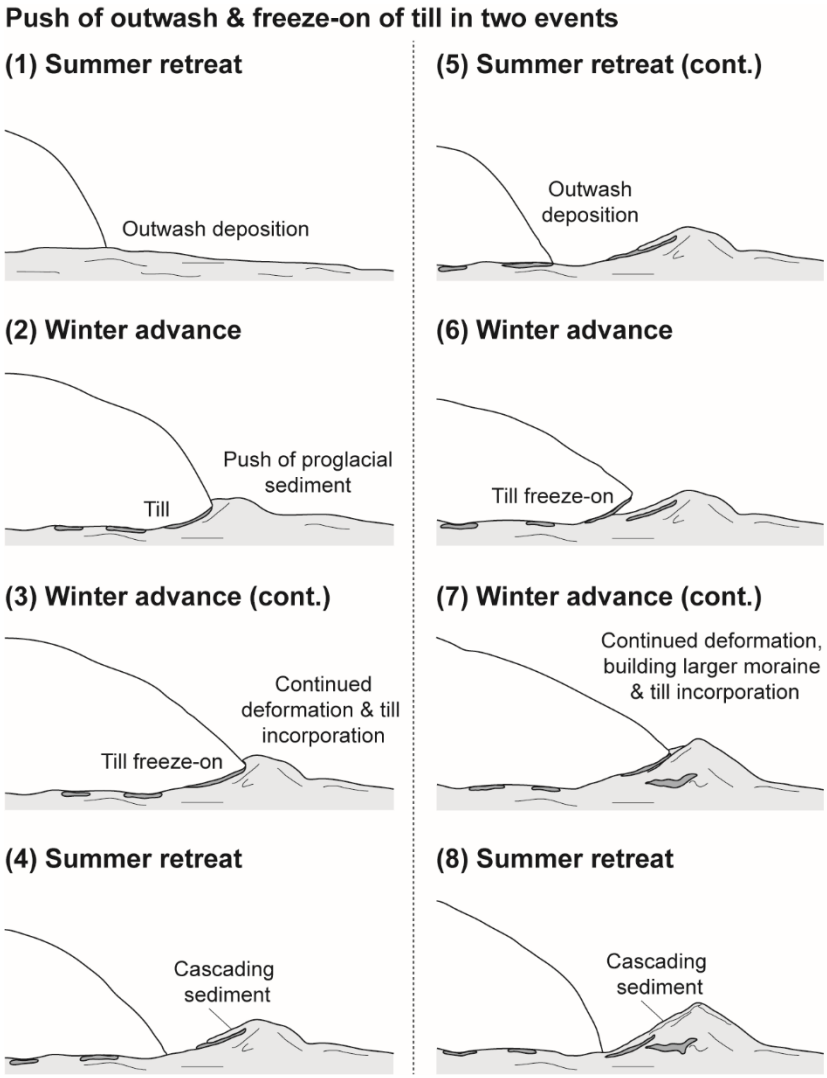

Figure 4.44. Conceptual diagram of minor moraine formation in the Schwarzensteinkees foreland through combined pushing and freezing mechanisms incorporating outwash sediment and till.

The two moraine building events present in this one composite moraine could have occurred during two continuous years or with a longer gap. Figure 4.27 assigns moraine construction during 1937, however if this represents two years, this moraine would be labelled 1937 and 1938, with the ages represented on the map extending to 1942. The exposure through the composite moraine continued deep enough to also expose the underlying sediment (that of the first moraine building event) and the relationships

between the two (Figure 4.33). The exposure log shows the till (diamicton) labelled as one FA because no boundaries within the FA were seen. However, the deformed core and very stark form of the individual till slab suggest that the core and slab are two separate FAs, and the boundary is not discernible at the macro scale.

This combined proglacial sediment push and till freeze-on mechanism of moraine formation is consistent with other previously described mechanisms of minor moraine formation (Andersen and Sollid, 1971; Krüger, 1995; Matthews et al., 1995; Winkler and Matthews, 2010; Reinardy et al., 2013; Hiemstra et al., 2015; Chandler et al., 2016a). This may incorporate one (Matthews et al., 1995; Hiemstra et al., 2015) or more sediment slabs in one season, with individual slabs melting out incrementally during moraine building (Krüger, 1995; Reinardy et al., 2013; Chandler et al., 2016a).

4.4.1.4 Review of minor moraine formation in the Schwarzensteinkees foreland

Five exposures reveal three potential mechanisms of minor moraine formation in the foreland, which share some similar sedimentological characteristics and ice front-sediment interactions. Pushing plays a role in all three conceptual models of minor moraine formation, and freeze-on mechanisms include stacking of proglacial sediment packages or incorporating subglacial till.

Other previously described mechanisms of minor moraine formation are not supported by the sedimentological composition of the minor moraines in the Schwarzensteinkees foreland. Till squeezing at the ice front implies high meltwater and/or pore water pressure beneath the glacier to saturate and extrude till. There is no evidence for changing dynamics responsible for these conditions in Exposure E, where till is present, and the till units here show no evidence of plastic flow or squeezing (Price 1970; Sharp 1984; Evans and Twigg 2002; Bradwell 2004; Chandler et al. 2016a). Other methods of formation suggest that supraglacial and/or subaerial sediment may be deposited into ice crevasses and eventually deposited at the ice front (Worsley, 1974), englacial channel fills may deliver sediment to the ice front (Krüger, 1995; Winkler and Matthews, 2010; Lukas, 2012), and supraglacial sediment, whether as debris cones or more general supraglacial cover, may be dumped off the ice front (Winkler and Matthews, 2010). The sedimentology of moraines in the Schwarzensteinkees foreland negates these ideas, as the clast shape measurements and roundness in the moraines are distinctly different from supraglacial control samples but show strong similarities to the modern glaciofluvial system (Figures 4.35-37 and Figure 4.41). The gravel sediments contained in the moraines at Schwarzensteinkees are consistent with clast measurements and observations of the

modern proglacial channel network, and can confidently be labelled as glaciofluvial outwash sediments.

Additionally, push moraine formation in the Schwarzensteinkees foreland can be described as "efficient bulldozing", using the term introduced by Lukas (2012), in which a steeper ice margin may push sediment as the ice advances so that the transfer of sediment onto the glacier tongue is negligible. Push moraine formation in the Schwarzensteinkees foreland is therefore most similar to one of three processes of formation Lukas (2012) describes in the Gornergletscher foreland.

4.4.2 The Little Ice Age and a proglacial lake

Historic maps clearly indicate the presence of an immediately proglacial lake in the Schwarzensteinkees valley at the beginning of the 19th century, as well as one or two moraines that had already been deposited. The first line of evidence for a proglacial lake is the obvious presence of a lake in maps of the upper Zemmgrund from 1807/08 and 1817 (Figure 4.2). The lake area appears to decrease as the glacier advances in the time elapsed between the productions of the two maps. This provides further support for a dynamic and short glacier response time (Bahr et al., 1998), demonstrated as the ice position shows significant retreat from the pre-1850 moraines, followed by a known advance to immediately upvalley of these moraines, creating the 1850 moraine. Such a dynamic response time is demonstrated for other small glaciers in the Alps as well (Haeberli, 1995; Hoelzle et al., 2003; Oerlemans, 2005; Zemp et al., 2006).

Although the accuracy of the maps cannot be established with confidence, it is important to recognize that this lake is drawn in the location of the modern IZ1-FZ1-LSZ area (Figures 4.1-4.2). This correlation and the geomorphology of the valley floor here support a former lacustrine setting, particularly in the relationship between FZ1 and the LSZ.

The prominent, shallow reflector on the GPR radargrams is interpreted as a strong boundary, which attenuates the signal so that no information is gained below this depth (Figure 4.25). Tracing this boundary reveals a vague basin shape within the upvalley and downvalley boundaries of FZ1 (approximately 71.0-310.5 m; Figure 4.45). The composition of this boundary cannot be known without further work that assess the material underlying the GPR01 transect, such as cores along the transect or shallow test pits. This reflector may, however, be representative of cohesive lakebed sediment (clay, and potentially silt) or bedrock, either of which may be related to the signature of a proglacial lake, as incorporated below.

The undulating shape could be the surface expression of now buried landforms, irregular bedrock topography, or data noise, however this cannot be ascertained without determining the material. Anything below the prominent reflector (RF1) is interpreted as noise or repetitions of the boundary, whereas anything above this reflector is interpreted as sediment fill (RF2). The homogeneous sediments of IZ1 (RF3) and LSZ (RF4) are interpreted as separate facies from those in FZ1, particularly as the prominent reflector generally does not extend through these zones.

FZ1 is devoid of landforms, contains few boulders, and is remarkably flat. The modern channel network grew considerably during a particularly rainy July in 2014; daily observations showed that the main channel overtopped its banks, creating many smaller channels across the Flat Zone. These channels remained surficial, i.e. grew laterally with increased rain, instead of cutting into the underlying sediment (similar to the fluvial system in 1942, Figure 4.16), and the surface remained significantly wet following the rainy period. These observations suggest fine grained (silt and clay), cohesive, and low-porosity underlying sediment (Lowe, 1975; Kumar, 2011), which may be indicative of a lake bed composed of fine particles (Church and Gilbert, 1975; Brodzikowski and van Loon, 1991; Ashley, 2002; Benn and Evans, 2010). The prominent boundary in the GPR profile may reflect this composition (Figure 4.45). An alternative explanation for the flatness here is lateral migration and planation of the modern channel, with channel bed material that may be represented by the prominent reflector (Figure 4.45), with the high points reflecting migrated gravel bars and the low points the former channels. Channel dynamics through time could also be responsible for eroding any landforms that may have been present, whether other minor moraines now erased from the record or other glaciogeomorphological features. Another explanation is that the prominent reflector could represent former topography, e.g. moraines, which have then been filled in with sediment. The underlying sediment was not visually investigated due to time constraints, financial constraints, and available tools. The hypothesis of a former lakebed is favoured as it most clearly accounts for the abnormally flat nature of the area relative to other areas of the Schwarzenstienkees foreland, which show more surface irregularity and surface cobbles and boulders that may be remnant of previously more prominent landforms predestined with low preservation potential.

The LSZ also supports the interpretation of a former lacustrine setting in the Schwarzensteinkees valley. This zone extends from 2,130 m elevation at its upvalley limit to 2,120 m elevation at its downvalley limit. The surface expression of this slope is consistent with a prograding delta (O'Cofaigh et al., 2005; Bennett and Glasser, 2009; Benn and Evans, 2010; Shroder, 2011), where FZ1 may contain some bottomsets, the LSZ surface with some boulders may represent foresets, and the IZ2 surface (which appears dominantly

flat with later glacial deposits overlying it) may represent topsets and/or an irregular lake margin surface.

Evidence for a lacustrine environment in the early 19th century in the Schwarzensteinkees foreland is firm, but evidence for why the lake formed, how it was constrained, and how it drained is less conclusive. Three mechanisms of proglacial lake formation may explain the presence of the Schwarzensteinkees proglacial lake:

1) **The pre-1850 moraines may have ponded meltwater.**

   This hypothesis is supported by geomorphological relationships of elevation. Firstly, the elevation of the moraines is conducive to damming of a lake: The modern altitude of these moraines is approximately 2,115 m near the modern channel and >2,130 m near the valley walls. FZ1, where this lake was drawn in 1807/08 and 1817, is at approximately 2,120 m at its up valley end, as extracted from visual comparison with these maps and modern DEM data (Figures 4.1-4.2). The pre-1850 moraines have likely eroded somewhat from 1800 to today, i.e. they may have been slightly higher in the past. Several prominent boulders in the modern channel where these moraines may have extended support this hypothesis, as any other fine sediment deposited in the moraines may have been eroded as the channel established itself, leaving behind only the largest boulders (Figure 4.46).

   The maps, however, show that the edge of the lake did not extend all the way to the moraines in 1807/08 and 1817 (Figure 4.2). This indicates that either the lake never reached the moraines and they were therefore not responsible for meltwater impoundment, or that the lake was more extensive prior to mapping. The lake may have been shrinking due to partial drainage, filling in with sediment, or ice overriding during glacier advance. Today, the moraines are fragmented, which could indicate palaeochannel incision and lake draining during this period, but could alternatively relate to deposition of the moraine ridges or later channel incision.

2) **A different moraine or landform, since eroded, may have trapped meltwater.**

   This hypothesis is supported by the unchanging downvalley extent of the lake and the known subsequent 1850 glacier advance. The edge of the lake appears consistent between the 1807/08 and 1817 maps (Figure 4.2), suggesting the influence of some topographic feature at that location constraining water. Furthermore, this topographic feature may not exist today due to subsequent ice advance. The 1850 moraine exists directly upvalley of the pre-1850 moraines, supporting that an ice advance to this position could have obliterated any pre-existing topographic feature. The maps do not, however, illustrate a prominent landform damming the lake.

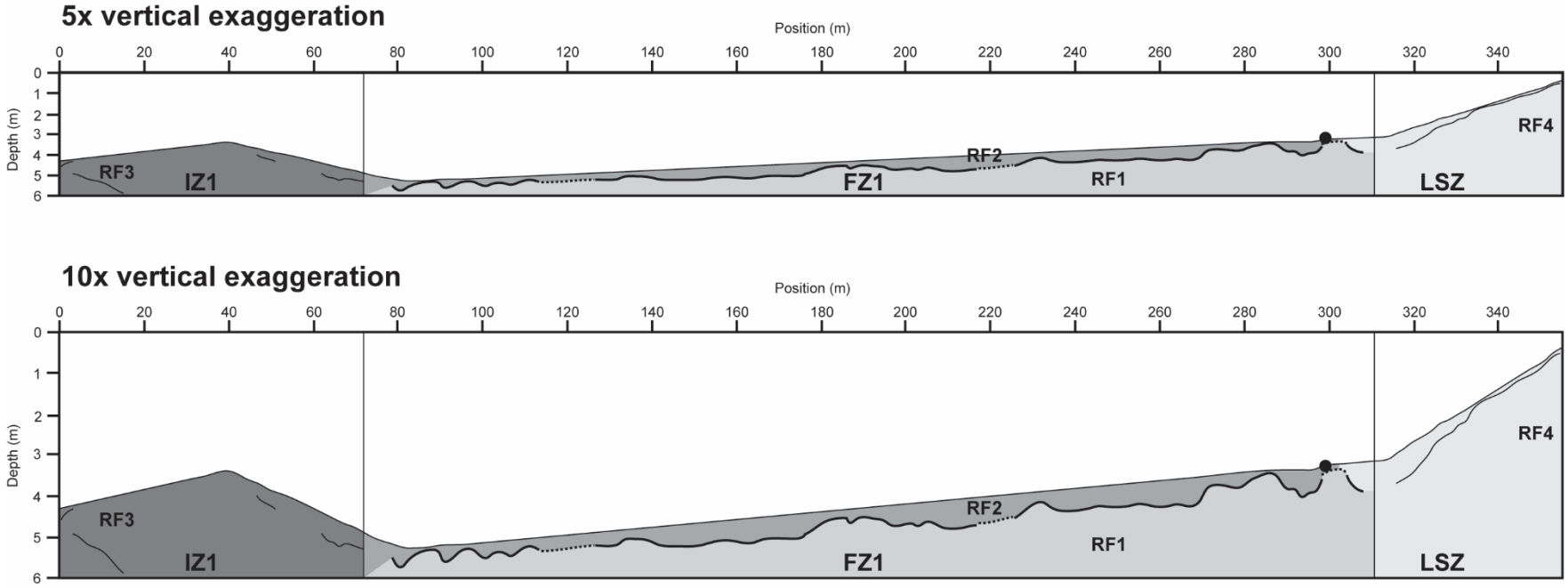

Figure 4.45. Interpretation of ground-penetrating radar reflection profiles along transect GPR01. Figure 4.25 shows radagrams used for this interpretation. Boundaries of zones on the geomorphological map (Figure 4.1) labelled and demarcated with vertical lines. Black circle indicates prominent surface boulder, as noted during data collection. Thick line shows prominent reflector, and dashed thick line shows inferred connection between visible prominent reflectors. Thin lines show other reflectors. Prominent radar facies labelled.

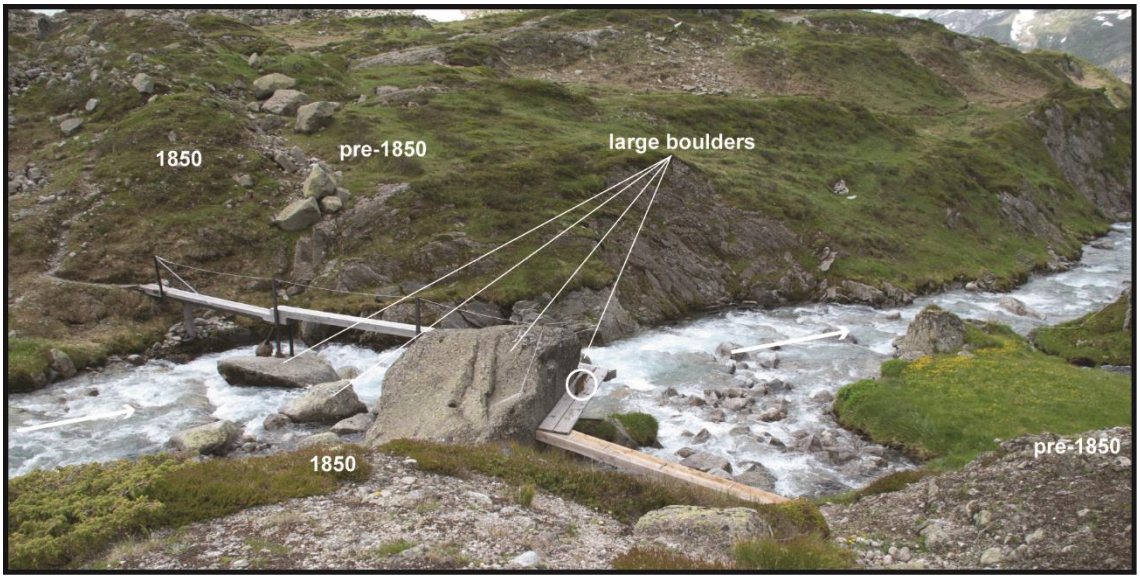

Figure 4.46. Large boulders in modern channel near 1850 moraine (1850 and pre-1850 labeled). Arrows indicate direction of channel flow. Marmot circled for scale. Photograph taken in July 2014 from crestline of 1850 moraine.

3) **A basin controlled by bedrock geometry or over-deepened trough filled with meltwater.**

The 1807/08 and 1817 maps do not show that a topographic feature dammed the lake (Figure 4.2). An over-deepened trough carved by previous glacier advance may therefore have accumulated meltwater. Alternatively, the natural level of the bedrock threshold, as seen by the level of the ice-moulded bedrock zone at the downvalley-most extent of the Schwarzensteinkees foreland (Figure 4.1), which varies locally from 2,117 m to 2,125 m elevation, may have been a barrier for meltwater draining completely from the valley. The position of the channel has been fixed and incising the ice-moulded bedrock since at least 1807 (Figure 4.2). Anything blocking the path of the channel (e.g. moraine sediment, see above) may have temporarily allowed for increasing lake level. Future work could test this hypothesis, and develop a better understanding of the bedrock morphology of the Schwarzensteinkees valley, by running further ground-penetrating radar (GPR) surveys throughout the foreland. The prominent reflector in the GPR profile, which exists within the limits of FZ1, may reflect the boundary of this basin, which then filled in with sediment of another signature (Figure 4.425). If this is the case, the lake was shallow, as the GPR transect through the approximate middle of the basin showed depths to this reflector ranging from 1.8 m to 2.8 m.

These three hypotheses show substantial evidence for some kind of basin that trapped meltwater, which may have also included a topographic barrier that dammed the water to a higher level than only the shallow basin would have allowed. The limits of this study,

however, cannot conclusively determine a damming landform, whether extant or since eroded.

Hypotheses regarding the termination of the Schwarzensteinkees proglacial lake are broader than those regarding its formation. As previously mentioned, infilling sediment and/or ice advance may have caused the lake to fill in. The difference in ice position between 1807/08 and 1817 shows an advancing ice front, further supported by the deposition of the 1850 terminal moraine (Figure 4.1-4.2). The known ice advance to the 1850 position may have compacted any underlying lacustrine and delta sediment, preserving the topography of the lake bottom as FZ1 and the delta as LSZ.

Alternatively or additionally, a channel may have drained the lake. The discontinuity of one of the pre-1850 moraines slightly north of the modern channel may support some channel incision, especially as the 1850 moraine is continuous in this location (Figure 4.1). This could, however, instead reflect original deposition of discontinuous moraine fragments. As previously mentioned, large boulders in the modern channel may have been part of the pre-1850 moraine arc and may persist as the only remnants, due to their size, of a more continuous landform across the main valley axis (Figure 4.46).

Historic maps and observations and several moraines show the dynamic ice front fluctuations of Schwarzensteinkees during the LIA. The most prominent of these moraines is the 1850 moraine, which is noted in valleys of varying sizes throughout the Alps as signifying the last advance of the LIA (e.g. Kerschner et al., 2006; Ivy-Ochs et al., 2009; Knoll et al., 2009; Kirkbride and Winkler, 2012; Schimmelpfennig et al., 2014). As a warming climate brought about the end of the LIA, Schwarzensteinkees has been in nearly continuous retreat and has not since advanced this far downvalley.

4.4.3 The former proglacial lake as the dominant influence on foreland evolution

The presence of two distinct groups of minor moraines in the Schwarzensteinkees foreland prompts inquiry into why these features exist in such separate groups and if these landforms were perhaps deposited during seasonal oscillations of the ice front (e.g. Hewitt, 1967; Beedle et al., 2009; Lukas, 2012; Bradwell et al., 2013; Chandler et al., 2016a). The first group of minor moraines begins immediately upvalley of the 1850 moraine and extends 75 m upvalley, or 150 m if including IZ1. The second group of minor moraines begins 475 m upvalley of the 1850 moraine and extends 325 m further upvalley. The two groups are separated by the IZ1-FZ1-LSZ-IZ2 sequence (Figure 4.1), although historical photographs show that the IZ1 may have once reflected more distinct moraine ridges than today (Figure 4.18). This area may therefore represent a part of MM1, albeit with smaller landforms than those closer to the 1850 moraine (Figure 4.1).

The 1850 moraine provides the basis of chronological constraint on minor moraine formation in the Schwarzensteinkees foreland as a maximum age of younger than 1850 for MM1. The aforementioned ages derived from lichenometry provide a constraint on depositional ages of MM2, beginning around 1890, with more specific ages on individual landforms of 1914 and 1926, formed during what Pindur and Heuberger (2008) refer to as a "stagnation phase." The only historical map to depict the moraines shows that they were deposited by 1932 (Figure 4.12).

The comparison of ice front variation measurements and the mapped moraines (Section 4.1.3; Figure 4.7, Table 4.2) suggests that the chronological constraint by Pindur and Heuberger (2008) may be accurate, and that age assignments for moraine exposures detailed in the present work may be warranted. In some instances, moraines that do not appear to match front variation measurement positions may be explain by minor advances that could have obliterated moraines at the ice front. This explanation is especially tangible for 1925, as 1926 shows an advance of 7.5 m, which would have overrun the 1925 ice position. Other non-matches may be explained by low preservation potential of small moraines, especially at the valley axis where the proglacial fluvial system may be eroding moraines, minor variations in ice front shape and the ability or lack thereof to form moraines due across the ice front, and years in which moraines may not have been formed. Similarly, Figure 4.7 shows some interpreted moraine chains that do not seem to link to specific years, which may reflect multiples moraines deposited in one year.

Although this analysis shows general correspondence of the moraine record and ice front variation measurements, some assumptions were used when comparing the datasets. The comparison was started using lichenometry-derived age assignments from Pindur and Heuberger (2008) on the larger later-frontal moraines, which some authors argue may be inaccurate or fraught with complications (e.g. Jochimsen, 1973; Osborn et al., 2014). These moraines were then extrapolated towards the valley axis and interpreted to connect to moraines nearer to the centre of the valley. Interpreted moraine connections throughout the valley may not be accurate, and should be treated as somewhat tenuous.

As previously described, minor moraines formed in two distinct groups in the Schwarzensteinkees foreland, rather than one continuous sequence of moraines. These moraines were formed during glacier retreat beginning at the termination of the LIA (Table 4.1). As these moraines were formed during a period of glacier retreat, they likely represent small ice-marginal fluctuations, perhaps reflecting seasonal (accumulation vs. ablation) changes on mass balance (e.g. Hewitt, 1967; Beedle et al., 2009; Lukas, 2012; Bradwell et al., 2013; Chandler et al., 2016a), or may be, in some cases, composite moraines formed through a series of two or more small ice-marginal fluctuations (e.g. Matthews et al., 1995; Hiemstra et al., 2015). Most of the minor moraines formed with a pushing component and

contain dominantly pre-existing proglacial outwash sediment, with one of five of the sampled moraines containing till, and two of the five sampled moraines showing the influence of basal freeze-on of sediment to the ice front. Part of this research therefore considers why the moraines exist as two separate groups, and how this may relate to the distinct lack of depositional landforms between the two clusters.

Ice front variation data for Schwarzensteinkees exist only from 1882 onwards (Figure 4.6; Table 4.1) (Zemp et al., 2012; Zemp et al., 2013). There is not, however, evidence for any large retreat or advance during the period separating the two groups of moraines, despite nearly 500 m separating these two groups. Only one year records this magnitude of ice advance or retreat (1966, 436 m retreat), which likely relates to a bedrock step in the upper reaches of the valley. The collective front variation data, as well as the specific data for the 1890-1930 time period, suggest that a rapid period of ice retreat or an extensive advance, which would have eroded pre-existing moraines, are not responsible for the gap between the two groups of minor moraines.

This then prompts consideration of smaller fluctuations that eventually totalled 500 m of retreat sometime after 1850 and before 1890, including the 37.9 m of total retreat from 1882 to 1893 (no data exist from 1885 to 1892) (Figure 4.6; Table 4.1). FZ1, which the ice must have occupied sometime during this period, shows no geomorphological features to interpret ice dynamics and ice front variations.

Three hypotheses may explain the lack of landforms in this area. Firstly, pre-existing sediments and landforms may not have been conducive to alteration. The glacier may not have been able to push any of the former lakebed (FZ1) due to its flat form and compacted sediments disallowing the initiation of push moraine formation (Boulton, 1986; Schlüchter et al., 1999) and any incorporation of lacustrine sediment into the moraines. The upvalley part of the proglacial deltaic system (i.e. LSZ and IZ2), in contrast, may show geomorphological evidence of ice fluctuations as these areas likely contained more surface perturbation to initiate bulldozing of sediments and associated glaciotectonic deformation, similar to the role of ice-contact fans described by Boulton (1986).

Alternatively, the advancing glacier may have planed-off and further compacted this sediment, allowing for the flat form seen today. Some lacustrine sediment may have therefore been incorporated into downvalley moraines, although this was not reflected in the composition of Exposure A.

Lastly, the preservation potential of subtle push moraines is fairly low (Boulton, 1986), implying that any features that may have been present in FZ1 may have been fully eroded by subtle channel shifts, gravitational processes, human and wildlife disturbance, or a combination of several factors. As previously discussed, no evidence shows that the channel fully sculpted FZ1. Similarly, the ice front variations do not support any major ice

advance between 1850 and 1890 that may have overridden and destroyed any landforms. An alternative explanation considers erosion by several smaller ice margin fluctuations that are not reflected in the data due to observation periods or that occurred prior to the beginning of measurement.

The first hypothesis introduces the role of the geomorphological geometry of the former proglacial lacustrine system in several different zones. Both of the irregular zones in the Schwarzensteinkees foreland (Figure 4.1) are characterized by a chaotic architecture that appears similar to the minor moraine zones in aerial view, but is less organized and contains lumpier and subtler ridges than in the two moraine zones, hence the "irregular" designation. Photographs in 1946 show that some ridges may have once been clearer, but that these moraines were also notably smaller than those further downvalley (Figure 4.18). Their positions in the valley in relation to FZ1, the mapped location of the proglacial lake (Figure 4.1-4.2), and GPR radargram interpretations (Figure 4.42) suggest that these regions of the foreland were the downvalley and upvalley lake margins. The rougher surface architecture of a lake margin compared to a lake bed may explain the jumbled surface expression seen today; the heterogeneous surface of the lake margins may have therefore promoted glacier bulldozing and landform formation as the glacier could push any surface perturbations during advances (Boulton, 1986; Schlüchter et al., 1999), in contrast to FZ1 in which no surface perturbations may have been present.

The second, smaller FZ2 interrupts the upvalley set of minor moraines (Figures 4.1, 4.13, 4.15, 4.18, 4.22B). The moraines clustered around 1890 exist on the downvalley end of FZ2 but are not present on valley right, whereas the moraines clustered around 1920 exist on the upvalley end on both sides of the valley. Field observations and aerial photographs show a distinct and clear boundary between the proximal slopes of moraines that rise sharply out of FZ2 on valley left. On valley right, a slope upwards out of the downvalley side of FZ2 leads to the sand pit and short step in which Exposure F was revealed, followed by another slope to the upper surface of IZ2.

Several hypotheses could explain the presence of FZ2. Firstly, the clear boundaries of FZ2 suggest a lacustrine environment similar to the downvalley FZ1 and associated geomorphological assemblage, albeit on a smaller scale. Sedimentological evidence in Exposure F further supports a former lacustrine environment of FZ2. This exposure is dominantly composed of sand, with some FAs that contain considerable laminations of silt and sand and some granules and pebbles, indicative of sedimentation into a standing body of water and variable deposition of different grain size classes, either directly at the ice front or from the proglacial channel system, where finer sediment is expected to be deposited towards the centre of the basin and coarser sediment towards the margins (Church and Gilbert, 1975; Brodzikowski and van Loon, 1991; Ashley, 2002; Benn and Evans, 2010). This

prolific amount of sand and silt is not seen in any of the moraines, composed of pushed outwash sediment, therefore suggesting a ponded environment trapping this finer sediment. Planar and deformed laminations both suggest a near-shore environment, where sediments may be more disturbed than in the centre of the basin (Ashley, 2002) or face the influence of freeze-thaw deformation of winter ice (Brodzikowski and van Loon, 1991). The planar cross-bedding of sand and silt laminations in FA6 near the top of the exposure may represent near-shore wave influence as ripple cross-bedding, although this cannot be conclusively interpreted with the limited amount of this FA exposed in the section. The slope up to IZ2 may therefore represent the slope out of the basin on the distal extent of the lake.

Secondly, FZ2 may represent a period of rapid retreat and no landform deposition. This mechanism of geomorphological evolution is not exclusive and could also include the formation of the proglacial lacustrine setting described above. Comparison of the relative ages of these two upvalley moraine clusters and ice front variation reveals connections between the ages assigned by Pindur and Heuberger (2008) for the "winter moraines", the larger more prominent moraines, and FZ2. The period of moraine formation "around 1890" mapped by Pindur and Heuberger (2008) includes 188.4 m of retreat from 1882 to 1914 (Figure 4.6; Table 4.1), their chronological designation for a prominent latero-frontal moraine, reflected in a comparison of front variation measurements and the moraines mapped in the present research (Figure 4.7; Table 4.2). This was followed by 20.7 m of overall retreat to 1926, which is the chronological designation of another prominent later-frontal moraine (Pindur and Heuberger, 2008; Figure 4.7; Table 4.2), with 0.3 m advances occurring in 1915 and 1920, and an advance of 7.5 m in 1926 (Figures 4.6-4.7; Tables 4.1-4.2). These data suggest that the prominent moraines may represent these larger advances, rather than smaller ice-marginal fluctuations that produced the smaller minor moraines nearby, therefore supporting the age designations. Unfortunately, only one front variation measurement (1905) appears to exist within FZ2, bound by moraines that may have been deposited in 1902 and 1913 (Figure 4.7). The period in between may then represent ice retreat with no seasonal readvances creating moraines, which may be reflected in the arc shape of FZ2 (Figure 4.1, Figure 4.23), perhaps preserving the shape of the ice front during the broader advance and intermediary retreat. A gap in photographs and maps from 1925 (Figure 4.11) to 1936 does not allow tg of FZ2, as FZ2 had already formed by 1936 (Figure 4.14).

The comparisons of historical observations, geomorphology, and front variation data presented here suggest that a previous lacustrine setting (FZ1) may have exerted a strong influence on minor moraine formation in the Schwarzensteinkees foreland, which may have also occurred on a smaller scale in later years (FZ2). The lacustrine setting did

not appear to influence the ice and sediment dynamics of minor moraine formation but may have controlled whether or not moraines were formed in specific sub-settings of the foreland. This research therefore emphasizes the necessity for a full understanding of the geomorphological evolution of a setting through time in understanding its present state. This research not only presents a relative timeline of proglacial lake formation and the end of the lacustrine environment, but also shows how different depositional regimes of a lacustrine environment may influence subsequent surficial deformation.

4.4.4 The timing of moraine formation and significance of minor moraines

The two groups of numerous closely spaced push or combined push and freeze-on moraines in the Schwarzensteinkees foreland were deposited during a broad period of retreat. The mechanisms of moraine formation show that these minor moraines are some signal of ice advance imprinted on overall ice retreat. A comparison of the geomorphological map and front variation measurements provides some chronological constraint in the valley and shows that many moraines may be connected to individual years. Unfortunately, due to the lack of historical climate data for the period of moraine formation, the specific relationships between temperature and precipitation on glacial mass balance changes and/or ice front variation cannot be examined. The close spacing of so many minor moraines in the foreland does, however, suggest that Schwarzensteinkees had a dynamic ice margin that may have responded rapidly to climate changes on a seasonal scale. A comparison of ice front variation measurements and the geomorphological record of minor moraines, possible in IZ2 and MM2, suggests that moraines may have been deposited during annual cycles. The minor moraines in the Schwarzensteinkees foreland may therefore be conservatively described as likely annual minor push or combined push and freeze-on moraines, with some caveats.

The evolution can be described in four periods of geomorphological development: 1) Late fluctuations of the LIA (1783-1820); 2) The terminal LIA advance (1820-1850); 3) Glacier retreat and minor moraines (1850-1940); and 4) Dominant glacier retreat (1940 to present). The glacial history of the Schwarzensteinkees foreland shows that a proglacial lake may have considerably influenced the geomorphological evolution of the valley. This research confirms the presence of a lake mapped in 1807/08 and 1817 through modern geomorphological relationships (i.e. IZ1, FZ1, LSZ, and IZ2) and GPR analysis that reveals a vague, small basin, or alternatively, a former braided channel system or pre-existing topography that has been filled in with sediment.

More importantly, this study shows how three primary environments of a proglacial lacustrine setting may have influenced the subsequent development of a valley, which

suggests the importance of the lake margins, the lakebed, and a prograding delta through the geomorphology of the different zones. The lake margins may have contributed to the unclear and chaotic glacial landforms in these zones, which may have otherwise been deposited as larger and sharper moraines seen elsewhere in the foreland. The lakebed likely disallowed the deposition of any glacial landforms through its smooth and compacted nature, creating the large flat zone preserved in the valley today. This lakebed, therefore, may have greatly influenced the ability of the glacier to push sediment during advance and exerted a primary control on landform deposition, specifically minor moraines, in this zone.

The evolution of the Schwarzensteinkees foreland since the late 18th Century presented here is the first study to discuss the influence of a proglacial lacustrine setting on minor moraines. The presence of these moraines signifies a rapid response time of Schwarzensteinkees to climatic changes. This work presents unique findings on the influence of a proglacial lake, during its existence and after it had drained, in shaping a high-mountain valley in the Alps through time. In presenting these findings, this research highlights the necessity of understanding the past sequence of geomorphological evolution of an area to unravel the subsequent sequence of development to what exists today.

CHAPTER 5. Mechanisms of minor moraine formation in the Silvrettagletscher, Switzerland, alpine foreland

5.1 Silvrettagletscher and the foreland

In contrast to Schwarzensteinkees (Chapter 4), the Silvrettagletscher ice front is easily accessible and the glacier is still producing landforms (Figure 5.1-5.2). The areas nearest to the modern glacier are characterised by bedrock, sometimes bare and sometimes with thin sediment cover (Figure 5.3).

5.1.1 Geomorphological features of the Silvrettagletscher foreland

The most prominent features of the Silvrettagletscher foreland are minor moraines, which have been forming in the foreland since before 1850, and the reverse bedrock slope that is present in most immediately proglacial areas (Figure 5.1-5.3). Additionally, flutings are present in two areas of the foreland.

Field observations of minor moraines include both ice-cored and non-ice-cored moraines. Crestlines of moraines without ice cores vary from defined, sharp ridges to subdued mounds. Ice-cored moraines feature defined crestlines that are dominantly oriented parallel to the ice front, however there is variability in these orientations and some are nearly perpendicular to the ice front (Figure 5.4). In some locations, the ice is exposed (Figure 5.4B-C), but in others, sediment was excavated to reveal the underlying buried ice. Sediment cover ranges from silty-sandy veneers the thickness of one grain to up to 1 m, and many pebbles and cobbles are found at the bases of these landforms. During fieldwork, sediment was seen rolling and slumping off of these landforms, and rills of silt and very fine sand were noticeable on top of ice and other sediment. Where observable, the base of the ice core was either in contact with underlying material in places or separated from underlying material with a void space (Figure 5.4C).

5.1.2 Glaciological features of Silvrettagletscher

5.1.2.1 Englacial debris septa

Regarding the glacier, englacial debris septa emerge at three locations, whereas most of the surrounding ice is clean, i.e. without considerable debris cover. Field observations in summer 2015 showed that three englacial debris septa emerged at the ice surface.

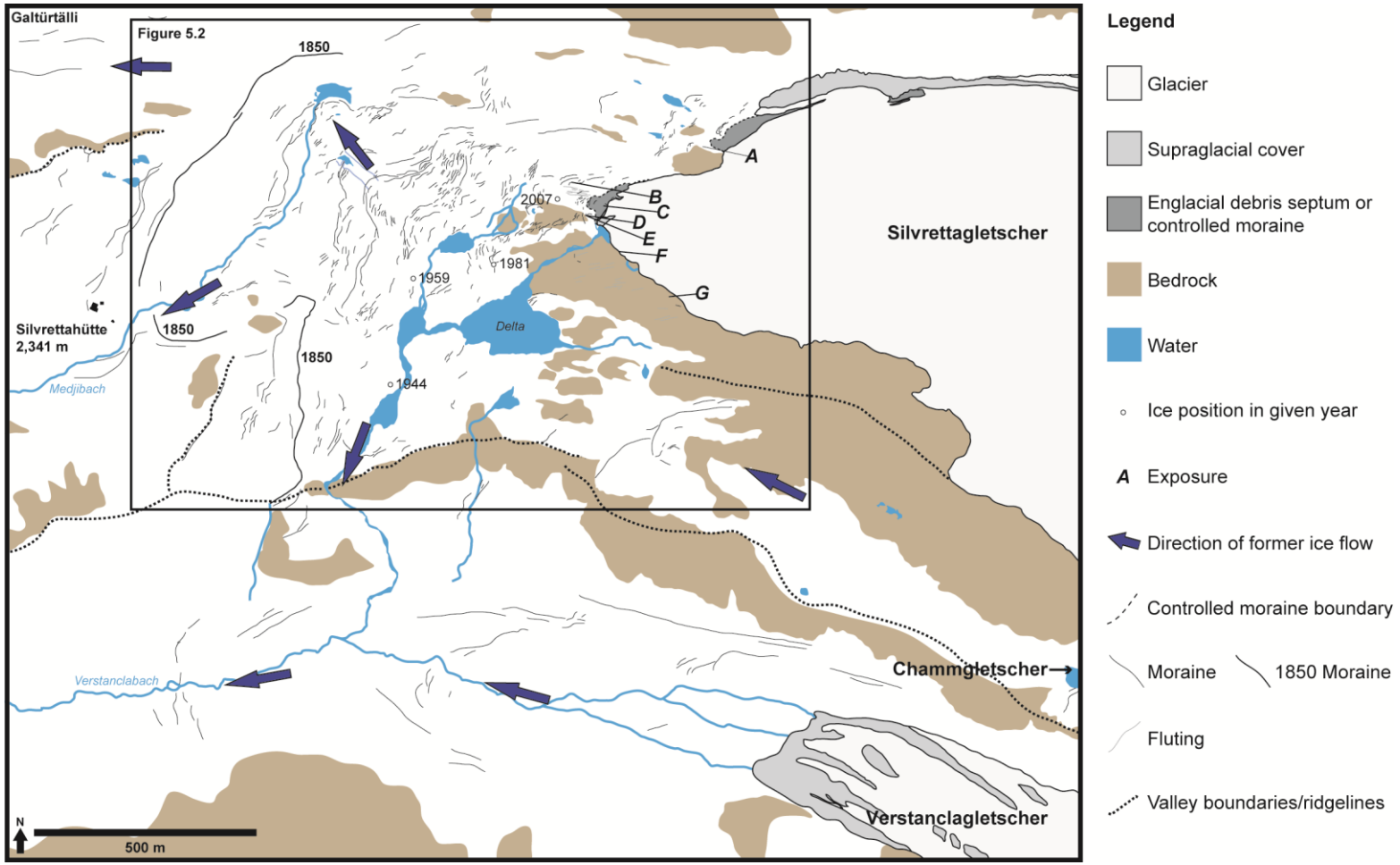

Figure 5.1. Geomorphological map of the Silvrettagletscher, Verstanclagletscher, and Chammgletscher forelands focusing on mapping moraines. Ice extent, exposed bedrock, and water (ponds, streams, and delta) based on 2013 aerial photograph as the newest available imagery. Moraines and fluting mapped using a combination of aerial photographs from 2012 and 2013 and field observations. Ice positions from marked locations along an educational path, the Gletscherlehrpfad (Silvrettahütte, 2016). Inset box shows location of Figure 5.2.

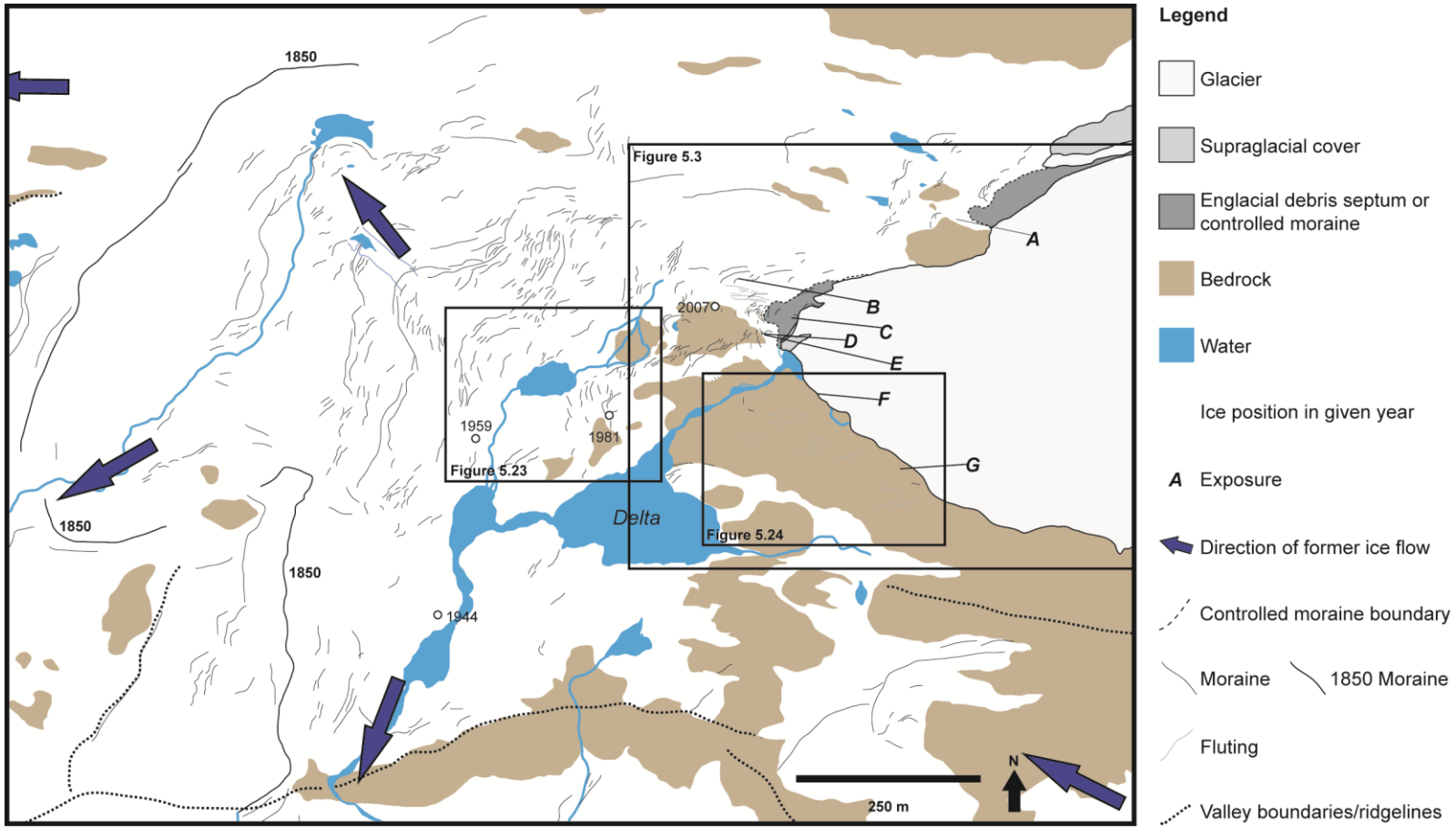

Figure 5.2. Geomorphological map of the Silvrettagletscher foreland focusing on mapping moraines, a closer view isolated from Figure 5.1. Ice extent, exposed bedrock, and water (ponds, streams, and delta) based on 2013 aerial photograph as the newest available imagery. Moraines and fluting mapped using a combination of aerial photographs from 2012 and 2013 and field observations. Ice positions from marked locations along an educational path, the Gletscherlehrpfad (Silvrettahütte, 2016). Inset boxes show locations of Figures 5.3, 5.23, and 5.24.

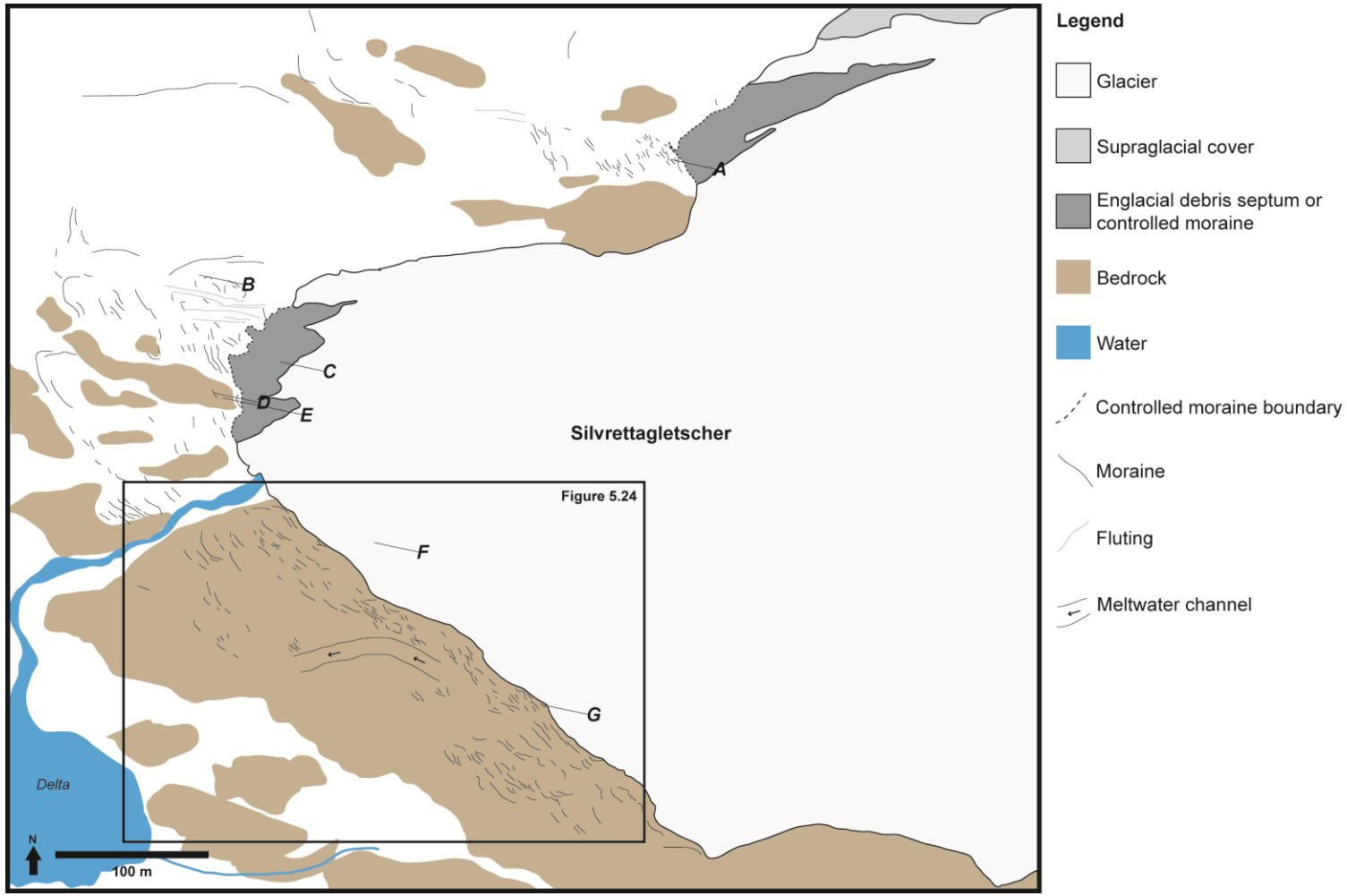

Figure 5.3. Geomorphological map of the Silvrettagletscher foreland focusing on mapping the most recent moraines. All mapping based on aerial photograph from 2009 (Google Earth, 2009) to serve as a comparison with the more recent map (Figures 5.1-5.2) and because moraines were more visible with this imagery. Inset box shows location of Figure 5.23.

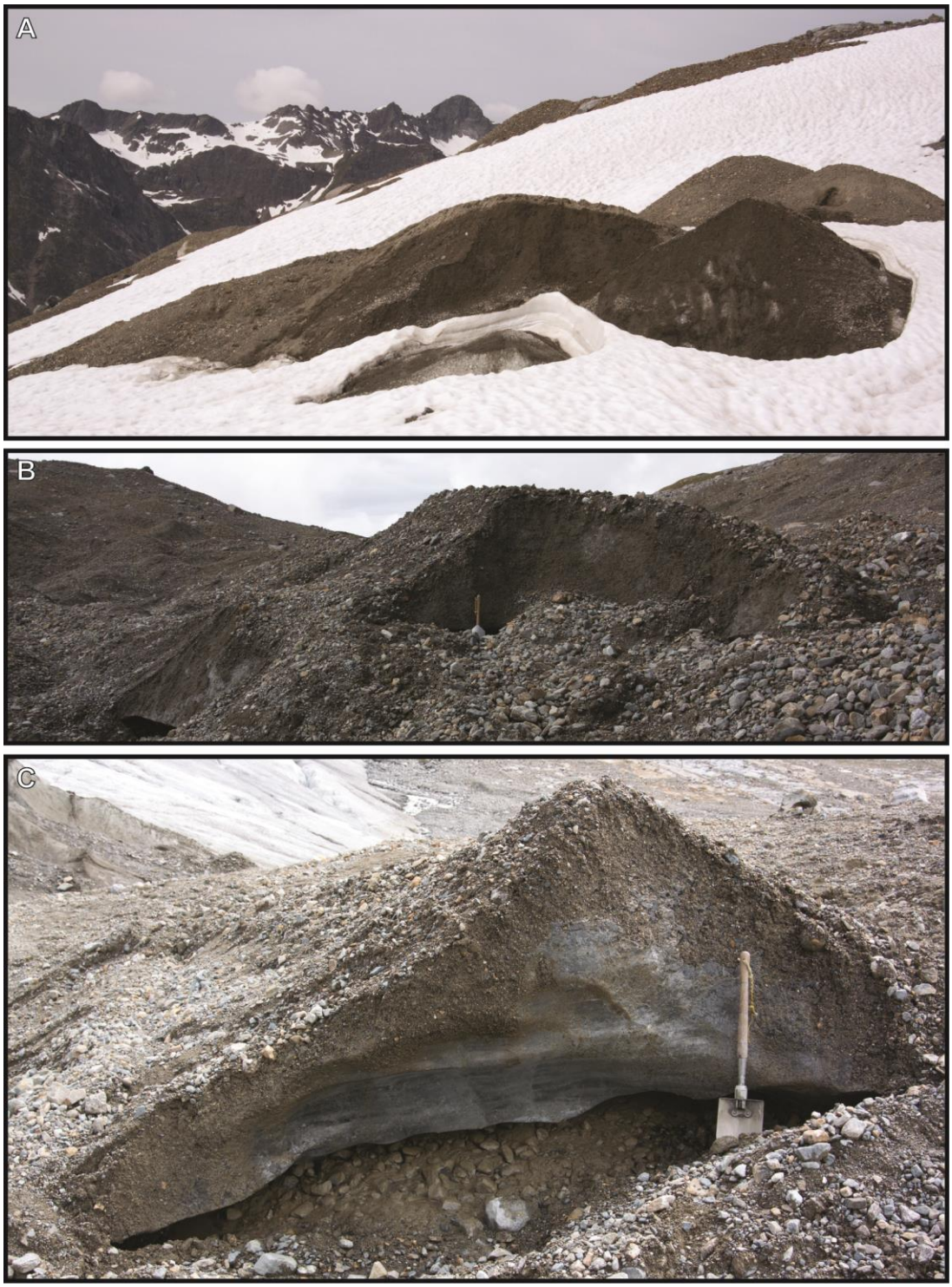

Figure 5.4. Ice-cored minor moraines in the Silvrettagletscher foreland. A) Three ice-cored moraines in the foreground and two in the middle ground of the photograph, with a noteworthy reverse bedrock slope in the background. The two prominent foreground moraines and the two middle ground moraines have ridges oriented approximately parallel to the ice front, whereas the other ridge is oblique to the ice front. Photograph taken in June 2015; B) Two ice-cored moraines. The lower moraine has a void space between the ice and underlying sediment and partially exposes an ice core. The upper ridge is oriented approximately parallel to the ice front, whereas the lower is oblique. Trenching tool for scale (49.5 cm long). Photograph taken in September 2015; C) An ice-cored moraine with the ice and sediment drape clearly exposed. This landform has a void space between the ice and underlying sediment at this exposed end. The ridge is oriented approximately parallel to the ice front. Trenching tool for scale (71 cm long). Photograph taken in September 2015.

Two of these septa existed in the lower portion of the ice front on the northern side of the channel and created debris cones on top of the glacier surface (Figure 5.5A). These are referred to here as the right debris septum or septa and left debris septum or septa, in relation to the valley axis and direction of ice movement. In the northernmost, higher portion of the ice front, several (greater than five) englacial debris septa created a complex of transverse linear debris concentrated on the glacier surface, hereafter referred to as a medial moraine (e.g. Evans, 2009), or the upper medial moraine (Figure 5.5B).

The morphologies of these englacial debris septa change through the timespan of 2003-2013 aerial imagery (Figure 5.6) and fieldwork observations in 2015 (Figure 5.5). These englacial debris septa also created controlled moraines at, and extending beyond the ice front during various periods. The term "controlled moraine" follows the definition of Evans (2009, p. 183), which states, "*Controlled moraines* are supraglacial debris concentrations that become hummocky moraine upon de-icing and possess clear linearity due to the inheritance of the former pattern of debris-rich folia in the parent ice." This process of controlled moraine formation is elaborated on in Section 5.4, whereas the dimensions and evolution of englacial debris septa emerging at the ice surface and controlled moraines are described here.

In 2015, the upper medial moraine extended quite far up-glacier and had multiple ridges in the direction of ice flow (Figure 5.5B). At this time, the medial moraine was easily distinguishable from clean ice on valley left. On valley right, a depression of clean ice with some supraglacial cover created a border between the medial moraine and ice with significant supraglacial cover, which extended to the valley walls. The two lower debris septa emerged near the ice front and were separated by surrounding clean ice (Figure 5.5A). The upper medial moraine, right debris septum, and left debris septum created controlled moraines in the foreland, but the boundaries between the controlled moraines and debris sources were unclear. At the ice front in all three locations, the contact between the ice of the controlled moraines and underlying surface varies. In places, ice was in contact with foreland sediment or bedrock. In other places, fluvial undercutting evacuated sediments, thereby producing void space between the ice and underlying surface, whether sediment or bedrock. For example, a small stream emerged from under the right controlled moraine and followed along and partially undercut the ice front before flowing beneath the left controlled moraine. Additionally, the ice of the controlled moraines contained numerous small caves and tunnels (Figure 5.5C).

Aerial photographs show the changing geometries of the englacial debris septa and associated medial and controlled moraines. In 2013 and 2012, the upper medial moraine complex extended approximately 380 m upvalley from the ice front and contained at least four distinct transverse linear debris ridges (Figure 5.6C-D).

Figure 5.5. Englacial debris septa and sediment delivery to the Silvrettagletscher ice front. A) The lower ice front. Ice extent indicated by dotted line. Englacial debris septa and debris fans indicated with dashed line. Left: right debris septa, right: left debris septa, in relation to the valley axis and direction of ice movement. Labelled asterisks indicate locations of B and C; B) The medial moraine at the upper ice front. This ice front exists behind the bedrock knob labelled in A. Extent of medial moraine indicated with dashed line; C) A portion of the right controlled moraine showing caves and cracks in the ice, which is draped in sediment. Trenching tool for scale (49.5 cm long). All photographs were taken in September 2015.

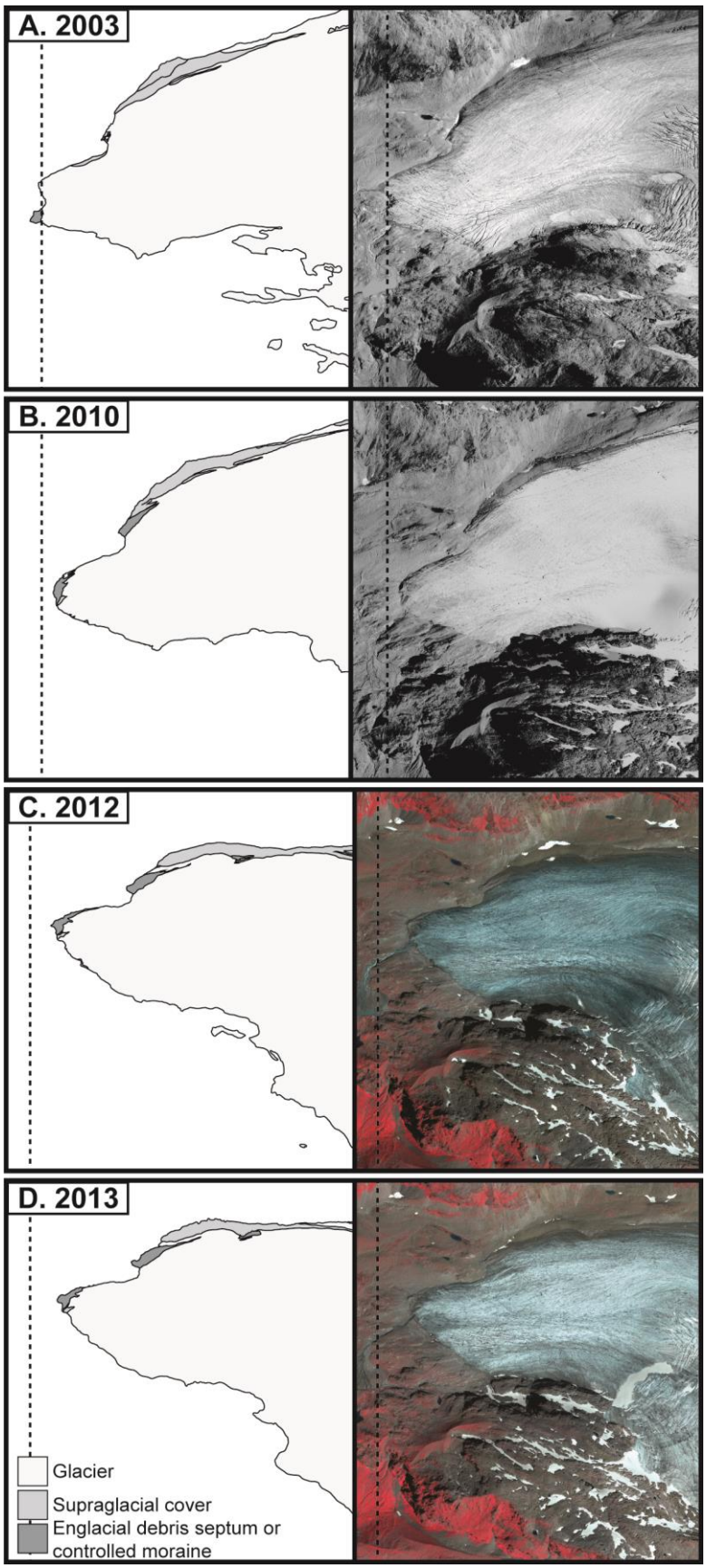

Figure 5.6. Evolution of the Silvrettagletscher ice front. A and B show the glacier in 2003 and 2010 based on aerial imagery at the same extent. C and D show the glacier in 2012 and 2013 based on infrared imagery at the same extent. No georeferencing has been applied, to present the most accurate depiction of ice front without skewing and stretching the images. Lines through the sketches and images show the location of alignment for image pairs (2003 and 2010, 2012 and 2013).

This upvalley extent was less than in 2015, by visual assessment. The upper controlled moraine was larger than in 2015 and covered approximately 2,200 m^2 of the foreland beyond the surrounding clean ice front. The right debris septum fed an extensive controlled moraine that covered over 6,000 m^2 of the foreland beyond the clean ice front, which was considerably larger than in 2015, by visual comparison. The right controlled moraine had some distinct ridges both parallel and perpendicular to ice flow. The left debris septum delivered debris to the ice surface as a debris cone (850 m^2), but did not create a controlled moraine. This debris cone was less extensive than in 2015, by visual assessment.

In 2010, the upper medial moraine had five ridges oriented parallel to ice flow and extended approximately 190 m upglacier (Figure 5.6B). The upper controlled moraine covered approximately 1,700 m^2 of the foreland beyond the surrounding clean ice front. The right debris septa created a clear transverse linear debris ridge that was approximately 75 m long and fed the controlled moraine complex, which was also fed by at least three other transverse linear debris ridges shorter (15-30 m) than the right debris septa complex. The right controlled moraine complex covered approximately 2,400 m^2 of the foreland beyond the surrounding clean ice. The left debris septum delivered debris to the ice surface as a small debris cone (880 m^2) and did not create a controlled moraine.

In 2003, the upper medial moraine was considerably smaller than later years and contained four ridges (15-30 m long) (Figure 5.6A). The medial moraine was producing a small controlled moraine, which covered approximately 210 m^2 of the foreland beyond the surrounding clean ice front and featured two prominent ridges. The right debris septum and controlled moraine either did not exist in 2003 or were covered by a pond. The left debris septum debris cone covered approximately 200 m^2 and was producing a controlled moraine that covered approximately 3,200 m^2 of the foreland beyond the surrounding clean ice front and featured several ridges parallel to the ice front.

Field observations also revealed highly saturated sediments immediately in front of the right controlled moraine and between the two lower controlled moraines. Small pools collected on the surface of proglacial gravel. Additionally, the presence of pockets of saturated, thixotropic till throughout the area were noticed when disturbing the overlying gravel layer. The 2003 imagery showed a proglacial lake in a depression in and extending beyond this saturated area, between a bedrock outcrop to the southwest, the glacier front along the south and east, a moraine to the northwest, and the valley walls to the north and northeast (Figure 5.6D). Subsequent photographs and field observations reveal the presence of flutings in this formerly ponded area.

5.1.2.2 The ice front

Unrelated to processes operating at medial and controlled moraines, incipient dead-ice bodies were noted across the ice front. These are occurring due to gravitational collapse of a thin ice front (Figure 5.7A), gravitational collapse when the ice tongue is not in contact with underlying material (Figure 5.7B), and/or fluvial undercutting (Figure 5.7C).

5.1.3 Sedimentological composition of the Silvrettagletscher minor moraines

The following descriptions detail the sedimentological composition of seven minor moraines without ice cores in the Silvrettagletscher foreland, labelled A-G from north to south. Interpretations for individual moraines are compiled and extrapolated on in the discussions of moraine formation (Section 5.5).

5.1.3.1 Exposure A

This moraine exists on a reverse bedrock slope in the northernmost, upper section of the ice front (46°51'26.75"N, 10°03'35.09"E; Figures 5.1-5.3). This moraine is 3.5 m long and 2.6 m wide with a straight crestline that trends 180°. The proximal slope is steeper (36°) than the distal slope (20°), as measured at the exposure. Aerial imagery shows that this moraine formed shortly before 2010 in front of the upper controlled moraine.

Bedrock is the lower boundary of most of the exposure (Figure 5.8). Seven different FAs were observed in the exposure. FA 1 consists of weathered bedrock in the lowest central area of the exposure. This bedrock is crumbling and splintering, with silt filling in some partings. Splintering follows foliation of constituent minerals, dominantly biotite sheets. The pore space between fragments also contains significant water, which leaks out when disturbed.

FAs 2-4 overlie intact bedrock and FA 1 weathered bedrock, and the most ice-distal zone of FA 3 partially overlies FA 2. FA 2 is composed of massive, moderately-sorted silt with little clay and fine sand (Fm). FA 3 contains very friable, massive, openwork, poorly-sorted cobbles with pebbles scattered throughout (Go, Gm; maximum a-axis 12.5 cm). Localised non-openwork zones contain coarse sand and granules in pore spaces. The contact between FA 2 and FA 3 is sharp, however the contact between this and the overlying FA 4 is more diffuse. The latter comprises very friable massive, openwork, poorly-sorted pebbles with frequent granules and some cobbles (Go, GRo).

Figure 5.7. Thin ice fronts of Silvrettagletscher. A) An example of the thin ice front in the upper portion of the valley, south of the upper controlled moraine. The ice here lies directly over a reverse bedrock slope. Trenching tool for scale (49.5 cm long); B) Example of the thin ice front in the lower portion of the valley, north of the right controlled moraine. The ice here partially overlies preexisting foreland sediment or has void space between the ice and underlying sediment. Trenching tool for scale (71 cm long); C) Example of the thin ice front in the lower portion of the valley, between the right and left debris septa, seen in the background. Some portions of the ice here are directly underlain by till, whereas fluvial undercutting has created void space between the ice front and underlying sediment in others. All photographs were taken in September 2016.

FAs 5-7 cap the uppermost portion of the exposure. FA 5 generally follows the shape of the ridge crest and contains massive, openwork, poorly-sorted cobbles with some pebbles (Go). The lower contact of this FA with FA 4 is diffuse, however the FAs are clearly distinguishable by dominant clast size. FA 6 follows the shape of the proximal slope as a veneer of massive, moderately-sorted coarse sand and granules. The contact between this FA and the surrounding FAs is sharp. FA 7 directly underlies the ridge crest and comprises massive, clast-supported, poorly-sorted pebbles and cobbles (Gm), with coarse sand, granules, and some medium sand in pore spaces. The lower contact of this FA with FA 5 is sharp, and this FA contains smaller clasts overall than FA 5 below.

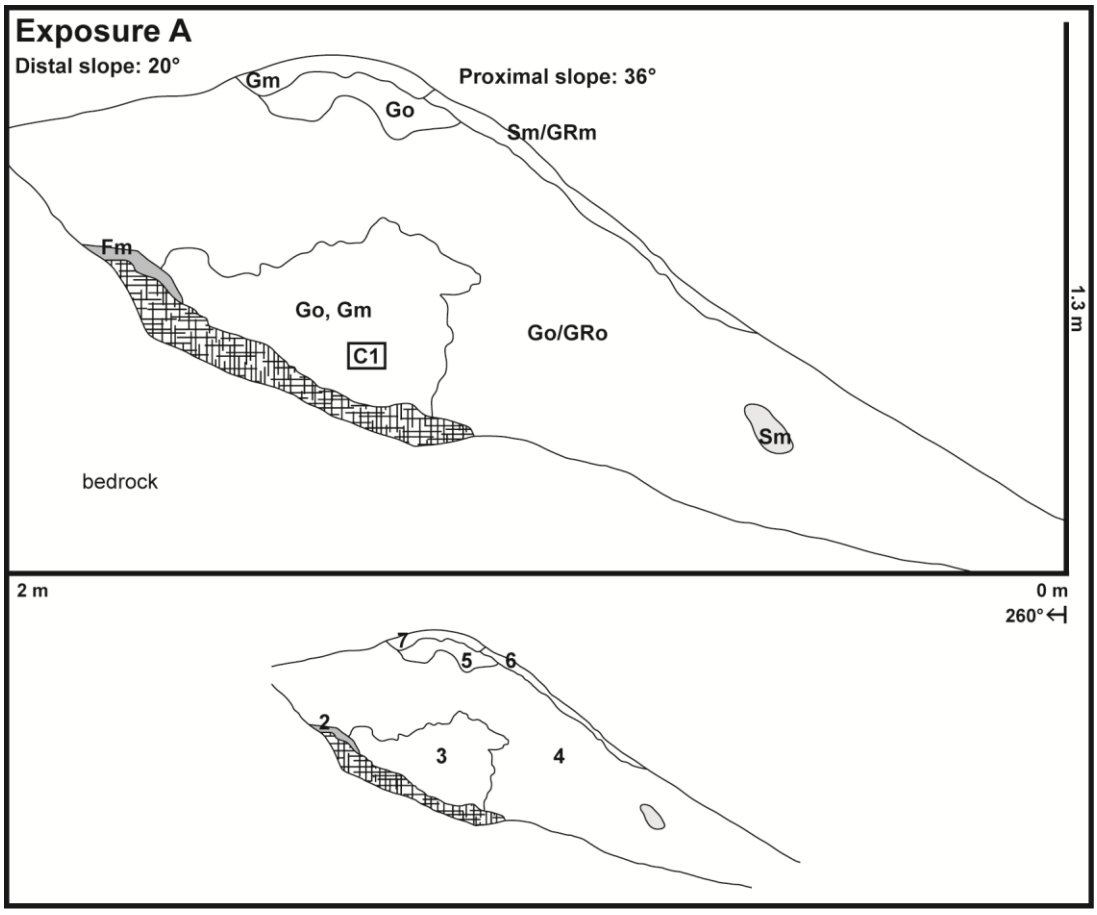

Figure 5.8. Exposure A representative log. FAs are labelled with facies codes (top) and FA numbers (bottom) and are described in the text in stratigraphic order from bottom to top. Figure 2.6 shows a facies codes and symbols key.

5.1.3.2 Exposure B

This moraine is located at the ice-distal extent of a proglacial lake observed in the 2003 aerial photograph (46°51'24.37"N, 10°03'20.82"E) and is 18.3 m long with an average width of 3.5 m and a semi-arcuate crestline that has an average trend of 29° (Figure 5.1). Overall, the proximal slope is slightly shallower (25°) than the distal slope (28°). This

moraine formed sometime before 2000, although a more specific estimate is not possible without older imagery.

Nine different FAs were observed (Figure 5.9). FA 1 forms the base of most of the exposure. This FA is composed of massive, matrix-supported, poorly-sorted cobbles with some pebbles (Gms; maximum a-axis 14.0 cm). FA 2 is the base of the remainder of the exposure and contains massive, moderately-sorted, very fine to fine sand with some silt and few and isolated pebbles (Sm, Fm). The contact between FA 2 and the surrounding parts of FA 1 is sharp.

FA 3 overlies the ice-proximal extent of FA 1 and is composed of similar sediments as FA 2 (Sm, Fm). The contact with underlying FA 1 is sharp. FA 4 follows the general trend of the distal slope and contains massive, poorly-sorted coarse sand (Sm). There is a sharp contact between FA 4 and the gravel FA 1 below. The contacts between FA 4 and the surrounding sand FAs are gradational, but the FAs are readily differentiated by grain size and the presence or absence of laminations. FA 5 is surrounded by sand FAs and contains massive, matrix-supported, poorly-sorted cobbles and some pebbles (Gms). The contact between this FA and the surrounding sand FAs is sharp. FA 6 contains poorly-sorted medium to coarse sand. The sand is laminated (Sl), and folded in places (Sd). The contact between this FA and gravel FA 1 below and FA 5 is sharp, but the contacts between this FA and the surrounding sand FAs are less so. The FAs are instead differentiated by presence or absence of laminations.

FA 7 directly underlies the lower part of the distal slope and contains massive, poorly-sorted, very fine to fine sand with some silt and few pebbles (Sm, Fm), similar to FA 2 and FA 3. The contact between this FA and others is sharp, and the FA is differentiated from the surrounding sand FAs by dominant grain size and presence or absence of laminations. FA 8 is a majority of the exposure and especially dominates the core of the moraine. This FA comprises moderately-sorted, medium sand that is horizontally laminated and bedded at the most proximal extent (Sh, Sl). Laminations and beds throughout the rest of the FA are folded with a dominant trend of laminations and fold axes following the orientation of the distal slope (Sd) (Figure 5.10). A prominent normal fault displaces a sand bed in the upper proximal zone of the FA. Larger portions of this sand FA frequently broke away from the exposure during excavation, suggesting the presence of other faults throughout the FA. The contact between this FA and the surrounding sand FAs is gradational, but grain size and the presence of laminations and bedding differentiate FA 8 from the others. FA 9 directly underlies the ridge crest and a majority of the distal slope. This FA contains moderately-sorted, medium sand with approximately horizontal laminations at the ridge crest (Sl). The rest of the FA is massive (Sm). The contact between this FA and the surrounding sand FAs is sharp.

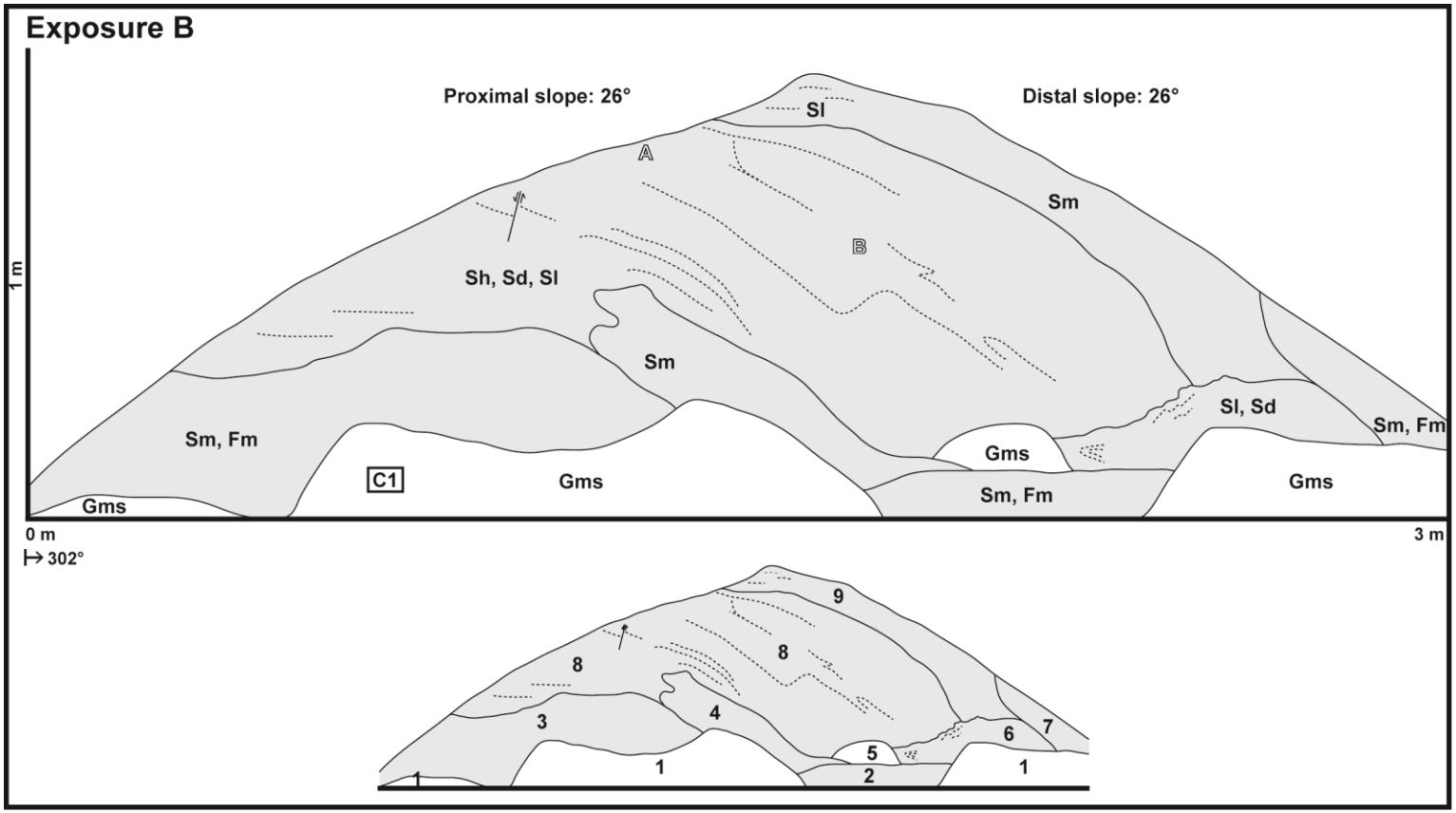

Figure 5.9. Exposure B representative log. FAs are labelled with facies codes (top) and FA numbers (bottom) and are described in the text in stratigraphic order from bottom to top. Figure 2.6 shows a facies codes and symbols key. Labelled photograph locations refer to the photographs in Figure 5.10.

Figure 5.10. Photographs from Exposure B. Photographs correspond to locations on Figure 5.9. These photographs highlight the zone of more horizontally laminated sand in FA 8 (A) compared to the deformed laminations in the core of FA 8 (B). Pencil for scale (14.7 cm long).

5.1.3.3 Exposure C

This moraine exists on the northern side of the main proglacial channel (46°51'22.59"N, 10°03'23.33"E; (Figures 5.1-5.3) and is 10.0 m long with an average width of 2.1 m and a generally straight crestline that has an average trend of 152°. Overall, the proximal slope is steeper (38°) than the distal slope (22°). The moraine exists on a reverse bedrock slope, however the exposure does not extend to the bedrock. A comparison of the 2013 aerial photograph and field observations in 2015 show that this moraine formed between 2013 and 2015 in front of the right controlled moraine.

Three different FAs and prominent underlying material (considered FA 1) were observed (Figure 5.11). FA 1 underlies the exposed portion of the moraine. The exposure was not cleared to include this FA due to its dense and very saturated nature making it difficult to excavate without flooding the base of the exposure. This is a massive, matrix-support diamicton (Dmm) with few clasts (maximum a-axis 5.5 cm). Sedimentary structures or lack thereof could not be ascertained due to the FA not lending itself to excavation. The matrix is composed dominantly of silt, with some clay. The contact between FA 1 and FA 2 is sharp and especially noticeable by the difficulty to pierce into FA 1 compared to the relative ease in excavating FA 2. FA 2 overlies FA 1 for most of the exposure and is a massive, matrix-supported, moderately-sorted diamicton (Dmm) with isolated zones that are clast-supported (Dcm) (maximum a-axis 19.0 cm). The matrix is composed dominantly of silt, with some very fine and fine sand. This diamicton contains significantly more clasts than FA 1 and is compact and cohesive but not as dense and saturated as FA 1.

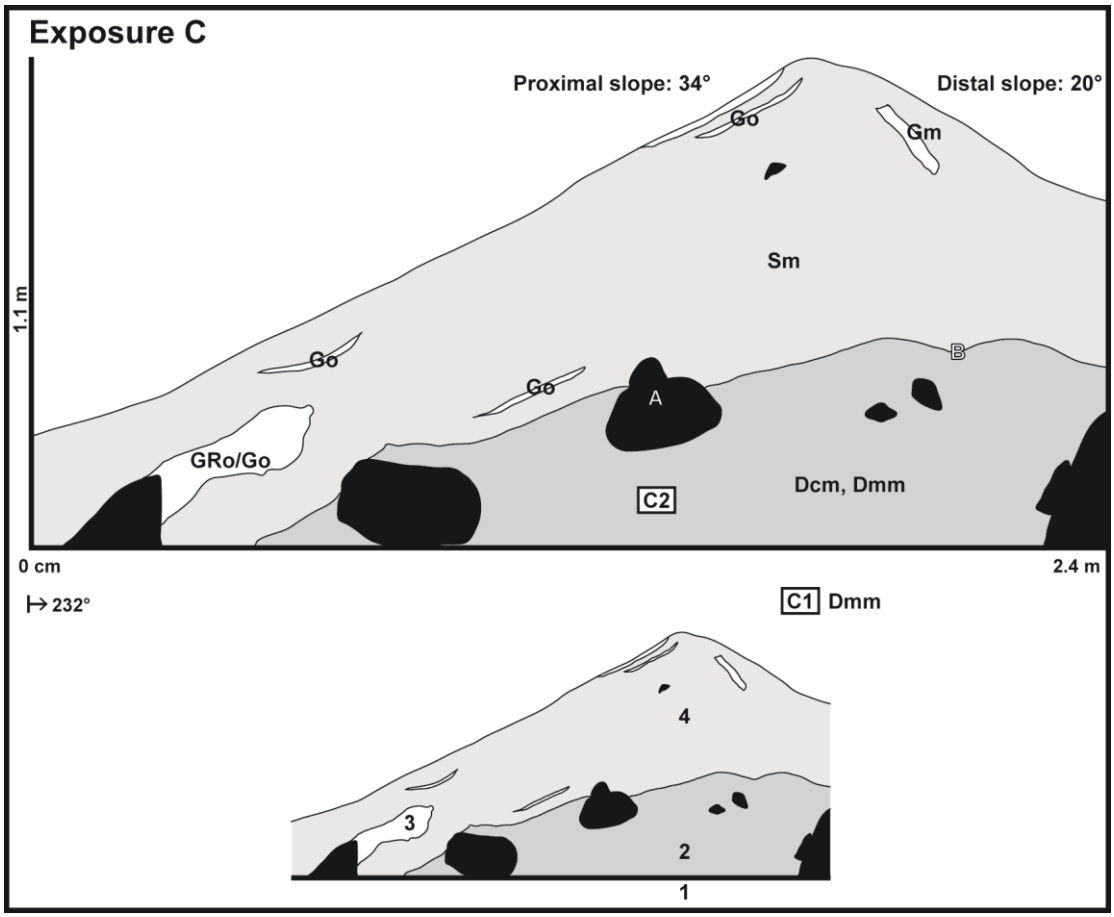

Figure 5.11. Exposure C representative log. FAs are labelled with facies codes (top) and FA numbers (bottom) and are described in the text in stratigraphic order from bottom to top. Figure 2.6 shows a facies codes and symbols key. Labelled photograph locations refer to the photograhs in Figure 5.12.

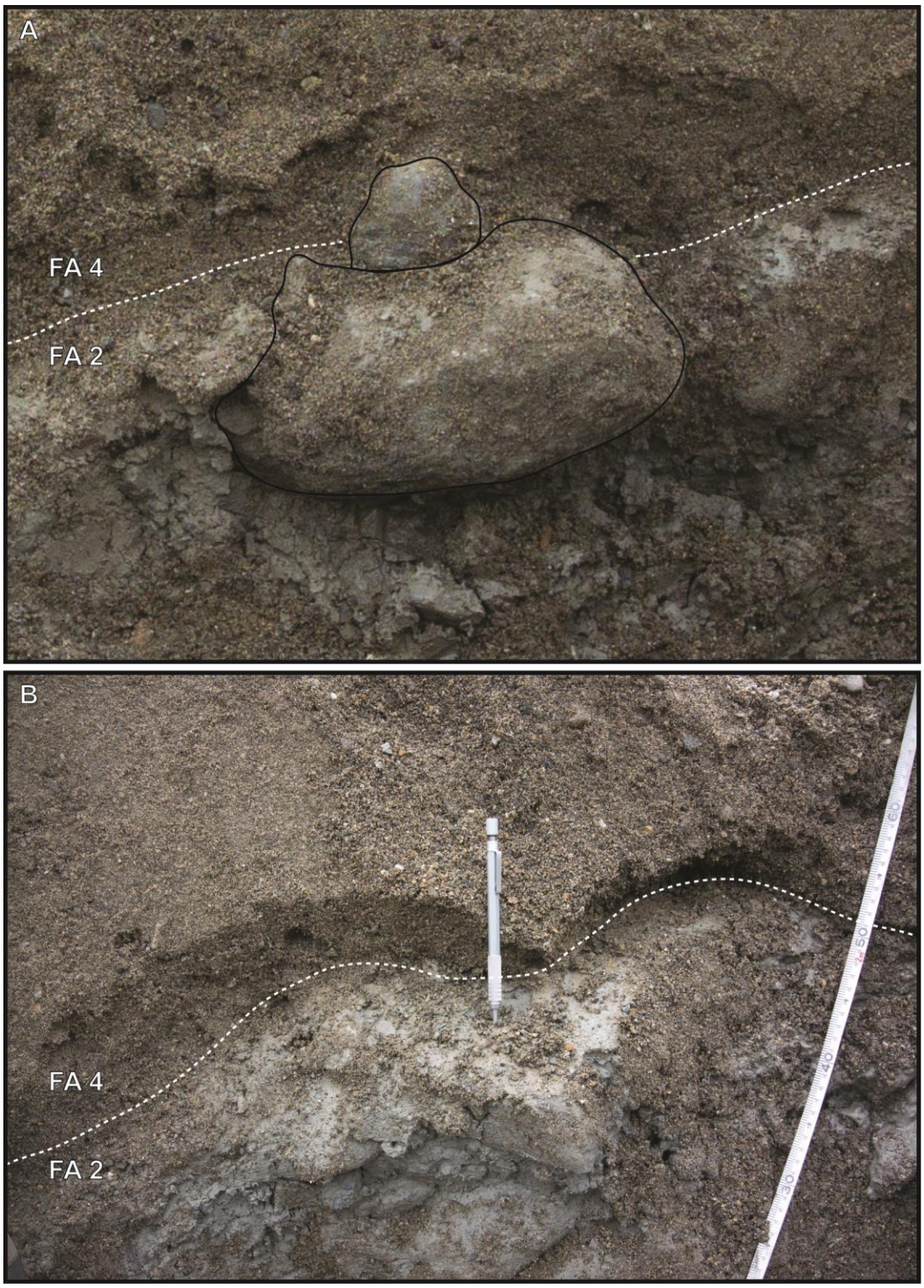

Figure 5.12. Photographs from Exposure C. Photographs correspond to locations on Figure 5.11. Dashed line shows the sharp contact between diamicton FA 2 and sand FA 3. Boulders outlined in black. Pencil for scale (14.7 cm long).

FA 3 is a distinct massive, openwork, poorly-sorted granule-pebble FA extending from a boulder and generally following the orientation of the proximal slope (Sm). The contact of this gravel FA and the surrounding sand FA is sharp. FA 4 comprises massive, poorly-sorted medium to coarse sand with some pebbles and few cobbles throughout (Sm)

and is very friable. FA 4 additionally contains several lenses of granules to pebbles, some of which are openwork (Go) and one of which is clast-supported and contains coarse sand in the pore spaces (Gm). The openwork lenses follow the general orientation of the proximal slope, whereas the clast-supported lenses follow the general orientation of the distal slope. The contact between FA 4 and FA 2 is sharp.

5.1.3.4 Exposure D

This moraine exists on a reverse bedrock slope on the northern side of the main proglacial channel (46°51'21.84"N, 10°03'21.37"E; Figures 5.1-5.3) and is 10.0 m long with an average width of 4.1 m and a semi-arcuate crestline that has an average trend of 204°. Overall, the proximal slope is steeper (30°) than the distal slope (15°). Aerial photographs show that this moraine formed shortly after 2003 in front of clean ice.

Bedrock marks the lower boundary of the exposure in a series of steps that resemble a staircase from the ice-proximal to the ice-distal extents of the landform (Figure 5.13). Sixteen different FAs were observed. FAs 1-3 exclusively overlie bedrock, as do portions of FA 4 and FA 9. FA 1 is a massive, matrix-supported, moderately-sorted diamicton (Dmm) that overlies a majority of the bedrock exposure base. Clasts are present but not prominent and are dominantly pebbles, with few cobbles (maximum a-axis 6.9 cm). The matrix is composed of clayey silt with some very fine sand in places and of silty clay in others. Consolidation varies throughout, but the FA is generally quite consolidated. FA 2 contains massive (Sm) and horizontally-laminated and low angle cross-laminated (Sl), well-sorted sand and overlies a portion of the bedrock exposure base. Laminations are individually ≤1 cm thick and alternate between moderately-sorted fine-medium sand and moderately-sorted coarse sand. FA 3 contains the same sediment as FA 1 (Dmm) and overlies bedrock at the distal extent of the exposure.

FA 4 overlies all of FA 1, and also a small portion of bedrock at the base of the exposure. This FA comprises massive, matrix-supported, moderately-sorted pebbles and cobbles (Gm). The matrix is composed dominantly of coarse sand with some granules and little medium sand. FA 5 overlies FA 4 with a sharp contact and contains massive, clast-supported, poorly-sorted cobbles and some pebbles (Gm). The pore space contains dominantly coarse sand with some granules. FA 6 is a small wedge of massive, openwork, moderately-sorted pebbles and some cobbles (maximum a-axis 7.9 cm). This FA has a sharp boundary.

The boundaries between FAs 7, 8, 9, and 11 are diffuse. FA 7 contains matrix-supported, poorly-sorted pebbles and cobbles, with a matrix composed dominantly of coarse sand and some medium sand. Faint horizontal bedding is noticeable on the lower ice-

proximal side of the exposure (Gh), but this FA is massive elsewhere (Gms). FA 8 comprises clast-supported, poorly-sorted pebbles and cobbles, with coarse sand, granules, and little medium sand in the pore spaces. Faint horizontal bedding is noticeable in places (Gh), but the FA is otherwise massive (Gm). FA 9 contains matrix-supported, moderately-sorted pebbles and some cobbles (Gms). The matrix coarsens upwards, with medium-coarse sand in the lower reaches, coarsening up to granules with some coarse sand (Gcu). Faint horizontal bedding is noticeable towards the middle of the FA (Gh), and planar bedding follows the shape of the contact with FA 3 below towards the lower ice-distal portion of the FA (Gp).

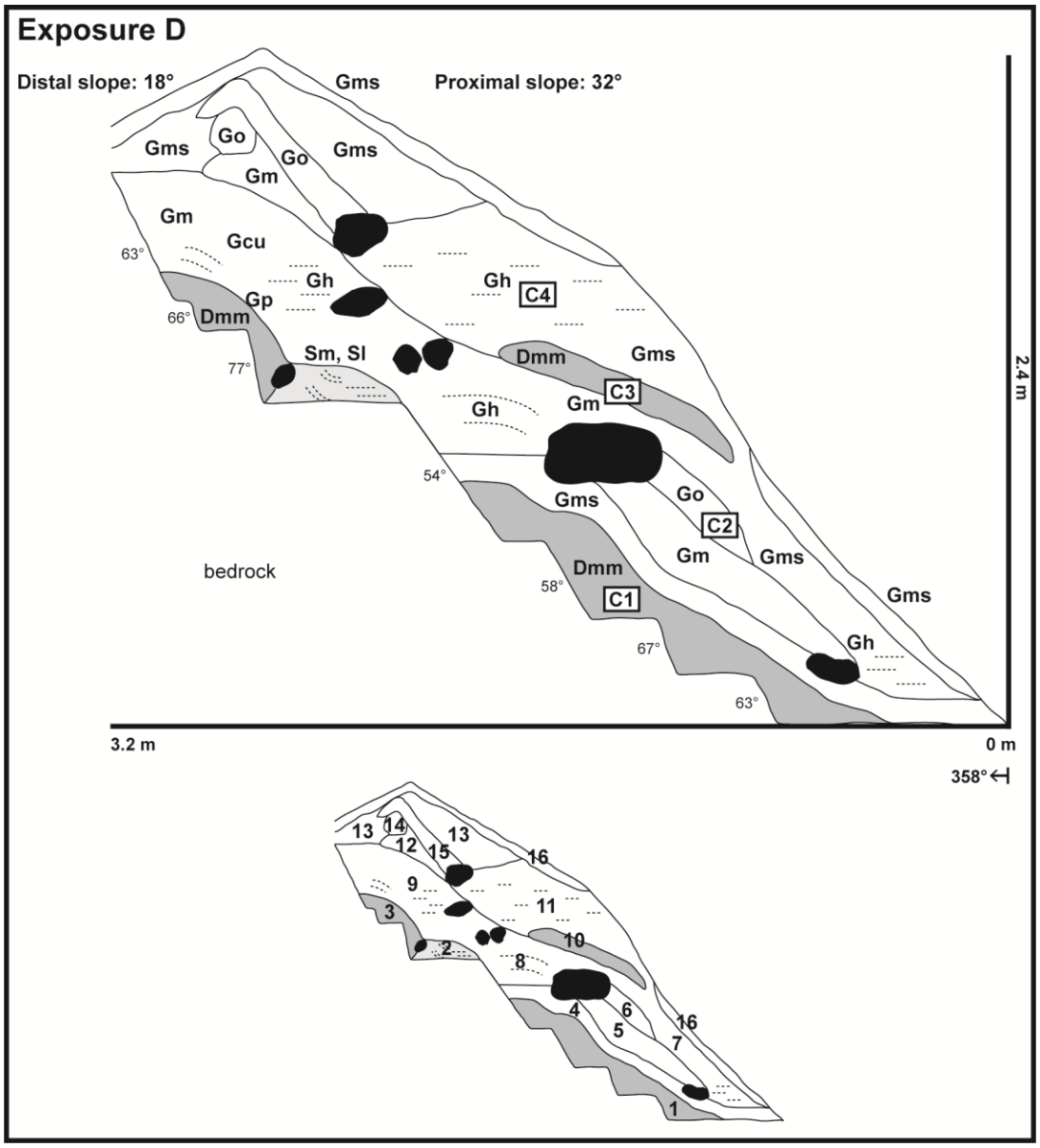

Figure 5.13. Exposure D representative log. FAs are labelled with facies codes (top) and FA numbers (bottom) and are described in the text in stratigraphic order from bottom to top. Figure 2.6 shows a facies codes and symbols key.

FA 10 is a distinct FA of massive, matrix-supported, moderately-sorted diamicton (Dmm) that has sharp contacts with surrounding FAs. Clasts are dominantly pebbles with some cobbles (maximum a-axis 9.5 cm) and are more abundant than in FA 1. The matrix is composed of silt with some clay and few zones of silty clay. The level of consolidation is similar to FA 1.

FA 11 comprises matrix-supported, moderately-sorted pebbles and cobbles (maximum a-axis 9.0 cm), with coarse sand and some medium sand as the matrix. Faint horizontal bedding is noticeable above the upper extent of FA 10 (Gh), however the lower portions of this FA are massive (Gms). FAs 12-16 make up the ridge crest portion of this exposure and have sharp contacts. FA 12 contains massive, clast-supported, moderately-sorted pebbles and some cobbles (Gm). Pore spaces contain coarse sand and granules with little medium sand. FA 13 contains massive, matrix-supported, moderately-sorted pebbles and cobbles, with coarse sand and some medium sand as the matrix (Gms). FA 14 is an isolated pod bound by FAs 12, 13, and 15 and contains massive, openwork, moderately-sorted cobbles and some pebbles (Go). FA 15 comprises massive, openwork, moderately-sorted pebbles and some cobbles, occasionally with a cobble as the entire thickness of the FA. FA 16 directly underlies the ridge crest, distal slope of the landform, and most of the proximal slope of the landform. This FA contains massive, matrix-supported, moderately-sorted pebbles and few cobbles, with medium to coarse sand and some granules as the matrix (Gms).

5.1.3.5 Exposure E

This moraine exists on a reverse bedrock slope on the northern side of the main proglacial channel (46°51'21.77"N, 10°03'21.63"E; Figures 5.1-5.3) and is 4.4 m long with an average width of 3.5 m and a generally straight crestline that has an average trend of 232°. Overall, the proximal slope is slightly steeper (34°) than the distal slope (30°). Aerial photographs show that this moraine formed sometime between 2003 and 2010 in front of an area of clean ice, and its location closer to the 2003 ice margin suggests formation nearer to 2003.

Nine different FAs were observed in the exposure (Figure 5.14). FA 1 and FA 2 extend below the exposure and are separated by approximately 2 m of bedrock. FA 1 contains massive, poorly-sorted gravel. The FA is clast-supported towards the left of the FA (Gm), with coarse sand and granules in pore space, and matrix-supported towards the right (Gms), with coarse sand, some medium sand, and few granules as the matrix.

FA 2 is the only non-gravel FA in this exposure, and is a massive, matrix-supported diamicton that contains poorly-sorted pebbles and cobbles (maximum a-axis 10.7 cm), with moderately-sorted silt and some clay as the matrix (Dmm).

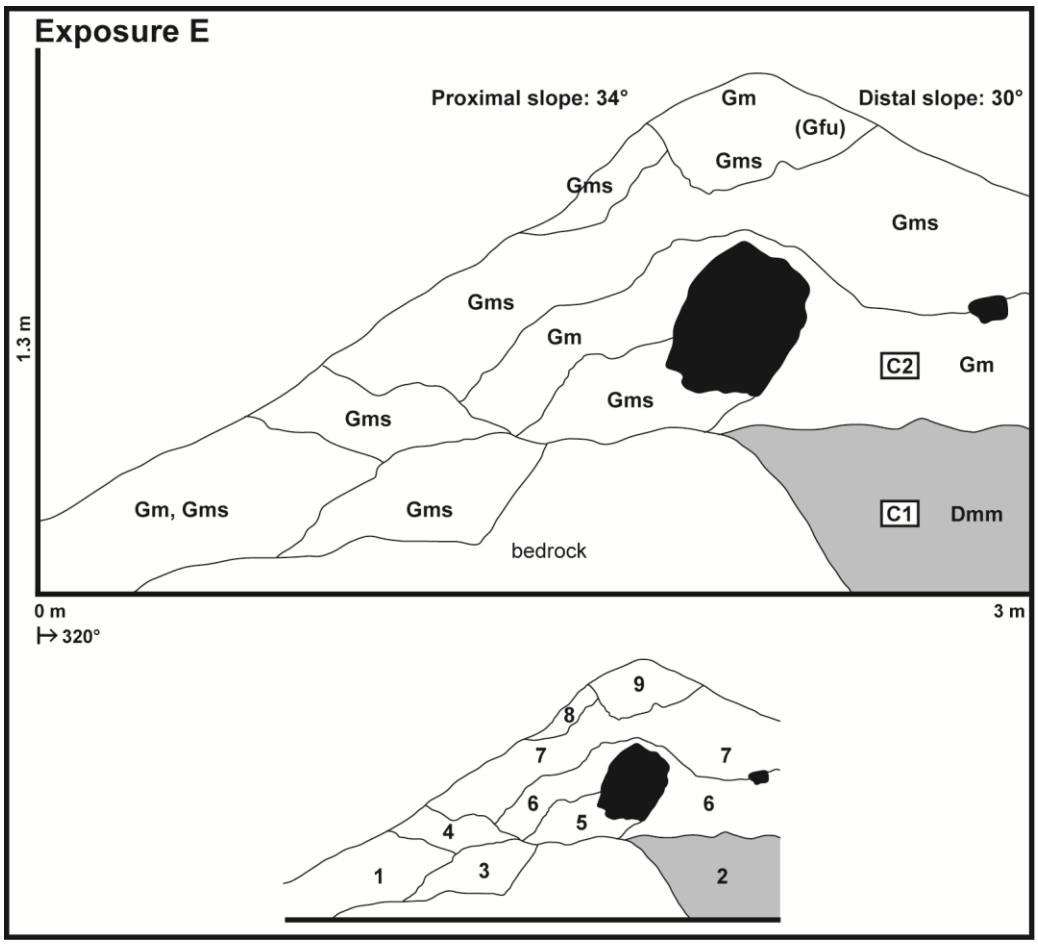

Figure 5.14. Exposure E representative log. FAs are labelled with facies codes (top) and FA numbers (bottom) and are described in the text in stratigraphic order from bottom to top. Figure 2.6 shows a facies codes and symbols key.

FAs 3-9 are composed dominantly of gravel and are the majority of the moraine. The boundaries between these FAs are somewhat diffuse, and FAs are differentiated by dominant clast size and composition. FA 3 overlies bedrock at the base of the exposure and contains massive, matrix-supported, poorly-sorted pebbles and cobbles (Gms). The matrix is dominantly coarse sand, with little medium sand. FA 4 contains massive, matrix-supported, moderately-sorted pebbles and few cobbles (Gms). The matrix is dominantly medium sand, with some coarse sand. FA 5 overlies bedrock at the base of the exposure and is partially bound at its upper end by a prominent boulder. This FA comprises massive, matrix-supported, poorly-sorted pebbles-cobbles, with coarse sand, some granules, and little medium sand as the matrix (Gms). FA 6 predominantly overlies FA 2 at the ice distal portion of exposure, but extends above and past the prominent boulder and forms the centre the exposure. This FA contains massive, clast-supported, moderately-sorted cobbles and some pebbles (Gm; maximum a-axis 10.5 cm). The pore space contains coarse sand and granules, with some medium sand. This FA also contains one prominent boulder in the centre of the exposure. FA 7 spans the width of the exposure in its upper half and is the most friable of the exposure. This FA comprises massive, matrix-supported, poorly-sorted

pebbles and some cobbles (Gms), with medium sand to granules and little fine sand as the matrix. FA 8 is a zone of gravel along the ice-proximal slope of the exposure and contains massive, matrix-supported, poorly-sorted pebbles to cobbles with medium sand, some coarse sand, and few granules as the matrix (Gms). FA 9 caps the exposure and immediately underlies the ridge crest and contains upward fining gravel. This FA comprises massive, matrix-supported, poorly-sorted cobbles with some pebbles towards the bottom (Gms), and clast-supported, moderately-sorted pebbles with some cobbles towards the top (Gm). The lower pore space contains coarse sand to granules, with some medium sand, which is the same composition as the overlying matrix.

5.1.3.6 Exposure F

This moraine exists on a reverse bedrock slope on the southern side of the main proglacial channel (46°51'18.90"N, 10°03'25.10"E; Figures 5.1-5.3) and is 8.0 m long and 2.9 m wide with a straight crestline that trends 290°. The proximal slope is shallower (33-37°) than the distal slope (43°). Aerial photographs show that this moraine formed around 2013 in front of an area of clean ice.

Six different FAs were observed. Bedrock forms the lower boundary of the exposure (Figure 5.15), and FA 1 consists of weathered bedrock, which is crumbling and splintering, with silt filling in some partings, rendering it easy to excavate. The splintering/dominant weathering planes follow foliation of constituent minerals, dominantly biotite. FA 2 is a zone of massive, matrix-supported diamicton (Dmm) within the weathered bedrock face of the exposure. The matrix is composed dominantly of silt, with some very fine sand. FA 3 is a massive, matrix-supported diamicton (Dmm) similar to FA 2. This FA caps the lower proximal extent of the exposure.

FA 4 comprises massive, poorly-sorted medium to coarse sand with few pebbles (Sm). This FA contains two distinct horizontal lenses of massive, moderately-sorted coarse sand. FA 5 is a massive, matrix-supported diamicton (Dmm) similar to FA 2 and FA 3. FA 6 caps the distal slope and ridge crest, as well as most of the proximal slope. The boundaries between FA 6 and underlying FAs are sharp. This FA contains massive, clast-supported pebbles and cobbles (maximum a-axis 12.6 cm) with poorly-sorted coarse sand and granules in the pore spaces (Gm).

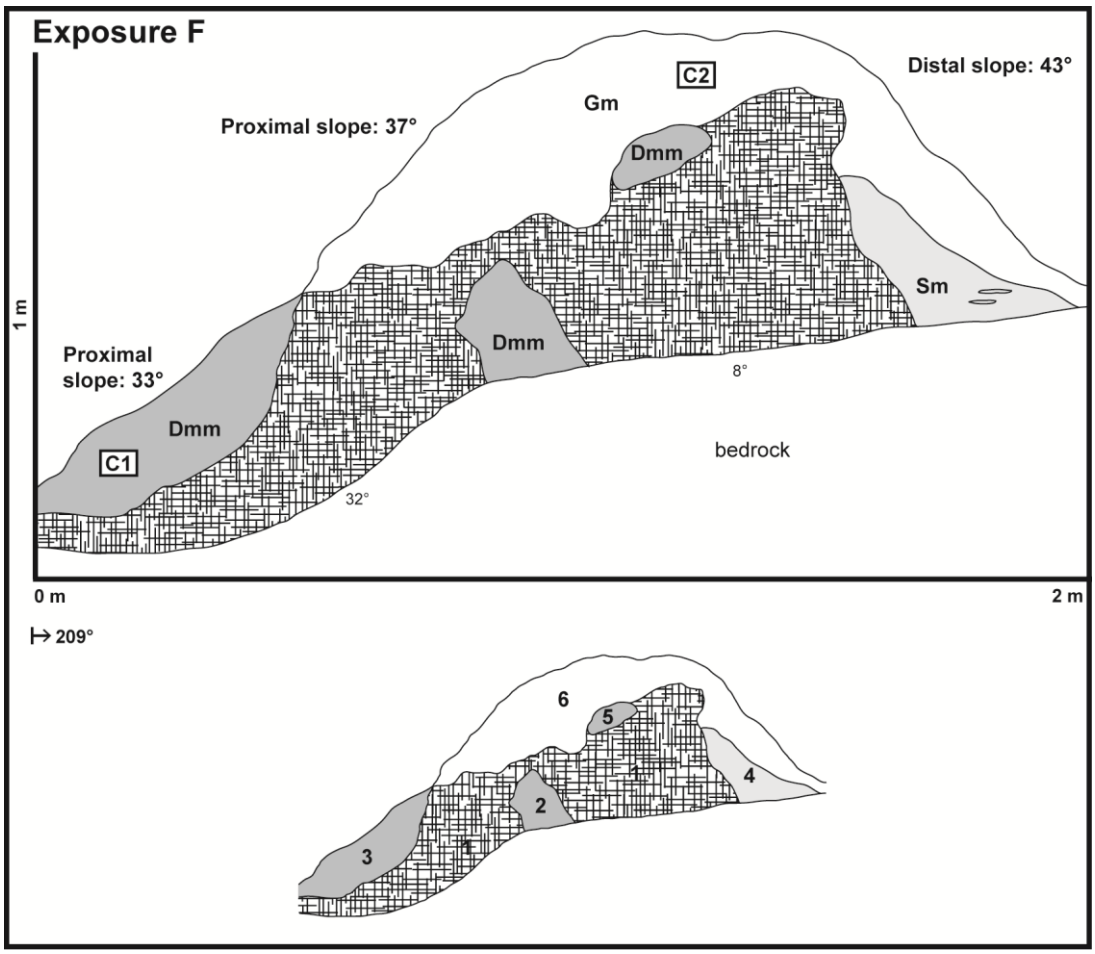

Figure 5.15. Exposure F representative log. FAs are labelled with facies codes (top) and FA numbers (bottom) and are described in the text in stratigraphic order from bottom to top. Figure 2.6 shows a facies codes and symbols key.

5.1.3.7 Exposure G

This moraine exists on a reverse bedrock slope on the southern side of the main proglacial channel (46°51'15.55"N, 10°03'31.24"E; (Figures 5.1-5.3) and is 6.0 m long and 2.3 m wide, with a straight crestline that trends 330°. The proximal slope is steeper (48°) than the distal slope (44°). Aerial photographs show that this moraine formed sometime between 2010 and 2013 in front of an area with clean ice.

Bedrock forms the lower boundary for most of the exposure (Figure 5.16). FA 1 delineates the base of exposure at its most proximal extent and overlies bedrock for the remainder of the exposure. This FA contains massive, clast-supported, poorly-sorted pebbles and cobbles with some granules and coarse sand in pore spaces (Gm/GRm; maximum a-axis 9.1 cm). The contact between FA 1 and FA 2 is sharp, and FA 2 dominates the exposure. This FA comprises massive, matrix-supported, clast-rich diamicton (Dmm). The matrix consists of silt and some very fine sand and contains some prominent boulders.

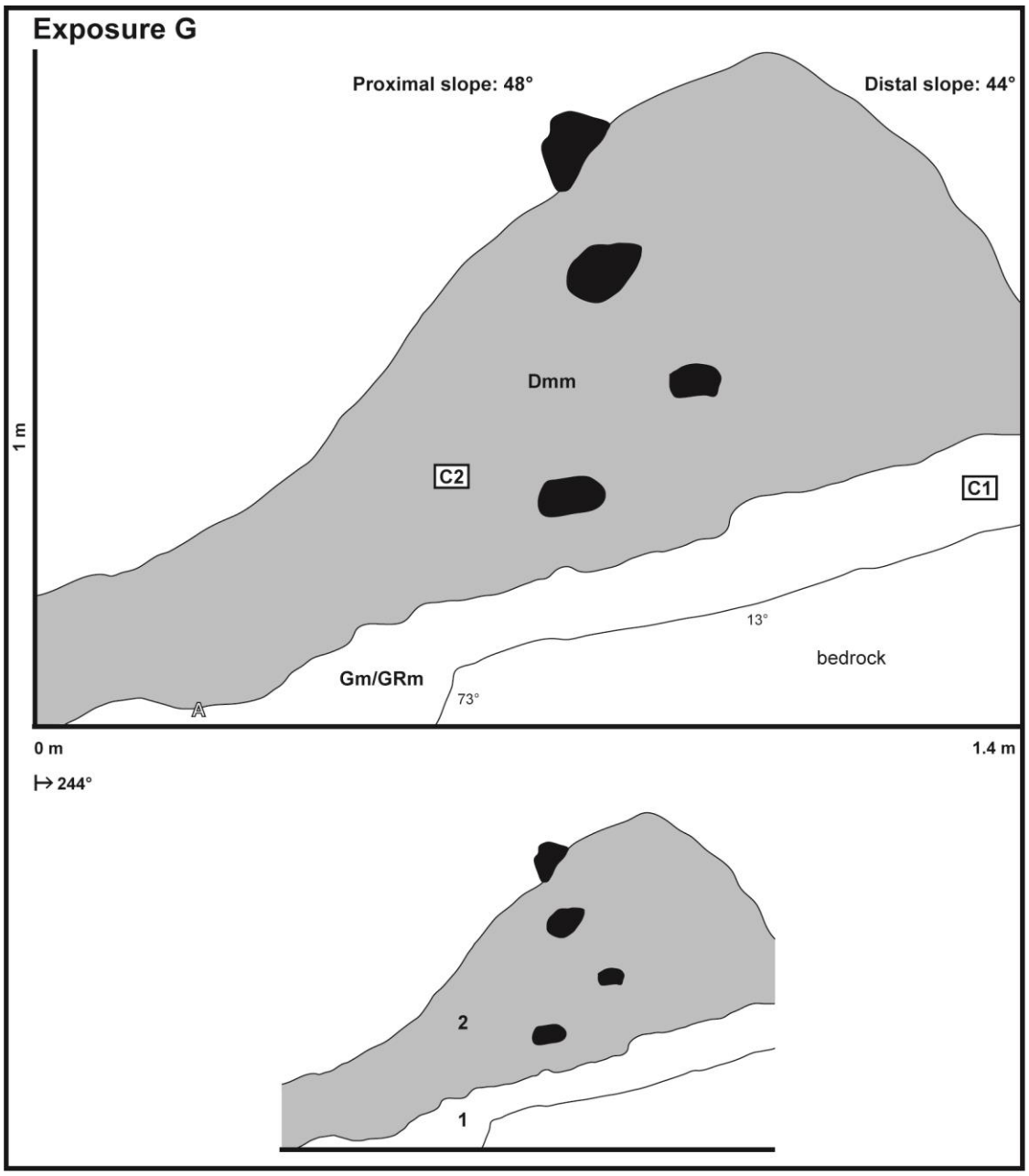

Figure 5.16. Exposure G representative log. FAs are labelled with facies codes (top) and FA numbers (bottom) and are described in the text in stratigraphic order from bottom to top. Figure 2.6 shows a facies codes and symbols key. Labelled photograph location refers to the photograph in Figure 5.17.

5.1.3.8 Clast characteristics of control and moraine samples

All clast measurement data can be found in Appendix B, and Figure 5.18 shows the location of all control samples. Medial moraines and debris cones may provide sediment to the ice front that may be incorporated into minor moraines, and are therefore included as control clasts (Chapter 2). Control clasts show several notable differences depending on environment (Figure 5.19). Supraglacial clasts have both the highest C_{40} (80%) and RA (90%) index values and notably no sub-rounded, rounded, or well rounded clasts (RWR =

0%). The average C_{40} index is similar for subglacial, controlled moraine, englacial debris cone, and channel clasts, around 33% (Figure 5.19).

Clast roundness somewhat differentiates these control clasts. Channel and subglacial clasts have similar RA index values, with averages of 14% and 9% respectively. The controlled moraine and englacial debris cone clasts are significantly less angular, with an average RA index value of 2.5%. However, none of the control sample clasts are particularly rounded, as the highest RWR index value of 6% represents the channel clasts, and subglacial, controlled moraine, and englacial debris cone clasts have average RA indices of 0.7%, 2%, and 1%, respectively (Figure 5.19).

Clasts were measured in 14 locations in the seven exposed moraines. Clasts from Exposures A and B were sampled from gravel FAs. Clasts from massive zones of FA 3 in Exposure A range from angular to rounded, but are dominantly sub-angular and sub-rounded, with an RA index of 2%, an RWR index of 4%, and a C_{40} index of 56% (Figure 5.20A). Clasts from FA 1 of Exposure B range from sub-angular to rounded, but are dominantly sub-angular, with an RWR index of 4% and a C_{40} index of 54% (Figure 5.20B).

Figure 5.17. Photograph from Exposure G. Photograph corresponds to location on Figure 5.16. Dashed line shows the sharp contact between FA 1 and FA 2. Solid line shows lower contact of moraine with bedrock. Trowel for scale (23 cm long).

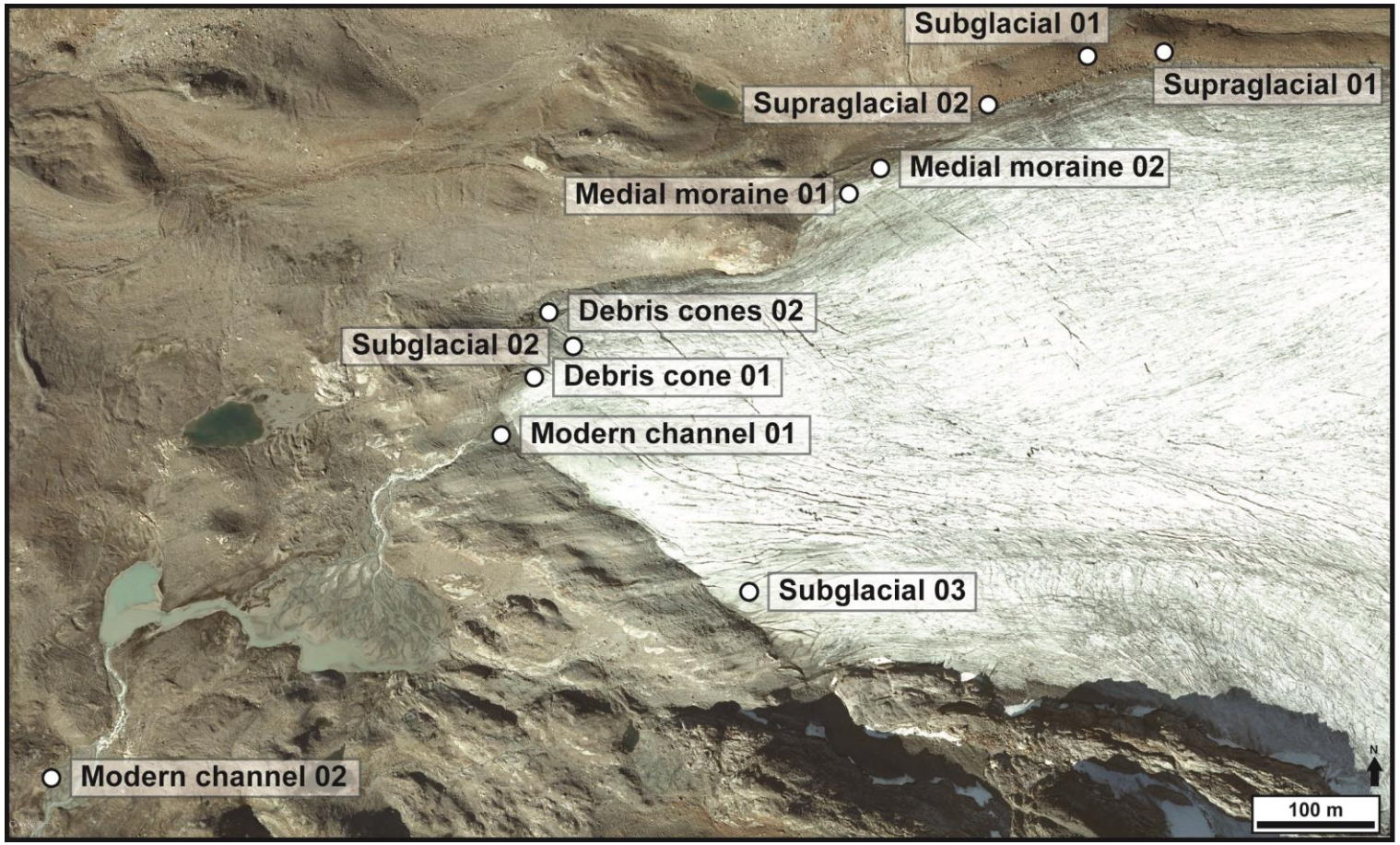

Figure 5.18. Locations of all clast control measurements from the Silvrettagletscher foreland. Environments sampled include: modern channel, subglacial, supraglacial, debris cones originating from englacial debris septa, and medial moraine. Fifty clasts were measured at each location. Figure 5.19 shows the ternary diagrams and histograms of all control samples**.** Imagery obtained from Google Earth (Google Earth, 2009).

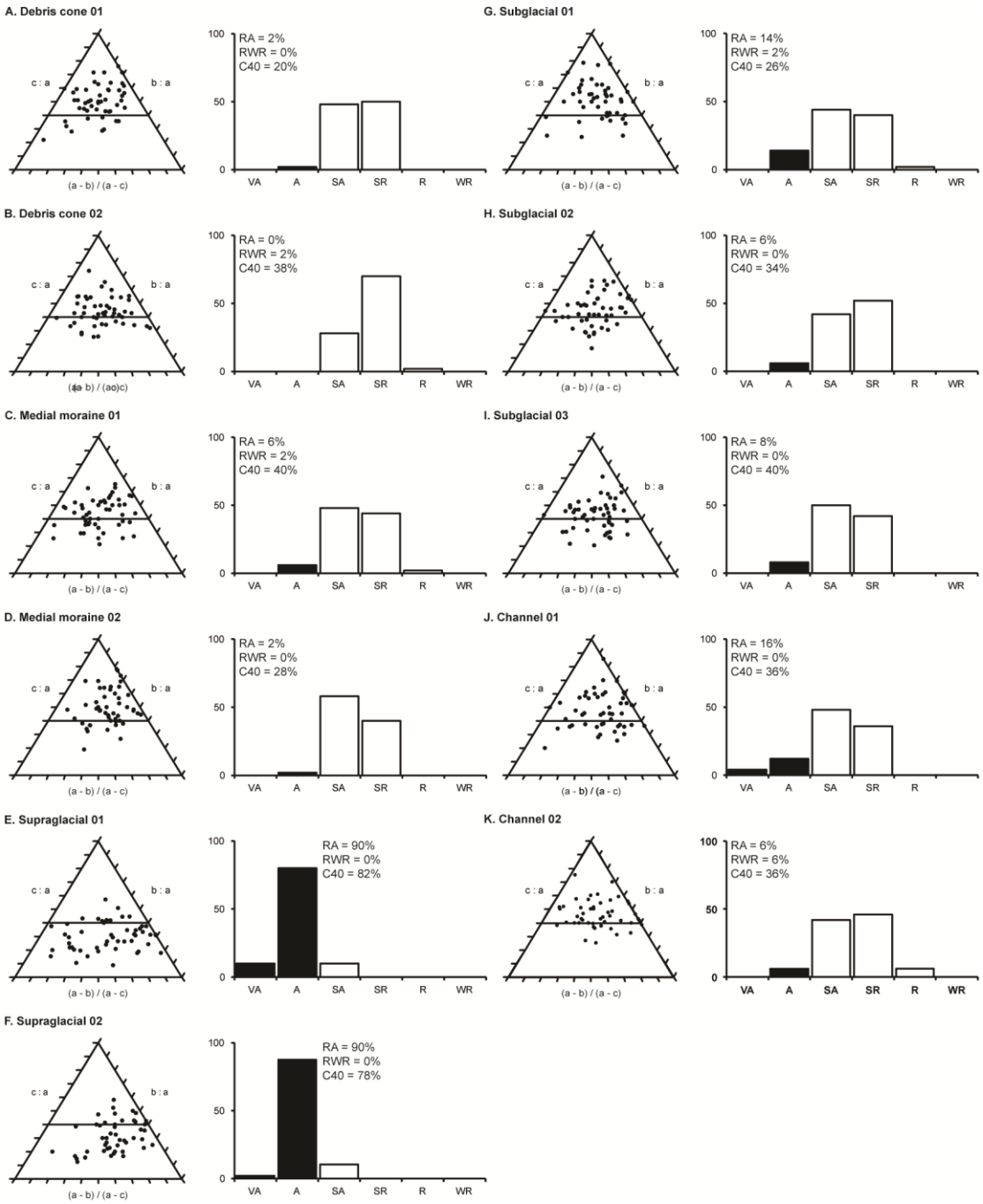

Figure 5.19. Clast measurement data for all control samples at Silvrettagletscher and in the foreland. Figure 5.18 shows sample locations.

Clasts from Exposure C were sampled from diamicton FAs. Clasts from FA 1 range from angular to rounded but are dominantly sub-angular and have an RA index of 14%, an RWR index of 4%, and a C40 index of 60% (Figure 5.20C). Clasts from FA 2 range from angular to rounded, but are dominantly sub-angular and sub-rounded, with an RA index of 8%, an RWR index of 4%, and a C_{40} index of 42% (Figure 5.20D).

Clasts from Exposures D-G were also sampled from diamicton FAs, as well as gravel FAs. Clasts from diamicton FA 1 of Exposure D range from angular to sub-rounded, but are dominantly sub-rounded, and have an RA index of 8% and a C_{40} index of 60% (Figure 5.20E). Clasts from gravel FA 6 range from angular to rounded, but are dominantly sub-rounded, and have an RA index of 2%, an RWR index of 4%, and a C_{40} index of 42% (Figure 5.20F). The clasts in diamicton FA 10 range from angular to sub-rounded, but are dominantly sub-rounded, and have an RA index of 4% and a C_{40} index of 34% (Figure 5.20), and those in gravel FA 11 range from angular to sub-rounded, but are dominantly sub-angular, and have an RA index of 2% and a C_{40} index of 50% (Figure 5.20G).

In Exposure E, clasts sampled from diamicton FA 2 range from angular to rounded, but are dominantly sub-angular, and have an RA index of 10% and a C_{40} index of 52% (Figure 5.20I), and clasts from gravel FA 6 range from angular to rounded, but are dominantly sub-rounded, and have an RA index of 2% and a C_{40} index of 42% (Figure 5.20J).

Clasts from diamicton FA 2 in Exposure F range from angular to sub-rounded, but are dominantly sub-angular and sub-rounded, with an RA index of 8%, a C_{40} index of 66%, and a maximum a-axis length of 12.8 cm (Figure 5.20K), and clasts from gravel FA 6 range from sub-angular to rounded, but are dominantly sub-rounded, with an RWR index of 2% and a C_{40} index of 58% (Figure 5.20L). In Exposure G, clasts from gravel FA 1 range from angular to rounded, but are dominantly sub-rounded, with an RA index of 2%, an RWR index of 2%, and a C_{40} index of 62% (Figure 5.20M), and clasts from diamicton FA 2 range from sub-angular to rounded, but are dominantly sub-rounded, with an RWR index of 2%, a C_{40} index of 52%, and a maximum a-axis length of 14.0 cm (Figure 5.20N).

Overall, clasts measured from the seven exposures are similar in shape but differ somewhat in roundness. The average C_{40} index for gravel clasts is 52% (7 samples, n = 350 clasts, 42-62%), and the average C_{40} index for diamicton clasts is 51% (6 samples, n = 300 clasts, 34-60%). Ternary diagrams represent these results as clusters in the middle of the diagrams, indicating a dominance of blade-shaped clasts for both gravel and diamicton samples. Elongated and platy clasts are also common, whereas blocky clasts are relatively rare (Figure 5.20). Clast roundness measurements differentiate gravel and diamicton clasts. Diamicton clasts are slightly more angular than gravel clasts, as indicated by average RA indices of 7% (0-14%) and 1% (0-2%) respectively. The RWR indices also show this difference as gravel clasts are very slightly more rounded than diamicton clasts, with RWR indices of 3% (0-8%) and 2% (0-4%), respectively (Figure 5.20).

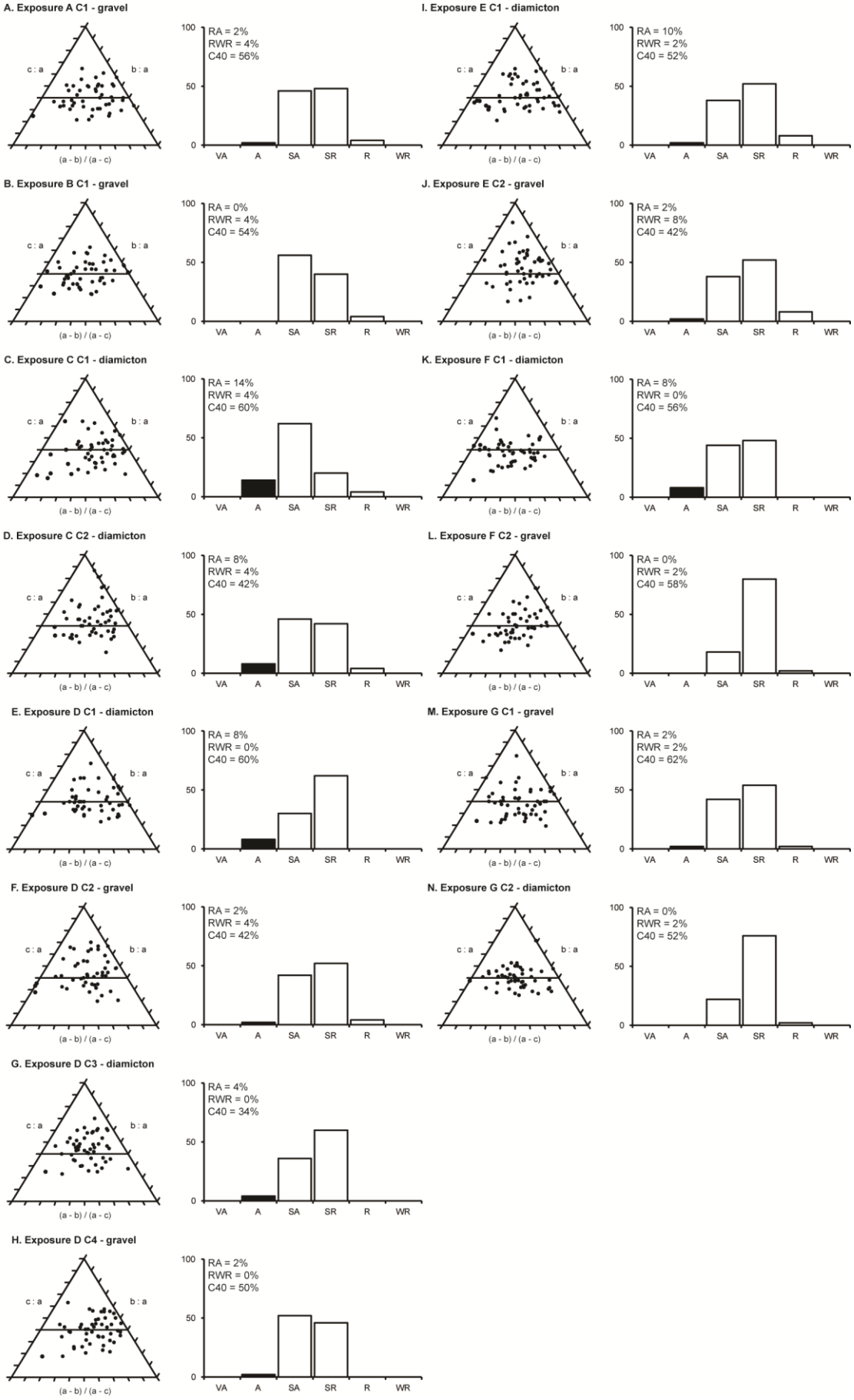

Figure 5.20. Clast measurement data for all exposures through moraines in the Silvrettagletscher foreland. Sample locations are indicated on corresponding exposure logs.

5.2 Climate, glacier measurements, and moraine spacing

As introduced in Chapter 2, Silvrettagletscher mass balance and front variation measurements were compared to local climate data for ablation, accumulation, and annual periods. Front variations show a period of retreat from 1957 to 2010, punctuated by minor advances (Figure 5.21; Table 5.1). In some instance, the net change in front position resulted in advances that would have overrun previous ice positions, and therefore likely self-censored the geomorphological record of minor moraines by obliterating any minor moraines than may have been formed (Sharp, 1984; Evans and Twigg, 2002; Chandler et al., 2016a), as seen between 1972 and 1981, and 1983 and 1984. Small variations in ice front position should be held with some degree of scepticism, as accuracy of GPS devices will have changed from 1957 to today, and the dataset does not specify where at the ice front the measurements were taken.

Moraine spacing, where annual deposition may be accurate but cannot be conclusively proven, was compared to climate data and the glacier measurement data as a potential proxy for ice margin retreat rates (Lukas, 2012; Chandler et al., 2016a). Chronological constraint on moraine ages is derived from counting moraine ridges from known ages for the periods 1957-1981 and 1993-2009 (Chapter 2) and a comparison of front variation measurements and the geomorphological map (Figures 5.22-5.23).

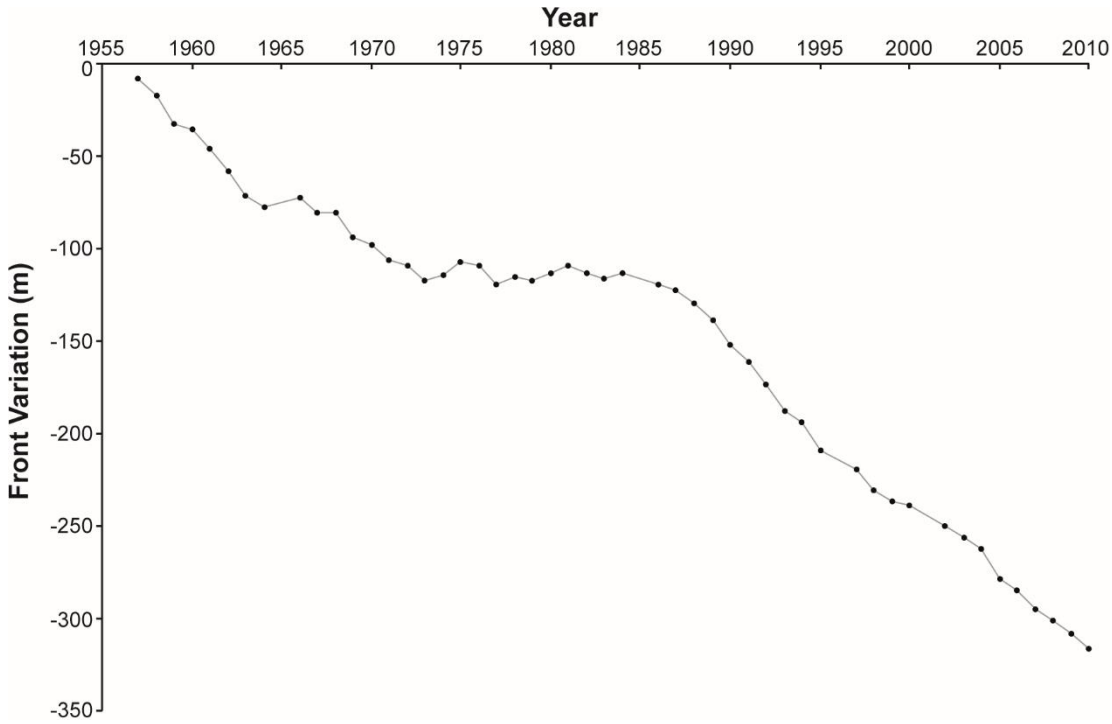

Figure 5.21. Front variation of Silvrettagletscher, 1957-2010. Data from the WGMS (Zemp et al., 2012; Zemp et al., 2013).

Table 5.1. Front variation of Silvrettagletscher, 1957-2010. This data set is missing some years (1965, 1996, 2001) and shows no measurement recorded in 1985 (Zemp et al., 2012; Zemp et al., 2013). The WGMS does not clarify what these spaces represent.

Year	Front Variation (m)	Year	Front Variation (m)
1957	-8	1984	3
1958	-9	1985	
1959	-16	1986	-6
1960	-3	1987	-3
1961	-10	1988	-8
1962	-12	1989	-9
1963	-13	1990	-13
1964	-7	1991	-9
1966	6	1992	-13
1967	-9	1993	-14
1968	0	1994	-6
1969	-13	1995	-15
1970	-4	1997	-10
1971	-8	1998	-12
1972	-3	1999	-6
1973	-8	2000	-2
1974	3	2002	-10.9
1975	7	2003	-6.6
1976	-2	2004	-5.8
1977	-10	2005	-15.9
1978	4	2006	-7
1979	-2	2007	-10
1980	4	2008	-6
1981	4	2009	-7
1982	-4	2010	-8
1983	-3		

The more detailed comparison of the Silvrettagletscher ice front variation measurements and geomorphological map of the foreland shows some agreement between the datasets, although more so for the more recent period (1993-2009; Figure 5.23) than the older period at the beginning of Silvrettagletscher ice front measurements (1957 onwards; Figure 5.22). Interpreted moraine chains that appear to match front variation measurement positions (16) match those in which the interpretations are uncertain (16), however both outnumber those that do not appear to match moraine positions (10) (Table 5.2). Measurements for four years are not reported, and eight years were omitted from analysis due to new variation yielding a positive advance period.

A comparison of the more recent period shows differences between assigning ages to moraines based on front variation measurements and moraine position in the foreland

as opposed to counting back from a known age (Figure 5.23). This comparison was conducted in two nearby areas, as they both have relatively continuous moraine chains out from the ice front. This mismatch in techniques suggests that it may not always be correct to interpret moraine changes by connecting individual landforms, some years may have had multiple moraines deposited (e.g. 2005 and 2009 of both transects), and some years may not have had moraines deposited along specific transects (e.g. 1993-1995 of southeastern transect).

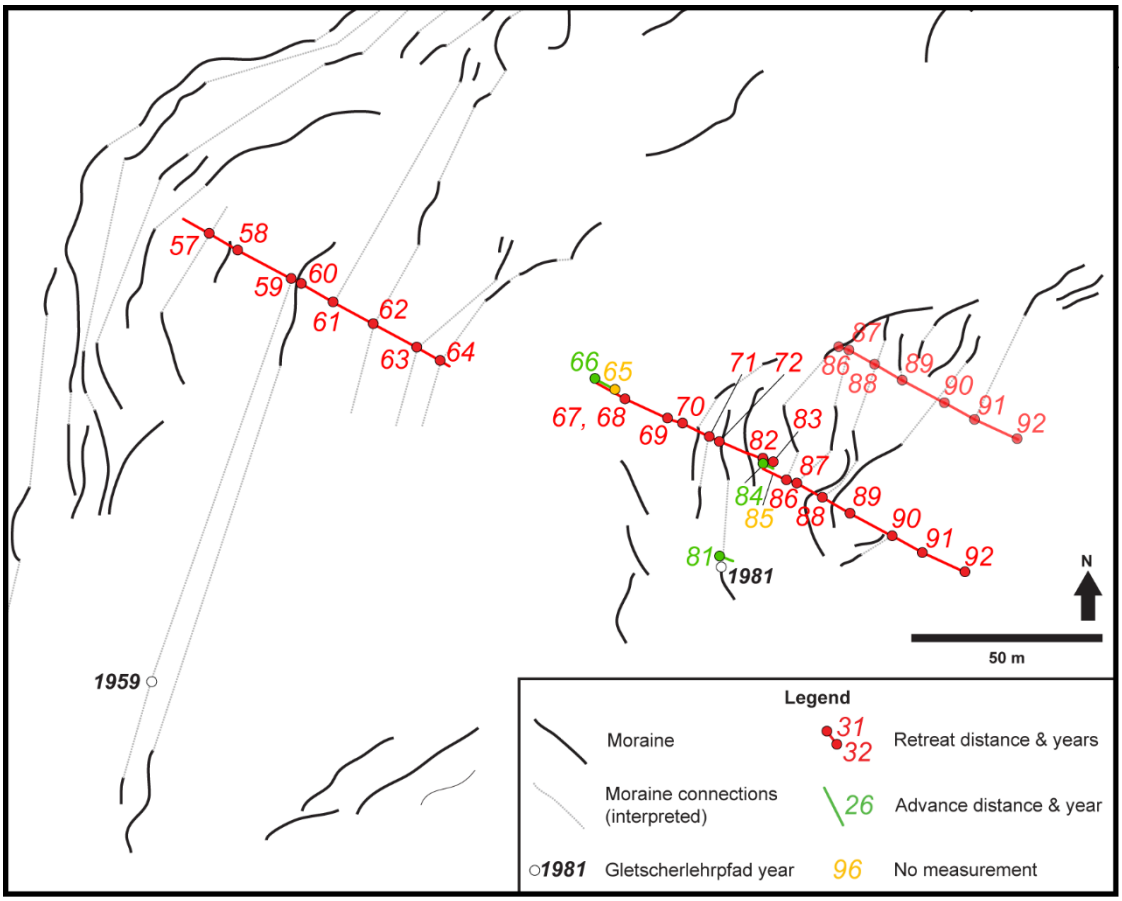

Figure 5.22. Front variation of Silvrettagletscher, 1957-1981, overlain on geomorphological map. Red points represent retreat measurements. Green points represent advance measurements. Light orange numbers represent interpreted moraine ages where front variation data are missing. See Figures 5.1-5.2 for larger geomorphological maps. Front variation data from the WGMS (Zemp et al., 2012; Zemp et al., 2013).

The strongest relationships between Silvrettagletscher mass balance and climate variables are average ablation season temperatures as measured at the Weissfluhjoch monitoring station (1960-2010; R^2 = 0.5210, p-value = 2.2733 x 10^{-9}) and the Davos monitoring station (1918-2010; R^2 = 0.5078, p-value = 7.9512 x 10^{-16}) (Table 5.3, Figures 5.24A and 5.25A). The relationship between Silvrettagletscher mass balance and average annual temperatures are also significant, but stronger at Weissfluhjoch (R^2 = 0.3042, p-value = 2.7297 x 10^{-5}) than Davos (R^2 = 0.1776, p-value = 2.3338 x 10^{-5}) (Table 5.3, Figures

5.24A and 5.25A). These data show the strongest relationship between Silvrettagletscher mass balance and average ablation season temperature as measured at Weissfluhjoch.

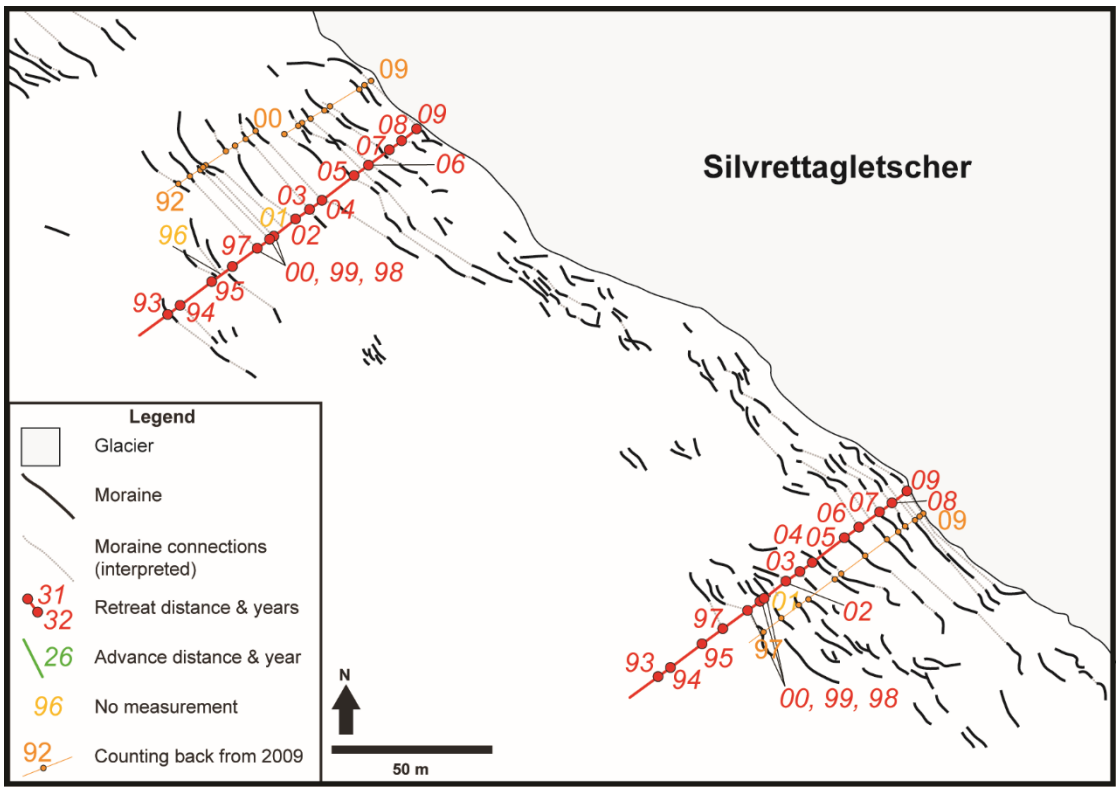

Figure 5.23. Front variation of Silvrettagletscher, 1992/3-2009, overlain on geomorphological map. Red points represent retreat measurements. Green points represent advance measurements. Light orange numbers represent interpreted moraine ages where front variation data are missing. Dark orange points represent moraine ages if counting back from 2009 ice position. See Figures 5.1-5.3 for larger geomorphological maps. Front variation data from the WGMS (Zemp et al., 2012; Zemp et al., 2013).

The strongest relationship between Silvrettagletscher front variation and climate variables as measured at the Weissfluhjoch monitoring station is average annual temperature (1960-2010; R^2 = 0.1356, p-value = 0.0109) (Table 5.3, Figure 5.24B). The relationships between Silvrettagletscher front variation and average ablation season temperatures (R^2 = 0.1287, p-value = 0.0133) and average accumulation season temperatures (R^2 = 0.1019, p-value = 0.0287) are also significant (Table 5.3, Figure 5.24B). The strongest relationship between Silvrettagletscher front variation and climate variables as measured at the Davos monitoring station is average ablation season temperature (1957-2010; R^2 = 0.1313, p-value = 0.0097) (Table 5.3, Figure 5.24B). These data show the strongest relationship between Silvrettagletscher front variation and annual average temperature at Weissfluhjoch.

Table 5.2. Comparison of front variation of Silvrettagletscher and mapped moraines derived from Figures 5.22-5.23. Grey shading indicates no net change between 1972 and 1981 ice positions. Front variation data from the WGMS (Zemp et al., 2012; Zemp et al., 2013).

Year	Match	Unlcear	No Match	No Data	Year	Match	Unclear	No Match	No Data
1957		x			1992			x	
1958	x				1993	x			
1959		x			1994		x		
1960	x				1995		x		
1961		x			1996				x
1962		x			1997		x		
1963		x			1998		x		
1964		x			1999	x			
1965				x	2000	x			
1966			x		2001				x
1967			x		2002	x			
1968			x		2003	x			
1969			x		2004	x			
1970			x		2005	x			
1971		x			2006		x		
1972	x				2007	x			
1973					2008		x		
1974					2009	x			
1975									
1976									
1977									
1978									
1979									
1980									
1981	x								
1982			x						
1983			x						
1984			x						
1985				x					
1986	x								
1987		x							
1988	x								
1989	x								
1990		x							
1991		x							
1992			x						

There are two statistically significant relationships between moraine spacing and glacier measurements spanning 1992-2009 when deriving chronological constraint from a comparison of front variation measurements and the geomorphological record of moraines (Figure 5.23). Front variation and moraine spacing of the southern transect show a highly statistically significant relationship (R^2 = 0.6091, p-value = 0.0046) (Table 5.3; Figure 5.26A). Mass balance and moraine spacing of the northern transect show a statistically significant relationship (R^2 = 0.6157, p-value = 0.0123) (Table 5.3; Figure 5.26B). Front

variation and mass balance measurements spanning 1960-2010 show a highly statistically significant relationship (R^2 = 0.3336, p-value = 1.1270 x 10^{-6}) (Table 5.3; Figure 5.26C).

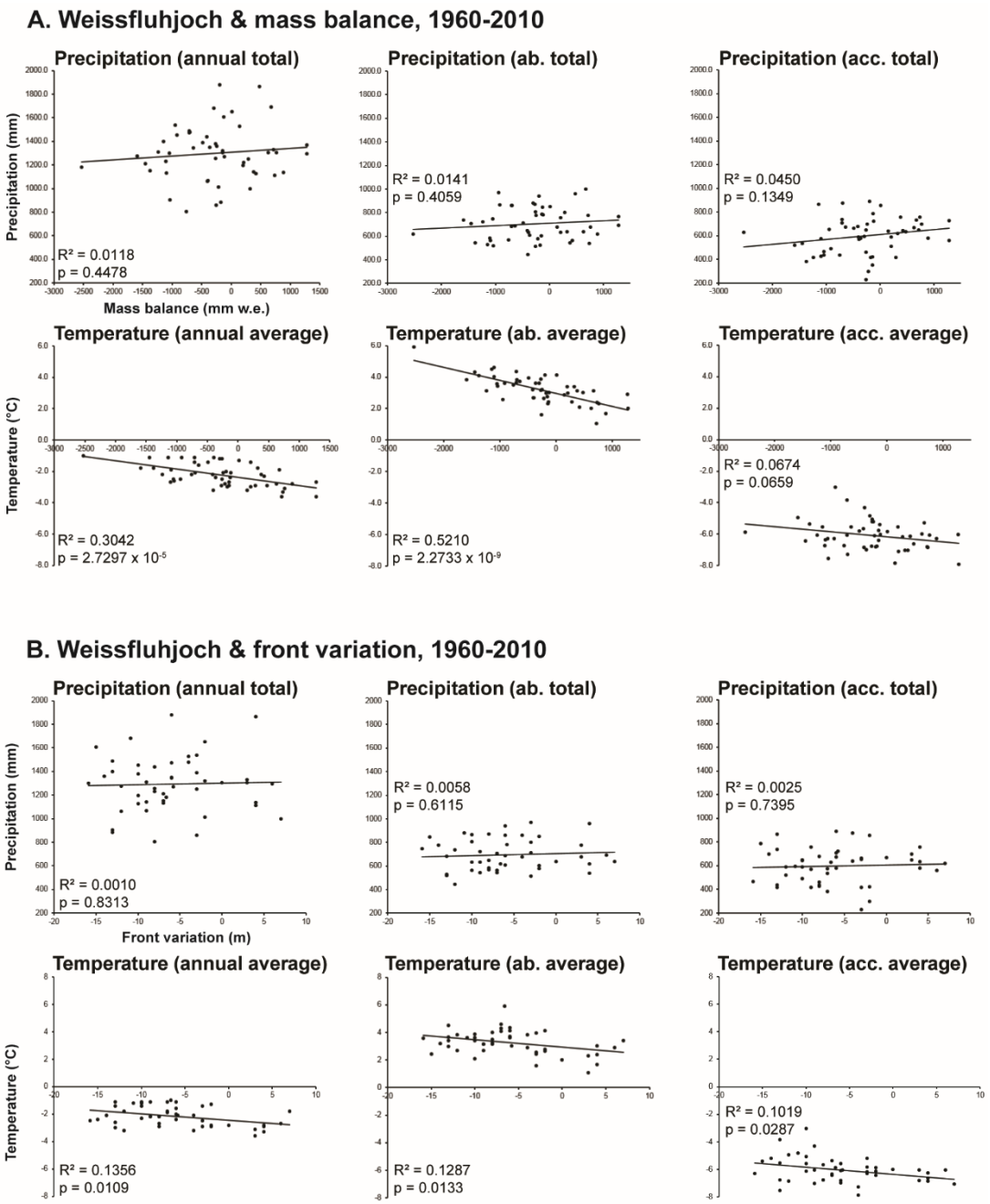

Figure 5.24. Correlation of Silvrettagletscher measurements and climate data from Weissfluhjoch. A) Silvrettagletscher mass balance measurements; B) Silvrettagletscher front variation measurements.

There are several statistically significant relationships between minor moraine spacing in the Silvrettagletscher foreland and climate variables spanning 1992-2009 (Table 5.3; Figures 5.27-5.30). When comparing moraine spacing with chronological constraint from the "counting back" approach from the 2009 ice front, average accumulation season temperature at Weissfluhjoch (R^2 = 0.4120, p-value = 0.0041) and Davos (R^2 = 0.3721, p-

value = 0.0077) both show highly statistically significant relationships with the northern transect (Figures 5.27A and 5.29A). When deriving chronological constraint from a comparison of front variation measurements and the geomorphological record of moraines, two statistically significant relationships between moraine spacing and climate variables are present; moraine spacing of the southern transect shows a statistically significant relationship to average annual temperature at Weissfluhjoch (R^2 = 0.4121, p-value = 0.0332) (Table 5.3; Figure 5.28B) and Davos (R^2 = 0.5153, p-value = 0.0129) (Table 5.3; Figure 5.30B).

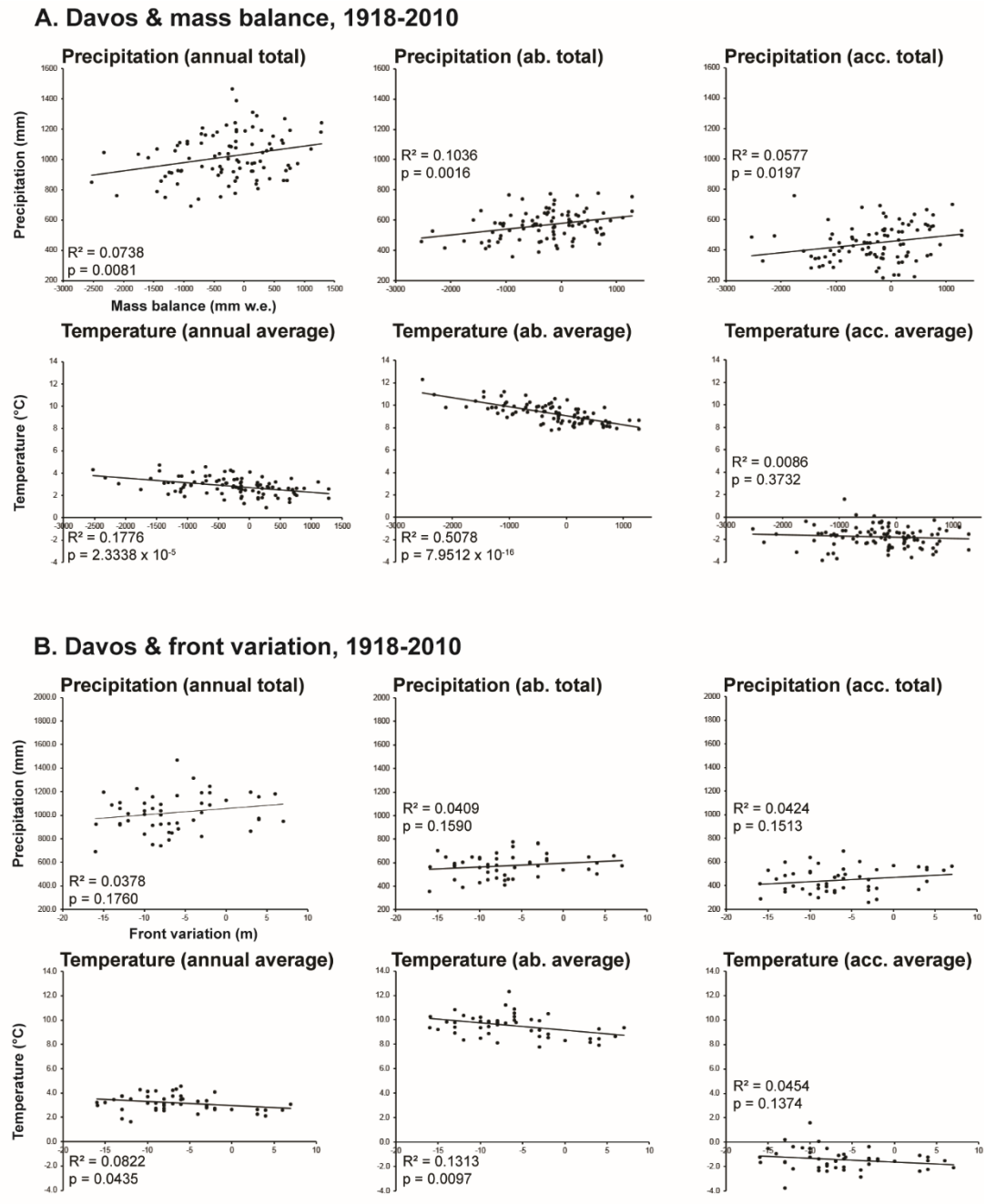

Figure 5.25. Correlation of Silvrettagletscher measurements and climate data from Davos. A) Silvrettagletscher mass balance measurements; B) Silvrettagletscher front variation measurements.

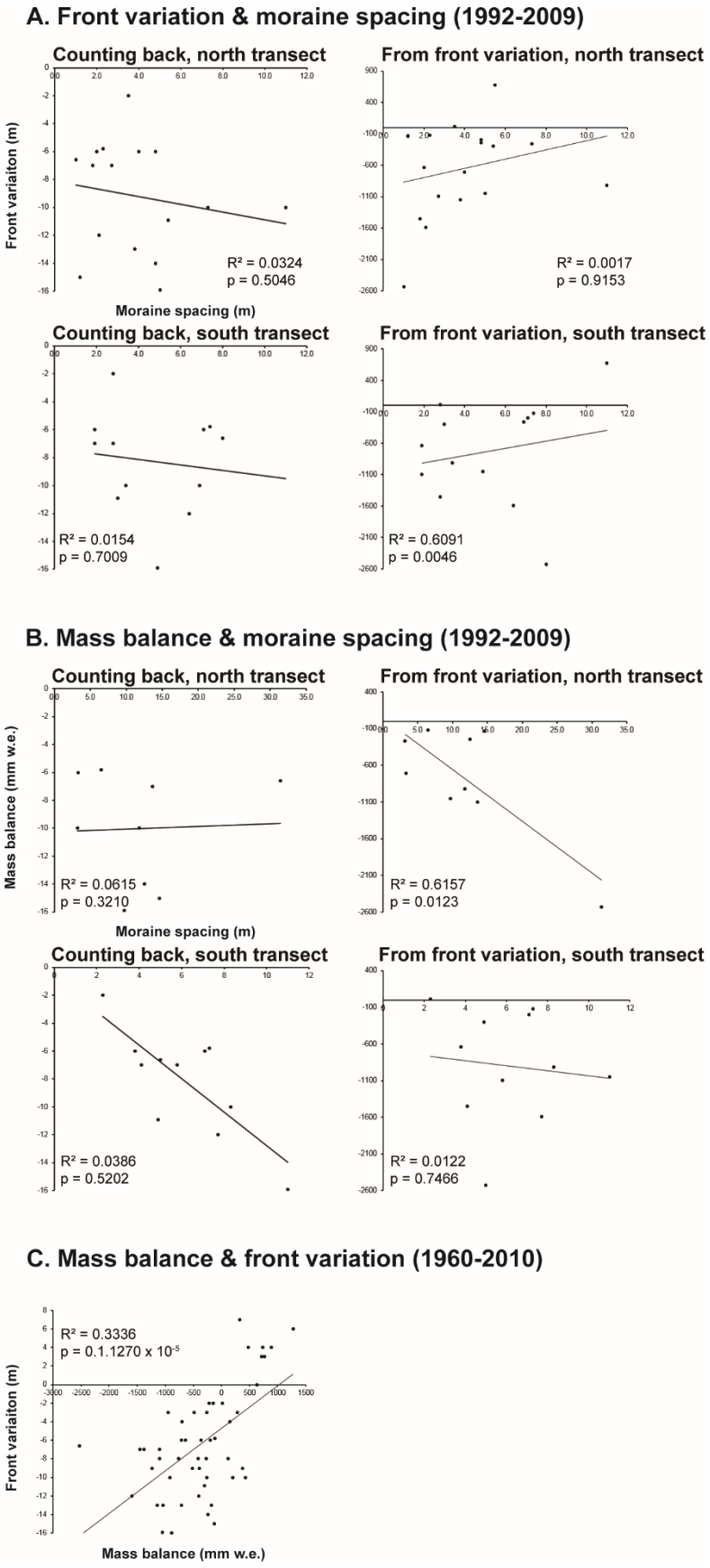

Figure 5.26. Correlation of minor moraine spacing in the Silvrettalgetscher foreland and glacier measurements. A) Correlation of moraine spacing and front variation measurements; B) Correlation of moraine spacing and mass balance measurements; C) Correlation of mass balance and front variation measurements. See Figure 5.23 for transect locations.

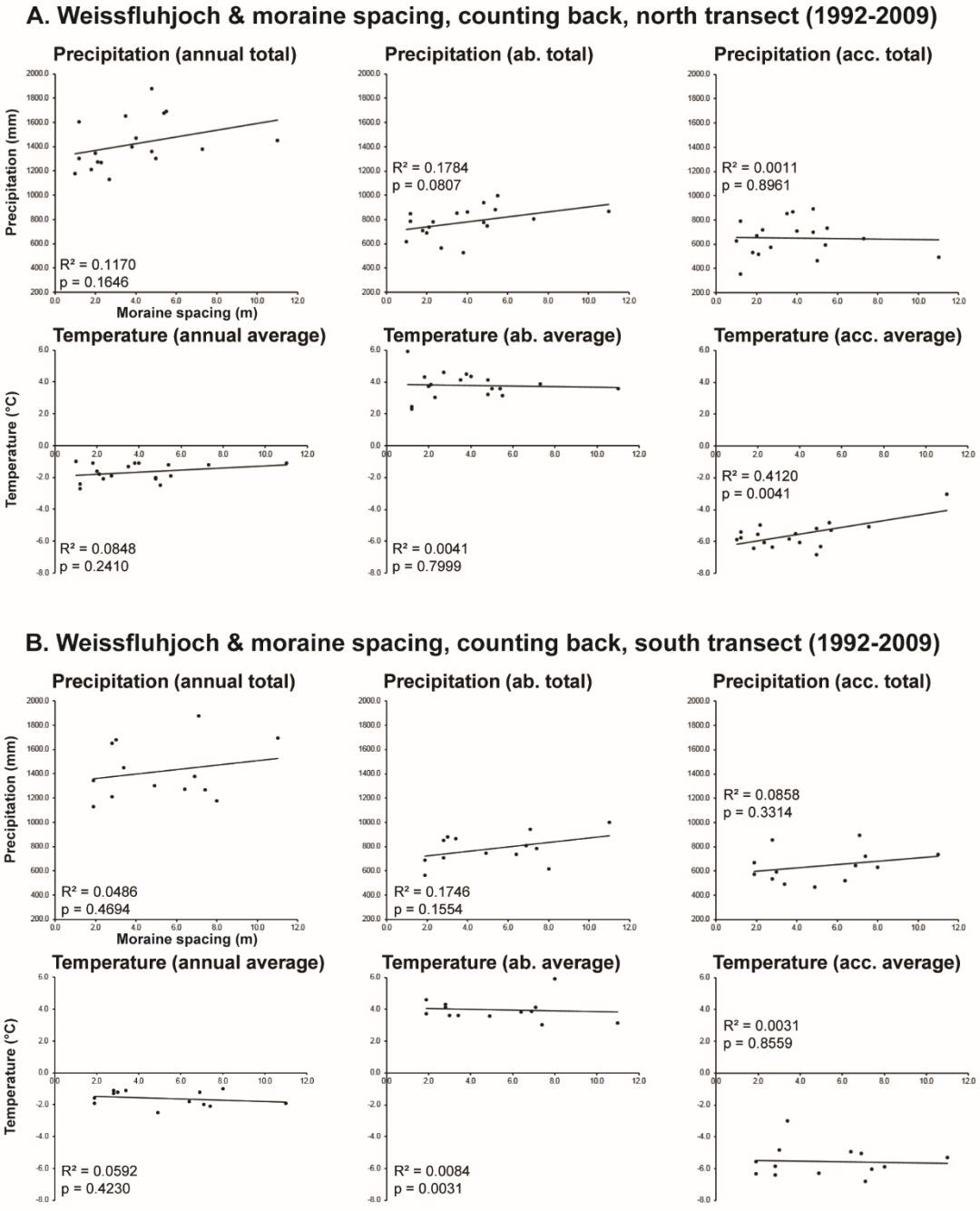

Figure 5.27. Correlation of minor moraine spacing in the Silvrettagletscher foreland with chronological constraint using a "counting back method" and Weissfluhjoch climate data. A) Moraine spacing of the north transect; B) Moraine spacing of the south transect. See Figure 5.23 for transect locations.

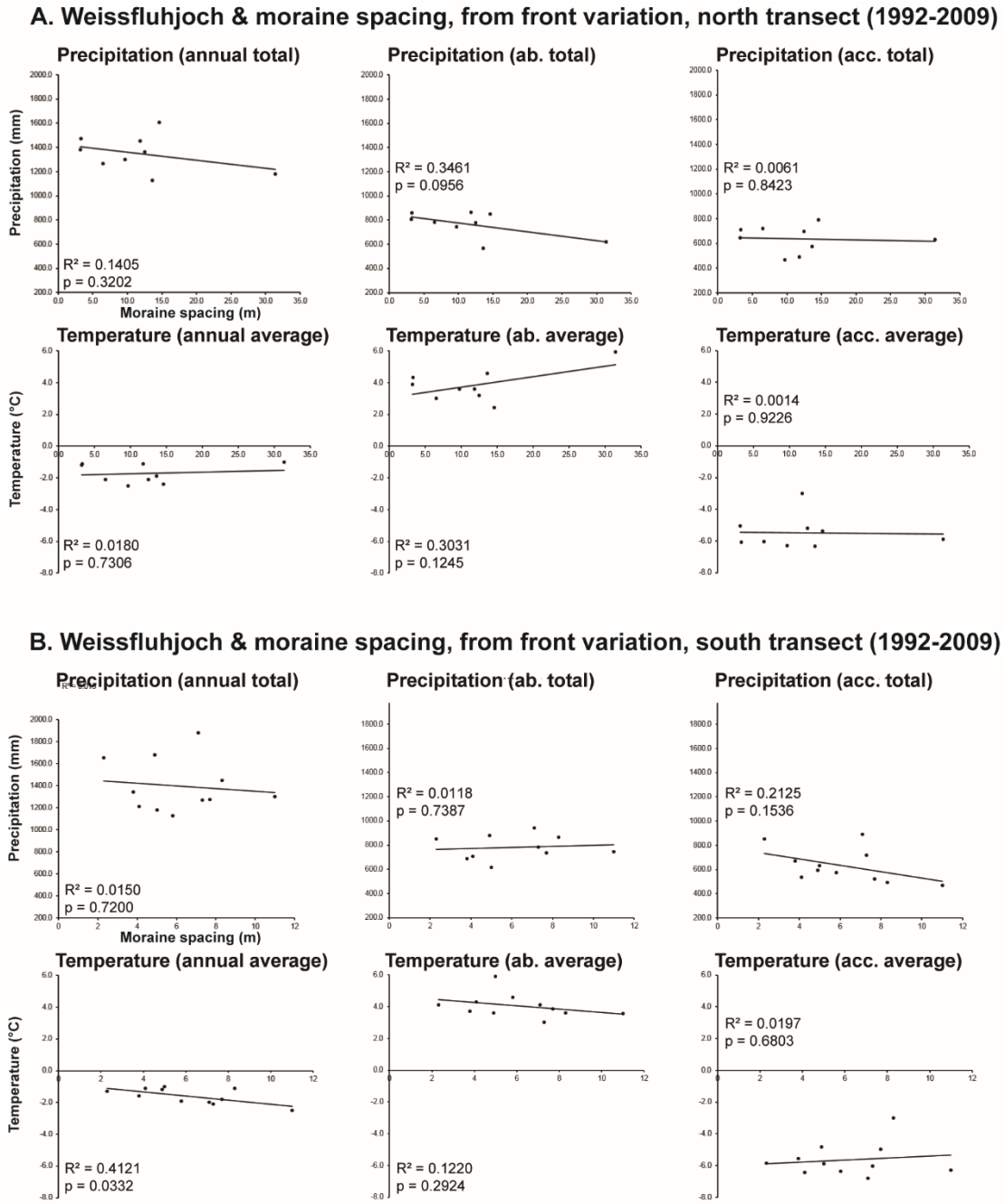

Figure 5.28. Correlation of minor moraine spacing in the Silvrettagletscher foreland with chronological constraint from comparisons with front variation measurements and Weissfluhjoch climate data. A) Moraine spacing of the north transect; B) Moraine spacing of the south transect. See Figure 5.23 for transect locations.

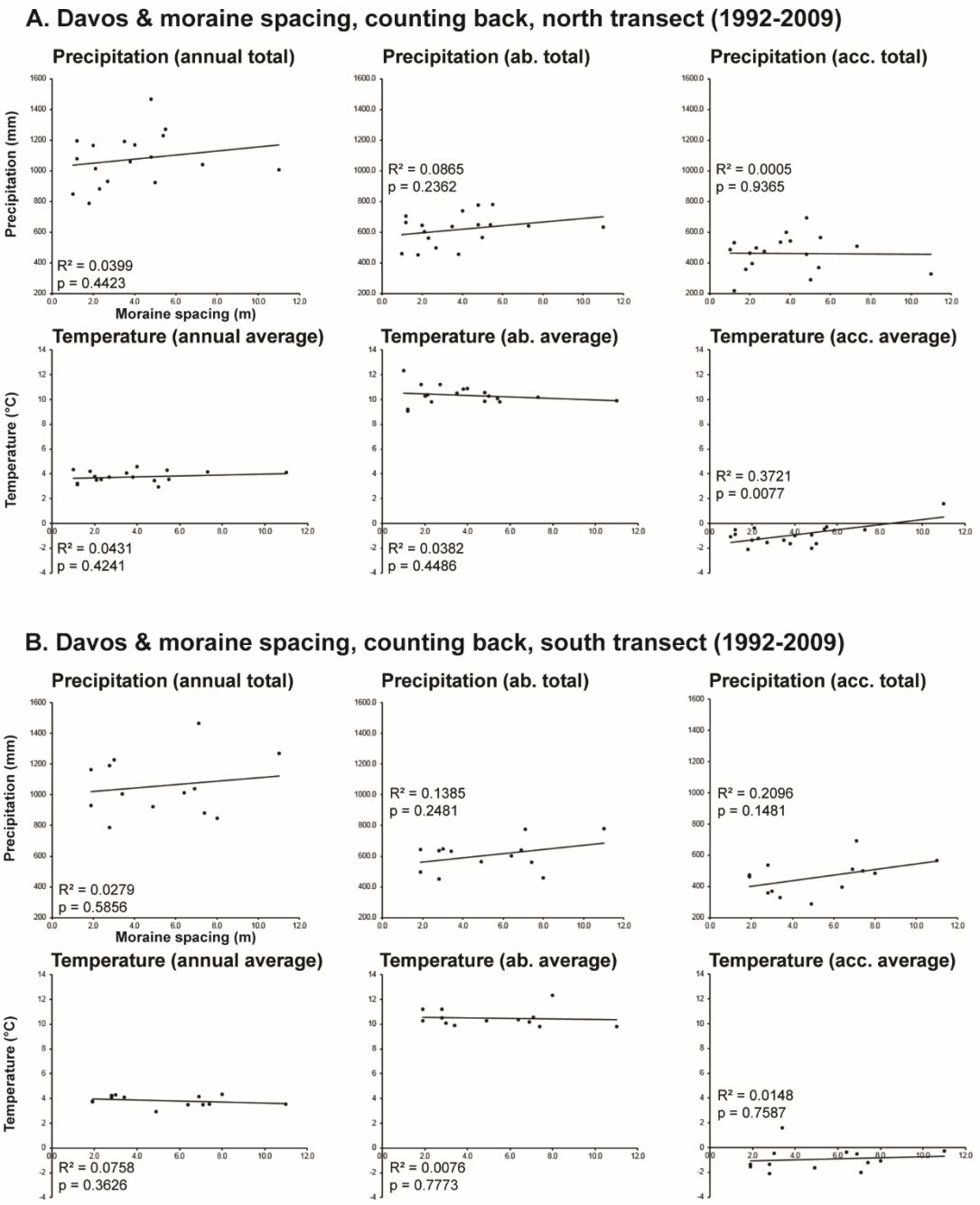

Figure 5.29. Correlation of minor moraine spacing in the Silvrettagletscher foreland with chronological constraint using a "counting back method" and Davos climate data. A) Moraine spacing of the north transect; B) Moraine spacing of the south transect. See Figure 5.23 for transect locations.

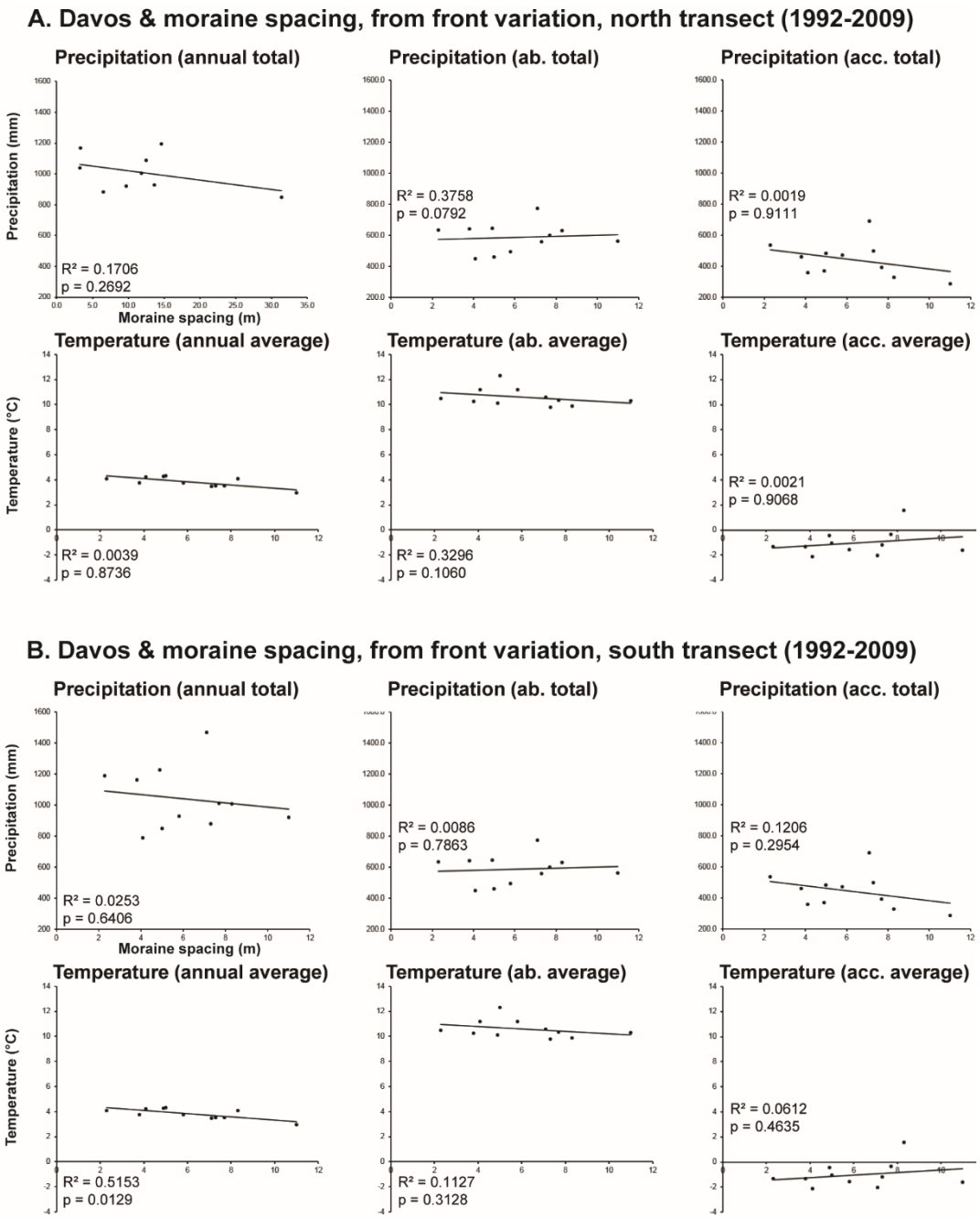

Figure 5.30. Correlation of minor moraine spacing in the Silvrettagletscher foreland with chronological constraint from comparisons with front variation measurements and Davos climate data. A) Moraine spacing of the north transect; B) Moraine spacing of the south transect. See Figure 5.23 for transect locations.

Table 5.3. Statistical assessment of Silvrettagletscher annual mass balance and front variation, climate data, and moraine spacing. R^2 values greater than 0.10 and statistically significant relationships are noted in bold, in which testing the statistical significance of the relationships follows the common convention of assessing p-values*.

Station	Time Period	Variable 1	Variable 2	R^2	p-value
WFJ[1]	1960-2010	Mass balance	P[3] (annual total)	0.0118	0.4478
			P[4] (ablation total)	0.0141	0.4059
			P (accumulation total)	0.0450	0.1349
			T (annual average)	**0.3042**	**2.7297×10^{-5}**
			T (ablation average)	**0.5210**	**2.2733×10^{-9}**
			T (accumulation average)	0.0674	0.0659
WFJ	1960-2010**	Front variation	P (annual total)	0.0010	0.8313
			P (ablation total)	0.0058	0.6115
			P (accumulation total)	0.0025	0.7395
			T (annual average)	**0.1356**	**0.0109**
			T (ablation average)	**0.1287**	**0.0133**
			T (accumulation average)	**0.1019**	**0.0287**
DAV[2]	1918-2010	Mass balance	P (annual total)	0.0738	**0.0081**
			P (ablation total)	**0.1036**	**0.0016**
			P (accumulation total)	0.0577	**0.0197**
			T (annual average)	**0.1776**	**2.3338×10^{-5}**
			T (ablation average)	**0.5078**	**7.9512×10^{-16}**
			T (accumulation average)	0.0086	0.3732
DAV	1957-2010**	Front variation	P (annual total)	0.0378	0.1760
			P (ablation total)	0.0409	0.1590
			P (accumulation total)	0.0424	0.1513
			T (annual average)	0.0822	**0.0435**
			T (ablation average)	**0.1313**	**0.0097**
			T (accumulation average)	0.0454	0.1374
n/a	1992-2009	Moraine spacing Counting back North	Front variation	0.0324	0.5046
n/a	1992-2009	Moraine spacing Counting back South	Front variation	0.0154	0.7009
n/a	1992-2009**	Moraine spacing Front variation North	Front variation	0.0017	0.9153
n/a	1992-2009**	Moraine spacing Front variation South	Front variation	**0.6091**	**0.0046**
n/a	1992-2009	Moraine spacing Counting back North	Mass balance	0.0615	0.3210
n/a	1992-2009	Moraine spacing Counting back South	Mass balance	0.0386	0.5202
n/a	1992-2009**	Moraine spacing Front variation North	Mass balance	**0.6157**	**0.0123**
n/a	1992-2009**	Moraine spacing Front variation South	Mass balance	0.0122	0.7466
n/a	1960-2010**	Front variation	Mass balance	**0.3336**	**1.1270×10^{-5}**

Station	Time Period	Variable 1	Variable 2	R^2	p-value
WFJ	1992-2009	Moraine spacing	P (annual total)	**0.1170**	0.1646
		Counting back	P (ablation total)	**0.1784**	0.0807
		North	P (accumulation total)	0.0011	0.8961
			T (annual average)	0.0848	0.2410
			T (ablation average)	0.0041	0.7999
			T (accumulation average)	**0.4120**	**0.0041**
WFJ	1992-2009	Moraine spacing	P (annual total)	0.0486	0.4694
		Counting back	P (ablation total)	**0.1746**	0.1554
		South	P (accumulation total)	0.0858	0.3314
			T (annual average)	0.0592	0.4230
			T (ablation average)	0.0084	0.7659
			T (accumulation average)	0.0031	0.8559
WFJ	1992-2009**	Moraine spacing	P (annual total)	**0.1405**	0.3202
		Front variation	P (ablation total)	**0.3461**	0.0956
		North	P (accumulation total)	0.0061	0.8423
			T (annual average)	0.0180	0.7306
			T (ablation average)	**0.3031**	0.1245
			T (accumulation average)	0.0014	0.9226
WFJ	1992-2009**	Moraine spacing	P (annual total)	0.0150	0.7200
		Front variation	P (ablation total)	0.0118	0.7387
		South	P (accumulation total)	**0.2125**	0.1536
			T (annual average)	**0.4121**	**0.0332**
			T (ablation average)	**0.1220**	0.2924
			T (accumulation average)	0.0197	0.6803
DAV	1992-2009	Moraine spacing	P (annual total)	0.0399	0.4423
		Counting back	P (ablation total)	0.0865	0.2362
		North	P (accumulation total)	0.0005	0.9365
			T (annual average)	0.0431	0.4241
			T (ablation average)	0.0382	0.4486
			T (accumulation average)	**0.3721**	**0.0077**
DAV	1992-2009	Moraine spacing	P (annual total)	0.0279	0.5856
		Counting back	P (ablation total)	**0.1385**	0.2481
		South	P (accumulation total)	**0.2096**	0.1481
			T (annual average)	0.0758	0.3626
			T (ablation average)	0.0076	0.7773
			T (accumulation average)	0.0148	0.7587
DAV	1992-2009**	Moraine spacing	P (annual total)	**0.1706**	0.2692
		Front variation	P (ablation total)	**0.3758**	0.0792
		North	P (accumulation total)	0.0019	0.9111
			T (annual average)	0.0039	0.8736
			T (ablation average)	**0.3296**	0.1060
			T (accumulation average)	0.0021	0.9068
DAV	1992-2009**	Moraine spacing	P (annual total)	0.0253	0.6406
		Front variation	P (ablation total)	0.0086	0.7863
		South	P (accumulation total)	**0.1206**	0.2954
			T (annual average)	**0.5153**	**0.0129**
			T (ablation average)	**0.1127**	0.3128
			T (accumulation average)	0.0612	0.4635

* $p < 0.05$ shows a statistically significant relationship between the regression line and data; $p < 0.01$ shows a highly statistically significant relationship; $p < 0.001$ shows a very highly statistically significant relationship

** 1965, 1985, 1996, and 2001 data absent from front variation measurements

[1] WFJ = Weissfluhjoch monitoring station (MeteoSwiss, 2015b)

[2] DAV = Davos monitoring station (MeteoSwiss, 2015a)

[3] P = precipitation

[4] T = temperature

5.3 Synthesis

Mechanisms of minor moraine formation are the primary focus of this research in the Silvrettagletscher foreland. All results and observations collectively enable minor moraine formation in the Silvrettagletscher foreland to be summarized into four mechanisms. The synthesis of formation processes includes consideration of the geology and geomorphological evolution of the Silvrettagletscher, which specifically considers the role of englacial debris sources, incipient dead ice associated with both controlled moraines and clean ice, highly saturated foreland sediment and flutings, and modern ice-cored ridges. This also inherently includes the information revealed by sedimentological investigation of moraines that did not contain ice cores in 2015 and comparison of clast measurements of samples from moraines and control locations. The following sections present conceptual models of minor moraine formation, by integrating interpretations of the sedimentological composition of individual moraines with each other, where applicable, and aerial photography and field observations.

5.3.1 Mechanisms of minor moraine formation in the Silvrettagletscher foreland

Most exposures contain recurring FAs, with gravel and diamicton facies dominating moraine composition and two moraines that contain primarily sand facies. Assessing clast form provides more information into the transport paths of clasts in the exposures, providing some support for mechanisms of moraine formation.

Covariance diagrams showing RA versus C_{40} and RWR versus C_{40} indices show that supraglacial clasts differ markedly from exposure clasts and all other samples (Figure 5.31). Although supraglacial material covers the northernmost flank of the glacier and other small, isolated areas of the glacier, the comparison with other control clasts shows that any clasts that may have originated supraglacially lost the dominant signature of hard angularity associated with this environment during their integration into and erosion as part of englacial, subglacial, and proglacial realms (Figure 5.31). Samples in debris cone, medial moraine, and glaciofluvial environments inherently would have originated as either sediment delivered supraglacially or derived subglacially. Covariance plots draw attention to outliers as individual samples, but the non-supraglacial samples are overall similar in form and roundness. The overlapping envelopes of these sediments and the subglacial control samples, on both RA and RWR versus C_{40} covariance plots, suggest that the debris cone, medial moraine, and modern channel samples originated in the subglacial realm or have spent considerable time subglacially, showing the interrelatedness among the transport environments in this glacial system (Figure

5.31). Some clasts from lateral moraines at Findelengletscher, Switzerland, similarly plot between supraglacial and subglacial envelopes on covariance plots, which Lukas et al. (2012) use as one line of evidence to interpret that the clasts had likely experienced the subglacial environment prior to deposition in lateral moraines.

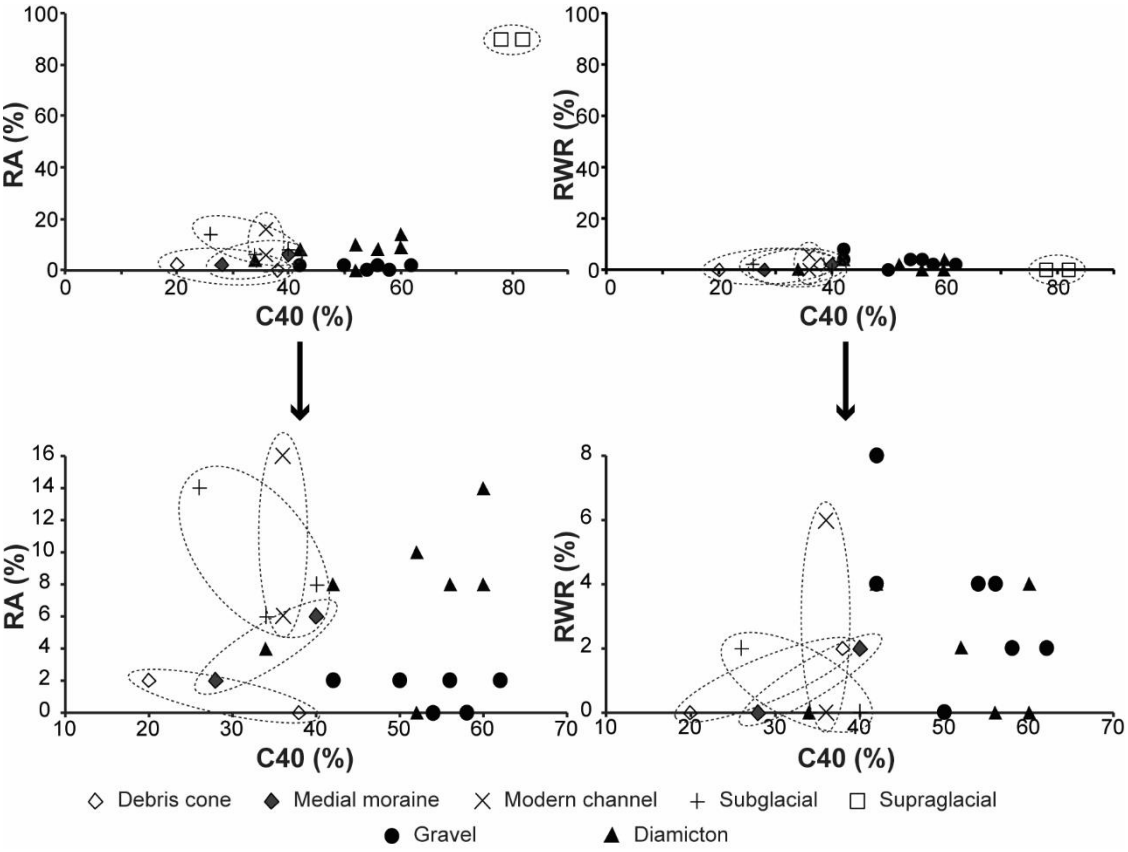

Figure 5.31. RA versus C_{40} and RWR versus C_{40} covariance plots for all clast measurements. Samples collected from minor moraine exposures are grouped by gravel samples and diamicton samples. Dashed lines group control samples as envelopes. Both upper and lower plots show the same data, with the lower plots constraining the y-axes to not include supraglacial samples. Refer to ternary diagrams and histograms for control data (Figure 5.18) and exposure data (Figure 5.20) for more specific information.

The covariance diagrams show that the clasts in the exposures are strikingly similar, although slight differences in roundness differentiate diamicton and gravel samples, where diamicton clasts are slightly more angular and gravel samples slightly more rounded (Figure 5.31). Clasts in the moraines show no evidence of pure supraglacial or subglacial origin, but also do not have a clear signature from other control environments, regardless of their location in diamicton or gravel units, and instead occupy a space on both covariance diagrams between the supraglacial and other control envelopes. This suggests that some of the clasts may have originated supraglacially but subsequently underwent some erosion, and therefore likely

experienced some other environment prior to deposition at the ice front, showing the interrelatedness among the transport environments in this glacial system. The clustering of clasts from moraine samples between the supraglacial and other control environments and overlapping subglacial and fluvial envelopes may both suggest minimal fluvial reworking of clasts emerging from the subglacial environment, perhaps due to short fluvial transport distances and a small basin size. Alternatively, these results may show that meta-granite clasts in this specific setting may not be an effective lithology to discriminate erosional and transportational environments.

Extending the number of samples may help differentiate these environments at Silvrettagletscher, however it appears that form and shape indicative of these specific environments are subdued either through the glacial dynamics of Silvrettagletscher or through the lithological control on clast morphology. Englacial conduits, faulting, and folding may transport subglacial and englacial sediment throughout the glacier, and may bring these sediments to the surface as englacial debris septa cones, transverse linear debris accumulations, or medial moraines (Evans, 2009; Lukas, 2012; Lukas et al., 2012). These sediments are similar to those that subglacial and proglacial channels may be transporting under, through, and in front of, the glacier. Alternatively, further targeted sampling of these environments, while also extending the sampling to other lithologies and comparing the results from multiple lithologies (e.g. Lukas et al., 2013), may help elucidate further details about erosional and transportational regimes in the Silvrettagletscher system.

The sedimentological analysis of moraine exposures provides more specific evidence and support for mechanisms of moraine formation. Although not all of the moraine in the Silvrettagletscher foreland could be exposed for sedimentological analyses, the seven moraines exposed for further analysis reveal four distinct mechanisms of formation: melt-out of controlled moraine ice cores, freeze-on of foreland and subglacial sediment on a reverse bedrock slope, push of pre-existing sediment on a reverse bedrocks lope, and push of pre-existing glaciolacustrine sediment. The following steps and conceptual models describe the mechanisms of formation in the Silvrettagletscher foreland, first describing deformation structures and lack of deformation structures as lines of evidence for the specific mechanism described.

5.3.1.1 Melt-out of controlled moraine ice cores

Sedimentological evidence and aerial photographs show that two of the investigated moraines formed through the degradation of controlled moraines at the ice front. The primary evidence

for moraines formed through the evolution of controlled moraines to hummocky topography is the emergence of these landforms in front of controlled moraines, as seen with the moraines that contain Exposures A and C. Aerial photographs show that the Exposure A moraine formed shortly before 2010 in front of the upper controlled moraine and the Exposure C moraine formed between 2013 and 2015 in front of the right controlled moraine. These types of moraines were observed forming during summer 2015, in various stages of evolution (Figure 5.5).

Geomorphological evidence supporting this mechanism of minor moraine formation is seen in the topography of the lower true right of the Silvrettagletscher foreland, which contains abundant sediment relative to the rest of the ice front and is similar to ice stagnation topography or hummocky terrain described in other studies that discuss extant ice-cored moraines (Sharp, 1949; Goldthwait, 1951; Boulton, 1972; Eyles, 1979; Rains and Shaw, 1981; Eyles, 1982; Kjær and Krüger, 2001; Everest and Bradwell, 2003; Schomacker and Kjær, 2008; Bennett et al., 2010; Ewertowski et al., 2011; Carrivick et al., 2012). The presence of sink holes (Sharp, 1949; Kjær and Krüger, 2001; Everest and Bradwell, 2003; Bennett et al., 2010) and patches of thixotropic till with thin gravel cover show the influence melting ice cores in this area saturating the sediment between moraines. The chaotic topography of this area also indicates the presence of melting ice cores, as gravitational collapse, slumping, and flowing of moraine sediment through backwasting and downwasting of the ice-cored moraines creates an area of constant re-sedimentation on and in the moraines and surrounding area (Sharp, 1949; Goldthwait, 1951; Lawson, 1979; Eyles, 1982; Krüger and Kjær, 2000; Kjær and Krüger, 2001; Everest and Bradwell, 2003; Lukas et al., 2005; Schomacker and Kjær, 2008; Ewertowski et al., 2011), which may diminish the appearance of once distinct and larger ice-cored landforms and any previous sedimentological architecture within the moraines (Sharp, 1949; Boulton, 1972; Kjær and Krüger, 2001; Evans, 2010; Carrivick et al., 2012). It is important to note that the process of de-icing of moraine cores is still active in the Silvrettagletscher foreland, as ice-cored moraines in areas formerly occupied by controlled moraines were noted during fieldwork in 2015.

The diamicton FAs in the Exposure C moraine (Figure 5.11), FA 1 and FA 2, are considered subglacial till deposits, which represent two different periods of deposition. The lowest till FA appears to be a remnant from a previous advance, preserved in a localised depression, whereas FA 2 was deposited during the moraine-building event. FA 1 is very saturated, reflecting its presence in a topographic depression and ability to collect meltwater from ice-cored moraines higher on the reverse bedrock slope, as well as snow melt and other precipitation, as observed during fieldwork.

The lack of structures in Exposure A (Figure 5.8) and a majority of Exposure C (FA4; Figure 5.11) suggests melt-out of an ice core and gravitational collapse of sediment (Goldthwait, 1951; Lawson, 1979; Kjær and Krüger, 2001; Everest and Bradwell, 2003; Lukas et al., 2005; Schomacker and Kjær, 2008; Reinardy et al., 2013), and can therefore be treated as evidence of deformation. Furthermore, most of the gravel of the Exposure A moraine has an open framework structure, which could be related to melt out of an ice core and fines washing away during progressive melting down through the moraine (Sharp, 1949; Boulton, 1972; Eyles, 1979; Lawson, 1979; Eyles, 1982; Lønne and Lysså, 2005; Lukas et al., 2005; Schomacker and Kjær, 2008; Ewertowski et al., 2011).

The shape of FA 6 in Exposure A, capping the proximal slope, shows that the sediment may have rolled down the steeper slope during melting (Lawson, 1979; Sharp, 1984), and FA 5 and FA 7 both follow the shape of the ridge crest and may indicate slumping down both slopes (Figure 5.8). Similarly, small lenses of openwork gravel in FA 4 of Exposure C follow the shape of the proximal slope (Figure 5.11), which suggest progressive melting of an ice core and gravitational reworking of these lenses down the steeper slope (Lawson, 1979; Sharp, 1984). Similarly, the one lens of massive gravel in FA 4 generally follows the shape of the distal slope.

Conceptual model of minor moraine formation through the melt-out of controlled moraine ice cores

This mechanism of moraine formation in the Silvrettagletscher foreland is detailed in the conceptual model below, as drawn from the aforementioned sedimentological analysis of Exposures A and C, aerial photographs, and field observations.

(1) Englacial debris septa emerge at the ice surface near the ice margin, delivering debris to the ice surface and ice front as debris flows. Differential ablation causes these debris flows to create distinct supraglacial ridges (e.g. Drewry, 1972; Goodsell et al., 2005; Lukas et al., 2005; Evans, 2009; Lukas et al., 2012). This may occur as a single debris septum, or multiple debris septa may create an ablation dominant medial moraine (Eyles and Rogerson, 1978; Evans, 2009; Benn and Evans, 2010).

(2) Englacial debris septa continue delivering debris to the ice surface. Differential ablation causes these features to be more pronounced than the surrounding clean ice, as the surface debris insulates the ice underlying debris flow material or medial moraines, relative to clean ice (Drewry, 1972), creating a controlled moraine complex near the ice front (Boulton, 1968; Boulton, 1972; Eyles, 1979; Rains and

Shaw, 1981; Evans, 2009a; Bennett et al., 2010a; Szuman and Kasprzak, 2010; Carrivick et al., 2012).

(3) Continued differential ablation further insulates the debris-covered zone, beginning to isolate a controlled moraine complex from the surrounding clean ice. Collapsing of ice caves and tunnels (Boulton, 1972; Eyles, 1979; Evans, 2009; Bennett et al., 2010; Carrivick et al., 2012) and fluvial undercutting (Boulton, 1972) may contribute to this process (Figure 5.7C). This area may either be chaotic or have recognizable linearity in plan form, showing the development of hummocky topography. This linearity and ridge formation can be attributed to englacial conduit locations and patterns (Boulton, 1968; Kjær and Krüger, 2001; Evans, 2009; Carrivick et al., 2012).

(4) The ice is eventually completely separated from the glacier, creating dead-ice topography with some individual ice-cored moraines (Gravenor and Kupsch, 1959; Evans, 2009; Lukas, 2011), and further evolution of hummocky topography. Sediment is redistributed through gravitational collapse, slumping, and flowing associated with melting ice cores, changing the morphology of moraines (Sharp, 1949; Boulton, 1972; Lawson, 1979; Lysså and Lønne, 2001; Sletten et al., 2001; Lukas et al., 2005; Ewertowski et al., 2011). Topographic inversion facilitates melting of ice cores by causing material on topographic highs, i.e. ridge crestlines, to roll or flow due to gravitational processes and meltwater, which then exposes ice cores and causes increased melting (Sharp, 1949; Boulton, 1972; Eyles, 1982; Schomacker and Kjær, 2007; Evans, 2009; Ewertowski et al., 2011).

(5) Multiple cycles of topographic inversion and continual downwasting cause ice cores to completely melt, creating an area of hummocky topography through topographic inversion where the controlled moraine once existed (Gravenor and Kupsch, 1959; Boulton, 1972; Eyles, 1979; Rains and Shaw, 1981; Evans, 2009; Benn and Evans, 2010). Distinct ridges may not be preserved, as the structure of englacial debris bands imparts linearity on the medial moraines or individual ridges of controlled moraines (Kjær and Krüger, 2001; Evans, 2009; Bennett et al., 2010; Carrivick et al., 2012).

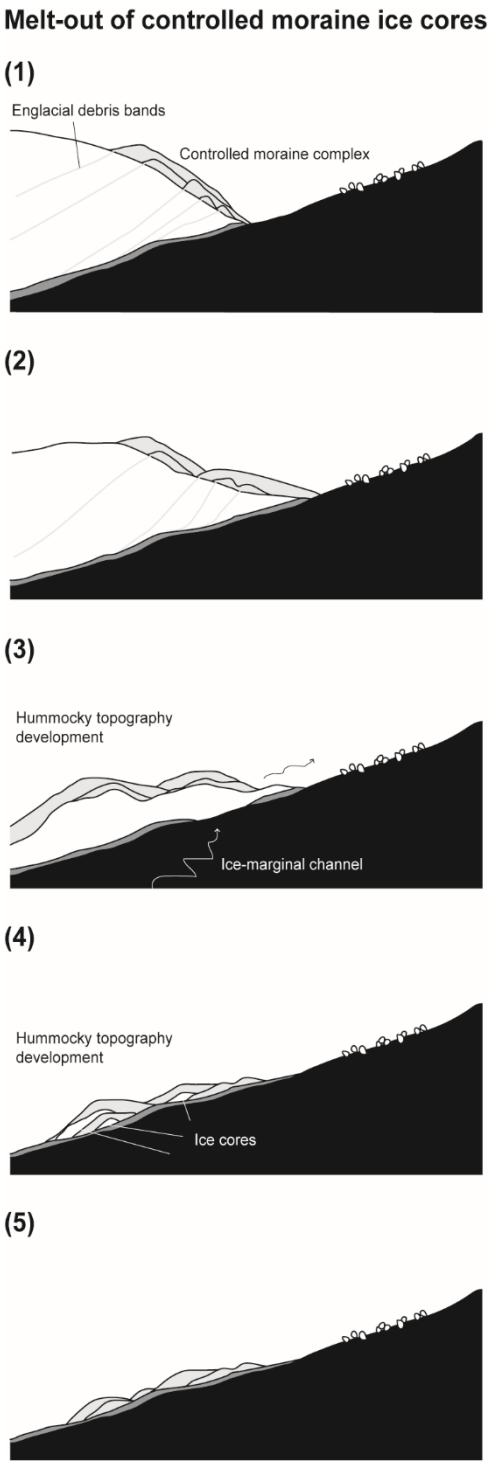

Figure 5.32 Conceptual diagram of minor moraine formation through melt-out of controlled moraine ice cores in the Silvrettagletscher foreland. The numbers follow steps described in Section 5.4.1.1.

The rock type and morphology of sediment delivered to the ice surface by individual englacial debris septa, and then subsequently to the foreland, inherently dictates the sedimentological composition of resultant moraines (Sharp, 1949; Bennett et al., 2010). Sediment composition,

local slopes, debris cover thickness, and meltwater amount then influence the morphology of resultant moraines (Sharp, 1949; Östrem, 1959; Østrem, 1964; Boulton, 1972; Lawson, 1979; Rains and Shaw, 1981; Schomacker and Kjær, 2007; Schomacker and Kjær, 2008; Ewertowski et al., 2016). The controlled moraines in the Silvrettagletscher foreland formed and are forming on reverse bedrock slopes, however this is not necessary.

These ridges are generally structureless, reflecting collapse/re-sedimentation of different layers during melt-out of the ice core (Goldthwait, 1951; Lawson, 1979; Kjær and Krüger, 2001; Everest and Bradwell, 2003; Lukas et al., 2005; Schomacker and Kjær, 2008; Reinardy et al., 2013). Lenses or layers that follow the shape of the proximal and distal slopes show flow, slump, or fall processes during melting or subsequent gravitational processes (Lawson, 1979; Sharp, 1984). The proximal slopes of these moraines are longer and steeper than the distal slopes, reflecting the geometric control of the underlying reverse bedrock slope. Finer sediments may be washed away during melting (Sharp, 1949; Boulton, 1972; Eyles, 1979; Lawson, 1979; Eyles, 1982; Lønne and Lysa, 2005; Lukas et al., 2005; Schomacker and Kjær, 2008; Ewertowski et al., 2011), which may explain why the moraines in the Silvrettagletscher foreland dominantly comprise gravel.

Controlled moraines have been known to form under similar processes in other settings, and have been linked to a high concentration of englacial debris bands created in polythermal glacier regimes (Evans, 2009; Evans, 2010; Szuman and Kasprzak, 2010; Evans, 2011; Ewertowski et al., 2011; Lakeman and England, 2012). The moraines formed by melting of ice cores as part of controlled moraines appear most similar to the processes described by Evans (2009) and Bennett et al. (2010) at Kvíárjökull, Iceland, albeit on a smaller scale, and conceptualised by Lukas (2011) as a mechanism of ice-cored moraine formation. Evans (2009) describes the evolution of a controlled moraine system from an origin of individual englacial debris septa emerging at the ice surface to eventually hummocky topography in the foreland, which has not been described in other studies. The similar processes of controlled moraine and minor moraine formation in the Silvrettagletscher and Kvíárjökull systems may be influenced by the glaciers both advancing up reverse bedrock slopes. This occurs at Kvíárjökull due to an over-deepened basin beneath the ice (Evans, 2009; Bennett et al., 2010). Controlled moraines at Ragnarbreen, Svalbard, also look similar to those at Silvrettagletscher, although on a larger scale (Ewertowski et al., 2011).

Previous work specifically in the temperate glacier regime of the Alps discusses the importance of englacial debris bands in delivering sediment to the glacier surface as “dirt cones” (Lukas, 2012; Lukas et al., 2012) or “pyramids” (Schlüchter, 1983) at Findelengletscher, which are described as similar, albeit larger, to the englacial debris septa at Silvrettagletscher.

The research at Silvrettagletscher presents the first description of the evolution of formerly and presently ice-cored moraines formed by the evolution of controlled moraines to hummocky topography in a high mountain setting.

5.3.1.2 Freeze-on of foreland and subglacial sediment on a reverse bedrock slope

One moraine shows evidence for a freeze-on mechanism of formation. The primary evidence supporting freeze-on in Exposure G is the moraine composed dominantly of till and a conformable, sharp contact between this till and underlying gravel. Aerial photographs show that this moraine formed sometime between 2010 and 2013 on a reverse bedrock slope and in front of an area with clean ice, both of which may have facilitated basal freezing. This freeze-on mechanism of minor moraine formation, specific to Silvrettagletscher, is detailed in the conceptual model below.

The Exposure G moraine formed on a reverse bedrock slope, and the contact between FA 1 and FA 2 reflects this geometry (Figure 5.16-5.17). This moraine shows massive till as the upper and majority FA (FA 2), which is unique to the field area, and shows that the glacier deposited till on top of proglacial gravel. The conformable and uniform contact between the underlying gravel and overlying till suggest a freezing mechanism that promoted maintaining this sharp contact. The gravel and till would have been thin enough to both freeze to a thin glacier front (Krüger, 1995; Lukas, 2012; Reinardy et al., 2013; Chandler et al., 2016a) and be carried up the slope during advance. Subsequent retreat deposited these layers maintaining a conformable contact and creating a ridge mimicking the shape of the wedge beneath the thin ice front (Reinardy et al., 2013).

Conceptual model of minor moraine formation through freeze-on of foreland and subglacial sediment on a reverse bedrock slope

This mechanism of moraine formation in the Silvrettagletscher foreland is detailed in the conceptual model below, as drawn from the sedimentological analysis of Exposure G and observations of aerial photographs.

(1) The glacier deposits sediment onto the foreland, creating a thin cover over a reverse bedrock slope.
(2) The glacier advances up the reverse bedrock slope, which may promote thinning of the ice front.

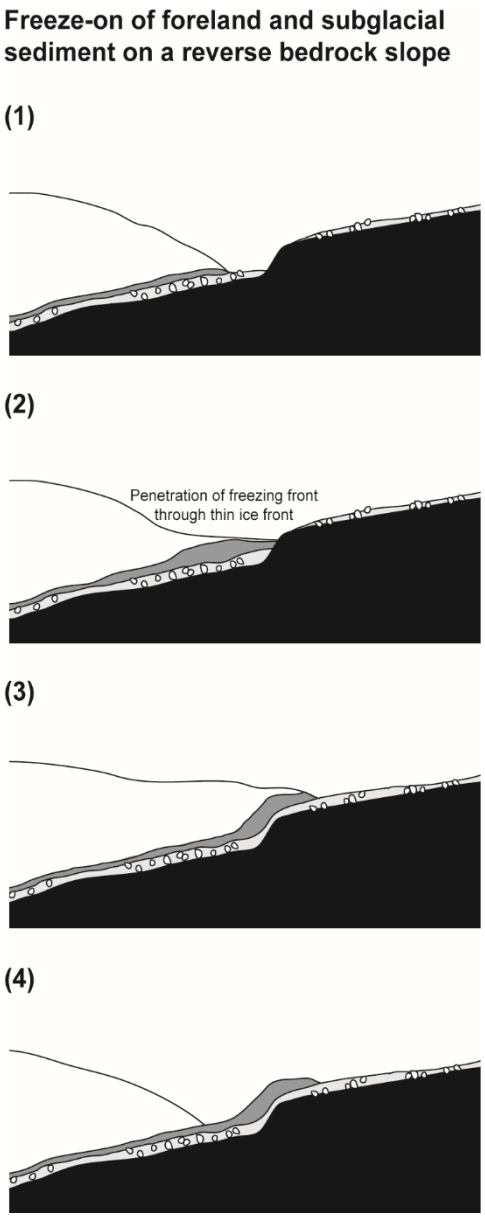

Figure 5.33. Conceptual diagram of minor moraine formation through freeze-on of foreland and subglacial sediment on a reverse bedrock slope. The numbers follow steps described in Section 5.4.1.2.

(3) A thin ice front and continued advance allow the freezing front to penetrate through the ice and underlying sediment, causing the underlying sediment (which may include till) to freeze on to the ice (Krüger, 1995; Lukas, 2012; Reinardy et al., 2013; Chandler et al., 2016a). The sediment cover on the bedrock slope and the till are both thin enough, due to the steep slope, for the freezing front to penetrate both layers of sediment. As the ice advances, it carries these two layers as a frozen unit, maintaining a conformable contact between the underlying gravel and overlying till.

(4) The glacier retreats, depositing sediment that was frozen to the bottom in an orientation similar to the wedge formed between the ice and bedrock (Reinardy et al., 2013). This leaves a ridge shape with a steeper proximal slope due to geometry of the underlying bedrock.

Basal freeze-on of till has previously only been described as a mechanism of minor moraine formation in lowland, maritime settings, e.g. Iceland (Krüger, 1995; Evans and Hiemstra, 2005; Chandler et al., 2016a) and Norway (Andersen and Sollid, 1971; Matthews et al., 1995; Winkler and Matthews, 2010; Reinardy et al., 2013; Hiemstra et al., 2015). Lukas (2012) also described basal freeze-on of sediment at Gornergletscher, although this does not seem to be prolific and does not include till, but instead proglacial debris-flow and outwash sediment. The results at Gornergletscher and Silvrettagletscher suggest that basal freeze-on mechanisms, whether exclusively incorporating extant proglacial sediment or also incorporating till, may be more prolific than the geographical collection of previous work presents.

This moraine appears different from others interpreted to have formed through freezing mechanisms, namely in that massive till constitutes and shapes the ridge. Other possible explanations could be till squeezing or push moraine formation. Push moraine formation is dismissed the till is very compact, and the thin ice front observed across the ice front would not likely have been able to push the rigid and strong sediment. Pushing would have presumably also disturbed the clear and sharp contact between two vastly different FAs seen here. Till squeezing is dismissed due to the high compaction of the till, which indicates it may not have been plastic enough for squeezing during formation. Additionally, a plastic FA may not have been able to maintain the steep slopes observed in Exposure G. Furthermore, till was not observed squeezing out along the ice front in 2015, and the sawtooth planform characteristic of many moraines formed through squeezing was not observed (Price, 1970; Sharp, 1984; Bradwell, 2004; Evans and Hiemstra, 2005; Chandler et al., 2016a). Sawtooth ridges reflect crenulations or pecten at the ice front, which provided accommodation space for till being squeezed out at the ice front and thus impart this particular geometry, typically following some pushing (Price, 1970; Sharp, 1984; Bennett, 2001; Evans and Hiemstra, 2005; Chandler et al., 2016a). Without this “mould” shape for the till to accumulate and eventually be deposited, any till squeezed out at the ice front may instead dissipate out at the ice front instead of forming a distinct ridge.

Reinardy et al. (2013) observe steeper distal slopes of minor moraines created through freeze-on processes, whereas the proximal slopes of nearly all Silvrettagletscher minor moraines are steeper, regardless of formation mechanism. This reflects the steep reverse

bedrock slopes on which most of the moraines formed, which cause proximal slopes to be steeper. Other studies that describe freeze-on report separate till slabs (Krüger, 1995; Evans and Hiemstra, 2005), perhaps stacked with other sediments (Reinardy et al., 2013; Chandler et al., 2016a), that dip up-glacier. The dip of the gravel layer and the contact between the gravel and till in the moraine at Silvrettagletscher reflects the dip of the bedrock slope, and therefore not necessarily moraine forming processes.

5.3.1.3 Push of pre-existing sediment on a reverse bedrock slope

Evidence for push of pre-existing sediment on a reverse bedrock slope is seen in Exposures D-F. A mix of sediment from control environments, other than purely supraglacial sediment, shows a mix of proglacial sediment deposited by the glacier and channels. Aerial photographs show that all three moraines formed in front of clean ice and on reverse bedrock slopes. The Exposure D moraine shows a clear influence of a "stair step" reverse bedrock slope (Figure 5.13). Although the full extent of underlying bedrock was not exposed, the Exposure E moraine does overlie a reverse bedrock slope (Figure 5.14). The Exposure F moraine is on a reverse bedrock slope, as seen for the entirety of the exposure base, and includes weathered bedrock (Figure 5.15).

The three moraines contain diamicton along portions of the base, overlying bedrock. In all three cases, the diamicton FAs are interpreted as subglacial till due to high compaction, fissility, and macroscopically massive structure (Evans et al., 2006). In Exposure D, FA 1 and FA3 are interpreted as subglacial till deposited when the glacier travelled up the reverse bedrock slope. The FA 2 diamicton in Exposure E is interpreted as a subglacial till. This would have been deposited during ice advance and was perhaps only deposited in this one location in the moraine as this area provided accumulation space at the front of the glacier. The bulldozed sediment would have subsequently been deposited above FA 2 and bedrock. The diamicton FAs (2, 3, and 5) of Exposure F are interpreted as true till and likely represent one depositional episode. FA 2 appears as an isolated pocket of till within bedrock due to bedrock geometry and where the moraine was excavated, but was exposed at the surface of the bedrock on the other side of the excavated trench. The weathered bedrock that is in contact with FA 3 and FA 5 has been filled in with matrix material similar to the FAs, further supporting glacier motion against the bedrock and till deposition through the planes of weakness in this crumbling and splintering zone of bedrock.

Evidence for formerly ice-cored moraines is seen in a lack of sedimentary structures throughout Exposure E and in FA 6 of Exposure F. This may suggest re-sedimentation during

de-icing (Goldthwait, 1951; Lawson, 1979; Kjær and Krüger, 2001; Everest and Bradwell, 2003; Lukas et al., 2005; Schomacker and Kjær, 2008; Reinardy et al., 2013), although is inconclusive. Similarly, most of the sediment in Exposure F is massive gravel (FA 6), consistent with push moraine formation of pre-existing foreland material and coarse, friable sediment that may not preserve deformation structures (Lukas, 2012; Chandler et al., 2016a). An alternative explanation could be dumping from englacial and supraglacial positions, however prolific englacial and supraglacial material was not seen in this area of the ice front.

Conversely, horizontal bedding in some exposures suggests moraines without ice cores. The presence of horizontal bedding in FA 9 and FA 11 of Exposure D supports formation without an ice core, as these FAs would have likely been altered from presumed original horizontality during melting and gravitational collapse. However, the shielded location of FA 4 in Exposure F and horizontal sand lenses suggest that it existed in this location prior to moraine formation.

Some FAs and contacts follow the shape of the ice proximal moraine slopes, as with the general orientations of all FAs and their contacts in Exposure D. In Exposure E, FA 8 and FA 9 cap the exposure and FA 8 follows the shape of the proximal slope. These orientations show gravitational reworking of sediments (Bennett, 2001; Lukas, 2005; Benn and Evans, 2010; Lukas, 2012; Reinardy et al., 2013; Chandler et al., 2016a), here specifically in the direction of the steeper and longer slope, as established by the reverse bedrock slope. This further supports a strong influence of the reverse bedrock slope on moraine formation, and is likely related to destabilization of the proximal slope following ice retreat (Bennett, 2001; Lukas, 2005; Benn and Evans, 2010; Lukas, 2012; Reinardy et al., 2013; Chandler et al., 2016a).

Conceptual model of minor moraine formation by pushing pre-existing sediment on a reverse bedrock slope

Push moraine formation on a reverse bedrock slope in the Silvrettagletscher foreland is detailed in the conceptual model below, following evidence from sedimentological analysis of Exposures D-F and aerial photographs.

(1) The glacier deposits sediment onto the foreland, creating a thin cover over a reverse bedrock slope. Steeper sections of the bedrock remain bare.
(2) The glacier advances up the reverse bedrock slope, pushing foreland sediment while it progresses (Lukas, 2012).

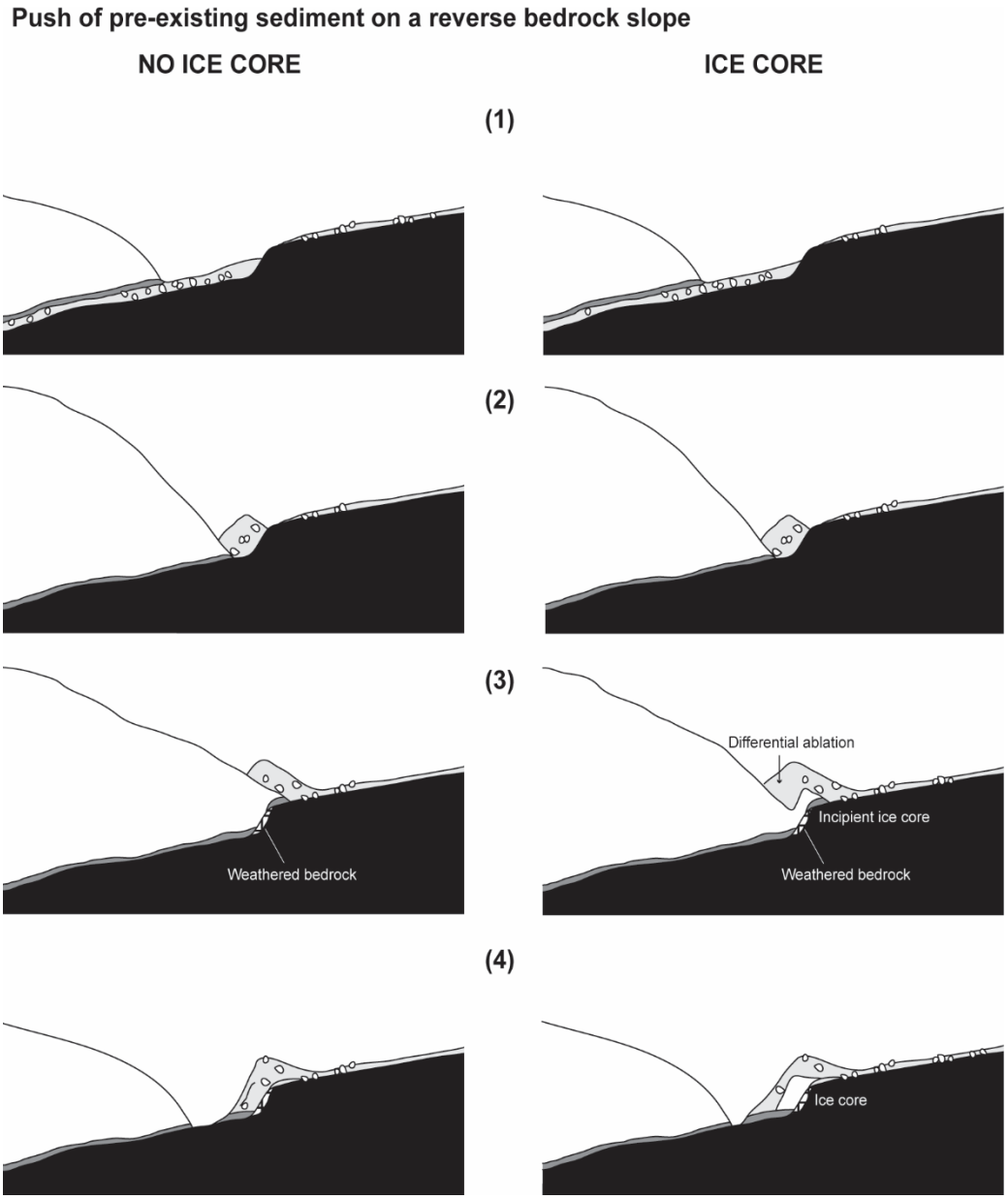

Figure 5.34. Conceptual diagram of minor moraine formation through push of pre-existing sediment on a reverse bedrock slope, without and with an ice core. The numbers follow steps described in Section 5.4.1.3.

(3) Continued advance creates a sediment pile at the ice front. Ice continues to advance, and when encountering steeper bedrock sections may weather those sections of bedrock by applying stress in the direction of ice movement. Some sediment may fall on top of the thin ice front, burying this localised portion and causing differential ablation, during which the sediment cover insulates underlying ice while more quickly melting clean ice (Lukas, 2012).

(4) The glacier retreats, depositing till overlying less steep sections of the reverse bedrock slope and the sediment pile as a push moraine. Gravitational collapse may steepen the slope angles (Bennett, 2001; Lukas, 2005; Benn and Evans, 2010; Lukas, 2012; Reinardy et al., 2013; Chandler et al., 2016a), particularly on the ice-proximal side dipping down the reverse bedrock slope. If a proto-ice core was forming during (3), retreat may cause this ice core to detach from the glacier, leaving an ice-cored moraine.

This specific mechanism of push moraine formation has previously been described only at Gornergletscher, where the steepness of the ice front exerts a strong control on moraine formation (Lukas, 2012). This mechanism of minor moraine formation at Silvrettagletscher conforms to the mechanisms of "efficient bulldozing" (no ice core) and "inefficient bulldozing" (with an ice core) described at Gornergletscher (Lukas, 2012). Together, these results show that a thin ice front and bedrock geometry play a crucial role in minor push moraine formation in the two study areas, which has been described in these two high-mountain settings in the Alps and two settings in Iceland (Bradwell et al., 2013; Chandler et al., 2016a).

These Silvrettagletscher push moraines do not show evidence of tight folding that appears in the minor moraines at Gornergletscher (Lukas, 2012). This likely reflects the size of sediment present in the two different forelands. Gravel dominates the Silvrettagletscher exposures, with some coarse sand. This coarser and friable sediment does not usually preserve deformation structures (Lukas, 2012; Chandler et al., 2016a; Chapter 4). Very few fine or diamicton FAs were recorded, aside from till where present, which are useful in tracing deformation of preserved bedding or stratification (Lukas, 2012). This could either relate generally to coarser outwash in the Silvrettagletscher foreland when compared to the outwash in the Gornergletscher foreland, washing away of finer sediment in ice-cored moraines during melting (Sharp, 1949; Boulton, 1972; Eyles, 1979; Lawson, 1979; Eyles, 1982; Lønne and Lysa, 2005; Lukas et al., 2005; Schomacker and Kjær, 2008; Ewertowski et al., 2011), or additionally to the reverse bedrock slope. Only a thin layer of gravel covers the steep slope, and the steepest parts remain bare, except in isolated pockets and on localised shallower sections. Any finer sediment that may have existed could have been washed away by snowmelt and rain.

Both the upper and lower foreland contain ice-cored moraines, which likely relate to a similar process of push moraine formation to that described by Lukas (2012) as "inefficient bulldozing" at Gornergletscher. Lukas (2012) was able to completely describe this mechanism of moraine formation, as he described an ice-cored moraine with ice still connected to the glacier. Unfortunately, this intermediate stage of ice-cored moraine formation was not observed in the Silvrettagletscher foreland; however, several lines of evidence suggest that

many moraines may have had ice cores, and that the moraines of Exposures E and F may have therefore also been ice cored.

Firstly, ice-cored ridges are present throughout the foreland, in both the upper zone and the lower zone (Figure 5.4). The location of these moraines away from controlled moraines, observed throughout the span of aerial photographs, suggest a mechanism of ice disconnecting from the glacier separate from that described as formerly ice-cored moraines once part of controlled moraines (Section 5.4.1.1). The sediment cover is consistent with that described in previous studies of ice-cored moraines, and coarser sediment collects at the bottoms of the landforms after rolling down moraine slopes (Carrara, 1975), in addition to mechanisms of re-sedimentation described in Section 5.4.1.1. Additionally, the ice-cored ridges in the Silvrettagletscher foreland occur in varying orientations, which is similar to those observed on Baffin Island (Goldthwait, 1951), and may reflect differences in the thickness of sediment cover and differential ablation through time.

Secondly, some previous work describing ice-cored moraines discusses the importance of a thin ice front in order for the ice core to separate from the glacier as dry calving (Goldthwait, 1951; Schomacker and Kjær, 2007; Lukas, 2012). The ice front of Silvrettagletscher is thin across the foreland (Figure 5.7), with some ice breaking off of the glacier during the course of summer fieldwork (e.g. Figure 5.7C). Lukas (2012) presents the method of sediment delivery onto a thin ice front most applicable to what likely occurred at Silvrettagletscher as "inefficient bulldozing" up a reverse bedrock slope, where bulldozing causes some of the foreland sediment to cover the thin ice front. This sediment then insulates the underlying ice, whereas the clean ice melts faster, causing this ice to detach from the glacier and therefore form an ice-cored moraine.

It is unknown how long the ice-cored moraines in the Silvrettagletscher foreland have existed, but the modern suite appears to have been deposited before 2003 and until at least 2013 based on aerial imagery. As the initial processes of ice-cored moraine formation, i.e. when the ice detaches from the glacier, were not observed, it is unknown whether these processes are no longer occurring in the foreland or if the short period of fieldwork was a period during which the processes of sediment cover and differential ablation were not observable.

5.3.1.4 Push of pre-existing glaciolacustrine sediment

The Exposure B moraine is an example of a moraine formed by the ice front pushing glaciolacustrine sediment into a ridge. The Exposure B moraine is also distinct from the other six excavated in both its location and its composition; the sedimentological composition is

dominantly sand, reflecting the position of the moraine in front of a former pond. This is the largest minor moraine of this study (Figure 5.9), which may reflect efficient bulldozing (Lukas, 2012) and increased sediment availability relative to the other minor moraines in the field area. This moraine exists in a lower area between a prominent reverse bedrock slope and valley wall, at the ice-distal edge of a lake that existed before 2003 to sometime before 2010. Subsequent draining of the pond in later aerial imagery reveals flutings (Figure 5.1-5.3), showing that ice had overrun this depression in the past, which may be coincident with formation of this moraine.

The dominance of sand in this moraine is consistent with a lacustrine source (Church and Gilbert, 1975; Brodzikowski and van Loon, 1991; Ashley, 2002; Benn and Evans, 2010), which suggests that the depression constraining the pond existed prior to moraine formation. The moraine also contains two gravel FAs, consistent with proglacial outwash (Church and Gilbert, 1975; Rust, 1975; Brodzikowski and van Loon, 1991; Knighton, 1998; Maizels, 2002; Benn and Evans, 2010).

The deformation structures and faulting of FA 8, the core and majority of this moraine, are indicative of push moraine formation, i.e. compressional stress from the glacier pushing a sediment pile from upvalley to its current position (e.g. Schlüchter et al., 1999; Lukas, 2012). FA 9, and the contact between FA 8 and FA 9, follows the shape of the distal slope. This orientation is consistent with sediment being pushed forward and rolling down the ice-free slope due to gravity and stress in a downvalley direction.

Conceptual model of minor moraine formation by pushing pre-existing glaciolacustrine sediment

This mechanism of minor push moraine formation through a proglacial pond, specific to the Exposure B moraine in the Silvrettagletscher foreland, is detailed in the conceptual model below, as elucidated from aerial photograph and sedimentological analyses.

(1) A proglacial pond forms in a depression in the foreland and captures meltwater from the ice front. The proglacial fluvial system deposits sediments onto the foreland in horizontal beds, where coarser sediment (gravel) is deposited closer to the ice front and finer sediment (sand) is deposited in the pond (Church and Gilbert, 1975; Brodzikowski and van Loon, 1991; Ashley, 2002; Benn and Evans, 2010).
(2) The glacier advances through the immediately proglacial foreland and pond, pushing sediments as it progresses.

(3) Continued ice advance faults and folds bedding and laminations in the core of the sediment pile, indicative of compressional stress (e.g. Schlüchter et al., 1999; Lukas, 2012).

(4) The glacier retreats, finally depositing the sediment as a push moraine.

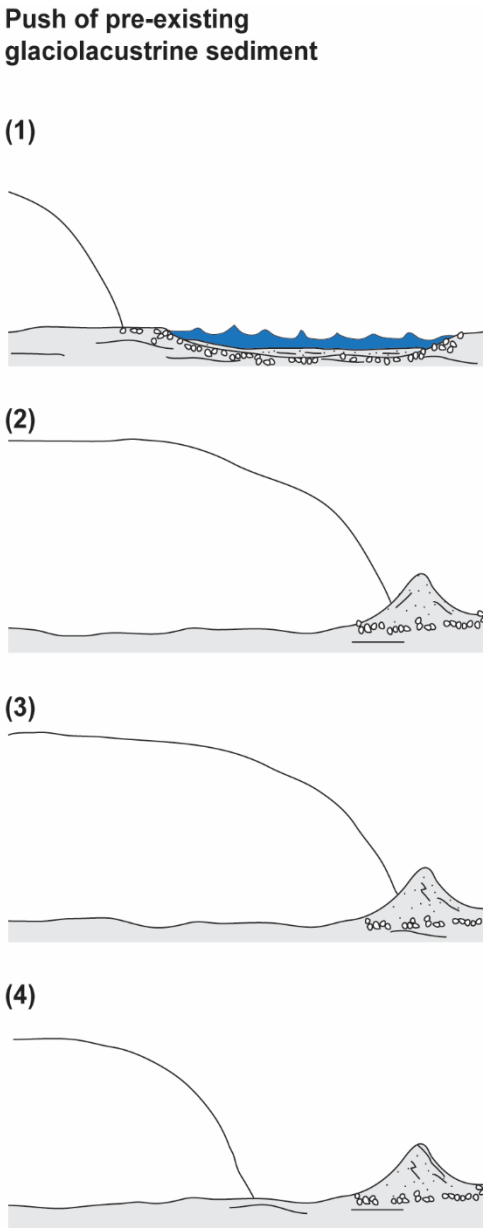

Figure 5.35. Conceptual diagram of minor moraine formation through push of pre-existing glaciolacustrine sediment. The numbers follow steps described in Section 5.5.1.4.

Several minor moraine studies describe push moraine formation mechanisms (Worsley, 1974; Birnie, 1977; Sharp, 1984; Ono, 1985; Boulton, 1986; Lukas, 2012; Bradwell et al., 2013;

Chandler et al., 2016a). The stress imposed by advancing ice compresses proglacial sediment at the ice front, shortening the pile and creating a moraine. Pre-existing foreland sediment or contemporaneously deposited sediment inherently dictate the composition of a push moraine, and therefore varies among study areas due to proglacial depositional processes prior to and during ice advance.

5.3.2 Preservation potential of minor moraines

A comparison of the geomorphological maps drawn using 2012 and 2013 imagery (Figure 5.1) and field observations in 2015 and the geomorphological map drawn using 2009 imagery (Figure 5.3) shows the limited preservation potential of minor moraines. The striking difference between these two maps is the number of extant minor moraines in the bedrock-dominated area immediately in front of the current ice front.

The preservation potential of minor moraines in the Silvrettagletscher foreland is limited primarily by size. These moraines are small (<1.5 m tall), suggesting that even minor erosion could obliterate traces of former ridges. Additionally, most of the moraines are composed dominantly of friable gravel and are therefore readily susceptible to erosion. Reverse bedrock slopes underlying most of the moraines may help accelerate erosion through enhanced gravitational processes of collapse, rolling, and sliding when compared to flatter settings. Additionally, water draining from higher areas on the reverse bedrock slope, as snowmelt, rain, or melt-out of ice cores, may accelerate erosion as it drains down the slopes towards the ice front or the main proglacial channel.

Preservation potential is further limited for ice-cored moraines, whether originating as controlled moraines or not. As ice melts, the sediment cover collapses and the ridge becomes smaller and less distinct through on-going re-sedimentation as gravitational collapse, slumping, and flowing, as described in Sections 5.4.1.1 and 5.4.1.3 (Sharp, 1949; Goldthwait, 1951; Boulton, 1972; Carrara, 1975; Lawson, 1979; Sharp, 1984; Kjær and Krüger, 2001; Lyså and Lønne, 2001; Sletten et al., 2001; Everest and Bradwell, 2003; Lukas et al., 2005; Schomacker and Kjær, 2007; Schomacker and Kjær, 2008; Evans, 2009; Ewertowski et al., 2011; Carrivick et al., 2012; Lukas, 2012; Reinardy et al., 2013). For example, individual mounds <1 m^2 were observed throughout the foreland, where all areas contain extant ice-cored moraines. Although it cannot be proven with the available aerial imagery, these mounds may be the remnants of moraines that were once more distinct. Many ridges in the foreland still contain ice cores, however the longevity of these ice cores is unknown.

Aerial imagery captures some moraines, but is not available for consecutive years, some photographs were taken with sun angles that do not show moraines well, and the photographs may not depict all of the smaller ridges and mounds. This study is therefore unable to count how many moraines, whether ice-cored, formerly ice-cored, or without ice cores, have existed in the foreland and how many of these have not been preserved.

The presence of controlled moraines stands somewhat separate from other ice-cored moraines. There is an inherent lag-time between the formation of dead ice and the formation of distinct moraine ridges due to the time required for ice to melt. This is dependent on the size of the original ice body, sediment cover distribution, and topographic inversion dynamics, whether insulating underlying ice or promoting melting (Sharp, 1949; Boulton, 1972; Eyles, 1982; Schomacker and Kjær, 2007; Evans, 2009; Ewertowski et al., 2011). Additionally, the degradation of a controlled moraine may form multiple moraines. Both of these issues highlight chronological implications if attempting to use moraines formed in this manner as chronological markers of ice extent and/or in comparing to glacier measurement and climate data. As these moraines may often not indicate ice front position, they should not be used for statistical analyses such as those used in this study. This additionally highlights complications in how simply counting ostensible moraines may not be a viable method of chronological constraint unless the processes of formation are pinpointed.

5.3.3 Climate influences on Silvrettagletscher mass balance and minor moraine formation

Measurements of Silvrettagletscher mass balance and front variation were statistically compared to ablation season, accumulation seasons, and annual temperature and precipitation data from two nearby weather stations. Moraine spacing, using two different methods for chronological constraint, was additionally compared to the glacier and climate data. Statistical analyses evaluated the correlation and significance of these datasets to assess potential influences of climate parameters on moraine formation.

The statistical data show relatively low R^2 values overall (0.0005-0.6157). Although these values are low, anomalously high values that are statistically significant ($R^2 > 0.1$, $p < 0.05$) are considered to represent some correlation between the variables. Similarly low values have been reported in other studies that investigate the relationships between climatic influences and moraine spacing used as a proxy for ice margin retreat rates. Bradwell (2004) and Beedle et al. (2009) conclude that ablation season air temperatures significantly influence glacier length changes at Lambatungnajökull and Castle Creek Glacier with R^2 values of 0.56 and 0.3025, respectively. Lukas (2012) concluded that accumulation season temperature

controlled ice-marginal retreat rates, with an R^2 value of 0.2026. Chandler et al. (2016a) conclude that ablation season Atlantic air temperature is a significant influence on ice margin retreat rates, with R^2 = 0.3464. Similar values from the analyses at Silvrettagletscher are therefore discussed here as being notable.

The results of statistical analyses show significant relationships between measurements of Silvrettagletscher and temperature and one significant relationship with precipitation (Table 5.3, Figures 5.24-5.25). These data suggest that average ablation season temperatures influence the mass balance of Silvrettagletscher most (R^2 = 0.5210 and 0.5078), and annual average temperature (R^2 = 0.3042 and 0.1776) and ablation season precipitation (R^2 = 0.1036) also show relationships to mass balance (Table 5.3, Figures 5.24-5.25). Average annual (R^2 = 0.1356), average ablation season (R^2 = 0.1287, and 0.1313), and average accumulation season (R^2 = 0.1019) temperatures may influence the front variation of Silvrettagletscher (Table 5.3).

Huss and Bauder (2009) compare mass balance and climate data from Silvrettagletscher to assess changes and relationships over a 93 year period using a mass balance model. The analyses of these datasets are more involved than those presented here, including corrections for measurement bias, varying observation dates, and gaps in data, as expected from more detailed and model-intensive assessment of climate forcings on mass balance. Huss and Bauder (2009) use a compilation of climate data from stations in Davos and Klosters. Although these stations are slightly closer to Silvrettagletscher (18 km and 13 km, respectively) than Weissfluhjoch (20 km), Weissfluhjoch (2,691 m) is more similar in elevation to Silvrettagletscher (2,732 m) than either the Davos (1,590 m) or Klosters (1,200 m) stations. Regardless of these differences, these models show that mass balance is primarily driven by summer ablation (Huss and Bauder, 2009), which agrees with the findings presented here (Table 5.3).

The dominant influence of ablation season temperature on mass balance at Silvrettagletscher (Table 5.3) is similar to several other studies that discuss climate influences on minor moraine formation. Sharp (1984), Bradwell (2004), and Chandler et al. (2016a) in Iceland discuss ablation season temperature as the primary influence on mass balance changes at the studied glaciers. This relationship between climate and mass balance contrasts the results from Gornergletscher, which show dominant influences of annual and accumulation season temperatures on minor moraine spacing, which is used as a proxy for ice-marginal retreat rates (Lukas, 2012).

The statistically significant relationship between front variation and mass balance may be manifesting itself two statistically significant relationships with moraine spacing in the

foreland during the 1992-2009 period assessed: front variation and moraine spacing of the southern transect (Figure 5.26A), and mass balance and moraine spacing of the northern transect (Figure 5.26C) (Table 5.3). In both cases, chronological constraints on moraines in the assessed transects are derived from comparing front variation measurements to the geomorphological map. The method of chronological constraint may, however, be the reason for this apparent significance.

Four statistically significant relationships between minor moraine spacing in the Silvrettagletscher foreland and climate variables spanning 1992-2009 show that average accumulation season temperature (when using the counting back approach to establish chronological control) and average annual temperature (when pairing the geomorphological record and front variation measurements as chronological control) appear related to moraine spacing measurements (Table 5.3, Figures 5.27-5.30). This relationship to accumulation season temperatures seems surprising, however, as there is only a weak relationship with this parameter in one other instance, when comparing front variation and temperatures at Weissfluhjoch (Table 5.3, Figure 5.24).

In summary, it appears that precipitation does not strongly influence Silvrettagletscher or the geomorphological record of minor moraines. Overall, ablation season temperature seems to play the dominant role on Silvrettagletscher measurements, whereas average annual temperature seems to influence the moraine record most.

The small amount of significant relationships between moraine spacing at Silvrettagletscher and front variation, mass balance changes, or climate factors and the similarities with lowland environments and dissimilarity with another setting in the Alps (Gornergletscher; Lukas, 2012) suggests that the formation of minor moraines here may not be primarily driven by climate factors. The data also suggest that changes in mass balance and front variation each year may not be reflected in shorter-term (i.e. seasonal) ice-marginal fluctuations that may create minor moraines.

Alternatively, the lack of correlation between moraine spacing in the Silvrettagletscher foreland and climatic influences may be due to difficulties in extracting a climate signal from moraine records, an incomplete moraine record, and lack of firm chronological constraint. Unfortunately, moraine spacing data are hindered by insufficient chronological control, the highly fragmented nature of moraines not allowing for long time series transects, different mechanisms of moraine formation, and isolated clusters of minor moraines in the foreland. The chronological constraint used in moraine spacing measurements was based on assumptions, as little firm chronological constraint exists. Associating moraines with individual years may not be correct at Silvrettagletscher, i.e. the glacier may not deposit one moraine every year or more

than one moraine may be deposited in a year. The analysis of moraine spacing may be further hindered by the lack of data available. More robust data could help more thoroughly assess these relationships, as the time period examined (17 years) is relatively short when compared to longer mass balance and front variation comparisons (50 years) and comparisons to climate data (70-92 years). Additionally, it should be noted that Figures 5.22 and 5.23 themselves point to potential inaccuracies in the attempted comparison of front variation and the moraine record. These figures show the older transect (Figure 5.22) ending around 1992, and the younger transects (Figure 5.23) beginning around 1992. However, the older transect and closest (northern) younger transect are separated by nearly 140 m, despite the overlain front variation measurements suggesting that they should be joined.

Both techniques (counting back and comparisons to front variation measurements) do, however, provide some valuable information. The technique of counting back from a known time (here, the 2009 ice front on aerial imagery) to establish moraine ages may not be strictly accurate due to the potential for obliterative overlap as self-censoring and other erosion as external-censoring (Gibbons et al., 1984; Kirkbride and Brazier, 1998; Kirkbride and Winkler, 2012; Barr and Lovell, 2014; Chandler et al., 2016a), multiple moraines formed in a single year, and years with no moraine formation. When considering using marked locations along the Gletscherlehrpfad, as seen in the older moraines compared to front variation measurements (1959 and 1981), the position could not be marked accurately on aerial imagery in the field due to the small size of the moraines. This location was transferred to the map using a GPS measurement with ± 3 m accuracy and therefore should be treated with caution. The lack of firm chronological constraint further hinders connecting moraines in different areas of the foreland to single ice positions, especially as moraine fragments are present in clusters (Figures 5.1-5.3).

The highly-fragmented nature of the moraines also poses problems in connecting fragments as longer chains, which may not be accurate, as subtle variations at the ice front, both as the shape of the ice front and potential topographic obstacles, could influence the location of moraine deposition relative to others deposited contemporaneously. Many of these fragments could not be connected with confidence. Without more detailed historical and modern high-resolution imagery or annual field observations, the precise timing of moraine formation in the foreland cannot be accurately known, and therefore the records of formation cannot be accurately compared to the climate and glacier measurement records.

A potentially incompletely mapped record, related to resources available for mapping and preservation potential of some moraines (see Section 5.4.2.), would also hinder accurate correlations between the moraine record and climate data. Simple counting of moraines,

without a detailed understanding of ice front position across the entire foreland, mechanisms of formation, and confidence in a complete record, may therefore produce errors when counting moraines deposited during any length of time.

Comparison is also complicated by the different mechanisms of formation operating across the ice front. Four primary mechanisms create minor moraines in this foreland. The available aerial imagery does not allow for these mechanisms to be differentiated, except perhaps where minor moraines are recognized forming in association with controlled moraines. These moraines were not used in moraine spacing measurements and subsequent statistical correlations, as they do not reflect individual ice front positions. Processes of moraine formation associated with the melt-out of controlled moraines also show that multiple ridges may form during the processes of de-icing, either through re-sedimentation or linearity of englacial debris septa (Section 5.4.1). The presence of multiple mechanisms of minor moraine formation in the foreland also suggests that several moraines may form along the ice front in any given year.

Despite these complications, an attempt was made to use techniques similar to those presented by Beedle et al. (2009) at Castle Creek Glacier, Lukas (2012) at Gornergletscher, and Chandler et al. (2016a) at Skálafellsjökull, using moraine spacing as a proxy for ice-marginal retreat rates and comparing this to climate data. These previous studies have also noted that extracting climate signals from the moraine record may be complicated by factors that are difficult to quantify, including patterns of snow cover (Beedle et al., 2009), topographic effects such as subglacial bed topography, differential shading across the glacier, and bedrock obstacles, and glaciological effects such as hypsometry and source areas (Lukas, 2012), and longer-term climate signals and internal glacier dynamics and structures (Chandler et al., 2016a), and a reverse bedrock slope at the ice front (Lukas, 2012; Chandler et al., 2016a). However, recognizing these complications also echoes support for detailed sedimentological investigation of minor moraines.

The comparisons between ice front variations measurements and mapped moraines and between techniques of pairing front variation data with the geomorphological record and counting back from a known age to establish chronological control on moraine formation provide examples of how different areas of the ice front may respond differently to change. This foreland is characterized by not having one dominant flow direction and valley axis, as well as considerable variation in bedrock and basin geometry, where some areas are characterised by reverse bedrock slopes (e.g. modern ice front), and others with steep bedrock slopes in the direction of ice flow (e.g. where the main proglacial channel exits the reverse bedrock slope zone) and some areas that are generally flat and infilled with sediment (e.g. delta) (Figure 5.1-

5.2). All such factors related to pre-existing topography may influence moraine formation (e.g. Section 5.4.1; Hewitt, 1967; Birnie, 1977; Schlüchter 1999; Ham and Attig, 2001; Lukas, 2010; Chandler et al., 2016a; Chapter 4).

5.3.4 Moraine classification

Exposures B, D, E, and F all show slightly different responses to pushing associated with small advances of the ice front, reflecting local differences in bedrock geometry, foreland sediment cover, and post-depositional alteration. These differences are reflected in the evidence for or against an ice core, the sedimentological composition of moraines, and the sedimentary structures observed in exposures. Across the ice front, any small changes in the shape and thickness could reflect local differences in the steepness of the underlying bedrock slope, which may affect push dynamics and moraine preservation. Similarly, although freeze-on is not a prolific mechanism of moraine formation in the study area, it was only observed in an area with a reverse bedrock slope and in only one of seven exposures studied in detail.

Some minor moraines in the Silvrettagletscher foreland may show localised responses to the presence of controlled moraines and bedrock geometry. Controlled moraines are dependent on englacial debris septa delivering sediment to the ice surface and subsequent accumulation at the ice front, so the minor moraines that occur following de-icing of controlled moraines would not exist without these processes operating and are also dictated by the orientation of englacial channels and amount of sediment.

Furthermore, the geomorphological maps compiled from several years of aerial imagery (Figures 5.1-5.3) show many short ridges that cannot be confidently connected to each other, ridges that are not in ice-parallel orientations, and clusters of ridges in certain areas of the foreland. The locations and orientations of minor moraines here show that local factors may strongly influence moraine formation processes. Alternatively or additionally, low preservation potential may signify that previous moraines may have been reworked or completely eroded, potentially explaining the absence of moraines in particularly areas.

Lastly, the aerial imagery through time is insufficient to track the development of minor moraines in the Silvrettagletscher foreland. Some moraines, mounds, and other landforms are too small to be noticeable at such large scales, and others are seen appearing and disappearing through time. This points to issues associated with varied resolution, sun angle, angles of photography (see Chapter 2 and Chapter 6), and georeferencing through time, as well as the images not spanning consecutive years.

The term “annual moraines” is quite specific, and should only be used when presented with sufficient evidence. Comparing ice front variation measurements, moraine positioning, and counting back from a known ice position to establish chronological constraint shows that many of the moraines from 1993-2009 may be annual, although this analysis is less conclusive for an older series of ridges (Table 5.2; Figures 5.22-5.23). Overall, the minor moraines in the Silvrettagletscher foreland should not be classified as “annual moraines,” because their presence cannot conclusively be tied to annual cycles of advance and retreat. Conservatively, however, the younger moraines and moraines in specific areas of the foreland may be referred to as potentially annual moraines, albeit with aforementioned caveats of inconsistent and interpreted moraine connections and, in some places, years in which multiple moraines may have formed. The most accurate way to assess if the moraines in this foreland are annual is to resurvey/monitor the foreland at a similar time annually while undertaking a comprehensive database of moraine formation, location, and degradation, as also suggested by Chandler et al. (2016a). Unfortunately, this level of detail does not exist for the period of minor moraine formation in the Silvrettagletscher foreland.

CHAPTER 6. Continued moraine formation and degradation in the Gornergletscher, Switzerland, alpine foreland

6.1 Minor moraine distribution in the Gornergletscher foreland since 2007

The geomorphological map of the Gornergletscher foreland drawn using aerial imagery from 2012, 2013, and 2014 shows numerous minor moraines formed after 1850 (Figure 6.1). This new geomorphological map shows that some moraines originally mapped by Lukas (2012) were not distinguishable on the 2012-2014 aerial images, including the GOR 1 moraine. At least 100 moraine fragments are present in the Gornergletscher foreland between the 2007 and 2014 ice front positions (Figure 6.2), which confirms that moraines formed since the time Lukas (2012) performed fieldwork. A comparison of the 2012, 2013, and 2014 aerial imagery reveals that six moraine fragments formed in 2013 and five moraine fragments formed in 2014 (Figure 6.3).

6.2 Discussion

6.2.1 Continued moraine formation in the Gornergletscher foreland since 2007

Aerial imagery shows that minor moraines have continued forming in the Gornergletscher foreland since the 2007 field investigation and image analysis by Lukas (2012). Most of these moraines have ridges oriented approximately parallel to the modern ice front, although some are nearly perpendicular. This may reflect small variations in the shape of the ice front, as seen in the most recent aerial image from 2014 (Figure 6.3). The new (2007-2014) moraines are notably discontinuous, with the longest moraine reaching 38 m, and cannot be connected to each other with confidence (Figure 6.2-6.3). This may reflect either discontinuous deposition along the ice front or post-depositional erosion. The 2013 and 2014 aerial images (Figure 6.3) support the former, as the moraines formed during these years are also discontinuous by the time of image capture.

Lukas (2012) presented that the minor moraines in the Gornergletscher foreland had been forming annually since 1977, based on an analysis of aerial images spanning 1977-2007. Example aerial photographs highlighting newly-formed moraines each year were not presented, however. Comparing the 2012, 2013, and 2014 aerial images confirms that some moraines in the Gornergletscher foreland form annually, as these images show that six moraines formed in 2013 and five moraines formed in 2014 (Figure 6.3). This study can, however, only specifically attribute annual formation to these 11 moraines, due to lack of aerial photography and/or field visits after 2007.

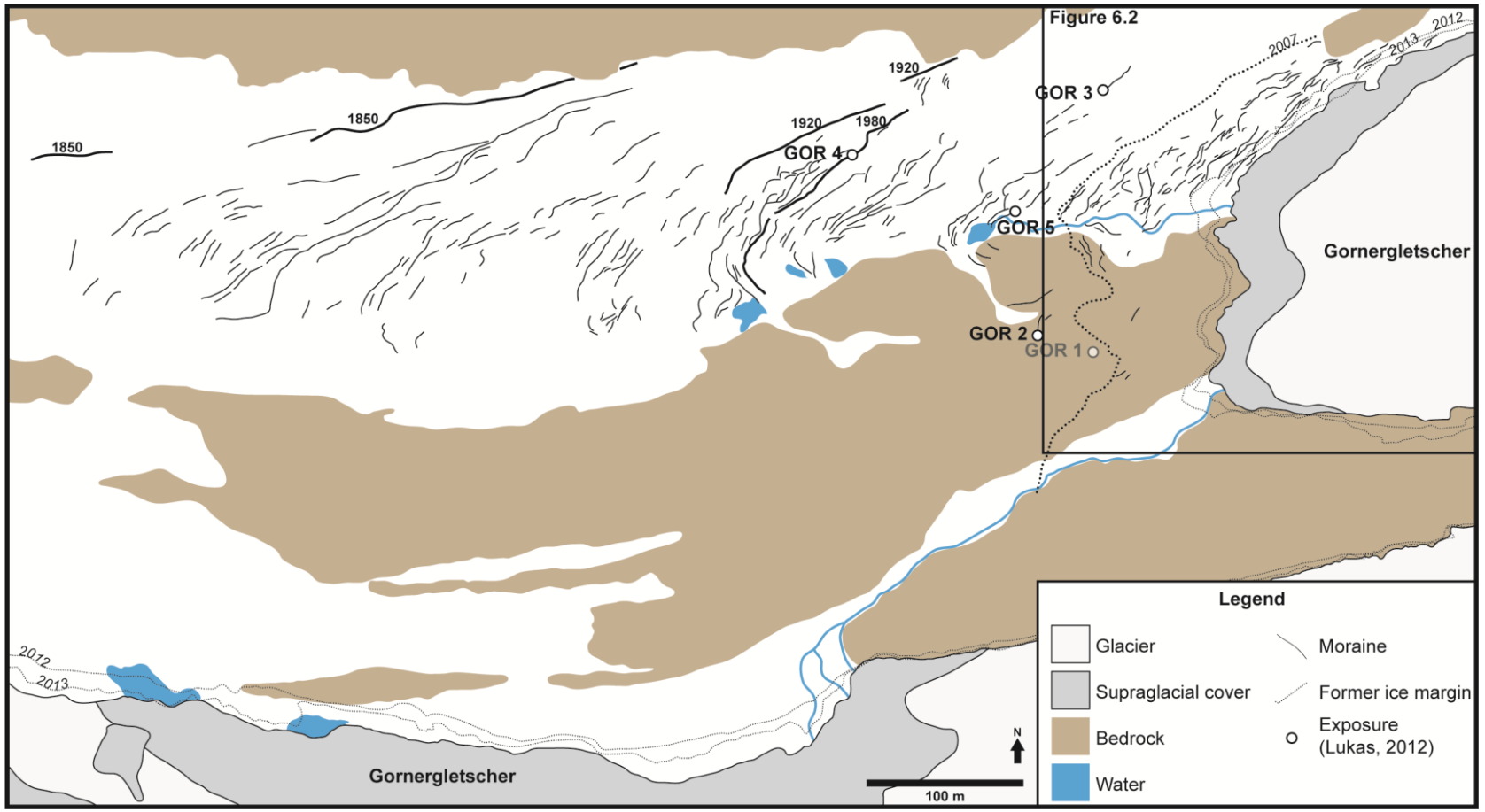

Figure 6.1. Geomorphological map of the Gornergletscher foreland focused on mapping moraines. Ice extent, exposed bedrock, and water (ponds and streams) based on 2014 air photo as the newest available imagery. Moraines mapped using a combination of aerial photographs from 2012, 2013, and 2014. Approximate extent of ice in 2007 shown with thicker dotted line based on mapping by Lukas (2012). Inset box shows extent of Figure 6.2.

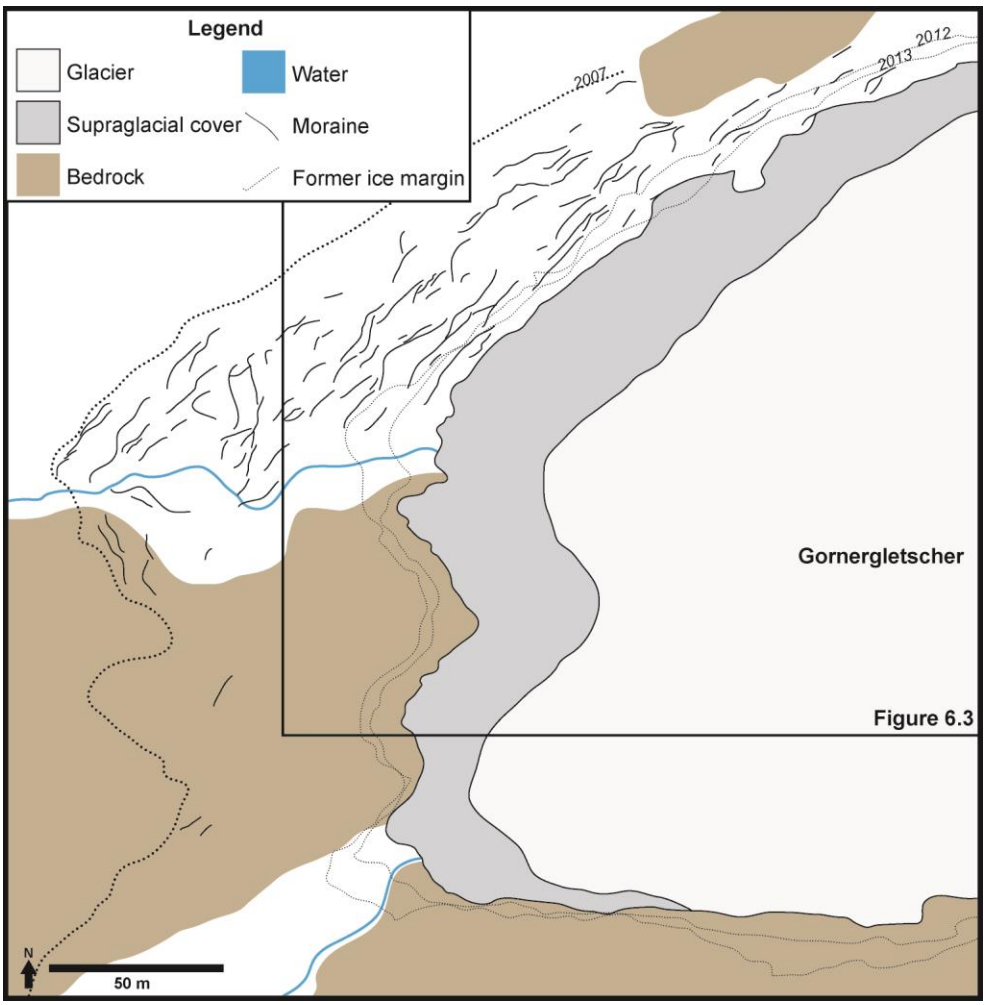

Figure 6.2. Geomorphological map of the Gornergletscher foreland showing only moraines between the 2007 and 2014 ice limits. Ice extent, exposed bedrock, and streams based on 2014 air photo as the newest available imagery. Moraines mapped using a combination of aerial photographs from 2012, 2013, and 2014. Approximate extent of ice in 2007 shown with thicker dotted line based on mapping by Lukas (2012). Inset box shows extent of Figure 6.3.

Annual deposition without conclusive evidence from each year would be an assumption, as multiple moraines may form in one year, some years may not have moraines formed, and some moraines may be missing from the record due to erosion or obliterative overlap (Gibbons et al., 1984; Kirkbride and Brazier, 1998; Kirkbride and Winkler, 2012; Barr and Lovell, 2014; Chandler et al., 2016a).

The mechanisms of minor moraine formation in the Gornergletscher foreland since 2007 cannot be known with confidence. Lukas (2012) described three mechanisms of minor moraine formation (Chapter 1), however discovering and understanding these mechanisms of formation was only possible with detailed fieldwork and observations. Both inefficient and efficient bulldozing could ostensibly happen across the ice front, whereas ice-contact fan formation as observed by Lukas (2012) necessitates an englacial conduit fill depositing sediment at the ice front. Although englacial conduit fills at the ice

front were not noticed on 2012-2014 aerial imagery, they may exist but not be noticeable from an aerial view or masked within clearly evident supraglacial cover.

Figure 6.3. Aerial images of the ice front in 2012, 2013, and 2014. Black lines show moraine crestlines. The images highlight the formation of three moraines between acquisition of the 2012 and 2013 photographs and two moraines between acquisition of the 2013 and 2014 photographs. Extracts taken from larger aerial photographs.

The detailed sedimentological and geomorphological research presented by Lukas (2012) and the updated work presented here through solely an analysis of aerial imagery highlights the importance of pairing field techniques with remote sensing in order to most thoroughly understand landform formation and landscape evolution.

The continued formation of minor moraines in the Gornergletscher foreland shows that the driving forces of ice-marginal fluctuations, and associated moraine formation, have been operating from 1977 (Lukas, 2012) until at least 2014. Minor moraines formed through push mechanisms inherently involve some oscillations of the ice margin. Lukas (2012) showed that moraine spacing in the Gornergletscher foreland correlates most strongly to annual and winter temperature climate signals. Specific mechanisms of moraine formation may be controlled by the steepness of the ice front and the presence of englacial conduit fills (Lukas, 2012). The research at Gornergletscher would benefit from continued observation to check the continued formation of moraines and if and when moraine formation ceases. The latter would provide further information about the fundamental mechanisms of minor moraine formation here, as related to climate, topography, and glacier dynamics.

6.2.2 Preservation potential of minor moraines in the Gornergletscher foreland

The preservation potential of minor moraines is discussed by several authors as a complication in most fully understanding the significance of minor moraines and the mechanisms of their formation (Andersen and Sollid, 1971; Evans et al., 1999; Bennett, 2001; Bradwell, 2004; Lukas, 2012; Schomacker et al., 2012; Bradwell et al., 2013; Reinardy et al., 2013; Chandler et al., 2016a; Ewertowski et al., 2016). This current study mapped moraines in the Gornergletscher foreland from 1850 to 2014 using exclusively aerial photographs from 2012, 2013, and 2014, and the previously published map of minor moraines at this study site mapped minor moraines from 1850 to 2007, using aerial imagery available at the time as well as field observations (Lukas, 2012). A comparison of these two maps shows that several moraines are missing when mapping using the most recent imagery, and that the sizes of some moraines are different between the two maps. For example, moraines mapped on bedrock by Lukas (2012), except for the GOR 2 moraine, are no longer visible by 2012, including moraine GOR 1. The differences in minor moraines mapped between the two studies may be due to resources available for mapping, operator experience, and/or preservation potential of minor moraines.

Firstly, differences in the minor moraine record in the Gornergletscher foreland, as displayed on geomorphological maps, may be related to resources available for mapping. The map produced by Lukas (2012) through combining field mapping and mapping from

aerial photographs likely benefited the final geomorphological map, as this provides two different lines of evidence to check the findings. This combined approach should be used when possible, as it can provide considerably more information than just one technique. The present study did not include visiting the foreland to compare the presence of moraines between aerial photographs and field observations.

Differences in the aerial photographs may have also influenced geomorphological mapping. All images used for mapping are portions of larger vertical aerial photographs. As these are extracts from larger images, they may be oblique to some degree. The obliquity will vary depending on where the centre of the original photograph is, leading to some level of geometric distortion (Boston, 2012). Even subtle variations in obliquity can cause complications in aligning photographs and landforms to each other, especially when focusing on small-scale landforms.

Other geometric distortion of aerial photographs can result from relief displacement due to varying distances between the terrain and the camera across a landscape in a single photograph due to elevation, which will be amplified in high relief settings (Lillesand et al., 2008), such as the high-mountain Alps environment of this study area. Distortion will be most prominent nearer the edges of an image, i.e. further from the directly overhead camera (Gibson, 2000; Campbell, 2002; Lillesand et al., 2008; Boston, 2012). Unfortunately, the location of the study area in relation to the original larger photographs is unknown, however the study area lies close to the edges of the 2012-2014 photographs available. Similarly, one photograph can have any number of scales, as terrain at higher elevations will be closer to the camera than lower elevation terrain, again resulting in geometric distortion (Gibson, 2000; Lillesand et al., 2008; Boston, 2012).

The larger images from 2012-2014 all show the same extent and are therefore aligned with confidence, however it is unknown whether this is due to matching extents of the original photographs or post-acquisition processing. Unfortunately, the full extent of the 2007 image used by Lukas (2012) is unavailable. A direct comparison of the 2007 map (Lukas, 2012) to the map presented in this study was complicated due to the underlying photograph not aligning well with the newer images. The presence and shapes of moraines mapped was therefore compared using notable stable features (large boulders on flat terrain and trails).

Furthermore, colour and tonal contrasts can complicate mapping from a single image. The time of day, time of year, and angle of acquisition can all influence shadows that can either accentuate or mask landforms. This suggests that unless all factors are kept constant (date the photograph was acquired and time of day/sunlight angle, distance from camera to ground control points, resolution of imagery) there may be complications in

aligning images taken in different years and comparing landforms mapped using different images.

Secondly, low preservation potential of these subtle landforms may mean that some of the younger minor moraines have been eroded since their deposition and since the 2007 aerial imagery was acquired. Low preservation potential likely explains the absence of the GOR 1 moraine on the 2012-2014 map. This moraine was ice-cored in 2007 (Lukas, 2012), which significantly limits preservation potential as the ice melts and redistributes overlying sediment into a small ridge or erodes the ridge completely (Sharp, 1984; Kjær and Krüger, 2001; Reinardy et al., 2013). Erosion may censor other moraines without ice cores as well. As Lukas (2012) noted, outwash fans, meltwater channels, and depressions separated many ridge fragments, suggesting post-depositional erosion of moraine chains that may have originally been more extensive. Ridges in the Gornergletscher foreland are also likely to be eroded due to gravitational redistribution of sediment down the ridge slopes, snowmelt, and freeze-thaw processes. Most moraines in the foreland, with the exception of the youngest moraines, are vegetated, which suggests stability and persistence through time. This therefore suggests that operator differences more likely account for the apparent "disappearance" of most moraines when comparing geomorphological maps.

Issues with preservation potential, especially of minor moraines, questions the recognition of these landforms in other study areas and their potential use in Pleistocene environments. The small size of these landforms and continued erosion through time may make them difficult to detect among larger, clearer landforms, which can pose risks when using techniques that relate moraine presence to climatological factors, e.g. the ice-marginal retreat rate studies conducted using minor moraines in Iceland (Bradwell, 2004; Chandler et al., 2016a), Switzerland (Lukas, 2012), and Canada (Beedle et al., 2009) and studies that count the number of moraines between landforms of known years to support annual deposition (Price, 1970; Andersen and Sollid, 1971; Bradwell et al., 2013; Hiemstra et al., 2015).

CHAPTER 7. Synthesis of research findings and comparison to minor moraines in other studies

> 'You know what I say to people when I hear they're writing anti-war books?'
> 'No, what *do* you say, Harrison Starr?'
> 'I say, "Why don't you write an anti-*glacier* book instead?"'
> What he meant, of course, was that there would always be wars, that they were as easy to stop as glaciers. I believe that too.
> *from* Slaughterhouse Five by Kurt Vonnegut (1969)

Chapter 1 provided a literature review of previously published studies on groups of closely spaced minor moraines interpreted to have formed by some degree due to seasonal ice front fluctuations. This chapter synthesizes the work of these previous studies in the context of findings from the new study areas of this thesis. Chapter 1 also introduced the research questions, objectives, and goals of this thesis, which are reviewed here.

7.1 The presence of minor moraines in the European Alps

The first research question asked if groups of closely spaced minor moraines exist in other high-mountain settings of the European Alps, extending the original research in this region by Lukas (2012). Minor moraines certainly do exist in other high-mountain settings of the European Alps, in both historical and modern environments. This study searched all of the currently glaciated valleys in the Alps to locate valleys that contain groups of minor moraines and revealed four valleys with at least ten minor moraines, from which two valleys were chosen for more detailed investigation as the primary study sites of this research. Minor moraines in the Schwarzensteinkees foreland, Austria, formed from 1850 to 1930. The minor moraines in the forelands of Silvrettagletscher and Gornergletscher, Switzerland, have been forming since before 1850.

It is important to reiterate that the record of minor moraines in the Alps presented in this thesis may be incomplete, for several reasons. Only valleys with extant glaciers were scanned for minor moraines, thus omitting the presence of any minor moraines in formerly glaciated areas. Additionally, only one suite of aerial imagery was used while searching for minor moraines, whereas other imagery may be more detailed for localised areas, potentially revealing minor moraines in other forelands. Furthermore, some moraines may have been eroded since their deposition, thereby censoring the geomorphological record. Extending the search beyond solely the Google Earth platform may help extend the findings of this study and present new study areas.

7.2 The importance of merging geomorphological and sedimentological observations

The second research question asked what the spatial arrangement, form, and sedimentological composition of minor moraines in glacier forelands in the European Alps reveals about glacier dynamics. This research has shown that analysing both the geomorphological form, i.e. external characteristics, and sedimentological composition, i.e. internal features, of minor moraines is imperative in understanding mechanisms of moraine formation. The presence of multiple distinct mechanisms of minor moraine formation in the two study areas (Chapter 4 and Chapter 5), as well as several variations of these mechanisms, highlights that this understanding would not have been possible using only remote-sensing methods and geomorphological investigations. It was crucial to metaphorically and physically dig deeper into these landforms.

The surface expression of minor moraines in both forelands, and how they record the geomorphological evolution of the valleys, extends the knowledge of moraine formation and subsequent degradation. The distribution of moraines in the Schwarzensteinkees foreland revealed how the geomorphological history of the valley influenced subsequent moraine formation, specifically regarding where minor readvances of the ice front were able to create moraines. This vein of investigation is also pertinent as extant ice-cored moraines and controlled moraines were observed during fieldwork at Silvrettagletscher. This provided a glimpse into sediment redistribution due to melting ice cores and "end-product" examples of when the ice had fully melted, adding to the discussion of preservation potential of minor moraines. This also inherently helps in understanding the evolution of controlled moraines to hummocky topography following de-icing, which may help inform other studies that encounter areas of hummocky topography in both modern and older settings.

Sedimentological and geomorphological investigation at Schwarzensteinkees, Silvrettagletscher, and Gornergletscher also informs the understanding of preservation potential of minor moraines overall, regardless of formation mechanisms, by providing insight into post-depositional evolution of these subtle landforms. Erosional processes include gravitational processes occurring without other external forces (e.g. rolling, sliding), snowmelt and rainfall contributing the gravitational processes and also mobilizing sediment as runoff down moraine slopes, and disturbance by people and animals. The latter is especially prevalent in the Schwarzensteinkees foreland, which is home to a team of horses and a herd of sheep in the summer that have been observed to create clear paths over ridges and collapse exposed faces of moraines. Fluvial processes may also erode moraines and evacuate sediment from the foreland. The main channel in the Schwarzensteinkees foreland has partially exposed several moraine faces and former

meltwater channels have cut through moraines in both the Schwarzensteinkees and Silvrettagletscher forelands. Additionally in the Schwarzensteinkees foreland, small streams sometimes run along the sides of minor moraines, potentially destabilizing the slope bases and increasing erosion.

Sedimentological investigation in the Schwarzensteinkees and Silvrettagletscher forelands shows that significant information would have been missed if only investigating the landforms geomorphologically. The minor moraines in the Schwarzensteinkees foreland are composed dominantly of outwash and were formed through a push mechanism, with an additional role of sediment freeze-on to the base of the ice front in some instances, showing the relationship between the advancing ice front and proglacial depositional environment. One moraine varied slightly in its composition by containing till, showing the relationships between subglacial and proglacial sediments. Any variation in push moraine formation may not have been noticed without the thorough investigation of multiple moraines. The presence of till in only one moraine of five investigated in detail in this foreland suggests that the greater number of moraines that can be excavated in any given setting, the more complete the understanding of moraine formation can be.

A detailed investigation of the moraine sediments in the Silvrettagletscher foreland was paramount in understanding mechanisms of moraine formation, as four distinct mechanisms, and some subtle variations of these four, were discovered. Three of these moraine types appear geomorphologically similar. Therefore, the differences in formation would not have been recognized without exposing the internal structures. Additionally, clast measurements revealed how different sediment transport pathways may interact in the subglacial, englacial, supraglacial, and proglacial realms. This includes the significant role that englacial channels may play in the evolution of the foreland, here by temporarily creating controlled moraines and hummocky topography. The three prominent englacial debris septa zones of Silvrettagletscher not only deliver sediment to the foreland, but also create landforms external to ice front fluctuations responsible for other mechanisms of moraine formation.

Another example of the importance of understanding the sedimentological composition of minor moraines is seen at a margin of the Laurentide Ice Sheet (LIS) in Iowa, U.S.A. Gwynne (1942) originally described the “swell and swale” topography at the margins of a LIS lobe as having formed through seasonal/annual push moraine formation. Gwynne (1942) only mentions that the moraines are composed of till and interprets a seasonal/annual pushing formation mechanism based on basic geomorphological relationships. Subsequent more detailed sedimentological investigation by Stewart et al. (1988) contradicts this previous research, however, and even suggests that the moraines may not reflect ice front positions, let alone seasonal fluctuations. Stewart et al. (1988)

present that these “corrugation ridges” instead reflect sedimentation into cracks and crevasses at the base of the glacier and deposition following retreat or melt. Whether this interpretation of moraine formation mechanism is correct or incorrect, this example of two contradictory studies, only one of which is supported through considerably detailed sedimentological analyses, shows the importance of extending research of moraine formation beyond just moraine distribution and form by literally digging deeper to assess sedimentological composition, as supported by the research in this thesis.

7.3 Mechanisms of minor moraine formation

The third research question asked how mechanisms of minor moraine formation in the Schwarzensteinkees and Silvrettagletscher study areas relate to the mechanisms of minor moraine formation in previously published work. The global minor moraines database (GLOMMAD16) and its utility were introduced in Chapter 1. The importance of this database lies in its availability to and use by other researchers. This compilation provides a quick summary of previously published research on minor moraines for other researchers, promoting efficient continuation of minor moraine studies. Two different formats of presentation provide a template for researchers to plan projects and update the database, promoting a larger collaborative effort. Both database formats contain the same information but aid investigation in different ways. The Google Earth database allows others to plainly view the global distribution of minor moraine studies and quickly view freely available imagery of the glaciers and their forelands, and in some cases, the minor moraines. The spread sheet database provides a simply organised collection of data in a free platform for viewers to easily extract key information regarding minor moraine studies. Both of these databases are publicly accessible, encouraging others to view the compiled information and to provide updates on previous studies or add new studies. This can be done by following the contact information provided with the files, which will allow me to moderate potential edits. The information in this database can also be paired with the literature review in Chapter 1 and the synthesis in Chapter 7 (this chapter) of this thesis, which provide more specific information than presented in the database itself.

GLOMMAD16 (.kmz)

https://drive.google.com/open?id=0B3ix2n-eHsw9TFV3T2JuSmVTVnM

For more information or to request edits or additions, please contact
Cianna E. Wyshnytzky at: moremoraines@gmail.com

GLOMMAD16 (.xlsx)

https://drive.google.com/open?id=0B3ix2n-eHsw9eG5uR3VzbnNCR3c

For more information or to request edits or additions, please contact
Cianna E. Wyshnytzky at: moremoraines@gmail.com

Making these databases publicly accessible will hopefully encourage others to create robust research projects when assessing minor moraines in the future and promote the significance of research on minor moraines. This may also help inspire new or updated methodological techniques in all study areas through revisiting previous studies, collaborating with other specialist researchers, or investigating other glaciological, topographical, or climatological factors more broadly across all study sites (Chapter 8). Any of this subsequent work will help further our understanding of glacier dynamics, geomorphological evolution, and the influence of climate on glacial landsystems.

The key findings in this thesis regarding specific mechanisms of minor moraine formation echo previous work with similar findings and also extend the understanding of specific formation mechanisms.

7.3.1 Push moraines

Pushing was the most common mechanism of minor moraine formation in the two new study areas of this thesis, interpreted for three or four of five moraines in the Schwarzensteinkees foreland and four of seven moraines in the Silvrettagletscher foreland (Table 7.1). This is also the most prolific formation mechanism interpreted in previous work, reported 22 times (Table 1.3).

Sedimentological evidence supporting push moraine formation agrees with, and also refines and extends, observations in previous studies. The conceptual models presented in this thesis incorporate destabilisation of the moraine slope and sediment pile, resulting in reworking/redistribution during pushing (distal slope) and more passive gravitational processes (both slopes) of sediment when the glacier retreats, reflected in bedding that mimic moraine slope orientations (Bennett, 2001; Lukas, 2005; Benn and Evans, 2010; Lukas, 2012; Reinardy et al., 2013; Chandler et al., 2016a). Where present, bed orientations, folding, and few faults indicate compressional stress from the glacier pushing the sediment pile, shortening the pile and eventually creating a moraine (Worsley, 1974; Birnie, 1977; Sharp, 1984; Ono, 1985; Boulton, 1986; Lukas, 2012; Bradwell et al., 2013; Chandler et al., 2016a).

Table 7.1. Mechanisms of minor moraine formation in this thesis. Grey shading indicates that a specific formation mechanism was not interpreted in the study area.

Formation Mechanism	SSK	SG	Total
Push	3-4	4	**7-8**
Freeze-on		1	**1**
Squeezing			
Combined push-squeeze			
Combined push-freeze on	1-2		**1-2**
Thrusting/shearing			
Englacial melt out			
Dumping			
Basal cracks and crevasses			
Controlled moraines		2	**2**
Total	**5**	**7**	**12**

SSK = Schwarzensteinkees
SG = Silvrettagletscher

Two studies discuss push moraine formation specifically on a reverse bedrock slope, as also described in the Silvrettagletscher foreland. In these particular settings, the previous researchers also specifically address the relative steepness of the ice front and its influence on push moraine formation on the reverse bedrock slopes. A thin ice margin, as well as reverse bedrock slope, may promote slumping of proglacial sediment, being pushed, onto the ice front, which would, in turn, bury the ice front and could create an ice-cored moraine (Lukas, 2012). Conversely, a relatively steep ice margin would not allow for sediment to bury the ice front during pushing (Chandler et al., 2016a). A thin ice front may also promote separation from the glacier due to dry calving (Goldthwait, 1951; Schomacker and Kjær, 2007; Lukas, 2012), and a thin margin and parts breaking off were seen in multiple locations along Silvrettagletscher. Similar relative differences in ice thickness may explain why some push moraines in the Silvrettagletscher foreland contain extant ice cores, why others may have once contained ice cores, and why some to not appear to have contained ice cores. These commonalities between among several studies show that bedrock geometry and ice front thickness may exert strong controls on push moraine formation (Lukas, 2012; Bradwell et al., 2013; Chandler et al., 2016a).

The role of ice cores in moraines, whether attributed specifically to pushing or not, has been previously highlighted in multiple studies and is discussed with regards to moraines in the Silvrettagletscher foreland. A lack of sedimentary structures may suggest re-sedimentation during de-icing (Goldthwait, 1951; Lawson, 1979; Kjær and Krüger, 2001; Everest and Bradwell, 2003; Lukas et al., 2005; Schomacker and Kjær, 2008; Reinardy et al., 2013), and this may result in coarser sediment collecting at the bottom of the moraines during melting (Carrara, 1975), and was observed in the Silvrettagletscher foreland. Where ice cores were observed, sediment overlying the ice cores was seen rolling and slumping

down the moraine slopes. Furthermore, ice-cored ridges in the foreland were seen in varying orientations, potentially reflecting variations in sediment cover thickness and consequent differential ablation through time (Goldthwait, 1951).

Some specific geomorphological and sedimentological observations refine and extend previous work that discusses mechanisms of minor push moraine formation. Both of the new study areas in this thesis contribute information on how prexisting topography and sedimentological dynamics may influence push moraine formation and resultant forms. The geomorphological signature of a lacustrine setting in the Schwarzensteinkees foreland, prior to the minor readvances interrupting an overall period of retreat, appears to have influenced where in the foreland pure push of combined push and freeze-on moraines were able to form. Although the ostensible need for some surface perturbation to generate push moraines has previous been mentioned (Schlüchter et al., 1999), the geomorphological evolution of the Schwarzensteinkees setting shows a concrete example of this concept. The moraine composition, interpreted mechanisms of formation, and differences in sediment cover thickness across the bedrock slope along the Silvrettagletscher ice front may influence if push moraines are able to form and if the moraines comprise ice cores. Intuitively, push moraines cannot form where the ice front encounters bare bedrock. Additionally, the amount of sediment available may also dictate how much may cover the advancing ice front, either promoting or inhibiting incorporation of an ice core through differential ablation dynamics dependent on sediment cover thickness. Although this has previously been described by Lukas (2012), the Silvrettagletscher foreland presents an environment of largely bare bedrock with very thin sediment cover.

Some previous studies of minor push moraines described sedimentological deformation structures that suggest a pushing mechanism of formation. More specifically, Lukas (2012) notes various types of folds and faults and locations within exposures that may indicate the unidirectional compressional stress of pushing, whereas Reinardy et al. (2013) use a lack of faulting as a line of evidence against push moraine formation. Most of the Schwarzensteinkees and Silvrettagletscher push moraines do not contain the tight folding at Gornergletscher (Lukas, 2012), and faults were noticed in few exposures. The lack of noticeable folding and faulting in these settings supports ideas promoted by other researchers addressing the sedimentological composition of minor push moraines, in that coarse and friable sediments may not readily preserve deformation structures (Lukas, 2012; Chandler et al., 2016a).

7.3.2 Freeze-on moraines

A pure freeze-on mechanism of minor moraine formation was interpreted in the Silvrettagletscher foreland for one moraine (Table 7.1). Freeze-on moraine formation is the second most prolific mechanism of moraine formation interpreted in previous research, reported seven times (Table 1.3). Observations of the moraine at Silvrettagletscher allowed for development of a conceptual mechanism of freeze-on moraine formation specific to this moraine, as drawn from previously described means of freeze-on. This mechanism requires a thin ice margin for the freezing front to penetrate through the ice and into the underlying sediment, whether subglacial till or proglacial sediment that the ice overrides during advance (Krüger, 1995; Lukas, 2012; Reinardy et al., 2013; Chandler et al., 2016a). The majority of the Silvrettagletscher margin was thin, as observed during the 2015 ablation season, suggesting that freezing could, in fact, penetrate through to underlying sediment during accumulation/ice advance periods. This would also necessitate thin sediment layers, particularly at Silvrettagletscher to conformably carry both packages. Observations of sediment cover on the bedrock slope shows that this gravel layer remains think in most places, except in isolated areas of shallower slopes or small concave-up pockets.

The shape of the freeze-on moraine at Silvrettagletscher appears to reflect what could have been the wedge shape between the ice front and bedrock, as also described by Reinardy et al. (2013). This wedge shape may be accentuated by the reverse bedrock slope in the Silvrettagletscher foreland, accounting for the steep slopes of the moraine. The reverse bedrock slope here also explains the direction of the contact between the till and underlying gravel, which mimics the underlying bedrock slope.

The freeze-on moraine in the Silvrettagletscher foreland is composed dominantly of till, with underlying proglacial gravel, which has been described in most other studies that interpret freeze-on (Andersen and Sollid, 1971; Krüger, 1995; Matthews et al., 1995; Evans and Hiemstra, 2005; Winkler and Matthews, 2010; Reinardy et al., 2013; Hiemstra et al., 2015; Chandler et al., 2016a). The only other study from the European Alps also describes an isolated freeze-on mechanism, but instead of till describes a moraine comprising proglacial debris-flow and outwash sediment (Lukas, 2012). These similarities show that freeze-on mechanisms may be more prolific than just the wealth Icelandic and Norwegian previous research shows, and that this mechanism of moraine formation can incorporate any sediment underlying the ice front.

7.3.3 Combined push and freeze-on moraines

In the Schwarzensteinkees foreland, a combination push and freeze-on mechanism formed moraines (Table 7.1), although in two distinct manners. Some combination of pushing and freeze-on was interpreted twice in previous research (Table 1.3). Where applicable, the freezing and pushing events occur similarly to the aforementioned pure push and freeze-on mechanisms of moraine formation, incorporating such concepts as sediment redistribution down moraine slopes during and after pushing and a lack of deformation features that may reflect the coarse and friable nature of the constituent sediment.

One conceptual mechanism of moraine formation specific to the Schwarzensteinkees foreland involves freeze-on of till to the ice front and pushing of proglacial sediment as the ice advances, which is similar to processes described in previous work (Andersen and Sollid, 1971; Krüger, 1995; Matthews et al., 1995; Winkler and Matthews, 2010; Reinardy et al., 2013; Hiemstra et al., 2015; Chandler et al., 2016a). In this moraine, this event appears to repeat, with advance to the position of the first combined freeze-push event. In this model of moraine formation, the shape and orientation of the till unit follows what would have been the up-arched ice front (Matthews et al., 1995; Reinardy et al., 2013) when pushing the proglacial sediment, creating the moraine ridge. The sharp contacts between the till units and surrounding sediment supports freezing as distinct slabs, as highlighted in previous work (Krüger, 1995; Matthews et al., 1995; Lukas, 2012; Reinardy et al., 2013; Chandler et al., 2016a).

The other conceptual mechanism of moraine formation specific to the Schwarzensteinkees foreland is presented as a plausible alternative to a purely pushing formation mechanism based on the sedimentological features of one moraine. This model involves freeze-on and stacking of distinct outwash sediment packages, followed by pushing to the position of the stacked sequence. This model of stacking distinct sediment packages in a sequence, by the ice front advancing to the approximate position during several periods has been described similarly in one other previous study (Matthews et al., 1995). Similar to the aforementioned till freezing, the shape of the sediment packages follows the shape of the up-arched ice front as it encountered a small moraine or other obstacle at the beginning of the stacking sequence, followed by the shapes of previously stacked sediment slabs (Matthews et al., 1995), consistent with the direction of ice movement and sediment transport from its originally horizontal position (Hiemstra et al., 2015). The sharp contacts, preserved as original depositional features, have been previously described for other moraines as evidence of freezing (Matthews et al., 1995; Hiemstra et al., 2015), consistent with the observations presented in this study.

The research in the Schwarzensteinkees foreland present some new developments to the overall concept of combined push and freeze on moraine formation. The combination of the stacking through freeze-on, followed by a changed to pushing, suggests that a change in ice front dynamics occurred, whether through increased temperature and/or increased ice front thickness, inhibiting further freeze-on and switching instead to pushing.

Comparing the two conceptual models of combined push and freeze-on minor moraine formation in the Schwarzensteinkees foreland present some new ideas to this category of moraine formation. In the till freeze-on and pushing combination, the moraine appears to record to combined push and freeze-on events. This would be explained by the glacier retreating enough following the first event to provide some accommodation space for sediment deposition between the proto-moraine of this first event and the ice front. This allowed some sediment for the next advance to also include a combined push and freeze-on mechanism, with advance to a position in close enough proximity to the proto-moraine of the first event, building a larger moraine that comprises two moraine-building events. Conversely, the stacked sequences of the other model of a freeze-on and pushing combination suggest shorter retreat distances. This may not have allowed for more sediment deposition at the ice front, resulting in stacked slabs with no additional pushing, or only enough sediment deposition to be incorporated as the next stacked slab.

7.3.4 Other minor moraines

The research in the Silvrettagletscher foreland has also revealed minor moraine formation through the larger mechanism of controlled moraine formation. Controlled moraines have been sparsely described in previous work (Boulton, 1968; Boulton, 1972; Eyles, 1979; Rains and Shaw, 1981; Evans, 2009; Bennett et al., 2010; Szuman and Kasprzak, 2010; Carrivick et al., 2012), and no other studies have specifically attributed minor moraine formation to the evolution of controlled moraines originating from englacial debris septa. While developing a conceptual model of minor moraine formation through the melt-out of controlled moraines, this research also describes a sequence of hummocky topography development by presenting observations and analyses of a modern glacial system, from the nascent stages of englacial debris septa to the creation of controlled moraines to eventual hummocky terrain. This research is in agreement with previous research that describes and/or interprets ice stagnation topography or hummocky terrain (Sharp, 1949; Goldthwait, 1951; Boulton, 1972; Eyles, 1979; Rains and Shaw, 1981; Eyles, 1982; Kjær and Krüger, 2001; Everest and Bradwell, 2003; Schomacker and Kjær, 2008; Bennett et al., 2010; Ewertowski et al., 2011; Carrivick et al., 2012).

The literature review in Chapter 1 and GLOMMAD16 describe several mechanisms of minor moraine formation that were not interpreted for the Schwarzensteinkees and Silvrettagletscher forelands. These mechanisms include till squeezing of at the ice front, thrusting/shearing of sediment from subglacial to proglacial positions, melt-out of englacial material, dumping of supraglacial sediment at the ice front, and deposition from infilled basal cracks and crevasses (Table 1.3).

7.4 Wider Quaternary and glaciological implications regarding minor moraines

Moraines can play an important role in investigating glacier dynamics and modern and paleoenvironmental records (Owen et al., 2009). Emphasis in minor/annual moraine research is frequently placed on the possibility of linking these landforms to specific ice front positions and thus potentially using the moraines as proxy climate and glacial behaviour indicators.

The classification of minor moraines as "annual moraines" provides further refinement to these groups of closely spaced ice margin indicators by implying a seasonal driver of ice margin fluctuations and moraine formation. This designation therefore holds important connotations related to climate drivers of glacier dynamics. As presented in Chapter 1, some authors provide strong evidence to support annual moraine formation in their study areas through example ground-level and aerial photographs (Beedle et al., 2009; Schomacker et al., 2012; Bradwell et al., 2013; Chandler et al., 2016a). Other authors mention good evidence supporting annual moraine formation, through field visits and/or aerial photographs, but do not provide examples (Worsley, 1974; Bradwell, 2004; Winkler and Matthews, 2010; Lukas, 2012), and some authors use the term "annual moraines" without mentioning evidence of annual formation (Andersen and Sollid, 1971; Birnie, 1977; Fushimi, 1977; Sharp, 1984; Boulton, 1986; Gordon and Timmis, 1992; Evans et al., 1999a; Evans et al., 1999b; Evans and Twigg, 2002; Reinardy et al., 2013). Some of these assumptions of annual formation may stem from this designation in previous work.

Even without some form of evidence, several of these authors voice reservations in attributing annual formation to the moraines in their study areas by mentioning that they are frequently, but not necessarily always, annually deposited (Evans and Twigg, 2002) or that the chronological control is not robust enough to conclusively support annual formation (Worsley, 1974; Birnie, 1977). Another modifier explained by several authors is that although the moraines may have formed annually, some moraines may have formed sub-annually (Krüger, 1995; Evans et al., 1999b; Chandler et al., 2016a) and some may have been occupied by the ice front multiple times (Bradwell et al., 2013).

These issues with ostensible, but not always, annual deposition of minor moraines show that a simple agreement of moraine ridges with years elapsed may lead to potentially dangerous assumptions of annual formation, as cautioned in other studies (Price, 1970; Chandler et al., 2016a). As previously discussed, this technique of counting moraines between known chronological markers or ice positions may be inaccurate. Other potential causes for inaccuracy using this method include assumptions connecting smaller moraines as larger moraine chains (e.g. Chapter 5 and Chapter 6), ensuring that moraines mark former ice extent (e.g. not controlled moraines, Chapter 5), and the low preservation potential of subtle proglacial landforms. Several authors have noted that these small-scale landforms are relatively erodible, in comparison to larger-scale landforms that may be present in a glacier foreland (Bennett, 2001; Schomacker et al., 2012; Bradwell et al., 2013; Reinardy et al., 2013; Chandler et al., 2016a; Ewertowski et al., 2016). Partial erosion or total eradication may occur due to either self-censoring or external censoring, or a combination of both. Self-censoring includes ice overriding previously deposited moraines (obliterative overlap) and superposition of multiple moraines as a larger composite moraine (Sharp, 1984; Evans and Twigg, 2002; Chandler et al., 2016a) and the melting of ice-cored moraines, which may or may not leave a moraine ridge or mound dependent on sediment redistribution (Andersen and Sollid, 1971; Sharp, 1984; Lukas, 2012; Reinardy et al., 2013; Chapter 5). External censoring may occur in several different ways, due to gravitational processes, human and animal disturbance, fluvial processes, and aeolian disturbance (Gwynne, 1942; Evans and Twigg, 2002; Schomacker et al., 2012; Bradwell et al., 2013; Chandler et al., 2016a). Two studies were able to assign periods of longevity to minor moraines, and showed only decadal existence of some of these landforms. Minor moraines in the Midtdalsbreen foreland last approximately 40 years (Reinardy et al., 2013) and those in the Fláajökull foreland persist for “decades” (Ewertowski et al., 2016).

7.4.1 Glacier and climate reconstructions using suites of minor moraines

The term “annual moraines” holds important implications in understanding glacial dynamics, and it is therefore crucial to be certain that each moraine in a group of closely spaced minor moraines represents a singular readvance in an accurately and precisely established year. Repeated seasonal moraine formation, creating groups of moraines that represent annual cycles of ice-margin fluctuation, allow for the most detailed insight into controls on glacial dynamics, as they may represent the most dynamic and quickest end-member of response time to climate forcing by potentially recording seasonal signals (Krüger, 1995; Bradwell, 2004; Beedle et al., 2009; Lukas, 2012; Bradwell et al., 2013; Reinardy et al., 2013; Chandler et al., 2016a). Annual moraines can therefore provide a high-

resolution geomorphological and climate archive to examine the controls on, patterns of, and rates of glacier retreat, the potential of which was recognized at the beginning of annual moraine research (Gwynne, 1942). Some studies have shown that these sequences of moraines, where chronological control is robust, can be used to reconstruct glacier length change and retreat rates by using moraine spacing as a proxy for retreat, which can further be connected to temperature and precipitation data (Beedle et al., 2009; Lukas, 2012; Bradwell et al., 2013; Chandler et al., 2016a). A robust chronological framework on continuous moraines or discontinuous moraine segments, and proven annual deposition, is inherently imperative to such work to most accurately analyse the driving mechanisms of moraine formation (Chandler et al., 2016a).

This then suggests that accurately ascribing annual formation to moraines in historical and Pleistocene or older settings, as presented by Ham and Attig (2001) and Gwynne (1942), and potentially extracting palaeoclimate information from these sequences, as proposed possible by Bradwell (2004), can be fraught with assumptions due to difficulties in obtaining high-resolution chronological constraint in the geological record (e.g. Fuchs and Owen, 2008; Balco, 2011; Osborn et al., 2014; Stokes et al., 2015; Wyshnytzky et al., 2015) and the potential for missing moraines and sub-annual moraines (Krüger, 1995; Evans et al., 1999b; Chandler et al., 2016a). Without the ability to obtain extremely accurate chronological control on older sequences of moraines, i.e. in association with varve records (De Geer, 1921; Hughen and Zolitschka, 2007; Zolitschka, 2007) or dendrochronological constraint (Schweingruber, 1988; Smith and Lewis, 2007a; Smith and Lewis, 2007b), it will not be feasible to identify groups of moraines as “annual moraines” and therefore high-resolution palaeoclimate connections and interpretations need to be approached with caution (Chandler et al., 2016a).

Even where chronological control may be able to assign precise and accurate years of formation on individual landforms and suites of minor moraines, few palaeoclimatic interpretations can be drawn from minor moraines. Firstly, the literature review (Chapter 1), GLOMMAD16, and new research presented here show that there is no agreement among researchers who interpreted the influences on minor moraine formation in their respective study areas as to what the dominant controls on the global record of minor moraines are, if any. The only studies that seems to place climatic influences on minor moraine formation into a global context are those by Beedle et al. (2009) and Chandler et al. (2016a), which extend statistical analyses of climatic factors to how the Southern Oscillation Index (SOI) and Pacific Decadal Oscillatin (PDO) and SST and NAO, respectively, may have controlled local climate data. Additionally, while some non-climatic controls may be observable in the palaeoenvironmental record, e.g. topography, geomorphological evolution, and bedrock setting, potential climatic controls on glacier metrics and landform formation are not

interpretable to the precision of individual years and certainly not individual ablation and accumulation seasons. This detail is only possible with the historic and modern network of weather stations and continued collection of data to produce climate records, which have allowed modern studies to compare the geomorphological record and this extant climate data. Even where modern studies are able to compare climate data and the moraine record, researchers rarely speculate as to why specifically clusters of minor moraines seem to form and cease to form (Reinardy et al., 2013; Chandler et al., 2016a, 2016b).

Secondly, some clusters of minor moraines have been interpreted to form unconnected with ice front positions, as with the crevasse and crack fill (Stewart et al., 1988) and controlled moraine degradation (Chapter 5). These examples call for a degree of scepticism when connecting moraine formation specifically to oscillations of the ice front that may be connected to climate. Therefore, some groups of minor moraines are not reliable for paleoclimate interpretations or modern connections to front variation, mass balance, climate forcings, etc. This echoes Section 7.2, showing a need to develop a strong understanding of moraine formation before beginning to think about these features in palaeoenvironmental or palaeoclimate contexts.

Previous work emphasises the possibility of using minor/annual moraines as proxy climate indicators. However, linking specific glacier behaviours to climate forcing is fraught with difficulties, especially when attempting to assess multiple glaciers. The emphasis of minor moraine studies should, perhaps, be placed foremost on the implications of minor moraines and their formation processes, then the corresponding implications for glacier dynamics (e.g. Reinardy et al., 2013, Chandler et al., 2016a). Although previous works speculates on the utility of comparing minor moraine studies in modern environments to similar landforms in paleoclimatic and Pleistocene contexts (Bennett, 2001; Ham and Attig, 2001; Evans et al., 2014), the utility of these comparisons will not be strong unless studies on modern minor moraines find commonalities in the driving forces on minor moraine formation mechanisms, period of formation, and cessation of formation.

7.4.2 Classification of moraines as “annual moraines”

As the previous paragraphs show, the term “annual moraines” holds important implications for our understanding of glacier dynamics. This term should therefore only be used where conclusive evidence that each moraine in a group of moraines represents one year exists. This evidence inherently involves seeing one moraine form each year, either in photographs or visits to the study area. Authors should present example evidence of annual formation (e.g. field photographs or remote-sensing imagery) when attributing annual formation, as presenting this evidence builds a stronger case for annual moraine formation than simply

mentioning said evidence. Independent chronological techniques and ice-front measurements, if available, would further strengthen the use of "annual moraines" in describing these landforms (Chandler et al., 2016a). Ideally, one moraine would form at the ice front each year, and this would be further supported with annual ice-front variation measurements, annual mass balance measurements, and annual climate data. However, these data are not available for all field areas, hindering confident assertion of annual moraine interpretations and creation of a robust research framework to connect annual moraines to glacier and climate dynamics. If annual formation cannot be proven, researchers can most accurately refer to moraines in the study area according to genetic processes of formation, which can provide a cautionary note for readers about ostensible correlations of high-resolution moraine records and climate records.

To summarise in the context of study areas in this thesis, the minor push and combined push and freeze-on moraines in the Schwarzensteinkees foreland and the minor push, freeze-on, and controlled moraines in the Silvrettagletscher foreland cannot be designated as annual moraines due to lack of chronological control on individual moraines (Chapter 4 and Chapter 5, respectively). The post-2007 moraines at Gornergletscher, however, may be annual moraines, but the present research can only conclusively show this for the years 2013 and 2014 (Chapter 6) and not the larger sequence of ridges.

7.4.3 Significance of understanding minor moraine genesis

As mentioned in Section 7.4.2, the genesis of minor moraines may provide particular utility in understanding the interaction between the glacier, sediment, and the foreland, and thus in better understanding how glaciers shape the landscape. Minor moraines provide a down-scaled view of moraine formation, as they frequently record only one event (Reinardy et al., 2013, Chandler et al., 2016a), therefore providing a simpler environment to extrapolate to larger, more complex moraines. The research presented here shows that many factors may influence where, when, and how suites of minor moraines are formed. However, some factors have only been speculated on by previous researchers, and other factors not previously mentioned may also play a role in minor moraine genesis. Lukas (2012) mentions that subglacial topography, which may pertain to reverse bedrock slopes mentioned in several studies (Lukas, 2012; Bradwell et al., 2013; Chandler et al., 2016a; Chapter 5) but also throughout the catchment, and catchment hypsometry and shape may affect minor moraine formation. The role of the shape and steepness of the ice front has also been mentioned in several studies, however any potential influence has not been discussed in detail (Hewitt, 1967; Birnie, 1977; Lukas, 2012; Chandler et al., 2016a). Other glaciological factors, such as retreat style and rates of glacier recession, ice flow velocities,

mass balance, and stability may influence the glaciogeomorphological controls on foreland evolution, but have not been discussed in the minor moraine/annual moraine literature. The preservation potential of minor moraines may also have implications for the understanding of preservation of other landforms, particularly as studies have been able to track moraine formation and complete eradication from the geomorphological record (Ewertowski et al., 2016). Exploring the preservation potential of these small landforms through the lens of sedimentological and geomorphological context may provide information about the longevity of other landforms in glacier forelands. The data presented here are by no means complete, but present a further avenue of research in assessing mechanisms of minor moraine formation globally and the potential controls on specific mechanisms of formation (Chapter 8).

CHAPTER 8. Conclusion

"Glaciers are no longer remote but just a phone call away."
(Carey et al., 2016)

8.1 Summary

This thesis investigated the presence of minor moraines in three valleys of the European Alps. Methods of investigation varied depending on study area and resources and data available. Fieldwork was conducted in the Schwarzensteinkees foreland, Austria, and the Silvrettagletscher foreland, Switzerland, whereas Gornergletscher, Switzerland, was not visited.

8.1.1 Schwarzensteinkees, Austria

Chapter 4 presented the history of the Schwarzensteinkees valley since the late 18th Century. The geomorphological evolution can be described in four periods: 1) Late fluctuations of the LIA (1783-1820); 2) The terminal LIA advance (1820-1850); 3) Glacier retreat and minor push moraines (1850-1940); and 4) Dominant glacier retreat (1940 to present).

The glacial history of the Schwarzensteinkees foreland shows that a proglacial lake may have had a strong influence in shaping the valley seen today. This research confirms the presence of a lake mapped in 1807/08 and 1817 through modern geomorphological relationships and GPR analysis. More importantly, this study shows how this former proglacial lacustrine setting may have influenced the subsequent development of a valley. Three primary environments of the lacustrine system may have influenced the development of the valley in different ways and show the importance of the lake margins, the lakebed, and a prograding delta through the geomorphology of the different zones. The lake margins may have contributed to the unclear and chaotic push moraines in these zones, which may have otherwise been deposited as sharper minor push moraines seen elsewhere in the foreland. The lakebed likely disallowed the deposition of any glacial landforms through its smooth and compacted nature, creating the large flat zone preserved in the valley today. This lakebed, therefore, may have greatly influenced the ability of the glacier to push sediment during advance and exerted a primary control on landform deposition, specifically push moraines, in this zone.

The Schwarzensteinkees foreland contains 189 minor moraine ridge fragments, which vary from 9 m to 108 m long and 1 m to 14 m wide, and most moraines are less than

1.5 m high. Five sections through these minor moraines have been excavated and described. These moraines contain facies indicative of a former glaciofluvial system, and are dominantly composed of gravel, with some sand and diamicton facies. Till is present in one exposure, in both moraine and underlying sediment. Sediments within the moraines show deformation structures produced by ice-marginal deformation and pushing during ice advance, including folds and units oriented in the shape of the ridge crest and dipping in the direction of the proximal moraine slopes, units that follow the shape of the proximal slope, water escape structures, and some maintained original horizontality.

Geomorphological and sedimentological investigations show that the minor moraines in the Schwarzensteinkees foreland were deposited as push moraines or through two different combined push and freeze-on mechanisms during glacier advance. Positive fluctuations of the ice front "efficiently bulldozed" proglacial outwash sediment into distinct moraine ridges and deposited this sediment when the ice retreated. Sediment then cascaded down the proximal slope when the supporting ice retreated. This study echoes mechanisms of minor moraine formation in the only other valley of the Alps in which these landforms are described (Lukas, 2012) but shows a comparative simplicity.

The evolution of the Schwarzensteinkees foreland since the late 18th Century presented here is the first paper to discuss the influence of a proglacial lacustrine setting on minor moraines. The presence of these moraines signifies a rapid response time of Schwarzensteinkees to climatic changes. This work presents unique findings on the influence of a proglacial lake, during its existence and after it had drained, in shaping a high-mountain valley in the Alps through time. In presenting these findings, this research highlights the necessity of understanding the past sequence of geomorphological evolution of an area to unravel the subsequent sequence of development to what exists today.

8.1.2 Silvrettagletscher, Switzerland

Chapter 5 showed that minor moraines in the Silvrettagletscher foreland have been forming since before 1850. The immediately ice-proximal foreland of Silvrettagletscher contains at least 100 minor moraine fragments. Seven sections through these minor moraines have been excavated and described. Detailed sedimentological investigation of these moraines and assessment of the ice front through time revealed four mechanisms of moraine formation:

(1) Melt-out of controlled moraines: englacial debris septa deliver sediment to the ice surface, which may accumulate at the ice front and create controlled moraines. This area is eventually separated from the glacier, creating dead-ice topography that

may still retain moraine crestlines associated with the linearity of englacial debris septa, manifest as ice-cored minor moraines. These crestlines may persist following melting of ice cores.

(2) Freeze-on of foreland and subglacial sediment on a reverse bedrock slope: The ice front thins when advancing up a reverse bedrock slope, allowing the freezing front to penetrate through to underlying sediment covering the bedrock and till. The ice carries this sediment and deposits it on the reverse bedrock slope.

(3) Push of pre-existing sediment on a reverse bedrock slope: The advancing ice front pushes foreland sediment while carrying till and then deposits these sediments as a ridge. This can, but does not have to, incorporate a dead-ice body, creating an ice-cored moraine.

(4) Push of pre-existing glaciolacustrine sediment: The glacier advances through a proglacial pond, pushing glaciolacustrine sediment into a ridge.

This study presented some new mechanisms of moraine formation to the Alps and globally, but also echoed mechanisms of minor moraine formation at other study sites. These findings showed primary controls of bedrock geometry on moraine formation in the study area and sediment delivery to the foreland, supporting observations and interpretations at another glacier in the Alps (Lukas, 2012). Processes of formation highlight that glacial landform deposition may not be primarily driven by climate and that pairing detailed understandings of internal sedimentological composition and external form is crucial to fully understanding foreland evolution.

8.1.3 Gornergletscher, Switzerland

The research presented in Chapter 6 accomplished the goal of checking whether minor moraines have formed in the Gornergletscher foreland since original investigation in 2007 by Lukas (2012). This research also provided some information regarding preservation potential of these subtle features, as the aerial photography shows that some moraines have likely been eroded since original mapping (Lukas, 2012). Specific mechanisms of formation of these minor moraines cannot be elucidated from geomorphological mapping alone, which emphasizes the need to visit the field area to verify results from year to year and to most thoroughly understand these subtle features. This research confirmed that minor moraine formation is actively happening in the Alps on a long timescale (1977 to 2014).

8.2 Review of research objectives and goals

The research presented in this thesis has successfully assessed mechanisms of minor moraine formation in the European Alps and connected these results to other study areas globally. The findings of these investigations are reviewed below in the context of the three original research objectives and goals presented in Chapter 1, by summarising both the findings and implications in the context of each.

(1) Do minor moraines exist in other high-mountain settings of the European Alps?

Yes. A thorough scouting of all currently glaciated valleys in the European Alps revealed two valleys with considerable groups of closely spaced minor moraines, which then provided the basis for this thesis. This thesis described two new settings to add to the original work on minor moraines in the Alps (Lukas, 2012) and showed that, despite dominant glacier retreat in the Alps, some glaciers record ice front fluctuations on short timescales. These examples from the Alps, along with others, show that minor moraines do exist in the high-mountain setting despite speculation that they should not (Bennett and Boulton, 1993; Bennett, 2001). The presence of these moraines in the Alps but lack of previous studies prompts consideration of how many more field areas may be missing from this field of research due to these field sites not yet having been investigated or lack of focus on these specific small-scale landforms in valleys that have been studied, e.g. Findelengletscher (see Chapter 1).

(2) What can the geomorphological presence and sedimentological composition of minor moraines in glacier forelands in the European Alps reveal about glacier dynamics?

The geomorphological relationships among minor moraines and their individual forms has revealed important information in both field areas. At Schwarzensteinkees, the geomorphological legacy of a proglacial lacustrine system may have dictated where subsequent minor moraines were able to form and what shape these moraines took in specific zones of the foreland. At Silvrettagletscher, a reverse bedrock slope affects the length and steepness of ice proximal moraine slopes and may also influence mechanisms of moraine formation. Additionally, de-icing across the foreland creates hummocky topography that is constantly evolving as ice continues to melt. Investigation of the composition of minor moraines revealed a pushing mechanism of moraine

formation and a combined push and freeze-on mechanisms of moraine formation in the Schwarzensteinkees foreland. Most moraines were composed of proglacial outwash, and one moraine additionally incorporated till. Four mechanisms of moraine formation operate in the Silvrettagletscher foreland: melt-out of controlled moraines fed by englacial debris septa, basal freeze-on of till and proglacial sediment, push of proglacial sediment up a reverse bedrock slope (either incorporating or not incorporating parts of the ice front as an ice core), and push through a proglacial pond. The mechanisms of minor moraine formation in the two field areas highlight the crucial need for sedimentological investigation of landforms to understand their formation, as the diversity of formation mechanisms would not have been noticed from the surface expression of the moraines.

(3) How do the mechanisms of minor moraine formation in study areas in the European Alps relate to the mechanisms of minor moraine formation in previously published work? Are there similarities linking minor moraine formation globally in terms of where, when, why, and how minor moraines form?

Most mechanisms of minor moraine formation in the Alps are similar to those described in previous work at multiple study sites. A pushing mechanism of minor moraine formation is the most common mechanism of formation in both the Alps and global suite of minor moraine research. Freeze-on has also been described as a mechanism of push moraine formation in both study areas of this thesis and other previously published work. There is notably no evidence for minor moraines in the Alps having formed through till squeezing or shearing/thrusting mechanisms, as reported in other forelands. The comparison of these formation mechanisms extends the knowledge of minor moraines in high-mountain settings and how similar processes may operate in both lowland and high-mountain forelands.

This research goal included compiling a global minor moraines database (GLOMMAD16), for use in this thesis as well as for future research on minor moraines. A thorough and robust comparison of minor moraine formation among study areas would not have been possible without this database, which revealed the following information, as summarised below in distinct categories of **where** minor moraines form, **when** minor moraines form, **why** minor moraines form, and **how** minor moraines form.

Where: Minor moraines are found in forelands globally, but with concentrations in Iceland, Norway, and the Alps, and on South Georgia. More telling, however, may be where minor moraines have not been reported. With a wide lens, this includes areas along the Pacific, the Arctic, and in Antarctica. Absence of evidence is not evidence of absence however, as this may simply reflect a lack of focus on these landforms.

When: Minor moraines have been prolifically noted in forelands after the Little Ice Age and are still forming today in many study areas. There are additionally Pleistocene examples of minor moraines, namely at the margins of the Laurentide Ice Sheet in the United States and Canada. Although these moraines cannot confidently be related to modern moraines due to lack of first-person observation on moraine formation and scant chronological constraints, the similarity of these features, both geomorphologically and sedimentologically, suggests that they may be related to modern groups of closely spaced minor moraines.

Why: Groups of closely spaced minor moraines suggest that particular ice margins react on very short time scales superimposed on a longer timeline of dominant glacier retreat. Climatological controls on glacier dynamics at these sites varies depending on study area and may be modulated by localised glaciological and topographical factors.

How: Minor moraines may be formed through several different mechanisms (see above). Localised glaciological, topographic, and sedimentological factors may influence distinct mechanisms of minor moraine formation by affecting where, when, why, and how moraines are produced at an ice front. Moraines at Schwarzensteinkees and Silvrettagletscher cannot be described as annual moraines with complete confidence, but these glaciers likely respond to seasonal climate changes and therefore record short-term climate drivers of ice front fluctuations.

In accomplishing these research goals, this thesis has highlighted the importance of minor moraines and continued study of these relatively small landforms in understanding glacial dynamics and landscape evolution.

8.3 Future work

The findings of this research have prompted several avenues for further research in individual study areas and in assessing minor moraine formation globally.

The following points outline future work in the Schwarzensteinkees foreland:

- Only a small portion of the foreland was investigated using GPR. This method was used only in the selected area (FZ1) due to time and funding constraints, equipment availability and malfunctions, and the selection of this area as providing critical evidence of the hypothesized former glaciolacustrine basin. The use of GPR could be extended throughout the other zones of the foreland, to investigate if other subsurface sedimentological relationships help further refine the geomorphological evolution of the valley. Furthermore, the composition of reflectors present in GPR radiograms was unknown. Obtaining several cores along the GPR transect would remedy this and allow for more thorough interpretations of GPR radagrams.
- Terrestrial laser scanning data were collected in two areas of the foreland. Unfortunately, these data have not yet been processed due to issues obtaining necessary software. When processed and analysed, this data will provide the highest resolution imagery of the foreland possible, allowing for very detailed measurements of geomorphological features, including minor moraine geometry. This may therefore help unravel the geomorphological evolution even more than the current study presents.
- Future work could excavate a clean exposure of the LSZ partially cut by the modern channel to assess the sedimentology and stratigraphic architecture of the LSZ. This, however, was not possible during fieldwork due to the presence of large boulders (>2 m a-axis), high water level of the modern channel, and available tools.
- Samples for optically stimulated luminescence (OSL) analysis were collected from moraine exposures in the Schwarzensteinkees foreland to assess if any signal properties can elucidate information about transportational and depositional processes of sediment in the foreland. These samples have been processed in the laboratory but no data have been collected.
- Two Masters of Science students from Queen Mary University of London conducted research in the valley. One project thoroughly mapped lateral moraines and explores mechanisms of lateral moraine formation, which included using clast measurements to elucidate sediment transport paths from source to lateral moraine. The other project assessed the use of lichenometric methods as a landform

chronometer in the upper Zemmgrund. Both projects offer more information to the overall evolution of the Schwarzensteinkees foreland, and will be incorporated into future collaborative publications.

The following points outline future work in the Silvrettagletscher foreland:

- GPR would be especially useful in determining the depth to bedrock, particularly in the two areas where controlled moraines are currently evolving. Calculating the volume of sediment in these areas, relative to the surrounding comparatively bare bedrock, may be used as a proxy for how long the controlled moraines have been present in their current locations, by comparing basin volume and modern rates of sediment delivery from englacial debris septa that create these moraines. Subsurface sedimentological relationships may also reveal more information about de-icing processes in these controlled moraine and hummocky moraine areas and would additionally show the extent of buried ice in the foreland.
- GPR may also be used to investigate the subglacial bedrock geometry, how far upvalley the glacier is advancing up a reverse bedrock slope, and what the relationship of this reverse slope is to the subglacial and foreland bedrock geology. This may reveal further important information about the influences of topography on minor moraine formation and glacier dynamics and help assess any other similarities between this high-mountain system and that at Kvíárjökull, with regards to controlled moraine formation.
- Minor moraines are currently forming in the Silvrettagletscher foreland, which also contains ice-cored moraines. This provides a prime study area to observe the continued formation of minor moraines, the development of the sedimentological composition of moraines, and the degradation of ice-cored and controlled moraines and their roles on the geomorphological evolution of the foreland. This would benefit from visual assessment by annually conducting fieldwork, but also provides an excellent location for annual monitoring through DEM-of-difference production to track foreland evolution through time. The only previous study to monitor the evolution of minor moraines consistently benefited from the efficiency and low cost of using UAVs and SfM for such work in Iceland (Ewertowski et al., 2016). This allowed for quantification of the preservation potential of minor moraines and other subtle proglacial landforms. The importance of repeat surveys through low-cost, yet effective, remote sensing methods was also mentioned by Chandler et al. (2016a), however this again pertained to an Icelandic setting. Extending these methods to a high mountain area would provide two different settings to compare data. The data obtained from these methods would also provide the high resolution imagery

needed to create a more detailed map of the subtle landforms in the Silvrettagletscher foreland, extending beyond just the presence of minor moraines, and could be conducted at optimal periods to reduce the ill effects of shading and snow cover that complicated mapping (Chapter 5). Furthermore, this would more broadly help advance the understanding of modern and former dead-ice topography and the de-icing of forelands (Kjær and Krüger, 2001; Schomacker and Kjær, 2007; Evans, 2009). To date, no study has continuously monitored the degradation of ice-cored minor moraines, however this type of research could benefit the understanding of the processes of minor moraine formation in modern settings, as well as the likelihood of their preservation in the Pleistocene record (e.g. Christiansen, 1956; Evans et al., 1999; Ham and Attig, 2001) where ice cores may have been present.

- The analysis of glacier measurements (front variation and mass balance) and climate factors (temperature and precipitation) did not test lagged responses of the ice to climate factors (e.g. Beedle et al., 2009). This could be fruitful in revealing delayed relationships between glacier response and climatic drivers, and therefore potentially relationships with minor moraine spacing. Further analyses could be conducted assessing larger scale atmospheric circulation patterns and their potential influences on Silvrettagletscher and the moraine record (Beedle et al., 2009; Chandler et al., 2016a).

The following points outline future work in other forelands of the European Alps:

- Revisiting Gornergletscher would be fruitful to assess the mechanisms of moraine formation after 2007, since original fieldwork was conducted by Lukas (2012). Not only would this provide more information about minor/annual moraine formation generally, but it would also check if the detailed dataset published by Lukas (2012) can be used to help predict formation mechanisms of new moraines and may therefore further reinforce the importance of assessing these landforms with considerable detail. Revisiting this foreland may also help quantify the preservation potential and degradation of moraines since 2007, particularly focusing on the single ice-cored moraine described by Lukas (2012) to test whether this mechanism has become more widespread.
- Findelengletscher can be visited to add to the suite of minor moraine studies in the Alps. The presence of minor moraines in this foreland has been noted but not investigated (Schlüchter, 1983; Lukas et al., 2012; personal communication, 2014). Access to the Findelengletscher foreland is relatively easy and would fit well with a visit to Gornergletscher, as they are adjacent.

This research has also identified the following avenues for future research on minor moraines more generally:

- Other forelands that contain minor moraines have been noted during Google Earth scanning, and these sites on South Georgia could be investigated as new study areas. Similarly, minor moraines have also been noted in the forelands of Hoffellsjökull, Skaftafelljökull, and Svínafelljökull, Iceland. These moraines at Skaftafelljökull appear to have been studied by a duo from the Creation Research Society (Klevberg and Oard, 2015), however their publication is not accessible with current means at Queen Mary University of London and a request for more information went unanswered. Furthermore, the veracity of earth science research performed by a creationist group should be examined. Additionally, Beedle et al. (2009) noted the presence of other forelands in Canada with minor moraines, but no research on minor moraines from this region has been subsequently published. An oral presentation by Nussbaumer et al. (2016) presented evidence for potentially annual moraines in the Loma Larga basin, Chile (33°44'49.3"S 70°03'02.9"W). The group is currently continuing more detailed investigation of these moraines to assess if these moraines are, in fact, annually formed. The moraines formed recently (during the past few 100 years), and some formed in the 20th century. Although similar moraines have not been noticed in the area, Nussbaumer (personal communication) recalls seeing similar moraines further north in the tropical Andes.
- Continued monitoring of minor moraine study areas in modern settings, as mentioned for Silvrettagletscher above, will help extend the knowledge of foreland evolution and allow for assessment of whether moraines are still forming. It would be quite exciting to extend observations to a period when minor or annual moraines cease forming, if possible, allowing for even more detailed glimpses into potential controls on formation.
- This thesis compiled previously published information about potential controls on minor moraine formation, however studies on minor moraines were not conducted with similar research questions in mind and methodologies in place. The comparison of minor moraines globally is therefore hindered by available information. Further investigation into minor moraines globally could therefore begin the significant undertaking of filling in empty spaces in the minor moraines database, allowing for even more robust comparisons among study areas. This would help extend the analyses conducted in Chapter 7, and should include obtaining temperature and precipitation data on monthly and annual scales for all study areas from the nearest long-term climate monitoring stations. This may be

complicated by study areas without nearby monitoring stations and the ability to obtain such data from various international governments and other organizations. Furthermore, several other factors that may influence moraine formation have not been assessed, including catchment hypsometry and shape (Lukas, 2012), subglacial topography (Lukas, 2012), shape and steepness of the ice front, ice flow velocities, rates of glacier recession, and glacier mass balance (Chapter 7). Assessing these potential factors may be possible remotely, depending on the availability and resolution of remote-sensing data for individual glacial systems. This substantial undertaking could provide a highly systematic and thorough investigation of all study sites containing groups of closely spaced minor moraines, contributing to the overarching theme of this thesis and extending the results from analysis based solely on previously published research.

8.4 Conclusion

Groups of closely spaced minor moraines provide a modern way to view terminal moraine formation and the interactions between the ice front and its proglacial setting, which is not typically possible during this current period of dominant global glacier retreat (Reinardy et al., 2013). A thorough understanding of how minor moraines form is critical in elucidating complex mechanisms of moraine formation and ice front fluctuations (Lukas, 2012; Reinardy et al., 2013). Furthermore, if correlations to distinct annual and seasonal cycles can be proven, annual moraines may provide a strong geomorphological climate archive.

To best understand how glaciers influence the landscape, we must understand their dynamics first through basic processes and on short timescales (Lawson, 1979; Owen et al., 2009). Minor moraines provide a scaled-down view into the mechanisms of and controls on moraine formation that may help us better understand formation on larger spatial and temporal scales, i.e. for ice caps and ice sheet margins and lobes in modern time and for various glacial systems throughout the Quaternary geomorphological record (Lukas, 2012; Chandler et al., 2016a). In the other direction, understanding minor moraine formation in the lens of climate influences and glacial response may help us to predict how glaciers and glaciated landscapes will react to future climate changes.

The compilation of a global database of minor moraine studies is one example of how collaboration is critical to extending our knowledge of glaciers. This includes integrated, multidisciplinary research efforts to most thoroughly understand glacier dynamics and elucidate connections between glacial processes and climate controls on glacial cycles and activity, and ultimately, to predict the outcome of our rapidly warming planet (Owen et al., 2009). A complete understanding of glacial dynamics will only occur

through a breadth and depth of research in glacial settings by communication between glaciologists, geomorphologists, sedimentologists, geochronologists, geologists, climatologists and atmospheric scientists. This idea, as well as the examples provided in this thesis, show the importance of focusing deeper on a couple of aspects, and keeping the larger research topic open for researchers with other specialised skillsets, forming the foundation of the minor moraines database and future work proposed in this thesis.

To conclude, and as with any worthy scientific endeavour, this project produces more questions and avenues for further research and will hopefully promote others to carry on similar work, ask analogous questions, and appreciate the stories that our natural world can reveal.

REFERENCES

Aizen, V., 2011, High Elevation Glacio-Climatology, *in* Singh, V., Singh, P., and Haritashya, U. eds., Encyclopedia of Snow, Ice and Glaciers: Dordrecht, Springer, p. 507–510.

Amt der Tiroler Landesregierung, 2007, Digitales Geländemodel 1 m.

Annan, A.P., 2009, Electromagnetic Principles of Ground Penetrating Radar, *in* Jol, H.M. ed., Ground Penetrating Radar Theory and Applications, Elsevier B.V., p. 3–40.

Annan, A.P., and Davis, J.L., 1976, Impulse radar soundings in permafrost: Radio Science, v. 11, no. 4, p. 383–394.

Andersen, J.L., and Sollid, J.L., 1971, Glacial Chronology and Glacial Geomorphology in the Marginal Zones of the Glaciers, Midtdalsbreen and Nigardsbreen, South Norway: Norsk Geografisk Tidsskrift, v. 25, no. 1, p. 1–38.

Ashley, G.M., 2002, Glaciolacustrine environments, *in* Menzies, J. ed., Modern and Past Glacial Environments: Oxford and Woburn, Butterworth-Heinemann, p. 335-359.

Auer, I., Böhm, R., Jurkovic, A., Lipa, W., Orlik, A., Potzmann, R., Schöner, W., Ungersböck, M., Matulla, C., Briffa, K., Jones, P., Efthymiadis, D., Brunetti, M., Nanni, T., Maugeri, M., Mercalli, L., Mestre, O., Moisselin, J., Begert, M., Müller-Westermeier, G., Kveton, V., Bochnicek, O., Stastny, P., Lapin, M., Szalai, S., Szentimrey, T., Cegnar, T., Dolinar, M., Gajic-Capka, M., Zaninovic, K., Majstorovic, Z., amd Nieplova, E., 2007, HISTALP - Historical instrumental climatological surface time series of the Greater Alpine Region: International Journal of Climatology, v. 27, p. 17-46.

Bahr, D.B., Pfeffer, W.T., Sassolas, C., and Meier, M.F., 1998, Response time of glaciers as a function of size and mass balance: Journal of Geophysical Research, v. 103, no. B5, p. 9777-9782.

Balco, G., 2011, Contributions and unrealized potential contributions of cosmogenic-nuclide exposure dating to glacier chronology, 1990-2010: Quaternary Science Reviews, v. 30, p. 3–27.

Ballantyne, C.K., 1982, Aggregate clast form characteristics of deposits at the margins of four glaciers in the Jotunheimen Massif, Norway: Norsk Geografisk Tidsskrift, v. 36, p. 103–113.

Barr, I.D., and Lovell, H., 2014, A review of topographic controls on moraine distribution: Geomorphology, v. 226, p. 44-64.

Bauder, A., Funk, M., and Huss, M., 2007, Ice-volume changes of selected glaciers in the Swiss Alps since the end of the 19th century: Annals of Glaciology, v. 46, no. 1, p. 145–149.

Bearth, P., 1953, Geologischer Atlas der Schweiz Blatt 29 (Zermatt) mit Erläuterungen [map], scale 1:25,000.

Beedle, M.J., Menounos, B., Luckman, B.H., and Wheate, R., 2009, Annual push moraines as climate proxy: Geophysical Research Letters, v. 36, no. L20501.

Benn, D.I., 1992, The genesis and significance of "hummocky moraine": Evidence from the Isle of Skye, Scotland: Quaternary Science Reviews, v. 11, no. 7-8, p. 781–799.

Benn, D.I., 2004, Clast Morphology, *in* Evans, D.J.A. and Benn, D.I. eds., A Practical Guide to the Study of Glacial Sediments: London, Arnold, p. 78–92.

Benn, D.I., and Ballantyne, C.K., 1993, The description and representation of clast shape: Earth Surface Processes and Landforms, v. 18, p. 665–672.

Benn, D.I., and Ballantyne, C.K., 1994, Reconstructing the transport history of glacigenic sediments: a new approach based on the co-variance of clast form indices: Sedimentary Geology, v. 91, p. 215–227.

Benn, D.I., and Evans, D.J.A., 2010, Glaciers & Glaciation: London, Hodder Education, 802 p.

Benn, D.I., and Lukas, S., 2006, Younger Dryas glacial landsystems in North West Scotland: an assessment of modern analogues and palaeoclimatic implications: Quaternary Science Reviews, v. 25, p. 2390-2408.

Benn, D.I., Warren, C.R., and Mottram, R.H., 2007, Calving processes and the dynamics of calving glaciers: Earth-Science Reviews, v. 82, p. 143–179.

Bennett, G.L., Evans, D.J.A., Carbonneau, P., and Twigg, D.R., 2010, Evolution of a debris-charged glacier landsystem, Kvíárjökull, Iceland: Journal of Maps, v. 6, no. 1, p. 40-67.

Bennett, M.R., 2001, The morphology, structural evolution and significance of push moraines: Earth-Science Reviews, v. 53, no. 3-4, p. 197–236.

Bennett, M.R., and Boulton, G.S., 1993, A reinterpretation of Scottish 'hummocky moraine' and its significance for the deglaciation of the Scottish Highlands during the Younger Dryas or Loch Lomond Stadial: Geological Magazine, v. 130, no. 3, p. 301-318.

Bennett, M.R., and Glasser, N.F., 2009, Glacial Geology: Ice Sheets and Landforms: Chicester, John Wiley & Sons, Ltd, 385 p.

Birnie, R. V., 1977, A snow-bank push mechanism for the formation of some "annual" moraine ridges: Journal of Glaciology, v. 18, no. 78, p. 77–85.

Blick auf den Schwarzenstein und den Schwarzensteinkees. 1880-1889 [photo], Deutscher Alpenverein; Historischer Alpenarchiv der Alpenvereine in Deutschland, Österreich und Südtirol.

Boston, C.M., 2012, A Lateglacial Plateau Icefield in the Monadhliath Mountains: reconstruction, dynamics and palaeoclimatic implications [Ph. D. thesis]: Queen Mary University of London, 291 p.

Boston, C.M., Lukas, S., and Carr, S.J., 2015, A Younger Dryas plateau icefield in the Monadhliath, Scotland, and implications for regional palaeoclimate: Quaternary Science Reviews, v. 108, p. 139-162.

Boulton, G.S., 1968, Flow tills and related deposits on some Vestspitsbergen glaciers: Journal of Glaciology, v. 7, no. 51, p. 391-412.

Boulton, G.S., 1972, Modern Arctic glaciers as depositional models for former ice sheets: Journal of the Geological Society of London, v. 128, p. 361-393.

Boulton, G.S., 1986, Push-moraines and glacier-contact fans in marine and terrestrial environments: Sedimentology, v. 33, p. 677–698.

Bradwell, T., 2004, Annual Moraines and Summer Temperatures at Lambatungnajökull, Iceland: Arctic, Antarctic, and Alpine Research, v. 36, no. 4, p. 502–508.

Bradwell, T., Sigurđsson, O., and Everest, J., 2013, Recent, very rapid retreat of a temperate glacier in SE Iceland: Boreas, v. 42, p. 959–973.

Brodzikowski, K., and van Loon, A.J., 1991, Developments in Sedimentology 49, Glacigenic Sediments: New York, Elsevier Science Publishers B.V., 674 p.

Bruneck (5248) 1 [map], 1925: Kartographisches, früher Militärgeographisches Institute; Bundesamt für Eich- und Vermessungswesen (Landesaufnahme), scale: 1:75,000.

Campbell, J.B., 2002, Introduction to remote sensing: London, Taylor and Francis, 621 p.

Carey, M., Jackson, M., Antonello, A., and Rushing, J., 2016, Glaciers, gender, and science : A feminist glaciology framework for global environmental change research: Progress in Human Geography, p. 1–24.

Carrara, P.E., 1975, The Ice-Cored moraines of Akudnirmuit Glacier, Cumberland Peninsula, Baffin Island, N. W. T., Canada: Arctic and Alpine Research, v. 7, no. 1, p. 61–67.

Carrivick, J.L., Davies, B.J., Glasser, N.F., Nývlt, D., and Hambrey, M.J., 2012, Late-Holocene changes in character and behavior of land-terminating glaciers on James Ross Island, Antarctica: Journal of Glaciology, v. 58, no. 212, p. 1176-1190.

Cassidy, N.J., 2009, Ground Penetrating Radar Data Processing, Modelling and Analysis, *in* Jol, H.M. ed., Ground Penetrating Radar Theory and Applications, Elsevier B.V., p. 141-176.

Chandler, B.M.P., Evans, D.J.A., and Roberts, D.H., 2016a, Characteristics of recessional moraines at a temperate glacier in SE Iceland: Insights into patterns, rates and drivers of glacier retreat: Quaternary Science Reviews, v. 135, p. 171–205.

Chandler, B.M.P., Evans D.J.A., and Roberts, D.H., 2016b, Recent retreat at a temperate Icelandic glacier in the context of the last ~80 years of climate change in the north Atlantic region: Arktos, 2: 24.

Chandler, B.M.P., Evans, D.J.A., Roberts, D.H., Ewertowski, M., and Clayton, A.I., 2015, Glacial geomorphology of the Skálafellsjökull foreland, Iceland: A case study of “annual” moraines: Journal of Maps, v. 5647, p. 1–13.

Christiansen, E.A., 1956, Glacial Geology of the Moose Mountain Area, Saskatchewan: Saskatchewan Department of Mineral Resources Report, v. 21, 35 p.

Church, M., and Gilbert, R., 1975, Proglacial Fluvial and Lacustrine Environments, *in* Jopling, A.V., and McDonald, B.C. eds., Glaciofluvial and Glaciolacustrine Sedimentation: Tulsa, Society of Economic Paleontologists and Mineralogists, Special Publication 23, p. 22-100.

Davis, J.L., and Annan, A.P., 1989, Ground-Penetrating Radar for High-Resolution Mapping of Soil and Rock Stratigraphy: Geophysical Prospecting, v. 37, p. 531-551.

De Geer, G., 1921, Correlation of late glacial clay-varves in North America with the Swedish time scale: Geologiska Föreningens i Stockholm Förhandlingar, v. 43, no. 1-2, p. 70-73.

Digital Globe, 2016, (none).

Drewry, D.J., 1972, A quantitative assessment of dirt-cone dynamics: Journal of Glaciology, vol. 11, no. 63, p. 431-446.

Drong, H.J., 1953, Schwarzensteinkees [photo], *in* Gletschermessungen aus Umgebung Berlinerhütte (Zillertal): Innsbruck, Österreichischen Alpenverein.

Ebert, A., 2001, Strukturgeologie und Petrographie im Gebiet von Zermatt and der Dent-Blanche-Decke in der Combin-Zone, in der Zone von Zermatt-Saas Fee und in der Monte Rosa-Decka [M. Sc. Thesis]: Universität Stuttgart, 156 p.

Eisen, O., Bauder, A., Lüthi, M., Riesen, P., and Funk, M., 2009, Deducing the thermal structure in the tongue of Gornergletscher, Switzerland, from radar surveys and borehole measurements: Annals of Glaciology, v. 50, no. 51, p. 63–70.

Ender, T., 1841a, Der Keesboden am Schwarzen Stein mit dem Horn und dem Rossrücken am Ursprung der Ziller im Ziller-Thale [painting]: Österreichischer Privatbesitz, Repro: Kurt Nicolussi.

Ender, T., 1841b, Ursprung der Ziller am Schwarzenstein-Gletscher [painting]: Österreichisches Alpenverein-Museum.

Esri, HERE, DeLorme, TomTom, Intermap, increment P Corp., GEBCO, USGS, FAO, NPS, NRCAN, GeoBase, IGN, Kadaster NL, Ordnance Survey, Esri Japan, METI, Esri China (Hong Kong), swisstopo, MapmyIndia, 2015, World Topographic Map.

Europa Technologies, Google, and SPOT IMAGE, 2013, (none).

European Soil Data Centre (ESDAC), 2005, Alpine region boundary [shapefile].

Evans D.J.A., 2005, Ice-Marginal Terrestrial Landsystems: Active Temperate Glacier Margins, *in* Evans, D.J.A., ed., Glacial Landsystems: London, Arnold, p. 12-43.

Evans, D.J.A., 2009, Controlled moraines: origins, characteristics and palaeoglaciological implications: Quaternary Science Reviews, v. 28, no. 3-4, p. 183–208.

Evans, D.J.A., 2010, Controlled moraine development and debris transport pathways in polythermal plateau icefields: Examples from Tungnafellsjökull, Iceland: Earth Surface Processes and Landforms, v. 35, p. 1430-1444.

Evans, D.J.A., 2011, Glacial landsystems of Satujökull, Iceland: A modern analogue for glacial landsystem overprinting by mountain icecaps: Geomorphology, v. 129, p. 225-237.

Evans, D.J.A., Archer, S., and Wilson, D.J.H., 1999a, A comparison of the lichenometric and Schmidt hammer dating techniques based on data from the proglacial areas of some Icelandic glaciers: Quaternary Science Reviews, v. 18, p. 13–41.

Evans, D.J.A., and Benn, D.I., 2004, A Practical Guide to the Study of Glacial Sediments: London, Hodder Education, 266 p.

Evans, D.J.A., and Hiemstra, J.F., 2005, Till deposition by glacier submarginal, incremental thickening: Earth Surface Processes and Landforms, v. 30, no. 13, p. 1633–1662.

Evans, D.J.A., Lemmen, D.S., and Rea, B.R., 1999b, Glacial landsystems of the southwest Laurentide ice sheet: Modern Icelandic analogues: Journal of Quaternary Science, v. 14, p. 673–691.

Evans, D.J.A., Phillips, E.R., Hiemstra, J.F., and Auton, C.A., 2006, Subglacial till: Formation, sedimentary characteristics and classification: Earth-Science Reviews, v. 78, p. 115-176.

Evans, D.J.A., and Twigg, D.R., 2002, The active temperate glacial landsystem: a model based on Breiðamerkurjökull and Fjallsjökull, Iceland: Quaternary Science Reviews, v. 21, p. 2143–2177.

Evans, D.J.A., Young, N.J.P., and O'Cofaigh, C., 2014, Glacial geomorphology of terrestrial-terminating fast flow lobes/ice stream margins in the southwest Laurentide Ice Sheet: Geomorphology, v. 204, p. 86-113.

Everest, J., and Bradwell, T., 2003, Buried glacier ice in southern Iceland and its wider significance: Geomorphology, v. 52, no. 3-4, p. 347–358.

Ewertowski, M., Evans, D., Roberts, D., Tomczyk, A., and Ewertowski, W., 2016, Preservation potential of subtle glacial landforms based on detailed mapping of recently exposed proglacial areas : application of unmanned aerial vehicle (UAV) and structure-from-motion (SfM): Geophysical Research Abstracts EGU2016-1034, EGU General Assembly, Vienna.

Ewertowski, M., Kasprzak, L., Szuman, I., and Tomczyk, A., 2011, Controlled ice-cored moraines: sediment and geomorphology. An example from Ragnarbreen, Svalbard: Zeitschrift für Geomorphologie, v. 56, no. 1, p. 53-74.

Eyles, N., 1979, Facies of supraglacial sedimentation on Icelandic and Alpine temperate glaciers: Canadian Journal of Earth Sciences, v. 16, p. 1341-1361.

Eyles, N., 1982, Modern Icelandic glaciers as depositional models for 'hummocky moraine' in the Scottish Highlands, *in* Evenson, E., Schlüchter, C., and Babassa, J., eds., Tills and Related Deposits; Genesis/Petrology/Applciations/Stratigraphy; Proceedings of the INQUA Symposia on the Genesis and Lithology of Quaternary Deposits/USA 1981/Argentina 1982: Rotterdam, A. A. Balkema, p. 47-59.

Eyles, N., and Rogerson, R.J., 1978, A framework for the investigation of medial moraine formation: Austerdalsbreen, Norway, and Berendon Glacier, British Columbia, Canada: Journal of Glaciology, v. 20, no. 82, p. 99–113.

Farinotti, D., Huss, M., Bauder, A., and Funk, M., 2009, An estimate of the glacier ice volume in the Swiss Alps: Global and Planetary Change, v. 68, no. 3, p. 225–231.

Felkel, E., and Rotter, W., 1946a, SCHWARZENSTEINKEES Die beiden Eisbruchsfelder GM46: 16 [photo], *in* Zillertaler Alpen 1946: Innsbruck, Österreichischen Alpenverein.

Felkel, E., and Rotter, W., 1946b, SCHWARZENSTEINKEES Eisbruch im Torgebiet Gm 46: 17 [photo], *in* Zillertaler Alpen 1946: Innsbruck, Österreichischen Alpenverein.

Felkel, E., and Rotter, W., 1946c, SCHWARZENSTEINKEES Vorfeld Gm 46: 14 [photo] *in* Zillertaler Alpen 1946: Innsbruck, Österreichischen Alpenverein,.

Felkel, E., and Rotter, W., 1946d, SCHWARZENSTEINKEES Vorfeld Gm 46: 15 [photo] *in* Zillertaler Alpen 1946: Innsbruck, Österreichischen Alpenverein.

Felkel, E., and Rotter, W., 1946e, Schwarzensteinkees (Zungenränder der Jahre: 1935, 1936, 1937, 1939, 1939) [sketch], *in* Zillertaler Alpen 1946: Innsbruck, Österreichischen Alpenverein.

Finlayson, A., Golledge, N., Bradwell, R., and Fabel, D., 2011, Evolution of a Lateglacial mountain icecap in northern Scotland: Boreas, v. 40, p. 536-554.

Flink, A.E., Noormets, R., Kirchner, N., Benn, D.I., Luckman, A., and Lovell, H., 2015, The evolution of a submarine landform record following recent and multiple surges of Tunabreen glacier, Svalbard: Quaternary Science Reviews, v. 108, p. 37–50.

Fliri, F., 1974, Niederschlag und Lufttemperatur im Alpenraum [data]: Innsbruck, Wagner.

Fox, P., 2013, Deep: The Story of Skiing and the Future of Snow: Jackson Hole, Rink House Productions, 288 p.

Frei, C., and Schär, C., 1998, A precipitation climatology of the Alps from high-resolution rain-gauge observations: International Journal of Climatology, v. 18, p. 873–900.

Fromm, H., and Wuczinicz, I., 1872, Gradkartenblatt Zone 17 Colonne V Section S.O. [map]: Bundesamt für Eich- und Vermessungswesen, scale 1:25,000.

Fuchs, M., and Owen, LA., 2008, Luminescence dating of glacial and associated sediments: review, recommendations and future directions: Boreas, v. 37, no. 4, p. 636–659.

Fushimi, H., 1977, Glaciations in the Khumbu Himal (1): Journal of the Japanese Society of Snow and Ice, v. 39, p. 60–67.

Generalkarte von Mitteleuropa [map], 1894: Bundesamt für Eich- und Vermessungswesen (Landesaufnahme), scale: 1:20,000. Generalkarte von Mitteleuropa [map], 1925: Kartographisches, früher Militärgeographisches Institute; Bundesamt für Eich- und Vermessungswesen (Landesaufnahme), scale 1:200,000.

Generalkarte von Mitteleuropa [map], 1937: Kartographisches, früher Militärgeographisches Institute; Bundesamt für Eich- und Vermessungswesen (Landesaufnahme), scale 1:200,000.

Geoimage Austria, and Google Earth, 2014, (none).

Geoimage Austria, and Google Earth, 2000, (none).

Geologische Bundesanstalt, 2005, 149-Lanersbach [map], 2005: Zusammenstellung ausgewählter Archiveunterlagen der Geologischen Bundesanstalt, scale 1:50,000.

Gibbons, A.B., Megeath, J.D., and Pierce, K.L., 1984, Probability of moraine survival in a succession of glacial advances: Geology, v. 12, p. 327-330.

Gibson, P.J., 2000, Introductory Remote Sensing: Principles and concepts: London, Routledge, 185 p.

Glasser, N.F, and Hambrey, M.J., 2005, Ice-Marginal Terrestrial Landsystems: Svalbard Polythermal Glaciers, *in* Evans, D.J.A. ed., Glacial Landsystems: London, Arnold, p. 65-88.

Goldthwait, R.P., 1951, Development of End Moraines in East-Central Baffin Island: The Journal of Glaciology, v. 95, no. 6, p. 567–577.

Goodsell, B., Hambrey. M.J., and Glasser, N.F., 2005, Debris transport in a temperate valley glacier: Haut Glacier d'Arolla, Valais, Switzerland: Journal of Glaciology, v. 51, no. 172, p. 139-146.

Google Earth, 2009, (none).

Google Earth, and Geoimage Austria, 2007, (none).

Gordon, J.E., and Timmis, R.J., 1992, Glacier fluctuations on South Georgia during the 1970s and early 1980s: Antarctic Science, v. 4, no. 2, p. 215–226.

Graham, D.J., and Midgley, N.G., 2000, Graphical representation of particle shape using triangular diagrams: an Excel spreadsheet method: Earth Surface Processes and Landforms, v. 25, p. 1473–1477.

Gravenor, C.P., and Kupsch, W.O., 1959, Ice-Disintegration Features in Western Canada: The Journal of Geology, v. 67, no. 1, p. 48–64.

Gwynne, C.S., 1942, Swell and Swale Pattern of the Mankato Lobe of the Wisconsin Drift Plain in Iowa: The Journal of Geology, v. 50, no. 2, p. 200–208.

Haeberli, W., and Penz, U., 1985, An attempt to reconstruct glaciological and climatological characteristics of 18 ka BP Ice Age glaciers in and around the Swiss Alps: Zeitschrift für Gletscherkunde und Glazialgeologie, v. 21, p. 351–361.

Ham, N.R., and Attig, J.W., 2001, Minor end moraines of the Wisconsin Valley Lobe, north-central Wisconsin, USA: Boreas, v. 30, no. 1, p. 31–41.

Heinrich, K., 1913, Matrei, Tirol 1 [map]: Militärgeographisches Institut; Bundesamt für Eich- und Vermessunswesen, scale 1:75,000.

Heiri, O., Koinig, K.A., Spötl, C., Barrett, S., Brauer, A., Drescher-Schneider, R., Gaar, D., Ivy-Ochs, S., Kerschner, H., Luetscher, M., Moran, A., Nicolussi, K., Preusser, F., Schmidt, R., Schoeneich, P., Schwörer, C., Sprafke, T., Terhorst, B., and Tinner, W., 2014, Palaeoclimate records 60-8 ka in the Austrian and Swiss Alps and their forelands: Quaternary Science Reviews, v. 106, p. 186–205.

Hewitt, K., 1967, Ice-Front Deposition and the Seasonal Effect: A Himalayan Example: Transactions of the Institute of British Geographers, v. 42, p. 93–106.

Hiemstra, J.F., Matthews, J.A., Evans, D.J., and Owen, G., 2015, Sediment fingerprinting and the mode of formation of singular and composite annual moraine ridges at two glacier margins, Jotunheimen, southern Norway: The Holocene, v. 25, p. 1–14.

Hippach und Wildgerlos-Spitze (5148) [map], 1925: Kartographisches, früher Militärgeographisches Institute; Bundesamt für Eich- und Vermessungswesen (Landesaufnahme), scale 1:75,000.

Hoelzle, M., Haeberli, W., Dischle, M., and Peschke, W., 2003, Secular glacier mass balances derived from cumulative glacier length changes: Global and Planetary Change, v. 36, no. 4, p. 295-306.

Hormes, A., Müller, B.U., and Schlüchter, C., 2001, The Alps with little ice: evidence for eight Holocene phases of reduced glacier extent in the Central Swiss Alps: The Holocene, v. 11, no. 3, p. 255–265.

Hubbard, B., and Glasser, N.F., 2005, Field Techniques in Glaciology and Glacial Geomorphology: West Sussex, John Wiley & Sons, Ltd, 400 p.

Hughen, K.A., and Zolitschka, B., 2007, Varved marine sediments, in Elias, S.A., ed., Encyclopedia of Quaternary Science, Elsevier, Amsterdam and Boston, p. 3114-3123.

Hugo, Victor, 1980, Les Misérables [Kindle edition]: Public Domain Books.

Huss, M., 2005, Gornergletscher: Gletscherseeaussbrüche und Massenbilanzabschätzungen [M. Sc. Thesis]: ETH Zürich, 204 p.

Huss, M., 2013, Density assumptions for converting geodetic glacier volume change to mass change: The Cryosphere, v. 7, no. 3, p. 877–887.

Huss, M., and Bauder, A., 2009, 20th-Century Climate Change Inferred From Four Long-Term Point Observations of Seasonal Mass Balance: Annals of Glaciology, v. 50, no. 50, p. 207–214.

Huss, M., Dhulst, L., and Bauder, A., 2015, New long-term mass-balance series for the Swiss Alps: Journal of Glaciology, v. 61, no. 227, p. 551-562.

Huss, M., Jouvet, G., Farinotti, D., and Bauder, A., 2010, Future high-mountain hydrology: a new parameterization of glacier retreat: Hydrology and Earth System Sciences, v. 13, no. 5, p. 815-829.

Huss, M., Sold, L., Hoelzle, M., Stokvis, M., Salzmann, N., Farinotti, D., and Zemp, M., 2013, Towards remote monitoring of sub-seasonal glacier mass balance: Annals of Glaciology, v. 54, no. 63, p. 75–83.

Icelandic Meteorological Office, 2012, Annual climatological data for Hólar í Hornafirði (1949-2011).

Ivy-Ochs, S., Kerschner, H., Maisch, M., Christl, M., Kubik, P.W., and Schlüchter, C., 2009, Latest Pleistocene and Holocene glacier variations in the European Alps: Quaternary Science Reviews, v. 28, no. 21-22, p. 2137–2149.

Ivy-Ochs, S., Kerschner, H., Reuther, A., Preusser, F., Heine, K., Maisch, M., Kubik, P.W., and Schlüchter, C., 2008, Chronology of the last glacial cycle in the European Alps: Journal of Quaternary Science, v. 23, no. 6-7, p. 559–573.

Jochimsen, M., 1973, Does the Size of Lichen Thalli Really Constitute a Valid Measure for Dating Glacial Deposits?: Arctic and Alpine Research, v. 5, no. 4, p. 417-424.

Joerin, U.E., Stocker, T.F., and Schlüchter, C., 2006, Multicentury glacier flucutations in the Swiss Alps during the Holocene: The Holocene, v. 16, p. 697-704.

Johannes, B., 1874, Schwarzensteingletscher, 1874-1883 (3) [photo]: Deutscher Alpenverein; Historischer Alpenarchiv der Alpenvereine in Deutschland, Österreich und Südtirol.

Johnson, W., and Menzies, J., 2002, Supraglacial and ice-marginal deposits and landforms, *in* Menzies, J. ed., Modern and Past Glacial Environments: Oxford and Woburn, Butterworth-Heinemann, p. 317-333.

Jónsson, S.A., Schomacker, A., Benediktsson, Í.Ö., Ingólfsson, Ó., and Johnson, M.D., 2014, The drumlin field and the geomorphology of the Múlajökull surge-type glacier, central Iceland: Geomorphology, v. 207, p. 213–220.

Karl, F., 1951, Schwarzensteink., 1951 [photo], *in* Gletschermessungen aus Umgebung Berlinerhütte (Zillertal) (5.8,-6.8.1951): Innsbruck, Österreichischen Alpenverein.

Karte der Zillertaler-Alpen Mittleres Blatt [map], 1932: Deutschen und Österreichischen Alpenvereins; Bundesamt für Eich- und Vermessungswesen (Landesaufnahme), scale 1:25,000.

Kerschner, H., Hertl, A., Gross, G., Ivy-Ochs, S., and Kubik, P.W., 2006, Surface exposure dating of moraines in the Kromer valley (Silvretta Mountains, Austria)-evidence for glacial response to the 8.2 ka event in the Eastern Alps?: The Holocene, v. 16, no. 1, p. 7–15.

Kerschner, H., and Ivy-Ochs, S., 2008, Palaeoclimate from glaciers: Examples from the Eastern Alps during the Alpine Lateglacial and early Holocene: Global and Planetary Change, v. 60, no. 1-2, p. 58–71.

Kinzl, H., 1951, Schwarzensteinkees [photo]: Innsbruck, Österreichischen Alpenverein.

Kirkbride, M.P., and Brazier, V., 1998, A Critical Evaluation of the Use of Glacier Chronologies in Climatic Reconstruction, with Reference to New Zealand: Quaternary Proceedings, v. 6, p. 55-64.

Kirkbride, M.P., and Winkler, S., 2012, Correlation of Late Quaternary moraines: impact of climate variability, glacier response, and chronological resolution: Quaternary Science Reviews, v. 46, p. 1–29.

Kinzl, H., 1929, Beiträge zur Geschichte der Gletscherschwankungen in den Ostalpen: Zeitschrift für Gletscherkunde, v. 17, p. 66–121.

Kjær, K.H., and Krüger, J., 2001, The final phase of dead-ice moraine development: processes and sediment architecture, Kötlujökull, Iceland: Sedimentology, v. 48, p. 935–952.

Klevberg, P., and Oard, M., 2015, The Little Ice Age in the North Atlantic Region: Creation Research Society Quarterly, v. 52, no. 2, p. 106-135.

Knighton, D., 1998, Fluvial forms and process: a new perspective: London, Arnold, 400 p.

Knoll, C., Kerschner, H., Heller, A., and Rastner, P., 2009, A GIS-based Reconstruction of Little Ice Age Glacier Maximum Extents for South Tyrol, Italy: Transactions in GIS, v. 13, no. 5-6, p. 449–463.

Kreidl, A., 1941, Granatengewinnung am Rossrücken: Unpublished chronicle, Zell am Ziller.

Kren, M., 2013, Blutgletscher [film]: Allegro Films, Filmfonds Wien, Filmstandor Austria (FISA), ORF Film/Fernseh-Abkommen, Österreichisches Filminstitut.

Krüger, J., 1994, Glacial processes, sediments, landforms, and stratigraphy in the terminus region of Myrdalsjökull, Iceland: Folia Geographica Danica, v. 21, p. 1-233.

Krüger, J., 1995, Origin, chronology and climatological significance of annual-moraine ridges at Myrdalsjökull, Iceland: The Holocene, v. 5, no. 4, p. 420–427.

Krüger, J., and Kjær, K.H., 2000, De-icing progression of ice-cored moraines in a humid, subpolar climate, Kötlujökull, Iceland: The Holocene, v. 10, no. 6, p. 737-747.

Kucera, R.E., 1972, Probing the Athabasca Glacier: Vancouver, Evergreen Press, 32 p.

Kucera, R.E., 1981, Exploring the Columbia Icefield: Canmore, High Country Press, 64 p.

Kumar, V., 2011, Bed strength, *in* Singh, V., Singh, P., and Haritashya, U.K. eds., Encyclopedia of Snow, Ice and Glaciers, Springer, Dordrecht, p. 94.

Lakeman, T., and England, J., 2012, Paleoglaciological insights from the age and morphology of the Jesse moraine belt, western Canadian Arctic: Quaternary Science Reviews, v. 47, p. 82-100.

Lässer, A., 1969, SCHWARZENSTEINKEES Sept 1969 [photo], *in* Gletschermessungen in den Zillertaler Alpen: Österreichischen Alpenverein, Innsbruck.

Lawson, D.E., 1979, Sedimentological analysis of the western terminus region of the Matanuska Glacier, Alaska: U.S. Army Cold Regions Research and Engineering Laboratory, CRREL Report 79-9, 112 p.

Lichtenecker, N., 1925, Schwarzensteinkees, Zillertal, 1925 [photo], *in* Beobachtungen an den Gletschern des Zemm- und Schlegeisgrundens in den Zillteraler Alpen 1924-1927, Zeitschrift für Gletscherkunde, v. 16, no. 1, Österreichischen Alpenverein, Innsbruck.

Lillesand, T.M., Kiefer, R.W., and Chipman, J.W., 2008, Remote Sensing and Image Interpretation, Sixth Edition: Hoboken, John Wiley & Sons, Ltd, 756 p.

Luckman, B.H., 1988, Dating the Moraines and Recession of Athabasca and Dome Glaciers, Alberta, Canada: Arctic and Alpine Research, v. 20, no. 1, p. 40-54.

Luckman, B.H., 2017, Glacier Landscapes in the Canadian Rockies, *in* Slaymaker, O. ed., Landscapes and Landforms of Western Canada: Cham, Springer International Publishing, p. 241-255.

Lukas, S., 2005, A test of the englacial thrusting hypothesis of 'hummocky' moraine formation: case studies from the northwest Highlands, Scotland: Boreas, v. 34, p. 287-307.

Lukas, S., 2007, Early-Holocene glacier fluctuations in Krundalen, south central Norway: palaeoglacier dynamics and palaeoclimate: The Holocene, v. 17, no. 5, p. 585–598.

Lukas, S., 2011, Ice-cored moraines, *in* Singh, V., Singh, P., and Haritashya, U.K. eds., Encyclopedia of Snow, Ice and Glaciers: Dordrecht, Springer, p. 616–619.

Lukas, S., 2012, Processes of annual moraine formation at a temperate alpine valley glacier: insights into glacier dynamics and climatic controls: Boreas, v. 41, no. 3, p. 463–480.

Lukas, S., and Benn, D. I., 2006, Retreat dynamics of Younger Dryas glaciers in the far NW Scottish Highlands reconstructed from moraine sequences: Scottish Geographical Journal, v. 122, no. 4, p. 308-325.

Lukas, S., Benn, D.I., Boston, C.M., Brook, M., Coray, S., Evans, D.J.A., Graf, A., Kellerer-Pirklbauer, A., Kirkbride, M.P., Krabbendam, M., Lovell, H., Machiedo, M., Mills, S.C., Nye, K., Reinardy, B.I., Ross, F.H., and Signer, M., 2013, Clast shape analysis and clast transport paths in glacial environments: A critical review of methods and the role of lithology: Earth-Science Reviews, v. 121, p. 96–116.

Lukas, S., Graf, A., Coray, S., and Schlüchter, C., 2012, Genesis, stability and preservation potential of large lateral moraines of Alpine valley glaciers – towards a unifying theory based on Findelengletscher, Switzerland: Quaternary Science Reviews, v. 38, p. 27–48.

Lukas, S., Nicholson, L.I., Ross, F., H., and Humlum, O., 2005, Formation, Meltout Proceses and Landscape Alteration of High-Arctic Ice-Cored Moraines—Examples From Nordenskiold Land, Central Spitsbergen: Polar Geography, v. 29, no. 3, p. 157-187.

Lukas, S., Preusser, F., Anselmetti, F.S., and Tinner, W., 2012, Testing the potential of luminescence dating of high-alpine lake sediments: Quaternary Geochronology, v. 8, p. 23–32.

Lukas, S., and Sass, O., 2011, The formation of Alpine lateral moraines inferred from sedimentology and radar reflection patterns: a case study from Gornergletscher, Switzerland: Geological Society of London, Special Publications, v. 354, no. 1, p. 77–92.

Lysså, A., and Lønne, I., 2001, Moraine development at a small High-Arctic valley glacier: Rieperbreen, Svalbard: Journal of Quaternary Science, v. 16, no. 6, p. 519-529.

Mahaney, W.C., Hancock, R.G.V., and Melville, H., 2011, Late glacial retreat and Neoglacial advance sequences in the Zillertal Alps, Austria: Geomorphology, v. 130, no. 3-4, p. 312–326.

Maizels, J., 2002, Sediments and landforms of modern proglacial terrestrial environments, *in* Menzies, J. ed., Modern and Past Glacial Environments: Oxford and Woburn, Butterworth-Heinemann, p. 279-316.

Martensteig, 1817, Zweiten oder Franziszeischen-Landesaufnahme von Tirol, Sektion 44 [map]: Österreichisches Staatsarchiv.

Matrei (5147) [map], 1925: Kartographisches, früher Militärgeographisches Institute; Bundesamt für Eich- und Vermessungswesen (Landesaufnahme), scale 1:75,000.

Matrei, Tirol [map], 1935: Kartographisches, früher Militärgeographisches Institute; Bundesamt für Eich- und Vermessungswesen (Landesaufnahme), scale 1:75,000.

Matthews, J.A., McCarroll, D., and Shakesby, R.A., 1995, Contemporary terminal-moraine ridge formation at a temperate glacier: Styggedalsbreen , Jotunheimen, southern Norway: Boreas, v. 24, p. 129–139.

Meltsch, C., 1889, Gradkartenblatt Zone 17 Colonne VI Section S.W. [map], scale 1:25,000.

Menzies, J., 2002, Glacial environments – modern and past, *in* Menzies, J. ed., Modern and Past Glacial Environments: Oxford and Woburn, Butterworth-Heinemann, p. 1-13.

MeteoSwiss: Federal Office of Meteorology and Climatology, 2015a, Davos climate data.

MeteoSwiss: Federal Office of Meteorology and Climatology, 2015b, Weissfluhjoch climate data.

MeteoSwiss: Federal Office of Meteorology and Climatology, 2015c, Zermatt climate data.

Moran, A.P., Ivy-Ochs, S., Schuch, M., Christl, M., and Kerschner, H., 2016, Evidence of central Alpine glacier advances during the Younger Dryas-early Holocene transition period: Boreas, v. 45, no. 3, p. 398-410.

Moser, M., and Pavlik, W., 2005, Zusammenstellung ausgewählter Archiveunterlagen der Geologischen Bundesanstalt, 150-Mayrhofen [map], scale 1:50,000.

Mühlberger, J., 1905, Generalkarte von Mitteleuropa [map]: Militär-geographisches Institute; Budesamt für Eich- und Vermessungswesen (Landesaufnahme), scale 1:200,000.

Neal, A., 2004, Ground-penetrating radar and its use in sedimentology: principles, problems and progress: Earth-Science Reviews, v. 66, no. 3-4, p. 261–330.

Nicolussi, K., and Schlüchter, C., 2012, The 8.2 ka event-Calendar-dated glacier response in the Alps: Geology, v. 40, no. 9, p. 819–822.

Nussbaumer, S.U., García, J.L., Gómez, G., Vega, R.M., Gärtner-Roer, I., and Salzmann, N., 2016, Reconstruction of cryospheric changes in the Maipo and Juncal river basins, central Andes of Chile: an integrative geomorphological approach: Geophysical Research Abstracts EGU2016-10824, EGU General Assembly, Vienna.

O'Cofaigh, C., Evans, D.J.A., and England, J., 2005, Ice-Marginal Terrestrial Landsystems: Sub-Polar Glacier Margins of the Canadian and Greenland High Arctic, *in* Evans, D.J.A., ed., Glacial Landsystems: London, Arnold, p. 44-64.

Oerlemans, J., 2005, Extracting a Climate Signal from 169 Glacier Records: Science, New Series, v. 308, no. 5722, p. 675-677.

Ono, Y., 1985, Recent Fluctuations of the Yala (Dakpatsen) Glacier, Langtang Himal, Reconstructed From Annual Moraine Ridges: Zeitschrift für Gletscherkunde und Glazialgeologie, v. 21, p. 251–258.

Osborn, G., McCarthy, D., LaBrie, A., and Burke, R., 2014, Lichenometric dating: Science or pseudo-science?: Quaternary Research, v. 83, no. 1, p. 1–12.

Österreichische Karte [map], 1964: Bundesamt für Eich- und Vermessungswesen (Landesaufnahme), scale 1:50,000.

Östrem, G., 1959, Ice Melting under a Thin Layer of Moraine, and the Existence of Ice Cores in Moraine Ridges: Geografiska Annaler, v. 41, no. 4, p. 228-230.

Østrem, G., 1964, Ice-Cored Moraines in Scandinavia: Geografiska Annaler, v. 46, no. 3, p. 282-337.

Owen, L.A., Thackray, G.D., Anderson, R.S., Briner, J., Kaufman, D., Roe, G., Pfeffer, W., and Yi, C., 2009, Integrated research on mountain glaciers: Current status, priorities and future prospects: Geomorphology, v. 103, p. 158–171.

Pernici, J., 1888a, Gradkartenblatt Zone 17 Colonne V Section S.O. [map], scale 1:25,000.

Pernici, J., 1888b, Gradkartenblatt Zone 18 Colonne V Section N.O. [map], scale 1:25,000.

Pfiffner, O.A., 2014, Geology of the Alps - Revised and translated second edition: West Sussex, John Wiley & Sons, Ltd, 368 p.

Pindur, P., and Heuberger, H., 2008, Zur holozänen Gletschergeschichte im Zemmgrund in den Zillertaler Alpen , Tirol / Österreich (Ostalpen): Zeitschrift für Gletscherkunde und Glazialgeologie, v. 42, no. 2, p. 21–89.

Price, R.J., 1970, Moraines at Fjallsjökull, Iceland: Arctic and Alpine Research, v. 2, no. 1, p. 27–42.

Rains, R.B., and Shaw, J., Some mechanisms of controlled moraine development, Antarctica: Journal of Glaciology, v. 27, no. 95, p. 113-128.

Rea, B.R., and Evans, D.J.A., 2011, An assessment of surge-induced crevassing and the formation of crevasse squeeze ridges: Journal of Geophysical Research, v. 116.

Reinardy, B.T.I., Leighton, I., and Marx, P.J., 2013, Glacier thermal regime linked to processes of annual moraine formation at Midtdalsbreen, southern Norway: Boreas, v. 42, no. 4, p. 896–911.

Riesen, P., Sugiyama, S., and Funk, M., 2010, The influence of the presence and drainage of an ice-marginal lake on the flow of Gornergletscher, Switzerland: Journal of Glaciology, v. 56, no. 196, p. 278–286.

Roux, O., 1888, Gradkartenblatt Zone 18 Colonne VI Section N.W. [map], scale 1:25,000.

Rust, B.R., 1975, Fabric and Structure in Glaciofluvial Gravels, *in* Jopling A.V., and McDonald, B.C. eds., Glaciofluvial and Glaciolacustrine Sedimentation: Tulsa, Society of Economic Paleontologists and Mineralogists, Special Publication 23, p. 238-248.

Sander, 1936, Schwarzensteinkees [photo]: Österreichischen Alpenverein.

Sandmeier, K.-J., 2010, Non-destructive test of concrete with electromagnetic and acoustic-elastic waves: data analysis, *in* Maierhofer, C., Reinhardt, H.-W., and Dobmann, G. eds., Non-destructive evaluation of reinforced concrete structures – Volume 2: Non-destructive testing methods: Cambridge, Woodhead Publishing, p. 125-143.

Schatz, H., 1942, 1942 [photo], *in* Zillertaler Alpen: Zeitschrift für Gletscherkunde (letzter Bericht): Innsbruck, Österreichischen Alpenverein.

Schimmelpfennig, I., Schaefer, J.M., Akçar, N., Koffman, T., Ivy-Ochs, S., Schwartz, R., Finkel, R.C., Zimmerman, S., and Schlüchter, C., 2014, A chronology of Holocene and Little Ice Age glacier culminations of the Steingletscher, Central Alps, Switzerland, based on high-sensitivity beryllium-10 moraine dating: Earth and Planetary Science Letters, v. 393, p. 220–230.

Schindelwig, I., Akçar, N., Kubik, P.W., and Schlüchter, C., 2012, Lateglacial and early Holocene dynamics of adjacent valley glaciers in the Western Swiss Alps: Journal of Quaternary Science, v. 27, no. 1, p. 114–124.

Schlüchter, C., 1983, The readvance of the Findelengletscher and its sedimentological imolications, *in* Evenson, E.B., Schlüchter, C., and Rabassa, J., eds., Tills and Related Deposits; Genesis/Petrology/Applciations/Stratigraphy; Proceedings of the INQUA Symposia on the Genesis and Lithology of Quaternary Deposits/USA 1981/Argentina 1982: Rotterdam, A. A. Balkema, p. 95-104.

Schlüchter, C., Gander, P., Lowell, T.V., and Denton, G.H., 1999, Glacially Folded Outwash Near Lago Llanquihe, Southern Lake District, Chile: Geografiska Annaler, v. 81 A, no. 2, p. 347–358.

Schomacker, A., Benediktsson, Í.Ö., Ingólfsson, Ó., Friis, B., Korsgaard, N.J., Kjær, K.H., and Keiding, J.K., 2012, Late Holocene and modern glacier changes in the marginal zone of Sólheimajökull, South Iceland: Jökull, v. 62, p. 111–130.

Schomacker, A., and Kjær, K.H., 2007, Origin and de-icing of multiple generations of ice-cored moraines at Brúarjökull, Iceland: Boreas, v. 36, p. 411–425.

Schomacker, A., and Kjær, K.H., 2008, Quantification of dead-ice melting in ice-cored moraines at the high-Arctic glacier Holmströmbreen, Svalbard: Boreas, v. 37, p. 211-225.

Schweingruber, F.H., 1988, Tree Rings: Basics and Applications of Dendrochronology: Dordrecht, Kluwer Academic Publishers, 276 p.

Sevestre, H., and Benn, D.I., 2015, Climatic and geometric controls on the global distribution of surge-type glaciers : implications for a unifying model of surging: Journal of Glaciology, v. 61, no. 228, p. 646–662.

Sharp, M., 1984, Annual moraine ridges at Skálafellsjökull, south-east Iceland: Journal of Glaciology, v. 30, no. 104, p. 82–93.

Sharp, R.P., 1949, Studies of superglacial debris on valley glaciers: American Journal of Science, p. 289-315.

Shroder, J. F., 2011, Landforms of glacial deposition, *in* Singh, V., Singh, P., and Haritashya, U.K. eds., Encyclopedia of Snow, Ice and Glaciers, Springer, Dordrecht, p. 690-692.

Shulmeister, J., Davies, T.R., Evans, D.J.A., Hyatt, O.M., and Tovar, D.S., 2009, Catastrophic landslides, glacier behaviour and moraine formation – A view from an active plate margin: Quaternary Science Reviews, v. 28, no. 11-12, p. 1085–1096.

Silvrettahütte, 2016, Gletscherlehrpfad: http://www.silvrettahuette.ch/de/aktivitaeten/gletscherlehrpfad (accessed May 2016).

SIO, NOAA, U.S. Navy, NGA, and GEBCO, 2015, Landsat Image *in* Google Earth.

Sletten, K., Lysså, A., Lønne, I., 2001, Formation and disintegration of a high-arctic ice-cored moraine complex, Scott Turnerbreen, Svalbard: Boreas, v. 30, p. 272-284.

Slupetzky, H., and Slupetzky, N., 1995, Betref des Wachsthums der Kletscher und Kälterwerdung des Klimas: Die Kreisamts-Präsidialakte, v. 84-89.

Smith, D., and Lewis, D., 2007a, Dendrochronology, *in* Elias, S.A., ed., Encyclopedia of Quaternary Science: Amsterdam and Boston, Elsevier, p. 459-465.

Smith, D., and Lewis, D., 2007b, Dendroglaciology, *in* Elias, S.A., ed., Encyclopedia of Quaternary Science: Amsterdam and Boston, Elsevier, p. 988-994.

Sneed, E.D., and Folk, R.L., 1958, Pebbles in the lower Colorado River, Texas, a study in particle morphogenesis: Journal of Geology, v. 66, p. 114–150.

Spedding, N., and Evans, D.J.A., 2002, Sediments and landforms at Kviárjökull, southeast Iceland: a reappraisal of the glaciated valley landsystem: Sedimentary Geology, v. 149, p. 21–42.

Steiger, R., and Mayer, M., 2008, Snowmaking and Climate Change: Future Options for Snow Production in Tyrolean Ski Resorts: Mountain Research and Development, v. 28, no. 3/4, p. 292-298.

Sterzing und Franzensfeste (5247) [map], 1925: Kartographisches, früher Militärgeographisches Institute; Bundesamt für Eich- und Vermessungswesen (Landesaufnahme), scale 1:75,000.

Stewart, E.J., Wilson, J., Espiner, S., Purdie, H., Lemieux, C., and Dawson, J., 2016, Implications of climate change for glacier tourism: Tourism Geographies, v. 18, no. 4, p. 377-398.

Stewart, R.A., Bryant, D., and Sweat, M.J., 1988, Nature and origin of corrugated ground moraine of the Des Moines Lobe, Story County, Iowa: Geomorphology, v. 1, no. 2, p. 111–130.

Stokes, C.R., Tarasov, L., Blomdin, R., Cronin, T.M., Fisher, T.G., Gyllencreutz, R., Hättestrand, C., Heyman, J., Hindmarsh, R.C.A., Hughes, A.L.C., Jakobsson, M., Kirchner, N., Livingstone, S.J., Margold, M., Murton, J.B., Noormets, R., Peltier, W.R., Peteet, D.M., Piper, D.J.W., Preusser, F., Renssen, H., Roberts, D.H., Roche, D.M., Saint-Ange, F., Stroeven, A.P., and Teller, J.T., 2015, On the reconstruction of palaeo-ice sheets: Recent advances and future challenges: Quaternary Science Reviews, v. 125, p. 15–49.

Sugiyama, S., Bauder, A., Huss, M., Riesen, P., and Funk, M., 2008, Triggering and drainage mechanisms of the 2004 glacier-dammed lake outburst in Gornergletscher, Switzerland: Journal of Geophysical Research: Earth Surface, v. 113, no. 4, p. 1–11.

Sugiyama, S., Bauder, A., Weiss, P., and Funk, M., 2007, Reversal of ice motion during the outburst of a glacier-dammed lake on Gornergletscher, Switzerland: Journal of Glaciology, v. 53, no. 181, p. 172–180.

Swisstopo, 2005, Geological Map of Switzerland, scale 1:500,000.

Szuman, I., and Kasprzak, L., 2010, Glacier ice structures influence on moraines development (Hørbye glacier, Central Spitsbergen): Quaestiones Geographicae, v. 29, no. 1, p. 65-73.

Timár, G., Molnár, G., Székely, B., Biszak, S., Varga, J., and Jankó, A., 2006, Zweiten oder Franziszeischen-Landesaufnahme von Salzburg, 1807-1808 [map]: Arcanum.

Triltsch, K., 1914, Generalkarte von Mitteleuropa [map]: Militärgeographisches Institut; Bundesamt für Eich- und Vermessunswesen, scale 1:200,000.

Van der Wateren, F.M., 1995, Structural Geology and Sedimentology of Push Moraines: Processes of soft sediment deformation in a glacial environment and the distribution of glaciotectonic styles: Mededelingen Rijks Geologische Dienst, no. 54, 170 p.

Van der Wateren, F.M., 2002, Processes of glaciotectonism, *in* Menzies, J. ed., Modern and Past Glacial Environments: Oxford and Woburn Butterworth-Heinemann, p. 417-443.

Van der Wateren, F.M., 2005, Ice-Marginal Terrestrial Landsystems: Southern Scandinavian Ice Sheet Margin, *in* Evans, D.J.A. ed., Glacial Landsystems: London, Arnold, p. 166-203.

Vonnegut, K., 1969, Slaughterhouse-Five, or The Children's Crusade: A Duty-Dance with Death: New York, Delacorte Press, 177 p.

Walter, F., Deichmann, N., and Funk, M., 2008, Basal icequakes during changing subglacial water pressures beneath Gornergletscher, Switzerland: Journal of Glaciology, v. 54, no. 186, p. 511-521.

Walter, F., Dreger, D.S., Clinton, J.F., Deichmann, N., and Funk, M., 2010, Evidence of Near-Horizontal Tensile Faulting at the Base of Gornerngletscher, a Swiss Alpine Glacier: Bulletin of the Seismological Society of America, v. 100, no. 2, p. 458–472.

Wanick, W., and Wuczinicz, I., 1872, Gradkartenblatt Zone 18 Colonne V Section N.O. [map]: Bundesamt für Eich- und Vermessungswesen, scale 1:25,000.

Welch, D.M., 1967, Slope evolution on recessional moraines [M. Sc. Thesis]: University of Alberta, 100 p.

WGMS, 2015, Global Glacier Change Bulletin No. 1 (2012-2013), *in* Zemp, M., Gärtner-Roer, I., Nussbaumer, S.U., Machguth, H., Mölg, N., Paul, F., and Hoelzle, M. eds., ICSU(WDS)/IUGG(IACS)/UNEP/UNESCO/WMO, World Glacier Monitoring Service, Zurich, Switzerland, p. 230.

Winkler, S., and Matthews, J.A., 2010, Observations on terminal moraine-ridge formation during recent advances of southern Norwegian glaciers: Geomorphology, v. 116, no. 1-2, p. 87–106.

Winkler, S., and Nesje, A., 1999, Moraine formation at an advancing temperate glacier: Brigsdalsbreen, western Norway: Geografiska Annaler, v. 81 A, no. 1, p. 17–30.

Wintges, T., 1985, Studies on crescentic fractures and crescentic gouges with the help of close-range photogrammetry: Journal of Glaciology, v. 31, no. 109, p. 340–349.

Worsley, P., 1974, Recent “annual” moraine ridges at Austre Okstindbreen, Okstindan, North Norway: Journal of Glaciology, v. 13, no. 68, p. 265–277.

Wuczinicz, I., 1872a, Gradkartenblatt Zone 17 Colonne VI Section S.W. [map]: Bundesamt für Eich- und Vermessungswesen, scale 1:25,000.

Wuczinicz, I., 1872b, Gradkartenblatt Zone 18 Colonne VI Section N.W. [map]: Bundesamt für Eich- und Vermessungswesen , scale 1:25,000.

Wyshnytzky, C.E., Rittenour, T.M., Summa Nelson, M., and Thackray, G.D., 2015, Luminescence dating of late Pleistocene proximal glacial sediments in the Southern Alps, New Zealand and Olympic Mountains, Washington: Quaternary International, v. 362, p. 116–123.

ZAMG Klimadaten von Österreich 1971-2000: Zentralanstalt für Meteorologie und Geodynamik.

Zemp, M., Frey, H., Gärtner-Roer, I., Nussbaumer, S.U., Hoelzle, M., Paul, F., and Haeberli, W., 2012, WGMS (2012): Fluctuations of Glaciers 2005-2010: ICSU (WDS)/ IUGG (IACS)/ UNEP/ UNESCO/ WMO, World Glacier Monitoring Service, Zurich, Switzerland.

Zemp, M., Nussbaumer, S.U., Naegeli, K., Gärtner-Roer, I., Paul, F., Hoelzle, M., and Haeberli, W., 2013, WGMS (2013): Glacier Mass Balance Bulletin: ICSU(WDS)/IUGG(IACS)/UNEP/UNESCO/WMO, World Glacier Monitoring Service, Zurich, Switzerland, v. 12, p. 106.

Zemp, M., Paul, F., Hoelzle, M., and Haeberlie, W., 2006, Glacier Fluctuations in the European Alps, 1850-2000: An overview and spatio-temporal analysis of available data, *in* The Darkening Peaks: Glacial Retreat in Scientific and Social Context: Berkeley, University of California Press, p. 152–167.

Zemp, M., Roer, I., Kääb, A., Hoelzle, M., Paul, F., and Haeberli, W., 2008, Global Glacier Changes: Facts and Figures: World Glacier Monitoring Service, Zürich.

Zolitschka, B., 2007, Varved lake sediments, *in* Elias, S.A., ed., Encyclopedia of Quaternary Science: Amsterdam and Boston, Elsevier, p. 3105-3114.

APPENDICES

"… not a soul was moving there, not a soul speaking, not a breath;
the silence was glacial and profound, and had it not been for that light, he might have thought himself next door to a sepulchre."
from Les Misérables by Victor Hugo (1980)

APPENDIX A. Database of minor moraine scanning in the European Alps

The Google Earth database (.kmz) of minor moraine scanning in the European Alps can be found at: https://drive.google.com/open?id=0B3ix2n-eHsw9LUh5OVFuNGJSaEk

APPENDIX B. Clast measurements for all field areas and samples

"Hören sie auf eine Banane zu fressen während sie weinen!"

– Ministerin Bodicek

from Blutgltescher (2013)

SCHWARZENSTEINKEES

Exposure A - C1

Latitude: N47°01'44.9"
Longitude: E011°49'26.0"
Elevation: 2116 ± 2 m

	VA	A	SA	SR	R	WR
True No.	0	10	23	17	0	0
%	0	20	46	34	0	0

	Clast axes				Clast axes		
Clast no.	**a-axis**	**b-axis**	**c-axis**	**Clast no.**	**a-axis**	**b-axis**	**c-axis**
1	4.2	3.0	1.5	**26**	3.0	1.2	1.2
2	4.3	2.0	2.0	**27**	3.2	2.5	1.8
3	5.0	3.3	2.9	**28**	4.5	2.2	1.8
4	3.0	2.1	1.2	**29**	3.5	2.7	0.9
5	3.3	2.0	1.7	**30**	2.9	1.7	0.8
6	5.0	3.4	2.2	**31**	4.0	3.2	2.7
7	9.8	6.0	4.0	**32**	3.3	2.6	1.8
8	4.5	4.5	2.9	**33**	3.0	1.5	1.0
9	4.5	2.1	2.0	**34**	3.5	1.5	1.0
10	5.1	3.5	2.3	**35**	3.5	2.8	1.2
11	3.4	2.2	1.0	**36**	3.0	2.0	1.0
12	3.3	2.2	1.5	**37**	3.0	1.8	1.0
13	3.2	2.8	2.0	**38**	2.2	1.9	1.0
14	2.5	2.1	1.6	**39**	3.5	3.3	2.0
15	4.9	2.5	2.2	**40**	2.5	1.5	1.2
16	5.0	3.3	2.2	**41**	3.1	2.7	1.2
17	3.5	2.0	1.5	**42**	2.5	2.0	1.2
18	4.5	2.2	2.1	**43**	2.2	1.9	0.9
19	4.0	3.8	2.5	**44**	2.9	2.0	1.5
20	2.5	1.9	1.0	**45**	2.8	1.4	1.2
21	3.3	2.0	1.1	**46**	2.5	1.6	1.0
22	5.0	3.8	2.2	**47**	2.5	1.4	1.2
23	2.7	1.4	1.2	**48**	2.7	1.8	1.2
24	3.0	2.5	2.0	**49**	2.5	1.6	0.8
25	3.8	3.0	1.2	**50**	2.1	1.1	1.0

Exposure A - C2

Latitude: N47°01'44.9"
Longitude: E011°49'26.0"
Elevation: 2116 ± 2 m

	VA	A	SA	SR	R	WR
True No.	0	3	30	17	0	0
%	0	6	60	34	0	0

	Clast axes				Clast axes		
Clast no.	**a-axis**	**b-axis**	**c-axis**	**Clast no.**	**a-axis**	**b-axis**	**c-axis**
1	3.3	3.0	1.8	**26**	3.5	2.9	2.0
2	7.5	6.5	5.5	**27**	4.9	4.0	3.4
3	7.5	6.0	5.6	**28**	3.0	2.3	2.0
4	3.5	2.6	1.7	**29**	2.8	2.0	2.0
5	4.8	3.8	3.0	**30**	5.1	4.0	3.4
6	5.5	4.5	3.7	**31**	4.0	3.4	2.2
7	3.5	2.5	2.2	**32**	4.0	3.5	3.5
8	8.5	6.8	5.9	**33**	4.0	2.5	2.0
9	4.5	3.9	2.8	**34**	4.0	3.7	3.0
10	4.0	3.1	2.3	**35**	3.5	2.8	1.6
11	4.6	3.6	2.7	**36**	3.0	2.4	1.9
12	7.0	4.0	4.0	**37**	6.6	4.9	4.5
13	6.9	5.1	4.5	**38**	4.6	3.9	3.9
14	3.5	2.8	2.0	**39**	5.0	4.4	3.5
15	3.6	2.5	2.5	**40**	3.5	3.0	2.5
16	2.7	2.0	1.5	**41**	3.9	2.7	2.1
17	2.8	2.4	2.0	**42**	3.5	2.8	1.8
18	8.5	4.9	4.8	**43**	3.1	2.5	1.5
19	5.2	3.9	2.5	**44**	7.5	7.0	4.5
20	6.5	4.0	3.0	**45**	4.9	3.5	2.7
21	5.0	3.7	2.7	**46**	4.3	2.4	2.1
22	2.4	1.4	0.8	**47**	4.2	3.1	3.0
23	4.0	3.5	3.0	**48**	3.5	2.9	2.0
24	9.0	7.5	6.0	**49**	3.5	3.2	1.8
25	6.0	5.0	4.2	**50**	3.8	3.1	2.0

Exposure B - C1

Latitude: N47°01'36.9"
Longitude: E011°49'53.1"
Elevation: 2121 ± 2 m

	VA	A	SA	SR	R	WR
True No.	0	9	26	14	1	0
%	0	18	52	28	2	0

	Clast axes				Clast axes		
Clast no.	**a-axis**	**b-axis**	**c-axis**	**Clast no.**	**a-axis**	**b-axis**	**c-axis**
1	9.5	6.3	6.3	**26**	3.5	2.7	2.7
2	4.0	2.3	2.3	**27**	4.4	3.5	3.5
3	5.5	3.0	3.0	**28**	3.7	3.0	2.0
4	3.0	3.0	3.0	**29**	4.5	3.4	1.8
5	4.2	3.2	3.2	**30**	6.5	6.0	3.6
6	4.5	4.0	4.0	**31**	4.2	3.5	2.3
7	4.5	2.3	2.3	**32**	3.3	3.0	1.3
8	3.7	3.3	3.3	**33**	3.0	2.2	1.0
9	7.0	5.0	5.0	**34**	3.5	2.6	2.0
10	3.5	2.9	2.9	**35**	4.5	3.9	2.0
11	2.5	1.7	1.7	**36**	5.1	3.0	1.7
12	2.5	2.0	2.0	**37**	8.5	6.5	6.5
13	4.5	3.3	3.3	**38**	12.5	7.8	7.8
14	2.0	1.8	1.8	**39**	8.0	7.7	4.4
15	10.5	5.6	5.6	**40**	12.5	12.0	9.3
16	3.7	3.0	3.0	**41**	10.5	8.5	6.1
17	4.0	3.5	3.5	**42**	7.0	5.0	3.4
18	3.1	2.9	2.9	**43**	3.5	3.0	1.5
19	4.0	2.7	2.7	**44**	16.0	12.0	9.5
20	3.5	3.2	3.2	**45**	3.5	2.2	1.5
21	3.5	2.3	2.3	**46**	12.2	12.0	7.5
22	2.0	1.5	1.5	**47**	4.5	2.4	1.5
23	1.5	1.3	1.3	**48**	5.0	3.7	3.3
24	2.9	1.6	1.6	**49**	3.5	3.0	1.5
25	2.5	1.5	1.5	**50**	7.0	5.0	3.0

Exposure B - C2

Latitude: N47°01'36.9"
Longitude: E011°49'53.1"
Elevation: 2121 ± 2 m

	VA	A	SA	SR	R	WR
True No.	0	15	27	10	0	0
%	0	28.846154	51.923077	19.230769	0	0

	Clast axes				Clast axes		
Clast no.	**a-axis**	**b-axis**	**c-axis**	**Clast no.**	**a-axis**	**b-axis**	**c-axis**
1	6.2	5.5	3.6	**26**	7.5	6.5	3.7
2	5.9	5.4	3.0	**27**	5.0	3.3	2.5
3	4.5	3.5	1.0	**28**	10.5	7.4	4.8
4	7.2	4.9	3.6	**29**	10.8	8.0	5.5
5	5.5	4.5	3.0	**30**	12.0	9.6	8.5
6	5.5	5.0	3.5	**31**	18.0	13.5	10.0
7	7.5	7.0	4.0	**32**	4.5	2.9	2.9
8	4.0	2.5	2.0	**33**	4.0	2.5	2.0
9	4.0	3.5	2.0	**34**	3.5	2.1	1.1
10	6.0	4.5	4.0	**35**	3.0	2.4	1.5
11	7.0	5.2	4.3	**36**	4.0	3.4	2.2
12	7.0	5.0	3.5	**37**	19.0	14.5	11.5
13	9.0	8.0	5.5	**38**	19.0	16.0	11.5
14	3.0	3.0	2.0	**39**	6.5	4.8	4.0
15	4.0	2.5	2.0	**40**	5.0	3.5	2.0
16	3.6	3.0	1.6	**41**	3.7	3.0	1.8
17	3.2	1.9	1.9	**42**	6.0	5.0	1.4
18	6.0	5.0	4.0	**43**	3.5	1.9	1.0
19	12.0	10.0	7.2	**44**	2.6	2.0	1.3
20	10.5	7.5	4.5	**45**	5.0	3.9	1.5
21	6.5	4.5	4.3	**46**	4.0	2.9	1.9
22	5.5	4.5	2.5	**47**	5.0	3.6	2.5
23	4.0	3.5	2.3	**48**	3.3	2.5	1.7
24	5.0	4.5	2.7	**49**	3.0	1.9	1.4
25	8.5	6.5	4.0	**50**	3.0	2.4	2.0

Exposure C - C1

Latitude: N47°01'36.5"
Longitude: E011°49'53.2"
2134 ±
Elevation: 4 m

	VA	A	SA	SR	R	WR
True No.	0	7	37	5	1	0
%	0	14	74	10	2	0

	Clast axes				Clast axes		
Clast no.	**a-axis**	**b-axis**	**c-axis**	**Clast no.**	**a-axis**	**b-axis**	**c-axis**
1	4.9	4.8	3.0	**26**	4.5	3.5	1.9
2	3.4	2.4	1.4	**27**	4.0	3.5	2.7
3	4.5	3.7	1.6	**28**	4.0	3.6	2.5
4	3.3	2.7	2.1	**29**	5.5	3.5	2.8
5	5.3	3.9	3.3	**30**	4.5	3.7	2.2
6	8.0	6.3	2.5	**31**	8.0	7.3	4.2
7	8.0	7.7	2.7	**32**	3.9	2.4	1.8
8	10.5	9.0	5.8	**33**	5.0	3.8	2.5
9	3.0	2.2	1.5	**34**	4.0	3.7	2.5
10	3.2	2.0	1.4	**35**	4.0	3.6	2.6
11	10.0	7.9	5.5	**36**	4.5	3.3	1.7
12	8.2	6.9	5.0	**37**	4.2	3.2	2.5
13	10.5	8.5	6.0	**38**	4.5	2.4	2.4
14	3.7	3.0	2.8	**39**	3.8	3.1	2.0
15	7.2	6.0	5.0	**40**	3.5	1.8	1.6
16	9.0	6.0	5.5	**41**	3.1	2.7	2.0
17	5.4	5.0	3.6	**42**	2.5	2.2	2.2
18	4.2	3.5	2.2	**43**	2.6	2.0	1.4
19	4.0	3.0	1.9	**44**	3.0	2.4	1.3
20	6.0	4.5	2.7	**45**	3.5	2.9	2.5
21	4.6	3.0	2.1	**46**	2.6	2.5	1.5
22	12.8	11.5	9.0	**47**	2.9	2.7	1.2
23	5.0	4.5	2.6	**48**	2.5	1.9	1.3
24	3.3	2.5	2.1	**49**	3.7	2.4	1.9
25	3.5	3.0	2.0	**50**	3.5	2.5	2.4

Exposure C - C2

Latitude: N47°01'36.5"
Longitude: E011°49'53.2"
2134 ±
Elevation: 4 m

	VA	A	SA	SR	R	WR
True No.	0	15	26	9	0	0
%	0	30	52	18	0	0

	Clast axes				Clast axes		
Clast no.	**a-axis**	**b-axis**	**c-axis**	**Clast no.**	**a-axis**	**b-axis**	**c-axis**
1	7.9	5.5	4.0	**26**	7.0	4.9	4.4
2	4.0	3.5	2.5	**27**	6.0	4.5	4.0
3	4.0	2.7	2.5	**28**	8.5	5.4	4.2
4	8.0	5.7	4.0	**29**	3.4	2.2	2.0
5	3.5	2.7	2.7	**30**	5.6	3.7	3.6
6	3.9	3.2	2.7	**31**	3.0	2.6	1.5
7	8.4	7.0	5.2	**32**	6.0	3.6	1.9
8	4.5	3.0	3.0	**33**	3.5	2.7	2.0
9	3.4	2.7	1.8	**34**	3.5	2.4	2.1
10	2.5	2.0	1.7	**35**	5.8	3.5	3.0
11	3.5	3.0	1.9	**36**	8.5	3.6	3.1
12	4.0	3.1	2.7	**37**	4.5	2.5	1.6
13	5.5	3.2	2.0	**38**	3.5	3.5	0.6
14	6.0	3.2	3.2	**39**	3.5	2.5	1.4
15	5.0	4.0	3.0	**40**	3.5	2.5	2.4
16	6.5	5.2	3.5	**41**	3.5	3.0	2.0
17	5.0	3.0	2.4	**42**	4.4	3.1	1.5
18	10.5	9.5	6.5	**43**	2.5	2.5	1.9
19	3.8	3.0	1.9	**44**	3.0	2.0	2.0
20	3.5	2.1	1.5	**45**	3.0	2.9	2.7
21	4.8	3.0	2.6	**46**	3.0	2.0	1.2
22	4.7	3.0	2.9	**47**	2.5	2.0	1.2
23	8.5	5.7	3.8	**48**	3.7	2.5	1.5
24	7.5	5.5	4.5	**49**	2.4	1.7	1.0
25	9.4	8.1	4.5	**50**	7.5	5.5	4.5

Exposure D - C1

Latitude: N47°01'35.6"
Longitude: E011°49'53.4"
Elevation: 2132 ± 3 m

	VA	A	SA	SR	R	WR
True No.	0	6	29	15	0	0
%	0	12	58	30	0	0

	Clast axes				Clast axes		
Clast no.	**a-axis**	**b-axis**	**c-axis**	**Clast no.**	**a-axis**	**b-axis**	**c-axis**
1	5.0	3.4	2.5	**26**	2.4	1.8	1.0
2	3.2	2.9	2.5	**27**	3.0	2.4	1.5
3	2.1	1.5	1.4	**28**	6.5	5.5	3.0
4	3.8	3.4	3.1	**29**	2.8	1.7	1.3
5	6.1	4.2	4.0	**30**	3.3	2.5	1.2
6	3.5	2.5	1.5	**31**	5.4	3.0	2.5
7	3.6	2.0	1.1	**32**	3.6	2.2	1.7
8	3.4	3.2	2.1	**33**	3.5	3.0	2.4
9	4.0	2.5	1.5	**34**	4.4	2.5	2.4
10	3.0	2.4	1.5	**35**	6.4	4.9	2.0
11	2.9	2.0	1.5	**36**	8.9	7.3	5.0
12	2.9	2.3	1.4	**37**	3.2	2.2	2.0
13	3.5	2.5	1.5	**38**	5.6	4.2	3.5
14	2.5	2.0	1.4	**39**	7.5	6.8	4.0
15	2.0	1.6	1.0	**40**	4.5	3.7	2.3
16	19.0	14.0	4.5	**41**	2.8	2.0	1.4
17	2.8	2.5	2.0	**42**	3.2	2.0	1.1
18	2.5	2.1	1.4	**43**	6.0	5.4	4.4
19	4.5	3.0	2.8	**44**	6.1	4.3	3.6
20	6.0	2.8	1.7	**45**	3.9	3.0	2.9
21	15.9	9.8	4.6	**46**	9.5	6.4	5.6
22	6.0	4.2	1.8	**47**	3.5	2.4	1.5
23	9.0	6.0	3.0	**48**	4.2	2.5	2.5
24	6.6	4.0	3.5	**49**	5.6	5.0	2.2
25	7.5	5.0	3.4	**50**	2.9	2.5	2.3

Exposure D - C2

Latitude: N47°01'35.6"
Longitude: E011°49'53.4"
Elevation: 2132 ± 3 m

	VA	A	SA	SR	R	WR
True No.	0	10	25	15	0	0
%	0	20	50	30	0	0

	Clast axes				Clast axes		
Clast no.	**a-axis**	**b-axis**	**c-axis**	**Clast no.**	**a-axis**	**b-axis**	**c-axis**
1	14.0	11.0	8.5	**26**	3.6	3.4	2.5
2	7.0	5.8	3.5	**27**	3.7	2.5	2.0
3	6.1	4.5	3.6	**28**	3.5	3.0	1.6
4	2.8	2.5	2.2	**29**	3.0	2.4	1.6
5	10.0	8.5	4.5	**30**	5.0	4.0	3.5
6	5.0	4.0	2.0	**31**	4.0	3.4	3.1
7	2.5	2.0	1.5	**32**	2.1	1.6	0.8
8	5.3	4.0	2.0	**33**	3.2	2.2	2.2
9	3.0	2.0	1.3	**34**	3.7	3.0	1.2
10	6.4	4.9	3.0	**35**	2.6	2.4	2.0
11	3.5	2.4	1.6	**36**	4.0	2.0	1.7
12	2.1	1.9	1.0	**37**	3.2	2.5	1.5
13	4.2	2.4	2.0	**38**	3.2	2.0	1.5
14	7.2	4.6	2.2	**39**	10.0	8.5	5.7
15	8.2	7.6	3.0	**40**	5.5	5.0	4.4
16	4.5	3.2	2.5	**41**	4.8	3.9	2.7
17	3.7	2.9	1.3	**42**	2.6	2.0	1.7
18	7.7	4.5	3.5	**43**	3.8	3.2	2.8
19	7.4	6.4	4.9	**44**	5.0	3.0	2.2
20	19.0	11.0	8.5	**45**	4.6	3.0	2.9
21	3.1	2.5	2.5	**46**	7.2	5.0	5.0
22	3.7	3.0	3.0	**47**	6.2	5.5	1.8
23	9.9	7.0	5.4	**48**	3.5	3.0	1.9
24	4.2	3.4	1.5	**49**	2.5	2.0	0.9
25	2.5	1.9	1.8	**50**	2.5	1.5	0.7

Exposure E - C1

Latitude: N47°01'32.6"
Longitude: E011°49'55.1"
Elevation: 2135 ± 3 m

	VA	A	SA	SR	R	WR
True No.	0	9	31	9	0	1
%	0	18	62	18	0	2

	Clast axes				Clast axes		
Clast no.	**a-axis**	**b-axis**	**c-axis**	**Clast no.**	**a-axis**	**b-axis**	**c-axis**
1	7.4	5.0	4.5	**26**	4.9	2.8	2.5
2	5.9	5.0	4.5	**27**	5.5	3.6	3.0
3	3.2	2.4	1.6	**28**	5.8	4.0	3.8
4	4.4	3.3	2.5	**29**	9.0	6.7	5.5
5	5.5	4.9	3.6	**30**	3.7	3.2	2.0
6	3.6	2.5	2.0	**31**	4.0	3.0	2.9
7	3.8	3.1	1.9	**32**	4.8	3.3	3.0
8	2.4	2.4	2.1	**33**	3.2	2.5	1.6
9	3.4	2.4	1.6	**34**	3.0	2.2	1.8
10	3.5	3.0	1.9	**35**	3.9	3.4	2.6
11	3.9	2.7	2.3	**36**	5.5	4.4	3.7
12	3.8	1.9	1.6	**37**	4.5	3.2	2.5
13	2.9	2.0	1.8	**38**	4.7	4.0	3.5
14	6.4	5.5	5.2	**39**	4.0	3.0	2.3
15	2.5	1.6	1.4	**40**	4.8	3.6	3.0
16	2.6	1.5	1.2	**41**	2.1	1.7	1.2
17	9.5	6.5	4.0	**42**	3.4	2.2	1.7
18	4.2	2.5	2.5	**43**	4.0	2.5	1.7
19	3.3	3.0	2.5	**44**	3.0	2.6	2.1
20	4.0	2.6	2.6	**45**	3.8	3.6	1.9
21	5.0	3.4	2.7	**46**	4.4	3.4	2.2
22	3.7	3.3	1.9	**47**	4.5	3.6	2.1
23	2.5	2.5	1.2	**48**	3.9	2.7	1.9
24	5.4	3.5	2.5	**49**	4.9	3.4	1.4
25	3.0	2.2	1.6	**50**	4.0	2.3	1.6

Exposure E - C2

Latitude: N47°01'32.6"
Longitude: E011°49'55.1"
Elevation: 2135 ± 3 m

	VA	A	SA	SR	R	WR
True No.	0	10	29	10	1	0
%	0	20	58	20	2	0

	Clast axes				Clast axes		
Clast no.	**a-axis**	**b-axis**	**c-axis**	**Clast no.**	**a-axis**	**b-axis**	**c-axis**
1	4.0	3.8	3.0	**26**	3.2	1.9	1.8
2	5.2	3.1	3.0	**27**	6.5	4.4	3.6
3	4.4	3.7	2.2	**28**	3.7	2.5	1.9
4	3.5	2.2	2.1	**29**	4.6	3.4	1.2
5	5.7	4.0	2.6	**30**	5.2	3.7	3.6
6	4.6	3.8	2.4	**31**	3.7	3.2	1.7
7	3.7	2.5	2.0	**32**	5.2	4.0	2.7
8	3.0	2.1	1.6	**33**	6.5	4.2	1.8
9	3.0	2.0	1.6	**34**	6.0	4.2	3.5
10	3.9	3.0	2.1	**35**	4.3	2.2	2.1
11	5.1	3.0	2.0	**36**	3.0	2.6	1.2
12	4.2	2.5	2.5	**37**	3.2	2.0	1.3
13	3.5	2.7	1.4	**38**	4.5	3.5	3.1
14	3.8	2.3	1.8	**39**	3.5	2.5	2.4
15	2.3	1.6	1.6	**40**	3.0	2.4	1.0
16	2.8	2.2	2.0	**41**	3.2	2.3	1.5
17	7.0	5.6	4.5	**42**	3.0	2.0	1.6
18	4.2	2.7	2.1	**43**	2.5	1.9	1.4
19	3.5	2.0	1.4	**44**	2.1	1.4	0.9
20	3.0	3.0	1.6	**45**	8.4	7.5	4.2
21	3.5	3.0	1.9	**46**	3.4	2.7	1.5
22	2.9	2.4	1.6	**47**	2.9	2.1	2.0
23	2.0	1.4	1.3	**48**	3.4	2.3	1.5
24	2.7	2.0	1.4	**49**	3.5	2.5	2.1
25	9.7	7.0	5.0	**50**	2.2	1.4	1.2

Alluvial Fan 01

Latitude: N47°01'28.9"
Longitude: E011°49'49.8"
2154 ±
Elevation: 3 m

	VA	A	SA	SR	R	WR
True No.	0	13	30	7	0	0
%	0	26	60	14	0	0

	Clast axes				Clast axes		
Clast no.	**a-axis**	**b-axis**	**c-axis**	**Clast no.**	**a-axis**	**b-axis**	**c-axis**
1	5.8	5.4	2.7	**26**	12.0	6.0	5.2
2	4.2	3.5	3.2	**27**	6.0	4.5	3.0
3	5.6	3.5	2.5	**28**	4.9	3.5	0.8
4	3.5	2.5	2.0	**29**	4.3	3.0	2.2
5	3.7	2.4	1.7	**30**	4.5	3.9	3.0
6	3.9	3.5	2.2	**31**	3.7	3.0	1.5
7	4.8	3.5	2.9	**32**	6.1	3.6	3.4
8	5.2	4.0	1.6	**33**	3.0	2.2	1.6
9	3.7	2.9	2.5	**34**	7.5	4.0	3.0
10	3.5	3.5	2.4	**35**	2.9	1.5	1.2
11	9.5	7.2	4.8	**36**	7.0	4.0	2.5
12	12.5	6.0	5.5	**37**	5.0	3.4	2.5
13	5.0	3.5	2.5	**38**	7.2	5.4	4.0
14	7.5	4.5	3.2	**39**	7.3	6.8	3.9
15	3.1	2.5	1.7	**40**	3.5	3.0	2.0
16	6.2	4.6	4.2	**41**	4.5	3.1	2.0
17	5.0	3.9	2.7	**42**	8.5	5.3	3.0
18	11.0	7.0	5.0	**43**	5.5	5.5	2.7
19	15.5	9.5	5.2	**44**	3.2	3.0	1.6
20	3.5	2.7	2.1	**45**	2.3	2.0	1.7
21	3.4	1.6	1.5	**46**	8.1	5.0	3.0
22	8.2	6.0	4.0	**47**	4.0	3.4	1.4
23	9.2	8.3	4.5	**48**	3.6	2.2	2.0
24	10.5	7.0	6.0	**49**	3.5	2.4	1.0
25	5.0	3.2	2.4	**50**	3.5	3.0	1.5

Alluvial Fan 02

Latitude: N47°01'21.6"
Longitude: E011°50'20.6"
Elevation: 2172 ± 2 m

	VA	A	SA	SR	R	WR
True No.	0	8	26	16	0	0
%	0	16	52	32	0	0

	Clast axes				Clast axes		
Clast no.	**a-axis**	**b-axis**	**c-axis**	**Clast no.**	**a-axis**	**b-axis**	**c-axis**
1	7.5	2.6	2.5	**26**	6.5	4.0	2.8
2	4.5	3.9	2.6	**27**	7.0	5.7	3.5
3	4.5	3.5	0.9	**28**	3.7	3.4	2.7
4	4.9	3.8	1.6	**29**	6.0	3.7	3.4
5	3.8	3.7	2.3	**30**	7.7	5.5	3.8
6	5.4	4.1	3.3	**31**	5.5	3.4	2.9
7	2.9	1.5	1.4	**32**	4.7	2.5	2.0
8	2.6	1.7	1.2	**33**	3.0	2.8	0.9
9	13.5	11.5	6.5	**34**	3.0	2.4	1.1
10	3.0	2.5	2.0	**35**	4.4	3.5	2.2
11	5.9	3.7	2.9	**36**	5.9	4.1	3.0
12	3.7	2.8	1.8	**37**	7.7	7.0	4.6
13	5.0	4.4	2.6	**38**	4.5	4.2	2.1
14	2.3	2.0	1.8	**39**	5.0	2.8	1.9
15	3.2	2.2	1.5	**40**	8.5	7.4	6.3
16	5.4	3.6	2.9	**41**	10.5	7.5	5.4
17	4.6	4.5	1.6	**42**	5.6	4.5	3.4
18	3.4	3.1	1.4	**43**	5.1	2.7	1.7
19	3.5	2.2	1.9	**44**	4.4	3.2	2.0
20	6.2	3.0	2.5	**45**	4.6	3.0	1.8
21	6.3	4.1	3.2	**46**	3.7	3.5	3.4
22	3.9	2.6	2.2	**47**	5.0	4.2	2.1
23	3.6	2.5	1.6	**48**	5.5	3.7	2.4
24	5.6	3.7	2.0	**49**	3.0	2.1	1.3
25	7.7	5.6	3.7	**50**	5.6	4.7	2.7

Modern Channel 01

Latitude: N47°01'36.7"
Longitude: E011°49'52.5"
Elevation: 2132 ± 3 m

	VA	A	SA	SR	R	WR
True No.	0	3	28	19	0	0
%	0	6	56	38	0	0

	Clast axes				Clast axes		
Clast no.	**a-axis**	**b-axis**	**c-axis**	**Clast no.**	**a-axis**	**b-axis**	**c-axis**
1	7.0	6.2	2.8	**26**	12.0	6.9	5.8
2	7.5	6.0	3.5	**27**	9.0	6.9	6.0
3	4.8	3.2	2.5	**28**	9.0	4.2	2.5
4	4.0	2.2	2.2	**29**	5.3	4.0	3.5
5	5.0	4.5	2.0	**30**	10.1	7.5	4.5
6	5.5	4.8	4.5	**31**	8.1	7.0	3.7
7	6.2	4.2	3.0	**32**	15.5	8.0	6.5
8	10.5	8.2	6.0	**33**	5.0	4.0	3.0
9	13.5	10.3	6.0	**34**	10.2	10.0	5.5
10	7.0	5.8	5.0	**35**	7.0	4.5	2.2
11	4.7	4.0	3.0	**36**	12.0	10.8	5.3
12	6.0	5.5	4.1	**37**	3.5	3.5	1.4
13	9.9	6.0	4.5	**38**	7.5	4.8	2.5
14	7.6	5.0	5.0	**39**	6.0	4.2	2.8
15	7.5	5.6	4.4	**40**	5.2	5.0	3.0
16	4.3	3.4	2.0	**41**	8.5	6.2	3.9
17	4.7	3.0	2.0	**42**	4.0	2.5	2.5
18	15.0	10.6	8.9	**43**	4.5	4.5	2.5
19	12.1	8.8	7.9	**44**	9.5	7.7	7.5
20	9.5	8.0	6.5	**45**	8.3	8.0	3.6
21	10.2	9.6	7.6	**46**	6.7	4.6	2.8
22	12.4	9.2	8.5	**47**	4.6	4.0	3.6
23	10.1	8.5	5.3	**48**	7.0	5.9	3.2
24	9.5	8.3	2.6	**49**	3.5	3.0	1.5
25	10.2	8.1	5.5	**50**	3.5	2.6	2.0

Modern Channel 02

Latitude: N47°01'31.5"
Longitude: E011°49'57.7"
Elevation: 2133 ± 3 m

	VA	A	SA	SR	R	WR
True No.	0	14	22	14	0	0
%	0	28	44	28	0	0

	Clast axes				Clast axes		
Clast no.	**a-axis**	**b-axis**	**c-axis**	**Clast no.**	**a-axis**	**b-axis**	**c-axis**
1	9.2	8.5	4.5	**26**	2.9	2.0	1.9
2	6.5	5.5	4.0	**27**	3.4	2.8	1.5
3	4.8	3.5	2.4	**28**	9.0	7.9	4.1
4	8.5	6.5	4.2	**29**	8.0	5.0	3.9
5	3.2	2.0	1.4	**30**	4.0	2.6	2.0
6	2.5	2.2	1.6	**31**	4.9	3.5	2.9
7	5.8	3.6	3.3	**32**	6.4	5.1	4.5
8	3.2	3.0	1.8	**33**	4.5	2.5	2.0
9	3.0	2.0	1.6	**34**	6.5	5.5	2.7
10	9.4	7.9	6.8	**35**	10.0	8.0	5.5
11	2.1	2.0	1.4	**36**	2.8	2.1	1.0
12	3.7	2.5	0.7	**37**	4.5	2.6	2.0
13	4.3	2.6	2.0	**38**	3.0	2.0	1.8
14	9.0	7.2	4.1	**39**	4.0	4.0	1.8
15	2.4	1.0	0.7	**40**	3.8	2.5	1.9
16	7.7	4.0	4.0	**41**	7.6	4.0	3.0
17	6.9	4.5	2.8	**42**	6.0	5.5	3.5
18	4.4	2.7	2.5	**43**	9.0	6.9	6.0
19	2.6	2.1	1.9	**44**	5.1	2.6	1.4
20	6.7	4.5	2.5	**45**	8.6	6.0	5.2
21	2.5	1.6	1.1	**46**	4.2	3.1	2.5
22	2.9	2.0	1.1	**47**	4.5	3.5	2.7
23	2.6	1.9	1.7	**48**	10.5	9.2	7.7
24	5.5	4.1	2.7	**49**	8.0	4.4	4.4
25	3.9	3.9	2.9	**50**	5.0	3.8	2.1

Talus 01

Latitude: N47°01'17.5"
Longitude: E011°50'19.9"
Elevation: 2190 ± 3 m

	VA	A	SA	SR	R	WR
True No.	0	15	26	9	0	0
%	0	30	52	18	0	0

	Clast axes				Clast axes		
Clast no.	**a-axis**	**b-axis**	**c-axis**	**Clast no.**	**a-axis**	**b-axis**	**c-axis**
1	4.4	4.0	3.0	**26**	5.0	3.8	2.5
2	4.3	4.0	2.5	**27**	4.1	3.3	3.2
3	5.0	4.0	3.5	**28**	4.1	3.4	2.5
4	3.9	3.5	2.0	**29**	3.7	3.1	2.0
5	8.9	6.0	5.0	**30**	3.1	2.2	1.4
6	5.0	2.4	1.3	**31**	3.2	2.1	1.5
7	6.7	4.6	4.5	**32**	6.0	5.2	3.6
8	2.3	2.0	0.9	**33**	3.2	2.9	2.0
9	4.5	2.4	1.5	**34**	5.0	3.2	2.8
10	2.8	2.0	1.1	**35**	2.9	2.4	1.8
11	7.2	5.0	4.0	**36**	3.1	2.5	1.7
12	4.2	3.1	1.2	**37**	4.0	2.6	1.4
13	5.5	4.5	2.2	**38**	3.0	1.6	1.4
14	3.6	3.0	2.7	**39**	2.9	1.5	0.8
15	6.4	4.4	2.4	**40**	11.5	9.7	6.4
16	6.5	5.9	4.0	**41**	8.8	6.0	3.5
17	2.6	2.1	1.7	**42**	4.2	3.8	2.7
18	3.2	2.3	1.1	**43**	3.2	2.6	2.1
19	2.2	2.0	1.8	**44**	3.5	3.0	1.9
20	13.8	9.5	8.5	**45**	3.0	1.4	1.2
21	6.4	4.9	3.9	**46**	3.3	2.5	1.7
22	6.5	4.1	4.0	**47**	4.5	3.6	2.4
23	5.5	3.2	2.7	**48**	12.0	9.0	9.0
24	7.0	5.6	3.9	**49**	8.4	6.5	2.7
25	5.0	3.5	3.5	**50**	11.5	7.9	3.7

Talus 02
Latitude: N47°01'17.4"
Longitude: E011°50'18.8"
2205 ±
Elevation: 3 m

	VA	A	SA	SR	R	WR
True No.	3	11	24	12	0	0
%	6	22	48	24	0	0

	Clast axes				Clast axes		
Clast no.	**a-axis**	**b-axis**	**c-axis**	**Clast no.**	**a-axis**	**b-axis**	**c-axis**
1	4.0	2.5	2.2	**26**	4.5	3.1	2.7
2	6.8	3.9	2.7	**27**	9.0	6.3	4.0
3	5.2	3.7	2.8	**28**	8.0	5.5	4.0
4	6.2	4.5	2.5	**29**	5.5	3.5	2.5
5	6.4	3.7	2.2	**30**	6.5	5.5	3.3
6	8.7	5.0	3.7	**31**	10.0	4.6	2.5
7	7.2	5.3	3.6	**32**	7.5	5.3	1.3
8	11.8	7.5	4.5	**33**	4.0	2.8	2.5
9	16.5	9.0	4.8	**34**	8.5	4.9	1.1
10	9.2	8.0	6.0	**35**	6.2	5.0	4.2
11	8.4	7.5	0.8	**36**	6.5	6.0	3.5
12	4.0	3.0	2.2	**37**	5.5	3.5	3.0
13	10.5	9.2	4.3	**38**	7.0	5.0	3.2
14	4.5	4.0	2.2	**39**	5.6	3.8	2.5
15	6.5	5.0	4.0	**40**	6.4	5.0	2.2
16	8.2	6.2	4.5	**41**	10.1	7.6	4.0
17	7.2	4.3	3.2	**42**	5.0	4.0	3.5
18	7.5	5.6	2.5	**43**	6.0	3.6	3.3
19	3.5	3.5	1.7	**44**	8.2	6.2	3.5
20	7.2	7.0	3.2	**45**	7.0	4.5	4.0
21	4.5	3.0	1.7	**46**	6.5	5.4	2.5
22	6.0	5.6	3.7	**47**	5.5	4.7	4.2
23	4.5	3.5	1.0	**48**	8.0	4.0	3.5
24	2.8	2.0	1.0	**49**	8.3	5.0	2.0
25	3.6	3.0	1.1	**50**	7.5	6.0	5.0

Supraglacial 01

Latitude: N47°00'36.4"
Longitude: E011°49'17.9"
2209 ±
Elevation: 4 m

	VA	A	SA	SR	R	WR
True No.	18	32	0	0	0	0
%	36	64	0	0	0	0

	Clast axes				Clast axes		
Clast no.	**a-axis**	**b-axis**	**c-axis**	**Clast no.**	**a-axis**	**b-axis**	**c-axis**
1	10.5	9.0	8.5	**26**	3.5	2.6	2.1
2	10.4	4.8	2.7	**27**	8.6	8.0	3.7
3	8.2	3.9	1.2	**28**	2.9	2.0	0.6
4	5.5	5.2	1.4	**29**	7.3	4.5	1.0
5	16.5	11.0	3.8	**30**	8.0	7.0	7.0
6	7.2	3.1	2.9	**31**	4.5	3.4	1.5
7	3.2	2.7	1.5	**32**	8.4	6.0	2.9
8	6.9	4.0	2.2	**33**	9.2	6.3	1.8
9	3.2	2.9	1.0	**34**	6.7	4.5	1.3
10	3.3	2.2	0.8	**35**	6.5	3.6	1.8
11	2.8	2.0	0.6	**36**	8.6	6.5	2.2
12	8.7	8.0	2.3	**37**	7.2	4.9	1.4
13	5.5	3.0	1.4	**38**	10.0	5.5	3.5
14	9.3	6.4	2.0	**39**	8.0	5.6	3.4
15	11.0	9.0	5.5	**40**	7.0	3.9	2.0
16	6.5	5.5	2.0	**41**	3.3	2.7	1.0
17	8.0	5.0	3.7	**42**	5.4	3.5	1.6
18	10.0	5.5	2.4	**43**	6.0	3.1	3.0
19	3.0	2.0	1.3	**44**	7.0	6.5	0.5
20	3.7	2.7	0.7	**45**	7.2	4.9	1.1
21	10.0	6.0	3.0	**46**	4.2	3.0	0.8
22	4.7	3.8	1.2	**47**	6.5	3.5	2.9
23	6.0	4.0	1.1	**48**	10.2	5.9	3.7
24	2.8	2.8	2.1	**49**	6.0	5.0	1.7
25	3.6	3.2	1.4	**50**	3.4	3.0	1.4

Supraglacial 02

Latitude: N47°00'35.2"
Longitude: E011°49'16.6"
Elevation: 2218 m

	VA	A	SA	SR	R	WR
True No.	0	42	7	1	0	0
%	0	84	14	2	0	0

	Clast axes				Clast axes		
Clast no.	**a-axis**	**b-axis**	**c-axis**	**Clast no.**	**a-axis**	**b-axis**	**c-axis**
1	9.1	7.6	1	**26**	4.0	3.8	1.6
2	13.5	8.5	2.5	**27**	6.2	5.5	0.4
3	10.2	8.5	1.8	**28**	5.2	2.6	2.5
4	4.6	2.5	1.3	**29**	6.0	2.1	2.1
5	8.2	5.8	3.2	**30**	4.0	3.1	1.5
6	10.1	6.7	1.5	**31**	5.4	3.9	2.0
7	7.5	6.4	2.7	**32**	6.0	3.4	1.0
8	5.0	2.8	1.0	**33**	11.0	7.4	2.3
9	7.2	5.5	4.3	**34**	9.0	5.0	2.0
10	7.5	5.0	3.8	**35**	4.6	2.7	1.3
11	7.5	5.9	3.3	**36**	11.0	4.8	2.2
12	7.3	6.1	5.0	**37**	6.5	3.3	3.3
13	4.1	3.7	2.2	**38**	4.1	2.4	1.0
14	6.5	4.0	3.8	**39**	5.9	3.6	2.1
15	3.8	3.4	2.0	**40**	8.0	3.6	1.8
16	5.8	2.6	2.4	**41**	6.4	4.5	2.6
17	6.3	4.5	1.0	**42**	6.0	4.1	2.8
18	10.0	6.0	1.5	**43**	4.4	3.0	0.6
19	8.0	4.9	4.1	**44**	4.8	3.0	1.3
20	10.0	4.5	3.7	**45**	4.5	4.0	0.8
21	7.4	6.0	3.0	**46**	3.4	2.5	1.5
22	5.5	4.1	1.2	**47**	3.7	2.6	2.0
23	9.4	5.2	4.5	**48**	4.6	2.0	2.0
24	8.6	5.5	0.8	**49**	4.5	4.0	1.0
25	7.0	5.8	1.4	**50**	9.7	8.0	2.1

Supraglacial 03

Latitude: N47°00'35.2"
Longitude: E011°49'16.6"
Elevation: 2218 m

	VA	A	SA	SR	R	WR
True No.	0	37	13	0	0	0
%	0	74	26	0	0	0

	Clast axes				Clast axes		
Clast no.	**a-axis**	**b-axis**	**c-axis**	**Clast no.**	**a-axis**	**b-axis**	**c-axis**
1	6.7	5	2.5	**26**	5.5	5.0	2.4
2	6	2.9	2.4	**27**	4.4	2.5	1.8
3	3.8	3.1	0.7	**28**	4.2	3.0	1.1
4	5.1	2.4	1.4	**29**	4.5	3.5	1.3
5	5.1	2.6	1.8	**30**	3.7	3.5	0.6
6	6.2	2.9	2.1	**31**	5.1	4.5	1.4
7	5.5	3.4	2.8	**32**	5.3	3.4	1.3
8	6.8	5.4	2.5	**33**	5.9	2.6	1.6
9	6.0	4.2	2.6	**34**	3.2	2.5	1.0
10	7.2	6.5	2.0	**35**	5.4	2.9	1.5
11	5.7	3.8	1.4	**36**	4.5	3.6	2.4
12	5.1	3.0	1.5	**37**	3.2	2.4	1.6
13	4.6	3.5	1.5	**38**	4.7	2.6	1.1
14	4.0	3.0	2.8	**39**	9.5	7.0	2.4
15	4.6	3.8	1.5	**40**	5.5	4.5	1.7
16	6.1	6.1	3.0	**41**	4.5	3.5	1.4
17	3.5	1.6	1.5	**42**	4.5	2.0	1.5
18	4.2	3.5	2.6	**43**	4.0	3.6	1.0
19	3.7	2.6	1.9	**44**	5.2	3.6	1.1
20	3.9	3.0	1.5	**45**	3.7	2.6	1.0
21	6.7	3.5	1.3	**46**	4.9	3.5	1.6
22	4.5	3.5	2.7	**47**	3.3	2.1	1.5
23	7.0	4.7	1.0	**48**	3.7	2.7	1.5
24	5.8	4.5	2.0	**49**	5.5	3.8	1.0
25	7.8	4.3	1.0	**50**	4.0	2.1	1.7

Subglacial 01

Latitude: N47°00'37.1"
Longitude: E011°49'18.3"
2202 ±
Elevation: 6 m

	VA	A	SA	SR	R	WR
True No.	0	15	27	8	0	0
%	0	30	54	16	0	0

	Clast axes				Clast axes		
Clast no.	**a-axis**	**b-axis**	**c-axis**	**Clast no.**	**a-axis**	**b-axis**	**c-axis**
1	4.4	3.7	2.8	**26**	7.2	5.1	2.0
2	6.5	4.9	4.0	**27**	7.5	6.0	3.0
3	7.0	5.0	3.6	**28**	8.8	8.2	3.1
4	10.0	4.5	3.9	**29**	3.5	2.9	2.5
5	5.0	3.0	2.9	**30**	5.2	4.0	3.5
6	10.3	5.0	3.6	**31**	5.0	4.5	3.5
7	5.5	3.6	2.0	**32**	8.8	4.7	2.5
8	5.0	4.7	2.5	**33**	7.0	5.6	4.5
9	6.0	4.4	4.0	**34**	8.0	5.0	3.0
10	5.0	3.5	2.9	**35**	7.0	5.0	2.7
11	5.2	3.9	2.2	**36**	4.0	3.5	1.5
12	7.0	4.6	4.3	**37**	7.1	5.2	3.0
13	7.8	5.5	3.9	**38**	5.3	4.0	2.5
14	11.6	7.5	5.5	**39**	6.6	4.7	3.0
15	7.5	5.0	3.5	**40**	12.5	9.0	7.0
16	12.0	8.0	6.7	**41**	3.5	2.0	2.0
17	6.0	3.0	2.8	**42**	4.8	3.5	3.2
18	8.6	4.2	4.0	**43**	6.5	4.0	3.7
19	6.0	5.5	3.7	**44**	7.0	5.5	4.0
20	6.6	5.0	3.5	**45**	5.5	5.0	3.2
21	12.0	7.5	4.5	**46**	7.0	4.0	3.5
22	5.0	3.3	2.4	**47**	9.0	6.0	3.5
23	6.0	4.5	2.5	**48**	4.0	2.0	1.7
24	6.0	3.7	2.9	**49**	6.5	5.0	3.0
25	10.0	6.5	3.5	**50**	10.0	6.0	4.5

Subglacial 02

Latitude: N47°00'36.6"
Longitude: E011°49'16.6"
Elevation: 2203 m

	VA	A	SA	SR	R	WR
True No.	0	1	25	23	1	0
%	0	2	50	46	2	0

	Clast axes				Clast axes		
Clast no.	**a-axis**	**b-axis**	**c-axis**	**Clast no.**	**a-axis**	**b-axis**	**c-axis**
1	5.0	3.9	3.1	**26**	6.7	5.3	2.4
2	9.0	5.5	3.7	**27**	5.0	4.5	2.5
3	4.2	3.6	1.7	**28**	5.0	3.5	2.4
4	3.9	2.5	1.5	**29**	5.5	3.4	2.4
5	3.7	2.1	2.1	**30**	7.0	5.4	3.0
6	6.3	5.5	3.6	**31**	4.5	2.9	2.9
7	7.2	4.5	3.6	**32**	5.0	4.5	3.4
8	6.8	4.5	4.0	**33**	4.4	3.5	3.0
9	6.0	3.9	3.0	**34**	4.5	4.3	3.3
10	5.0	3.5	2.7	**35**	6.4	3.2	2.9
11	4.2	3.0	2.7	**36**	6.2	3.5	3.0
12	5.0	3.7	2.0	**37**	5.1	4.1	2.6
13	3.5	2.4	2.0	**38**	4.4	3.4	2.5
14	7.4	4.0	3.0	**39**	5.2	3.5	2.8
15	5.5	3.6	2.6	**40**	6.5	4.0	3.1
16	4.5	3.5	3.0	**41**	5.2	3.1	2.0
17	6.0	4.2	2.5	**42**	5.6	4.3	3.0
18	5.0	4.5	3.0	**43**	4.6	3.3	3.0
19	5.0	2.5	2.5	**44**	4.3	4.2	1.3
20	4.6	3.5	3.4	**45**	4.6	4.0	3.0
21	3.9	2.5	2.3	**46**	5.5	5.4	2.0
22	7.5	3.9	3.3	**47**	3.7	2.5	1.5
23	4.5	4.1	4.0	**48**	3.5	2.6	2.5
24	5.9	5.5	3.0	**49**	4.0	1.5	1.5
25	5.5	4.2	2.5	**50**	4.0	3.1	1.4

Subglacial 03
Latitude: N47°00'37.2"
Longitude: E011°49'17.0"
Elevation: 2203 m

	VA	A	SA	SR	R	WR
True No.	0	0	23	27	0	0
%	0	0	46	54	0	0

	Clast axes				Clast axes		
Clast no.	**a-axis**	**b-axis**	**c-axis**	**Clast no.**	**a-axis**	**b-axis**	**c-axis**
1	5.5	3.5	3.1	**26**	7.6	6.0	5.5
2	7.4	7.0	5.0	**27**	6.8	5.5	4.1
3	12.5	6.0	5.1	**28**	5.0	3.5	2.1
4	10.0	8.0	6.1	**29**	4.0	3.5	2.6
5	7.4	4.5	3.3	**30**	6.2	4.5	3.0
6	6.0	4.1	3.0	**31**	7.0	4.0	3.5
7	6.0	4.4	3.6	**32**	5.5	4.0	3.3
8	5.5	5.0	3.2	**33**	6.8	6.0	5.1
9	6.0	3.9	3.9	**34**	6.5	4.0	3.0
10	5.5	4.8	2.6	**35**	7.0	4.8	4.1
11	5.0	4.1	3.0	**36**	4.0	2.9	2.5
12	5.0	3.4	2.0	**37**	6.0	3.6	3.5
13	7.5	5.0	3.1	**38**	5.2	3.9	3.0
14	3.4	3.0	2.0	**39**	5.5	4.2	2.9
15	7.4	4.0	3.0	**40**	5.5	3.6	3.1
16	6.0	4.6	3.8	**41**	5.6	3.9	3.9
17	5.0	3.0	3.0	**42**	8.1	6.2	3.5
18	7.0	4.5	3.5	**43**	7.6	5.1	3.5
19	4.1	4.0	1.5	**44**	5.0	3.9	3.0
20	4.7	4.1	2.6	**45**	4.5	4.5	2.6
21	5.1	3.0	2.5	**46**	6.5	5.1	2.8
22	4.5	3.5	2.5	**47**	7.0	7.0	4.0
23	4.2	3.5	2.6	**48**	6.0	3.2	2.5
24	7.0	5.6	3.1	**49**	6.0	4.4	3.5
25	6.5	4.5	3.5	**50**	5.0	4.0	2.9

SILVRETTAGLETSCHER

Exposure A - C1

Latitude: N46°51.446’

Longitude: E010°03.585’

Elevation: 2538 m

	VA	A	SA	SR	R	WR		
True No.	0	1	23	24	2	0	0	
%	0	2	46	48	4	0	0	

	Clast axes				Clast axes		
Clast no.	a-axis	b-axis	c-axis	Clast no.	a-axis	b-axis	c-axis
1	4.9	4.1	1.6	26	8.0	6.7	2.6
2	12.5	8.5	7.6	27	4.2	2.2	1.7
3	11	7	5.5	28	9.0	5.2	2.2
4	12.2	12	3	29	3.7	1.6	1.4
5	6.5	3.8	1.4	30	4.5	3.4	1.6
6	6.9	5	3.4	31	3.5	2.5	2.0
7	9	7.5	4.5	32	9.0	5.0	4.5
8	6.0	4.9	2.0	33	8.1	5.7	3.0
9	5.0	2.2	2.0	34	6.0	4.0	3.0
10	7.5	5.0	1.6	35	7.0	4.0	3.6
11	3.0	2.7	1.1	36	5.5	3.6	2.5
12	9.0	6.8	3.0	37	4.0	2.4	1.7
13	3.5	2.1	1.4	38	6.5	3.0	1.6
14	3.7	2.9	1.4	39	4.9	2.5	1.7
15	4.0	2.0	1.5	40	3.6	1.2	1.2
16	3.6	2.4	1.7	41	4.5	3.0	2.3
17	3.6	2.9	2.0	42	3.4	2.5	1.7
18	6.5	5.5	4.2	43	3.9	2.6	2.0
19	5.0	3.0	1.5	44	6.5	5.5	3.0
20	8.5	4.5	2.9	45	6.5	3.6	2.0
21	5.2	4.0	2.2	46	8.5	7.5	4.3
22	3.5	2.0	2.0	47	4.5	2.1	1.2
23	6.6	5.0	2.0	48	6.5	3.7	2.0
24	7.5	3.0	2.2	49	6.5	5.0	3.0
25	3.7	2.5	1.2	50	12.2	10.2	4.5

Exposure B - C1

Latitude: N46°51.406’

Longitude: E010°03.348’

Elevation: 2490 m

	VA	A	SA	SR	R	WR		
True No.	0	0	28	20	2	0	0	
%	0	0	56	40	4	0	0	

	Clast axes				Clast axes		
Clast no.	a-axis	b-axis	c-axis	Clast no.	a-axis	b-axis	c-axis
1	14	10	5	26	5.2	3.0	1.9
2	7.3	6	2.6	27	6.0	3.5	3.1
3	5.9	4	2.6	28	3.1	2.8	1.4
4	4	2.5	2	29	3.0	2.5	0.7
5	4	1.9	1.9	30	6.4	5.0	3.7
6	3.5	2.5	1.1	31	4.2	2.6	1.4
7	5.5	4.4	2	32	3.2	3.0	1.6
8	3.5	2.5	1.7	33	7.6	6.0	3.2
9	4.5	2.9	2.5	34	4.5	3.2	1.4
10	6.8	6.5	2.0	35	3.5	2.0	0.8
11	10.5	6.8	4.6	36	3.7	3.0	1.2
12	8.5	4.5	2.7	37	3.6	1.5	1.5
13	9.5	7.7	3.6	38	3.2	2.5	2.0
14	3.8	3.7	1.6	39	2.6	2.1	0.8
15	4.5	3.9	2.6	40	3.5	2.0	1.2
16	4.0	3.0	1.1	41	3.5	2.4	1.0
17	3.3	2.6	1.5	42	3.5	2.0	1.2
18	8.0	6.0	4.0	43	2.9	2.0	1.4
19	3.5	2.6	1.1	44	3.5	2.7	2.0
20	6.4	3.1	2.2	45	3.5	2.0	1.5
21	10.0	5.5	2.5	46	3.0	2.4	1.2
22	3.0	2.0	0.8	47	3.0	1.4	1.4
23	5.0	4.1	1.9	48	3.0	1.7	1.1
24	14.0	7.2	6.0	49	2.6	1.5	0.6
25	2.5	1.8	1.1	50	2.5	1.7	0.7

Exposure C - C1

Latitude: N46°51.376’

Longitude: E010°03.389’

Elevation: 2483 m

	VA	A	SA	SR	R	WR	
True No.	0	7	31	10	2	0	0
%	0	14	62	20	4	0	0

	Clast axes				Clast axes		
Clast no.	a-axis	b-axis	c-axis	Clast no.	a-axis	b-axis	c-axis
1	5.2	3	2.9	26	3.3	2.1	1.5
2	3.5	2.3	1.9	27	2.5	1.7	1.1
3	4	2.1	1.6	28	2.5	1.5	1.2
4	2.4	1.8	1	29	3.5	1.5	1.3
5	4	3	2.5	30	3.5	2.2	1.2
6	5.2	2.5	1.2	31	2.7	1.5	1.3
7	3.8	2.4	1.2	32	2.6	1.1	1.0
8	5.4	3.0	1.8	33	2.7	1.2	1.1
9	3.5	2.6	1.5	34	3.2	1.4	0.9
10	3.0	2.0	1.2	35	3.0	1.6	1.1
11	3.0	2.5	1.2	36	3.1	1.0	0.6
12	2.5	2.1	0.5	37	2.5	2.3	0.9
13	4.0	2.1	2.1	38	2.5	2.1	1.6
14	5.5	2.6	1.9	39	2.9	1.7	0.6
15	4.5	3.5	2.0	40	3.0	2.0	1.1
16	3.5	2.0	1.4	41	3.2	2.5	1.5
17	3.0	2.0	0.7	42	3.1	1.8	0.9
18	3.6	2.0	0.9	43	2.7	2.5	0.5
19	4.5	3.0	1.9	44	3.0	2.0	1.0
20	3.4	1.8	1.0	45	3.5	2.0	1.0
21	2.6	2.0	1.5	46	2.5	2.4	1.6
22	3.3	2.0	1.5	47	2.6	1.5	1.2
23	3.0	1.6	1.3	48	2.5	1.9	0.7
24	3.6	2.5	0.7	49	3.1	1.5	1.1
25	2.5	2.1	0.4	50	2.9	1.4	1.0

Exposure C – C2

Latitude: N46°51.376’

Longitude: E010°03.389’

Elevation: 2483 m

	VA	A	SA	SR	R	WR	
True No.	0	4	23	21	2	0	0
%	0	8	46	42	4	0	0

	Clast axes				Clast axes		
Clast no.	a-axis	b-axis	c-axis	Clast no.	a-axis	b-axis	c-axis
1	8	5.5	4.5	26	5.6	3.2	2.4
2	4.7	3.5	3.4	27	4.1	3.7	1.6
3	7.6	6.5	3.5	28	11.0	8.5	5.0
4	15	10	3.9	29	3.7	2.2	1.5
5	8.2	5.9	3.6	30	6.2	3.0	2.3
6	5	4.1	2.8	31	5.0	3.5	2.7
7	3.1	2.5	1	32	5.1	3.0	2.7
8	4.0	2.5	1.4	33	3.5	2.5	1.1
9	6.2	3.9	2.7	34	6.5	3.5	3.5
10	3.4	1.5	0.6	35	7.5	4.2	3.6
11	5.8	3.5	3.0	36	19.0	9.5	8.0
12	3.9	3.5	2.4	37	15.0	10.5	7.0
13	4.6	3.1	1.9	38	9.7	4.4	3.0
14	11.0	8.4	5.0	39	3.1	1.6	1.1
15	3.5	2.5	1.4	40	3.2	2.6	2.6
16	4.4	3.8	1.4	41	5.0	3.5	3.2
17	5.9	3.5	2.0	42	2.7	1.6	1.1
18	4.0	3.0	1.2	43	4.0	3.0	1.3
19	3.4	2.5	2.5	44	5.5	3.0	2.9
20	7.5	6.5	6.5	45	4.5	3.7	2.6
21	3.2	2.0	1.6	46	3.5	1.9	1.1
22	5.6	3.5	1.8	47	4.5	2.5	2.0
23	5.2	2.4	1.5	48	7.5	5.5	2.2
24	3.2	2.0	1.2	49	4.0	2.9	1.6
25	6.0	5.4	3.1	50	4.6	2.2	1.6

Exposure D – C1

Latitude: N46°51.364’

Longitude: E010°03.356’

Elevation: 2492 m

	VA	A	SA	SR	R	WR		
True No.	0	4	15	31	0	0	0	
%	0	8	30	62	0	0	0	

	Clast axes				Clast axes		
Clast no.	a-axis	b-axis	c-axis	Clast no.	a-axis	b-axis	c-axis
1	4.5	3.5	2	26	3.8	2.9	1.5
2	3.1	1.6	1.2	27	3.6	2.0	1.5
3	4	3.3	2.4	28	3.0	1.5	1.5
4	5	4.6	1.5	29	2.5	1.6	0.7
5	3.5	3.5	1	30	2.5	1.0	0.7
6	2.9	2.5	1.7	31	3.0	2.2	1.2
7	3	2.1	1.2	32	2.5	1.6	1.2
8	2.5	2.0	1.0	33	2.7	1.7	0.9
9	3.7	1.5	1.0	34	2.6	1.3	0.6
10	4.4	3.0	1.5	35	4.9	2.6	2.6
11	3.4	1.4	1.0	36	3.1	1.6	1.6
12	6.5	5.3	4.7	37	3.6	3.0	1.4
13	6.9	5.0	2.5	38	4.0	1.7	1.5
14	2.7	2.0	0.9	39	3.7	2.0	1.2
15	3.8	2.0	2.0	40	2.5	2.0	1.1
16	5.0	3.6	2.5	41	3.1	2.0	0.9
17	2.5	1.0	1.0	42	3.5	1.6	0.9
18	2.5	1.4	1.1	43	2.5	2.0	1.5
19	3.0	1.7	1.1	44	2.7	1.5	1.4
20	4.7	3.4	1.5	45	3.0	2.5	1.5
21	3.0	2.1	1.8	46	2.7	1.6	1.6
22	2.6	2.0	1.1	47	3.0	1.4	1.0
23	2.8	1.9	1.0	48	2.7	1.0	1.0
24	3.0	1.5	1.4	49	3.6	2.6	1.2
25	2.7	1.2	1.0	50	2.5	1.8	1.0

Exposure D – C2

Latitude: N46°51.364’

Longitude: E010°03.356’

Elevation: 2492 m

	VA	A	SA	SR	R	WR		
True No.	0	1	21	26	2	0	0	
%	0	2	42	52	4	0	0	

	Clast axes				Clast axes		
Clast no.	a-axis	b-axis	c-axis	Clast no.	a-axis	b-axis	c-axis
1	4.2	2.9	1.8	26	5.9	3.5	2.0
2	2.5	2.3	1.4	27	3.0	2.0	2.0
3	4.5	4	2.9	28	3.6	3.1	1.5
4	7.9	4	1.6	29	2.9	1.5	1.4
5	3	2.4	2.1	30	3.0	2.0	1.0
6	7.5	5.5	5	31	3.2	2.0	1.4
7	2.6	1.5	0.9	32	3.7	2.5	1.5
8	3.9	3.0	2.5	33	3.0	1.8	1.6
9	3.0	2.1	1.2	34	2.5	1.8	1.6
10	3.4	3.4	1.2	35	3.8	2.6	1.6
11	3.6	3.5	1.0	36	3.8	1.4	0.8
12	3.4	2.2	2.0	37	3.5	1.6	1.0
13	3.5	2.0	1.1	38	3.1	1.8	1.3
14	7.1	4.5	2.9	39	2.6	2.0	0.8
15	3.9	2.9	2.1	40	2.6	2.1	1.3
16	3.6	2.0	1.5	41	2.7	1.5	1.2
17	3.9	3.5	1.6	42	2.5	1.5	0.7
18	3.2	2.5	2.0	43	2.7	1.6	1.3
19	4.0	2.0	1.0	44	2.7	1.6	1.2
20	3.4	2.6	1.3	45	2.8	2.0	1.1
21	3.6	2.4	1.3	46	2.6	1.6	0.9
22	3.5	2.7	1.9	47	2.5	2.0	1.3
23	3.7	3.0	1.2	48	2.6	2.0	0.8
24	3.8	3.5	2.5	49	2.5	1.3	1.2
25	3.0	3.0	1.0	50	4.0	2.0	1.0

Exposure D – C3

Latitude: N46°51.364’

Longitude: E010°03.356’

Elevation: 2492 m

	VA	A	SA	SR	R	WR		
True No.	0	2	18	30	0	0	0	
%	0	4	36	60	0	0	0	

	Clast axes				Clast axes		
Clast no.	a-axis	b-axis	c-axis	Clast no.	a-axis	b-axis	c-axis
1	4.4	2.9	2	26	2.5	1.7	1.1
2	6	5.1	3.6	27	3.4	2.5	2.0
3	5.6	3.1	2.5	28	3.7	2.5	1.5
4	3	2.3	1.6	29	3.7	2.5	1.1
5	4.9	3.2	3	30	4.5	2.9	2.4
6	3.3	2.1	1.2	31	4.8	2.5	1.6
7	2.8	2.2	1.1	32	3.0	2.6	1.6
8	3.1	2.4	1.5	33	3.5	2.7	1.5
9	2.6	1.5	0.8	34	2.6	2.0	1.2
10	4.0	3.0	1.4	35	3.0	2.6	1.5
11	5.4	4.2	2.5	36	3.1	2.0	1.5
12	5.0	3.9	3.5	37	2.5	1.6	1.5
13	2.8	2.5	0.7	38	2.7	2.2	1.3
14	3.0	2.0	0.9	39	9.0	5.0	3.3
15	3.7	3.0	1.9	40	2.5	1.7	1.2
16	3.7	3.0	2.3	41	2.5	1.3	0.7
17	3.1	2.0	1.3	42	8.0	2.7	2.2
18	9.5	7.0	5.5	43	4.9	3.5	3.0
19	4.5	2.6	2.1	44	3.0	2.8	1.4
20	2.6	2.0	1.5	45	3.5	2.1	0.9
21	3.5	2.5	2.1	46	3.5	2.5	1.5
22	4.6	3.5	2.0	47	6.1	4.5	2.1
23	2.8	1.4	1.0	48	5.1	3.5	2.1
24	2.6	2.0	0.6	49	3.5	3.0	1.4
25	2.8	1.5	0.7	50	3.3	2.6	1.5

Exposure D – C4

Latitude: N46°51.364’

Longitude: E010°03.356’

Elevation: 2492 m

	VA	A	SA	SR	R	WR		
True No.	0	1	26	23	0	0	0	
%	0	2	52	46	0	0	0	

	Clast axes				Clast axes		
Clast no.	a-axis	b-axis	c-axis	Clast no.	a-axis	b-axis	c-axis
1	5.5	2.6	2.5	26	2.7	2.5	1.7
2	4.2	2	1.3	27	3.8	2.1	1.6
3	3.8	2.8	1.6	28	2.9	2.0	0.7
4	5.9	3.8	2.5	29	2.5	1.8	1.4
5	3.7	2.5	1.5	30	3.0	1.5	0.8
6	3.4	2.5	0.6	31	3.9	2.5	1.0
7	4.4	2.5	1.5	32	3.0	2.0	1.1
8	5.1	3.3	2.5	33	6.7	4.3	2.1
9	3.4	1.5	1.3	34	5.4	2.3	1.9
10	3.9	2.2	2.1	35	5.4	3.5	3.1
11	2.7	2.0	1.2	36	8.5	7.0	2.9
12	6.2	4.1	3.0	37	2.6	2.2	1.1
13	5.2	3.6	2.1	38	4.0	3.0	2.3
14	4.7	3.0	2.6	39	5.5	3.5	2.1
15	4.5	2.7	2.5	40	5.6	2.6	2.2
16	3.0	1.6	1.5	41	4.3	3.0	1.1
17	4.5	3.0	2.0	42	4.4	3.5	1.7
18	4.5	2.7	2.0	43	3.4	1.5	1.0
19	5.0	2.7	1.7	44	3.5	1.7	0.8
20	9.0	4.8	4.0	45	4.4	2.6	0.9
21	3.8	2.5	2.1	46	2.8	1.2	0.6
22	4.0	3.5	0.7	47	2.7	2.4	1.2
23	3.0	1.5	1.1	48	2.6	1.5	0.9
24	4.8	2.9	2.4	49	3.1	2.0	1.4
25	4.2	3.3	1.6	50	2.5	1.5	0.7

Exposure E – C1

Latitude: N46°51.363’

Longitude: E010°03.361’

Elevation: 2489 m

	VA	A	SA	SR	R	WR	
True No.	0	5	25	19	1	0	0
%	0	10	50	38	2	0	0

	Clast axes				Clast axes		
Clast no.	a-axis	b-axis	c-axis	Clast no.	a-axis	b-axis	c-axis
1	6.5	3	2	26	6.5	4.2	4.2
2	3	2.5	0.9	27	3.6	3.0	2.1
3	7	2.9	2.5	28	6.0	4.9	2.5
4	5.1	2	1.7	29	5.0	3.5	2.0
5	4.8	3.5	1	30	4.6	2.5	1.8
6	3.4	1.6	1.4	31	3.0	2.1	1.2
7	10.7	7.2	4.5	32	3.0	1.7	1.4
8	6.0	5.3	3.6	33	2.5	2.0	1.5
9	5.5	3.5	2.4	34	3.0	2.0	1.2
10	2.7	1.9	1.4	35	3.0	1.1	1.0
11	6.9	4.6	4.3	36	2.6	2.0	1.5
12	5.9	3.7	2.5	37	3.0	1.7	1.0
13	4.2	2.0	2.0	38	2.6	1.8	1.4
14	3.0	2.5	1.8	39	2.7	1.1	1.1
15	3.2	1.9	1.0	40	2.5	2.1	0.8
16	4.3	2.5	2.0	41	7.5	2.5	2.1
17	4.5	3.7	2.9	42	4.7	3.0	2.0
18	3.5	2.5	1.0	43	4.0	3.8	1.5
19	3.5	2.2	1.8	44	4.5	3.9	1.5
20	3.6	2.2	1.9	45	4.3	4.0	1.6
21	3.7	2.9	1.9	46	3.8	2.0	1.4
22	3.4	2.0	1.1	47	2.5	2.4	0.9
23	3.3	2.4	1.0	48	3.8	3.0	1.4
24	2.9	1.9	1.0	49	3.5	1.9	1.0
25	2.5	2.0	1.4	50	3.0	1.5	1.2

Exposure E – C2

Latitude: N46°51.363’

Longitude: E010°03.361’

Elevation: 2489 m

	VA	A	SA	SR	R	WR		
True No.	0	1	19	26	4	0	0	
%	0	2	38	52	8	0	0	

	Clast axes				Clast axes		
Clast no.	a-axis	b-axis	c-axis	Clast no.	a-axis	b-axis	c-axis
1	3	1.9	1	26	4.0	2.2	0.7
2	10.5	7.4	6	27	3.0	1.6	1.2
3	6.9	4	3.5	28	2.6	1.6	1.3
4	5.2	3.6	2.2	29	3.0	1.8	1.6
5	3.3	2	1.4	30	3.0	2.8	2.5
6	5	2.9	1.6	31	4.0	2.9	2.0
7	6.5	4.4	2.9	32	7.0	5.4	5.0
8	2.1	1.7	1.0	33	10.5	4.0	3.5
9	5.5	4.4	1.6	34	3.6	2.5	2.0
10	5.9	3.4	3.0	35	8.5	6.5	3.5
11	5.0	3.8	2.9	36	3.5	2.5	2.1
12	4.5	3.0	1.2	37	5.0	3.2	2.0
13	7.8	3.7	3.4	38	3.5	2.5	1.1
14	3.0	2.5	2.0	39	3.0	2.1	1.0
15	3.7	2.0	1.2	40	3.9	2.4	1.4
16	3.0	2.1	1.6	41	4.0	3.0	2.1
17	3.8	3.3	2.5	42	4.1	2.1	2.0
18	3.0	2.5	1.4	43	3.0	1.9	0.5
19	4.1	3.0	2.0	44	3.4	3.0	2.0
20	2.8	2.4	0.9	45	5.0	2.5	1.0
21	3.1	3.0	1.6	46	3.7	2.0	1.4
22	7.2	4.1	3.7	47	2.8	1.3	1.1
23	2.5	1.9	1.0	48	2.5	1.5	1.3
24	5.0	2.5	1.9	49	2.7	2.0	1.6
25	3.4	1.3	1.1	50	3.4	2.0	1.3

Exposure F – C1

Latitude: N46°51.315’

Longitude: E010°03.435’

Elevation: 2475 m

	VA	A	SA	SR	R	WR		
True No.	0	4	22	24	0	0	0	
%	0	8	44	48	0	0	0	

	Clast axes				Clast axes		
Clast no.	a-axis	b-axis	c-axis	Clast no.	a-axis	b-axis	c-axis
1	12.8	10	5	26	3.8	2.0	1.0
2	7.9	6	3.6	27	2.7	1.8	1.4
3	10.8	6.5	4.8	28	3.0	2.0	0.9
4	9.9	7.4	2.6	29	2.5	2.0	1.1
5	3	3	1.3	30	2.9	1.7	1.1
6	4	2.5	1.5	31	2.7	2.6	1.8
7	3.8	2.5	1.5	32	2.9	1.6	0.7
8	4.6	3.0	1.4	33	3.0	1.6	1.0
9	3.6	3.0	1.6	34	3.5	3.2	2.0
10	3.5	3.3	1.4	35	3.3	2.5	1.4
11	5.8	3.0	1.8	36	2.7	1.5	0.9
12	4.2	3.6	1.5	37	3.7	2.0	1.2
13	4.0	2.8	1.5	38	2.7	1.5	1.0
14	2.5	2.4	1.1	39	2.8	2.0	0.7
15	4.2	3.6	0.6	40	2.5	2.1	1.2
16	3.8	2.5	1.0	41	3.3	1.9	1.6
17	3.1	2.0	1.2	42	6.0	5.5	2.5
18	3.0	2.1	1.1	43	4.0	3.0	1.4
19	3.2	1.5	1.1	44	5.5	3.7	1.6
20	2.5	1.5	1.0	45	9.7	8.0	4.5
21	4.1	3.0	1.6	46	4.6	3.5	1.0
22	4.0	3.4	1.4	47	6.9	4.0	3.5
23	3.4	2.8	1.4	48	4.5	3.5	1.0
24	3.2	1.7	1.2	49	9.3	5.4	4.6
25	3.1	2.1	0.8	50	7.5	6.6	3.0

Exposure F – C2

Latitude: N46°51.315’

Longitude: E010°03.435’

Elevation: 2475 m

	VA	A	SA	SR	R	WR		
True No.	0	0	9	40	1	0	0	
%	0	0	18	80	2	0	0	

	Clast axes				Clast axes		
Clast no.	a-axis	b-axis	c-axis	Clast no.	a-axis	b-axis	c-axis
1	5	3.5	1.3	26	7.0	4.9	2.4
2	8	5.4	2.1	27	2.7	1.9	1.1
3	8.4	6.2	5.4	28	2.6	1.5	1.0
4	5	3.4	1.5	29	6.0	3.5	2.8
5	12	11.5	4	30	7.2	5.5	3.6
6	5	3.5	2.7	31	3.0	2.1	1.1
7	4.5	2.5	1.7	32	4.4	2.7	2.2
8	3.0	2.4	1.0	33	2.8	2.6	1.4
9	4.5	3.6	1.5	34	3.6	2.5	0.7
10	3.4	2.2	1.0	35	4.6	2.5	1.4
11	4.6	3.5	2.0	36	5.1	3.5	2.0
12	12.5	8.0	6.0	37	3.2	2.5	1.5
13	6.1	4.4	2.0	38	4.0	3.0	2.0
14	6.5	5.0	2.2	39	12.6	7.0	7.0
15	6.5	4.5	3.0	40	6.5	3.1	2.6
16	4.3	3.5	2.6	41	5.7	4.1	4.1
17	5.0	3.2	2.2	42	3.1	2.6	1.0
18	5	3.5	1.3	43	3.4	2.1	1.0
19	8	5.4	2.1	44	5.0	3.0	1.6
20	8.4	6.2	5.4	45	4.1	3.5	1.1
21	5	3.4	1.5	46	2.9	2.0	1.0
22	12	11.5	4	47	7.0	3.5	3.0
23	5	3.5	2.7	48	5.0	3.0	1.9
24	4.5	2.5	1.7	49	4.5	3.1	1.8
25	3.0	2.4	1.0	50	3.0	2.5	1.5

Exposure G – C1

Latitude: N46°51.259’

Longitude: E010°03.521’

Elevation: 2501 m

	VA	A	SA	SR	R	WR		
True No.	0	1	21	27	1	0	0	
%	0	2	42	54	2	0	0	

	Clast axes				Clast axes		
Clast no.	a-axis	b-axis	c-axis	Clast no.	a-axis	b-axis	c-axis
1	4.5	4	2.1	26	7.0	4.5	3.5
2	4	3.1	2.4	27	3.4	3.0	0.8
3	4.5	3.2	1	28	4.5	3.1	1.9
4	5	4.5	2.2	29	5.6	3.5	1.7
5	6.5	3	3	30	3.7	2.9	1.5
6	3.5	2.8	1.4	31	4.1	2.2	1.2
7	4	2.8	1.1	32	5.2	2.6	1.5
8	2.5	2.2	1.0	33	6.5	4.2	2.2
9	6.8	5.0	2.5	34	3.6	2.5	0.9
10	4.2	2.4	2.1	35	8.5	5.4	4.1
11	6.2	3.1	3.0	36	5.5	3.0	2.0
12	9.1	5.0	2.1	37	2.5	2.5	1.5
13	8.0	6.2	4.5	38	3.5	2.5	1.5
14	3.5	2.4	1.5	39	6.0	2.7	1.5
15	5.1	4.5	4.0	40	3.0	2.4	1.3
16	3.4	2.0	1.0	41	3.2	2.4	1.6
17	4.5	2.9	1.3	42	4.9	3.5	1.2
18	5.5	3.0	1.8	43	2.6	1.0	0.5
19	3.2	2.5	1.2	44	3.5	1.7	1.4
20	4.5	3.5	1.0	45	3.0	1.5	1.2
21	3.5	2.0	1.0	46	3.0	1.8	1.1
22	2.9	1.5	1.5	47	3.4	2.4	1.0
23	8.0	3.6	2.5	48	2.7	1.5	0.7
24	3.6	3.0	1.4	49	2.5	2.2	1.4
25	5.5	3.0	2.2	50	2.9	1.5	1.1

Exposure G – C2

Latitude: N46°51.259’

Longitude: E010°03.521’

Elevation: 2501 m

	VA	A	SA	SR	R	WR		
True No.	0	0	11	38	1	0	0	
%	0	0	22	76	2	0	0	

	Clast axes				Clast axes		
Clast no.	a-axis	b-axis	c-axis	Clast no.	a-axis	b-axis	c-axis
1	4.9	3.4	1.5	26	3.9	3.5	1.7
2	5.5	2.5	2.1	27	3.5	2.5	2.5
3	9.8	7.5	2.7	28	4.2	2.0	2.0
4	7.5	4.5	1.9	29	11.0	8.5	4.5
5	6	4.4	3	30	5.7	4.5	3.0
6	10.5	6.4	3.5	31	7.6	3.2	2.4
7	3.7	2.6	1.5	32	14.0	5.5	4.0
8	3.3	2.1	1.2	33	6.5	4.5	2.5
9	3.5	3.0	1.1	34	4.1	2.9	2.0
10	9.5	6.0	3.5	35	8.5	3.6	2.6
11	3.5	2.4	1.3	36	4.9	2.9	2.0
12	10.5	5.5	3.0	37	3.8	3.0	1.8
13	3.2	2.0	1.5	38	4.0	2.2	1.5
14	2.8	2.1	1.2	39	5.0	3.0	1.7
15	9.5	7.6	4.0	40	4.0	3.0	2.1
16	4.5	3.6	1.6	41	5.7	4.1	2.4
17	5.0	3.1	1.6	42	5.5	3.0	2.5
18	11.6	5.5	3.1	43	6.0	4.5	3.0
19	5.6	4.0	2.1	44	5.5	4.0	2.0
20	4.0	4.0	1.5	45	7.3	6.0	3.0
21	2.5	1.5	0.8	46	7.7	7.0	3.5
22	4.5	3.0	1.7	47	4.1	2.6	1.1
23	6.0	4.5	2.4	48	3.0	2.5	1.5
24	6.0	4.1	2.8	49	3.5	3.0	1.6
25	3.0	2.0	1.3	50	2.7	2.5	1.1

Debris cone 01

Latitude: N46°51.361’

Longitude: E010°03.396’

Elevation: 2519 m

	VA	A	SA	SR	R	WR		
True No.	0	1	24	25	0	0	0	
%	0	2	48	50	0	0	0	

	Clast axes				Clast axes		
Clast no.	a-axis	b-axis	c-axis	Clast no.	a-axis	b-axis	c-axis
1	7	4.4	3.8	26	4.7	4.0	1.5
2	4.9	4.4	2.5	27	2.5	2.0	0.7
3	6	4.7	2.6	28	3.1	2.6	1.4
4	5.5	4.4	2.8	29	4.2	2.4	1.5
5	3	2.8	1.7	30	4.7	3.5	2.3
6	5.5	4.2	3	31	2.5	1.9	1.9
7	8.8	5	4	32	4.2	3.4	2.1
8	8.4	5.2	2.4	33	4.9	4.3	2.5
9	6.5	4.0	3.3	34	2.8	2.3	2.0
10	3.0	2.2	1.5	35	3.5	3.1	2.5
11	4.7	3.5	3.0	36	4.8	3.2	2.8
12	3.5	2.5	1.8	37	5.4	3.5	2.3
13	4.3	3.5	2.7	38	4.8	4.2	1.7
14	4.5	3.7	2.2	39	4.4	2.7	1.3
15	5.5	4.4	2.8	40	4.2	4.2	2.5
16	7.5	5.8	3.5	41	3.4	2.5	2.0
17	7.5	6.5	4.4	42	4.5	3.8	2.9
18	7.0	4.7	3.0	43	3.2	3.0	0.7
19	6.0	4.5	3.0	44	4.7	3.8	2.1
20	2.6	1.7	1.6	45	6.0	4.0	2.3
21	4.5	2.5	1.6	46	5.2	3.8	2.3
22	4.8	3.5	2.8	47	4.0	3.0	1.5
23	8.0	5.0	3.8	48	3.2	2.0	1.8
24	5.2	3.5	3.3	49	2.8	1.8	1.2
25	4.2	3.0	3.0	50	2.7	2.5	1.6

Debris cone 02

Latitude: N46°51.394’

Longitude: E010°03.407’

Elevation: 2521 m

	VA	A	SA	SR	R	WR		
True No.	0	0	14	35	1	0	0	
%	0	0	28	70	2	0	0	

	Clast axes				Clast axes		
Clast no.	a-axis	b-axis	c-axis	Clast no.	a-axis	b-axis	c-axis
1	10	3.5	3.2	26	5.2	3.2	2.1
2	3.8	3.4	2.1	27	3.0	2.5	1.0
3	5.5	4.5	3	28	3.5	2.2	0.9
4	5	3.6	3	29	3.0	2.0	1.4
5	8	5.4	3.5	30	3.5	1.8	1.5
6	4.8	3.8	3	31	3.8	2.2	2.0
7	5.5	3.5	3	32	3.8	2.2	1.4
8	5.5	4.0	2.2	33	4.5	2.5	1.8
9	5.1	3.6	2.0	34	5.5	4.5	2.6
10	5.4	3.2	3.0	35	4.6	2.9	2.1
11	6.4	4.0	2.2	36	9.5	7.0	2.6
12	5.8	4.0	2.8	37	5.7	3.0	2.0
13	4.0	3.5	2.0	38	2.7	2.5	2.0
14	4.5	3.1	1.5	39	4.0	3.6	2.2
15	3.0	2.5	1.6	40	4.2	2.6	1.8
16	6.0	3.5	2.5	41	3.5	2.4	1.5
17	3.5	3.0	1.5	42	3.8	3.0	2.5
18	4.8	1.8	1.6	43	4.0	3.2	1.6
19	5.5	3.6	1.4	44	3.5	2.6	1.0
20	5.0	3.8	2.4	45	3.3	2.4	1.6
21	3.9	2.6	1.6	46	3.8	3.6	1.5
22	5.5	3.8	3.0	47	3.8	2.7	1.6
23	4.0	3.4	2.2	48	4.4	2.0	1.5
24	5.0	2.8	2.2	49	2.8	2.3	1.0
25	4.6	3.0	1.6	50	3.5	2.8	1.5

Medial moraine 01

Latitude: N46°51.454’

Longitude: E010°03.633’

Elevation: 2531 m

	VA	A	SA	SR	R	WR		
True No.	0	3	24	22	1	0	0	
%	0	6	48	44	2	0	0	

	Clast axes				Clast axes		
Clast no.	a-axis	b-axis	c-axis	Clast no.	a-axis	b-axis	c-axis
1	9.9	5.9	5	26	3.5	2.1	2.0
2	5	3.6	2.6	27	5.0	4.5	2.6
3	8	6	4.2	28	5.0	3.5	2.0
4	7	5.5	3	29	4.1	3.9	2.0
5	3.5	2.5	2.2	30	4.2	3.0	2.5
6	12	8	6	31	4.5	3.5	2.0
7	7.5	4.5	1.6	32	8.5	8.0	3.0
8	4.5	3.4	1.6	33	5.6	4.0	3.1
9	5.0	3.7	1.8	34	3.5	2.2	0.9
10	6.0	3.5	3.4	35	3.9	3.5	1.0
11	3.9	3.0	1.5	36	2.8	2.0	1.6
12	3.0	2.2	1.6	37	4.4	3.5	1.8
13	5.0	3.5	1.8	38	4.8	4.5	2.3
14	3.5	2.0	1.5	39	5.5	4.0	3.6
15	4.0	3.0	1.6	40	4.2	3.5	2.0
16	10.8	8.0	4.0	41	4.5	3.6	2.4
17	5.9	2.5	1.6	42	4.5	3.0	2.1
18	4.0	3.4	2.0	43	4.5	2.5	1.6
19	6.2	3.0	1.6	44	5.5	3.0	2.1
20	6.0	4.0	2.0	45	4.0	3.5	2.5
21	4.0	2.5	2.0	46	3.7	2.4	2.0
22	5.0	2.5	2.2	47	4.0	2.0	1.5
23	8.5	6.4	2.5	48	3.2	2.2	1.5
24	4.0	3.0	2.0	49	4.5	3.9	2.0
25	3.4	2.1	1.0	50	3.4	2.5	1.0

Medial moraine 02

Latitude: N46°51.467’

Longitude: E010°03.655’

Elevation: 2534 m

	VA	A	SA	SR	R	WR		
True No.	0	1	29	20	0	0	0	
%	0	2	58	40	0	0	0	

	Clast axes				Clast axes		
Clast no.	a-axis	b-axis	c-axis	Clast no.	a-axis	b-axis	c-axis
1	4	2.6	1.7	26	6.5	6.0	4.5
2	4.1	3	1.5	27	5.3	3.5	3.0
3	6	5	3.1	28	10.5	6.0	4.2
4	6.8	5.3	5.3	29	10.0	7.0	5.0
5	8.5	4.5	4.1	30	6.0	5.1	2.5
6	5.5	4	2.6	31	6.0	4.5	3.0
7	4.2	3.3	1.6	32	10.0	7.0	6.5
8	9.0	5.5	3.0	33	6.0	4.4	2.2
9	9.5	5.0	4.5	34	4.5	2.1	2.0
10	4.5	3.4	2.2	35	5.5	3.5	2.5
11	7.0	5.5	4.5	36	5.5	3.3	2.4
12	3.5	2.6	2.2	37	4.0	2.5	1.6
13	2.6	2.2	1.8	38	3.7	2.0	1.4
14	5.0	3.3	2.2	39	2.7	2.5	1.3
15	4.0	3.0	2.3	40	3.8	2.2	1.4
16	4.5	3.2	3.1	41	3.0	1.5	0.8
17	6.3	3.8	2.6	42	3.5	2.4	1.6
18	5.0	3.5	3.0	43	4.1	3.2	2.2
19	5.0	3.7	1.7	44	5.3	3.6	1.0
20	6.5	5.0	5.0	45	5.3	4.3	3.4
21	3.5	2.0	1.4	46	3.9	2.4	2.3
22	5.5	2.7	2.5	47	3.6	2.3	1.9
23	6.0	4.5	3.9	48	4.4	3.2	2.1
24	6.2	4.5	2.0	49	2.6	1.9	1.9
25	7.6	4.5	3.0	50	2.6	1.5	1.3

Supraglacial 01

Latitude: N46°51.519’

Longitude: E010°03.857’

Elevation: 2560 m

	VA	A	SA	SR	R	WR	
True No.	5	40	5	0	0	0	5
%	10	80	10	0	0	0	10

	Clast axes				Clast axes		
Clast no.	a-axis	b-axis	c-axis	Clast no.	a-axis	b-axis	c-axis
1	5	3.3	2.1	26	7.5	4.3	1.8
2	8	3.8	2.1	27	6.8	3.5	1.8
3	3.2	3.1	1.2	28	4.0	3.2	1.0
4	5.1	4.5	2	29	4.0	1.7	1.5
5	14	4.5	3.4	30	4.0	1.6	1.5
6	7.5	4.2	2.2	31	4.5	1.6	0.8
7	7	3	2.5	32	5.2	2.6	1.8
8	3.5	2.6	2.0	33	7.9	5.9	1.6
9	3.5	3.0	1.1	34	9.5	6.5	1.0
10	5.5	3.5	2.8	35	8.5	3.0	1.6
11	3.8	2.2	1.0	36	6.0	4.0	2.4
12	6.0	3.7	1.3	37	11.5	3.6	3.6
13	6.5	2.8	2.0	38	5.6	3.0	2.5
14	6.5	5.6	1.0	39	7.9	3.6	0.7
15	5.1	3.6	1.0	40	7.5	3.0	2.5
16	6.0	2.6	1.6	41	4.5	2.6	1.4
17	14.0	3.0	2.5	42	7.9	3.5	2.5
18	5.5	3.5	2.3	43	3.4	2.8	1.0
19	6.5	2.0	2.0	44	3.2	2.5	0.7
20	4.0	3.5	0.8	45	4.2	2.5	0.8
21	3.5	2.5	1.5	46	16.0	5.5	5.0
22	6.3	4.3	2.6	47	14.5	6.5	5.0
23	3.7	3.0	1.6	48	7.3	5.6	1.6
24	7.8	5.0	1.2	49	12.0	6.0	2.5
25	6.0	4.6	2.0	50	9.0	5.2	4.0

Supraglacial 02

Latitude: N46°51.495’

Longitude: E010°03.732’

Elevation: 2545 m

	VA	A	SA	SR	R	WR	
True No.	1	42	5	0	0	0	1
%	2	88	10	0	0	0	2

	Clast axes				Clast axes		
Clast no.	a-axis	b-axis	c-axis	Clast no.	a-axis	b-axis	c-axis
1	9.5	4	3.8	26	5.4	3.8	0.8
2	3.1	1.6	1.5	27	9.4	4.0	4.0
3	4.7	2	1.7	28	11.0	6.0	2.5
4	7.5	5	3.1	29			
5	6	3.5	1.6	30			
6	7	3.8	3.5	31	5.0	3.0	2.0
7	6.4	3.1	1.8	32	4.5	1.8	1.6
8	10.0	3.0	2.5	33	5.1	3.5	2.0
9	6.7	4.5	3.5	34	4.3	2.4	1.4
10	9.5	7.0	4.5	35	6.0	3.0	1.2
11	5.2	4.3	2.0	36	7.6	4.5	2.9
12	4.5	2.1	1.2	37	9.0	6.5	1.5
13	8.0	3.5	2.4	38	7.0	3.5	1.3
14	7.0	4.0	3.0	39	10.0	6.0	3.0
15	5.0	3.2	2.4	40	4.4	2.5	0.9
16	4.5	2.5	1.0	41	4.4	1.5	1.0
17	6.4	4.4	0.8	42	2.7	1.6	0.9
18	7.5	3.4	1.5	43	3.5	1.8	1.0
19	5.5	2.1	1.6	44	8.0	7.0	1.6
20	4.3	3.0	2.5	45	15.0	10.0	3.0
21	6.5	3.3	1.1	46	16.0	10.5	2.5
22	7.0	4.6	1.1	47	4.5	3.2	1.8
23	6.0	2.6	1.0	48	6.5	3.3	1.6
24	6.0	3.5	1.5	49	7.0	3.5	3.0
25	7.4	3.6	3.1	50	8.0	5.0	2.4

Subglacial 01

Latitude: N46°51.517'

Longitude: E010°03.802'

Elevation: 2552 m

	VA	A	SA	SR	R	WR		
True No.	0	7	22	20	1	0	0	
%	0	14	44	40	2	0	0	

	Clast axes				Clast axes		
Clast no.	a-axis	b-axis	c-axis	Clast no.	a-axis	b-axis	c-axis
1	6.5	4.5	3	26	5.5	3.6	3.0
2	7	6.6	5.5	27	3.2	2.5	2.0
3	4.5	3.5	3.5	28	5.0	3.0	2.0
4	11.8	5.5	4	29	4.0	3.5	2.4
5	6	3	2.4	30	3.0	2.2	1.6
6	5	3.4	1.2	31	3.1	2.2	1.8
7	7	4	3.5	32	4.0	3.5	2.5
8	2.6	2.2	2.0	33	4.0	3.0	2.0
9	3.6	2.5	2.0	34	5.0	4.1	2.5
10	3.5	3.5	2.5	35	4.0	3.0	2.5
11	4.0	3.0	2.1	36	3.5	3.0	2.0
12	12.5	7.1	4.5	37	3.1	3.0	1.2
13	6.0	5.5	3.0	38	5.6	5.0	1.4
14	8.0	3.5	2.0	39	5.0	3.9	2.3
15	5.0	3.5	3.0	40	3.0	2.0	1.5
16	11.0	5.5	4.1	41	4.0	3.0	1.4
17	4.5	3.5	2.5	42	4.0	2.5	1.5
18	5.0	2.5	2.0	43	3.5	3.1	2.3
19	4.5	3.5	2.5	44	3.5	2.0	2.0
20	5.0	3.4	2.7	45	3.0	2.5	2.0
21	6.0	3.7	2.5	46	3.0	1.5	1.5
22	4.5	4.0	2.5	47	3.6	2.0	1.5
23	4.0	3.0	2.5	48	3.3	2.0	1.3
24	6.0	3.5	3.1	49	4.0	2.0	2.0
25	6.0	3.6	2.5	50	3.8	3.0	2.1

Subglacial 02

Latitude: N46°51.377'

Longitude: E010°03.427'

Elevation: 2473 m

	VA	A	SA	SR	R	WR		
True No.	0	3	21	26	0	0	0	
%	0	6	42	52	0	0	0	

	Clast axes				Clast axes		
Clast no.	a-axis	b-axis	c-axis	Clast no.	a-axis	b-axis	c-axis
1	9	8.5	4	26	5.7	4.5	2.8
2	10	9	3.7	27	4.5	4.0	2.2
3	8.5	4.8	4	28	4.1	2.4	0.7
4	7.5	5	3.5	29	3.6	2.5	1.5
5	3	2.5	1.5	30	4.5	4.5	2.0
6	6.5	4	3	31	4.1	3.0	2.2
7	3.8	2	2	32	3.0	2.5	2.0
8	4.5	3.0	1.5	33	3.7	1.9	1.6
9	6.7	5.0	2.5	34	6.0	4.0	2.5
10	3.8	2.6	1.1	35	4.4	2.7	2.5
11	3.4	2.0	1.4	36	4.0	2.5	1.1
12	4.0	2.9	2.4	37	5.0	3.0	1.6
13	4.7	2.6	2.2	38	3.8	3.0	1.6
14	3.3	2.5	2.2	39	3.5	2.7	1.1
15	3.0	2.2	1.5	40	3.2	2.6	2.0
16	4.0	3.5	1.6	41	3.3	2.5	2.2
17	6.2	4.5	2.6	42	3.1	2.5	1.5
18	5.0	3.5	3.3	43	3.6	2.0	1.1
19	6.5	3.6	3.5	44	3.6	2.0	2.0
20	3.4	2.1	1.4	45	3.1	2.4	1.5
21	4.3	3.5	2.5	46	5.0	3.6	1.9
22	5.5	4.0	3.5	47	2.5	2.1	1.0
23	3.0	2.2	1.6	48	3.1	2.0	0.8
24	4.0	2.4	1.5	49	2.8	1.9	0.8
25	4.6	2.4	1.6	50	3.5	2.2	1.0

Subglacial 03

Latitude: N46°51.252’

Longitude: E010°03.560’

Elevation: 2496 m

	VA	A	SA	SR	R	WR		
True No.	0	4	25	21	0	0	0	
%	0	8	50	42	0	0	0	

	Clast axes				Clast axes		
Clast no.	a-axis	b-axis	c-axis	Clast no.	a-axis	b-axis	c-axis
1	5.2	2.5	2	26	4.6	3.5	1.9
2	6.5	4.2	3.1	27	4.6	3.4	1.0
3	3	2	1.5	28	5.0	4.0	2.0
4	5	4.4	2.5	29	4.5	2.5	1.6
5	5.7	4.8	3	30	2.8	2.2	1.5
6	4.9	3.1	2.7	31	3.8	2.6	1.2
7	4.5	2.8	2	32	4.5	3.1	1.8
8	3.4	2.5	1.6	33	3.6	2.5	2.1
9	6.5	3.5	3.0	34	3.6	2.6	1.4
10	3.5	3.1	1.6	35	3.6	2.8	1.2
11	3.1	2.0	2.0	36	3.6	2.9	1.1
12	3.8	3.0	2.7	37	3.4	2.0	1.3
13	7.0	4.2	2.9	38	4.0	2.4	1.9
14	3.2	2.6	1.5	39	3.6	2.4	2.0
15	7.8	6.5	3.5	40	4.2	2.6	2.5
16	7.6	4.0	2.0	41	4.0	2.4	1.4
17	6.0	5.0	2.8	42	3.5	2.5	1.6
18	4.3	2.5	1.6	43	2.7	2.0	1.6
19	3.8	2.6	1.8	44	2.8	1.8	1.2
20	3.1	2.7	1.5	45	3.5	1.5	1.0
21	4.6	2.5	1.4	46	3.4	2.0	0.7
22	7.0	5.3	3.0	47	2.5	1.8	1.2
23	4.6	3.8	1.4	48	3.1	1.6	0.8
24	6.0	3.7	3.0	49	2.5	1.4	0.7
25	3.5	3.5	1.5	50	2.7	1.5	0.8

Channel 01

Latitude: N46°51.332’

Longitude: E010°03.371’

Elevation: 2469 m

	VA	A	SA	SR	R	WR	
True No.	2	6	24	18	0	0	2
%	4	12	48	36	0	0	4

	Clast axes				Clast axes		
Clast no.	a-axis	b-axis	c-axis	Clast no.	a-axis	b-axis	c-axis
1	5	2.6	1.8	26	9.0	6.5	5.5
2	2.9	2.5	1.2	27	16.5	9.0	7.5
3	5	3.9	3.5	28	4.0	3.0	2.3
4	7	3.6	2.6	29	3.1	2.0	1.1
5	3	2.4	1.7	30	4.2	2.6	1.6
6	4	2.4	1.8	31	3.0	2.4	1.1
7	3.1	2.6	1.9	32	3.0	3.0	1.5
8	3.5	2.3	1.6	33	2.7	1.2	1.0
9	3.7	2.7	2.2	34	3.2	2.8	1.1
10	4.5	4.3	2.4	35	2.7	1.8	1.2
11	5.5	3.4	2.5	36	7.0	4.5	3.5
12	3.5	3.0	2.0	37	6.5	5.4	3.8
13	3.1	2.5	2.0	38	2.5	2.2	0.5
14	3.7	2.2	2.1	39	5.5	2.0	2.0
15	3.6	2.8	1.6	40	3.2	2.0	1.2
16	2.9	1.5	1.5	41	3.5	3.0	3.0
17	4.2	3.4	1.5	42	2.5	1.5	1.5
18	6.7	4.0	2.0	43	8.3	4.6	4.4
19	7.5	3.9	2.4	44	9.0	5.5	5.5
20	3.3	1.5	1.0	45	5.0	3.9	3.0
21	3.5	2.7	1.6	46	3.6	2.5	2.5
22	4.2	3.5	2.0	47	6.8	4.0	3.6
23	4.4	2.4	2.0	48	5.5	2.6	1.4
24	5.6	2.7	2.0	49	3.4	2.0	1.4
25	5.0	3.0	1.4	50	4.0	2.9	1.5

Channel 02

Latitude: N46°51.120'

Longitude: E010°03.009'

Elevation: 2410 m

	VA	A	SA	SR	R	WR	
True No.	0	3	21	23	3	0	0
%	0	6	42	46	6	0	0

	Clast axes				Clast axes		
Clast no.	a-axis	b-axis	c-axis	Clast no.	a-axis	b-axis	c-axis
1	9.5	6	4.5	26	3.1	1.9	1.4
2	3.5	2.5	1.9	27	5.6	2.4	2.4
3	3.8	2.9	1.6	28	6.7	4.4	2.4
4	3.6	1.5	1.5	29	3.6	2.9	1.6
5	5.3	2.8	2.2	30	3.5	2.5	1.4
6	3.6	2	2	31	2.5	2.0	1.0
7	5	3.6	3.5	32	3.1	1.9	1.5
8	3.5	2.7	1.4	33	5.1	3.9	3.1
9	3.5	1.6	1.4	34	3.2	3.0	1.6
10	4.0	2.5	1.5	35	3.0	2.2	1.5
11	3.4	2.2	1.5	36	3.6	3.5	2.7
12	2.5	2.0	1.5	37	3.1	1.2	1.2
13	3.7	2.3	1.5	38	4.5	3.0	1.2
14	8.4	6.3	4.2	39	3.5	2.8	2.0
15	4.7	4.0	1.9	40	3.0	2.0	1.7
16	3.9	3.7	2.0	41	3.1	1.3	1.0
17	3.5	2.7	1.5	42	3.2	1.6	1.0
18	3.3	2.9	1.9	43	4.1	1.9	1.9
19	3.8	2.9	1.6	44	3.0	2.0	1.1
20	3.8	2.6	1.5	45	3.2	2.5	1.5
21	4.0	3.0	2.0	46	3.5	2.3	1.5
22	4.9	4.0	2.5	47	2.7	2.5	1.4
23	3.7	2.0	2.0	48	2.7	1.7	1.6
24	3.2	1.9	0.8	49	3.1	2.3	1.6
25	4.5	2.5	1.6	50	2.9	2.6	1.1